

THE UNIVERSITY OF CHICAGO

PALLADIUM-CATALYZED β -C-H FUNCTIONALIZATION OF KETONES AND AMINES

A DISSERTATION SUBMITTED TO
THE FACULTY OF THE DIVISION OF THE PHYSICAL SCIENCES
IN CANDIDACY FOR THE DEGREE OF
DOCTOR OF PHILOSOPHY

DEPARTMENT OF CHEMISTRY

BY

ZHONGXING HUANG

CHICAGO, ILLINOIS

AUGUST 2017

Copyright © 2017 by Zhongxing Huang

All rights reserved

To my mother

TABLE OF CONTENTS

LIST OF SCHEMES.....	ix
LIST OF TABLES.....	xvi
LIST OF FIGURES.....	xviii
LIST OF ABBREVIATIONS.....	xxiii
ACKNOWLEDGEMENT.....	xxv
CHAPTER 1 Site-Selectivity Control in Organic Reactions.....	1
1.1 Introduction.....	1
1.2 Undirected Control of Site-Selectivity.....	5
1.3 Directed Control of Site-Selectivity.....	8
1.4 Conclusion and Outlook.....	12
1.5 References.....	14
CHAPTER 2 Transition Metal-Catalyzed Ketone-Directed or Mediated C–H Functionalization	16
2.1 Introduction.....	16
2.2 Ketone as the Directing Group.....	18
2.2.1 Coupling with Alkenes and Alkynes.....	20
2.2.2 Arylation.....	39

2.2.3 Carbon-Heteroatom (C–X) Bond Formation	44
2.3 β -C–H Functionalization of Simple Ketones	50
2.4 Addition of α -C–H Bonds to Unactivated Alkenes or Alkynes	55
2.4.1 Addition to Alkenes	55
2.4.2 Addition to Alkynes	63
2.5 Conclusion	66
2.6 References.....	67
 CHAPTER 3 Catalytic C–C Bond Forming Transformations via Direct β -C–H Functionalization of Carbonyl Compounds	 74
3.1 Introduction	74
3.2 Cyclometallation via Directing Groups.....	75
3.2.1 General Mechanisms	76
3.2.2 Type A. Bidentate Directing Group	77
3.2.2.1 Arylation	77
3.2.2.2 Alkylation	85
3.2.2.3 Alkynylation	87
3.2.2.4 Carbonylation.....	88
3.2.2.5 Application in Total Synthesis	89
3.2.3 Type B. Weaker coordinating directing group.....	93
3.3 Migratory Coupling.....	101

3.4 Organocatalysis	105
3.5 Conclusion	108
3.6 References	110
CHAPTER 4 Catalytic Direct β -Arylation of Simple Ketones with Aryl Iodides	114
4.1 Introduction	114
4.2 Results and Discussion	122
4.3 Conclusion	142
4.4 Experimental	143
4.5 ^1H -NMR and ^{13}C -NMR Spectra	162
4.6 References	184
CHAPTER 5 Palladium-Catalyzed Direct β -Arylation of Ketones with Diaryliodonium Salts: A Stoichiometric Heavy Metal-Free and User-Friendly Approach	187
5.1 Introduction	187
5.2 Results and Discussion	190
5.3 Conclusion	208
5.4 Experimental	209
5.5 ^1H -NMR and ^{13}C -NMR Spectra	248
5.6 References	279

CHAPTER 6 Hydrazone-Based <i>exo</i> -Directing Groups for β -C–H Oxidation of Aliphatic Amines	281
6.1 Introduction	281
6.2 Results and Discussion	287
6.3 Conclusion	312
6.4 Experimental	314
6.5 ^1H -NMR and ^{13}C -NMR Spectra	368
6.6 References	423
CHAPTER 7 Further Exploration of Palladium-Catalyzed Direct β -Arylation of Ketones	425
7.1 Stoichiometric Heavy Metal-Free β -Arylation of Ketones with Aryl Iodides	425
7.1.1 Introduction	425
7.1.2 Results and Discussion	427
7.2 β -Arylation of Ketones with Aryl Bromides	439
7.2.1 Introduction	439
7.2.2 Results and Discussion	440
7.3 Enantioselective β -Arylation of Ketones	447
7.3.1 Introduction	447
7.3.2 Results and Discussion	448
7.4 Conclusion	462
7.5 Experimental	463

7.6 References 474

LIST OF SCHEMES

Scheme 1.1 Chemoselectivity and Site-selectivity: Concepts and Examples	2
Scheme 1.2 Alkyl C–H Bromination Using a Bulky Bromination Reagent	6
Scheme 1.3 White’s C–H Oxidation Using Iron Catalysts	7
Scheme 1.4 Site-Selectivity Control of Dirhodium-Catalyzed C–H Functionalization	8
Scheme 1.5 Peptide-Based Catalysts for Site-Selective Epoxidation of Polyenes	9
Scheme 1.6 Ligand-Controlled α - and β -Arylation of <i>N</i> -Boc Amines	10
Scheme 1.7 Site-Selective Acylation of Mannopyranose Derivatives	12
Scheme 2.1 Functionalization of Ketones	18
Scheme 2.2 C–H Functionalization Directed by Ketones	19
Scheme 2.3 Ruthenium-Catalyzed <i>ortho</i> -Alkylation of Aromatic Ketones	21
Scheme 2.4 Proposed Catalytic Cycle for the Ruthenium-Catalyzed <i>ortho</i> -Alkylation of Aromatic Ketones	22
Scheme 2.5 Formation of Active Catalyst of Ruthenium-Catalyzed <i>ortho</i> -Alkylation	23
Scheme 2.6 RuH ₂ (H ₂) ₂ (PCy ₃) ₂ -Catalyzed <i>ortho</i> -Ethylation with Ethylene	24
Scheme 2.7 Ketone-Directed <i>ortho</i> -Alkylation Using Ru(II) Precursors	25
Scheme 2.8 Ketone-Directed <i>ortho</i> -Alkylation of Olefinic C–H Bonds	25
Scheme 2.9 Rhodium-Catalyzed <i>ortho</i> -Alkylation of Aromatic Ketones with Olefins	26
Scheme 2.10 Amine-Assisted <i>ortho</i> -Alkylation of Aromatic Ketones and Enones	27
Scheme 2.11 Iridium-Catalyzed <i>ortho</i> -Alkylation of Aromatic Ketones with Olefins	28
Scheme 2.12 Branch-Selective <i>ortho</i> -Alkylation of Aromatic Ketones with Olefins	29
Scheme 2.13 Rhodium-Catalyzed <i>ortho</i> -Olefination of Aromatic Ketones with Olefins	30
Scheme 2.14 Catalytic Cycle of Rhodium-Catalyzed <i>ortho</i> -Olefination	31
Scheme 2.15 Rhodium-Catalyzed <i>ortho</i> -Alkylation/Aldol Condensation Cascade	32
Scheme 2.16 Ruthenium-Catalyzed <i>ortho</i> -Alkenylation of Aromatic Ketones or Enones with Alkynes	33
Scheme 2.17 Rhodium-Catalyzed Fulvene and Indenol Synthesis	34
Scheme 2.18 Rhodium-Catalyzed Cyclization of Diynes and Aromatic Ketones or Chalcones ..	35
Scheme 2.19 Rhodium-Catalyzed Cyclization of Enynes and Aromatic Ketones	36

Scheme 2.20 Cobalt-Catalyzed Cyclization of Enynes and Aromatic Ketones	37
Scheme 2.21 Ruthenium-Catalyzed Alkylation of Aromatic Diterpenoid	37
Scheme 2.22 Ruthenium-Catalyzed Synthesis and Modification of Polymers	38
Scheme 2.23 Ruthenium-Catalyzed <i>ortho</i> -Arylation of Aromatic Ketones with Arylboronates	39
Scheme 2.24 Proposed Catalytic Cycle of Ruthenium-Catalyzed <i>ortho</i> -Arylation	40
Scheme 2.25 Ruthenium-Catalyzed <i>ortho</i> -Arylation Using Pinacolone as Solvent	41
Scheme 2.26 Palladium-Catalyzed Multi-Arylation of Ketones	42
Scheme 2.27 Palladium-Catalyzed <i>ortho</i> -Arylation with Aryl Iodides	43
Scheme 2.28 Palladium-Catalyzed <i>ortho</i> -Arylation and Tandem Cyclization	43
Scheme 2.29 Palladium-Catalyzed Fluorenone Synthesis via Sequential C–H Activation	44
Scheme 2.30 General Mechanism of the Ketone-Directed <i>ortho</i> -C–X Bond Formation	45
Scheme 2.31 Palladium-Catalyzed Ketone-Directed <i>ortho</i> -Hydroxylation Reaction	46
Scheme 2.32 Ruthenium and Rhodium-Catalyzed Ketone-Directed <i>ortho</i> -Hydroxylation Reaction	47
Scheme 2.33 Palladium-Catalyzed Ketone-Directed <i>ortho</i> -Bromination and Iodination	48
Scheme 2.34 Palladium-Catalyzed Ketone-Directed <i>ortho</i> -Chlorination	48
Scheme 2.35 Palladium-Catalyzed Ketone-Directed <i>ortho</i> -Amination Using Sulfonamides	49
Scheme 2.36 Palladium-Catalyzed Ketone-Directed <i>ortho</i> -Amination Using Sulfonyl Azides	49
Scheme 2.37 Direct β -C–H Functionalization of Ketones	50
Scheme 2.38 Direct β -Arylation of Ketones via Photoredox Organocatalysis	51
Scheme 2.39 Proposed Catalytic Cycle of Direct β -Arylation of Ketones	52
Scheme 2.40 β -Aldol Coupling of Cyclic Ketones with Aryl Ketones via Photoredox Catalysis	53
Scheme 2.41 Photocatalyzed β -Alkylation and Acylation of Cyclopentanones	55
Scheme 2.42 α -Alkylation of Ketones	56
Scheme 2.43 Palladium-Catalyzed Intramolecular α -Alkylation of Ketones with Olefins	57
Scheme 2.44 Proposed Pathway of Palladium-Catalyzed Intramolecular α -Alkylation	58
Scheme 2.45 Gold-Catalyzed Intramolecular α -Alkylation of Ketones with Olefins	59
Scheme 2.46 Copper-Catalyzed Intermolecular α -Alkylation of Ketones with Olefins	60
Scheme 2.47 Manganese-Catalyzed Intermolecular α -Alkylation of Ketones with Olefins	61
Scheme 2.48 Proposed Strategy of α -Alkylation of Ketones Using Bifunctional Catalysis	62

Scheme 2.49 Rhodium-Catalyzed α -Alkylation of Ketones with Bifunctional Ligand	63
Scheme 2.50 Gold-Catalyzed Intramolecular α -Alkenylation of Ketones with Alkynes	64
Scheme 2.51 Palladium-Catalyzed Intramolecular α -Alkenylation of Ketones with Alkynes	65
Scheme 3.1 Conventional Synthesis of β -substituted Carbonyl Compounds	75
Scheme 3.2 Cyclometallation-type β -C–H Functionalization via Oxidative Addition of Electrophiles	76
Scheme 3.3 Cyclometallation-type β -C–H Functionalization via Transmetalation of Organometallic Reagents	77
Scheme 3.4 Palladium-Catalyzed β -Arylation of Amides using 8-Aminoquinoline as the Directing Group	78
Scheme 3.5 Synthesis of Non-natural Amino Acid Derivatives	79
Scheme 3.6 Palladium-Catalyzed β -Arylation Directed by 2-Methylthio Aniline or 8-Aminoquinoline Auxiliary	80
Scheme 3.7 Palladium-Catalyzed β -Monoarylation of Alanine Derivatives at Room Temperature	81
Scheme 3.8 Palladium-Catalyzed Synthesis of α -Amino- β -lactams via a Monoarylation/Amidation Sequence	81
Scheme 3.9 Palladium-Catalyzed Intramolecular β -Arylation	82
Scheme 3.10 Palladium-Catalyzed β -Arylation with Aryl Bromides or Diaryliodonium Salts	83
Scheme 3.11 Iron-Catalyzed β -Arylation Directed by 8-Aminoquinoline Auxiliary	84
Scheme 3.12 Iron-Catalyzed β -Arylation Directed by Triazolylmethylmethyl Auxiliary	84
Scheme 3.13 Nickel-Catalyzed β -Arylation Directed by 8-Aminoquinoline Auxiliary	84
Scheme 3.14 Early Examples of β -Alkylation Reaction	85
Scheme 3.15 Palladium-Catalyzed β -Alkylation with α -Halideacetates	86
Scheme 3.16 Nickel-Catalyzed β -Alkylation with Alkyl Halides	87
Scheme 3.17 Palladium-Catalyzed β -Alkynylation Directed by 8-Aminoquinoline Auxiliary	88
Scheme 3.18 Ruthenium-Catalyzed Synthesis of Succinimides via β -Carbonylation	89
Scheme 3.19 Synthesis of Celogentin C via Palladium-Catalyzed β -Arylation	90
Scheme 3.20 Synthesis of Piperarborenine B and D via Sequential β -Arylation	91

Scheme 3.21 Synthesis of Pipericyclobutanamide A via Palladium-Catalyzed β -Arylation/Olefination Sequence	92
Scheme 3.22 Synthesis of Podophyllotoxin via Palladium-Catalyzed β -Arylation	92
Scheme 3.23 Palladacycles from Bidentate or Monodentate Directing Groups	93
Scheme 3.24 Palladium-Catalyzed β -Arylation of Simple Carboxylic Acids	94
Scheme 3.25 Palladium-Catalyzed β -Arylation with Aryl Organoboron Reagents	94
Scheme 3.26 Palladium-Catalyzed β -Alkylation of <i>O</i> -Methyl Hydroxamic Acids	95
Scheme 3.27 Palladium-Catalyzed β -Arylation Using Acidic <i>N</i> -Arylamide Directing Groups ..	96
Scheme 3.28 Palladium-Catalyzed Synthesis of Succinimides via β -Carbonylation	97
Scheme 3.29 Palladium-Catalyzed β -Olefination with Benzyl Acrylates	97
Scheme 3.30 Palladium-Catalyzed β -Arylation of Methylene C–H Bonds	98
Scheme 3.31 Palladium-Catalyzed β -Alkynylation Directed by <i>N</i> -Arylamide	99
Scheme 3.32 Palladium-Catalyzed Ligand-controlled Synthesis of β -Hetero-diaryl Amino Acid Derivatives	100
Scheme 3.33 Palladium-Catalyzed Enantioselective β -Arylation	101
Scheme 3.34 Hartwig's Observation of β -Arylation	102
Scheme 3.35 Palladium-Catalyzed β -Arylation of Carboxylic Esters	102
Scheme 3.36 Palladium-Catalyzed Enantioselective β -Arylation of Carboxylic Esters	103
Scheme 3.37 Proposed Mechanism of the Palladium-Catalyzed β -Arylation of Carboxylic Esters	103
Scheme 3.38 Palladium-Catalyzed β -Arylation of Silyl Ketene Acetals	104
Scheme 3.39 β -C–C Bond Formation via Oxidative Enamine Catalysis	106
Scheme 3.40 Synthesis of β -Substituted γ -Nitro Aldehydes via Oxidative Enamine Catalysis	106
Scheme 3.41 β -Functionalization/Cyclization of Aldehydes via Oxidative NHC Catalysis	107
Scheme 3.42 Generation of a Nucleophilic β -Carbon with NHC	108
Scheme 3.43 NHC-Catalyzed β -Functionalization of Aldehydes with Electrophiles	108
Scheme 4.1 Buchwald-Hartwig-Miura α -Arylation of Ketones	115
Scheme 4.2 β -Arylation of Ketones with Aryl Halides	116
Scheme 4.3 Examples of Classical Approach towards β -Aryl Carbonyl Compounds	118
Scheme 4.4 Proposed Palladium-Catalyzed Redox Cascade	120

Scheme 4.5 Precedents of Possible Side-reactions	121
Scheme 4.6 Extraction of Halide Ligand	121
Scheme 4.7 Early Result of β -Arylation Reaction	122
Scheme 4.8 Early Result of β -Arylation Reaction (continued)	123
Scheme 4.9 Early Result of β -Arylation without Silver Additives	124
Scheme 4.10 Discovery of α -Arylation of Cyclopentanone	125
Scheme 4.11 Better Performance of Cyclohexanone than Cyclopentanone	125
Scheme 4.12 Effects of HFIP as a co-solvent	126
Scheme 4.13 Origin of Di-arylation	133
Scheme 4.14 β -Arylation with Aryl Bromides under Standard Conditions	136
Scheme 4.15 Gram-scale Reactions and Copper Salt as Promoter	137
Scheme 4.16 Synthesis of an Intermediate for SERT Antagonists	138
Scheme 4.17 Comparison between ‘One-cycle’ and ‘Two-cycle’ Mechanism	139
Scheme 4.18 Cross-over Experiments with Exotic Enones	140
Scheme 4.19 Stoichiometric Dehydrogenation Reactions	141
Scheme 5.1 An Alternative Mechanism Consisting of Two Separate Cycles	188
Scheme 5.2 Use of Diaryliodonium Salt as the Aryl Source	189
Scheme 5.3 β -Arylation of Cyclohexanone with Diphenyliodonium Triflate	190
Scheme 5.4 Comparison between Diphenyliodonium and Mesitylphenyliodonium Salt	191
Scheme 5.5 β -Arylation of Cyclohexanone with Mesitylphenyliodonium Triflate	191
Scheme 5.6 Simplified Reaction Conditions	192
Scheme 5.7 Synthesis of Bis- <i>N</i> -sulfilimine Ligand 5.5	196
Scheme 5.8 Reactions at Lower Temperature	198
Scheme 5.9 Analysis of Redox Property	200
Scheme 5.10 Pyrolysis of Ligand 5.5	205
Scheme 5.11 Hot Filtration Test	205
Scheme 5.12 Mercury Poisoning Test	207
Scheme 5.13 Methods for the Synthesis of Mesitylaryliodonium Salts	213
Scheme 6.1 α -C–H Functionalization of Aliphatic Amines	282
Scheme 6.2 Directing Group Strategy for γ -C–H Functionalization of Amines	283

Scheme 6.3 Functionalization of δ - or ϵ -C–H Bond of Amines via Hydrogen Shift.....	284
Scheme 6.4 Site-selective Nitrene Insertion for the Synthesis of 1,2-Diamine Derivatives	285
Scheme 6.5 Free Amine-directed β -C–H Functionalization of Strained Secondary Amines ...	286
Scheme 6.6 Synthesis of Sulfinate Amide.....	289
Scheme 6.7 Decomposition of Sulfinate Amide.....	290
Scheme 6.8 Potential Phosphoramidite-based Directing Group	291
Scheme 6.9 Hartwig’s Discovery of a Metallated Iridium-Phosphoramidite Complex	291
Scheme 6.10 Attempts for Catalytic β -C–H Functionalization of Phosphoramidite	292
Scheme 6.11 Oxime-based <i>exo</i> Directing Group.....	294
Scheme 6.12 Proposed Hydrazone-based Directing Group Strategy.....	295
Scheme 6.13 Synthesis of Hydrazone Substrate.....	296
Scheme 6.14 Initial Attempts for β -Acetoxylation Reaction	297
Scheme 6.15 Scaled up β -Acetoxylation Reaction.....	306
Scheme 6.16 Removal of Protecting and Directing Group	307
Scheme 6.17 A β -tosyloxylation Strategy to Access Amphetamine Derivatives.....	308
Scheme 6.16 Synthesis of Phthalazinones from Alkyl Amines	310
Scheme 6.17 β -Acetoxylation Using Phthalazinone-based Directing Group	311
Scheme 6.18 β -Acetoxylation of <i>tert</i> -Butyl Substituted Phthalazinone.....	311
Scheme 6.19 β -Acetoxylation of Cyclopentyl Substituted Phthalazinone.....	312
Scheme 6.20 Substrate Synthesis for Functional Group Tolerance Test.....	329
Scheme 7.1 Use of Non-redox-active Salts as the Iodide Scavenger.....	427
Scheme 7.2 Early Results Using KTFA as Iodide Scavenger	428
Scheme 7.3 Kinetic Profile of Early Reaction Conditions	429
Scheme 7.4 Kinetic Profile of Early Reaction Conditions	430
Scheme 7.5 Effects of a Mixture of KTFA and KOTf as the Additive	433
Scheme 7.6 Use of Ligated Palladium Chloride as Precatalyst	436
Scheme 7.7 Optimized Stoichiometric Heavy Metal-Free Conditions with Aryl Iodides.....	438
Scheme 7.8 Preliminary Screening of Various Free NHC Ligands	440
Scheme 7.9 Competing Complexation with NHC ligand of Palladium and Silver Salt	441
Scheme 7.10 <i>In Situ</i> Generation of Pd-NHC Catalyst	442

Scheme 7.11 Reaction with Methyl 4-Iodobenzoate under Conditions with IMes Ligand	446
Scheme 7.12 Palladium-Catalyzed Asymmetric Conjugate Addition.....	448
Scheme 7.13 Attempts for Enantioselective β -arylation with Diaryliodonium Salts	449
Scheme 7.14 Preliminary Results with Chiral Pyox-type Ligand.....	452
Scheme 7.15 Performance of Different Pyox-type Ligands	454
Scheme 7.16 Performance of Pyox-type Ligands with Benzyl Side Chain	455
Scheme 7.17 Screening of Quinox-type Ligands.....	456
Scheme 7.18 Screening of Quinox-type Ligands (Continued)	457
Scheme 7.19 Screening of Other Types of Ligands.....	458
Scheme 7.20 Reaction Pathways by Computation	461

LIST OF TABLES

Table 4.1 Ligand Screening of β -Arylation of Cyclohexanone	128
Table 4.2 Control Experiments for the Optimized Conditions	130
Table 4.3 Substrate Scope of Aryl Iodides	132
Table 4.4 Substrate Scope of Ketones	133
Table 5.1 Screening of Sulfide and Sulfoxide Ligands.....	193
Table 5.2 Screening of Sulfide and Sulfoxide Ligands.....	194
Table 5.3 Screening of Non-sulfur-based Ligands.....	195
Table 5.4 Effects of Sulfilimine Ligands	196
Table 5.5 Control Experiments	199
Table 5.6 Scope of Diaryliodonium Salts	201
Table 5.7 Scope of Ketone	203
Table 5.8 Full Details of the Control Reactions	211
Table 5.9 Results of Hot Filtration Test	226
Table 6.1 Beneficial Effect of Lithium Acetate	297
Table 6.2 Inhibition of Aldehyde Formation from Hydrolysis.....	298
Table 6.3 Effects of Reaction Temperature and Concentration	299
Table 6.4 Comparison between Low and High Loading of Palladium Catalyst	300
Table 6.5 Control Experiments	301
Table 6.6 Compatibility of Different Protecting Groups.....	302
Table 6.7 Substrate Scope	304
Table 7.1 Replacement of Silver Salts in Previous Conditions	427
Table 7.2 Combination of Catalytic PdCl ₂ and Silver Salts as Precatalysts.....	431
Table 7.3 Selected Screening of Ligands.....	432
Table 7.4 Screening of Salt Combination	434
Table 7.5 Screening of the Amount and Ratio of Salt Additives	436
Table 7.6 Portion-wise Addition of Catalyst and Additives	437
Table 7.7 Effects of Pd(Ph ₂ SO) ₂ Cl ₂ as Precatalyst.....	437
Table 7.8 Effects of IMes-ligated Palladium Precatalyst	442

Table 7.9 Examination of PEPPSI-type Ligands	443
Table 7.10 Screening of a Secondary Ligand.....	444
Table 7.11 Effects of Bidentate NHC Ligands	445
Table 7.12 Reaction with Different NHC-ligated Palladium Precatalysts.....	447
Table 7.13 Investigation of Chiral Phosphine Ligands.....	450
Table 7.14 Effects of 2,2'-Bipyridine as An Additional Ligand	451
Table 7.15 Effects of Related Achiral Diamine Ligands	452
Table 7.16 Effects of Different Amount of Pyox-type Ligand.....	453
Table 7.17 Effects of Acid or Base Additives	459
Table 7.18 Detailed Analysis of Reactions with Acid or Base Additives	460

LIST OF FIGURES

Figure 4.1 Selected Bioactive Compounds with β -Aryl Moiety.....	116
Figure 4.2 Price Comparisons between Saturated and Unsaturated Ketones	117
Figure 4.3 Representative Examples of Failed Substrates.....	135
Figure 4.4 ^{31}P -NMR study of Complexation of Phosphine Ligand.....	142
Figure 4.5 Crystal Structure of 4.3u	160
Figure 4.6 ^1H -NMR Spectrum of 4.3a	162
Figure 4.7 ^1H -NMR Spectrum of 4.3b	162
Figure 4.8 ^1H -NMR Spectrum of 4.3c	163
Figure 4.9 ^1H -NMR Spectrum of 4.3d	163
Figure 4.10 ^1H -NMR Spectrum of 4.3e	164
Figure 4.11 ^1H -NMR Spectrum of 4.3f	164
Figure 4.12 ^1H -NMR Spectrum of 4.3g	165
Figure 4.13 ^1H -NMR Spectrum of 4.3h	165
Figure 4.14 ^1H -NMR and ^{13}C -NMR Spectrum of 4.3i	166
Figure 4.15 ^1H -NMR Spectrum of 4.3j	167
Figure 4.16 ^1H -NMR Spectrum of 4.3k	167
Figure 4.17 ^1H -NMR Spectrum of 4.3l	168
Figure 4.18 ^1H -NMR and ^{13}C -NMR Spectrum of 4.3m	169
Figure 4.19 ^1H -NMR and ^{13}C -NMR Spectrum of 4.3n	170
Figure 4.20 ^1H -NMR and ^{13}C -NMR Spectrum of 4.3o	171
Figure 4.21 ^1H -NMR Spectrum of 4.3p	172
Figure 4.22 ^1H -NMR and ^{13}C -NMR Spectrum of 4.3q	173
Figure 4.23 ^1H -NMR and ^{13}C -NMR Spectrum of 4.3r	174
Figure 4.24 ^1H -NMR Spectrum of 4.3s	175
Figure 4.25 ^1H -NMR and ^{13}C -NMR Spectrum of 4.3t	176
Figure 4.26 ^1H -NMR and ^{13}C -NMR Spectrum of 4.3u	177
Figure 4.27 ^1H -NMR and ^{13}C -NMR Spectrum of 4.3v	178
Figure 4.28 ^1H -NMR and ^{13}C -NMR Spectrum of 4.3w	179

Figure 4.29 $^1\text{H-NMR}$ and $^{13}\text{C-NMR}$ Spectrum of 4.3x	180
Figure 4.30 $^1\text{H-NMR}$ Spectrum of 4.3y-mono	181
Figure 4.31 $^1\text{H-NMR}$ and $^{13}\text{C-NMR}$ Spectrum of 4.3y-di	182
Figure 4.32 $^1\text{H-NMR}$ Spectrum of 4.3z	183
Figure 4.33 $^1\text{H-NMR}$ Spectrum of 4.20	183
Figure 5.1 Kinetic Profile.....	204
Figure 5.2 Dynamic Light Scattering Data	206
Figure 5.3 Crystal Structure of <i>Racemic 5.5</i>	242
Figure 5.4 Crystal Structure of <i>Meso 5.5</i>	244
Figure 5.5 Crystal Structure of 5.13d/DNP Adduct	246
Figure 5.6 $^1\text{H-NMR}$ and $^{13}\text{C-NMR}$ Spectra of 5.22	248
Figure 5.7 $^1\text{H-NMR}$ and $^{13}\text{C-NMR}$ Spectra of 5.27	249
Figure 5.8 $^1\text{H-NMR}$ and $^{13}\text{C-NMR}$ Spectra of 5.30	250
Figure 5.9 $^1\text{H-NMR}$ and $^{13}\text{C-NMR}$ Spectra of 5.31	251
Figure 5.10 $^1\text{H-NMR}$ and $^{13}\text{C-NMR}$ Spectra of 5.33	252
Figure 5.11 $^1\text{H-NMR}$ and $^{13}\text{C-NMR}$ Spectra of 5.34	253
Figure 5.12 $^1\text{H-NMR}$ and $^{13}\text{C-NMR}$ Spectra of 5.5-meso	254
Figure 5.13 $^1\text{H-NMR}$ and $^{13}\text{C-NMR}$ Spectra of 5.5-racemic	255
Figure 5.14 $^1\text{H-NMR}$ and $^{13}\text{C-NMR}$ Spectra of 5.14	256
Figure 5.15 $^1\text{H-NMR}$ and $^{13}\text{C-NMR}$ Spectra of 5.15	257
Figure 5.16 $^1\text{H-NMR}$ Spectrum of 5.12a	258
Figure 5.17 $^1\text{H-NMR}$ Spectrum of 5.12b	258
Figure 5.18 $^1\text{H-NMR}$ Spectrum of 5.12c	259
Figure 5.19 $^1\text{H-NMR}$ Spectrum of 5.12d	259
Figure 5.20 $^1\text{H-NMR}$ Spectrum of 5.12e	260
Figure 5.21 $^1\text{H-NMR}$ Spectrum of 5.12f	260
Figure 5.22 $^1\text{H-NMR}$ Spectrum of 5.12g	261
Figure 5.23 $^1\text{H-NMR}$ Spectrum of 5.12h	261
Figure 5.24 $^1\text{H-NMR}$ Spectrum of 5.12i	262
Figure 5.25 $^1\text{H-NMR}$ Spectrum of 5.12j	262

Figure 5.26 ^1H -NMR Spectrum of 5.12k	263
Figure 5.27 ^1H -NMR Spectrum of 5.12l	263
Figure 5.28 ^1H -NMR and ^{13}C -NMR Spectrum of 5.12m	264
Figure 5.29 ^1H -NMR and ^{13}C -NMR Spectrum of 5.12n	265
Figure 5.30 ^1H -NMR Spectrum of 5.12o	266
Figure 5.31 ^1H -NMR and ^{13}C -NMR Spectrum and of 5.12p	267
Figure 5.32 ^1H -NMR and ^{13}C -NMR Spectrum of 5.12q	268
Figure 5.33 ^1H -NMR and ^{13}C -NMR Spectrum of 5.13a	269
Figure 5.34 ^1H -NMR and ^{13}C -NMR Spectrum of 5.13b	270
Figure 5.35 ^1H -NMR and ^{13}C -NMR Spectrum of 5.13c	271
Figure 5.36 ^1H -NMR and ^{13}C -NMR Spectrum of 5.13d	272
Figure 5.37 ^1H -NMR and ^{13}C -NMR Spectrum of 5.13e	273
Figure 5.38 ^1H -NMR and ^{13}C -NMR Spectrum of 5.13f	274
Figure 5.39 ^1H -NMR and ^{13}C -NMR Spectrum of 5.13g	275
Figure 5.40 ^1H -NMR and ^{13}C -NMR Spectrum of 5.13h	276
Figure 5.41 ^1H -NMR Spectrum of 5.13i	277
Figure 5.43 ^1H -NMR Spectrum of 5.13k	278
Figure 6.1 Site-selective C–H Functionalization of Aliphatic Amines.....	281
Figure 6.2 Four-membered and Five-membered Metallacycle.....	287
Figure 6.3 Sulfinate Amide Directing Groups.....	288
Figure 6.4 Selected Unsuccessful Substrates.....	305
Figure 6.5 Comparison between Hydrazone and Phthalazinone.....	309
Figure 6.6 ^1H -NMR and ^{13}C -NMR Spectrum of 6.14a	368
Figure 6.7 ^1H -NMR and ^{13}C -NMR Spectrum of 6.14b	369
Figure 6.8 ^1H -NMR and ^{13}C -NMR Spectrum of 6.14c	370
Figure 6.9 ^1H -NMR and ^{13}C -NMR Spectrum of 6.14d	371
Figure 6.10 ^1H -NMR and ^{13}C -NMR Spectrum of 6.14e	372
Figure 6.11 ^1H -NMR and ^{13}C -NMR Spectrum of 6.14f	373
Figure 6.12 ^1H -NMR and ^{13}C -NMR Spectrum of 6.14g	374
Figure 6.13 ^1H -NMR and ^{13}C -NMR Spectrum of 6.14h	375

Figure 6.14 ^1H -NMR and ^{13}C -NMR Spectrum of 6.14i	376
Figure 6.15 ^1H -NMR and ^{13}C -NMR Spectrum of 6.14j	377
Figure 6.16 ^1H -NMR and ^{13}C -NMR Spectrum of 6.14k	378
Figure 6.17 ^1H -NMR and ^{13}C -NMR Spectrum of 6.14l	379
Figure 6.18 ^1H -NMR and ^{13}C -NMR Spectrum of 6.14m	380
Figure 6.19 ^1H -NMR and ^{13}C -NMR Spectrum of 6.14n	381
Figure 6.20 ^1H -NMR and ^{13}C -NMR Spectrum of 6.14o	382
Figure 6.21 ^1H -NMR and ^{13}C -NMR Spectrum of 6.14p	383
Figure 6.22 ^1H -NMR and ^{13}C -NMR Spectrum of 6.14q	384
Figure 6.23 ^1H -NMR and ^{13}C -NMR Spectrum of 6.14r	385
Figure 6.24 ^1H -NMR and ^{13}C -NMR Spectrum of 6.14s	386
Figure 6.25 ^1H -NMR and ^{13}C -NMR Spectrum of 6.14t	387
Figure 6.26 ^1H -NMR and ^{13}C -NMR Spectrum of 6.14u	388
Figure 6.27 ^1H -NMR and ^{13}C -NMR Spectrum of 6.14v	389
Figure 6.28 ^1H -NMR and ^{13}C -NMR Spectrum of 6.32	390
Figure 6.29 ^1H -NMR and ^{13}C -NMR Spectrum of 6.18	391
Figure 6.30 ^1H -NMR and ^{13}C -NMR Spectrum of 6.15a	392
Figure 6.31 ^1H -NMR and ^{13}C -NMR Spectrum of 6.15b	393
Figure 6.32 ^1H -NMR and ^{13}C -NMR Spectrum of 6.15c	394
Figure 6.33 ^1H -NMR and ^{13}C -NMR Spectrum of 6.15d	395
Figure 6.34 ^1H -NMR and ^{13}C -NMR Spectrum of 6.15e	396
Figure 6.35 ^1H -NMR and ^{13}C -NMR Spectrum of 6.15f	397
Figure 6.36 ^1H -NMR and ^{13}C -NMR Spectrum of 6.15g	398
Figure 6.37 ^1H -NMR and ^{13}C -NMR Spectrum of 6.15h	399
Figure 6.38 ^1H -NMR and ^{13}C -NMR Spectrum of 6.15i	400
Figure 6.39 ^1H -NMR and ^{13}C -NMR Spectrum of 6.15j-mono	401
Figure 6.40 ^1H -NMR and ^{13}C -NMR Spectrum of 6.15j-di	402
Figure 6.41 ^1H -NMR and ^{13}C -NMR Spectrum of 6.15k	403
Figure 6.42 ^1H -NMR and ^{13}C -NMR Spectrum of 6.15l	404
Figure 6.43 ^1H -NMR and ^{13}C -NMR Spectrum of 6.15m	405

Figure 6.44 ^1H -NMR and ^{13}C -NMR Spectrum of 6.15n	406
Figure 6.45 ^1H -NMR and ^{13}C -NMR Spectrum of 6.15o	407
Figure 6.46 ^1H -NMR and ^{13}C -NMR Spectrum of 6.15p	408
Figure 6.47 ^1H -NMR and ^{13}C -NMR Spectrum of 6.15q	409
Figure 6.48 ^1H -NMR and ^{13}C -NMR Spectrum of 6.15r	410
Figure 6.49 ^1H -NMR and ^{13}C -NMR Spectrum of 6.15s	411
Figure 6.50 ^1H -NMR and ^{13}C -NMR Spectrum of 6.15t	412
Figure 6.51 ^1H -NMR and ^{13}C -NMR Spectrum of 6.15u	413
Figure 6.52 ^1H -NMR and ^{13}C -NMR Spectrum of 6.15v	414
Figure 6.53 ^1H -NMR and ^{13}C -NMR Spectrum of 6.19	415
Figure 6.54 ^1H -NMR and ^{13}C -NMR Spectrum of 6.20a	416
Figure 6.55 ^1H -NMR and ^{13}C -NMR Spectrum of 6.20b	417
Figure 6.56 ^1H -NMR and ^{13}C -NMR Spectrum of 6.20c	418
Figure 6.57 ^1H -NMR and ^{13}C -NMR Spectrum of 6.20d	419
Figure 6.58 ^1H -NMR and ^{13}C -NMR Spectrum of 6.16	420
Figure 6.59 ^1H -NMR and ^{13}C -NMR Spectrum of 6.20b'	421
Figure 6.60 ^1H -NMR and ^{13}C -NMR Spectrum of 6.17	422

LIST OF ABBREVIATIONS

Ac	acetyl
Ac ₂ O	acetic anhydride
acac	acetylacetonate
BARF	tetrakis(3,5-tris(trifluoromethyl)phenyl)borate
Bn	benzyl
Boc	<i>t</i> -butoxycarbonyl
BQ	benzoquinone
CFL	compact fluorescent light
Cp*	1,2,3,4,5-pentamethylcyclopentadienyl
DABCO	1,4-diazabicyclo[2.2.2]octane
dba	dibenzylideneacetone
DCE	1,2-dichloroethane
DCM	dichloromethane
DDQ	2,3-dichloro-5,6-dicyano-1,4-benzoquinone
DG	directing group
DMF	<i>N,N</i> -dimethylformamide
DMPU	1,3-dimethyl-3,4,5,6-tetrahydro-2-pyrimidinone
DMSO	dimethylsulfoxide
DNP	2,4-dinitrophenylhydrazine
dppb	1,4-bis(diphenylphosphino)butane
dppe	1,2-bis(diphenylphosphino)ethane
dppf	1,1'-bis(diphenylphosphino)ferrocene
EDG	electron-donating group
EWG	electron-withdrawing group
FG	functional group
HFIP	hexafluoro-2-propanol
IBX	2-iodoxybenzoic acid

KPS	potassium persulfate
Mes	2,4,6-trimethylphenyl
MS	molecular sieve
NCS	<i>N</i> -chlorosuccinimide
NHC	<i>N</i> -heterocyclic carbenes
OTf	trifluoromethanesulfonate
P(<i>i</i> -Pr) ₃	triisopropylphosphine
PCy ₃	tricyclohexylphosphine
Phth	phthaloyl
PivOH	pivalic acid
PTFE	polytetrafluoroethylene
<i>t</i> -amylOH	2-methylbutan-2-ol
TBS	<i>tert</i> -butyldimethylsilyl
TEMPO	(2,2,6,6-tetramethylpiperidin-1-yl)oxyl
TFA	trifluoroacetic acid
TFAA	trifluoroacetic anhydride
TIPS	triisopropylsilyl
TLC	thin layer chromatography
TMEDA	tetramethylethylenediamine
TMS	trimethylsilyl
TsOH	<i>p</i> -toluenesulfonic acid
XantPhos	4,5-bis(diphenylphosphino)-9,9-dimethylxanthene

ACKNOWLEDGEMENT

Of all the parts of the dissertation, I feel the acknowledgement is the most difficult one to write. I'm afraid that the words I write are not able to adequately express my gratitude to those who offered their help for the completion of my thesis, for my career, and for my life. But on second thought, nothing and no words are ever enough, as I'm forever indebted to their advices, love, and kindness.

I think my graduate research would be much less exciting without Professor Guangbin Dong as my advisor. Working with Guangbin significantly broadened my horizon of organic chemistry and chemistry at large. Since our first contact, Guangbin has constantly infused me with amazing and creative new ideas of organic chemistry. What's more wonderful is that we were able to make some of these ideas into reality. Guangbin is also the biggest cheerleader for my chemistry. There were moments when I wanted to walk away from my chemistry, when I was about to give up a seemingly hopeless project, and when I felt pessimistic because of the comments from others. It is Guangbin who kept reminding me of the significance of my reactions and pushing me to be a stronger person concentrating on what I really want. Being able to design a new reaction, realize that reaction, and continuously extend and optimize that reaction is a truly rewarding experience in my life time, and I sincerely thank Guangbin for that.

I would also like to thank Professor Jianbo Wang for his mentorship during my undergraduate years. Professor Wang is the instructor of my introductory organic chemistry who sparked my interest in organic synthesis. He also took a risk when allowing me, an inexperienced undergraduate who has only took one semester of organic chemistry, to join his group. In my last year of college, he also had a great trust in me and let me finish one project by myself. I believe

these knowledge and training obtained in Professor Wang's lab laid a solid foundation for my graduate study, as well as my future career.

Professor Michael Krische has been a huge supporter for me and my chemistry, from whom I got many great advices and encouragement. His organometallics class has laid the ground work for my graduate research and I always marveled at his passionate and informative teaching style. Professor Stephen Martin has taught me a great amount of knowledge in classic organic synthesis that helped me analyze synthetic problems in better ways. He is also a mentor that really cares about his students and always willing to help me when I asked. I would also like to thank Professor Scott Snyder and John Anderson, who agreed to serve on my defense committee on a very short notice. And I truly appreciate their help and suggestions.

I also got guidance from a lot of senior members from the lab. I'm lucky enough to have a close relationship with Dr. Fanyang Mo 'Momo' and his family. Momo is a role model with a clear line between what is right and what is wrong, and he's not afraid of any outside pressure to reinforce this standard to himself, his friends, and anybody around him. Dr. Tao Xu is a great guy to work with and offered me a lot of help in my early years, especially when I was involved in C-C bond activation projects. For my last two years in the lab, Dr. Dong Xing has been supportive of me, and a short visit with him to the coffee shop in the afternoon has always been a pleasure. I also had the honor to join the OBC ('old boy club') consisting of three post-docs from the lab, Dr. Xuan Zhou, Dr. Michael Young, and Dr. Heenam Lim. Xuan is a true friend of mine who gave help to me for several times when I was in difficult situations. Michael made the lab happier, and is always a good listener for my complaint. Heenam, on the other hand, is a true gentleman and gave me a lot of advices on research. Besides research, as the youngest member

of the club, I feel I had also learned a great deal of experience for life from these ‘old boys’. Seeing how each of them handled both lab work and personal life in balance with their perseverance, patience, and hardworking, I feel more ready for my future life and career.

Graduate school is not easy, and you need a support system. I feel blessed to have forged great friendship with many of the lab members. Chengpeng worked with me on the hydrazone project and has since become one of my best friends and the receiving end of my complaint and grumbling. I appreciate Jianchun, Lin, Renhe, and Jiaxin’s friendship and accompany. Hanging out with them after a day or a week’s lab work really cheers me up and clears my mind. I also enjoyed my time with Brent, Alex, Tatsuhiro, and Kiyoung, as they are all very kind, and interesting to talk with. Special thanks are dedicated to John, Rachel, Nik, Brandon, and Zack, Guangbin’s first class of students. Their experience and willingness to help have made my adaption to the lab, course work, and preparation of candidacy exam much easier.

Last, I attribute all my success and achievement to my mother. From my early age, my mother has instilled in me the value of hardworking, responsibility, and kindness. As a role model, my mother has constantly inspired me to be steadfast in work and life, and to make the right choice instead of the easy one. Witnessing her striving to give me the best she could afford and bring us out of difficult situations with extreme perseverance has encouraged me to never give up, even in the darkest moment. It is to her that I dedicate this dissertation.

CHAPTER 1

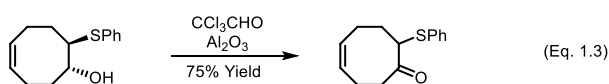
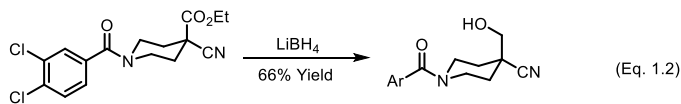
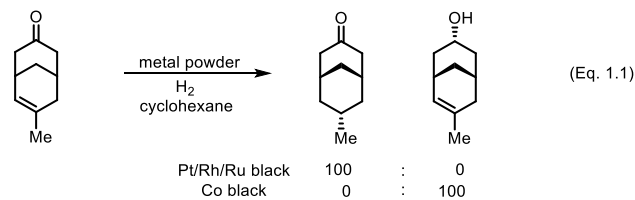
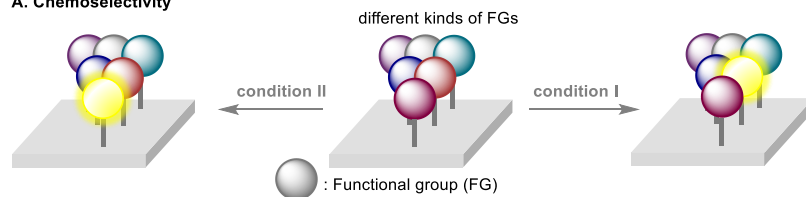
Site-Selectivity Control in Organic Reactions

1.1 Introduction

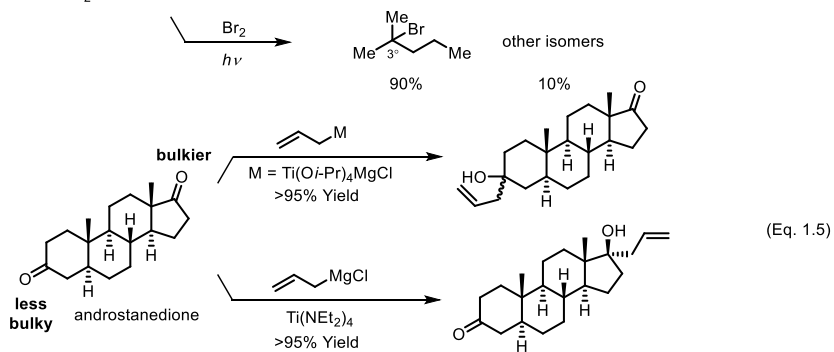
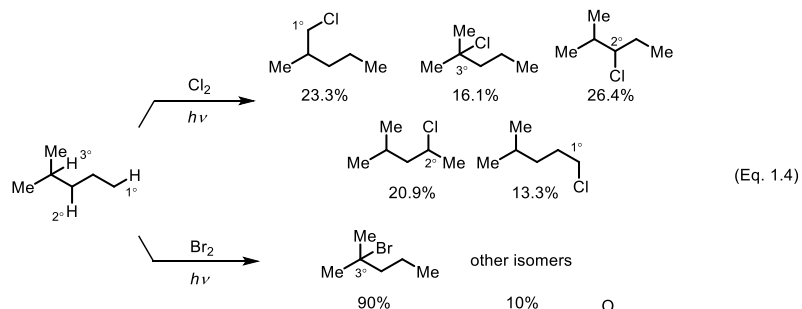
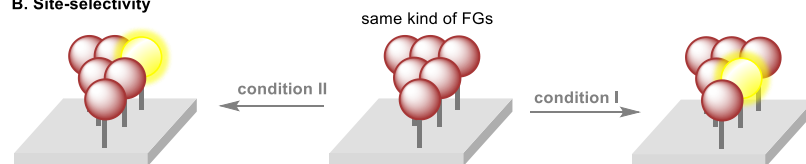
In its *Glossary of Terms Used in Physical Organic Chemistry*, the IUPAC defined chemoselectivity as “the preferential reaction of a chemical reagent with one of two or more different functional groups (FGs)” (Scheme 1.1A).¹ While this definition was only introduced in 1979, distinguishing reactivity among different kinds of FGs through selective transformations has been a constant quest in the history of organic chemistry.² The endeavors towards this goal have led to the development of important methods or approaches that are now archetypes in synthesis.

Scheme 1.1 Chemoselectivity and Site-selectivity: Concepts and Examples

A. Chemoselectivity



B. Site-selectivity



For example, controlled hydrogenation between alkene and ketone moieties was realized using different metal powders as catalysts (Eq. 1.1);³ selective reduction of one carbonyl moiety in the presence of other carboxylic acid derivatives has been made available by choosing specific hydride reagents (Eq. 1.2);⁴ without affecting alkene or sulfide moieties, oxidation of a hydroxyl group can be achieved through a unique hydride transfer pathway (Eq. 1.3).⁵ Hence, by taking advantage of the difference in inherent reactivity among different kinds of FGs, one can choose a certain method, reagent or catalyst to manipulate one FG while keeping others intact.

While efforts to pursue selective reactions among different kinds of FGs continue to pay off, there awaits a more formidable task on the path towards the perfection of synthesis: to differentiate reactivity among the same kind of FGs that have different chemical environments, namely site-selectivity (Scheme 1.1B). As a special scenario of chemoselectivity, site-selectivity is more difficult to control because, constituted by the same atoms and bonds, the same kind of FGs possess nearly identical chemical properties and tend to undergo the same transformation under given conditions. In other words, the activation-energy difference between the reactions of the same kind of FGs within the same molecule can be quite small. However, the rewards of developing site-selective transformations can be enormous. For example, protecting group strategy has been ubiquitously employed to allow reactions with one specific FG (e.g. hydroxyl or carbonyl group) through masking others of the same kind. Clearly, the availability of site-selective methods can eliminate ‘protection/deprotection’ sequences and enhance the overall synthetic efficiency. In addition, compounds with repeating structural motifs, such as polyols, polyenes, and polyketides, are common feedstocks from nature and privileged building blocks in complex molecule synthesis. Thus, selective functionalization or derivatization of these

compounds is highly valuable. Moreover, considering that C–H bonds are arguably the most abundant FGs in organic molecules, direct and site-selective conversion of specific C–H bonds to new FGs would greatly streamline the synthesis of complex target molecules from readily available starting materials.

Clearly, to control site-selectivity, one must find a way to utilize or amplify the difference of chemical environments among the same kind of FGs at different sites of the molecule, which are generally influenced by the electronic and steric properties of other FGs nearby. It can be envisaged that through the induction effect, Coulombic interaction, conjugation and hyperconjugation, a certain bond would be weaker or a certain intermediate would be more stabilized. Thus, these electronic factors provide an opportunity for a selective transformation. A classic example is the bromination of alkanes, where tertiary C–H bonds are preferred to be brominated over secondary and primary ones (Eq. 1.4).⁶ Such a site-selectivity is attributed to the generation of a more stable tertiary alkyl radical intermediate as a result of increased hyperconjugation, as well as having a late transition state by choosing bromine as the reagent instead of chlorine.⁷ Alternatively, sterics provide another handle for site-selectivity control. Depending on the sizes of surrounding moieties, the same kind of FGs in a molecule can have different degrees of spatial accessibility. These differences often enable a chemical reaction to preferentially occur at the less sterically hindered site. For example, treatment of androstanedione with an allyl nucleophile resulted in a selective addition at the more accessible cyclohexanone site instead of the cyclopentanone site that contains α,α -di-substituents (Eq. 1.5).⁸ In contrast, selective reaction at the bulkier site can also be realized through preferentially “masking” or protecting the less crowded one. Still in the case of androstanedione, the site-

selectivity was reversed when a titanium complex was added to mask the cyclohexanone carbonyl *in situ*.

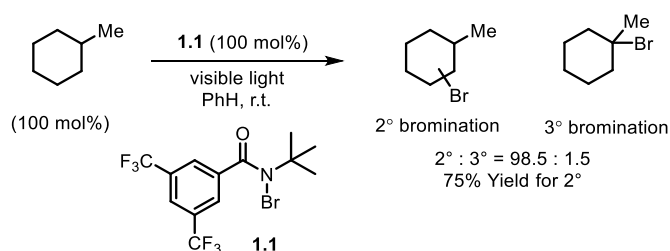
While universally applicable methods for site-selectivity control remain to be found, numerous elegant approaches have been developed over the past few decades for site-selective reactions of certain FGs or within certain family of compounds. Based on innovative designs of new reagents, catalysts and/or reaction pathways, these methods can discriminate the subtle difference in reactivity among the same kind of FGs, and sometimes even override the conventional bias of selectivity. Here, rather than being comprehensive, this chapter aims to offer case studies on some more recent site-selective methods. These examples are organized into two categories, undirected and directed control of site-selectivity, depending on whether the site selection is assisted by temporary reaction or complexation with other FGs in the molecule. Cases in the former category are exemplified by novel C–H functionalization approaches without the aid of directing groups. The key is to design specific reagents or catalysts that can recognize the intrinsic reactivity variance from site to site by matching the steric, electronic and/or stereoelectronic properties of the target position. Reactions in the latter category utilize an existing FG as an anchor to either enable proximity effect typically through temporary complexation or alter the reaction pathway under specific reaction conditions.

1.2 Undirected Control of Site-Selectivity

C–H bromination: Alkane halogenation via a free radical approach is one of the most important ways to functionalize aliphatic C–H bonds. The aforementioned bromination of

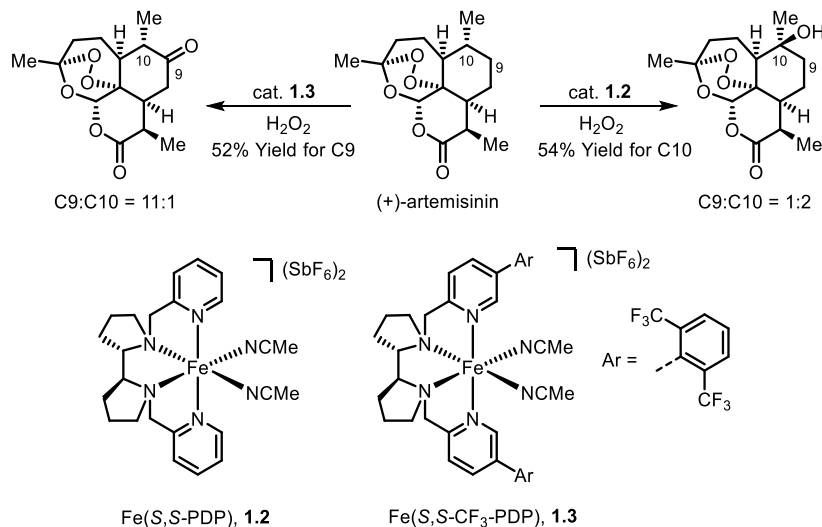
alkanes inherently prefers to form tertiary alkyl bromide (*vide supra*, Eq. 1.4). In 2014, Alexanian and coworkers developed a bulky bromination reagent (**1.1**) that can override the preference for tertiary C–H bonds and switch the selectivity to methylene groups (Scheme 1.2).⁹ The efficacy is proposed to mainly stem from the steric hindrance of the amidyl radical intermediate that is slow to abstract hydrogen from a tertiary position.

Scheme 1.2 Alkyl C–H Bromination Using a Bulky Bromination Reagent



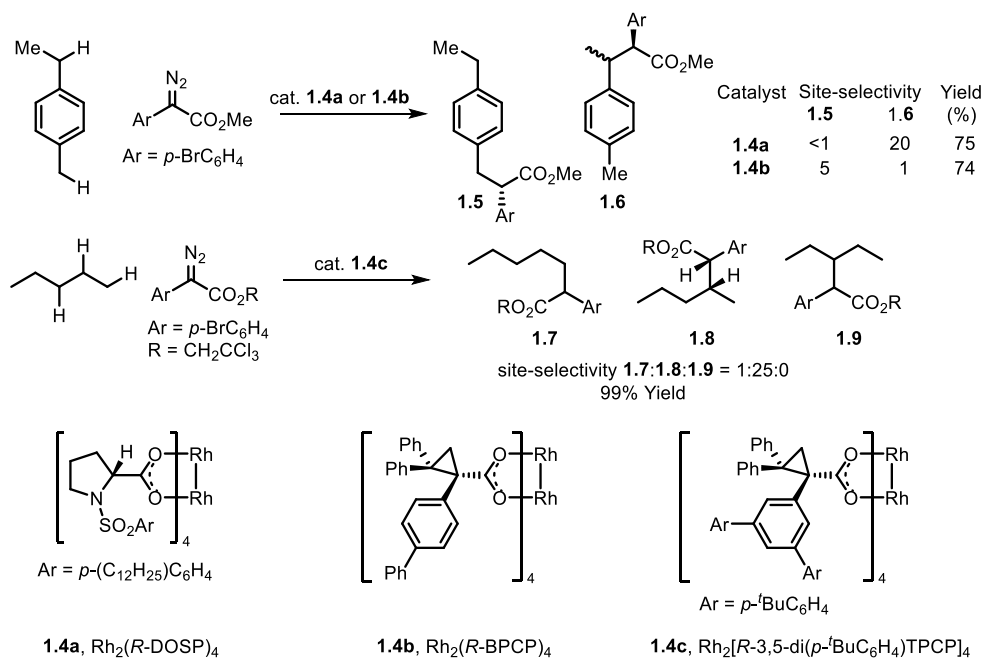
C–H oxidation: Besides controlled by the reagents used, site-selectivity of C–H functionalization can also be guided through modifying the structure of the catalysts. The seminal work from the White group shows that iron-based catalyst Fe(*S,S*-PDP) **1.2** affords mild oxidation of aliphatic C–H bonds in complex molecules (Scheme 1.3). The C–H oxidation proceeds through an iron-oxo intermediate and the site-selectivity generally biases towards the more electron-rich tertiary C–H bonds. Recently, the same team was able to change the preference from tertiary to secondary C–H bonds using a bulkier Fe(*S,S*-CF₃-PDP) (**1.3**) as the catalyst.¹⁰ Exemplified in the oxidation of (+)-artemisinin, the Fe(*S,S*-PDP) prefers the more electron-rich tertiary C10 position, whereas the Fe(*S,S*-CF₃-PDP) prefers to oxidize the more accessible C9 methylene.

Scheme 1.3 White's C–H Oxidation Using Iron Catalysts



Carbenoid Insertion: Complementary site-selectivity in the dirhodium-catalyzed C–H functionalization of alkanes with donor/acceptor carbenes can be achieved by tuning the electronic and steric properties of the spectator ligands (Scheme 1.4). For example, shown by the Davis group, the carbene insertion with *para*-ethyl toluene occurred almost exclusively at the secondary benzylic position with the $\text{Rh}_2(\text{R-DOSP})_4$ (**1.4a**) catalyst that contains a proline-derived ligand;¹¹ however, with the more sterically demanding $\text{Rh}_2(\text{R-BPCP})_4$ catalyst **1.4b**, reaction at the less hindered methyl group became predominant. In addition, the amazing C2-selectivity was achieved on functionalization of unactivated C–H bonds in *n*-alkanes, enabled by an even bulkier dirhodium catalyst (**1.4c**).¹²

Scheme 1.4 Site-Selectivity Control of Dirhodium-Catalyzed C–H Functionalization

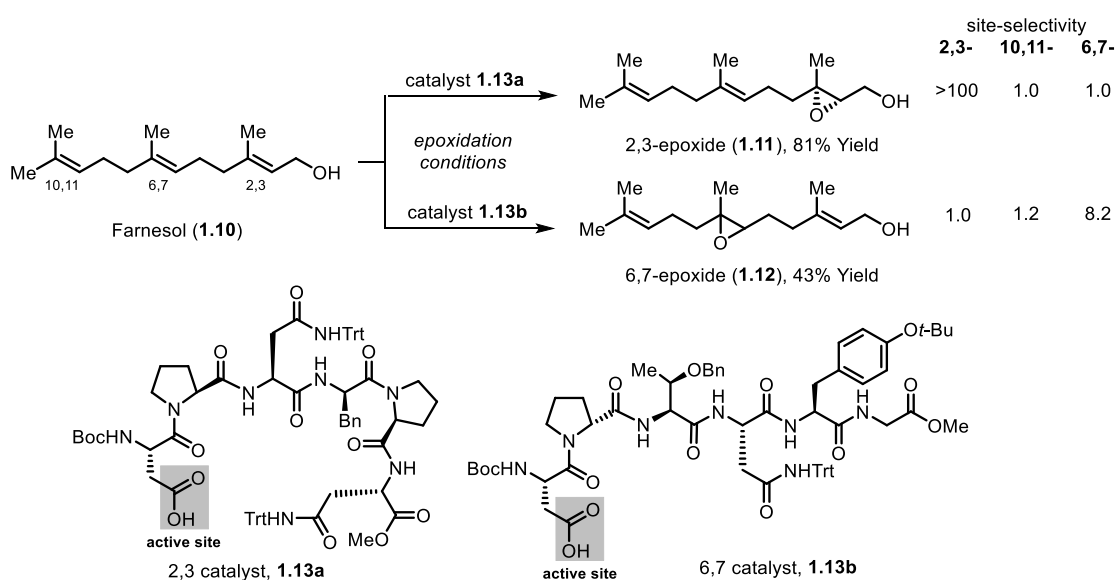


1.3 Directed Control of Site-Selectivity

Peptide Catalysis: As a mimic of enzyme-catalyzed reactions, peptide-based catalytic methods have emerged as a powerful tool to control the enantio- and site-selectivity of organic transformations. The peptide catalysts typically consist of a backbone chain of amino acids and a single acidic or basic residue that can act as the reactive site. The steric hindrance, hydrogen bonding, π -interactions, and other characters of the backbone can be fine-tuned by replacing the amino-acid residues. The modularity together with mature protocols for peptide synthesis allow for convenient preparation of diversified catalyst libraries. A representative example of site-selective epoxidation of polyenes using a peptide-based catalyst was reported by the Miller group in 2012 (Scheme 1.5).¹³ Through directed screening of low-molecular-weight peptides,

two catalysts (**1.13a** and **1.13b**) were discovered for selective epoxidation of the 2,3- or 6,7-olefins of farnesol (**1.10**). The free carboxylic acid moiety in both catalysts is *in situ* transformed to a peracid and serves as a reaction site. The observed contrary site-selectivity is attributed to the conformational difference of the backbones of the two catalysts upon forming hydrogen bonds with the hydroxyl group in the substrate.

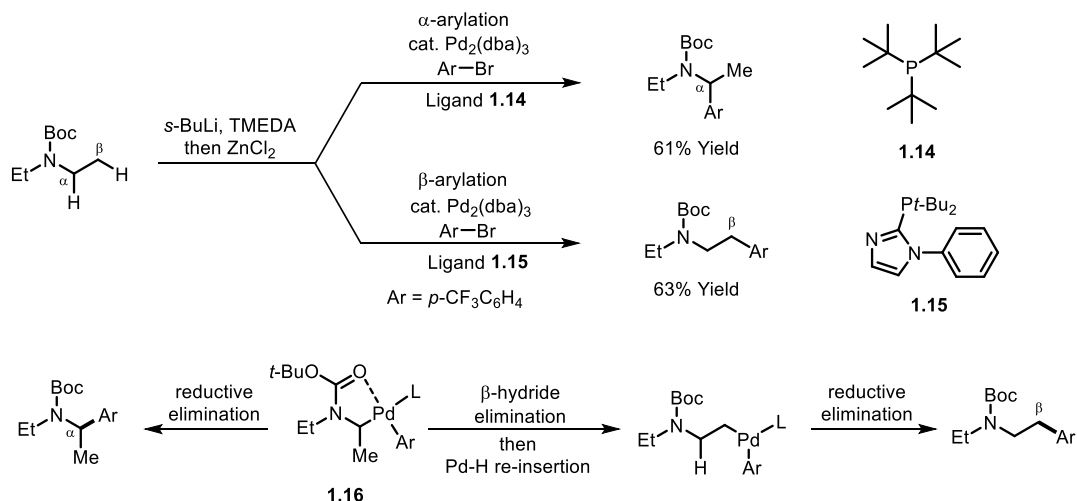
Scheme 1.5 Peptide-Based Catalysts for Site-Selective Epoxidation of Polyenes



Ligand Effect: For transition metal-catalyzed reactions, ligands have been known to play a critical role in controlling the reactivity and selectivity of the metal. Scheme 1.6 illustrates a case that divergent C–H arylation reactions of *N*-Boc amines can be realized by properly choosing the ligand for palladium.^{14,15} The work by Baudoin and coworkers shows that upon directed lithiation and transmetalation, the arylation can occur at either the α - or β -position of the amines depending on the property of the phosphine ligand. It was rationalized that, although a bulky and rigid $P(t\text{-Bu})_3$ (**1.14**) ligand favored the direct reductive elimination of intermediate

1.16 to give the α -arylated amine, a more flexible ligand, such as **1.15**, promoted a β -hydrogen elimination/Pd–hydride re-insertion sequence to eventually yield the β -arylation product.

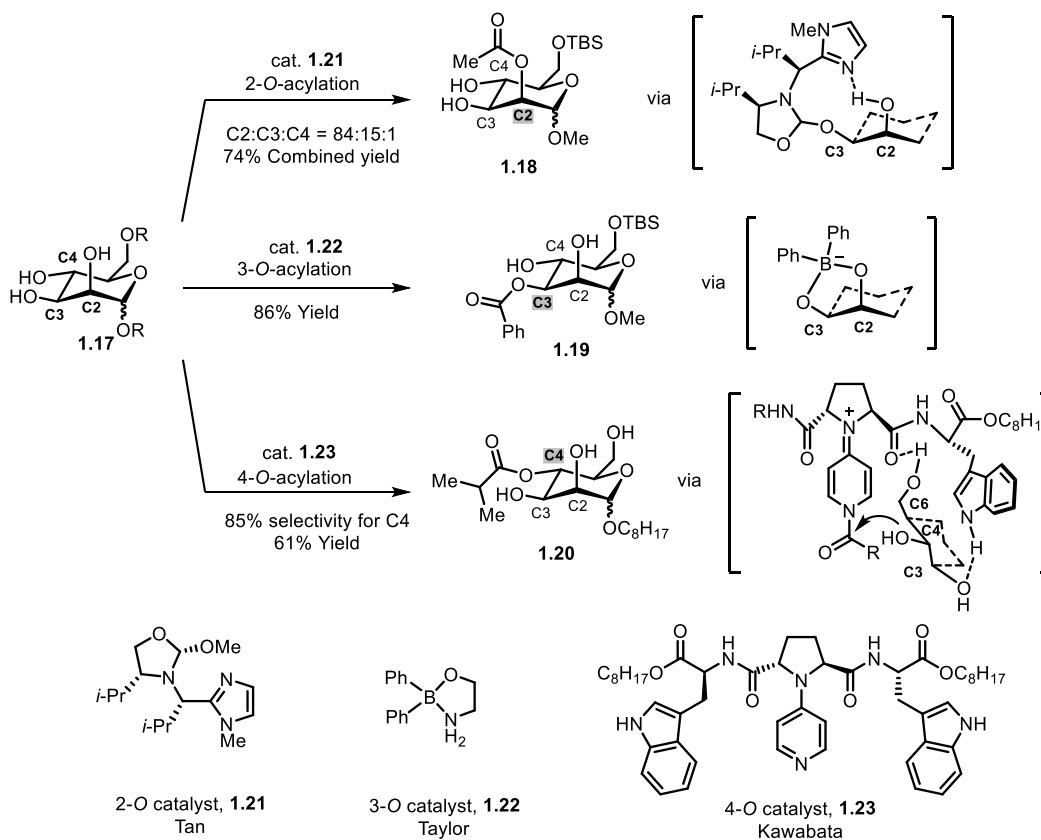
Scheme 1.6 Ligand-Controlled α - and β -Arylation of *N*-Boc Amines



Sugar Chemistry: The vigorous development of carbohydrate chemistry has also given rise to a number of site-selective transformations of saccharides. As naturally occurring polyols, saccharides contain multiple hydroxyl groups that are close to each other and thus share similar chemical environments. Site-selective transformation of one alcohol in a sugar molecule without affecting others represents a huge advantage over traditional protecting group-based approaches. To date, a number of excellent approaches have been developed. For instance, peptide catalysis (*vide supra*) has been an effective tool for site-selective functionalization of carbohydrates.^{16,17} Here, we mainly focus on some recent developments on site-selective acylation of mannopyranose derivative **1.17**, which contains three consecutive secondary alcohols at C2, C3, and C4 positions (Scheme 1.7). First, the C2-selective acylation was achieved using Tan's catalyst **1.21** whereas the C3 OH was proposed to form a single dynamic covalent bond with the

catalyst.¹⁸ Such an interaction would deliver the imidazole motif in close proximity to the C2 OH, which then triggers the acylation at this site. A similar recognition of *cis*-1,2-diol (C2, C3) was realized by catalyst **1.22**.¹⁹ In this case, a diphenylborinate adduct is selectively formed between the *cis*-C2,C3-diols and the catalyst, which consequently enhances the reactivity of these two sites over the free C4 alcohol. Influenced by the substrate conformation, the acylation subsequently takes place selectively at the less bulky, equatorial C3 alcohol. In contrast, the 4-pyrrolidinopyridine-derived catalyst (**1.23**) led to selective C4 acylation.²⁰ A transition state was proposed containing two hydrogen bonds between the catalyst and the C6/C3 hydroxyl groups. Consequently, the spatially close relationship between the C4 OH and the acylpyridinium ion promoted the site-selective acylation.

Scheme 1.7 Site-Selective Acylation of Mannopyranose Derivatives



1.4 Conclusion and Outlook

With no doubt, the control of site-selectivity remains an ineluctable challenge to our quests for the perfection of synthesis. In this chapter, a number of recent efforts have been summarized; however, due to the space constraint, many excellent works are unfortunately omitted such as directed remote C–H functionalization and site-selective olefin metathesis reactions. Compared with the advancement of selectivity control among different kinds of FGs as well as the monument of controlling regio-, diastereo- and enantioselectivity, the development of

site-selective approaches is still in its infant stage. To breed more general, practical and broadly applicable methods, it is envisaged that future endeavors will focus on 1) expanding the substrate scope that can undergo site-selective transformations and 2) precisely controlling the site of reaction in less biased settings. Clearly, the needs cannot be met without the availability of more powerful catalysts, reagents, strategies and even new tactics. It is expected that Mother Nature will continue providing inspirations to design biomimetic or supramolecular catalysts. To enable more precise site-selectivity control and broader reaction scope would require better modeling and deeper mechanistic understanding of these catalytic processes. In addition, cooperative catalysis through combining two or more activation modes might be another trend for the incoming efforts. Vigorous development in recent years has demonstrated that merger of multiple catalysis is able to activate substrates once considered inert or functionalize sites previously inaccessible. Furthermore, practical applications of site-selective transformations in complex molecule synthesis are anticipated to be illustrated more frequently in the future.

1.5 References

1. Muller, P. *Pure & Appl. Chem.* **1994**, *66*, 1077.
2. Trost, B.M. *Science* **1983**, *219*, 245.
3. Ishiyama, J.; Senda, Y.; Imaizumi, S. *Chem. Lett.* **1983**, 1243.
4. Vacher, B.; Bonnaud, B.; Funes, P.; Jubault, N.; Koek, W.; Assié, M.-B.; Cosi, C.; Kleven, M. *J. Med. Chem.* **1999**, *42*, 1648-1660.
5. Posner, G. H.; Chapdelaine, M. J. *Tetrahedron Lett.* **1977**, *37*, 3227.
6. Russell, G. A.; Brown, H. C. *J. Am. Chem. Soc.* **1955**, *77*, 4025.
7. Estel, D.; Mateew, K.; Pritzkow, W.; Schmidt-Renner, W. *J. Prakt. Chem.* **1981**, *323*, 262.
8. Reetz, M. T.; Wenderoth, B.; Peter, R. *J. Chem. Soc., Chem. Commun.* **1983**, 406.
9. Schmidt, V. A.; Quinn, R. K.; Brusoe, A. T.; Alexanian, E. J. *J. Am. Chem. Soc.* **2014**, *136*, 14389.
10. Gormisky, P. E.; White, M. C. *J. Am. Chem. Soc.* **2013**, *135*, 14052.
11. Qin, C.; Davies, H. M. L. *J. Am. Chem. Soc.* **2014**, *136*, 9792.
12. Liao, K.; Negretti, S.; Musaev, D. G.; Bacsa, J.; Davies, H. M. L. *Nature* **2016**, *533*, 230.
13. Lichtor, P. A.; Miller, S. J. *Nat. Chem.* **2012**, *4*, 990.
14. Millet, A.; Dailler, D.; Larini, P.; Baudoin, O. *Angew. Chem. Int. Ed.* **2014**, *53*, 2678.
15. For an earlier case where the site-selectivity was controlled by substrates, see: Seel, S.; Thaler, T.; Takatsu, K.; Zhang, C.; Zipse, H.; Straub, B. F.; Mayer, P.; Knochel, P. *J. Am. Chem. Soc.* **2011**, *133*, 4774.
16. Griswold, K. S.; Miller, S. J. *Tetrahedron* **2003**, *59*, 8869.
17. Lewis, C. A.; Miller, S. J. *Angew. Chem. Int. Ed.* **2006**, *45*, 5616.
18. Sun, X.; Lee, H.; Lee, S.; Tan, K. L. *Nat. Chem.* **2013**, *5*, 790.
19. Lee, D.; Taylor, M. S. *J. Am. Chem. Soc.* **2011**, *133*, 3724.

20. Kawabata, T.; Muramatsu, W.; Nishio, T.; Shibata, T.; Schedel, H. *J. Am. Chem. Soc.* **2007**, *129*, 12890.

CHAPTER 2

Transition Metal-Catalyzed Ketone-Directed or Mediated C–H Functionalization

2.1 Introduction

Transition metal-catalyzed C–H functionalization has emerged as an increasingly important tool for organic synthesis; however, control of site-selectivity remains a challenging and ongoing task.¹ Among all of the approaches developed hitherto, the use of a directing group (DG) represents a versatile and reliable strategy to govern which C–H bond will be functionalized.² Through coordination of a DG to a transition metal, the proximity effect can often override the inherent steric/electronic preferences and ultimately dictate the site-selectivity of C–H bond activation. Consequently, nitrogen-based functional groups (FGs) and heterocycles, as well as soft elements (e.g. sulfur and phosphorus), are widely employed as DGs due to their excellent coordination ability with transition metals. In contrast, the use of a more common FG as DG, such as regular ketones is much rarer due to their relatively low coordinating ability.

Undoubtedly the C–H functionalization reactions involving these common FGs as DGs or substrates are highly attractive. For example, ketone moieties are widely found in various bioactive molecules and functional materials;³ they can also be readily transformed into a diverse range of other FGs, and are thus often employed as versatile synthetic intermediates. For this reason simple ketone-directed or mediated C–H functionalization is of high synthetic value.

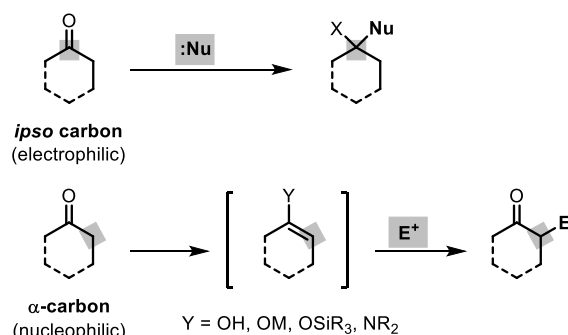
Conventional ketone-functionalization methods take advantage of the intrinsic electrophilicity of the carbonyl and acidity of the α -C–H bonds (Scheme 2.1A). Carbonyl attack by various nucleophiles allows functionalization at the *ipso* carbon, whereas deprotonation of the α -hydrogen or enolization with a strong (Lewis) acid permits substitution at the α -positions by reaction with various electrophiles. Alternatively, recent advancements in transition-metal chemistry enable novel ketone-based C–H bond transformations that do not occur under traditional conditions. This field has taken off since Murai's pioneering work on ketone-directed Ru-catalyzed C–H/olefin coupling reactions in 1993 (*vide infra*).⁴ To date, a number of innovative approaches and methods have been developed.

This chapter focuses on the simple-ketone-directed or mediated C–H functionalization reactions that are catalyzed by transition metals, covered through January of 2015 (Scheme 2.1B). The content is organized into three parts: use of ketone carbonyl as the DG, direct β -functionalization, and α -alkylation/alkenylation with unactivated olefins and alkynes. It is noteworthy that transition metal enolate-mediated cross coupling reactions, e.g. Buchwald-Hartwig-Miura α -arylation,⁵ and Lewis acid-mediated enolate chemistry with regular electrophiles⁶ will not be included. Reactions with related ketone derivatives, such as silyl enol ethers, oximes, β -keto esters and α,β -unsaturated ketones, will also not be discussed. While not

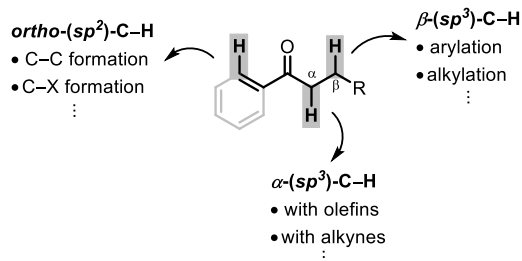
intended to be comprehensive, this chapter summarizes major developments from the perspective of strategic design and reaction discovery.

Scheme 2.1 Functionalization of Ketones

A. Conventional Ketone Functionalization



B. Transition-Metal-Catalyzed C–H Functionalization



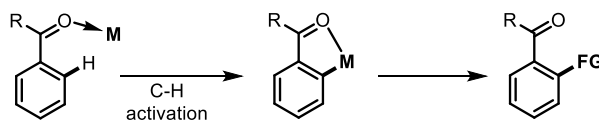
2.2 Ketone as the Directing Group

Based on the reaction type, this section is divided into three subsections: carbon–carbon (C–C) bond formation via addition to alkenes and alkynes, C–H arylation, and carbon–heteroatom (C–X) bond formation. While a large number of transformations have been reported using ketone as the directing group, it should be noted that the substrate scopes of these reactions are limited to sp^2 C–H bonds in aromatic, and in some cases, vinyl ketones. Applications of the DG-based strategy to other types of ketones, such as alkyl ketones (β - sp^3 C–H bonds, *vide infra*), are largely underdeveloped, likely due to the weak coordinating ability of ketones.

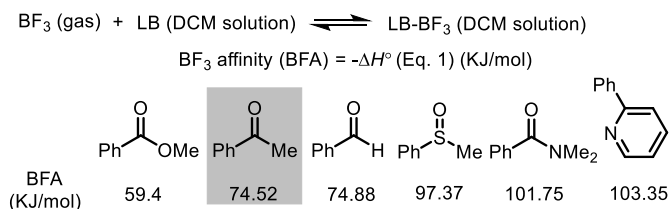
Over the past two decades, the DG-based strategy has been established as one prominent approach for C–H functionalization.² One common mode of reactivity consists of coordination of the DG to a transition metal before C–H cleavage and subsequent formation of stable metallacycles (Scheme 2.2A). To date, a diverse range of DGs are available, among which ketones are often considered weakly coordinating due to their relatively low Lewis basicity. As demonstrated by the BF₃ affinity scale, ketones' coordinating capability is considerably lower than other directing groups, including pyridines, sulfoxides and amides (Scheme 2.2B).⁷ However, from a chronological viewpoint, ketones are actually one of the earliest DGs employed in transition metal-catalyzed C–H functionalization.

Scheme 2.2 C–H Functionalization Directed by Ketones

A. Ketone-Directed C–H Functionalization



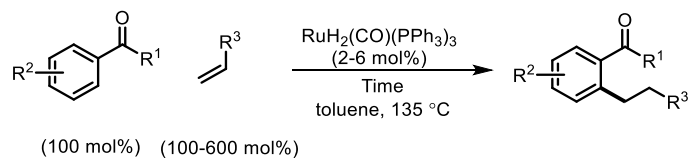
B. Lewis Basicity of Ketone and other DGs



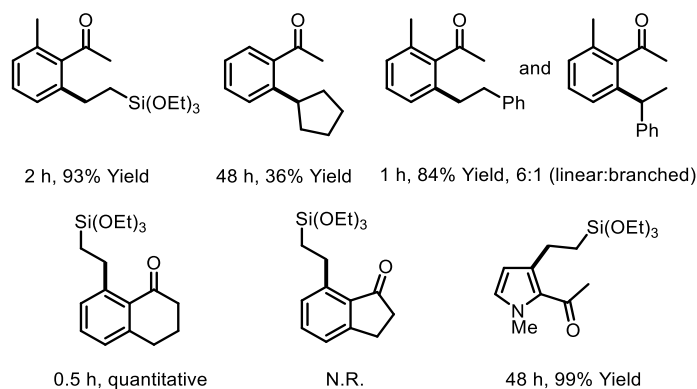
2.2.1 Coupling with Alkenes and Alkynes

In 1993, Murai and coworkers reported the first Ru-catalyzed *ortho*-alkylation reaction of aromatic ketones with olefins, also known as the hydroarylation of olefins (Scheme 2.3).⁴ The *ortho*-C–H bond of the ketone was selectively coupled with the olefin to afford the alkylation product in up to quantitative yield with $\text{RuH}_2(\text{CO})(\text{PPh}_3)_3$ as the catalyst in toluene at 135 °C. Detailed studies of the substrate scope revealed that a large collection of olefins can participate in this reaction.⁸ Vinylsilanes proved to be superior substrates that gave complete linear selectivity. In the case of styrene, a 6:1 ratio between linear and branched products was obtained. Despite the good reactivity with terminal olefins, internal, isomerizable terminal, and acrylate-type olefins gave poor yields or no reaction. Regarding the scope of ketones, aromatic ketones bearing various alkyl, aryl, or heteroaryl substituents were all alkylated smoothly under the reaction conditions. It is interesting to note that while α -tetralone afforded the product in quantitative yield, 1-indanone showed no reactivity. As explained by the authors, the loss of reactivity with 1-indanone was attributed to the difficulty of forming the five-membered ring metallacycle due to the strained benzofused structure.

Scheme 2.3 Ruthenium-Catalyzed *ortho*-Alkylation of Aromatic Ketones

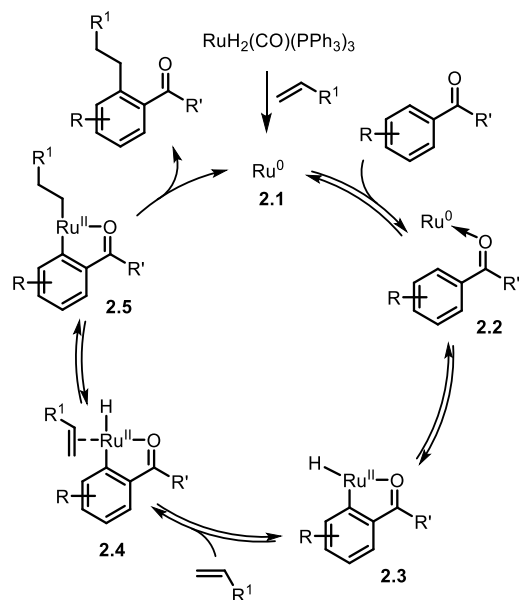


Selected examples:



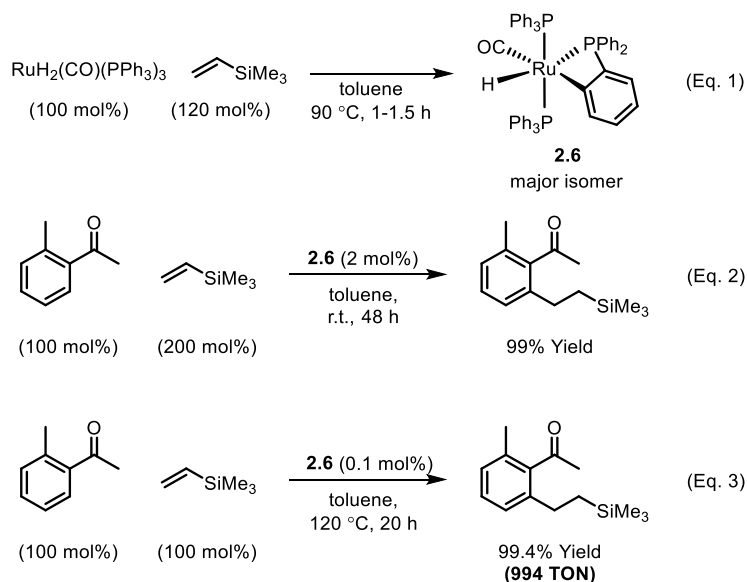
The proposed catalytic cycle, supported by both mechanistic studies^{9,10,11,12} and DFT calculations,¹³ is initiated by the generation of a Ru(0) species through the reduction of $\text{RuH}_2(\text{CO})(\text{PPh}_3)_3$ with olefin substrates (Scheme 2.4). The ketone moiety coordinates to and delivers the Ru(0) within proximity of the *ortho*-C–H bond, followed by oxidative addition to generate ruthenium hydride **2.3**. Subsequent migratory insertion of olefin into the Ru–H bond proceeds in a highly regio- and chemoselective manner to give intermediate **2.5**, which after reductive elimination gives the alkylation product and restores the active Ru(0) catalyst. The reductive elimination of complex **2.5** proved to be the rate determining step of the catalytic cycle. While the reaction was run at 135 °C, the oxidative addition of Ru(0) to the aryl C–H bond was found to proceed even at 50 °C.

Scheme 2.4 Proposed Catalytic Cycle for the Ruthenium-Catalyzed *ortho*-Alkylation of Aromatic Ketones



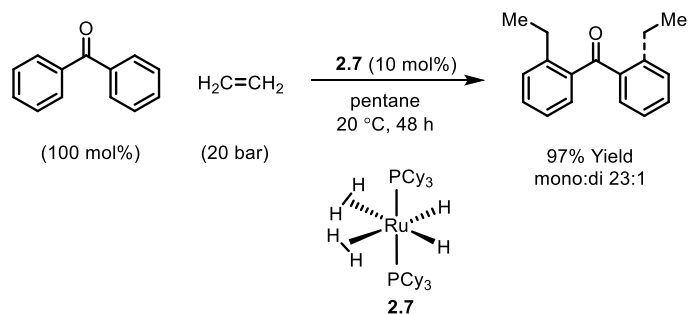
A more reactive precatalyst was discovered during the mechanistic studies by Kakiuchi, Murai, and coworkers.¹⁴ The spectroscopic evidence supported the generation of a Ru-hydride complex (**2.6**) from the reaction of $\text{RuH}_2(\text{CO})(\text{PPh}_3)_3$ and trimethylvinylsilane (Scheme 2.5, Eq. 1). This species, once used as the catalyst, could enable the *ortho*-alkylation to proceed even at room temperature (Eq. 2). When the alkylation was run at 120 °C, complex **2.6** achieved a turnover number (TON) close to 1000 (Eq. 3).

Scheme 2.5 Formation of Active Catalyst of Ruthenium-Catalyzed *ortho*-Alkylation



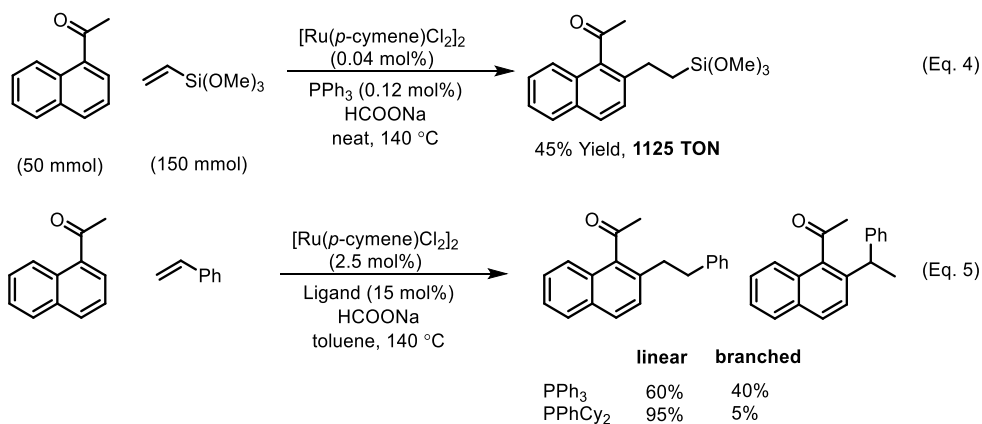
Other groups have also developed improved catalysts for this transformation. Using $\text{RuH}_2(\text{H}_2)_2(\text{PCy}_3)_2$ (**2.7**) as the catalyst, the Chaudret^{15,16} and Leitner^{17,18} groups reported *ortho*-alkylation with ethylene that proceeded at room temperature (Scheme 2.6). A variant ruthenium complex with two tricyclopentylphosphine (PCyp_3) ligands was also synthesized, characterized, and demonstrated to possess outstanding catalytic activity towards the same ethylation reaction.¹⁹ Compared to Murai's original precatalyst $\text{RuH}_2(\text{CO})(\text{PPh}_3)_3$, these modified ruthenium species have two dihydrogen and two tricycloalkylphosphine ligands. The lability of dihydrogen and strongly electron-donating tricyclohexylphosphine ligand were proposed to generate an active and electron-rich $\text{Ru}(0)$ catalyst promptly. However, coupling with olefins other than ethylene was not demonstrated using these modified catalysts.

Scheme 2.6 RuH₂(H₂)₂(PCy₃)₂-Catalyzed *ortho*-Ethylation with Ethylene



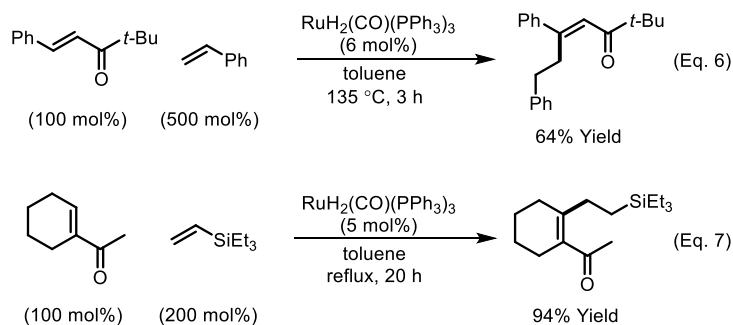
Another important contribution for the catalyst modification came from the Darses group.^{20,21,22,23} They developed several protocols for the *ortho*-alkylation of aromatic ketones using a combination of less expensive Ru salts, such as [RuCl₂(*p*-cymene)]₂ and RuCl₃, along with triarylphosphine ligands and formate salts (Scheme 2.7). The formate salts were proposed to reduce the Ru(II) or Ru(III) catalyst *in situ* to generate the active Ru(0) catalyst. This strategy turned out to be highly efficient and the TON could reach more than 1000 (Eq. 4). Besides the lower cost of the precatalysts, the addition of phosphine ligands as a separate reagent presents another advantage over the original catalytic system using RuH₂(CO)(PPh₃)₃. This is because the ruthenium dihydride complexes are often nontrivial to synthesize and sensitive to air and moisture, thus the addition of ligand as a separate reagent makes it easier to evaluate the ligand effect. The authors discovered that the ligand played a vital role in controlling the regioselectivity. For example, the coupling between 1-acetonaphthone and styrene with dicyclohexyl(phenyl)-phosphine significantly enhanced linear selectivity compared to triphenylphosphine (Eq. 5).²⁰

Scheme 2.7 Ketone-Directed *ortho*-Alkylation Using Ru(II) Precursors



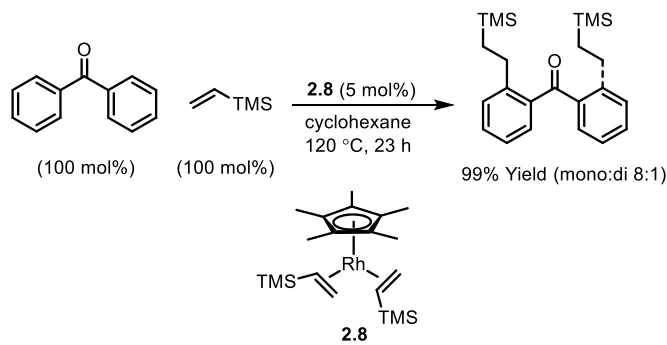
Besides aromatic C–H bonds, the olefinic C–H bond can also participate in the Ru-catalyzed alkylation with alkenes (Scheme 2.8). Trost²⁴ and Kakiuchi/Murai^{25,26} independently demonstrated that both linear (Eq. 6) and cyclic vinyl ketones (Eq. 7) are suitable substrates for the alkylation reaction, although *E/Z* isomerization from linear enone substrates was observed in some cases.²⁴ With regard to the alkene scope, vinyl silanes and styrene-type olefins proved to be superior substrates for the coupling. Alkyl olefins and acrylate derivatives also participated in the reaction, although a large excess was required to obtain good yields.

Scheme 2.8 Ketone-Directed *ortho*-Alkylation of Olefinic C–H Bonds



In addition to ruthenium catalysts, *ortho*-alkylation of aromatic ketones with olefins has also been reported using other transition-metal catalysts. The rhodium bis-olefin complex **2.8** was used by Brookhart and coworkers for the hydroarylation of olefins (Scheme 2.9).²⁷ A distinct feature of this rhodium catalysis is the non-site-selective oxidative addition of rhodium into aromatic C–H bonds before the migratory insertion. Chelation of the ketone moiety was proposed to lower the barrier of reductive elimination, which is the rate-determining step, thus affording the *ortho*-selective alkylation product. Besides the distinct mechanism, this rhodium-catalyzed alkylation can accommodate isomerizable olefins (e.g. 1-pentene) that were hard to react under Murai’s ruthenium catalysis.

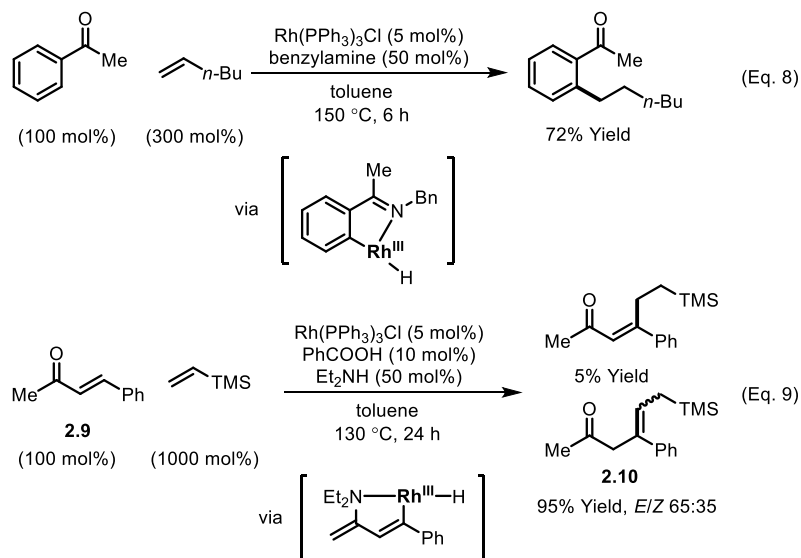
Scheme 2.9 Rhodium-Catalyzed *ortho*-Alkylation of Aromatic Ketones with Olefins



In 2002, Jun and coworkers reported a benzylamine-assisted *ortho*-alkylation of aromatic ketones catalyzed by Wilkinson’s catalyst (Scheme 2.10).²⁸ A substoichiometric amount (50 mol%) of benzylamine acts as a co-catalyst through transient condensation with the substrate, which converts ketones to stronger coordinating ketimines. After the rhodium-catalyzed *ortho*-alkylation, the resulting alkylated ketimine would be hydrolyzed to release the product and regenerate the benzylamine (Eq. 8). A similar strategy was later applied to the β -alkylation of 4-

phenyl-3-buten-2-one (**2.9**) (Eq. 9).²⁹ In this case, a secondary amine was employed to form a transient enamine with **2.9**, followed by directed olefinic C–H activation with a rhodium catalyst. It is interesting to note that after the alkylation reaction, an olefin migration was proposed to take place to give β,γ -enone **2.10** as the major product. Although the substrate scopes of these amine-assisted alkylations were only briefly investigated, the reaction conditions were compatible with a variety of olefins, including vinyl silanes, styrene-type olefins and even isomerizable α -olefins, which represent a key advantage over the Ru-catalyzed *ortho*-alkylation reactions.

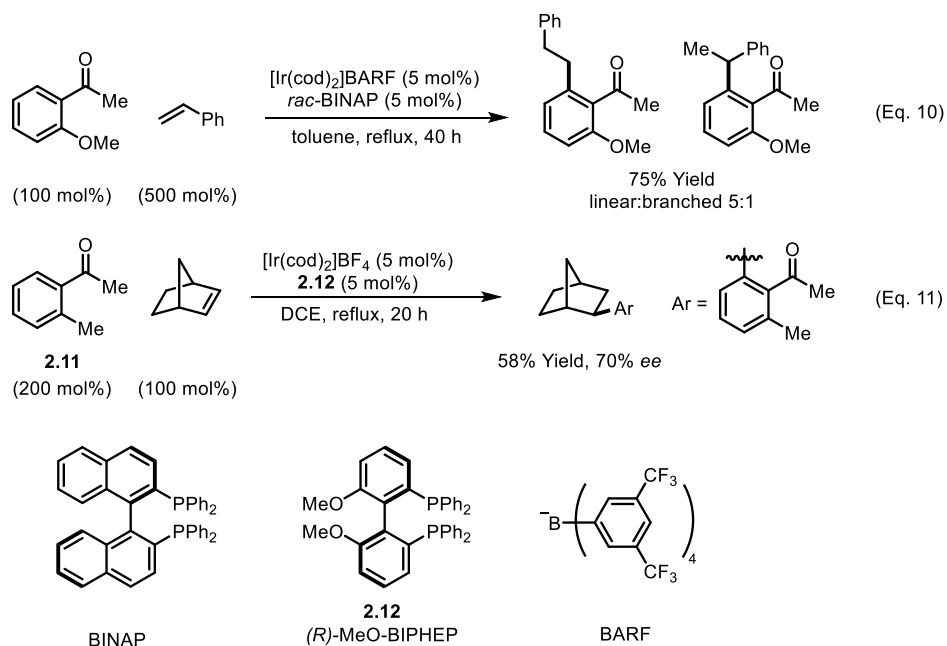
Scheme 2.10 Amine-Assisted *ortho*-Alkylation of Aromatic Ketones and Enones



An iridium-catalyzed hydroarylation of olefins was reported by Shibata and coworkers in 2008 (Scheme 2.11).³⁰ In their study, the cationic iridium complex [Ir(cod)₂]BARF was used as the catalyst to promote *ortho*-alkylation of aromatic ketones with styrene-type olefins, giving the linear products as the major isomers (Eq. 10). It is noteworthy that when the chiral bidentate

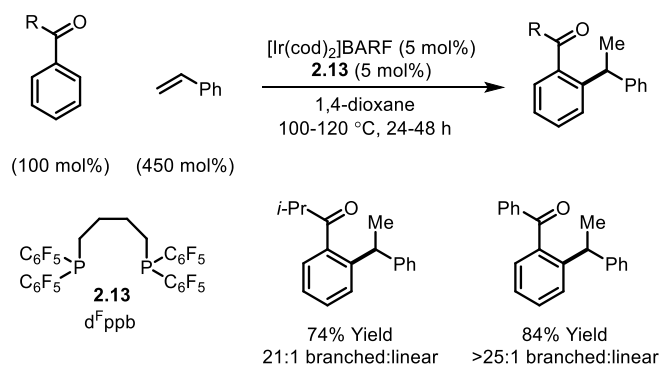
phosphine ligand (*R*)-MeO-BIPHEP (**2.12**) was used, the coupling between norbornene and **2.11** afforded the product with moderate enantioselectivity (Eq. 11).

Scheme 2.11 Iridium-Catalyzed *ortho*-Alkylation of Aromatic Ketones with Olefins



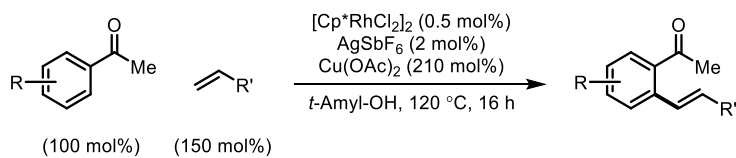
With Murai's protocols, formation of linear alkylation products is favored over branched ones. In 2014, Bower and coworkers reported an alternative iridium-catalyzed system that is highly selective for branched products (Scheme 2.12).³¹ The key for the inversion of the selectivity is the use of an electron-deficient bis-phosphine ligand (**2.13**), which can presumably accelerate the reductive elimination. Under their reaction conditions, various aromatic ketones were coupled with styrenes giving better than 20:1 branched/linear selectivity.

Scheme 2.12 Branch-Selective *ortho*-Alkylation of Aromatic Ketones with Olefins

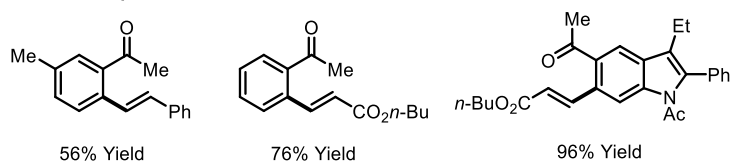


An important variation of Murai's ketone-directed alkylation reaction is the oxidative *ortho*-olefination of aromatic ketones with alkenes. While Murai's reaction is viewed as a redox-neutral addition of a C–H bond to an olefin, the olefination reaction can be considered as a formal dehydrogenative coupling, also known as the oxidative Heck reaction.³² It is noteworthy to mention that an olefination product was also observed by Murai and coworkers in the $\text{Ru}_3(\text{CO})_{12}$ -catalyzed addition of C–H bonds to olefins, although the dehydrogenative coupling was directed by imidates instead of ketones.³³ In 2011, Glorius and coworkers reported a rhodium-catalyzed C–H olefination reaction directed by ketones (Scheme 2.13).³⁴ When styrene-type olefins were coupled with acetophenone derivatives, 1,2-disubstituted *trans*-alkenes were generated as the sole regioisomer. This selectivity represents a distinct feature from Murai's ruthenium catalysis, where a mixture of branched and linear alkylation products was produced with styrene-type olefins. In addition, acrylate-type olefins, previously unreactive under Murai's conditions, afforded the alkenylation products in good yields with this rhodium catalysis.

Scheme 2.13 Rhodium-Catalyzed *ortho*-Olefination of Aromatic Ketones with Olefins

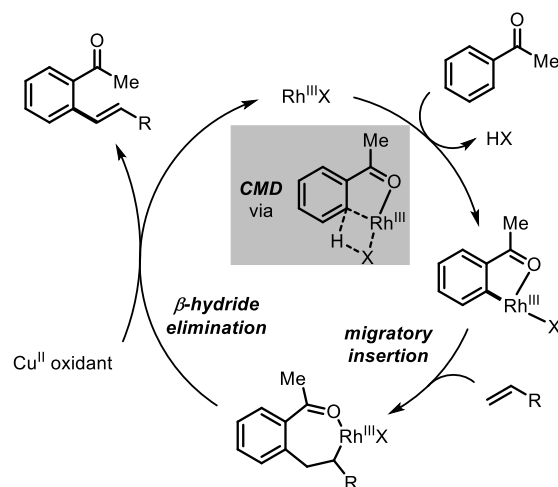


Selected examples:



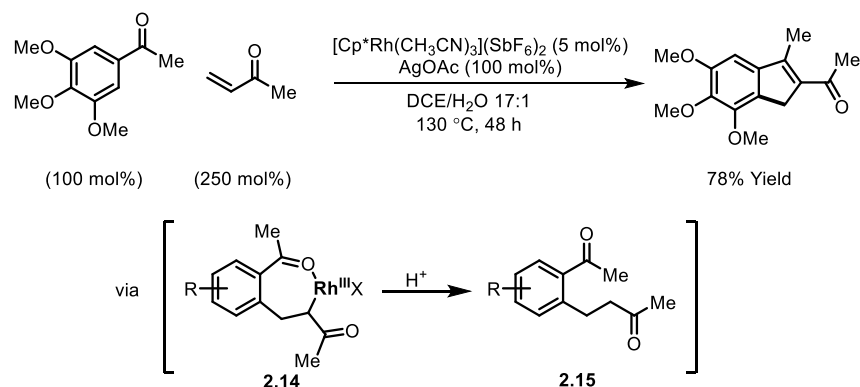
The use of a cationic rhodium catalyst, in conjunction with a stoichiometric Cu(II) oxidant, triggered a different reaction pathway from Murai's original alkylation reaction (Scheme 2.14). The activation of the *ortho*-C-H bond was proposed to proceed through a concerted metalation-deprotonation (CMD) pathway with the Rh(III) catalyst. Unlike the oxidative addition pathway observed with Ru(0), however, the CMD mechanism yielded a Rh(III)-aryl complex and an acid instead of a metal-hydride species. Subsequent migratory insertion of the olefin into the Rh(III)-aryl bond and β -hydride elimination afforded the olefination product. The Cu(II) oxidant was proposed to be responsible for regenerating the active Rh(III) catalyst. An analogous Ru(III)-catalyzed *ortho*-alkenylation with olefins was reported by Jeganmohan and coworkers.³⁵

Scheme 2.14 Catalytic Cycle of Rhodium-Catalyzed *ortho*-Olefination



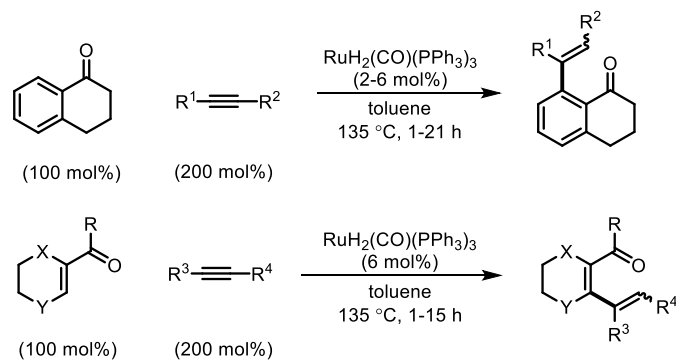
When a cationic rhodium catalyst $[Cp^*Rh(CH_3CN)_3](SbF_6)_2$ was used with stoichiometric silver acetate, Li and coworkers discovered aromatic ketones and enones underwent a C–H alkylation/aldol condensation sequence instead of an oxidative olefination reaction (Scheme 2.15).³⁶ The cascade reaction was proposed to proceed through **2.14**, a similar intermediate as in Glorius's olefination reaction. However, instead of β -hydride elimination, intermediate **2.14** would be protonated under the reaction conditions to give **2.15**, followed by silver-mediated aldol condensation to give an indene as the product. The possibility of direct aldol condensation with intermediate **2.14** cannot be excluded. A small amount of water was demonstrated to be beneficial to the cascade reaction, probably by facilitating the protonation step.

Scheme 2.15 Rhodium-Catalyzed *ortho*-Alkylation/Aldol Condensation Cascade

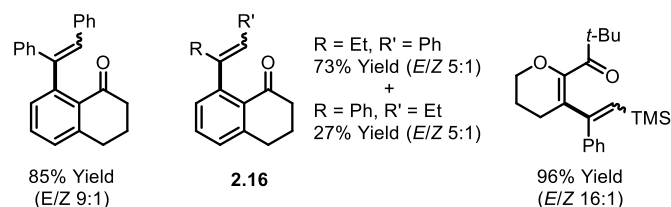


Although less studied than coupling with olefins, ketone-directed addition of the *ortho*-C–H bonds to alkynes also proves to be efficient. Murai and coworkers demonstrated that both aromatic³⁷ and olefinic³⁸ C–H bonds can react with alkynes to give the alkenylation products using the same ruthenium catalyst (Scheme 2.16). While internal alkynes gave good yields, terminal alkynes failed to provide access to the desired products, presumably due to competing side reactions, e.g. dimerization. When unsymmetrical ethylphenylacetylene was submitted to the reaction, all four possible stereo- and regioisomers (**2.16**) were isolated. However, reactions with trimethylsilyl-substituted acetylenes all gave 1-trimethylsilyl-2-aryl alkenes as the exclusive regioisomers. Besides ruthenium catalysis, Shibata and coworkers also reported the same transformation with a cationic iridium catalyst, although only diphenylacetylene and trimethylsilylphenylacetylene were employed.³⁰

Scheme 2.16 Ruthenium-Catalyzed *ortho*-Alkenylation of Aromatic Ketones or Enones with Alkynes



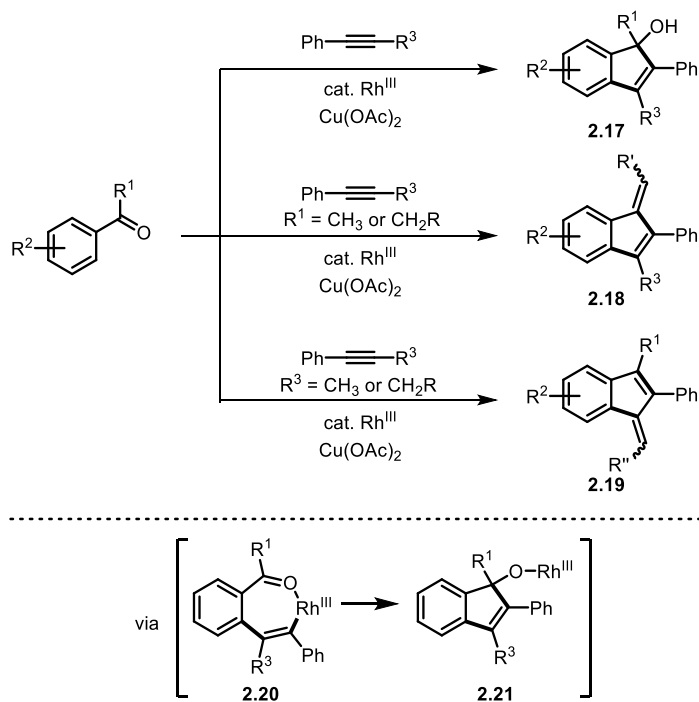
Selected examples:



In 2011, Glorius and coworkers reported that the coupling between aromatic ketones and alkynes can undergo a different pathway, leading to indenol and fulvene derivatives when a cationic Rh(III) catalyst and stoichiometric Cu(II) salt are used (Scheme 2.17).³⁹ Similar to the coupling with olefins (*vide supra*, Scheme 2.14), *ortho*-C–H activation with Rh(III) proceeds through a CMD mechanism and the following migratory insertion of alkyne gives vinyl-Rh(III) species **2.20**. Subsequently, an intramolecular addition of vinyl group to the ketone carbonyl yields the intermediate **2.21**, which upon protonation gives the indenol (**2.17**) as the final product. However, if a methyl or methylene group is present at the α -position of the ketone (R^1) or the γ -position of the alkyne (R^3), dehydration takes place affording the fulvene derivatives (**2.18** and

2.19, respectively). Similar transformations have also been reported by Cheng,⁴⁰ Jeganmohan,⁴¹ and Shibata⁴² using rhodium, ruthenium, and iridium catalysts respectively.

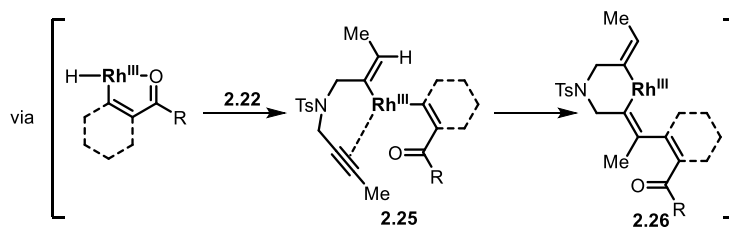
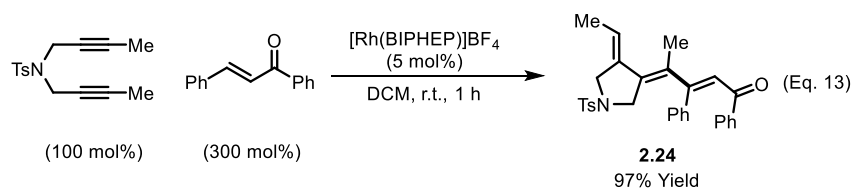
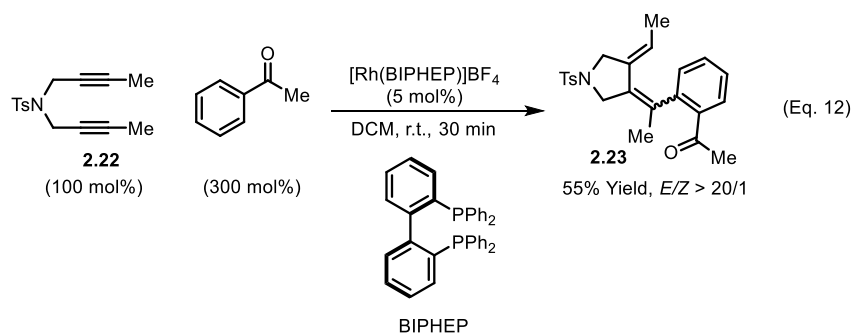
Scheme 2.17 Rhodium-Catalyzed Fulvene and Indenol Synthesis



Another interesting tandem reaction that involves ketone-directed C–H bond activation is the rhodium-catalyzed cyclization of aromatic ketones and diynes (Scheme 2.18). In 2007, Shibata and coworkers reported the formation of cyclic 1,3-diene product **2.23** from the coupling of diynes and aromatic ketones catalyzed by $[\text{Rh}(\text{BIPHEP})]\text{BF}_4$ (Eq. 12).⁴³ When *trans*-chalcone was used as the substrate, monocyclic trienone **2.24** was generated (Eq. 13). The tandem process was proposed to initiate via the ketone-directed *ortho*-C–H activation with the rhodium catalyst. Intermolecular hydro-rhodation of one of the alkyne moieties and subsequent intramolecular

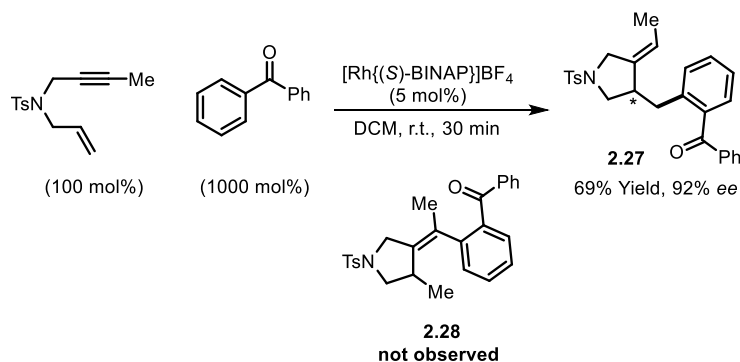
carbo-rhodation of the other would give the six-membered rhodacycle **2.26**. The final reductive elimination generates the product and releases the active catalyst.

Scheme 2.18 Rhodium-Catalyzed Cyclization of Diynes and Aromatic Ketones or Chalcones



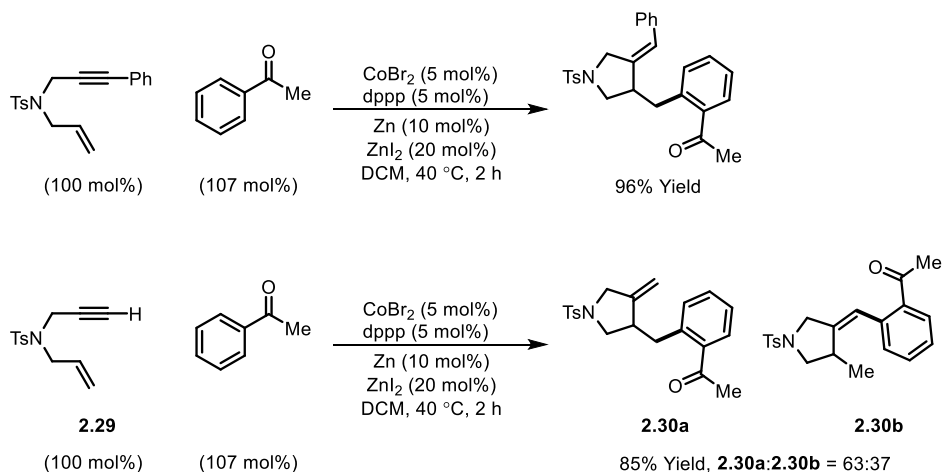
When an enyne was employed as the substrate, the metallated intermediate added to the alkyne first to give the monocyclic product **2.27** (Scheme 2.19). The product descended from the initial addition to alkene and subsequent carbo-rhodation of alkyne (**2.28**) was not observed. When a chiral rhodium complex was used as the catalyst, good enantioselectivity was obtained. Similar tandem reactions with enynes and diynes as the coupling partners have also been published by Tanaka and coworkers using cationic rhodium catalysts.^{44,45}

Scheme 2.19 Rhodium-Catalyzed Cyclization of Enynes and Aromatic Ketones



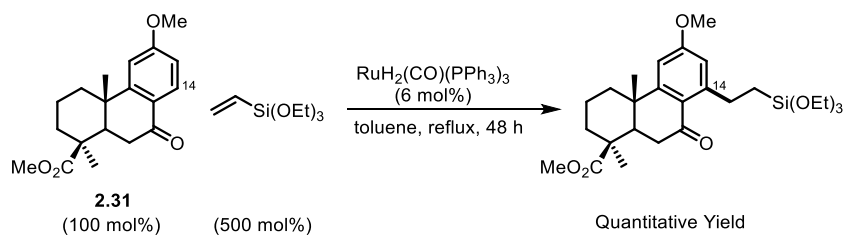
Recently, Cheng and coworkers reported a similar hydroarylation cyclization of enynes and aromatic ketones with a cobalt catalyst (Scheme 2.20).⁴⁶ In their case, $\text{CoBr}_2/1,3$ -bis(diphenylphosphino)propane (dppp) was used as the precatalyst and the combination of zinc and zinc iodide was proposed to reduce the cobalt salt to the active Co(I) catalyst. A large collection of functionalized pyrrolidines, dihydrofurans, and cyclopentanes were accessed as single regioisomers in good yields from simple aromatic ketones and enynes. While examples with terminal alkynes were not shown with rhodium catalysts (*vide supra*, Scheme 2.19), enyne **2.29** proceeded to give the cyclization product **2.30** as a mixture of regioisomers under the cobalt catalysis.

Scheme 2.20 Cobalt-Catalyzed Cyclization of Enynes and Aromatic Ketones



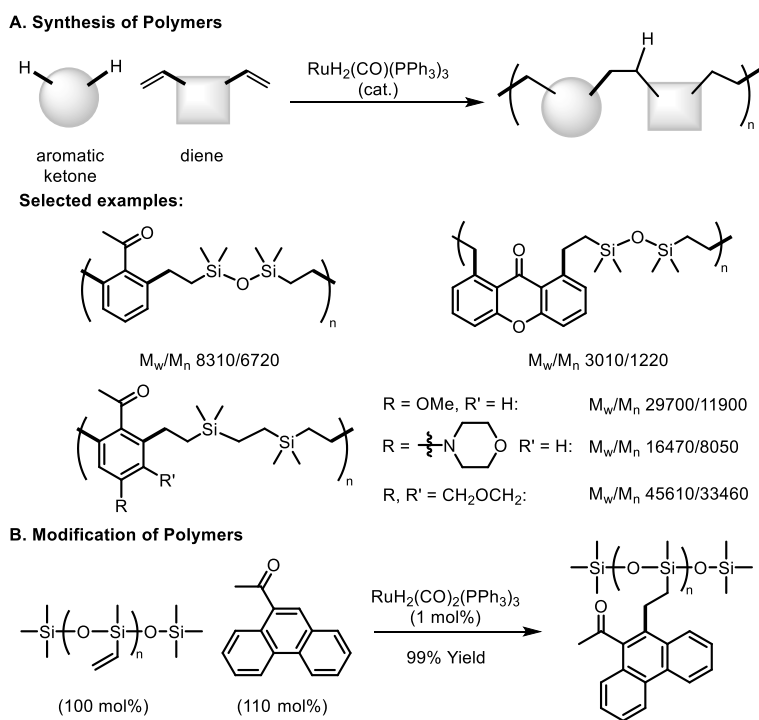
Although this chapter focuses on reaction discovery and strategy design, ketone-directed C–H bond addition to alkenes and alkynes has found many synthetic applications. For example, ketone-directed hydroarylation reactions were employed by Woodgate and coworkers in the synthesis of various aromatic diterpenoids (Scheme 2.21). In their study, the C14 C–H bond of diterpenoid **2.31** was selectively alkylated in quantitative yield with triethoxyvinylsilane using $\text{RuH}_2(\text{CO})(\text{PPh}_3)_3$ as the catalyst.⁴⁷ The authors also demonstrated the resulting alkylalkoxysilane moiety could serve as a handle to access a diverse range of analogues.⁴⁸

Scheme 2.21 Ruthenium-Catalyzed Alkylation of Aromatic Diterpenoid



Due to its high efficiency, the ketone-directed hydroarylation reaction has also found applications in the field of polymer chemistry. Shortly after Murai's original discovery, Weber and coworkers applied the ruthenium-catalyzed *ortho*-alkylation of ketones to the copolymerization of aromatic ketones and diene derivatives (Scheme 2.22A). Copolymers with various backbones and functional groups, such as amines and acetals, were synthesized in high efficiency using $\text{RuH}_2(\text{CO})(\text{PPh}_3)_3$ as the catalyst.^{49,50,51,52,53} The Weber group also reported the modification of poly-(vinylmethylsiloxane) (PVMS) using the ruthenium-catalyzed hydroarylation reaction (Scheme 2.22B). The *ortho*-C–H bond of the ketone in 9-acetylphenanthrene added to the pendant vinyl groups in PVMS with anti-Markovnikov selectivity and afforded the modified polymer in an excellent yield.⁵⁴

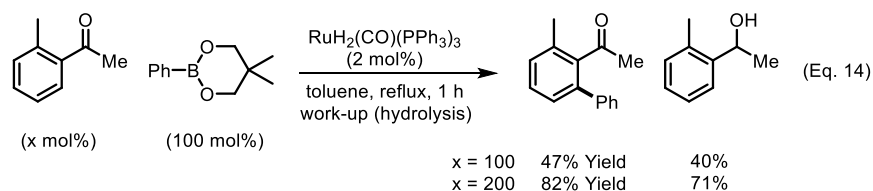
Scheme 2.22 Ruthenium-Catalyzed Synthesis and Modification of Polymers



2.2.2 Arylation

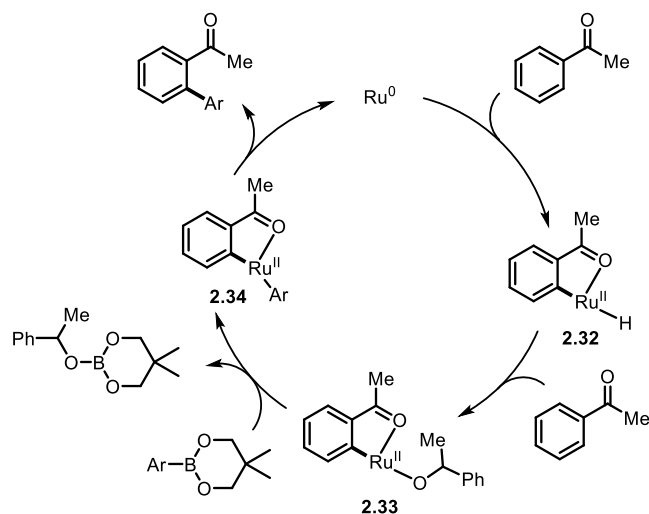
In 2003, Kakiuchi and coworkers successfully extended ruthenium-catalyzed *ortho*-functionalization to the arylation of aromatic ketones (Scheme 2.23).⁵⁵ With $\text{RuH}_2(\text{CO})(\text{PPh}_3)_3$ as the catalyst, a wide panel of aromatic ketones were arylated in good yields with arylboronates as the arene source. To ensure good yields, two equivalents of ketone substrate were required.

Scheme 2.23 Ruthenium-Catalyzed *ortho*-Arylation of Aromatic Ketones with Arylboronates



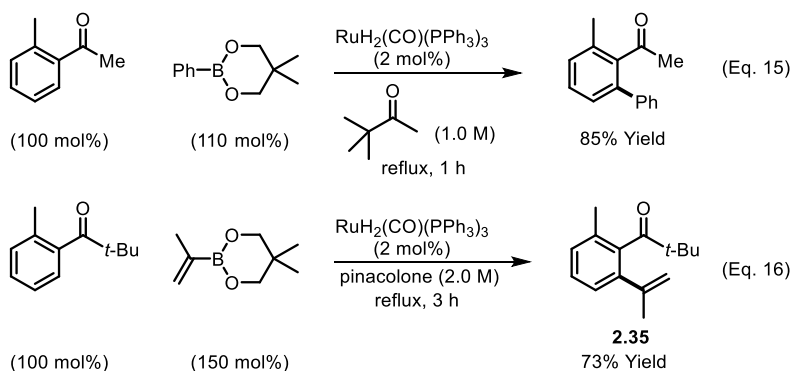
Murai's original ruthenium-catalyzed addition of C–H bonds across olefins is a redox-neutral process requiring no external oxidant or reductant. However, in the case of arylation with arylboronates, additional reductants are necessary to trap the hydride generated after the oxidative addition. This is supported by the authors' observation that an equal amount of benzyl alcohol was isolated as a byproduct after workup (Eq. 14).⁵⁶ In the proposed catalytic cycle, addition of Ru(II)-hydride **2.32** to another ketone substrate generates Ru(II)-alkoxide **2.33** (Scheme 2.24). Subsequent transmetalation between **2.33** and arylboronate transfers the aryl group to the Ru(II) and meanwhile generates a stoichiometric amount of boronic ester, which is hydrolyzed during the workup to give the benzyl alcohol. Reductive elimination of complex **2.34** would give the arylation product and restore the active Ru(0) catalyst.

Scheme 2.24 Proposed Catalytic Cycle of Ruthenium-Catalyzed *ortho*-Arylation



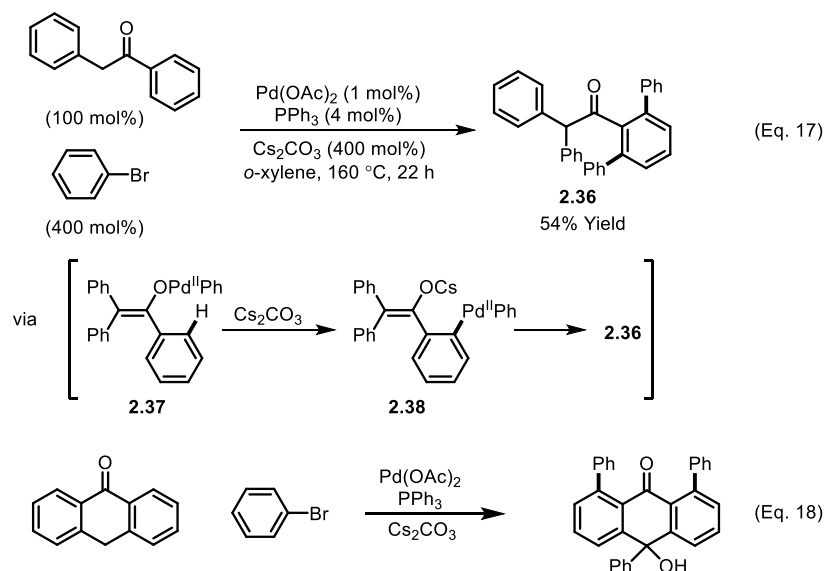
The issue of using excess ketone substrates was later resolved by employing pinacolone as the solvent (Scheme 2.25, Eq. 15). The efficiency of the arylation reaction can be sustained with aromatic ketones as the limiting reagent, and excess pinacolone serves as the hydride scavenger instead of the aryl ketone substrate. The coupling with alkenylboronates was also reported under similar reaction conditions by the same group (Eq. 16).^{57,58} This new olefination reaction can be considered as a complementary approach to the previous C–H addition to alkynes (*vide supra*, Scheme 2.16), since products like **2.35** cannot be accessed directly from coupling with alkynes.

Scheme 2.25 Ruthenium-Catalyzed *ortho*-Arylation Using Pinacolone as Solvent



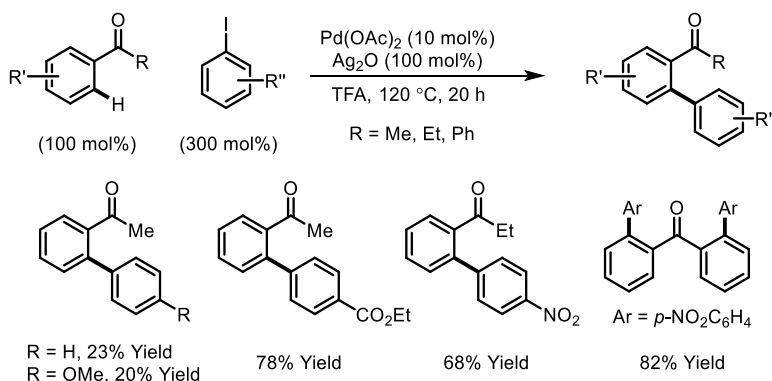
On the other hand, the *ortho*-arylation of aromatic ketones using aryl halides as the coupling partner was achieved using palladium catalysis. The *ortho*-arylation of aromatic ketones with aryl bromides was first discovered by Miura and coworkers (Scheme 2.26).⁵⁹ In the presence of a palladium catalyst and a stoichiometric base, benzylphenyl ketone reacted with excess bromobenzene to give poly-arylated ketone **2.36** as the major product (Eq. 17). Instead of a ketone-directed pathway, the authors proposed an enolate-directed palladation assisted by Cs_2CO_3 . In a following study by the same group, the *ortho*-C–H bonds of anthrone were also arylated under similar reaction conditions (Eq. 18).⁶⁰

Scheme 2.26 Palladium-Catalyzed Multi-Arylation of Ketones

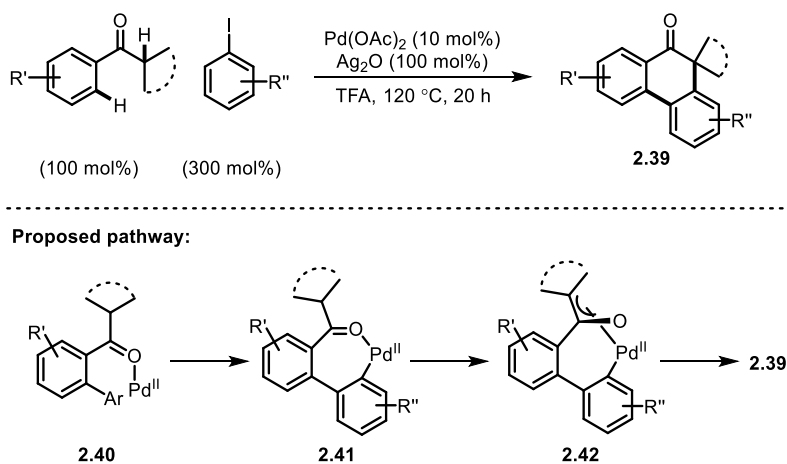


In 2010, Cheng and coworkers reported a ketone-directed *ortho*-arylation with aryl iodides (Scheme 2.27).⁶¹ Contrary to Miura's basic conditions, trifluoroacetic acid was used as the solvent for this reaction. In addition, although excess aryl iodides were employed, only mono arylation products were observed for a range of aromatic ketones. However, when electron-neutral or rich aryl iodides were used as the substrates, the yields were largely compromised. It is interesting to note that the use of *sec*-alkyl aryl ketones triggered a tandem process that gave phenanthrone products (Scheme 2.28). It was proposed that after the *ortho*-arylation, a second ketone (or enolate)-directed C–H activation occurs to form a seven-membered palladacycle (**2.41**). Subsequent enolate formation, rearrangement, and reductive elimination results in formation of phenanthrone **2.39**.

Scheme 2.27 Palladium-Catalyzed *ortho*-Arylation with Aryl Iodides



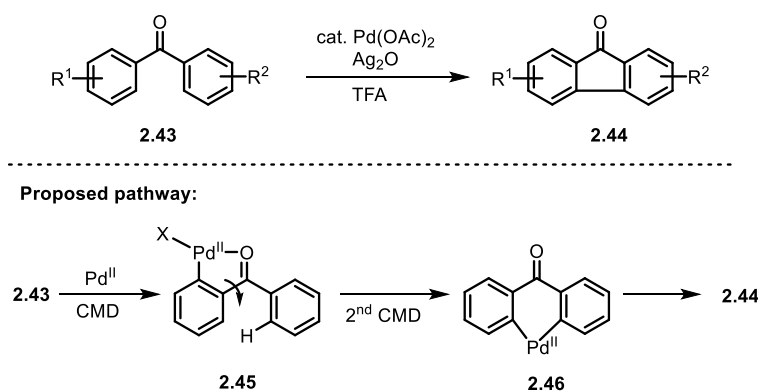
Scheme 2.28 Palladium-Catalyzed *ortho*-Arylation and Tandem Cyclization



Besides coupling with pre-functionalized aryl sources (i.e. arylboronates and aryl halides), ketone-directed arylation can also occur through the coupling between two aryl C–H bonds. In 2012, the Cheng⁶² and Shi⁶³ groups independently reported the synthesis of fluorenone derivatives from diaryl ketones using palladium acetate as the catalyst and silver oxide as the oxidant (Scheme 2.29). The proposed pathway begins with *ortho*-C–H palladation via a CMD mechanism directed by the ketone carbonyl. Due to the weak coordinating ability of the ketone, de-chelation followed by C–C bond rotation can occur, allowing the Pd(II) center to rotate

towards the *ortho*-C–H on the other arene. A second C–H palladation would lead to a six-membered pallacycle (**2.46**), which upon reductive elimination would give fluorenone **2.44** as the product and a Pd(0) species. The silver salt was proposed to oxidize the Pd(0) intermediate and restore the active Pd(II) catalyst.

Scheme 2.29 Palladium-Catalyzed Fluorenone Synthesis via Sequential C–H Activation



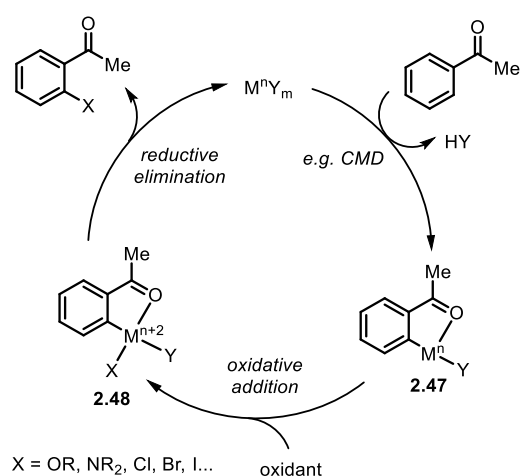
2.2.3 Carbon-Heteroatom (C–X) Bond Formation

Compared to C–C bond forming reactions, ketone-directed *ortho*-C–X (X: heteroatom) bond formation is relatively less studied. Nevertheless, direct and efficient assembly of *ortho*-heteroatom-substituted ketones via C–H functionalization is of great value to the synthetic community as *o*-acyl phenols, anilines, and haloarenes are prevalent motifs in bioactive compounds.

The general catalytic cycle for ketone-directed C–X bond formation is illustrated in Scheme 2.30. The reaction starts with a directed *ortho*-C–H metalation to give a five-membered metallacycle (**2.47**), where the oxidation state of the metal remains unchanged. The following

oxidation with various oxidants first delivers an anionic heteroatom ligand (X) to the metal, and second increases the oxidation state of the metal by two. Depending on the oxidant employed, different heteroatom ligands can be introduced to the metal. The final reductive elimination of the higher-oxidation state metal complex (**2.48**) affords the product with a newly formed C–X bond and regenerates the active metal catalyst.

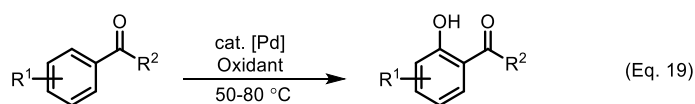
Scheme 2.30 General Mechanism of the Ketone-Directed *ortho*-C–X Bond Formation



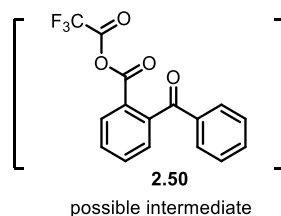
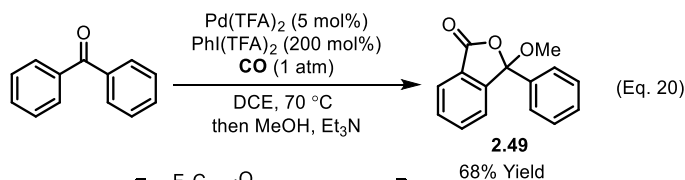
In 2012, the Rao⁶⁴ and Dong⁶⁵ groups independently reported a palladium-catalyzed *ortho*-hydroxylation reaction directed by ketones (Scheme 2.31, Eq. 19). A wide range of *ortho*-acylphenols were synthesized using palladium acetate or trifluoroacetate as the catalyst in good yields. Both organic and inorganic oxidants, e.g. hypervalent iodine compounds and potassium persulfate, can be used to promote the C–O bond formation. Dong and coworkers further discovered an unusual *ortho*-carbonylation reaction when running the hydroxylation reaction under CO atmosphere (Eq. 20).⁶⁵ While the exact pathway remains unclear, the ethyl-ketal lactone was proposed to come from mixed-anhydride intermediate **2.50**. A similar palladium-

catalyzed hydroxylation reaction was later reported by Kwong and coworkers.⁶⁶ In addition to palladium catalysis, the ketone-directed hydroxylation reaction can also be catalyzed by ruthenium^{67,68} and rhodium⁶⁸ under similar conditions (Scheme 2.32). The study of substrate scopes indicated that, while ruthenium- and rhodium-catalyzed hydroxylation reactions shared similar chemoselectivity (electron-rich arenes are favored), the ruthenium catalysts gave better performance in terms of yields.

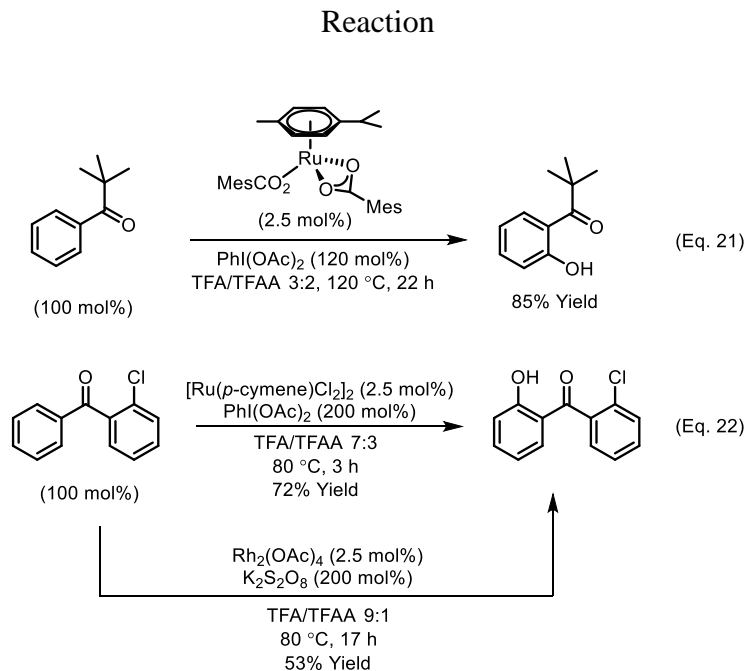
Scheme 2.31 Palladium-Catalyzed Ketone-Directed *ortho*-Hydroxylation Reaction



[Pd]: Pd(OAc)₂, Pd(TFA)₂
Oxidant: PhI(OAc)₂, PhI(TFA)₂, K₂S₂O₈

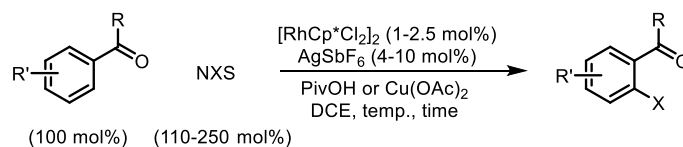


Scheme 2.32 Ruthenium and Rhodium-Catalyzed Ketone-Directed *ortho*-Hydroxylation

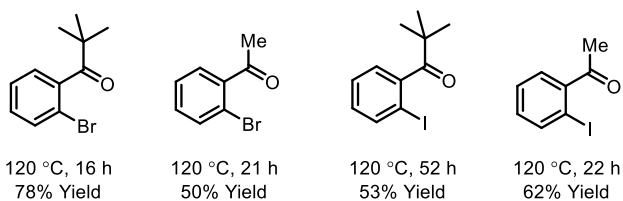


Halogenation is also possible, and *N*-halo succinimides proved to be efficient oxidants for carbon-halogen bond formation directed by ketones. In 2012, Glorius and coworkers reported rhodium-catalyzed *ortho*-bromination and iodination reactions with aromatic ketones, using *N*-bromo and *N*-iodosuccinimide as the oxidant respectively (Scheme 2.33).⁶⁹ The reaction conditions utilize a cationic rhodium catalyst and stoichiometric pivalic acid or copper acetate, presumably to facilitate the metalation step. The chlorination with *N*-chlorosuccinimide was reported later by Rao and coworkers using palladium catalysis (Scheme 2.34).⁷⁰ Both triflic acid and potassium persulfate additives play a vital role in sustaining the reactivity. While triflic acid facilitates coordination of the ketone by *in situ* generation of a more electrophilic palladium catalyst Pd(OTf)₂, potassium persulfate is believed to promote the oxidation of Pd(II) to Pd(IV) as a co-oxidant.

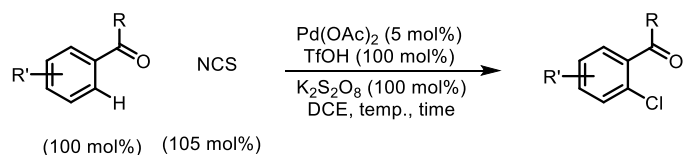
Scheme 2.33 Palladium-Catalyzed Ketone-Directed *ortho*-Bromination and Iodination



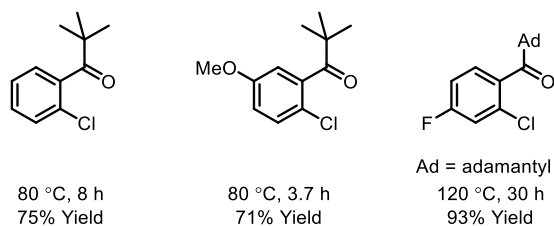
Selected examples:



Scheme 2.34 Palladium-Catalyzed Ketone-Directed *ortho*-Chlorination

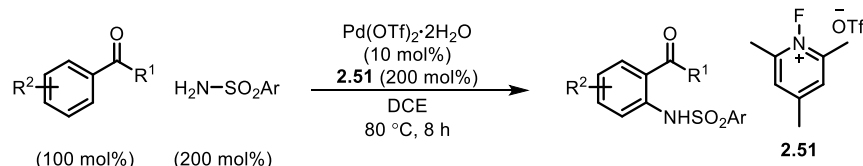


Selected examples:

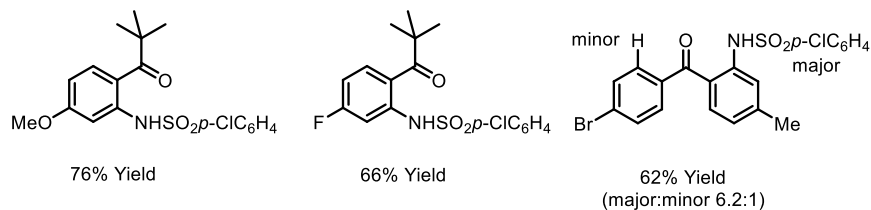


Ketone-directed *ortho*-amination was first accomplished by Liu and coworkers using sulfonamides or amides as the amine source (Scheme 2.35).⁷¹ *N*-Fluoro-2,4,6-trimethylpyridinium triflate **2.51** or sodium persulfate can be used as the terminal oxidant. Mechanistic studies revealed that during the reaction the sulfonamide competes with the weakly coordinating ketone for complexation with palladium, which results in lower efficiency during the reaction.

Scheme 2.35 Palladium-Catalyzed Ketone-Directed *ortho*-Amination Using Sulfonamides

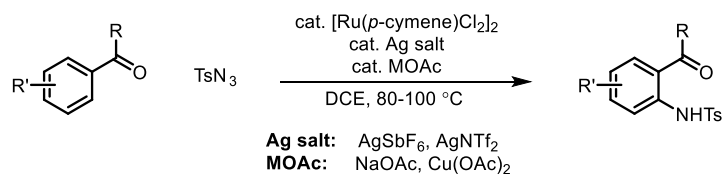


Selected examples:



The corresponding *ortho*-amination with sulfonyl azides was independently reported by the Chang,⁷² Jiao,⁷³ and Sahoo⁷⁴ groups in 2013 using $[\text{Ru}(p\text{-cymene})\text{Cl}_2]_2$ as the catalyst (Scheme 2.36). Besides the use of cationic silver salts, additional copper or sodium acetate is indispensable for all three reactions. The silver salt is proposed to generate a more electrophilic ruthenium catalyst allowing better complexation with ketone. The basic acetate ligands are expected to facilitate C–H metalation via a CMD mechanism.

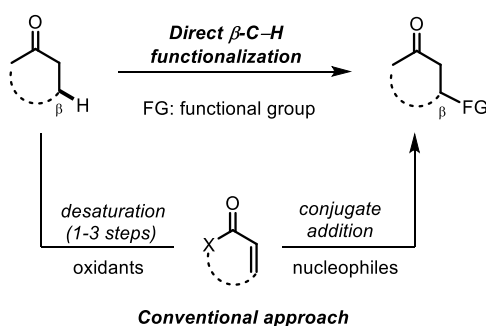
Scheme 2.36 Palladium-Catalyzed Ketone-Directed *ortho*-Amination Using Sulfonyl Azides



2.3 β -C–H Functionalization of Simple Ketones

β -Substituted ketones represent an important class of prevalent motifs in bioactive compounds, such as drug candidates, anti-oxidants, and pesticides. Nevertheless, compared to the α -C–H bond, the more distal β -(sp^3)C–H bonds of ketones are usually considered intrinsically unreactive. Conventionally, β -functionalized ketones are prepared through the conjugate addition of nucleophiles to α,β -unsaturated ketones (Scheme 2.37).⁷⁵ As efficient as this protocol is, α,β -unsaturated ketones are often synthesized from the corresponding saturated ketones via dehydrogenation, which takes 1-3 steps and requires stoichiometric oxidants.⁷⁶ The direct β -C–H functionalization of the carboxylic acid derivatives, e.g. amides and esters, using a DG-based strategy have been extensively studied and reviewed:⁷⁷ in contrast, β -functionalization of simple ketones is nontrivial to develop due to their higher reactivity but lower coordinating ability. In the past two years, several transition-metal-catalyzed approaches have emerged that enable the direct β -C–H functionalization of simple ketones.

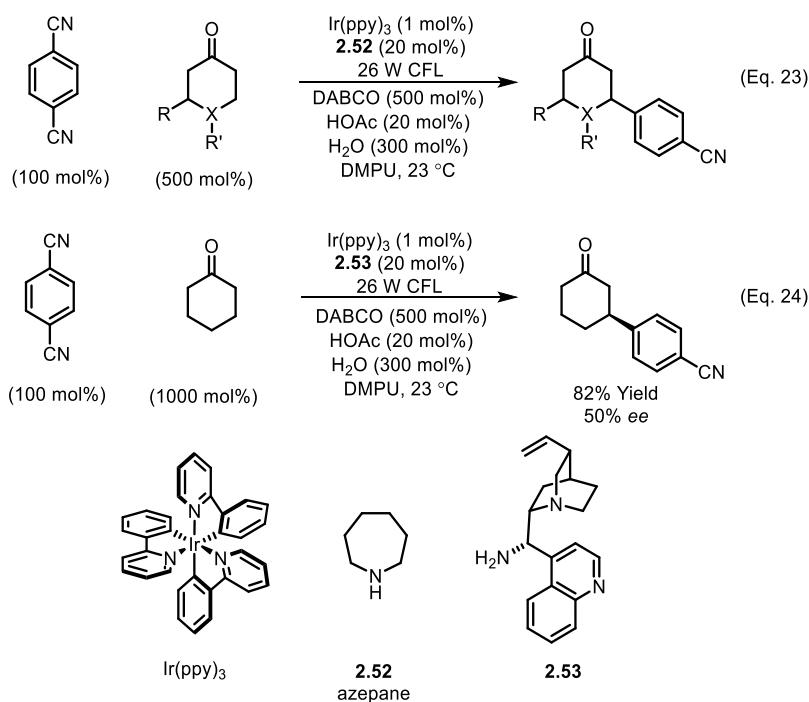
Scheme 2.37 Direct β -C–H Functionalization of Ketones



In 2013, MacMillan and coworkers reported a direct β -arylation of cyclic ketones with electron-deficient aryl nitriles via the combination of photo- and enamine catalysis (Scheme

2.38).⁷⁸ With a photocatalyst, i.e. Ir(ppy)₃, and amine catalyst, i.e. azepane, various cyclic ketones were coupled with 1,4-dicyanobenzene selectively at the β-position in the presence of a 26W light bulb (CFL: compact fluorescent light) (Eq. 23). This transformation is amenable for enantioselective catalysis. When a cinchona-based chiral amine (**2.53**) was employed, a moderate *ee* value was obtained for the β-arylation of cyclohexanone (Eq. 24).

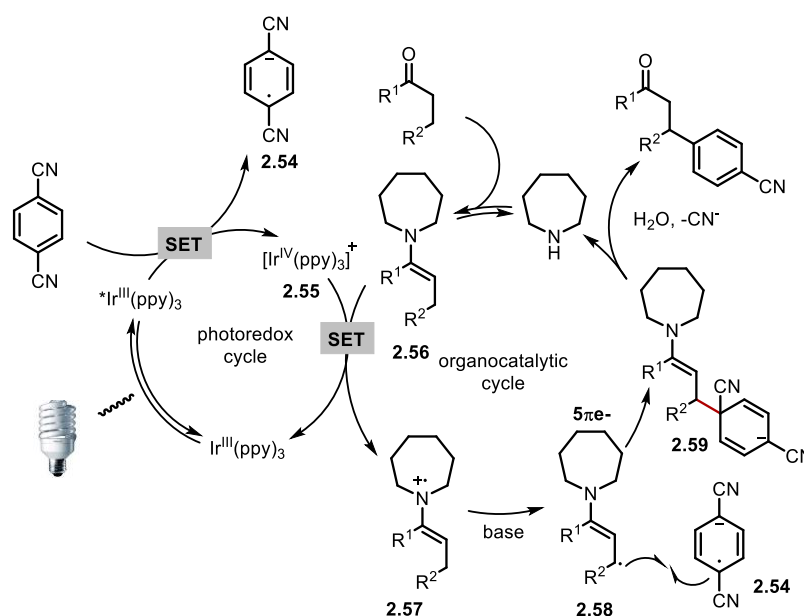
Scheme 2.38 Direct β-Arylation of Ketones via Photoredox Organocatalysis



The proposed mechanism for the β-arylation reaction consists of two catalytic cycles mediated by the photo- and amine catalyst, respectively (Scheme 2.39). In the photocatalytic cycle, the Ir(ppy)₃ catalyst is first activated by light to generate an excited *Ir(ppy)₃. A subsequent single electron transfer (SET) between the electron-deficient 1,4-dicyanobenzene and the activated catalyst reduces the arene to a radical anion (**2.54**) and yields an Ir(IV) intermediate

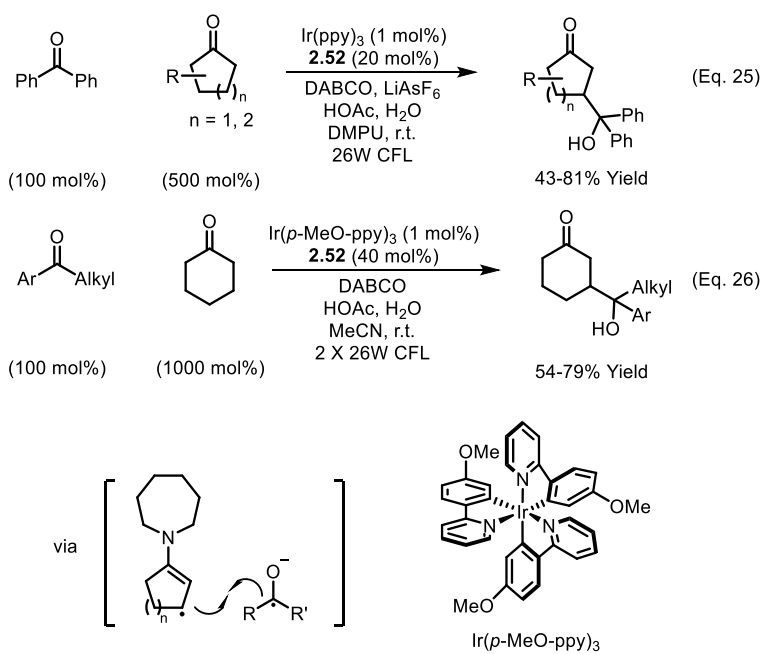
2.55. In the second cycle, the amine catalyst condenses with the ketone substrate to give an electron-rich enamine intermediate (**2.56**). The two catalytic cycles then merge through a single electron transfer process, where the enamine gets oxidized to a nitrogen-centered radical cation (**2.57**) and the Ir complex (**2.55**) is reduced back to Ir(ppy)₃. The formation of the radical cation increases the acidity of the allylic β-C–H bond, which can be deprotonated by a base to give a 5π-electron system that has significant radical character at the β-carbon. Coupling between electron-rich β-radical **2.58** and electron-deficient radical anion **2.54** provides intermediate **2.59** bearing a new β-C–C bond. The following re-aromatization and hydrolysis affords the β-arylated ketone, releases a cyanide anion, and regenerates the amine catalyst. The use of electron-deficient aryl nitriles as the coupling partner is important because the radical anion intermediate **2.54** generated from the aryl nitrile is long living and reluctant to dimerize due to its electron deficiency, which is the key for high chemo and site-selectivity for the β-C–C bond formation.

Scheme 2.39 Proposed Catalytic Cycle of Direct β-Arylation of Ketones



Later, the same group extended this activation mode to other ketone β -C-H functionalization reactions. With the use of the same photocatalyst $[\text{Ir}(\text{ppy})_3]$ and amine catalyst (azepane), cyclic ketones can be coupled with diarylketones to give γ -hydroxyketone adducts (Scheme 2.40, Eq. 25).⁷⁹ This transformation can be considered as a formal β -aldol reaction. A similar mechanism as the β -arylation reaction was proposed by the authors, where the major difference is that a ketyl radical is used as the coupling partner instead of the aryl radical anion. A stoichiometric amount of LiAsF_6 salt was found important to sustain the efficiency of the coupling, presumably due to its capability of prohibiting the dimerization of ketyl radicals. When an alkyl aryl ketone was employed as the substrate, a more reducing photocatalyst $\text{Ir}(p\text{-OMe-ppy})_3$, a higher loading of the amine catalyst, and an additional light bulb are necessary to promote the transformation (Eq. 26). This can be attributed to a higher reduction potential for the alkyl aryl ketones compared to the diaryl ketones.

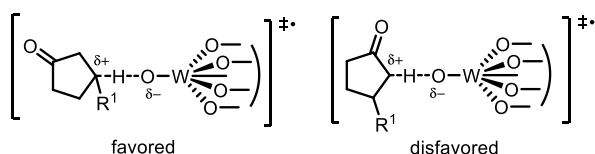
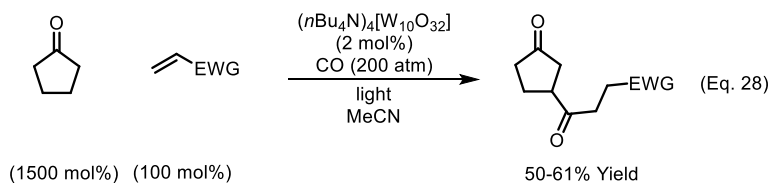
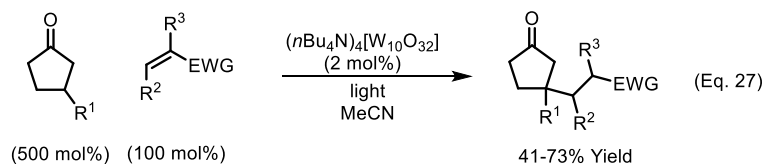
Scheme 2.40 β -Aldol Coupling of Cyclic Ketones with Aryl Ketones via Photoredox Catalysis



Another interesting ketone β -functionalization was reported by Fagnoni and coworkers in 2014 using a different transition-metal-catalyzed photoredox approach (Scheme 2.41).⁸⁰ Using tetrabutylammonium decatungstate (TBADT) as the catalyst and a Xe lamp or sunlight as the light source, various cyclopentanones can be coupled with electron-deficient alkenes to give β -alkylated products (Eq. 27). The light source was proposed to excite the TBADT catalyst to a state containing electronegative oxygen-centered radicals. The activated catalyst can directly abstract a β -hydrogen of the cyclopentanone to generate a carbon-centered radical. Subsequent 1,4-addition to a Michael acceptor, followed by hydrogen transfer back from the catalyst, results in the β -alkylation product.

The β -selectivity of this transformation is determined during the hydrogen abstraction step. When the electronegative oxygen-centered radical approaches a C–H bond, a partial positive charge will build on the carbon atom in the transition state. Because the partial positive charge is destabilized by the neighboring carbonyl group, the abstraction of the α -hydrogen is disfavored, resulting in a high β -selectivity. In addition to the alkylation, a β -acylation of cyclopentanones was also achieved when the reaction was run under high pressure of carbon monoxide (Eq. 28). Despite the high β -selectivity for cyclopentanone, other cyclic ketones, e.g. cyclohexanone, gave a mixture of β - and γ -C–H functionalization products.

Scheme 2.41 Photocatalyzed β -Alkylation and Acylation of Cyclopentanones



2.4 Addition of α -C-H Bonds to Unactivated Alkenes or Alkynes

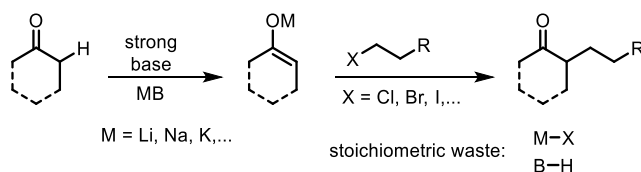
2.4.1 Addition to Alkenes

Direct addition of the α -C-H bond of ketones across unactivated alkenes represents a transformation of significant synthetic value. Traditionally, α -alkylation of ketones is realized through enolate formation and subsequent substitution with an alkylating reagent, e.g. alkyl halides in most cases (Scheme 2.42A). Efficient as this reaction is, it suffers from several drawbacks, including highly basic conditions, generation of stoichiometric waste, lack of regioselectivity, high cost of the alkylation reagents and over-alkylation.⁸¹ The Stork enamine reaction can also be used to prepare α -alkylated ketones,⁸² although the use of highly reactive

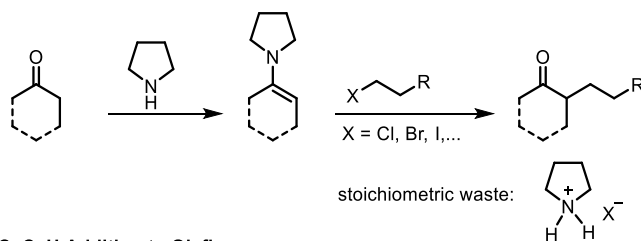
alkylating reagents ('hot electrophiles'), as well as the formation of stoichiometric amine salts is inevitable (Scheme 2.42B).

Scheme 2.42 α -Alkylation of Ketones

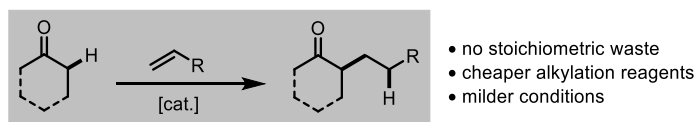
A. Enolate Alkylation



B. Stork Enamine Alkylation



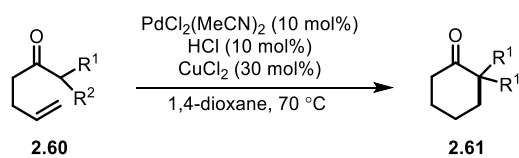
C. C-H Addition to Olefins



Compared to conventional alkylation reagents, such as alkyl halides and Michael acceptors, simple olefins are more accessible and generally less expensive. Moreover, the addition of the α -C-H bond of ketones to olefins ostensibly generates no stoichiometric waste, thus maximizing the atom economy of the alkylation reaction (Scheme 2.42C). Although the addition of activated methylene compounds (e.g. α -C-H bond of 1,3-dicarbonyl compounds) to olefins has been well studied,⁸³ examples of using less-acidic simple ketones as substrate are limited.

In 2003, Widenhoefer and coworkers reported an intramolecular cyclization with a γ,σ -enone using palladium catalysis (Scheme 2.43).⁸⁴ A catalytic amount of hydrochloric acid was employed to promote enol formation, and CuCl_2 was used to stabilize the Pd(II) catalyst. A number of γ,δ -enones (**2.60**) cyclized efficiently in a 6-*endo-trig* fashion to afford 2-substituted cyclohexanones (**2.61**). When a tertiary substituent is present on the ketone, a spirocyclic structure can be formed in a similar yield. Based on deuterium-labeling studies, the authors proposed that after intramolecular nucleophilic attack of the enol to the olefin, the resulting Pd(II)-alkyl species (**2.63**) would undergo a “chain walk” to place palladium on the α -position through a series of β -hydride elimination/re-insertion steps (Scheme 2.44). Protonation of the Pd(II)-enolate (**2.66**) would release the product and regenerate the active palladium catalyst.⁸⁵

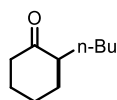
Scheme 2.43 Palladium-Catalyzed Intramolecular α -Alkylation of Ketones with Olefins



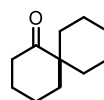
Selected examples:



79% Yield

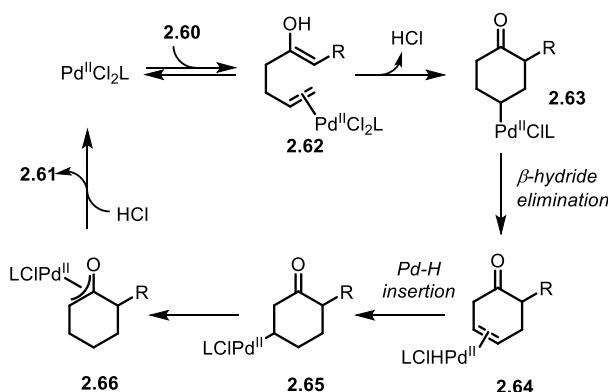


65% Yield



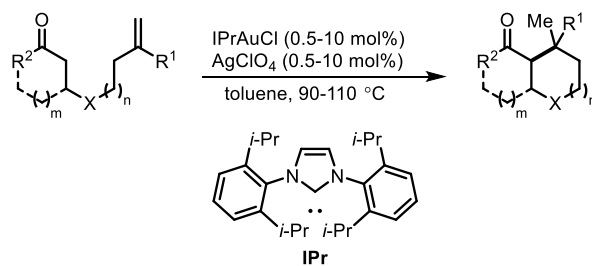
59% Yield

Scheme 2.44 Proposed Pathway of Palladium-Catalyzed Intramolecular α -Alkylation

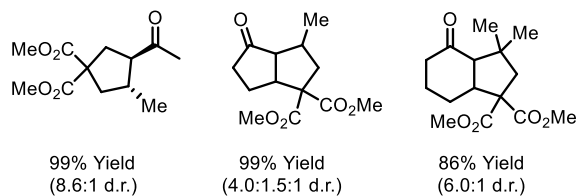


In 2011, an efficient gold-catalyzed intramolecular α -alkylation with aliphatic olefins was developed by Che and coworkers (Scheme 2.45).⁸⁶ Compared to Widenhoefer's protocol, the gold-catalyzed method has several distinct features. First, no additional protic acids are employed because the cationic gold is Lewis acidic enough to facilitate enol formation. Second, the *5-exo-trig* cyclization to give five-membered rings is favored over the *6-endo-trig* pathway. Mechanistically, the alkyl-Au(I) species generated from the enol addition step was proposed to undergo direct protonation to give the alkylation product as opposed to the aforementioned "chain walk" process. No coupling with aromatic olefins was reported with either Widenhoefer or Che's catalytic system, which can likely be attributed to the acid-lability of aryl olefins.

Scheme 2.45 Gold-Catalyzed Intramolecular α -Alkylation of Ketones with Olefins

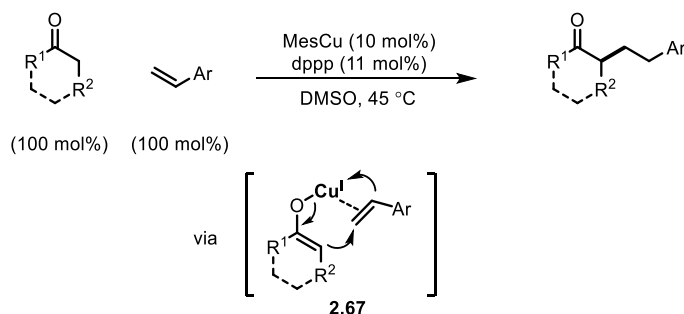


Selected examples:



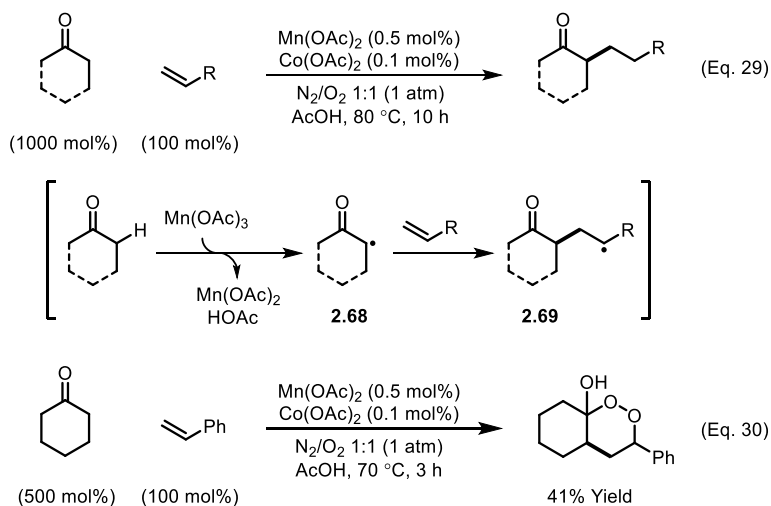
Besides intramolecular alkylation reactions, several approaches for the more challenging intermolecular α -alkylation of ketones with simple olefins have also emerged. Intermolecular alkylation with aryl olefins, e.g. styrene, is known to be catalyzed by strong bases such as KO^tBu in polar solvents such as DMSO.^{87,88,89} In 2012, Kanai and coworkers reported a copper-catalyzed addition of ketone α -C-H bonds to styrene derivatives (Scheme 2.46).⁹⁰ Mesityl cuprate and CuOⁱPr were both found to be efficient precatalysts. Ketones with diverse structures can be coupled with styrene derivatives to afford linear alkylation products. While the exact mechanism remains unclear, a dual role of the copper catalyst was proposed: 1) it acts as a strong base to generate a Cu(I)-enolate; 2) it serves as a π acid to activate the styrene.

Scheme 2.46 Copper-Catalyzed Intermolecular α -Alkylation of Ketones with Olefins



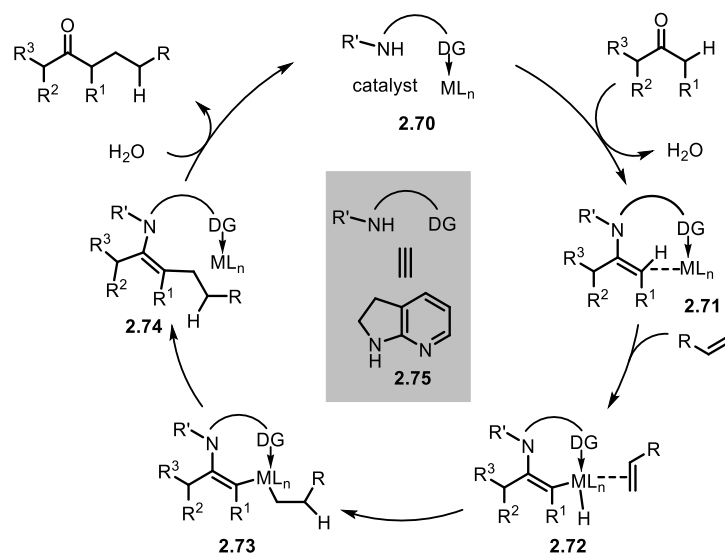
An unusual radical approach also proved to be feasible for the addition of α -C–H bonds of ketones to aliphatic olefins.⁹¹ In 2000, Ishii and coworkers reported an α -alkylation reaction of ketones with alkenes using a combination of catalytic $\text{Mn}(\text{OAc})_2$ and $\text{Co}(\text{OAc})_2$ (Scheme 2.47, Eq. 29). Both cyclic and linear ketones can couple with 1-octene or isopropenyl acetate to give the alkylation products. Acetic acid was used as solvent, and the reaction was run under a mixed atmosphere of nitrogen and oxygen. In the proposed mechanism, the ketone substrate was first oxidized by *in situ* generated $\text{Mn}(\text{OAc})_3$ to give an α -keto radical species (**2.68**). Subsequent radical addition to the alkene, followed by hydrogen abstraction from either the solvent or another ketone, would provide the alkylation product. The presence of oxygen was critical, suggesting an oxidative process. Although the cobalt salt is not necessary for product formation, it is believed to assist the re-oxidation of $\text{Mn}(\text{OAc})_2$ by oxygen. A major drawback of this approach is the use of excess ketone, presumably to sustain the efficiency of the radical generation. When styrene was used as the substrate, an interesting peroxo bicycle was formed (Eq. 30).

Scheme 2.47 Manganese-Catalyzed Intermolecular α -Alkylation of Ketones with Olefins



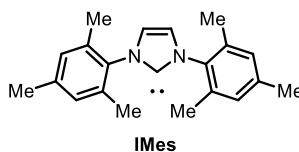
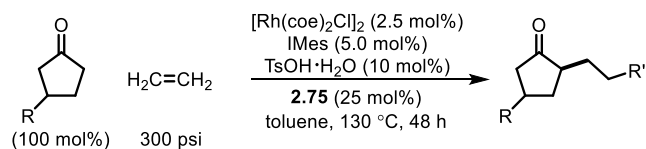
In 2014, Mo and Dong reported a Rh(I)-catalyzed α -alkylation of ketones with various alkenes via bifunctional catalysis (Scheme 48).⁹² The dual activation of the ketone and olefin was achieved through the use of Rh(I)/7-azaindoline as the bifunctional catalyst. In the proposed catalytic cycle, the secondary amine motif in 7-azaindoline (**2.75**) would first condense with ketone to form enamine **2.71**, which converts a ketone sp^3 α -C–H bond to an sp^2 C–H bond. One benefit of the transient enamine formation is that sp^2 C–H bonds are generally easier to be activated than sp^3 bonds both thermodynamically and kinetically.⁹³ Directed by the pyridine moiety, oxidative addition of Rh(I) into the α -C–H bond would then yield six-membered rhodacycle **2.72**. Subsequent migratory insertion of the olefin into the Rh-hydride bond, followed by reductive elimination to form the C–C bond and hydrolysis of the enamine, furnished the alkylation product and re-generated the bifunctional catalyst.

Scheme 2.48 Proposed Strategy of α -Alkylation of Ketones Using Bifunctional Catalysis

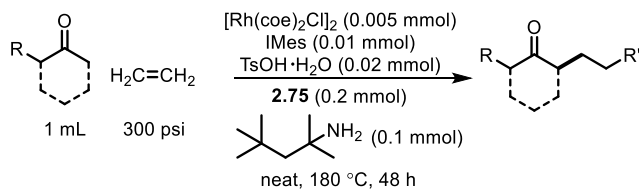
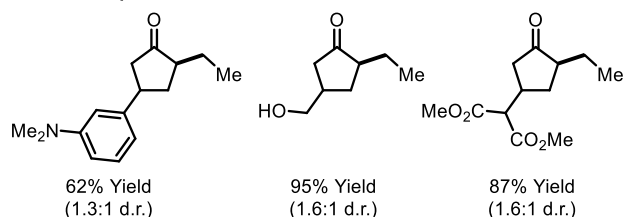


Based on the proposed strategy, the optimized conditions consist of $[\text{Rh}(\text{coe})_2\text{Cl}]_2/\text{Bis}[1,3\text{-bis}(2,4,6\text{-trimethylphenyl})\text{imidazol-2-ylidene}]$ (IMes) as the precatalyst, and catalytic tosylsulfonic acid to promote enamine formation (Scheme 2.49). This strategy enabled coupling of both aliphatic and aromatic alkenes giving the alkylation products with linear selectivity. Both cyclic and linear ketones can be coupled with various α -olefins to give the corresponding alkylation products. In addition, due to the pH- and redox-neutral conditions, many sensitive functional groups, such as free alcohols, amines and malonates etc., were found compatible.

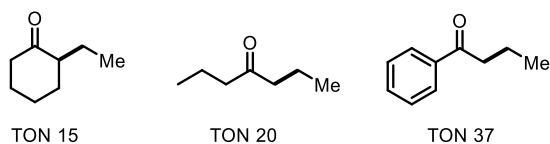
Scheme 2.49 Rhodium-Catalyzed α -Alkylation of Ketones with Bifunctional Ligand



Selected examples:



Selected examples:



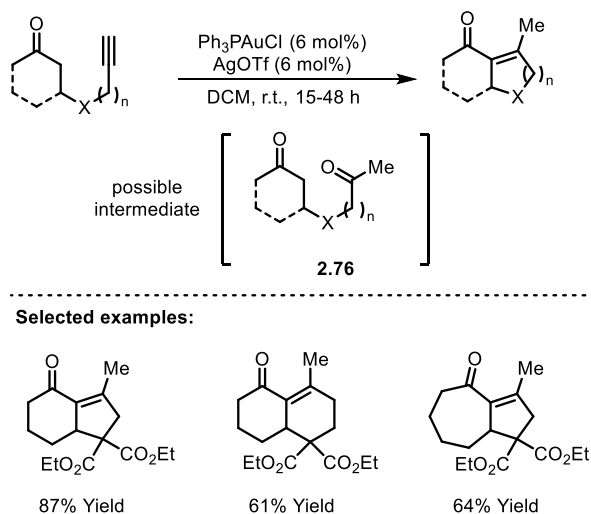
2.4.2 Addition to Alkynes

The direct addition of ketone α -C-H bonds to alkynes represents a promising approach to access enone derivatives. For example, the intramolecular ketone-alkyne cyclization has been extensively studied and employed to construct cyclic enone structures.⁹⁴ Although a large collection of catalysts and reaction conditions have been developed to facilitate this cyclization,

the substrate scope is primarily focused on 1,3-dicarbonyl compounds. Nevertheless, π -acid-catalyzed ketone-mediated transformations have been recently developed.

In 2010, Davies and coworkers reported a gold-catalyzed intramolecular cycloisomerisation of alkynes and simple ketones (Scheme 2.50).⁹⁵ A number of tethered keto-alkynes could cyclize in the presence of a cationic gold catalyst to give fused or spiro-enone derivatives. While the direct addition of the α -C-H bond to the alkyne represents a possible pathway, mechanistic studies indicate an alkyne hydration/aldol condensation pathway seems to be more reasonable. In the proposed reaction pathway, gold-catalyzed alkyne hydration with adventitious water would first generate diketone **2.76**, which upon intramolecular aldol condensation gives the enone product.

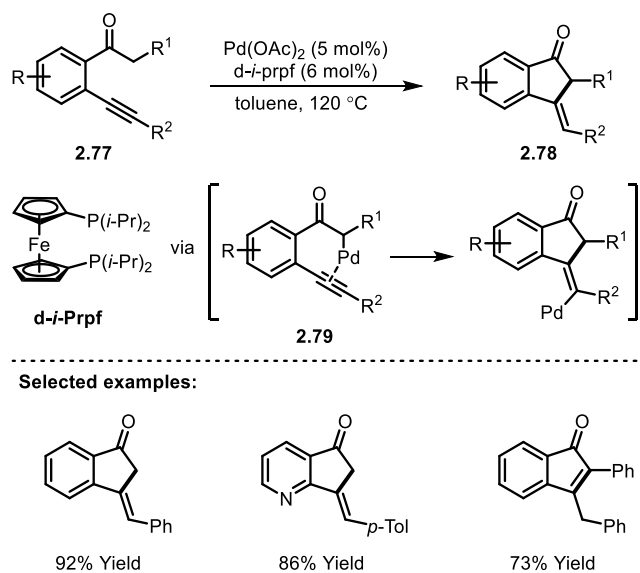
Scheme 2.50 Gold-Catalyzed Intramolecular α -Alkenylation of Ketones with Alkynes



A palladium-catalyzed cyclization of keto-alkynes was later reported by Gevorgyan and coworkers. 2-Alkynyl acetophenone derivatives can readily cyclize to form β -alkylidene indanone structures (Scheme 2.51).⁹⁶ Complete stereoselectivity for the *E* isomers was observed

for the cyclization. Interestingly, when the ketone possesses an α -aryl substituent, a conjugated indenone structure was formed instead of the indanone. DFT calculation implied the reaction proceeded through palladium enolate **2.79**, a similar intermediate to that proposed in Kanai's alkylation reaction with olefins (*vide supra*, Scheme 2.46).

Scheme 2.51 Palladium-Catalyzed Intramolecular α -Alkenylation of Ketones with Alkynes



The intermolecular addition of ketones to alkynes has limited success using simple ketones as the substrate. No transition metal-catalyzed example has been reported. To date, stoichiometric Lewis acid-mediated addition of silyl enol ethers into terminal alkynes⁹⁷ and strong base-promoted addition of potassium enolates into aryl terminal acetylenes^{98,99} represent the only known examples.

2.5 Conclusion

In summary, the transition metal-catalyzed ketone-directed or mediated C–H functionalization has been a rapidly growing field over the past two decades. While the mode of activation varies from case to case, the use of transition metals has driven transformations of ketones beyond the intrinsic reactivity allowing C–H functionalization to occur at the less reactive position or with unactivated coupling partners. Among all the topics covered in this chapter, the aromatic *ortho* C–H functionalization using ketone DGs has been most well studied. Future endeavors are expected to demonstrate more applications with these methods and introduce more types of FGs. Although the functionalization of ketone aliphatic C–H bonds using transition-metal catalysis is a relatively new area, an avalanche of novel approaches have sprung up recently. While it is still too early to assess the synthetic potential of these methods, they nonetheless offer new perspectives on how strategy and catalyst design can enable the reactivity and selectivity that are not expected from conventional viewpoints.

2.6 References

1. For recent reviews on transition metal-catalyzed C–H functionalization, see: (a) Davies, H. M. *L. J. Mol. Catal. A: Chem.* **2002**, *189*, 125. (b) Kakiuchi, F.; Murai, S. *Acc. Chem. Res.* **2002**, *35*, 826. (c) Chen, X.; Engle, K. M.; Wang, D.-H.; Yu, J.-Q. *Angew. Chem. Int. Ed.* **2009**, *48*, 5094. (d) Ackermann, L.; Vicente, R.; Kapdi, A. R. *Angew. Chem. Int. Ed.* **2009**, *48*, 9792. (e) Jazzar, R.; Hitce, J.; Renaudat, A.; Sofack-Kreutzer, J.; Baudoin, O. *Chem. Eur. J.* **2010**, *16*, 2654. (f) Daugulis, O. *Top. Curr. Chem.* **2010**, *292*, 57. (g) Colby, D. A.; Bergman, R. G.; Ellman, J. A. *Chem. Rev.* **2010**, *110*, 624. (h) Mkhaliid, I. A. I.; Barnard, J. H.; Marder, T. B.; Murphy, J. M.; Hartwig, J. F. *Chem. Rev.* **2010**, *110*, 890. (i) Baudoin, O. *Chem. Soc. Rev.* **2011**, *40*, 4902. (j) Li, B.-J.; Shi, Z.-J. *Catal. Sci. Technol.* **2011**, *1*, 191. (k) Lu, H.; Zhang, X. P. *Chem. Soc. Rev.* **2011**, *40*, 1899. (l) Wencel-Delord, J.; Dröge, T.; Liu, F.; Glorius, F. *Chem. Soc. Rev.* **2011**, *40*, 4740. (m) Arockiam, P. B.; Bruneau, C.; Dixneuf, P. H. *Chem. Rev.* **2012**, *112*, 5879. (n) Song, G.; Wang, F.; Li, X. *Chem. Soc. Rev.* **2012**, *41*, 3651.
2. For recent reviews on directing group strategy, see: (a) Lyons, T. W.; Sanford, M. S. *Chem. Rev.* **2010**, *110*, 1147. (b) Rousseau, G.; Breit, B. *Angew. Chem. Int. Ed.* **2011**, *50*, 2450. (c) Zhang, M.; Zhang, Y.; Jie, X.; Zhao, H.; Li, G.; Su, W. *Org. Chem. Front.* **2014**, *1*, 843.
3. For selected examples, see: (a) Mancha, S. R.; Regnery, C. M.; Dahlke, J. R.; Miller, K. A.; Blake, D. J. *Bioorg. Med. Chem. Lett.* **2013**, *23*, 562. (b) Roth, G. N.; Chandra, A.; Nair, M. G. *J. Nat. Prod.* **1998**, *61*, 542. (c) Misawa, N.; Nakamura, R.; Kagiya, Y.; Ikenaga, H.; Furukawa, K.; Shindo, K. *Tetrahedron* **2005**, *61*, 195. (d) Melvin, L. S.; Johnson, M. R.; Harbert, C. A.; Milne, G. M.; Weissman, A. *J. Med. Chem.* **1984**, *27*, 67. (e) Hamon, D. P. G.; Hayball, P. J.; Massy-Westropp, R. A.; Newton, J. L.; Tamblyn, J. G. *Tetrahedron: Asymmetry* **1996**, *7*, 263.
4. Murai, S.; Kakiuchi, F.; Sekine, S.; Tanaka, Y.; Kamatani, A.; Sonoda, M.; Chatani, N. *Nature* **1993**, *366*, 529.
5. For recent reviews on α -arylation of ketones, see: (a) Johansson, C. C. C.; Colacot, T. J. *Angew. Chem., Int. Ed.* **2010**, *49*, 676. (b) Bellina, F.; Rossi, R. *Chem. Rev.* **2010**, *110*, 1082. (c) Culkin, D. A.; Hartwig, J. F. *Acc. Chem. Res.* **2003**, *36*, 234.
6. For selected reviews, see: (a) R. C. Larock, In *Comprehensive Organic Transformation*, 2nd Edn, Wiley-VCH, New York, 1999, pp 709. (b) Mahrwald, R. *Chem. Rev.* **1999**, *99*, 1095. (c) Palomo, C.; Oiarbide, M.; Garcia, J. M. *Chem. Soc. Rev.* **2004**, *33*, 65.
7. Laurance, C.; Gal, J.-F. *Lewis Basicity and Affinity Scales: Data and Measurement*, Wiley-VCH, Weinheim, 2010.
8. Kakiuchi, F.; Sekine, S.; Tanaka, Y.; Kamatani, A.; Chatani, N.; Murai, S. *Bull. Chem. Soc. Jpn.* **1995**, *68*, 62.

-
9. Murai, S.; Kakiuchi, F.; Sekine, S.; Tanaka, Y.; Kamatani, A.; Chatani, N. *Pure Appl. Chem.* **1994**, *66*, 1527.
 10. Sonoda, M.; Kakiuchi, F.; Chatani, N.; Murai, S. *J. Organomet. Chem.* **1995**, *504*, 151.
 11. Sonoda, M.; Kakiuchi, F.; Chatani, N.; Murai, S. *Bull. Chem. Soc. Jpn.* **1997**, *70*, 3117.
 12. Hiraki, K.; Ishimoto, T.; Kawano, H. *Bull. Chem. Soc. Jpn.* **2000**, *73*, 2099.
 13. Matsubara, T.; Koga, N.; Musaev, D. G.; Morokuma, K. *J. Am. Chem. Soc.* **1998**, *120*, 12692.
 14. Kakiuchi, F.; Kochi, T.; Mizushima, E.; Murai, S. *J. Am. Chem. Soc.* **2010**, *132*, 17741.
 15. Guari, Y.; Sabo-Etienne, S.; Chaudret, B. *J. Am. Chem. Soc.* **1998**, *120*, 4228.
 16. Guari, Y.; Castellanos, A.; Sabo-Etienne, S.; Chaudret, B. *J. Mol. Catal. A: Chem.* **2004**, *212*, 77.
 17. Busch, S.; Leitner, W. *Chem. Commun.* **1999**, 2305.
 18. Busch, S.; Leitner, W. *Adv. Synth. Catal.* **2001**, *343*, 192.
 19. Grellier, M.; Vendier, L.; Chaudret, B.; Albinati, A.; Rizzato, S.; Mason, S.; Sabo-Etienne, S. *J. Am. Chem. Soc.* **2005**, *127*, 17592.
 20. Martinez, R.; Chevalier, R.; Darses, S.; Genet, J.-P. *Angew. Chem. Int. Ed.* **2006**, *45*, 8232.
 21. Martinez, R.; Simon, M.-O.; Chevalier, R.; Pautigny, C.; Genet, J.-P.; Darses, S. *J. Am. Chem. Soc.* **2009**, *131*, 7887.
 22. Simon, M.-O.; Martinez, R.; Genet, J.-P.; Darses, S. *J. Org. Chem.* **2010**, *75*, 208.
 23. Simon, M.-O.; Genet, J.-P.; Darses, S. *Org. Lett.* **2010**, *12*, 3038.
 24. Trost, B. M.; Imi, K.; Davies, I. W. *J. Am. Chem. Soc.* **1995**, *117*, 5371.
 25. Kakiuchi, F.; Tanaka, Y.; Sato, T.; Chatani, N.; Murai, S. *Chem. Lett.* **1995**, *24*, 679.
 26. Sato, T.; Kakiuchi, F.; Chatani, N.; Murai, S. *Chem. Lett.* **1998**, *27*, 893.
 27. Lenges, C. P.; Brookhart, M. *J. Am. Chem. Soc.* **1999**, *121*, 6616.

-
28. Jun, C.-H.; Moon, C. W.; Hong, J.-B.; Lim, S.-G.; Chung, K.-Y.; Kim, Y.-H. *Chem. Eur. J.* **2002**, *8*, 485.
29. Jun, C.-H.; Moon, C. W.; Kim, Y.-M.; Lee, H.; Lee, J. H. *Tetrahedron Lett.* **2002**, *43*, 4233.
30. Tsuchikama, K.; Kasagawa, M.; Hashimoto, Y.-K.; Endo, K.; Shibata, T. *J. Organomet. Chem.* **2008**, *693*, 3939.
31. Crisenze, G. E. M.; McCreanor, N. G.; Bower, J. F. *J. Am. Chem. Soc.* **2014**, *136*, 10258.
32. For a recent review, see: Yeung, C. S.; Dong, V. M. *Chem. Rev.* **2011**, *111*, 1215.
33. Kakiuchi, F.; Sato, T.; Yamauchi, M.; Chatani, N.; Murai, S. *Chem. Lett.* **1999**, *28*, 19.
34. Patureau, F. W.; Besset, T.; Glorius, F. *Angew. Chem. Int. Ed.* **2011**, *50*, 1064.
35. Padala, K.; Jeganmohan, M. *Org. Lett.* **2011**, *13*, 6144.
36. Shi, X.-Y.; Li, C.-J. *Org. Lett.* **2013**, *15*, 1476.
37. Kakiuchi, F.; Yamamoto, Y.; Chatani, N.; Murai, S. *Chem. Lett.* **1995**, *24*, 681.
38. Kakiuchi, F.; Uetsuhara, T.; Tanaka, Y.; Chatani, N.; Murai, S. *J. Mol. Catal. A: Chem.* **2002**, *182*, 511.
39. Patureau, F. W.; Besset, T.; Kuhl, N.; Glorius, F. *J. Am. Chem. Soc.* **2011**, *133*, 2154.
40. Muralirajan, K.; Parthasarathy K.; Cheng, C.-H. *Angew. Chem. Int. Ed.* **2011**, *50*, 4169.
41. Chinnagolla, R. K.; Jeganmohan, M. *Eur. J. Org. Chem.* **2012**, 417.
42. Tsuchikama, K.; Kasagawa, M.; Endo, K.; Shibata, T. *Synlett.* **2010**, *1*, 97.
43. Tsuchikama, K.; Kuwata, Y.; Tahara, Y.-K.; Yoshinami, Y.; Shibata, T. *Org. Lett.* **2007**, *9*, 3097.
44. Tanaka, K.; Otake, Y.; Wada, A.; Noguchi, K.; Hirano, M. *Org. Lett.* **2007**, *9*, 2203.
45. Tanaka, K.; Otake, Y.; Sagae, H.; Noguchi, K.; Hirano, M. *Angew. Chem. Int. Ed.* **2008**, *47*, 1312.
46. Santhoshkumar, R.; Mannathan, S.; Cheng, C.-H. *Org. Lett.* **2014**, *16*, 4208.

-
47. Harris, P. W. R.; Woodgate, P. D. *J. Organomet. Chem.* **1997**, *530*, 211.
48. Harris, P. W. R.; Woodgate, P. D. *Tetrahedron* **2000**, *56*, 4001.
49. Guo, H.; Weber, W. P. *Polym. Bull.* **1994**, *32*, 525.
50. Guo, H.; Tapsak, M. A.; Weber, W. P. *Polym. Bull.* **1994**, *34*, 49.
51. Londergan, T. M.; You, Y.; Thompson, M. E.; Weber, W. P. *Macromolecules* **1998**, *31*, 2784.
52. Huang, D.; Yang, J.; Weber, W. P. *Polym. Bull.* **2000**, *43*, 465.
53. Guo, H.; Tapsak, M. A.; Weber, W. P. *Polym. Bull.* **1994**, *33*, 417.
54. Gupta, S. K.; Weber, W. P. *Macromolecules* **2002**, *35*, 3369.
55. Kakiuchi, F.; Kan, S.; Igi, K.; Chatani, N.; Murai, S. *J. Am. Chem. Soc.* **2003**, *125*, 1698.
56. Kakiuchi, F.; Matsuura, Y.; Kan, S.; Chatani, N. *J. Am. Chem. Soc.* **2005**, *127*, 5936.
57. Ueno, S.; Chatani, N.; Kakiuchi, F. *J. Org. Chem.* **2007**, *72*, 3600.
58. Ueno, S.; Kochi, T.; Chatani, N.; Kakiuchi, F. *Org. Lett.* **2009**, *11*, 855.
59. Satoh, T.; Kametani, Y.; Terao, Y.; Miura, M.; Nomura, M. *Tetrahedron Lett.* **1999**, *40*, 5345.
60. Terao, Y.; Kametani, Y.; Wakui, H.; Satoh, T.; Miura, M.; Nomura, M. *Tetrahedron* **2001**, *57*, 5967.
61. Gandeepan, P.; Parthasarathy, K.; Cheng, C.-H. *J. Am. Chem. Soc.* **2010**, *132*, 8569.
62. Gandeepan, P.; Hung, C.-H.; Cheng, C.-H. *Chem. Commun.* **2012**, *48*, 9379.
63. Li, H.; Zhu, R.-Y.; Shi, W.-J.; He, K.-H.; Shi, Z.-J. *Org. Lett.* **2012**, *14*, 4850.
64. Shan, G.; Yang, X.; Ma, L.; Rao, Y. *Angew. Chem. Int. Ed.* **2012**, *51*, 13070.
65. Mo, F.; Trzepakowski, L. J.; Dong, G. *Angew. Chem. Int. Ed.* **2012**, *51*, 13075.
66. Choy, P. Y.; Kwong, F. Y. *Org. Lett.* **2013**, *15*, 270.
67. Thirunavukkarasu, V. S.; Ackermann, L. *Org. Lett.* **2012**, *14*, 6206.

-
68. Shan, G.; Han, X.; Lin, Y.; Yu, S.; Rao, Y. *Org. Biomol. Chem.* **2013**, *11*, 2318.
69. Schröder, N.; Wencel-Delord, J.; Glorius, F. *J. Am. Chem. Soc.* **2012**, *134*, 8298.
70. Sun, X.; Shan, G.; Sun, Y.; Rao, Y. *Angew. Chem. Int. Ed.* **2013**, *52*, 4440.
71. Xiao, B.; Gong, T.-J.; Xu, J.; Liu, Z.-J.; Liu, L. *J. Am. Chem. Soc.* **2011**, *133*, 1466.
72. Kim, J.; Kim, J.; Chang, S. *Chem. Eur. J.* **2013**, *19*, 7328.
73. Zheng, Q.-Z.; Liang, Y.-F.; Qin, C.; Jiao, N. *Chem. Commun.* **2013**, *49*, 5654.
74. Bhanuchandra, M.; Yadav, M. R.; Rit, R. K.; Kuram, M. R.; Sahoo, A. K. *Chem. Commun.* **2013**, *49*, 5225.
75. For selected reviews on transition-metal-catalyzed conjugate addition, see: (a) Rossiter, B. E.; Swingle, N. M. *Chem. Rev.* **1992**, *92*, 771. (b) Gutnov, A. *Eur. J. Org. Chem.* **2008**, 4547. (c) Hayashi, T.; K. Yamasaki, *Chem. Rev.* **2003**, *103*, 2829.
76. (a) Buckle, D. R.; Pinto, I. L. In *Comprehensive Organic Synthesis*; Trost, B. M.; Fleming, I. Eds.; Pergamon Press: Oxford, U.K., 1991; Vol. 7, pp 119-149. (b) Larock, R. C. In *Comprehensive Organic Transformations*; John Wiley & Sons: New York, 1999, pp 251-256. (c) Muzart, J. *Eur. J. Org. Chem.* **2010**, 3779.
77. For recent reviews on β -C-H functionalization, see: (a) Rouquet, G.; Chatani, N. *Angew. Chem. Int. Ed.* **2013**, *52*, 11726. (b) Huang, Z.; Dong, G. *Tetrahedron Lett.* **2014**, *55*, 5869. (c) Qiu, G.; Wu, J. *Org. Chem. Front.* **2015**, *2*, 169.
78. Pirnot, M. T.; Rankic, D. A.; Martin, D. B. C.; MacMillan, D. W. C. *Science* **2013**, *339*, 1593.
79. Petronijević, F. R.; Nappi, M.; MacMillan, D. W. C. *J. Am. Chem. Soc.* **2013**, *135*, 18323.
80. Okada, M.; Fukuyama, T.; Yamada, K.; Ryu, I.; Ravelli, D.; Fagnoni, M. *Chem. Sci.* **2014**, *5*, 2893.
81. (a) Smith, M. B. and March, J. *March's Advanced Organic Chemistry*, Wiley, New York, 2001. (b) Anastas, T. and Warner, J. C. *Green Chemistry: Theory and Practice*, Oxford Univ. Press, Oxford, 1998. (c) von Oettingen, W. F. *The Halogenated Hydrocarbons of Industrial and Toxicological Importance*, Elsevier, Amsterdam, New York, 1964.
82. (a) Stork, G.; Terrell, R.; Szmuszkovicz, J. *J. Am. Chem. Soc.* **1954**, *76*, 2029. (b) Stork, G.; Landesman, H. *J. Am. Chem. Soc.* **1956**, *78*, 5128.

-
83. For a recent review, see: Dénès, F.; Pérez-Luna, A.; Chemla, F. *Chem. Rev.* **2010**, *110*, 2366.
84. Wang, S.; Pei, T.; Han, X.; Widenhoefer, R. A. *Org. Lett.* **2003**, *5*, 2699.
85. Han, X.; Wang, X.; Pei, T.; Widenhoefer, R. A. *Chem. Eur. J.* **2004**, *10*, 6333.
86. Xiao, Y.-P.; Liu, X.-Y.; Che, C.-M. *Angew. Chem. Int. Ed.* **2011**, *50*, 4937.
87. Pines, H.; Kannan, S. V.; Simonik, J. *J. Org. Chem.* **1971**, *36*, 2311.
88. Rodriguez, A. L.; Bunlaksananusorn, T.; Knochel, P. *Org. Lett.* **2000**, *2*, 3285.
89. Gaudin, J.-M.; Millet, P. *Chem. Commun.* **2008**, 588.
90. Majima, S.; Shimizu, Y.; Kanai, M. *Tetrahedron Lett.* **2012**, *53*, 4381.
91. Iwahama, T.; Sakaguchi, S.; Ishii, Y. *Chem. Commun.* **2000**, 2317.
92. Mo, F.; Dong, G. *Science* **2014**, *345*, 68.
93. Hartwig, J. F. *Organotransition Metal Chemistry: From Bonding to Catalysis*; University Science Books: Sausalito, 2010.
94. (a) Conia, J. M.; Le Perchec, P. *Synthesis* **1975**, *1*. (b) Corkey, B. K.; Toste, F. D. *J. Am. Chem. Soc.* **2005**, *127*, 17168. (c) Ochida, A.; Ito, H.; Sawamura, M. *J. Am. Chem. Soc.* **2006**, *128*, 16486. (d) Itoh, Y.; Tsuji, H.; Yamagata, K.-I.; Endo, K.; Tanaka, I.; Nakamura, M.; Nakamura, E. *J. Am. Chem. Soc.* **2008**, *130*, 17161. (e) Yang, T.; Ferrali, A.; Sladojevich, F.; Campbell, L.; Dixon, D. J. *J. Am. Chem. Soc.* **2009**, *131*, 9140. (f) Matsuzawa, A.; Mashiko, T.; Kumagai, N.; Shibasaki, M. *Angew. Chem. Int. Ed.* **2011**, *50*, 7616. (g) Boominathan, S. S. K.; Hu, W.-P.; Senadi, G. C.; Wang, J.-J. *Adv. Synth. Catal.* **2013**, *355*, 3570. (h) Shaw, S.; White, J. D. *J. Am. Chem. Soc.* **2014**, *136*, 13578.
95. Davies, P. W.; Detty-Mambo, C. *Org. Biomol. Chem.* **2010**, *8*, 2918.
96. Chernyak, N.; Gorelsky, S. I.; Gevorgyan, V. *Angew. Chem. Int. Ed.* **2011**, *50*, 2342.
97. (a) Yamaguchi, M.; Hayashi, A.; Hiram, M. *J. Am. Chem. Soc.* **1993**, *115*, 3362. (b) Yamaguchi, M.; Sehata, M.; Hayashi, A.; Hiram, M. *J. Chem. Soc., Chem. Commun.* **1993**, 1708. (c) Hayashi, Y.; Yamaguchi, M.; Hiram, M. *Synlett.* **1995**, 51. (d) Yamaguchi, M.; Tsukagoshi, T.; Arisawa, M. *J. Am. Chem. Soc.* **1999**, *121*, 4074.
98. Trofimov, B. A.; Schmidt, E. Y.; Ushakov, I. A.; Zorina, N. V.; Skital'tseva, E. V.; Protsuk, N. I.; Mikhaleva, A. I. *Chem. Eur. J.* **2010**, *16*, 8516.

99. Trofimov, B. A.; Schmidt, E. Y.; Zorina, N. V.; Ivanova, E. V.; Ushakov, I. A. *J. Org. Chem.* **2012**, *77*, 6880.

CHAPTER 3

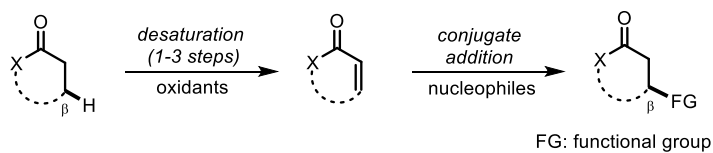
Catalytic C–C Bond Forming Transformations via Direct β -C–H Functionalization of Carbonyl Compounds

3.1 Introduction

Functionalization of carbonyl compounds represents a cornerstone of organic chemistry. The inherent electrophilicity of the carbonyl group and acidity of the α -C–H bond provide convenient handles for the installation of various functional groups at the *ipso* and α -position of carbonyl compounds, respectively. However, the β -C–H bond is usually considered inert and thus less facile to functionalize directly. On the other hand, such β -substituted motifs are frequently found in a wide array of bioactive compounds, including pesticides, anti-oxidants and drug candidates.¹ Traditionally, functionalization of the β -position is often accomplished with conjugate addition of nucleophiles to the corresponding α,β -unsaturated carbonyl compounds (Scheme 3.1).² However, α,β -unsaturated carbonyl compounds are often prepared from their

saturated derivatives using a stoichiometric amount of oxidant.³ Thus, direct methods to convert the β -C–H bond to the desired functional group would considerably increase the efficiency of preparing β -substituted carbonyl compounds. During the last decade, significant efforts have been devoted towards direct β -C–H functionalization of carbonyl compounds. This chapter primarily focuses on discussing the transformations that directly replace a β -C–H bond of carbonyl compounds with a C–C bond. While not intended to comprehensively cover all literature references, it rather offers a perspective on strategy design and discovery through selected examples to highlight representative reaction types.

Scheme 3.1 Conventional Synthesis of β -substituted Carbonyl Compounds



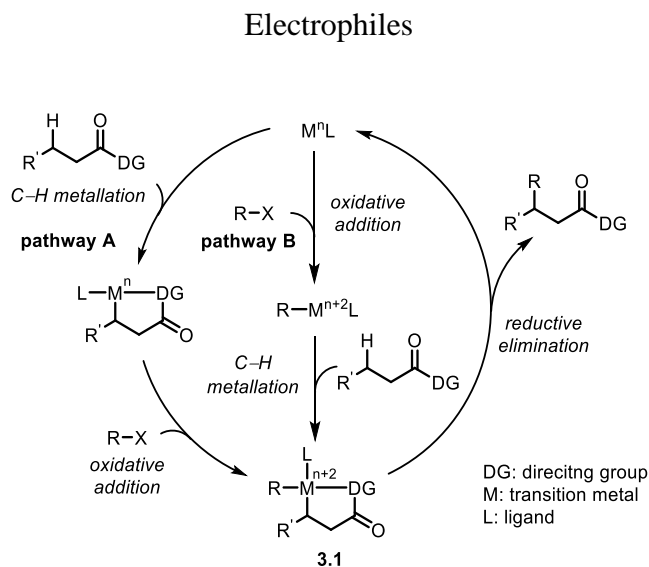
3.2 Cyclometallation via Directing Groups

Directing group strategies have been widely applied in transition-metal-mediated site-selective C–H activation, through which an avalanche of catalytic transformations has been developed. Nevertheless, compared with sp^2 C–H bonds, the sp^3 -hybridized β -C–H bond of carbonyl compounds is less prone to be cleaved by transition metals from both kinetic and thermodynamic prospective,⁴ which presents a significant challenge for design and development of new directing groups.

3.2.1 General Mechanisms

Regarding the mechanism of these cyclometallation-type transformations, two general classes can be imagined based on the coupling partners employed. When an electrophile, such as an aryl halide, is involved, a typical reaction pathway proceeds through a selective metallation at the β -position assisted by the directing group, followed by oxidative addition of the electrophile to the metal giving intermediate **3.1** (Scheme 3.2, pathway A). It is also possible for the C-H metallation and oxidative addition to occur in a reverse order. Under either pathway, reductive elimination of intermediate **3.1** delivers the β -functionalization product and restores the active catalyst.

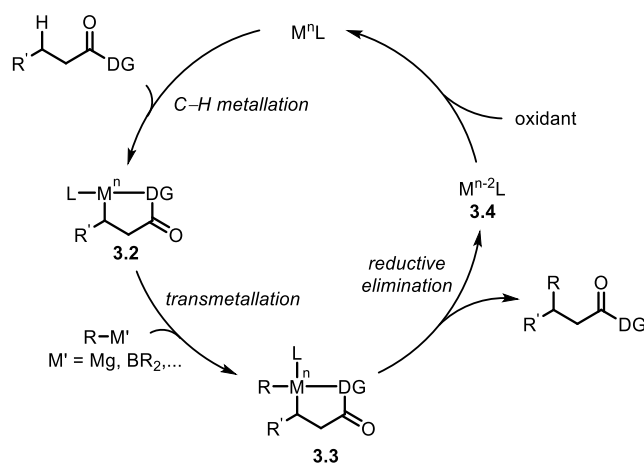
Scheme 3.2 Cyclometallation-type β -C-H Functionalization via Oxidative Addition of



When an organometallic reagent (i.e. arylboronic acids) is used, the coupling proceeds through a different mechanism (Scheme 3.3). After the C-H metallation step, transmetalation between the organometallic reagent and intermediate **3.2** installs the functional group on the

metal center while the oxidation state of the metal remains unchanged. Subsequent reductive elimination affords the product, and oxidation of the reduced catalyst (**3.4**) by an external oxidant regenerates the catalyst.

Scheme 3.3 Cyclometallation-type β -C–H Functionalization via Transmetalation of Organometallic Reagents



According to the types of the directing groups employed, the β -functionalization through cyclometallation can be classified into two categories: type A is with strong bidentate directing groups; type B is with weaker coordinating directing groups.

3.2.2 Type A. Bidentate Directing Group

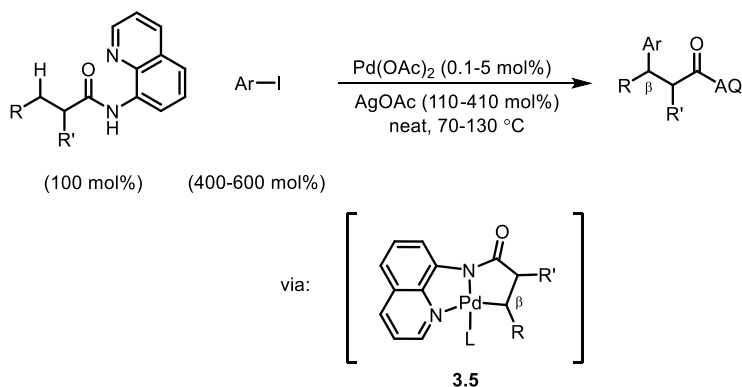
3.2.2.1 Arylation

In 2005, Daugulis and co-workers disclosed a palladium-catalyzed β -arylation of amides using 8-aminoquinoline (AQ) as a directing group (Scheme 3.4).⁵ In their proposed intermediate,

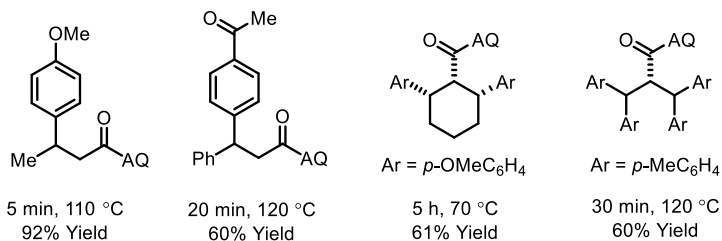
the 8-aminoquinoline auxiliary provides an L-type (quinoline) and an X-type (amide) ligand to chelate with palladium in a bidentate fashion. The 5-5 fused palladacycle **3.5** was formed after the selective palladation of the β -C–H bond. Methyl, methylene and benzylic C–H bonds β to the carbonyl can be arylated selectively with aryl iodides as the aryl source under neat conditions. Silver salts are likely used as an iodide scavenger. When activating a methyl group, the arylation occurred twice to give diarylation products.

Scheme 3.4 Palladium-catalyzed β -Arylation of Amides using 8-Aminoquinoline as the

Directing Group



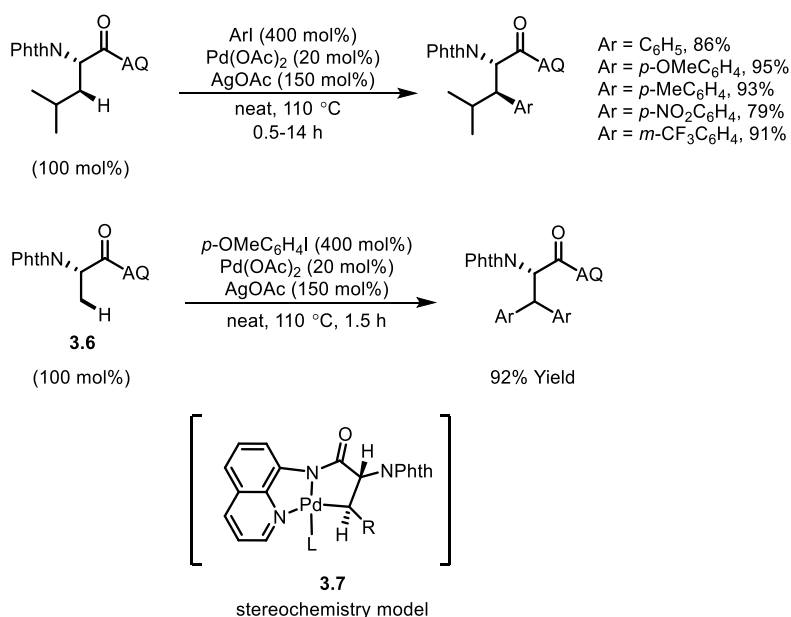
Selected examples:



Soon after the seminal work by Daugulis, Corey and coworkers successfully applied this strategy to prepare non-natural amino acids (Scheme 3.5).⁶ With the 8-aminoquinoline moiety as the directing group, *N*-phthaloyl valine and phenylalanine derivatives underwent diastereoselective β -arylation through coupling with a range of aryl iodides. The

diastereoselectivity could be explained by formation of a less sterically hindered *trans*-palladacycle (**3.7**). When alanine derivative **3.6** was submitted to the reaction conditions, a diarylation product was selectively formed, which is consistent with the observation by Daugulis.⁵

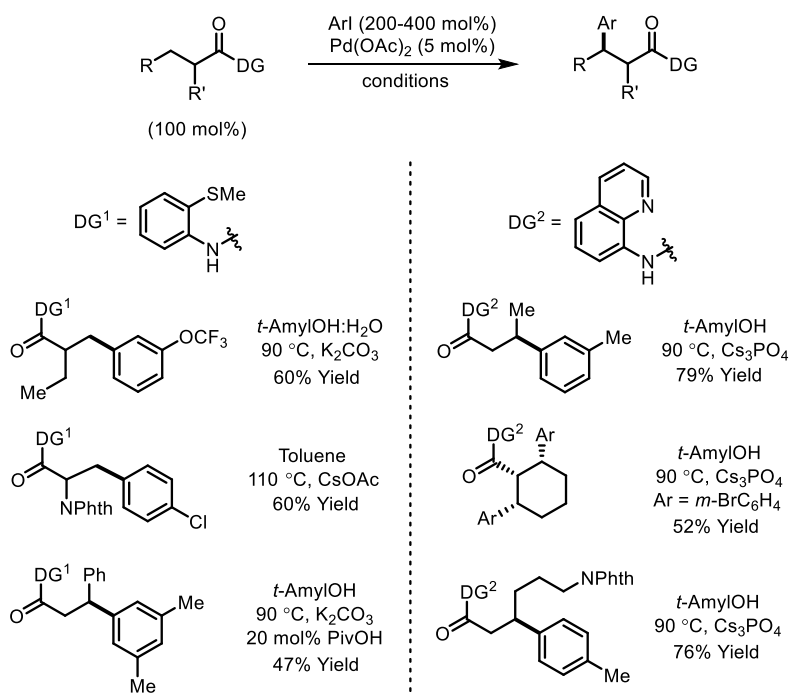
Scheme 3.5 Synthesis of Non-natural Amino Acid Derivatives



Daugulis and coworkers subsequently discovered that the use of silver salts and neat conditions can be avoided by using a combination of main-group inorganic salts and alcoholic solvents (Scheme 3.6).⁷ In addition, while the diarylation product dominates when 8-aminoquinoline was used as the directing group, 2-methylthio aniline was found to afford selective monoarylation of primary β -C–H bonds. This new directing group also works for a secondary benzylic C–H bond albeit with a moderate yield when a catalytic amount of pivalic acid was employed as a proton shuttle. In contrast, the 8-aminoquinoline directing group is more efficient for secondary C–H bonds; a number of cyclic and acyclic methylene β -C–H bonds can

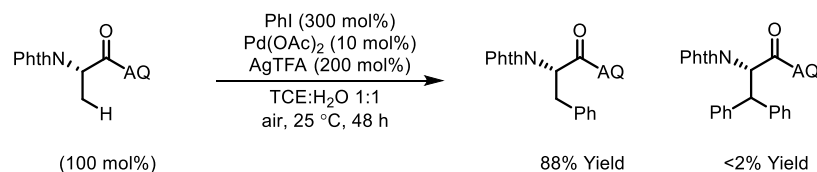
be arylated in good yields. Notably, Daugulis and coworkers later demonstrated that these complementary reaction conditions could also be nicely applied to the syntheses of non-natural amino acids via diastereoselective β -C-H arylation of *N*-protected amino acid derivatives.⁸

Scheme 3.6 Palladium-catalyzed β -Arylation Directed by 2-Methylthio Aniline or 8-Aminoquinoline Auxiliary



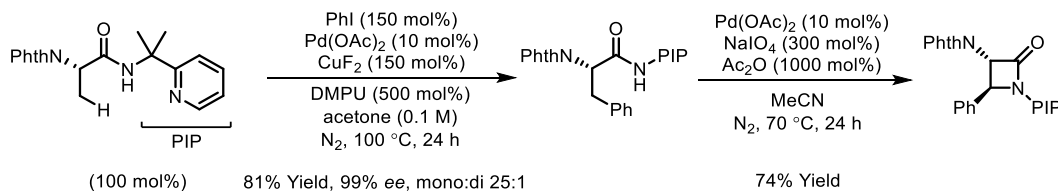
Recently, Chen and coworkers reported a mono-selective β -arylation of *N*-phthaloyl alanine derivatives using 8-aminoquinoline as the directing group (Scheme 7).⁹ With the assistance of the trifluoroacetate anion, the β -arylation reaction proceeded under room temperature to afford the monoarylation product in a high selectivity. The authors also demonstrated that the monoarylation products could be further arylated, alkylated or amidated at the β -position using the same directing group under different reaction conditions.

Scheme 3.7 Palladium-catalyzed β -Monoarylation of Alanine Derivatives at Room Temperature



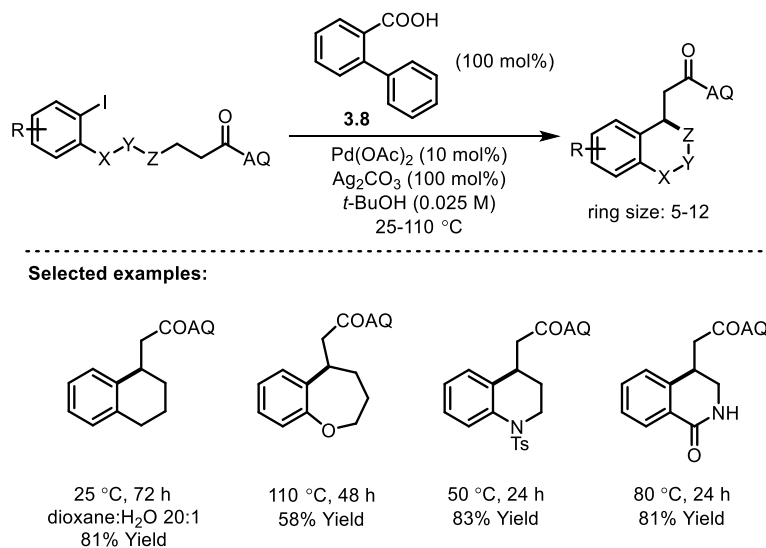
A strategy to synthesize chiral α -amino- β -lactams was developed by B. Shi and coworkers using a palladium-catalyzed monoarylation/amidation sequence with 2-(pyridine-2-yl)isopropyl (PIP) as the auxiliary (Scheme 3.8).¹⁰ The PIP directing group is critical for the success of the sequence, because first it displays a high selectivity for the monoarylation step (mono:di > 25:1) and second it is robust enough to survive during the subsequent oxidative amidation step.

Scheme 3.8 Palladium-catalyzed Synthesis of α -Amino- β -lactams via a Monoarylation/Amidation Sequence



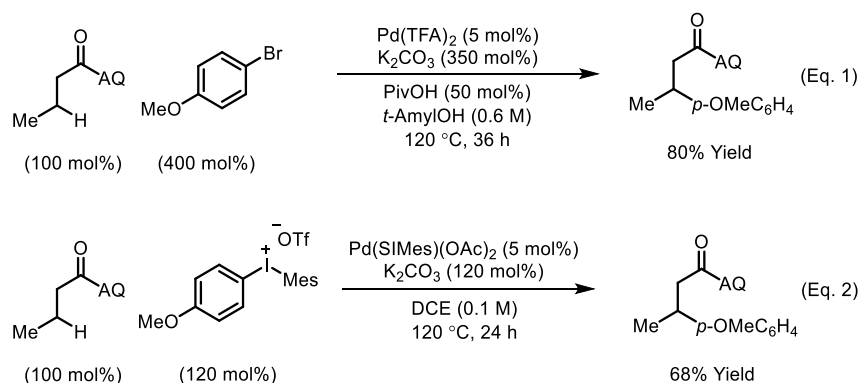
Chen and coworkers developed the first intramolecular version of the β -arylation reaction to construct benzo-fused rings in a rapid fashion using 8-aminoquinoline as the directing group (Scheme 3.9).^{11,12} Through the selective intramolecular coupling of aryl iodides and β -methylene C–H bonds, benzo-bicycles with different ring sizes were prepared, bearing ether, amine or amide linkages. The *ortho*-phenyl benzoic acid (*o*-PBA) ligand **3.8** was found to enhance the overall efficiency, which was proposed to facilitate the oxidative addition of aryl iodides.

Scheme 3.9 Palladium-catalyzed Intramolecular β -Arylation



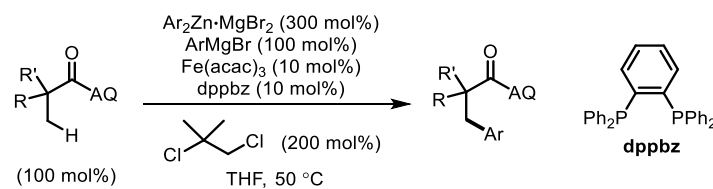
Besides using aryl iodides, Zeng and coworkers demonstrated that less reactive aryl bromides are also suitable aryl sources for the palladium-catalyzed β -arylation reactions. (Scheme 3.10, Eq. 1).¹³ 8-Aminoquinoline was employed as the directing group. Use of potassium carbonate as the base and pivalic acid as the additive were shown to be critical for the high efficiency. Diaryliodonium salts can be used as an alternative aryl source, reported by Z. Shi and coworkers (Eq. 2).¹⁴ In this case, the NHC-ligated Pd(SIMes)(OAc)₂ [SIMes = 1,3-bis(2,4,6-trimethylphenyl)imidazole-2-ylidene] complex was employed as the catalyst and only a slight excess of diaryliodonium salt was required, which is a notable difference from the reactions with aryl halides.

Scheme 3.10 Palladium-catalyzed β -Arylation with Aryl Bromides or Diaryliodonium Salts

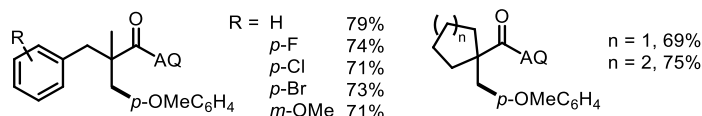


The 8-aminoquinoline auxiliary later proved to be a versatile directing group and readily applicable to C–H activation reactions catalyzed by metals other than palladium. An iron-catalyzed version of the β -arylation reaction was developed by Ilies, Nakamura and coworkers in 2013 (Scheme 3.11).¹⁵ The iron-catalyzed arylation utilized *in situ* generated diarylzinc reagents as the aryl source, 1,2-dichloroisobutane (DCIB) as a terminal oxidant and additional Grignard reagent to deprotonate the amides. A transmetalation-based mechanism was proposed (*vide supra*, Scheme 3.3). A high selectivity for methyl over benzylic C–H bonds was observed without “over arylation” of methyl groups, which is distinct from the palladium-catalyzed reactions. In 2014, Ackermann and coworkers demonstrated the iron-catalyzed β -arylation can be carried out using triazolylmethylmethyl (TAM) as the directing group,¹⁶ which can be easily accessed via click cyclization (Scheme 3.12).¹⁷

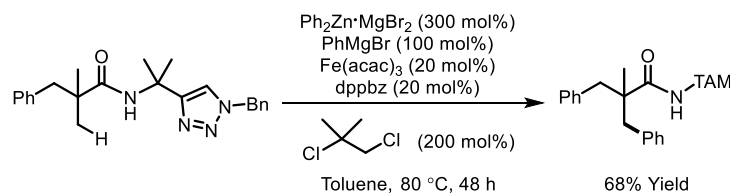
Scheme 3.11 Iron-catalyzed β -Arylation Directed by 8-Aminoquinoline Auxiliary



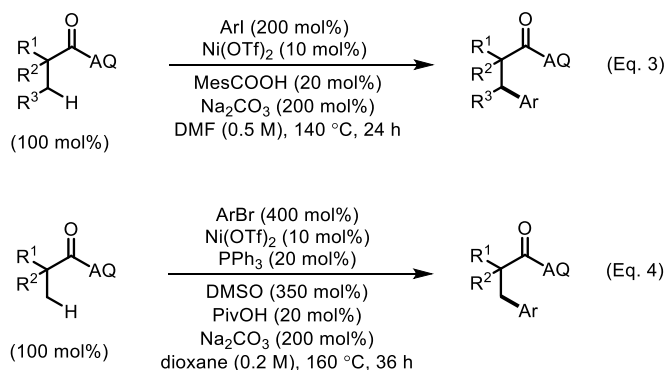
Selected examples:



Scheme 3.12 Iron-catalyzed β -Arylation Directed by Triazolylmethylmethyl Auxiliary



Scheme 3.13 Nickel-catalyzed β -Arylation Directed by 8-Aminoquinoline Auxiliary

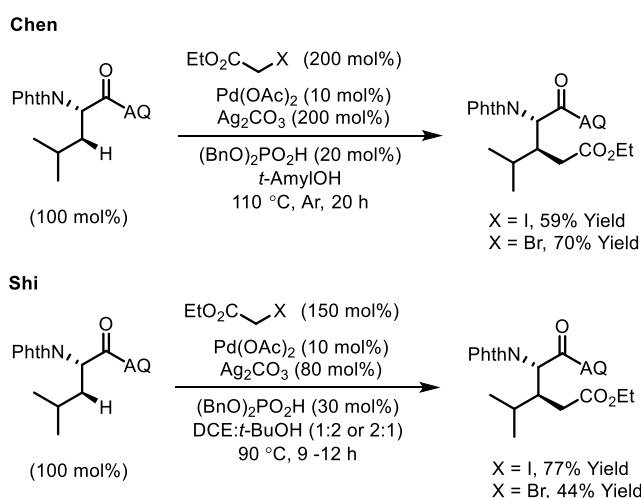


Recently, a nickel-catalyzed β -arylation of amides was reported by the Chatani group using 8-aminoquinoline as the directing group (Scheme 3.13, Eq. 3).¹⁸ A wide spectrum of sensitive functional groups was tolerated under the reaction conditions, including amines, iodides,

catalyzed coupling of the β -methyl C–H bond of propionic amide and *i*-butyl or *n*-octyl iodide was successful with K_2CO_3 as the base and a catalytic amount of pivalic acid. An example of an intramolecular alkylation of a more challenging β -methylene C–H bond was achieved by Chen and coworkers (Eq. 6).¹²

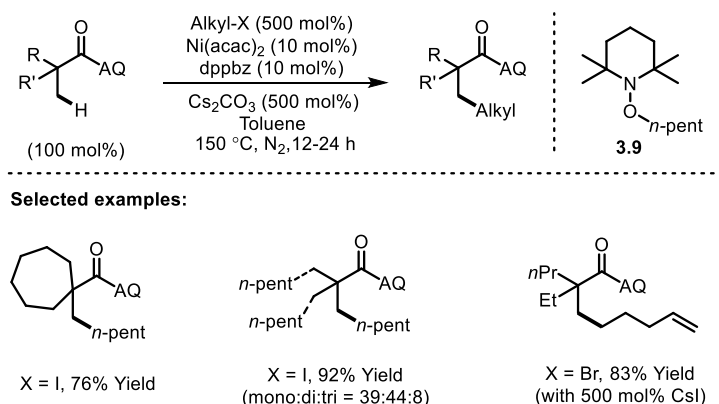
A general solution to the challenging β -alkylation of methylene groups was independently provided by the Chen and B. Shi groups in 2013 (Scheme 3.15).^{20,21} A wide range of methylene groups, cyclic or acyclic, were alkylated using α -iodoacetate, methyl iodide or ethyl iodide. The combination of Ag_2CO_3 and $(BnO)_2PO_2H$, which was first introduced by Chen, appeared to be the key for the success. When alkylating a methyl C–H bond, B. Shi and coworkers were able to expand the alkyl-halide scope to alkyl iodides or bromides that contain various sensitive functional groups including alkenes, esters and acetals.²¹ Reactions with secondary alkyl iodides didn't proceed under either Chen or B. Shi's conditions.

Scheme 3.15 Palladium-catalyzed β -Alkylation with α -Halideacetates



Recently, Ge and coworkers reported that β -alkylation can also be achieved via nickel catalysis using 8-aminoquinoline as the directing group (Scheme 3.16).²² A tertiary α -carbon is necessary for the amide substrates to be alkylated. Activation of methyl groups tends to be more favorable than methylene groups. It was found that the reaction was sensitive to the sterics of the alkyl halides, as isobutyl iodide and secondary halides didn't give any alkylation product. Addition of TEMPO suppressed the reaction and a TEMPO/alkyl adduct (**3.9**) was also isolated along with the desired product. Therefore, a Ni(II)/Ni(III) catalytic cycle involving alkyl radicals was proposed by the authors for this reaction.

Scheme 3.16 Nickel-catalyzed β -Alkylation with Alkyl Halides

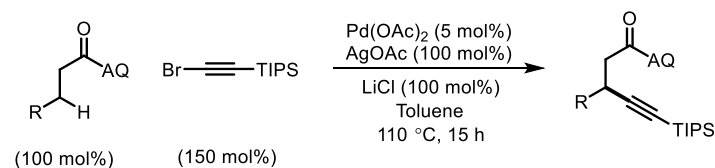


3.2.2.3 Alkynylation

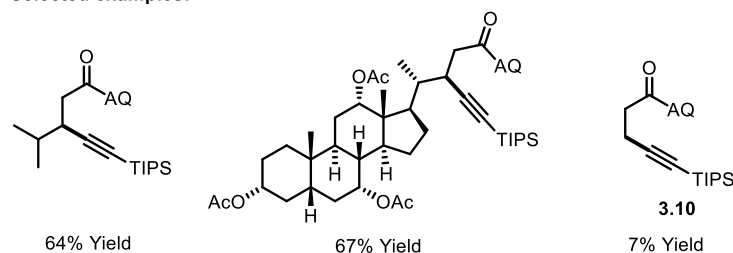
A palladium-catalyzed β -alkynylation reaction with the 8-aminoquinoline directing group was published by Tobisu, Chatani and coworkers in 2011 (Scheme 3.17).²³ Bromotriisopropylsilylacetylene was used as the alkyne source. Interestingly, while secondary C–H bonds reacted effectively under the reaction conditions, reactions with methyl C–H bonds

only gave a trace amount of product (**3.10**). This method offered a straightforward and site-selective approach to install alkyne motifs onto the carboxylic derivatives.

Scheme 3.17 Palladium-catalyzed β -Alkynylation Directed by 8-Aminoquinoline Auxiliary



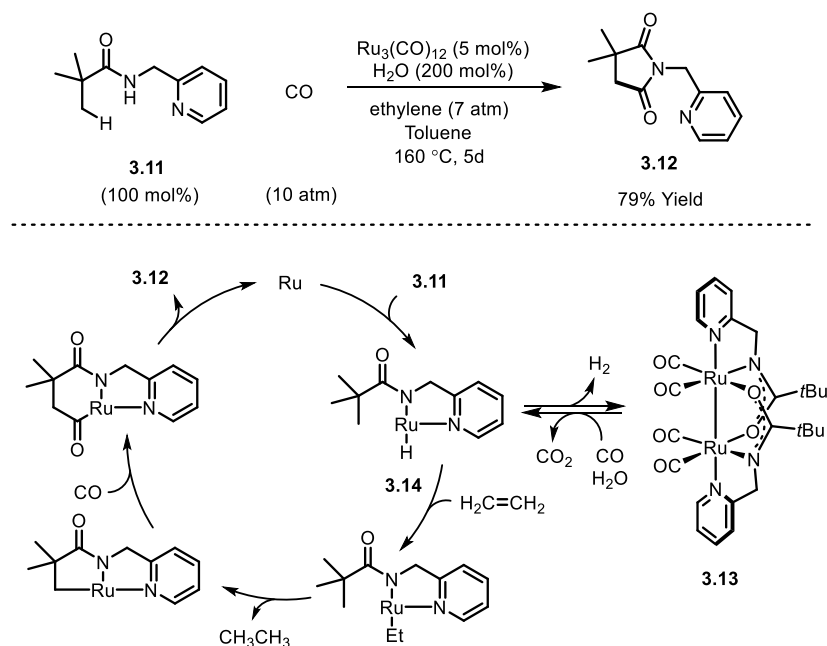
Selected examples:



3.2.2.4 Carbonylation

The Chatani group also published a ruthenium-catalyzed β -carbonylation reaction directed by a 2-pyridylmethylamine auxiliary (Scheme 3.18).²⁴ A range of succinimide derivatives were formed using this approach. The reaction was proposed to go through a sequence of β -C–H activation, CO migratory insertion and C–N reductive elimination. In the proposed catalytic cycle, ethylene serves as the H₂ acceptor, and water reacts with complex **3.13** (the resting state of the catalyst) to generate active species **3.14**.

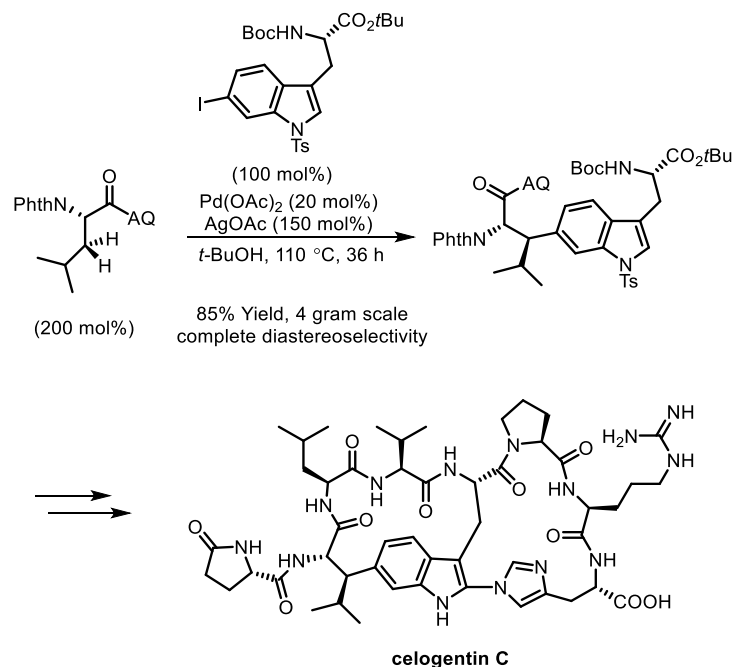
Scheme 3.18 Ruthenium-catalyzed Synthesis of Succinimides via β -Carbonylation



3.2.2.5 Application in Total Synthesis

When applied in a much more complex setting, the bidentate directing-group strategy still proved to be versatile and reliable. The first total synthesis using this transition-metal-catalyzed direct β -C–H functionalization was reported by Feng and Chen in 2010 (Scheme 3.19).²⁵ In the synthesis of the bicyclic peptide natural product, celogentin C, 8-aminoquinoline was used as the directing group in the palladium-catalyzed β -arylation reaction to construct the key C–C bond between the Leu C β and Trp C6 position. This β -arylation reaction proceeded smoothly to give the coupling product on a multi-gram scale with complete diastereoselectivity.

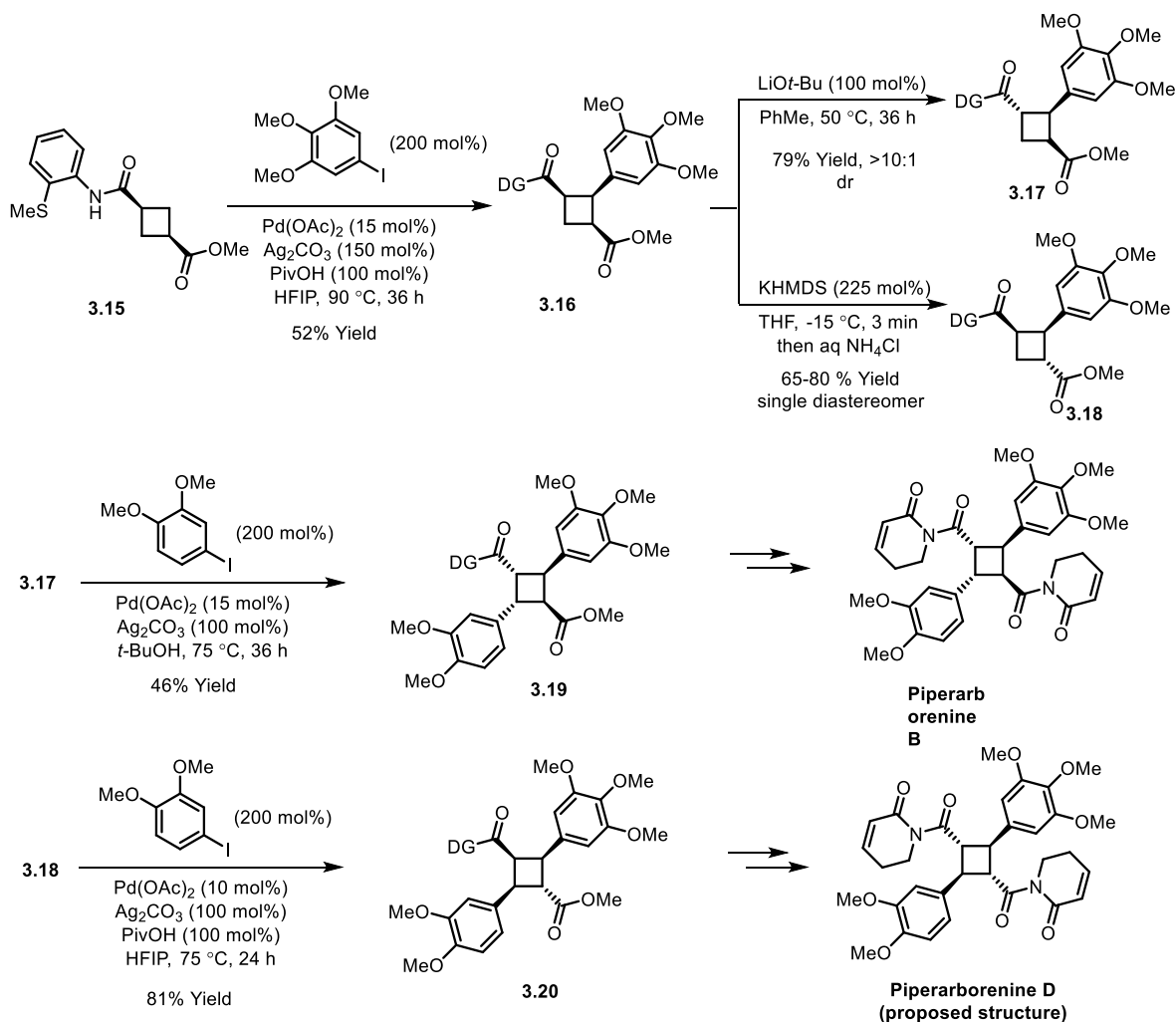
Scheme 3.19 Synthesis of Celogentin C via Palladium-catalyzed β -Arylation



Similar C–H functionalization strategies were utilized by Baran and coworkers in construction of the unsymmetrical cyclobutane cores of piperarborenines (Scheme 3.20).²⁶ Cyclobutane **3.15** containing a 2-methylthio aniline directing group underwent efficient β -arylation with 3,4,5-trimethoxyiodobenzene under the optimized conditions. Bis-arylation on both methylene groups was not observed presumably due to the sterically hindered all-*cis* orientation of the tri-substituted cyclobutanes **3.16**. Different epimerization conditions were then applied to invert either the ester or amide stereocenter on the cyclobutane ring to afford diastereoisomers **3.17** and **3.18**. With reduced steric hindrance, the second arylations with 3,4-dimethoxyiodobenzene proceeded smoothly to give tetra-substituted cyclobutane core structures **3.19** and **3.20**, which, upon further modifications, led to piperarborenine B and the proposed structure of piperarborenine D, respectively. Later, the same group applied this C–H

functionalization logic to the synthesis of the proposed structure of pipericyclobutanamide A, where a C–H arylation/olefination sequence was accomplished (Scheme 3.21).²⁷

Scheme 3.20 Synthesis of Piperarborenine B and D via Sequential β -Arylation

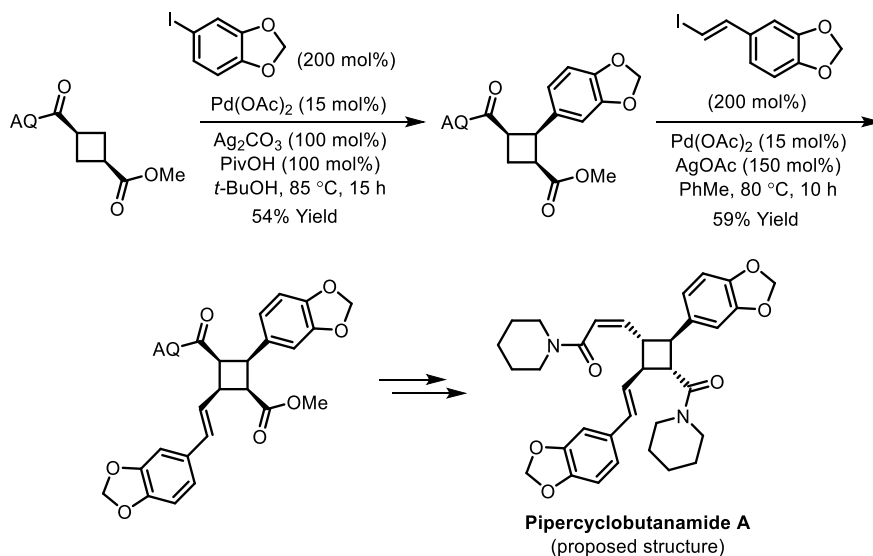


Recently, Ting and Maimone reported a concise synthesis of aryltetralin lignan podophyllotoxin via a palladium-catalyzed β -C–H arylation reaction (Scheme 3.22).²⁸ The major competing reaction of the arylation step was the β -lactam formation through a C–N bond reductive elimination. The authors discovered that the conformation of the rigid polycyclic

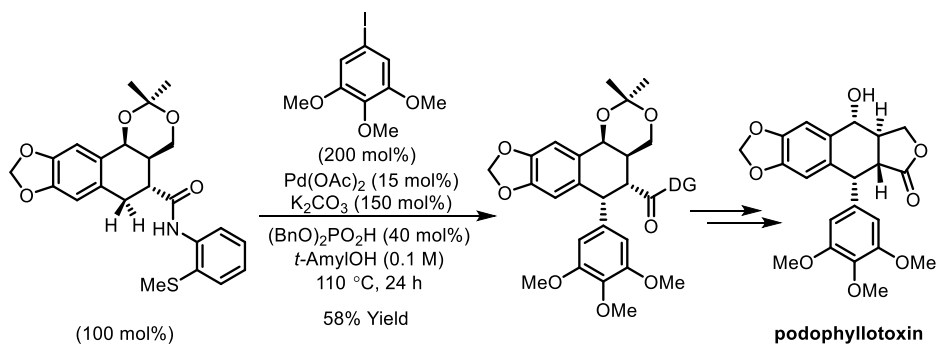
system was important to control the selectivity between the C–C bond formation and C–N bond formation.

Scheme 3.21 Synthesis of Pipericyclobutanamide A via Palladium-catalyzed β -

Arylation/Olefination Sequence



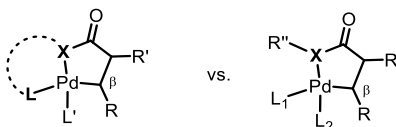
Scheme 3.22 Synthesis of Podophyllotoxin via Palladium-Catalyzed β -Arylation



3.2.3 Type B. Weaker coordinating directing group

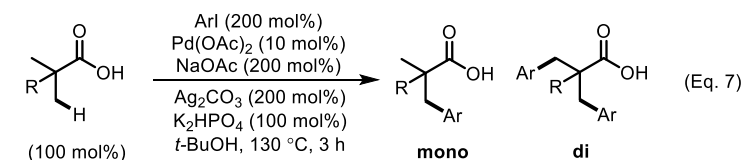
The use of weaker coordinating non-pyridine-type directing groups in β -C(sp^3)-H functionalization of carbonyl compounds was pioneered by Yu and coworkers.²⁹ Compared to bidentate directing groups, such as 8-aminoquinoline, using a monodentate directing group should form a less thermodynamically stable thus more reactive metallacycle after the C-H metallation (Scheme 3.23). The enhanced reactivity of the metallated intermediate has enabled a collection of challenging C-H functionalization transformations. Furthermore, since an extra coordination site becomes available when using monodentate directing groups, the role of ligand is expected to be more important in controlling the reactivity and selectivity of the C-H functionalization reaction.

Scheme 3.23 Palladacycles from Bidentate or Monodentate Directing Groups

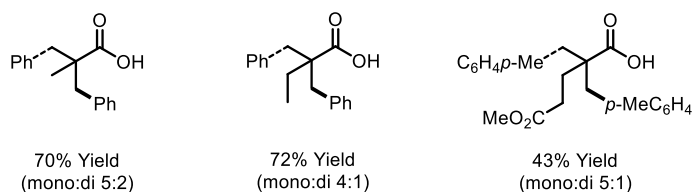


In 2007, Yu and coworkers reported the first β -arylation reaction of simple carboxylic acids with aryl iodides (Scheme 3.24, Eq. 7).³⁰ As proposed by the authors, the *in situ* generated potassium carboxylate guides palladium insertion into the β -C-H bond through a five-membered palladacycle, which, upon oxidative addition of aryl iodide and subsequent C-C bond reductive elimination, gives the β -arylation product. Phenylboronic acid pinacol ester (PhBpin) could also be coupled with the β -C-H bonds in the presence of benzoquinone (BQ) and Ag_2CO_3 as oxidants, albeit with lower efficiency (Scheme 3.25, Eq. 8).

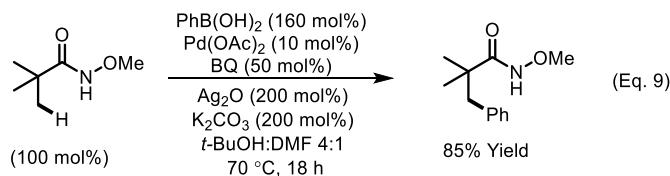
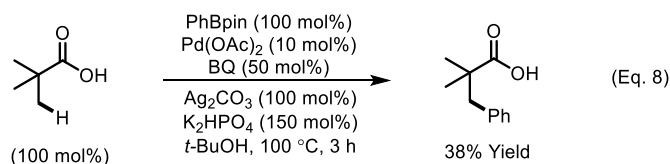
Scheme 3.24 Palladium-catalyzed β -Arylation of Simple Carboxylic Acids



Selected examples:

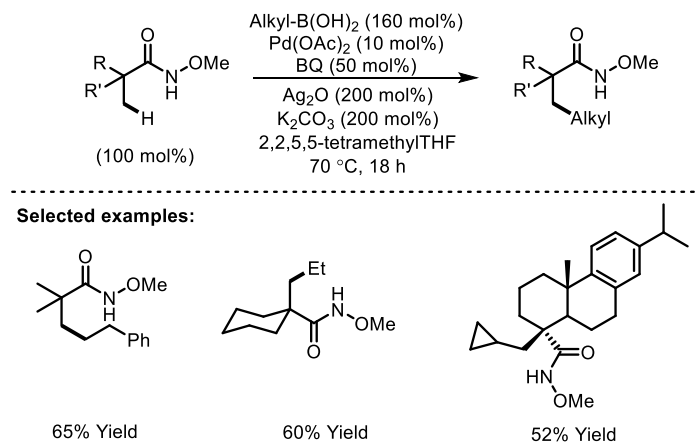


Scheme 3.25 Palladium-catalyzed β -Arylation with Aryl Organoboron Reagents



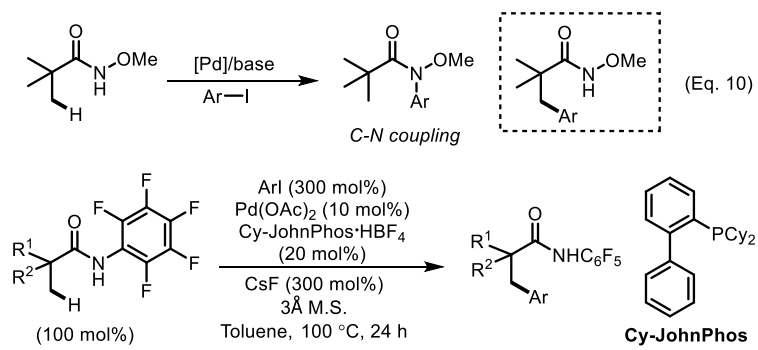
Later, by employing *O*-methyl hydroxamic acids as the directing group, Yu and coworkers improved the yield of the β -arylation reaction with organoboron reagents (Scheme 3.25, Eq. 9).³¹ Notably, an analogous β -alkylation reaction with alkyl boronic acids was also achieved. In this transformation, 2,2,5,5-tetramethyltetrahydrofuran was used as solvent, which might act as a bulky ligand to inhibit undesired homo-coupling and β -hydride elimination (Scheme 3.26). Besides silver salts, air was also demonstrated to be a suitable terminal oxidant for the β -arylation and alkylation reactions.

Scheme 3.26 Palladium-catalyzed β -Alkylation of *O*-Methyl Hydroxamic Acids

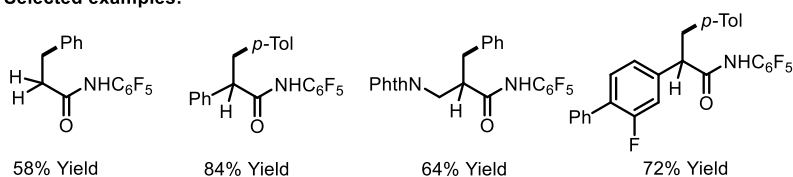


Unfortunately, when the authors attempted the hydroxamic acid-directed β -arylation using aryl iodides as the aryl source, a C–N bond coupling between the amide and aryl iodide proceeded readily (Scheme 3.27, Eq. 10).³² To suppress the C–N bond formation pathway, an acidic but less-nucleophilic *N*-pentafluorophenyl amide was used and found superior as the directing group. A range of β -methyl C–H bonds were arylated efficiently with Pd(OAc)₂/Cy-JohnPhos as a precatalyst and CsF as a base.

Scheme 3.27 Palladium-catalyzed β -Arylation Using Acidic *N*-Arylamide Directing Groups

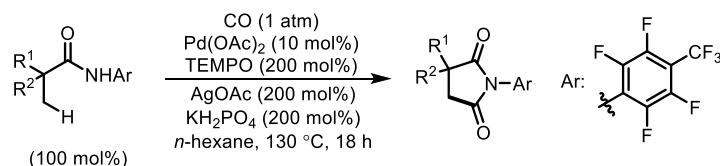


Selected examples:

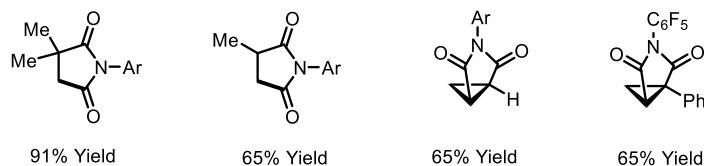


The acidic *N*-arylamide directing groups later found broad applications in the palladium-catalyzed β -functionalization reactions. A straightforward synthesis of succinimide derivatives via C–H carbonylation was reported by Yu and coworkers in 2010 (Scheme 3.28).³³ Note that a ruthenium-catalyzed analogue was reported by Chatani with a bidentate directing group (*vide supra*, Scheme 3.18). Besides primary C–H bonds, cyclopropyl methylene groups are also suitable substrates. A palladium-catalyzed coupling between β -C–H bonds and benzyl acrylates was later developed by the same group (Scheme 3.29). The *in situ* generated vinylation intermediate (the oxidative Heck product) underwent an intramolecular 1,4-addition affording the lactam products.³⁴

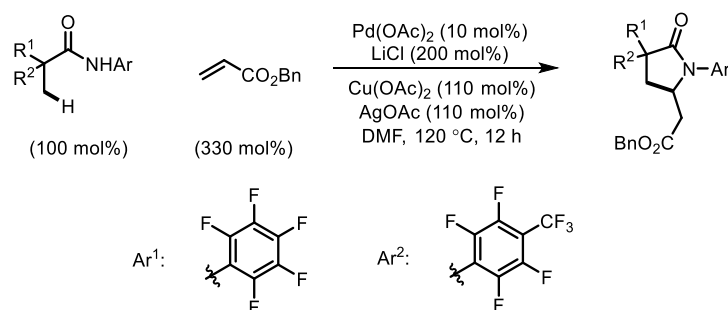
Scheme 3.28 Palladium-catalyzed Synthesis of Succinimides via β -Carbonylation



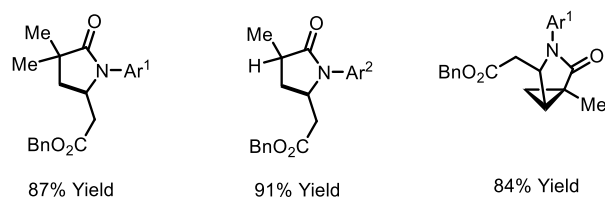
Selected examples:



Scheme 3.29 Palladium-catalyzed β -Olefination with Benzyl Acrylates



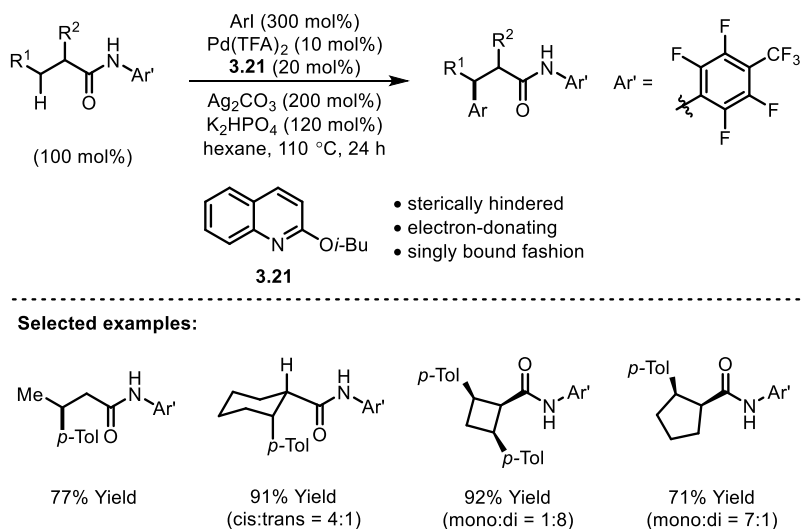
Selected examples:



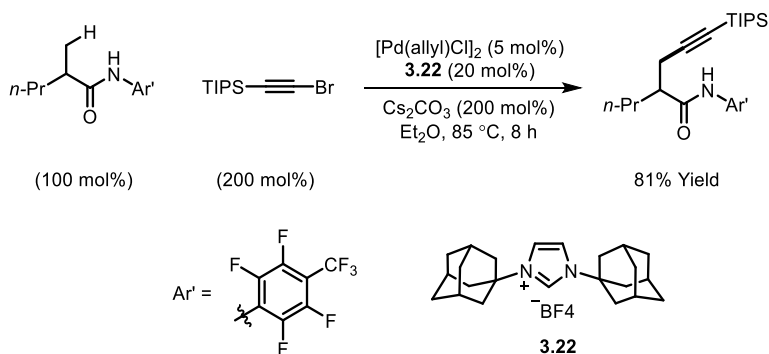
The aforementioned studies with the weaker *N*-arylamide directing groups mainly focused on primary (methyl group) and activated secondary C–H bonds in cyclopropanes. In contrast, methylene C–H bonds are more inert towards palladium insertion due to the unfavorable steric hindrance and enhanced risk for undesired β -hydride elimination.³⁵ Thus, to achieve a general β -methylene C–H functionalization with the weaker *N*-arylamide directing

group, these challenges must be addressed. In 2012, a significant breakthrough was achieved by Yu and coworkers (Scheme 3.30).³⁶ The *N*-arylamide-directed β -arylation of various methylene groups was enabled by a bulky and electron-donating quinoline ligand **3.21**. Only a single ligand was proposed to strongly coordinate to the palladium center due to its steric hindrance, which leaves room for palladium to bind with the *N*-arylamide directing group. Methylene C-H bonds in both cyclic and acyclic substrates were arylated efficiently under the reaction conditions. Later, a Pd(0)-catalyzed alkynylation of β -methylene and methyl C-H bonds with alkynyl bromides was accomplished by the same group. In this case, the bulky and electron-donating NHC ligand **3.22** was used (Scheme 3.31).³⁷

Scheme 3.30 Palladium-catalyzed β -Arylation of Methylene C-H Bonds

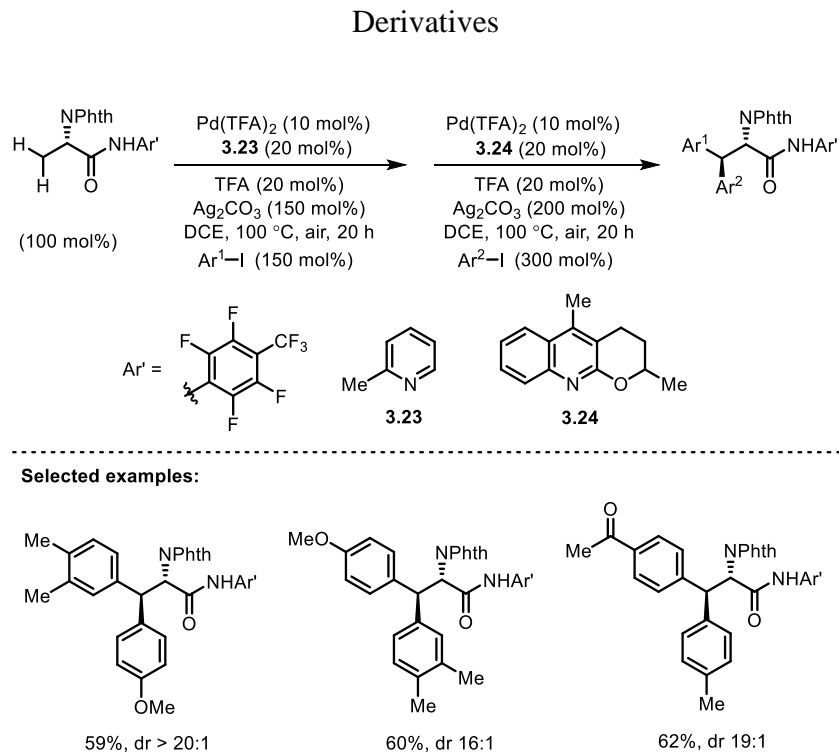


Scheme 3.31 Palladium-catalyzed β -Alkynylation Directed by *N*-Arylamide



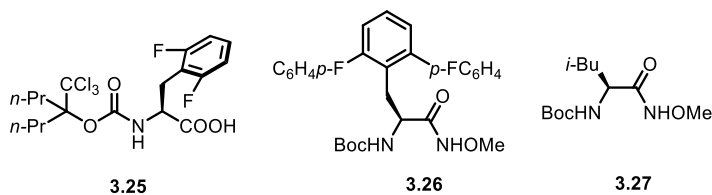
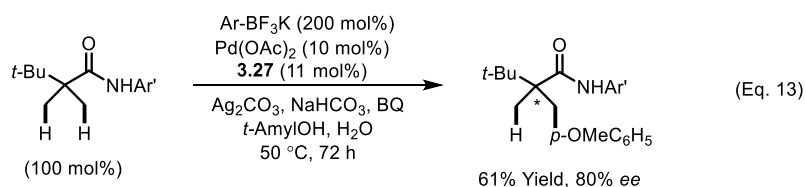
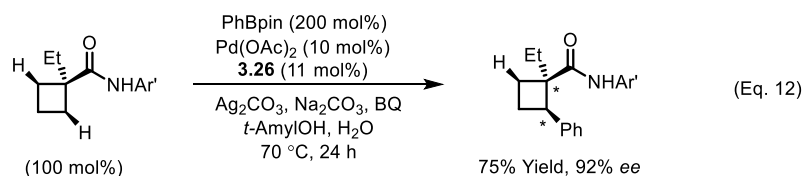
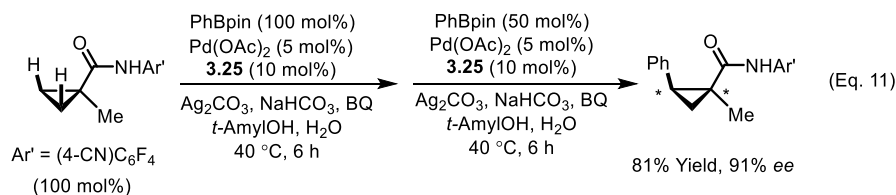
Recently, towards the synthesis of β -Ar- β -Ar'- α -amino acids with the *N*-arylamide directing group, Yu and coworkers demonstrated that selectivity for mono- versus di-C-H arylation can be determined by the choice of ligands (Scheme 3.32).³⁸ Simple 2-picoline ligand **3.23** afforded the β -monoarylation products with high yield and selectivity while the quinoline-type ligand (**3.24**) with rigidified oxygen lone pairs was required for the more challenging β -methylene arylation. With this pair of ligands, a sequence to incorporate two different aryl groups at the β -position of amino acid derivatives was accomplished in a one-pot fashion without isolating the monoarylation intermediate.

Scheme 3.32 Palladium-catalyzed Ligand-controlled Synthesis of β -Hetero-diaryl Amino Acid Derivatives



Enantioselective β -C–H functionalization reactions have also been achieved with the acidic *N*-arylamide directing groups (Scheme 3.33). In 2011, Yu and coworkers reported a desymmetrization-type arylation of cyclopropane methylene C–H bonds with organoboron reagents (Eq. 11).³⁹ The mono-*N*-protected amino acid ligand (**3.25**) was found to induce high enantioselectivity for the β -arylation. In contrast, the coupling of alkylboron reagents with the same ligand resulted in a compromised enantioselectivity. An enantioselective β -arylation of cyclobutane methylene groups was later developed by the same group (Eq. 12).⁴⁰ In this case, the chiral *O*-methyl hydroxamic acid ligand **3.26** was employed, which is more Lewis basic than the corresponding amino acid ligands. The desymmetrization of the prochiral β -methyl groups was also demonstrated using a similar ligand **3.27** (Eq. 13).

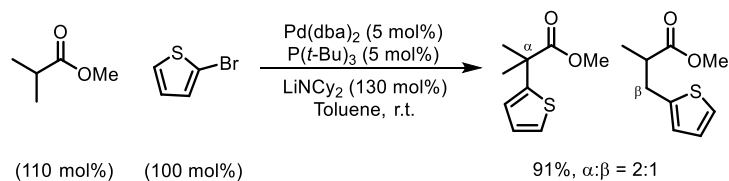
Scheme 3.33 Palladium-catalyzed Enantioselective β -Arylation



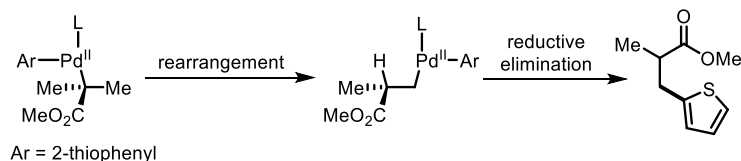
3.3 Migratory Coupling

In 2002, while studying the scope of the palladium-catalyzed α -arylation of esters, Hartwig and coworkers discovered that the coupling between methyl isobutyrate and 2-bromothiophene gave an unexpected 2:1 mixture of α - and β -arylation products (Scheme 3.34).⁴¹ The novel β -arylation product, as speculated by the authors, came from reductive elimination of a palladium homoenolate, which was rearranged from the hindered palladium enolate.

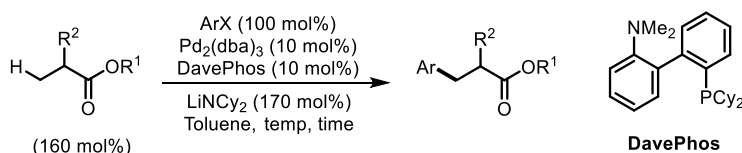
Scheme 3.34 Hartwig's Observation of β -Arylation



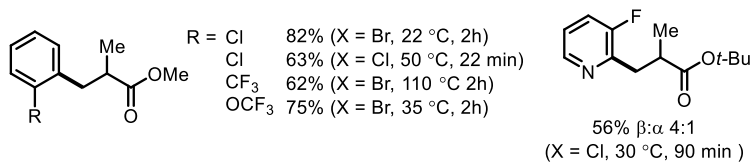
Proposed pathway:



Scheme 3.35 Palladium-Catalyzed β -Arylation of Carboxylic Esters



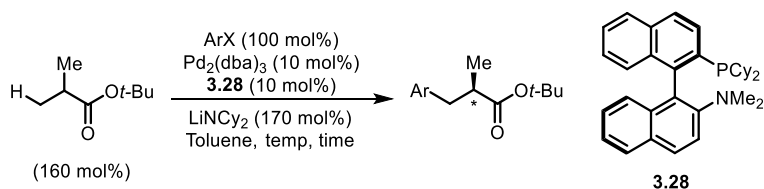
Selected examples:



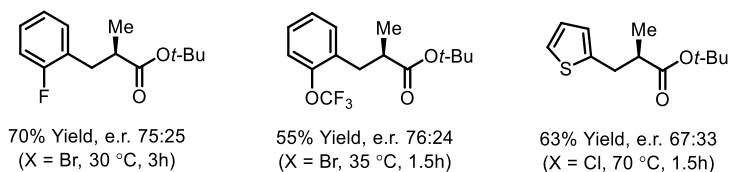
After Hartwig's seminal discovery, Baudoin and coworkers reported a systematic study of the palladium-catalyzed β -arylation reaction of carboxylic esters with aryl halides (Scheme 3.35).⁴² The optimized conditions feature the use of Pd(0)/DavePhos as the precatalyst and lithium dicyclohexylamide as the stoichiometric base to generate enolate species. Aryl halides bearing an *ortho* electron-withdrawing group tended to give a high or complete selectivity for the β -arylation instead of the α -arylation. Regarding the ester scope, a tertiary α -carbon is required for the β -selectivity, presumably because the resulting palladium enolate would disfavor a direct

reductive elimination to give α -arylation due to the steric hindrance. Notably, moderate *er* values were obtained when a chiral version of the DavePhos ligand (**3.28**) was used (Scheme 3.36).

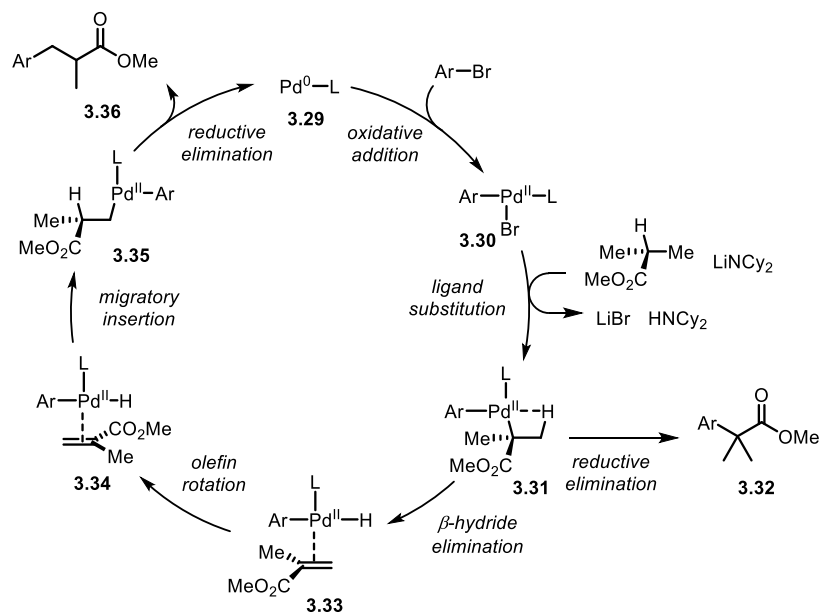
Scheme 3.36 Palladium-Catalyzed Enantioselective β -Arylation of Carboxylic Esters



Selected examples:



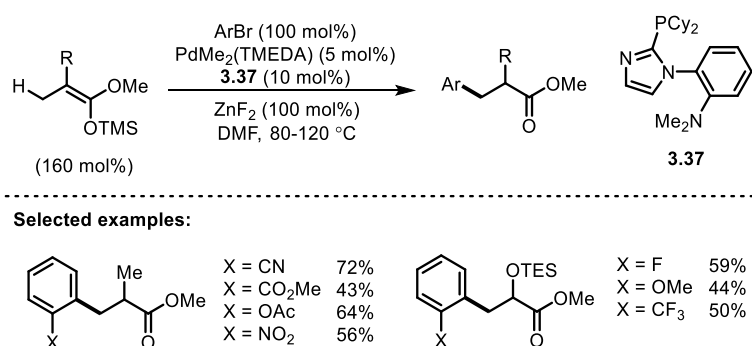
Scheme 3.37 Proposed Mechanism of the Palladium-Catalyzed β -Arylation of Carboxylic Esters



A plausible catalytic cycle, supported by both experimental and computational studies, was proposed by the authors (Scheme 3.37).⁴³ Initially, Pd(0) would undergo oxidative addition with aryl bromides and subsequent ligand exchange with the lithium enolate to give palladium enolate **3.31**. Direct reductive elimination of **3.31** would afford the α -arylation product **3.32**. To access the β -arylation product, palladium homoenolate **3.35** is expected to form via a sequence of β -hydride elimination, olefin rotation and Pd–H reinsertion. Subsequent reductive elimination of the less hindered palladium homoenolate would give the β -arylation product (**3.36**) and regenerate the Pd(0) catalyst.

This migratory-coupling type of β -arylation approach has been readily applied to the modification of amino esters utilizing dibenzyl-protected alanine esters as the substrates.⁴⁴ Baudoin and coworkers further demonstrated that silyl ketene acetals, surrogates for lithium enolates, can be also adopted for the β -arylation.⁴⁵ Under the optimized conditions, a wide range of sensitive functional groups are tolerated, including methyl esters, ketones, acetates and triflates (Scheme 3.38).

Scheme 3.38 Palladium-Catalyzed β -Arylation of Silyl Ketene Acetals

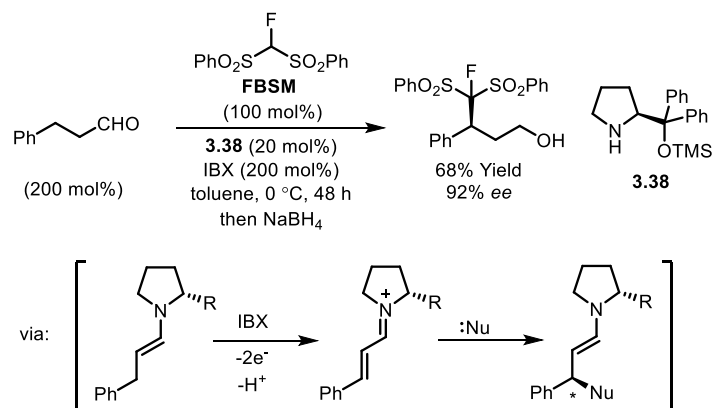


3.4 Organocatalysis

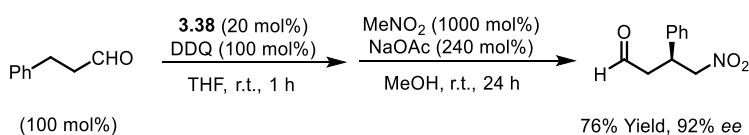
The field of using organic molecules as catalysts has experienced explosive growth during the past decade, which has led to the discovery of a number of new transformations. For the functionalization of carbonyl compounds, amines⁴⁶ and *N*-heterocyclic carbenes (NHCs)⁴⁷ have been extensively applied as catalysts due to their facile reactions with carbonyl groups, highly modifiable structures and capability to induce enantioselectivity. Recently, new modes of activation have been developed to allow β -functionalization directly from saturated carbonyl compounds based on amine or NHC catalysis.

In 2011, Wang and coworkers reported an oxidative enamine catalysis for the direct β -functionalization of aldehydes (Scheme 3.39).⁴⁸ They discovered that the enamine produced by the condensation of the aldehyde and the secondary amine catalyst was first oxidized by *o*-iodoxybenzoic acid (IBX) to give an α,β -unsaturated iminium ion; subsequently, the conjugate addition of carbon nucleophiles followed by hydrolysis afforded the β -substituted aldehydes. Using a chiral amine catalyst (**3.38**), a range of aldehydes coupled with fluorobis(phenylsulfonyl)methane (FBSM) selectively at the β -position with high enantioselectivity. Shortly after, Hayashi and coworkers published a cross-coupling of aldehydes and nitromethanes using a similar strategy.^{49,50} With 2,3-dichloro-5,6-dicyanoquinone (DDQ) as the stoichiometric oxidant, a sequential enamine oxidation and conjugate addition, in which both steps are catalyzed by the same chiral amine (**3.38**), proceeds to give a range of β -substituted γ -nitro aldehydes in a one-pot fashion with high enantioselectivity (Scheme 3.40).

Scheme 3.39 β -C–C Bond Formation via Oxidative Enamine Catalysis

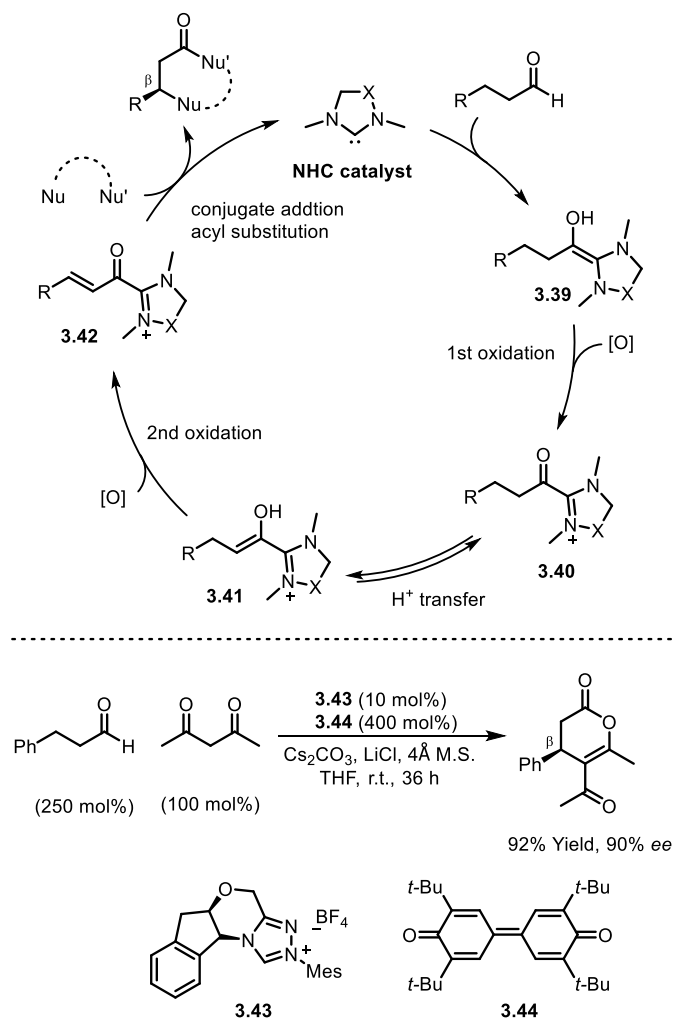


Scheme 3.40 Synthesis of β -Substituted γ -Nitro Aldehydes via Oxidative Enamine Catalysis



Recently, an oxidative NHC catalysis was developed by Chi and coworkers for the direct β -functionalization of aldehydes (Scheme 41).⁵¹ They proposed the Breslow intermediate (**3.39**) can be oxidized first to an NHC-bound ester (**3.40**), which is a tautomer of enol **3.41**, and a second oxidation process leads to an α,β -unsaturated ester (**3.42**). The interception of such a Michael acceptor with a carbon nucleophile is expected to introduce a C–C bond at the β -position. Based on this concept, the authors demonstrated an enantioselective synthesis of enol δ -lactones via coupling between saturated aldehydes and 1,3-dicarbonyl nucleophiles. In this transformation, NHC **3.43** was used as the catalyst and quinone **3.44** was used as the oxidant.

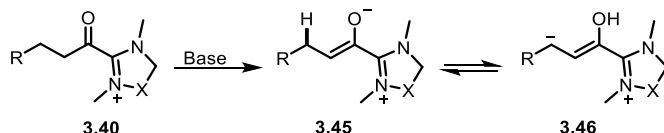
Scheme 3.41 β -Functionalization/Cyclization of Aldehydes via Oxidative NHC Catalysis



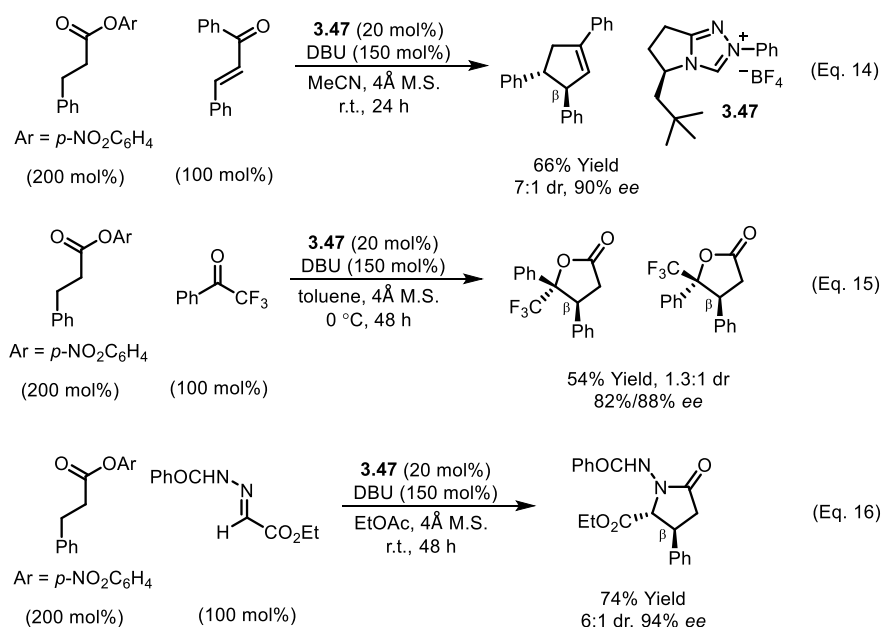
Later, the same group found that treatment of intermediate **3.40** with a base (instead of an oxidant) would trigger a α - then β -C–H deprotonation sequence resulting in a nucleophilic β -carbon (Scheme 3.42).⁵² The acidity of the β -C–H bonds in intermediate **3.45** might stem from the electron-withdrawing nature of the triazolium group, as well as the conjugated system. The reaction of intermediate **3.46** with chalcone derivatives afforded cyclopentene products through a cascade process involving Michael addition, aldol reaction, lactonization and decarboxylation

(Scheme 3.43, Eq. 14). Trifluoroketones and hydrazones can also serve as electrophiles to give corresponding lactones and lactams (Eqs. 15 and 16). With chiral NHC **3.47** as the catalyst, all these products were formed with high enantioselectivity.

Scheme 3.42 Generation of a Nucleophilic β -Carbon with NHC



Scheme 3.43 NHC-Catalyzed β -Functionalization of Aldehydes with Electrophiles



3.5 Conclusion

During the past decade, the challenge of direct β -functionalization of carbonyl compounds has been a stimulus for new methodology development in organic synthesis. While

the toolbox for the direct β -functionalization has been extended dramatically, general and practical methods with broader substrate scope and better functional group tolerance remain to be further developed. Considering the great potential of using direct β -functionalization to streamline complex molecule synthesis, it is expected there will be continuing and vigorous development in this area.

3.6 References

1. For representative examples, see: (a) Fujiwara, M.; Marumoto, S.; Yagi, N.; Miyazawa, M. *J. Nat. Prod.* **2011**, *74*, 86. (b) Mancha, S. R.; Regnery, C. M.; Dahlke, J. R.; Miller, K. A.; Blake, D. J. *Bioorg. Med. Chem. Lett.* **2013**, *23*, 562. (c) Misawa, N.; Nakamura, R.; Kagiya, Y.; Ikenaga, H.; Furukawa, K.; Shindo, K. *Tetrahedron* **2005**, *61*, 195.
2. Selected reviews on transition-metal-catalyzed conjugate addition: (a) Rossiter, B. E.; Swingle, N. M. *Chem. Rev.* **1992**, *92*, 771. (b) Gutnov, A. *Eur. J. Org. Chem.* **2008**, 4547. (c) Hayashi, T.; Yamasaki, K. *Chem. Rev.* **2003**, *103*, 2829.
3. (a) Buckle, D. R.; Pinto, I. L. In *Comprehensive Organic Synthesis*; Trost, B. M., Fleming, I., Eds.; Pergamon Press: Oxford, U.K., 1991; Vol. 7, pp 119-149. (b) Larock, R. C. In *Comprehensive Organic Transformations*; John Wiley & Sons: New York, 1999; pp 251-256.
4. Hartwig, J. F. In *Organotransition Metal Chemistry: From Bonding to Catalysis*; University Science Books: Sausalito, 2010.
5. Zaitsev, V. G.; Shabashov, D.; Daugulis, O. *J. Am. Chem. Soc.* **2005**, *127*, 13154.
6. Reddy, B. V. S.; Reddy, L. R.; Corey, E. J. *Org. Lett.* **2006**, *8*, 3391.
7. Shabashov, D.; Daugulis, O. *J. Am. Chem. Soc.* **2010**, *132*, 3965.
8. Tran, L. D.; Daugulis, O. *Angew. Chem. Int. Ed.* **2012**, *51*, 5188.
9. Wang, B.; Nack, W. A.; He, G.; Zhang, S.-Y.; Chen, G. *Chem. Sci.* **2014**, *5*, 3952.
10. Zhang, Q.; Chen, K.; Rao, W.; Zhang, Y.; Chen, F.-J.; Shi, B.-F. *Angew. Chem. Int. Ed.* **2013**, *52*, 13588.
11. A selected example of palladium-catalyzed intramolecular α -arylation: Iwama, T; Rawal, V. H. *Org. Lett.* **2006**, *8*, 5725.
12. Feng, Y.; Wang, Y.; Landgraf, B.; Liu, S.; Chen, G. *Org. Lett.* **2010**, *12*, 3414.
13. Wei, Y.; Tang, H.; Cong, X.; Rao, B.; Wu, C.; Zeng, X. *Org. Lett.* **2014**, *16*, 2248.
14. Pan, F.; Shen, P.-X.; Zhang, L.-S.; Wang, X.; Shi, Z.-J. *Org. Lett.* **2013**, *15*, 4758.
15. Shang, R.; Ilies, L.; Matsumoto, A.; Nakamura, E. *J. Am. Chem. Soc.* **2013**, *135*, 6030.

-
16. Ye, X.; He, Z.; Ahmed, T.; Weise, K.; Akhmedov, N. G.; Petersen, J. L.; Shi, X. *Chem. Sci.* **2013**, *4*, 3712.
 17. Gu, Q.; Al Mamari, H. H.; Graczyk, K.; Diers, E.; Ackermann, L.; *Angew. Chem. Int. Ed.* **2014**, *53*, 3868.
 18. Aihara, Y.; Chatani, N. *J. Am. Chem. Soc.* **2014**, *136*, 898.
 19. Li, M.; Dong, J.; Huang, X.; Li, K.; Wu, Q.; Song, F.; You, J. *Chem. Commun.* **2014**, *50*, 3944.
 20. Zhang, S.-Y.; Li, Q.; He, G.; Nack, W. A.; Chen, G. *J. Am. Chem. Soc.* **2013**, *135*, 12135.
 21. Chen, K.; Hu, F.; Zhang, S.-Q.; Shi, B.-F. *Chem. Sci.* **2013**, *4*, 3906.
 22. Wu, X.; Zhao, Y.; Ge, H. *J. Am. Chem. Soc.* **2014**, *136*, 1789.
 23. Ano, Y.; Tobisu, M.; Chatani, N. *J. Am. Chem. Soc.* **2011**, *133*, 12984.
 24. Hasegawa, N.; Charra, V.; Inoue, S.; Fukumoto, Y.; Chatani, N. *J. Am. Chem. Soc.* **2011**, *133*, 8070.
 25. Feng, Y.; Chen, G. *Angew. Chem. Int. Ed.* **2010**, *49*, 958.
 26. Gutekunst, W. R.; Baran, P. S. *J. Am. Chem. Soc.* **2011**, *133*, 19076.
 27. Gutekunst, W. R.; Gianatassio, R.; Baran, P. S. *Angew. Chem. Int. Ed.* **2012**, *51*, 7507.
 28. Ting, C. P.; Maimone, T. J. *Angew. Chem. Int. Ed.* **2014**, *53*, 3115.
 29. Engle, K. M.; Mei, T.-S.; Wasa, M.; Yu, J.-Q. *Acc. Chem. Res.* **2012**, *45*, 788.
 30. Giri, R.; Mangel, N.; Li, J.-J.; Wang, D.-H.; Breazzano, S.-P.; Saunders, L.-B.; Yu, J.-Q. *J. Am. Chem. Soc.* **2007**, *129*, 3510.
 31. Wang, D.-H.; Wasa, M.; Giri, R.; Yu, J.-Q. *J. Am. Chem. Soc.* **2008**, *130*, 7190.
 32. Wasa, M.; Engle, K. M.; Yu, J.-Q. *J. Am. Chem. Soc.* **2009**, *131*, 9886.
 33. Yoo, E. J.; Wasa, M.; Yu, J.-Q. *J. Am. Chem. Soc.* **2010**, *132*, 17378.
 34. Wasa, M.; Engle, K. M.; Yu, J.-Q. *J. Am. Chem. Soc.* **2010**, *132*, 3680.

-
35. (a) Baudoin, O. *Chem. Soc. Rev.* **2011**, *40*, 4902-4911. (b) Wasa, M.; Engle, K. M.; Yu, J.-Q. *Isr. J. Chem.* **2010**, *50*, 605.
36. Wasa, M.; Chan, K. S. L.; Zhang, X.-G.; He, J.; Miura, M.; Yu, J.-Q. *J. Am. Chem. Soc.* **2012**, *134*, 18570.
37. He, J.; Wasa, M.; Chan, K. S. L.; Yu, J.-Q. *J. Am. Chem. Soc.* **2013**, *135*, 3387.
38. He, J.; Li, S.; Deng, Y.; Fu, H.; Laforteza, B. N.; Spangler, J. E.; Homs, A.; Yu, J.-Q. *Science* **2014**, *343*, 1216.
39. Wasa, M.; Engle, K. M.; Lin, D. W.; Yoo, E. J.; Yu, J.-Q. *J. Am. Chem. Soc.* **2011**, *133*, 19598.
40. Xiao, K.-J.; Lin, D. W.; Miura, M.; Zhu, R.-Y.; Gong, W.; Wasa, M.; Yu, J.-Q. *J. Am. Chem. Soc.* **2014**, *136*, 8138.
41. Jørgensen, M.; Lee, S.; Liu, X.; Wolkowski, J. P.; Hartwig, J. F. *J. Am. Chem. Soc.* **2002**, *124*, 12557.
42. Renaudat, A.; Jean-Gérard, L.; Jazzar, R.; Kefalidis, C. E.; Clot, E.; Baudoin, O. *Angew. Chem. Int. Ed.* **2010**, *49*, 7261.
43. Larini, P.; Kefalidis, C. E.; Jazzar, R.; Renaudat, A.; Clot, E.; Baudoin, O. *Chem. Eur. J.* **2012**, *18*, 1932.
44. Aspin, S.; Goutierre, A.-S.; Larini, P.; Jazzar, R.; Baudoin, O. *Angew. Chem. Int. Ed.* **2012**, *51*, 10808.
45. Aspin, S.; López-Suárez, L.; Larini, P.; Goutierre, A.-S.; Jazzar, R.; Baudoin, O. *Org. Lett.* **2013**, *15*, 5056.
46. Mukherjee, S.; Yang, J. W.; Hoffmann, S.; List, B.; *Chem. Rev.* **2007**, *107*, 5471.
47. Enders, D.; Niemeier, O.; Henseler, A. *Chem. Rev.* **2007**, *107*, 5606.
48. Zhang, S.-L.; Xie, H.-X.; Zhu, J.; Li, H.; Zhang, X.-S.; Li, J.; Wang, W.; *Nat. Commun.* **2011**, *2*, 211.
49. Hayashi, Y.; Itoh, T.; Ishikawa, H. *Angew. Chem. Int. Ed.* **2011**, *50*, 3920.
50. Hayashi, Y.; Itoh, T.; Ishikawa, H. *Adv. Synth. Catal.* **2013**, *355*, 3661.

51. Mo, J.; Shen, L.; Chi, Y. R.; *Angew. Chem. Int. Ed.* **2013**, *52*, 8588.

52. Fu, Z.; Xu, J.; Zhu, T.; Leong, W. W. Y.; Chi, Y. R. *Nat. Chem.* **2013**, *5*, 835.

CHAPTER 4

Catalytic Direct β -Arylation of Simple Ketones with Aryl Iodides

4.1 Introduction

Functionalization and transformation of carbonyl compounds are essential to organic synthesis. While the α -position of the carbonyl group can be readily functionalized through enolate chemistry (*vide supra*, Scheme 2.1), the corresponding β -C–H bonds are typically not reactive. As an important class of carbonyl compound functionalization, arylation has been achieved at the α -position through Pd-catalyzed couplings of carbonyl compounds and aryl halides¹ (Scheme 4.1, pioneered by Buchwald, Hartwig, and Miura), preparing structural motifs frequently found in pharmaceutical, material and agrochemical products.² The practicality and wide applicability of the α -arylation reactions are likely attributed to the use of readily available starting materials (simple carbonyl compounds, aryl halides), the efficient and tunable Pd catalysts, the scalable reaction conditions and high functional group tolerance. However, the

corresponding β -arylation, while equally important for accessing bioactive compounds (Figure 4.1),³ has remained largely underdeveloped.

Scheme 4.1 Buchwald-Hartwig-Miura α -Arylation of Ketones

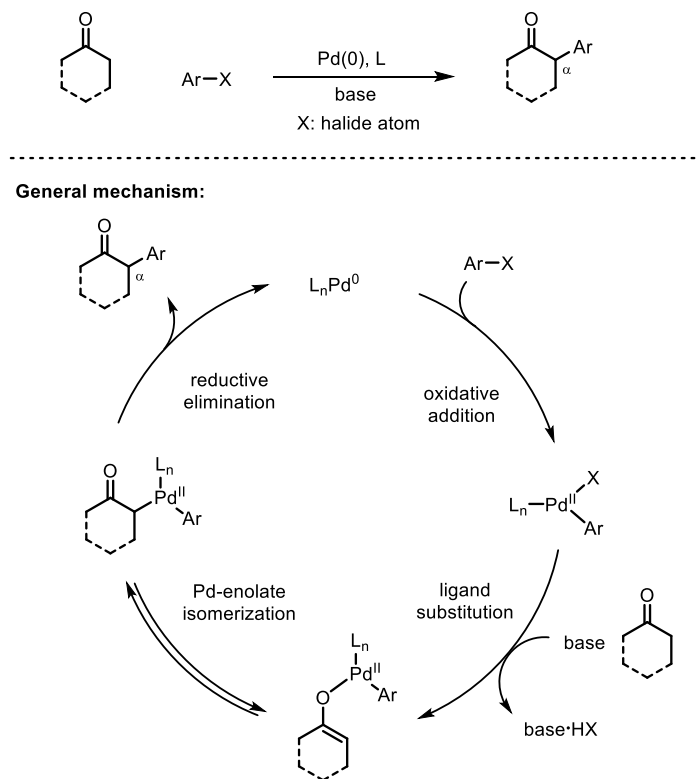
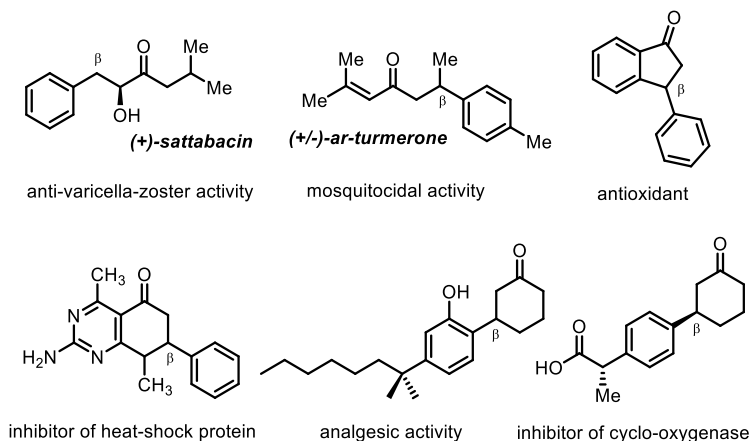
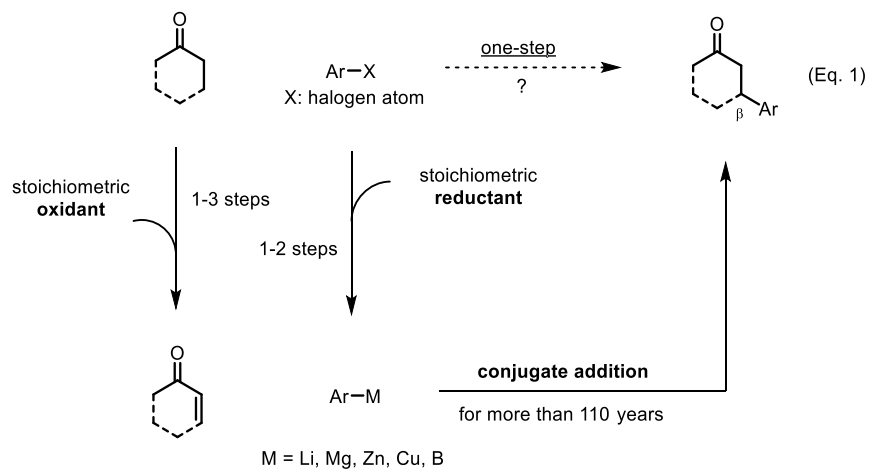


Figure 4.1 Selected Bioactive Compounds with β -Aryl Moiety



Conventionally, β -C-C forming reactions largely rely on conjugate addition of a soft nucleophile (e.g. organocuprates) to an α,β -unsaturated carbonyl substrate (e.g. conjugated enones) with or without a transition-metal (TM) catalyst (Scheme 4.2).⁴

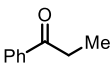
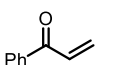
Scheme 4.2 β -Arylation of Ketones with Aryl Halides



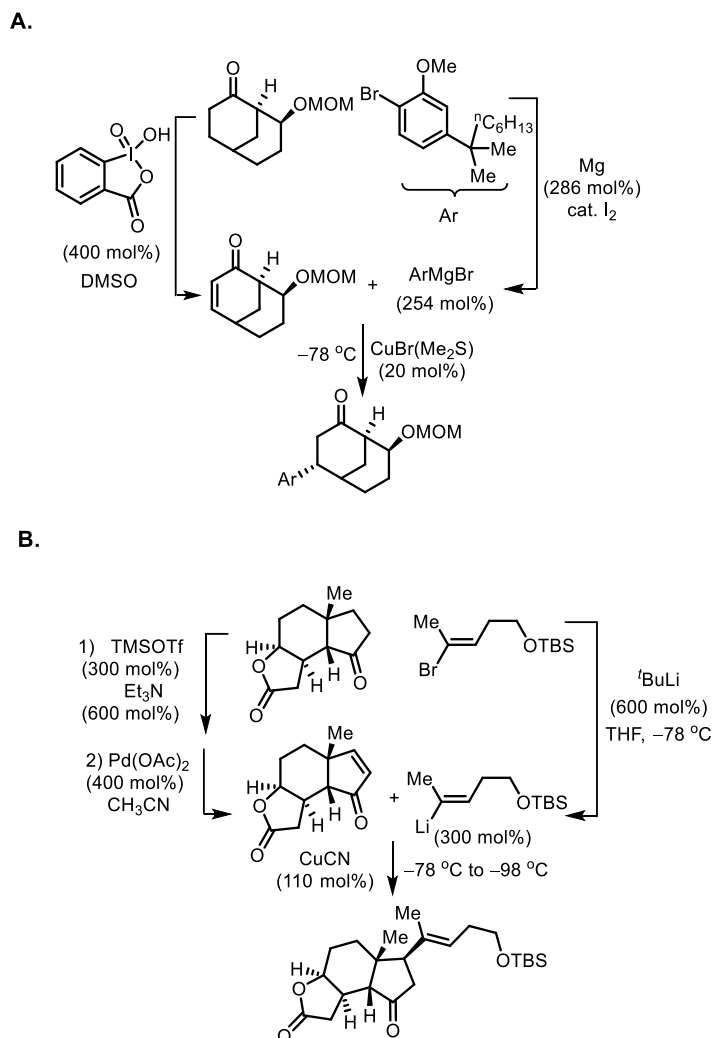
While effective, this approach typically requires use of unsaturated carbonyls and metallated nucleophiles (R-M; M = Li, Mg, Cu, Zn, Sn, B, Si etc). Compared with their

saturated counterparts, α,β -unsaturated carbonyl compounds are typically less accessible, more expensive (Figure 4.2), and often prepared from the corresponding saturated compounds through desaturation (1-3 steps) with stoichiometric oxidants (e.g. examples in Scheme 4.3).^{5,6} Metallated nucleophiles are usually generated from the corresponding more available organohalides (RXs) using stoichiometric low-valent metals as reductant. From a viewpoint of process-chemistry, it is known that oxidation reactions are problematic on scales ⁷ due to cost, safety, and chemoselectivity issues. Another concern is the use of stoichiometric or excess basic and nucleophilic metallated reagents, which are often incompatible with electrophilic and/or acidic FGs, such as aldehyde, ester, and ketone with α -protons.

Figure 4.2 Price Comparisons between Saturated and Unsaturated Ketones

				
n = 1	<u>\$0.032/g</u>	<u>\$7.6/g</u>	R = 3,3-Me,Me	<u>\$1.51/g</u> <u>N/A</u>
n = 2	<u>\$0.017/g</u>	<u>\$1.2/g</u>	R = 4-Ph	<u>\$1.30/g</u> <u>N/A</u>
n = 3	<u>\$0.49/g</u>	<u>\$39/g</u>	R = 4-Me	<u>\$0.20/g</u> <u>N/A</u>
n = 4	<u>\$0.94/g</u>	<u>N/A</u>		
* Lowest prices from Aldrich. N/A: not available				
				
	<u>\$0.046/g</u>	<u>\$108/g</u>		

Scheme 4.3 Examples of Classical Approach towards β -Aryl Carbonyl Compounds



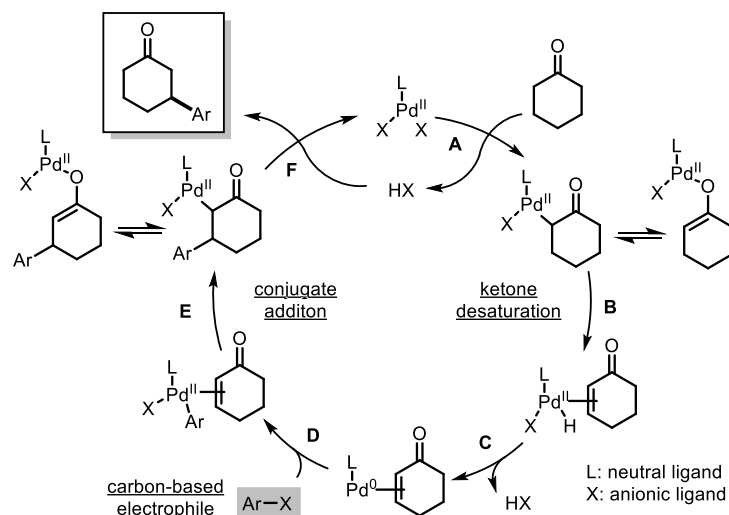
During the past decade, several β -arylation strategies that can directly employ saturated carbonyl compounds have emerged (*vide supra*, Chapter 3). The palladium-catalyzed direct β -arylation of amides was first achieved with a bidentate directing auxiliary.⁸ This strategy was pioneered by Daugulis, Corey and Chen, and further extended with the use of iron and nickel catalysts.⁹ Yu and coworkers also reported successful β -arylation reactions of weakly coordinating carboxylic acids and *N*-aryl amides.¹⁰ The β -arylation of esters via a migratory

coupling pathway was first discovered by Hartwig,¹¹ and later systematically developed by Baudoin and coworkers.¹² The β '-arylation of 1,3-dicarbonyl compounds has also been reported using an oxidative palladium catalysis, albeit with limited substrate scopes.¹³ In 2013, combining photo-redox and enamine catalysis, MacMillan and coworkers disclosed a novel β -arylation of cyclic ketones with electron-deficient aryl nitriles (ArCN) as the aryl source.¹⁴ Thus, a general solution to the β -arylation problem possessing the broadly applicable feature of Buchwald-Hartwig-Miura α -arylation, which includes direct use of readily accessible substrates, high functional group compatibility and scalability, would be transformative but remains to be discovered.

We conceived the idea of merging Pd-catalyzed ketone α,β -desaturation, Ar-X bond activation (X: halogen) and conjugate addition to realize a redox-neutral β -arylation reaction. Our proposed strategy is depicted in Scheme 4.4. First, since the seminal discovery of Theissen,¹⁵ Pd-mediated ketone desaturation has been known to activate carbonyl β C-H bonds, following a sequence of Pd(II)-enolate formation, β -H elimination and reductive elimination of an acid (HX) to give an enone and a Pd(0) species (steps A-C).¹⁶ While a number of oxidants can be used to enable catalytic desaturations through regenerating the active Pd(II) species, we envisioned that the versatile Pd(0) intermediate can be harnessed for further cascade transformation. Here, we hypothesize that, first, aryl halides can serve as stoichiometric oxidants to promote ketone oxidation to conjugated enones as the oxidative addition of Pd(0) into Ar-X bonds to give Ar-Pd(II)-X is a well-established process (step D).¹⁷ Second, the resulting Ar-Pd(II) species would undergo migratory insertion into the conjugated enone olefin to provide a Pd(II)-enolate (step E), which upon protonation by HX would give the β -arylated product and regenerate the Pd(II) catalyst (step F). A key feature of this palladium-catalyzed redox cascade is

that ketone oxidation and conjugate addition are incorporated into a single catalytic cycle using aryl halides as both the oxidant and aryl-substituent source, thus the proposed transformation would not need an external oxidant or reductant.

Scheme 4.4 Proposed Palladium-Catalyzed Redox Cascade

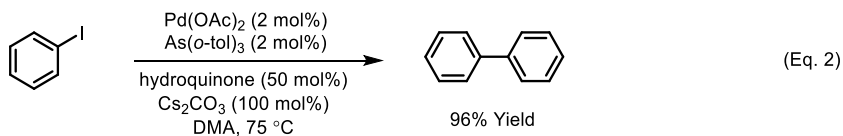


The success of this strategy relies on addressing the following key challenges: First, an electrophilic Pd complex is generally required for ketone oxidation (Steps A and B) while oxidative addition into carbon-halide bonds (Step D) prefers electron-rich catalysts. Thus, developing a catalyst system that is able to accommodate both needs during the catalytic cycle is nontrivial. Second, dimerization of aryl halides (Scheme 4.5, Eq. 2) and over-oxidations to phenols¹⁸ (Eq. 3) and/or to β -aryl enones¹⁹ (Eq. 4), which are known side reactions, must be inhibited. Third, given that the Pd-mediated dehydrogenation works most efficiently with carboxylate ligands,⁵ a suitable promoter must be found to extract halides from the Pd and deliver carboxylate anions to restore the active catalyst.

Scheme 4.5 Precedents of Possible Side-reactions

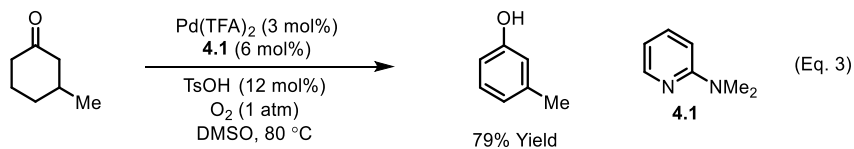
Dimerization of aryl halides

Rawal, 1999



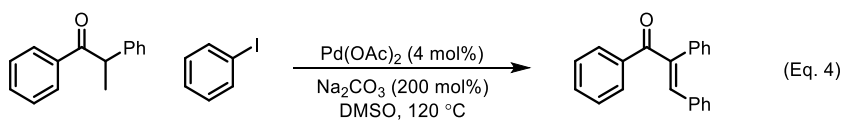
Oxidation of cyclohexanone to phenol

Stahl, 2011

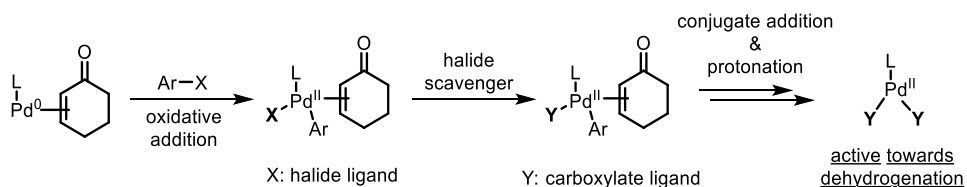


Dehydrogenative β -arylation

Cheng, 2014



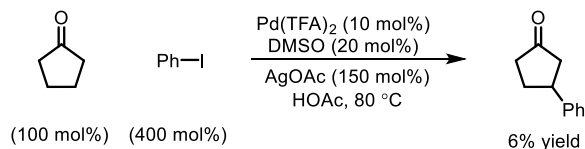
Scheme 4.6 Extraction of Halide Ligand



4.2 Results and Discussion

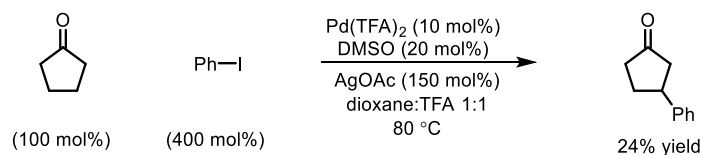
We set out to examine the feasibility of the proposed β -arylation reaction using cyclopentanone and iodobenzene as substrates. To our delight, the desired arylation product, 3-phenylcyclopentanone was identified and isolated in our first trials (Scheme 4.7). In these early reaction conditions, the combination of $\text{Pd}(\text{TFA})_2$ and DMSO was used as the precatalyst, and AgOAc supposedly acted as the iodide scavenger.

Scheme 4.7 Early Result of β -Arylation Reaction



An extensive screening of reaction parameters, including precatalysts, ligands, additives, and solvents, was able to further increase the efficiency of the β -Arylation Reaction (Scheme 4.8). And several trends can be summarized based on the results of the optimization.

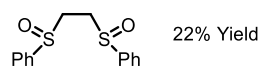
Scheme 4.8 Early Result of β -Arylation Reaction (continued)



Ligand effect:

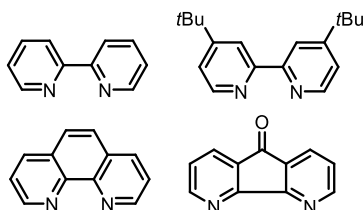
phosphine ligands 9-15% Yield

PPh3
PCy3
dppe
dppf
dppb
tBuXPhos
XantPhos



nitrogen-based ligands trace

Ar-N=C=N-Ar Ar = mesityl
 Ar = 2,6-diisopropylphenyl



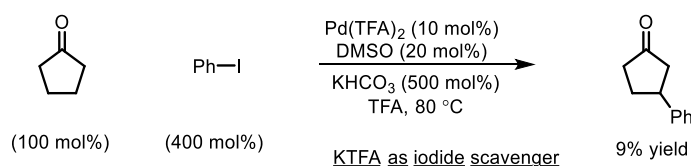
First, acidic and coordinating solvents are both important for the reaction, as a mixed solvent consisting of equal volumes of dioxane and trifluoroacetic acid was found beneficial for the arylation reaction. Trifluoroacetic acid is proposedly critical for the last protonation step while the dioxane can stabilize the Pd(0) intermediate as a weak ligand.

Second, silver salt can greatly promote the reaction. In our design of the catalytic cycle, the role of silver salt is to scavenge the iodide ligand and restore the active Pd(II) catalyst.

Third, acetate or trifluoroacetate counter anion is indispensable for the reaction. In the catalytic cycle, while the silver scavenges iodide from the palladium center, it also delivers its counter anion to the palladium. Since the acetate-type ligand on palladium is crucial to maintain palladium an electron-deficient species, silver acetate or silver trifluoroacetate is favored for the reaction. It did turn out that other silver salt only gave marginal amount of product.

Fourth, although different sorts of ligands are screened, they seemed to have undifferentiated effects on the reaction outcome. We hypothesize this is reasonable, as under extremely acidic reaction condition (TFA), almost every phosphine, phosphite or nitrogen-based ligand can be protonated, making them sluggish to coordinate to the palladium center.

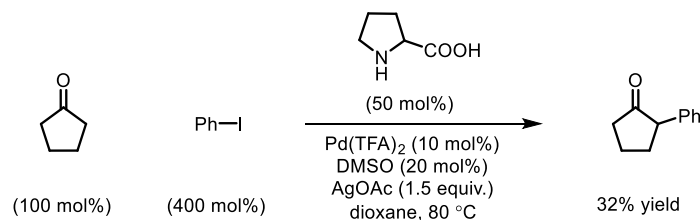
Scheme 4.9 Early Result of β -Arylation without Silver Additives



Finally and notably, when potassium trifluoroacetate was used (i.e. the combination of KHCO_3 , TFA) as iodide scavenger, the reaction can still afford the product in 9% yield (Scheme 4.9). This result is quite promising because it indicates we may be able to develop a β -arylation protocol without the use of stoichiometric transition-metal salt.

During our optimization of the β -arylation of cyclopentanone, we found that the site-selectivity of the arylation can be completely switched to the α -position of cyclopentanone when 50 mol% of proline was used as an additive. Control reactions indicated both $\text{Pd}(\text{TFA})_2$ and proline are essential for the α -arylation, implying a merger of organo- and transition metal catalysis.

Scheme 4.10 Discovery of α -Arylation of Cyclopentanone

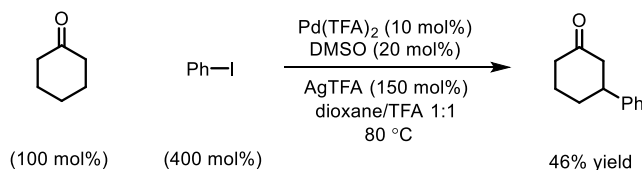


Control reactions:

w/o Pd(TFA) ₂ :	no product
w/o Proline:	no product
w/o DMSO:	34% Yield
w/o AgOAc:	26% Yield
pyrrolidine instead of proline	25% Yield

As our optimization continued for the β -arylation reaction, we discovered that when cyclohexanone was used as the substrate in place of cyclopentanone, the yield significantly increased (Scheme 4.11). As plain and substituted cyclohexanones are often preferred substrates over cyclopentanone in the studies of palladium-catalyzed dehydrogenation, the better performance of cyclohexanones for the β -arylation may be attributed to the faster dehydrogenation step.

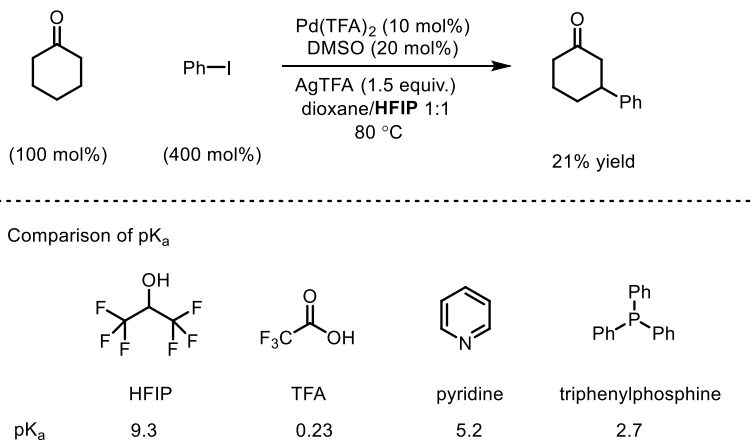
Scheme 4.11 Better Performance of Cyclohexanone than Cyclopentanone



Another breakthrough of the reaction conditions optimization was the use of hexafluoro-2-propanol (HFIP) as a co-solvent (Scheme 4.12). At the first glance, HFIP didn't give yield as high as TFA did. Nevertheless, the pK_a of HFIP is only 9.3. This indicated HFIP is acidic enough to give the desired β -arylation product but not acidic enough to protonate the majority of

phosphine and pyridine-based ligands. Thus, we expected different types of phosphine- or nitrogen-based ligands, in their free forms under conditions with HFIP, should impose different effects on the outcome of the β -arylation reactions.

Scheme 4.12 Effects of HFIP as a co-solvent

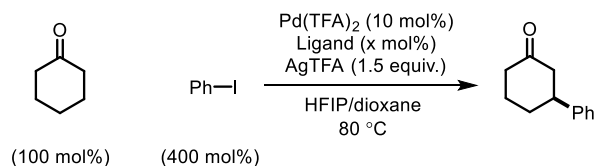


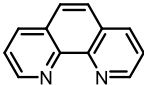
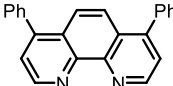
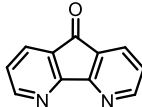
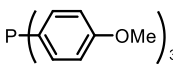
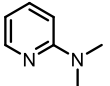
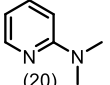
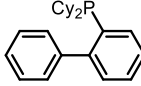
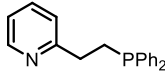
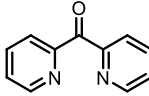
Indeed, when HFIP was used as a co-solvent for the ligand screening, the difference among various types of ligands was revealed to be dramatic (Table 4.1). It was discovered that pyridine-based ligands, while still capable of giving β -arylation product, gave relatively low yields. And it is noteworthy that simple triphenylphosphine outperformed DMSO to deliver the β -arylation product in 42% yield. Further screening of phosphine ligands demonstrated electron-rich trialkylphosphine, especially PCy_3 and $P(i-Pr)_3$, are the best candidates for the reaction, while most bidentate phosphine ligands gave very low conversion.

After we chose $P(i-Pr)_3$ as the ligand, the next improvement of the reaction was the reverse ratio of cyclohexanone and iodobenzene. When excess amount of cyclohexanone was used compared with iodobenzene, the yield significantly increased to above 75%, probably due to the faster initiation of dehydrogenation of ketones, as demonstrated in Stahl's mechanistic

studies of palladium-catalyzed aerobic dehydrogenation. Finally, with further fine-tuning of the reaction condition, including the scale, concentration and equivalence of additive and catalyst, the yield of the β -arylation reaction reaches 76% (Table 4.2, Eq. 5). Under the optimized conditions, neither over-oxidation to 3-phenyl-cyclohexenone nor the α -arylation product was observed. Note that the combination of electron-rich phosphine-Pd complexes and aryl halides has been extensively employed in the ketone α -arylation reactions (*vide supra*, Scheme 4.1); however, while a similar combination is employed here, this reaction proceeded with complete site-selectivity for the β -position. This can likely be explained that the Buchwald-Hartwig-Miura arylation typically uses stoichiometric bases to generate the corresponding enolates, but our reaction operates under acidic conditions, which triggered a different activation mode.

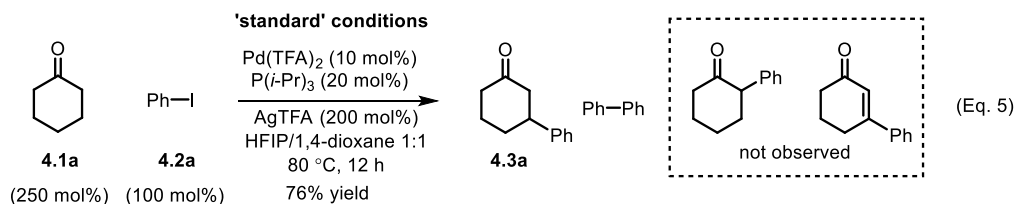
Table 4.1 Ligand Screening of β -Arylation of Cyclohexanone



Ligand	yield (%)	conversion (%)	Ligand	yield (%)	conversion (%)
2,2'-Bipyridine(10)	19	22	 (10)	<5%	6%
dtbpy(10)	11	~10	 (10)	8%	8%
 (10)	27	55	P(2-furyl) ₃ (20)	12%	17%
Mes-N  -Mes (10)	7	16	PCy₃ (20)	48%	~50%
PPh₃ (20)	42	51	P(o-tol) ₃ (20)	5%	16%
DMSO (20)	21	51	P(2,6-dimethoxy) ₃ (20)	4%	17%
P() ₃ (20)	27	48	P(p-tol) ₃ (20)	27%	43%
P(C ₆ F ₅) ₃ (20)	10	31	P(i-Pr)₃ (20)	51%	~50%
no ligand	12	41	P(n-Bu) ₃ (20)	30%	31%
 (20)	trace	6	P(t-Bu) ₃ (20)	7%	19%
 (20)	trace	28	BPh ₃ (20)	10%	34%
 + TsOH (40)	trace	31	 (20)	12%	28%
 (10)	trace	5	 (10)	31%	32%
dppm (15)	26	32	 (20)	2%	53%
dppe (15)	trace	--	PPh ₃ (10)/bipyridine (10)	11%	12%
dppb (15)	trace	--			
dppf (15)	trace	--			

* 2.0 equiv. of AgTFA was used for the right side of the table

A set of control experiments were consequently conducted (Table 4.2). In the absence of Pd, no product was obtained, suggesting the pivotal position of Pd in the catalytic cycle (entry 1). Electron-rich ligands were uncommon for the palladium-catalyzed dehydrogenation reactions. However, for this β -arylation reaction, electron-rich phosphines play an important role in inhibiting the aryl dimerization and promoting formation of the desired product, though the exact reason is unclear (entries 2-8). In the absence of $P(i\text{-Pr})_3$ or use of triisopropyl phosphine oxide, biphenyl was observed as the major product with only a trace amount of the β -arylated ketone formed (entries 2 and 8). Other electron-rich phosphines, such as PMe_3 and PCy_3 , also proved to be efficient (entries 3 and 4). In contrast, use of less electron-rich PPh_3 or sterically hindered $P(t\text{-Bu})_3$ led to formation of a considerable amount of biphenyl (entries 5 and 6). Silver salts were utilized to facilitate iodide-carboxylate exchange, which is expected to be crucial for regenerating the active Pd(II) catalyst (entry 9). Replacing the trifluoroacetate counterion of the silver salts with acetate resulted in decreased yields (entries 10 and 11). Interestingly, substitution of the Ag salt with strong bases, such as NaOt-Bu , gave a complex reaction mixture without forming any β - or α -arylation product (entry 12). Solvent effects were also surveyed (entries 13-16): while 1,4-dioxane is most suitable for this transformation, addition of mildly acidic HFIP is beneficial likely because it accelerates the protonation of Pd-enolates to regenerate the Pd(II) catalysts (Step F, Scheme 4.4), which in turn should diminish side reactions, e.g., over-oxidations. On the other hand, HFIP is not acidic enough to protonate phosphine ligands, whereas using stronger acids, such as trifluoroacetic acid (TFA), as a co-solvent was found detrimental. Finally, when cyclohexanone and iodobenzene were added in an equimolar ratio, the desired 3-phenyl-cyclohexanone was still provided in 67% yield (entry 17).

Table 4.2 Control Experiments for the Optimized Conditions^a

entry	variations from the 'standard' conditions	yield of 4.3a (%) ^b	yield of Ph-Ph (%) ^b
1	w/o Pd(TFA) ₂	0	0
2	w/o P(<i>i</i> -Pr) ₃	4	56
3	PMe ₃ instead of P(<i>i</i> -Pr) ₃	56	9
4	PCy ₃ instead of P(<i>i</i> -Pr) ₃	51	8
5	PPh ₃ instead of P(<i>i</i> -Pr) ₃	30	25
6	P(<i>t</i> -Bu) ₃ instead of P(<i>i</i> -Pr) ₃	4	48
7	(<i>i</i> -Pr) ₃ P=O instead of P(<i>i</i> -Pr) ₃	3	47
8	w/o AgTFA	0	0
9	AgOAc instead of AgTFA ^c	56	20
10	Pd(OAc) ₂ /AgOAc instead of Pd(TFA) ₂ /AgTFA	51	11
11	1,4-dioxane only, no HFIP	66	21
12	<i>t</i> -BuOH instead of HFIP	65	15
13	TFA instead of HFIP	23	7
14	toluene instead of 1,4-dioxane	19	6
15	Ph-I : cyclohexanone = 1:1	67	17

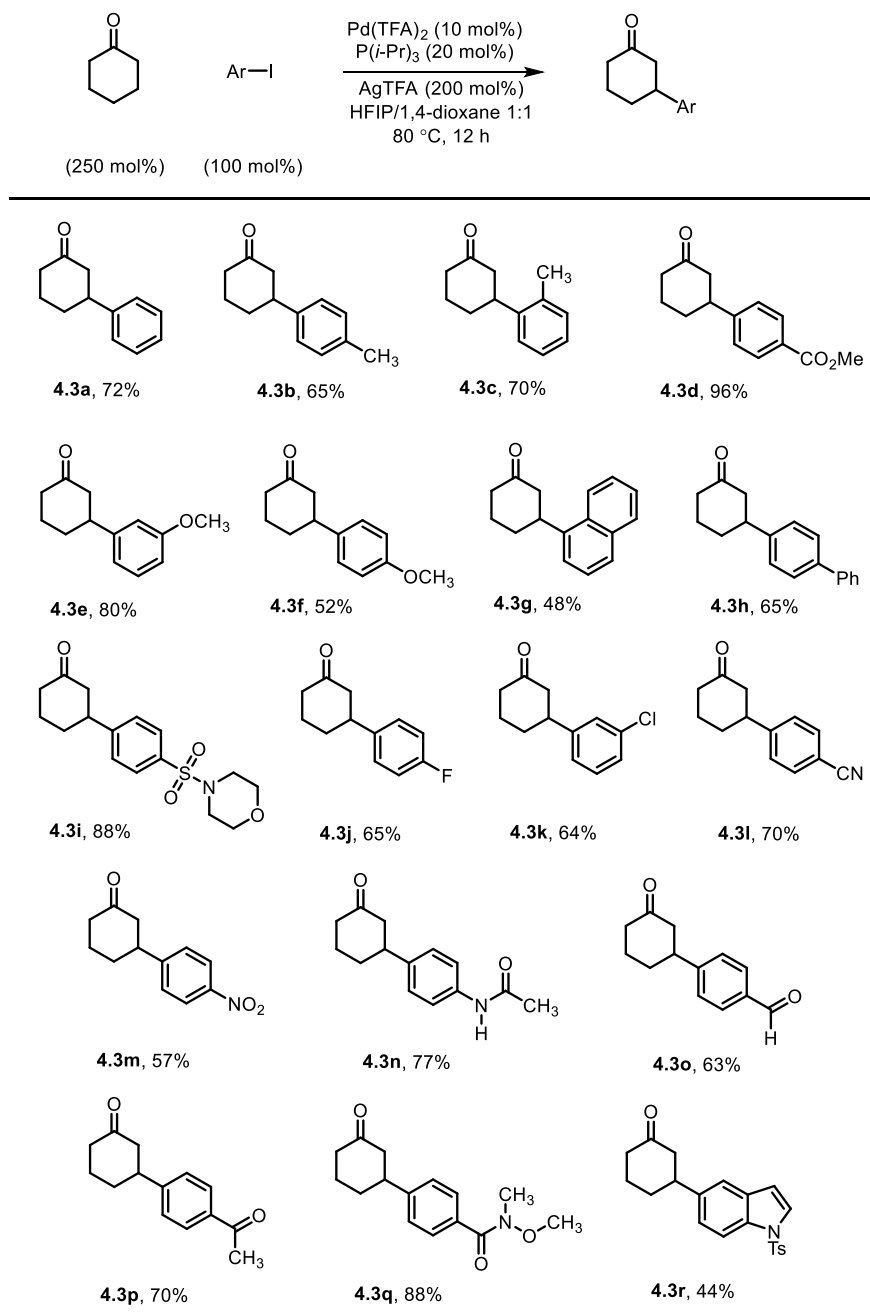
^aReaction conditions: all the reactions were run on a 0.2 mmol scale with 1.0 mL solvents in 12 h. ^bGC yield determined using dodecane as the internal standard. ^cHFIP was not added.

With the optimized conditions in hand, the substrate scope was then investigated (Table 4.3). Aryl iodides containing arenes with different electronic properties (electron-rich and -poor) all participated to give the corresponding β -arylated ketones (**4.3a-4.3m**). In addition, substitutions on the aryl group at the *ortho*-, *meta*- or *para* positions are all tolerated. Furthermore, a broad range of functional groups, including aryl ethers, cyanides, aryl chlorides, fluorides, naphthalene, protected indoles, carboxylic esters, nitro group, and sulfonamides, are

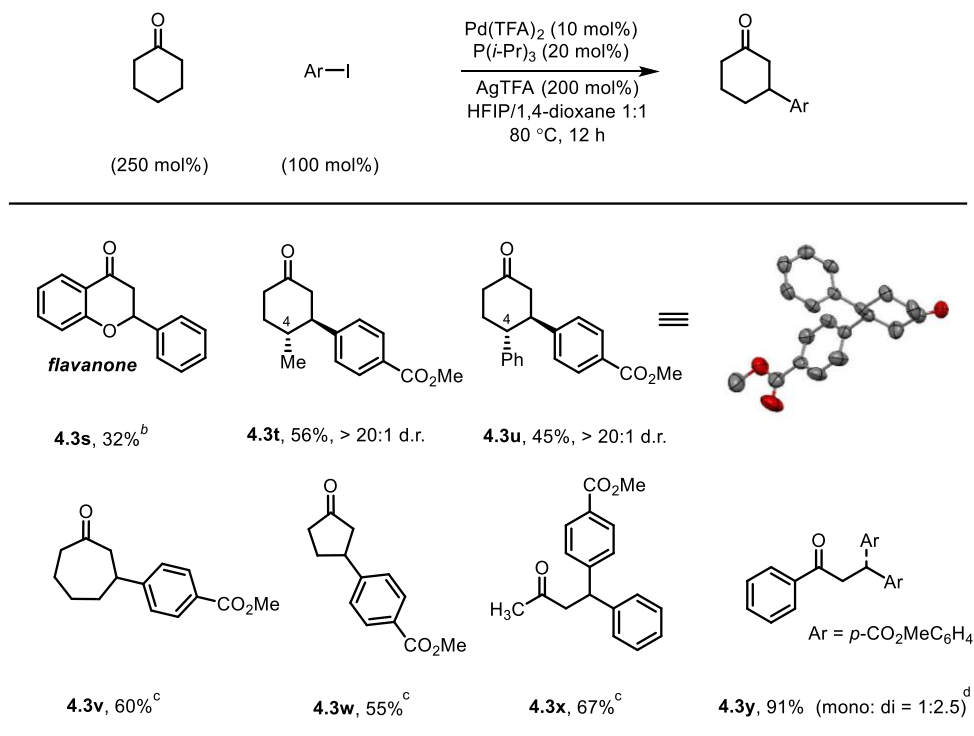
compatible under the reaction conditions. These features indicate that this Pd-catalyzed direct β -arylation exhibits comparable reactivity and scope as the aryl-conjugate additions but using fewer steps or redox operations. Perhaps, it is more encouraging to note that products that are more difficult to prepare via conventional 1,4-additions, such as *arenes that contain base- or nucleophile-sensitive groups* (*i.e.* amide protons **4.3n**, ketones with enolizable hydrogens **4.3p**, aldehydes **4.3o**, Weinreb amide **4.3q**), can also be accessed using this method. The high chemoselectivity is likely due to the mild reaction conditions (base-free) as well as the absence of stoichiometric aryl-metal nucleophiles.

The scope of the ketone component was also examined (Table 4.4). The β -arylation of ketones bearing a stereocenter at the C4 position proceeded with excellent diastereoselectivity (>20:1) giving the *trans* products (**4.3t**, **4.3u**). Besides the 6-membered ring ketones, cyclopentanone and cycloheptanone also provided the desired β -arylation products (**4.3v**, **4.3w**). Acyclic ketones also proved to be suitable substrates (**4.3x**, **4.3y**). Given the broad substrate scope, this approach is clearly complementary to the previous directing group and photo-redox β -arylation methods. Interestingly, when propiophenone was employed as the substrate, a mixture of mono- and di-arylated products was isolated in 91% yield with a 1:2.5 ratio. The tendency of propiophenone to give diarylation products is likely due to its flexible conformation permitting free bond rotation, which in turn, results in a second ketone dehydrogenation via β -H elimination (Scheme 4.13).

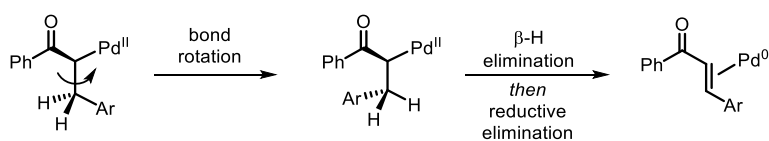
Table 4.3 Substrate Scope of Aryl Iodides^a



^aReaction conditions: aryl iodide (0.4 mmol), ketone (1.0 mmol), Pd(TFA)₂ (0.04 mmol), P(*i*-Pr)₃ (0.08 mmol), AgTFA (0.8 mmol), HFIP (1 mL), dioxane (1 mL), 80°C, 12 h.

Table 4.4 Substrate Scope of Ketones^a

^aReaction conditions: aryl iodide (0.4 mmol), ketone (1.0 mmol), Pd(TFA)₂ (0.04 mmol), P(*i*-Pr)₃ (0.08 mmol), AgTFA (0.8 mmol), HFIP (1 mL), dioxane (1 mL), 80°C, 12 h. ^b1.0 equiv. of the ketone and 2.5 equiv. of iodobenzene were used. ^c5.0 equiv. of the ketone was used. ^d10.0 equiv. of the ketone was used.

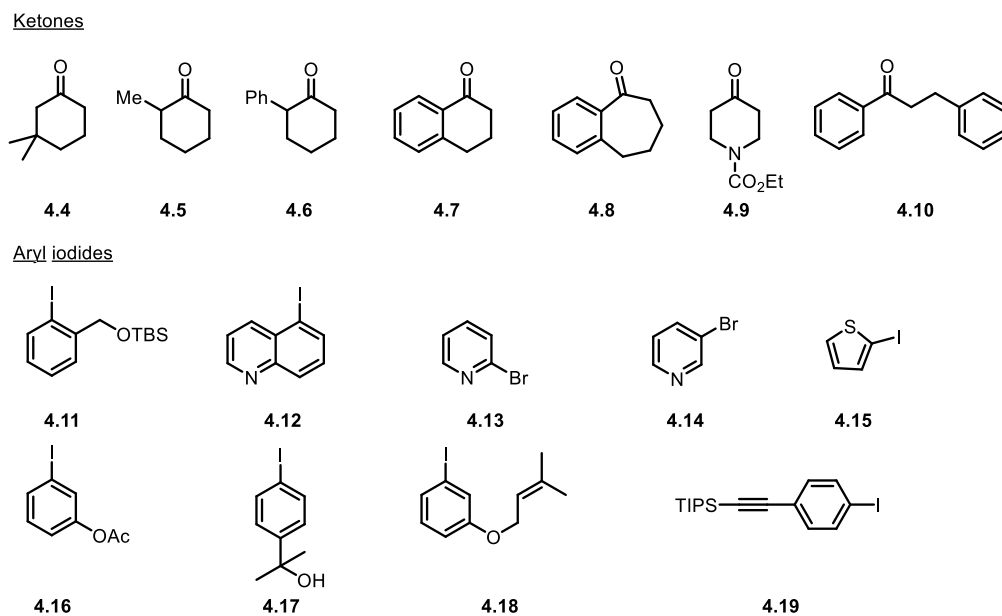
Scheme 4.13 Origin of Di-arylation

Besides these successful examples, a list of representative failed substrates is shown below (Figure 4.3). For the scope of ketones, the reaction conditions are sensitive to the steric hindrance and conformation of the ketone structures. For example, substituents at 2- or 3-position of cyclohexanone will greatly diminish the yield (**4.4-4.7**). Also, benzo-fused cyclic ketones, including 5, 6 and 7-membered cyclic ketones (**4.7**, **4.8**), will only give a trace amount

of desired products. In addition, cyclic ketones with heteroatom incorporated make the reaction quite sluggish and give little product (**4.9**). The high sensitivity to the steric hindrance can also be demonstrated by the comparison of the reactions with propiophenone and β -phenyl propiophenone (**4.10**); while propiophenone gave excellent yield, a β -phenyl group highly inhibits the reaction. It is also necessary to mention that the high yield of the diarylation product of the reaction with propiophenone doesn't contradict such comparison because the second arylation is facile since the palladium is already on the α -position once the first arylation is complete (*vide supra*, Scheme 4.13).

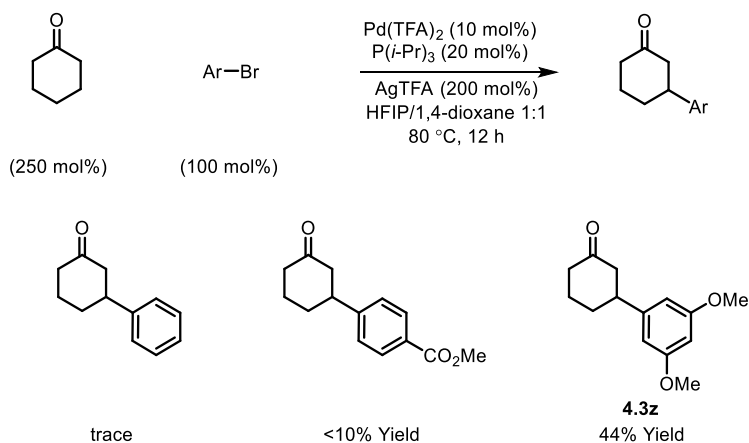
For the substrates of aryl halide, heteroaryl halides are not good coupling partners. Thiophene and furan moieties are not tolerated probably due to the inclination to oxidation (**4.15**). Nitrogen-contained heterocycles tend to bind to the palladium catalyst, thus giving no product (**4.12-4.14**). Acetate (**4.16**), tertiary alcohol (**4.17**), and TBS-protected alcohol (**4.11**) being not tolerated might be attributed to the acidic reaction conditions. Also due to the acidic medium, as well as the electrophilic palladium catalyst, alkene (**4.18**) and alkyne (**4.19**) are not tolerated.

Figure 4.3 Representative Examples of Failed Substrates



A wide range of aryl electrophiles (ArX, X = I, Br, Cl, OTf etc) are known to participate in palladium-catalyzed cross couplings via oxidative addition with Pd(0).¹⁷ There is a pressing need to extend the scope of the aryl source to aryl bromides and triflates (even chlorides) due to their general availability and cost advantage. The challenge of using ArBr or ArOTf is due to their slow oxidative addition with Pd(0) species, which can lead to catalyst decomposition to Pd black in the absence of excess ligands. Our preliminary studies indicate that aryl bromides still hold great promise as suitable substrates (Scheme 4.14). While simple bromobenzene only gave trace amount of β -arylation product under the standard conditions, certain electron-deficient aryl bromides could afford the desired product in a much higher yield. This is also consistent with our hypothesis that oxidative addition is the main obstacle.

Scheme 4.14 β -Arylation with Aryl Bromides under Standard Conditions

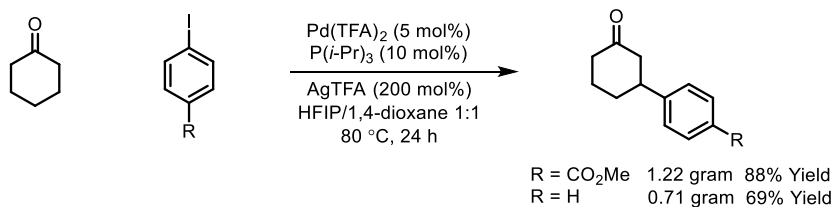


This β -arylation method proved to be readily scalable; on a gram scale, the β -arylation product was isolated in 88% yield using methyl 4-iodobenzoate and 69% yield using phenyl iodide with a lower catalyst loading (Scheme 4.15A).

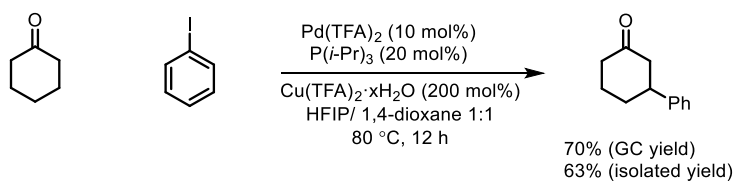
Efforts have also been set forth to examine whether the silver promoter can be substituted with more economically viable reagents. It is encouraging to note that replacement of silver trifluoroacetate with copper(II) trifluoroacetate only slightly reduced the yield (Scheme 4.15B).

Scheme 4.15 Gram-scale Reactions and Copper Salt as Promoter

A. Gram-scale reaction

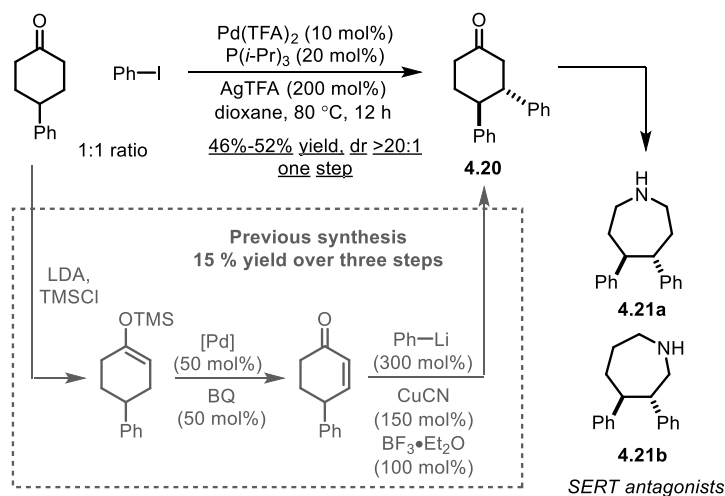


B. Substitution of silver salts



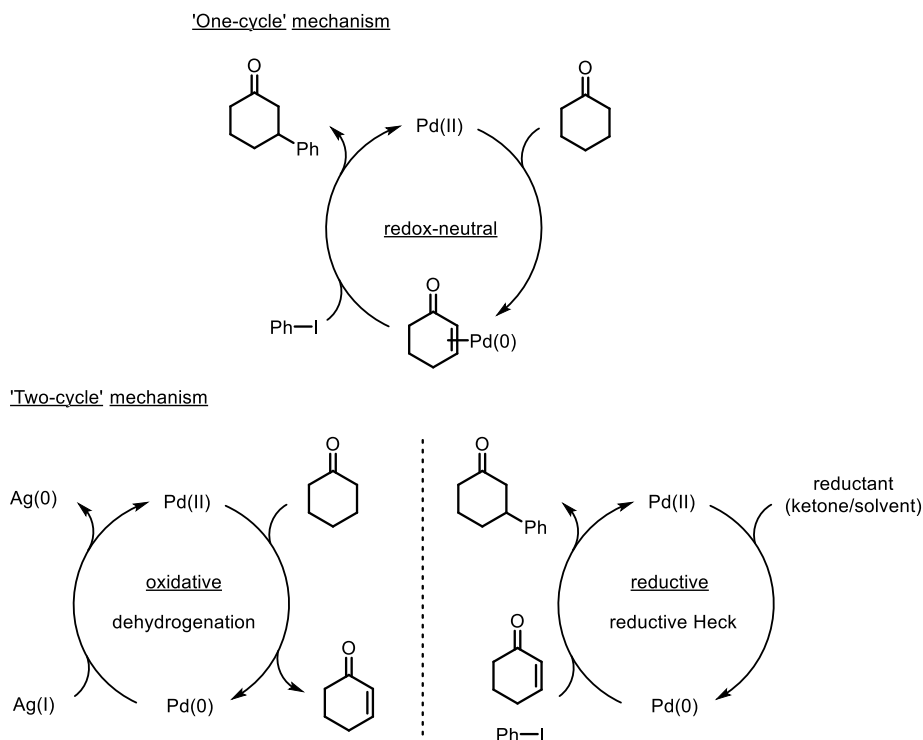
Application of this Pd-catalyzed direct β -arylation in the synthesis of a key intermediate (**4.20**) for SERT antagonist **4.21a/b** (serotonin reuptake inhibitors) is illustrated in Scheme 4.16. The previous approach, using classical dehydrogenation and conjugate addition, required three steps and provided a 15% overall yield.²⁰ With this β -arylation method, ketone **4.20** was obtained in one single step with a 3-fold increase in yield from the same ketone material and just one equiv of iodobenzene.

Scheme 4.16 Synthesis of an Intermediate for SERT Antagonists



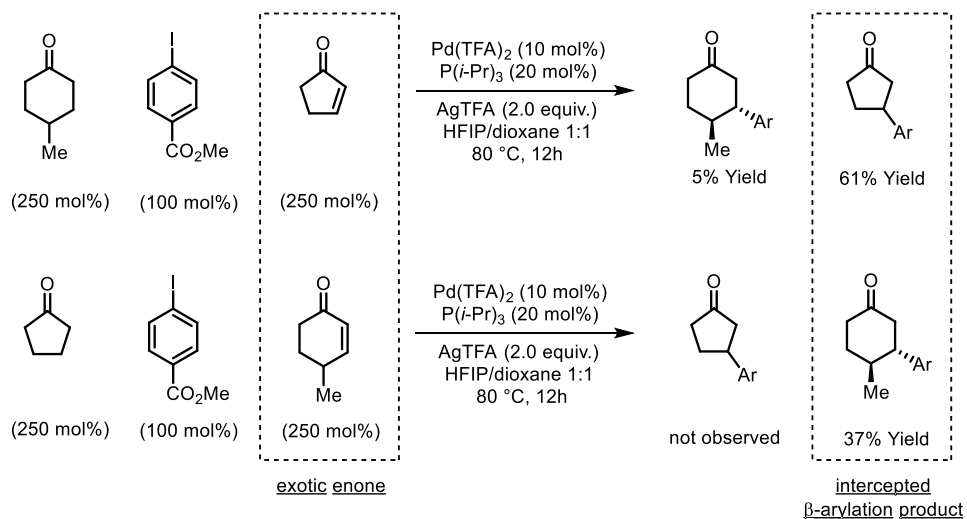
Although systematic studies of the reaction mechanism haven't been carried out, some preliminary results have been obtained and offered insights into the reaction pathway. A major concern regarding the mechanism is whether the β -arylation reaction proceeds through a 'two-catalytic-cycle' pathway consisting of palladium-catalyzed dehydrogenation and reductive Heck reaction (Scheme 4.17). In this alternative mechanism, the Ag(I) additive serves as a stoichiometric oxidant for the palladium-catalyzed dehydrogenation, and the resulting enone enters the second catalytic cycle to undergo the palladium-catalyzed reductive Heck reaction, where excess ketones or solvents could serve as the reductant. In order to probe the possibility of this mechanism, we designed a cross-over reaction where an exotic enone was added to the β -arylation reaction. Thus, if the reaction runs through two separate catalytic cycles, the exotic enone would be intercepted by the cycle of reductive Heck reaction, and eventually gives a different β -aryl ketone as the product.

Scheme 4.17 Comparison between ‘One-cycle’ and ‘Two-cycle’ Mechanism



It turned out the β -aryl ketones from the exotic enones are the major products of the cross-over experiments (Scheme 4.18). This result is consistent with the ‘two-cycle’ mechanism. However, it is also possible the exotic enones undergo a ligand exchange with the Pd(0)-enone complex generated from the dehydrogenation before the conjugate addition step. Because the ingenious enone is only produced in a catalytic amount, such a ligand replacement should be facile. Thus, at the current stage, the cross-over results are not able to distinguish between the two mechanisms conclusively.

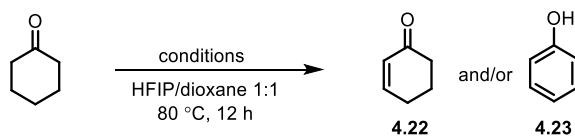
Scheme 4.18 Cross-over Experiments with Exotic Enones



Another direction for mechanistic study is to elucidate the role of phosphine ligand. One particularly intriguing question about the conditions is how electron-rich trialkylphosphine ligand is compatible with the dehydrogenation, as electrophilic palladium catalysts are often required for that step. A set of stoichiometric dehydrogenation reactions were therefore devised to probe the influence of silver salt and phosphine ligand on the reactivity and selectivity. As shown in Scheme 4.19, the dehydrogenation of cyclohexanone can be mediated alone by $\text{Pd}(\text{TFA})_2$ (entry 1) to give phenol as the only oxidation product. And AgTFA is not capable of giving any dehydrogenation products (entry 2). On the other hand, the combination of $\text{Pd}(\text{TFA})_2$ and AgTFA largely increased the conversion of ketone, and a complete selectivity towards phenol was also observed (entry 3). When 200 mol% $\text{P}(i\text{-Pr})_3$ was used alone with $\text{Pd}(\text{TFA})_2$, the dehydrogenation was completely shut down (entry 4), indicating the incapability of an electron-rich palladium complex to oxidize ketones. However, it is interesting to note that when AgTFA was added to $\text{Pd}(\text{TFA})_2/\text{P}(i\text{-Pr})_3$, the reactivity of dehydrogenation was revived, and the

selectivity was switched to the enone (entry 5). These results clearly implied the role of phosphine ligand to inhibit the over-oxidation of cyclohexanone to phenol, as well as the indispensable role of AgTFA to maintain the reactivity of palladium-catalyzed dehydrogenation in the presence of $P(i\text{-Pr})_3$.

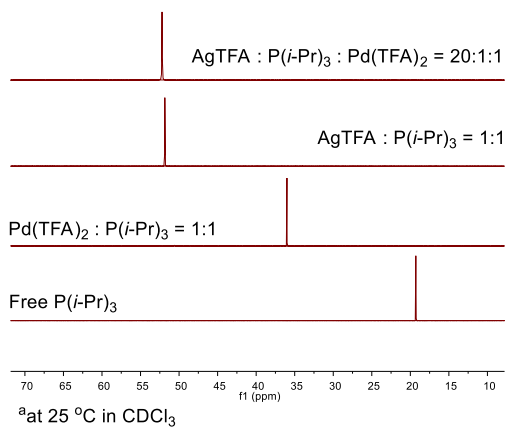
Scheme 4.19 Stoichiometric Dehydrogenation Reactions



Entry	condition (mol%)			conversion (%)	4.22 (%)	4.23 (%)
	Pd(TFA) ₂	AgTFA	P(<i>i</i> -Pr) ₃			
1	100	0	0	37	0	19
2	0	100	0	0	0	0
3	100	200	0	80	0	23
4	100	0	200	0	0	0
5	100	200	200	68	38	5

One possible explanation for the revived dehydrogenation reactivity is that AgTFA could act as a ‘phosphine shuttle’ during the catalytic reaction. During the palladium-mediated dehydrogenation step, it is hypothesized the electron-rich phosphine ligand may complex with AgTFA instead of Pd(TFA)₂. Thus, the electrophilicity of the palladium catalyst remains. This hypothesis was supported by a brief ³¹P-NMR study of the complexation among Pd(TFA)₂, AgTFA, and P(*i*-Pr)₃ (Figure 4.4). The spectrum of the mixture of these three components in a similar ratio as the catalytic β-arylation indicated the phosphine ligand coordinated to AgTFA in a complete selectivity. Nevertheless, it is still unclear whether and how this complexation mode might change during the course of the catalytic arylation, and how these events could affect the reactivity of the palladium catalyst.

Figure 4.4 ^{31}P -NMR study of Complexation of Phosphine Ligand



4.3 Conclusion

In summary, this Pd-catalyzed direct β -arylation of simple ketones overcomes several limitations and complements the scope of β -functionalization of carbonyl compounds. It has significant advantages over the conventional conjugate additions, because this approach not only circumvents use of conjugated enones and aryl nucleophiles, which need additional steps and redox procedures to prepare, but also tolerates base/nucleophile-sensitive moieties. It is distinct from the amide/ester-based C–H activation strategy by allowing both linear and cyclic ketones to react; direct coupling of the readily available aryl halides also distinguishes this work from the photoredox strategy. Furthermore, this methodology is scalable and chemoselective. Although still in its infancy, this approach has shown great potential to streamline complex-molecule synthesis. Finally, the unique tandem Pd-redox system discovered here is expected to shed lights on developing other β -functionalization transformations.

4.4 Experimental

Unless stated otherwise, all reactions were carried out in vials sealed with PTFE lined caps, purchased from Qorpak. 1,4-Dioxane was distilled from Na and freeze-pump-thawed three times prior to use. Hexafluoro-2-propanol (HFIP) was purchased from Oakwood Chemical and used as received. Pd(TFA)₂ was prepared following literature procedures.²¹ Silver trifluoroacetate and copper trifluoroacetate hydrate were purchased from Alfa and used as received. Tri-isopropyl phosphine was purchased from Strem, stored and used in a glovebox. All commercially available substrates were used without further purification. Thin layer chromatography (TLC) analysis was run on silica gel plates purchased from EMD Chemical (silica gel 60, F254). Gas chromatography (GC) data was obtained from Agilent 7820A GC system, equipped with Agilent 19091J-413 column and a FID detector. GC yield of 3-phenyl cyclohexanone and conversion of cyclohexanone and iodobenzene were determined using standard curves with dodecane as internal standard. Mass spectra were recorded on an Autospec or Agilent 6150. Accurate masses from high-resolution mass spectra were reported for the molecular ion [M+Na]⁺, [M]⁺ or [M+H]⁺. ¹H NMR and ¹³C NMR spectra were recorded on a Varian Gemini (400 MHz for ¹H, 100 MHz for ¹³C). Chemical shifts are reported as parts per million (ppm) using residual solvent signals as internal standard (CHCl₃, δ = 7.26 ppm for ¹H NMR, δ = 77.00 ppm for ¹³C NMR). Data for ¹H NMR were presented as following: chemical shifts (δ, ppm), multiplicity (br = broad, s = singlet, d = doublet, t = triplet, q = quartet, dd = doublet of doublets, tt = triplet of triplets, td = triplet of doublets, m = multiplet), coupling constant (Hz), and integration. The chemical shifts of peaks found were reported for ¹³C NMR spectra. Infrared spectra were obtained from a Nicolet 380 FTIR spectrometer.

Typical procedure for reaction condition screening

The reaction was run at a 0.2 mmol scale based on the limiting reagent. A 4 mL vial was charged with palladium salt, silver salt, cyclohexanone, iodobenzene, ligand and 1 mL solvent. The vial was sealed with a PTFE lined cap and heated at 80 °C for 12 hours under stirring. Then the mixture was allowed to cool to room temperature. Appropriate amount of dodecane (~10 mg) was added to the reaction mixture as internal standard and the mixture was stirred for an additional 5 min to fully mix. ~0.3 mL of the resulting mixture was filtered through a small plug of silica gel, eluted with diethyl ether. The filtrate was directly used for GC analysis.

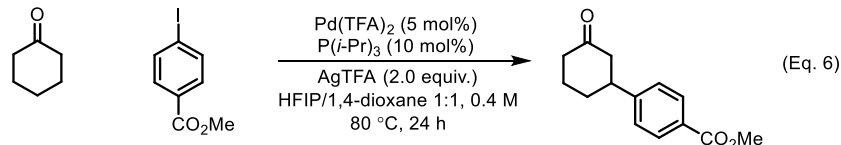
GC instrument conditions: inlet temperature: 250 °C, detector temperature: 300 °C, hydrogen flow: 40 mL/min, air flow: 400 mL/min, column + makeup flow: 30 mL/min. Method: 50 °C hold for 0 min, followed by a temperature increase of 10°C/min to 300 °C, hold 0 min (total run time: 25 min). Retention times were as follows: cyclohexanone (3.67), iodobenzene (5.71), dodecane (7.99) and 3-phenylcyclohexanone (12.54).

Typical procedure for substrate scope

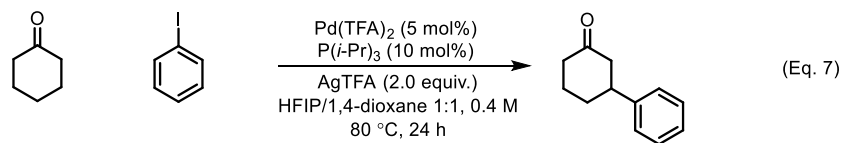
Unless stated otherwise, an 8 mL vial was charged with Pd(TFA)₂ (13.3 mg, 0.1 equiv.), AgTFA (176 mg, 2.0 equiv.), hexafluoroisopropanol (1 mL), ketone (1.0 mmol, 2.5 equiv.) and aryl iodide/bromide (0.4 mmol). The vial was sealed with a PTFE lined cap and transferred to a glove box. The vial was opened and 1,4-dioxane (1 mL) and P(*i*-Pr)₃ (16 µL, 0.2 equiv.) were

added under N₂ purging. The vial was then sealed again and heated in a pie-block at 80 °C for 12 hours under stirring. Then, the vial was allowed to cool to room temperature and the mixture was filtered through a small plug of silica gel, eluted with diethyl ether. The solvent was then removed *in vacuo* and flash column chromatography (hexane/ethyl acetate or DCM/methanol) of the residue gave the arylation product.

Procedures for large-scale synthesis

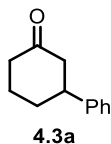


A flame-dried 50 mL Schlenk flask was charged with methyl 4-iodobenzoate (1.57 g, 6.0 mmol), cyclohexanone (1.54 mL, 15 mmol), Pd(TFA)₂ (100 mg, 0.30 mmol) and AgTFA (2.65 g, 12 mmol). The flask was then transferred to glove-box under N₂. 7.5 mL of HFIP and 1,4-dioxane were added to the flask (15 mL solvent in total, 0.4 M concentration). P(*i*-Pr)₃ (114 μL, 0.60 mmol) was then added to the mixture. The flask was sealed with a rubber cap and heated in an oil bath at 80 °C for 24 hours under stirring. The mixture was then allowed to cool to room temperature and passed through a small plug of silica gel, eluted with diethyl ether. The solvent was removed *in vacuo* and flash column chromatography of the residue afforded the product as a white solid (1.22 g, 88% yield).

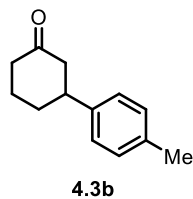


A flame-dried 25 mL Schlenk flask was charged with iodobenzene (1.22 g, 6.0 mmol), cyclohexanone (1.54 mL, 15 mmol), Pd(TFA)₂ (100 mg, 0.30 mmol) and AgTFA (2.65 g, 12 mmol). The flask was then transferred to glove-box under N₂. 7.5 mL of HFIP and 1,4-dioxane were added to the flask (15 mL solvent in total, 0.4 M concentration). P(*i*-Pr)₃ (114 μL, 0.60 mmol) was then added to the mixture. The flask was sealed with a rubber cap and heated in an oil bath at 80 °C for 24 hours under stirring. The mixture was then allowed to cool to room temperature and passed through a small plug of silica gel, eluted with diethyl ether. The solvent was removed *in vacuo* and flash column chromatography of the residue afforded the product as a colorless oil (714 mg, 69% yield).

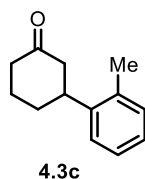
Characterization data



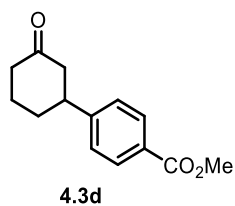
3-Phenylcyclohexanone (4.3a)²²: 72% Yield. Colorless oil. R_f = 0.7 (Hex/EA = 5:1). ¹H NMR (400 MHz, CDCl₃) δ 7.35-7.32 (m, 2H), 7.25-7.22 (m, 3H), 3.01 (tt, *J* = 11.6, 3.6 Hz, 1H), 2.63-2.34 (m, 4H), 2.19-2.07 (m, 2H), 1.91-1.72 (m, 2H). HRMS calcd C₁₂H₁₄O [M]⁺: 174.1045. Found: 174.1045.



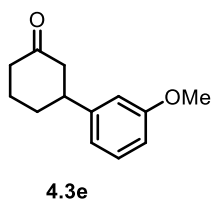
3-(*p*-Tolyl)cyclohexanone (4.3b)²²: 65% Yield. Colorless oil. $R_f = 0.7$ (Hex/EA = 5:1). **¹H NMR** (400 MHz, CDCl₃) δ 7.16-7.10 (m, 4H), 3.02-2.94 (m, 1H), 2.57-2.32 (m, 4H), 2.33 (s, 3H), 2.18-2.11 (m, 1H), 2.10-2.03 (m, 1H), 1.89-1.70 (m, 2H). **HRMS** calcd C₁₃H₁₆O [M]⁺: 188.1201. Found: 188.1201.



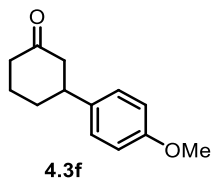
3-(*o*-Tolyl)cyclohexanone (4.3c)²³: 70% Yield. Colorless oil. $R_f = 0.7$ (Hex/EA = 5:1). **¹H NMR** (400 MHz, CDCl₃) δ 7.25-7.12 (m, 4H), 3.25-3.17 (m, 1H), 2.53-2.37 (m, 4H), 2.33 (s, 3H), 2.21-2.14 (m, 1H), 2.04-1.99 (m, 1H), 1.90-1.74 (m, 2H). **HRMS** calcd C₁₃H₁₆O [M]⁺: 188.1201. Found: 188.1199.



Methyl 4-(3-oxocyclohexyl)benzoate (4.3d)²²: 96% Yield. White solid. $R_f = 0.5$ (Hex/EA = 5:1). **¹H NMR** (400 MHz, CDCl₃) δ 7.99 (d, $J = 8.4$ Hz, 2H), 7.28 (d, $J = 8.4$ Hz, 2H), 3.90 (s, 3H), 3.10-3.03 (m, 1H), 2.62-2.34 (m, 4H), 2.19-2.13 (m, 1H), 2.11-2.06 (m, 1H), 1.92-1.73 (m, 2H). **HRMS** calcd C₁₄H₁₆O₃ [M]⁺: 232.1099. Found: 232.1096.

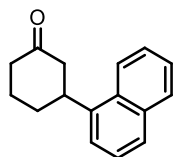


3-(3-Methoxyphenyl)cyclohexanone (4.3e)²⁴: 80% Yield. Colorless oil. $R_f = 0.4$ (Hex/EA = 5:1). **¹H NMR** (400 MHz, CDCl₃) δ 7.27-7.23 (m, 1H), 6.83-6.76 (m, 3H), 3.80 (s, 3H), 2.98 (tt, $J_1 = 11.7$ Hz, $J_2 = 3.9$ Hz, 1H), 2.62-2.57 (m, 1H), 2.55-2.51 (m, 1H), 2.49-2.43 (m, 1H), 2.41-2.33 (m, 1H), 2.18-2.06 (m, 2H), 1.90-1.71 (m, 2H). **HRMS** calcd C₁₃H₁₆O₂ [M]⁺: 204.1150. Found: 204.1148.



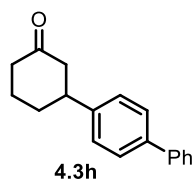
3-(4-methoxyphenyl)cyclohexanone (4.3f)²²: 52% Yield. Colorless oil. $R_f = 0.5$ (Hex/EA = 5:1). **¹H NMR** (400 MHz, CDCl₃) δ 7.15-7.12 (m, 2H), 6.88-6.85 (m, 2H), 3.79 (s,

3H), 2.96 (tt, $J_1 = 11.7$ Hz, $J_2 = 4.0$ Hz, 1H), 2.60-2.32 (m, 4H), 2.16-2.10 (m, 1H), 2.08-2.02 (m, 1H), 1.86-1.70 (m, 2H). **HRMS** calcd $C_{13}H_{16}O_2$ $[M]^+$: 204.1150. Found: 204.1148.



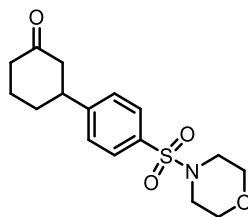
4.3g

3-(Naphthalen-1-yl)cyclohexanone (4.3g)²²: 48% Yield. White solid. $R_f = 0.6$ (Hex/EA = 5:1). **1H NMR** (400 MHz, $CDCl_3$) δ 8.04 (d, $J = 8.3$ Hz, 1H), 7.88 (d, $J = 7.9$ Hz, 1H), 7.76 (d, $J = 8.1$ Hz, 1H), 7.56-7.45 (m, 3H), 7.40 (d, $J = 6.4$ Hz, 1H) 3.86 (tt, $J_1 = 11.7$ Hz, $J_2 = 3.6$ Hz, 1H), 2.80-2.74 (m, 1H), 2.70-2.63 (m, 1H), 2.59-2.53 (m, 1H), 2.51-2.42 (m, 1H), 2.28-2.17 (m, 2H), 2.06-1.87 (m, 2H). **HRMS** calcd $C_{16}H_{16}O$ $[M]^+$: 224.1201. Found: 224.1208.



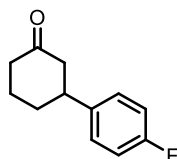
4.3h

3-([1,1'-Biphenyl]-4-yl)cyclohexanone (4.3h)²³: 65% Yield. White solid. $R_f = 0.7$ (Hex/EA = 5:1). **1H NMR** (400 MHz, $CDCl_3$) δ 7.60-7.55 (m, 4H), 7.46-7.42 (m, 2H), 7.37-7.29 (m, 3H), 3.11-3.03 (m, 1H), 2.67-2.62 (m, 1H), 2.60-2.54 (m, 1H), 2.52-2.46 (m, 1H), 2.45-2.36 (m, 1H), 2.21-2.11 (m, 2H), 1.95-1.78 (m, 2H). **HRMS** calcd $C_{18}H_{18}O$ $[M]^+$: 250.1358. Found: 250.1363.



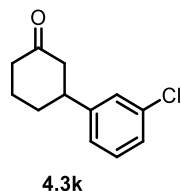
4.3i

3-(4-(morpholinylsulfonyl)phenyl)cyclohexanone (4.3i): 88% Yield. White solid. Mp. 95-98 °C. $R_f = 0.3$ (Hex/EA = 2:1). $^1\text{H NMR}$ (400 MHz, CDCl_3) δ 7.71 (d, $J = 8.4$ Hz, 2H), 7.40 (d, $J = 8.4$ Hz, 2H), 3.76-3.73 (m, 4H), 3.15-3.07 (m, 1H), 3.01-2.99 (m, 4H), 2.64-2.36 (m, 4H), 2.21-2.09 (m, 2H), 1.93-1.75 (m, 2H). $^{13}\text{C NMR}$ (100 MHz, CDCl_3) δ 209.81, 149.71, 133.44, 128.39, 127.40, 66.08, 48.28, 45.94, 44.46, 41.04, 32.40, 25.33. **IR** (KBr, cm^{-1}) 2957, 2863, 1707, 1452, 1345, 1166, 1114, 944, 738. **HRMS** calcd $\text{C}_{16}\text{H}_{21}\text{NNaO}_4\text{S}$ $[\text{M}+\text{Na}]^+$: 346.1089. Found: 346.1081.

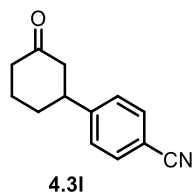


4.3j

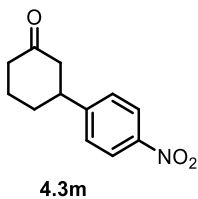
3-(4-Fluorophenyl)cyclohexanone (4.3j)²²: 65% Yield. Colorless oil. $R_f = 0.6$ (Hex/EA = 5:1). $^1\text{H NMR}$ (400 MHz, CDCl_3) δ 7.18-7.14 (m, 2H), 7.02-6.97 (m, 2H), 3.02-2.94 (m, 1H), 2.59-2.31 (m, 4H), 2.16-2.10 (m, 1H), 2.08-2.04 (m, 1H), 1.85-1.69 (m, 2H). **HRMS** calcd $\text{C}_{12}\text{H}_{13}\text{FO}$ $[\text{M}]^+$: 192.0950. Found: 192.0946.



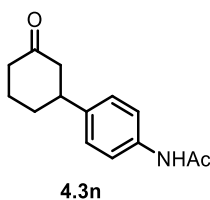
3-(3-chlorophenyl)cyclohexanone (4.3k)²²: 64% Yield. Colorless oil. $R_f = 0.7$ (Hex/EA = 5:1). **¹H NMR** (400 MHz, CDCl₃) δ 7.26-7.18 (m, 3H), 7.09-7.06 (m, 1H), 3.01-2.93 (m, 1H), 2.60-2.28 (m, 4H), 2.17-2.11 (m, 1H), 2.09-2.04 (m, 1H), 1.87-1.70 (m, 2H). **HRMS** calcd C₁₂H₁₃O³⁵Cl [M]⁺: 208.0655. Found: 208.0653.



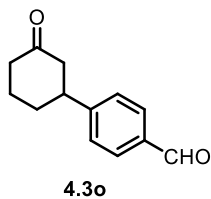
4-(3-Oxocyclohexyl)benzonitrile (4.3l)²⁵: 70% Yield. White solid. $R_f = 0.4$ (Hex/EA = 2:1). **¹H NMR** (400 MHz, CDCl₃) δ 7.64-7.61 (m, 2H), 7.34-7.31 (m, 2H), 3.07 (tt, $J_1 = 11.7$ Hz, $J_2 = 4.0$ Hz, 1H), 2.61-2.56 (m, 1H), 2.53-2.45 (m, 2H), 2.43-2.34 (m, 1H), 2.20-2.13 (m, 1H), 2.11-2.05 (m, 1H), 1.90-1.73 (m, 2H). **HRMS** calcd C₁₃H₁₃NNaO [M+Na]⁺: 222.0895. Found: 222.0894.



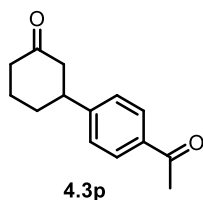
3-(4-Nitrophenyl)cyclohexanone (4.3m): 57% Yield. Light yellow solid. Mp. 75-78 °C. $R_f = 0.2$ (Hex/EA = 5:1). **$^1\text{H NMR}$** (400 MHz, CDCl_3) δ 8.19 (d, $J = 8.5$ Hz, 2H), 7.39 (d, $J = 8.5$ Hz, 2H), 3.17-3.10 (m, 1H), 2.63-2.36 (m, 4H), 2.21-2.09 (m, 2H), 1.93-1.75 (m, 2H). **$^{13}\text{C NMR}$** (100 MHz, CDCl_3) δ 209.56, 151.50, 127.51, 124.04, 48.21, 44.44, 41.01, 32.34, 25.29. **IR** (KBr, cm^{-1}) 2939, 1707, 1596, 1346, 1224, 1109, 852. **HRMS** calcd $\text{C}_{12}\text{H}_{14}\text{NO}_3$ $[\text{M}+\text{H}]^+$: 220.0974. Found: 220.0973.



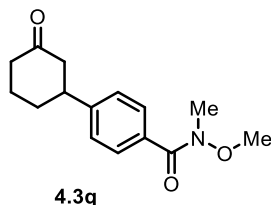
N-(4-(3-oxocyclohexyl)phenyl)acetamide (4.3n): 77% Yield. White solid. Mp. 108-110 °C. $R_f = 0.2$ (Hex/EA = 2:1). **$^1\text{H NMR}$** (400 MHz, CDCl_3) δ 7.44 (d, $J = 8.5$ Hz, 2H), 7.24 (br, 1H), 7.16 (d, $J = 8.5$ Hz, 2H), 3.01-2.94 (m, 1H), 2.59-2.33 (m, 4H), 2.17 (s, 3H), 2.14-2.01 (m, 2H), 1.87-1.73 (m, 2H). **$^{13}\text{C NMR}$** (100 MHz, CDCl_3) δ 211.03, 168.25, 140.37, 136.33, 127.08, 120.26, 48.95, 44.19, 41.16, 32.78, 25.45, 24.55. **IR** (KBr, cm^{-1}) 3309, 2934, 1701, 1669, 1537, 1516, 1413, 1317, 829. **HRMS** calcd $\text{C}_{14}\text{H}_{18}\text{NO}_2$ $[\text{M}+\text{H}]^+$: 232.1338. Found: 232.1328.



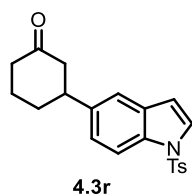
4-(3-Oxocyclohexyl)benzaldehyde (4.3o): 63% Yield. Colorless oil. $R_f = 0.2$ (Hex/EA = 5:1). $^1\text{H NMR}$ (400 MHz, CDCl_3) δ 9.98 (s, 1H), 7.85 (d, $J = 8.2$ Hz, 2H), 7.39 (d, $J = 8.2$ Hz, 2H), 3.14-3.06 (m, 1H), 2.63-2.36 (m, 4H), 2.20-2.13 (m, 1H), 2.13-2.08 (m, 1H), 1.94-1.74 (m, 2H). $^{13}\text{C NMR}$ (100 MHz, CDCl_3) δ 210.19, 191.80, 151.16, 135.14, 130.26, 127.32, 48.31, 44.79, 41.08, 32.37, 25.39. **IR** (KBr, cm^{-1}). 2938, 2864, 1699, 1606, 1424, 1310, 1211, 1170, 823. **HRMS** calcd $\text{C}_{13}\text{H}_{14}\text{O}_2$ $[\text{M}]^+$: 202.0994. Found: 202.0993.



3-(4-Acetylphenyl)cyclohexanone (4.3p)²²: 70% Yield. White solid. $R_f = 0.3$ (Hex/EA = 5:1). $^1\text{H NMR}$ (400 MHz, CDCl_3) δ 7.90 (d, $J = 8.4$ Hz, 2H), 7.29 (d, $J = 8.4$ Hz, 2H), 3.10-3.02 (m, 1H), 2.56 (s, 3H), 2.54-2.33 (m, 4H), 2.17-2.11 (m, 1H), 2.10-2.05 (m, 1H), 1.90-1.71 (m, 2H). **HRMS** calcd $\text{C}_{14}\text{H}_{16}\text{O}_2$ $[\text{M}]^+$: 216.1150. Found: 216.1151.



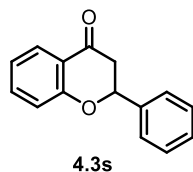
***N*-Methoxy-*N*-methyl-4-(3-oxocyclohexyl)benzamide (4.3q):** 88% Yield. Colorless oil. $R_f = 0.4$ (Hex/EA = 2:1). $^1\text{H NMR}$ (400 MHz, CDCl_3) δ 7.65 (d, $J = 8.4$ Hz, 2H), 7.24 (d, $J = 8.4$ Hz, 2H), 3.56 (s, 3H), 3.35 (s, 3H), 3.08-3.00 (m, 1H), 2.62-2.34 (m, 4H), 2.18-2.07 (m, 2H), 1.90-1.72 (m, 2H). $^{13}\text{C NMR}$ (100 MHz, CDCl_3) δ 210.62, 169.60, 146.91, 132.41, 128.69, 126.26, 61.06, 48.57, 44.54, 41.13, 32.53, 25.43. **IR** (KBr, cm^{-1}) 2930, 1711, 1639, 1421, 1377, 1224, 977, 840. **HRMS** calcd $\text{C}_{15}\text{H}_{20}\text{NO}_3$ $[\text{M}+\text{H}]^+$: 262.1443. Found: 262.1444.



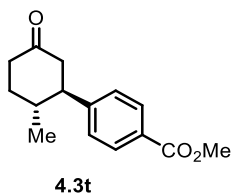
3-(1-Tosyl-1H-indol-5-yl)cyclohexanone (4.3r): 44% Yield. White solid. Mp. 95-97 °C. $R_f = 0.3$ (Hex/EA = 5:1). $^1\text{H NMR}$ (400 MHz, CDCl_3) δ 7.92 (d, $J = 8.4$ Hz, 1H), 7.77 (d, $J = 8.4$ Hz, 2H), 7.55 (d, $J = 3.6$ Hz, 1H), 7.36 (d, $J = 1.6$ Hz, 1H), 7.23 (d, $J = 8.4$ Hz, 2H), 7.17 (dd, $J_1 = 8.6$ Hz, $J_2 = 1.8$ Hz, 1H), 6.61 (d, $J = 4.0$ Hz, 1H), 3.11-3.03 (m, 1H), 2.62-2.37 (m, 4H), 2.34 (s, 3H), 2.17-2.06 (m, 2H), 1.91-1.71 (m, 2H). $^{13}\text{C NMR}$ (100 MHz, CDCl_3) δ 211.02, 144.94, 139.53, 135.31, 133.58, 130.99, 129.89, 126.82, 126.70, 123.54, 118.89, 113.60, 108.83, 49.28,

44.61, 41.18, 33.12, 25.48, 21.57. **IR** (KBr, cm^{-1}) 2960, 1706, 1647, 1368, 1172, 813, 682.

HRMS calcd $\text{C}_{21}\text{H}_{21}\text{NNaO}_3\text{S}$ $[\text{M}+\text{Na}]^+$: 390.1140. Found: 390.1130.

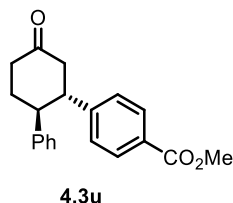


Flavanone (4.3s)²⁶: 32% Yield. White solid. $R_f = 0.8$ (Hex/EA = 5:1). **$^1\text{H NMR}$** (400 MHz, CDCl_3) δ 7.93 (dd, $J_1 = 8.0$ Hz, $J_2 = 1.6$ Hz, 1H), 7.52-7.35 (m, 6H), 7.07-7.03 (m, 2H), 5.48 (dd, $J_1 = 13.4$ Hz, $J_2 = 2.9$ Hz, 1H), 3.09 (dd, $J_1 = 16.9$ Hz, $J_2 = 13.4$ Hz, 1H), 2.89 (dd, $J_1 = 16.9$ Hz, $J_2 = 2.9$ Hz, 1H). **HRMS** calcd $\text{C}_{15}\text{H}_{12}\text{O}_2$ $[\text{M}]^+$: 224.0837. Found: 224.0828.

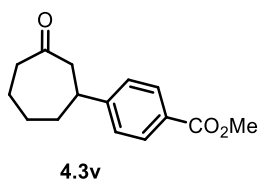


Methyl 4-(2-methyl-5-oxocyclohexyl)benzoate (4.3t): 56% Yield. White solid. Mp. 59-62 °C. $R_f = 0.5$ (Hex/EA = 5:1). **$^1\text{H NMR}$** (400 MHz, CDCl_3) δ 8.00 (d, $J = 8.4$ Hz, 2H), 7.25 (d, $J = 8.4$ Hz, 2H), 3.91 (s, 3H), 2.67-2.45 (m, 5H), 2.19-2.04 (m, 2H), 1.61-1.50 (m, 1H), 0.77 (d, $J = 6.4$ Hz, 3H). **$^{13}\text{C NMR}$** (100 MHz, CDCl_3) δ 210.22, 166.85, 148.78, 130.11, 128.76, 127.28, 52.08, 51.99, 48.64, 41.29, 36.58, 34.51, 19.18. **IR** (KBr, cm^{-1}) 2954, 2926, 1717, 1610, 1280,

1111, 770, 709. **HRMS** calcd C₁₅H₁₈NaO₃ [M+Na]⁺: 269.1154. Found: 269.1148. Relative stereochemistry (*trans*) is determined by NOE studies.

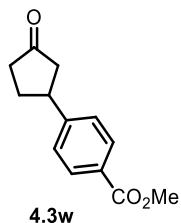


Methyl 4-(5-oxo-2-phenylcyclohexyl)benzoate (4.3u): 45% Yield. White solid. Mp. 106-108 °C. R_f = 0.3 (Hex/EA = 5:1). **¹H NMR** (400 MHz, CDCl₃) δ 7.83-7.80 (m, 2H), 7.14-7.03 (m, 5H), 7.01-6.99 (m, 2H), 3.84 (s, 3H), 3.33-3.18 (m, 2H), 2.78-2.58 (m, 4H), 2.35-2.27 (m, 1H), 2.16-2.05 (m, 1H). **¹³C NMR** (100 MHz, CDCl₃) δ 209.47, 166.79, 147.77, 142.21, 129.75, 128.39, 127.31, 126.58, 51.99, 50.64, 49.11, 48.86, 41.50, 34.33. **IR** (KBr, cm⁻¹) 2952, 1717, 1611, 1181, 1114, 702. **HRMS** calcd C₂₀H₂₀NaO₃ [M+Na]⁺: 331.1310. Found: 331.1296. Relative stereochemistry (*trans*) is determined by X-ray structure of crystal.

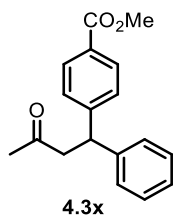


Methyl 4-(3-oxocycloheptyl)benzoate (4.3v): 60% Yield. White solid. Mp. 68 °C. R_f = 0.5 (Hex/EA = 5:1). **¹H NMR** (400 MHz, CDCl₃) δ 7.95 (d, *J* = 8.4 Hz, 2H), 7.22 (d, *J* = 8.4 Hz, 2H), 3.88 (s, 3H), 2.94-2.88 (m, 2H), 2.62-2.55 (m, 3H), 2.07-1.95 (m, 3H), 1.77-1.66 (m, 2H),

1.53-1.43 (m, 1H). ^{13}C NMR (100 MHz, CDCl_3) δ 212.84, 166.86, 152.01, 130.03, 128.33, 126.46, 52.02, 50.73, 43.88, 42.72, 38.88, 29.15, 24.04. IR (KBr, cm^{-1}) 2928, 1717, 1699, 1610, 1436, 1282, 1113, 770, 707. HRMS calcd $\text{C}_{15}\text{H}_{18}\text{O}_3$ $[\text{M}]^+$: 246.1256. Found: 246.1261.

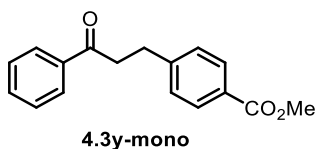


Methyl 4-(3-oxocyclopentyl)benzoate (4.3w): 55% Yield. White solid. Mp. 69 °C. R_f = 0.4 (Hex/EA = 5:1). ^1H NMR (400 MHz, CDCl_3) δ 8.01 (d, J = 8.8 Hz, 2H), 7.33 (d, J = 8.4 Hz, 2H), 3.92 (s, 3H), 3.52-3.44 (m, 1H), 2.73-2.67 (m, 1H), 2.52-2.44 (m, 2H), 2.39-2.28 (m, 2H), 2.05-1.95 (m, 1H). ^{13}C NMR (100 MHz, CDCl_3) δ 217.55, 166.81, 148.30, 130.00, 128.70, 126.77, 52.10, 45.45, 42.20, 38.73, 30.96. IR (KBr, cm^{-1}) 2953, 1739, 1717, 1609, 1432, 1100, 773. HRMS calcd $\text{C}_{13}\text{H}_{14}\text{O}_3$ $[\text{M}]^+$: 218.0943. Found: 218.0946.

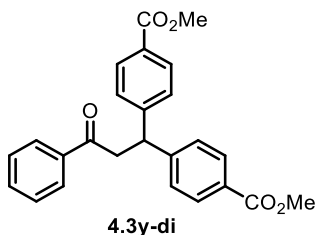


Methyl 4-(3-oxo-1-phenylbutyl)benzoate (4.3x): 67% Yield. Colorless oil. R_f = 0.4 (Hex/EA = 5:1). ^1H NMR (400 MHz, CDCl_3) δ 7.94-7.92 (m, 2H), 7.29-7.25 (m, 4H), 7.19-7.18

(m, 3H), 4.63 (t, $J = 7.5$ Hz, 1H), 3.86 (s, 3H), 3.19 (d, $J = 7.5$ Hz, 2H), 2.08 (s, 3H). ^{13}C NMR (100 MHz, CDCl_3) δ 206.27, 166.86, 149.14, 143.00, 129.92, 128.72, 128.37, 127.76, 127.68, 126.73, 52.04, 49.25, 45.85, 30.66. **IR** (KBr, cm^{-1}) 3028, 2952, 1719, 1610, 1435, 1281, 1110, 1018, 709. **HRMS** calcd $\text{C}_{18}\text{H}_{18}\text{NaO}_3$ $[\text{M}+\text{Na}]^+$: 305.1154. Found: 305.1154.

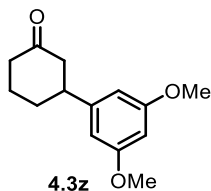


Methyl 4-(3-oxo-3-phenylpropyl)benzoate (4.3y-mono)²⁷: 15% Yield. White solid. $R_f = 0.6$ (Hex/EA = 5:1). ^1H NMR (400 MHz, CDCl_3) δ 7.98-7.94 (m, 4H), 7.59-7.54 (m, 1H), 7.48-7.44 (m, 2H), 7.34-7.31 (m, 2H), 3.90 (s, 3H), 3.33 (t, $J = 7.5$ Hz, 2H), 3.13 (t, $J = 7.5$ Hz, 2H). **HRMS** calcd $\text{C}_{17}\text{H}_{16}\text{NaO}_3$ $[\text{M}+\text{Na}]^+$: 291.0997. Found: 291.0991.

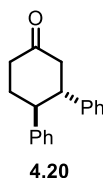


Dimethyl 4,4'-(3-oxo-3-phenylpropane-1,1-diyl)dibenzoate (4.3y-di): 76% Yield. White solid. $R_f = 0.2$ (Hex/EA = 5:1). ^1H NMR (400 MHz, CDCl_3) δ 7.95-7.90 (m, 6H), 7.57-7.53 (m, 1H), 7.44 (t, $J = 7.7$ Hz, 2H), 7.31 (d, $J = 8.3$ Hz, 4H), 4.93 (t, $J = 7.3$ Hz, 1H), 3.86 (s, 6H), 3.76 (d, $J = 7.3$ Hz, 2H). ^{13}C NMR (100 MHz, CDCl_3) δ 197.09, 166.76, 148.49, 136.65,

133.40, 130.04, 128.71, 128.61, 128.01, 127.88, 52.07, 45.81, 44.02. **IR** (KBr, cm^{-1}) 2952, 1717, 1688, 1607, 1436, 1281, 1111, 758. **HRMS** calcd $\text{C}_{25}\text{H}_{22}\text{NaO}_5$ $[\text{M}+\text{Na}]^+$: 425.1365. Found: 425.1360.



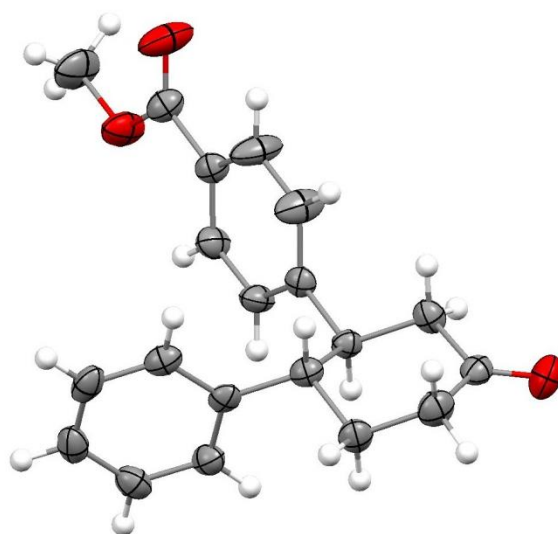
3-(3,5-Dimethoxyphenyl)cyclohexanone (4.3z)²⁸: 44% Yield. Colorless oil. $R_f = 0.5$ (Hex/EA = 5:1). **$^1\text{H NMR}$** (400 MHz, CDCl_3) δ 6.37 (d, $J = 2.2$ Hz, 2H), 6.34 ($J = 2.2$ Hz, 1H), 3.79 (s, 6H), 2.94 (tt, $J_1 = 11.8$ Hz, $J_2 = 3.9$ Hz, 1H), 2.61-2.51 (m, 1H), 2.53-2.49 (m, 1H), 2.48-2.42 (m, 1H), 2.41-2.33 (m, 1H), 2.18-2.11 (m, 1H), 2.10-2.06 (m, 1H), 1.88-1.70 (m, 2H). **HRMS** calcd $\text{C}_{14}\text{H}_{19}\text{O}_3$ $[\text{M}+\text{H}]^+$: 235.1334. Found: 235.1329.



trans-3,4-Diphenylcyclohexanone (4.20)²⁰: 46% Yield. White solid. $R_f = 0.6$ (Hex/EA = 5:1). **$^1\text{H NMR}$** (400 MHz, CDCl_3) δ 7.14-7.10 (m, 4H), 7.06-6.99 (m, 6H), 3.25-3.15 (m, 2H), 2.77-2.54 (m, 4H), 2.32-2.26 (m, 1H), 2.13-2.02 (m, 1H). **HRMS** calcd $\text{C}_{18}\text{H}_{18}\text{O}$ $[\text{M}]^+$: 250.1358. Found: 250.1358.

X-ray data for 4.3u

Figure 4.5 Crystal Structure of **4.3u**



Empirical formula	C ₂₀ H ₂₀ O ₃	
Formula weight	308.36	
Temperature	153(2) K	
Wavelength	0.71073 Å	
Crystal system	Orthorhombic	
Space group	P212121	
Unit cell dimensions	a = 8.1378(2) Å	α = 90°.
	b = 14.7951(5) Å	β = 90°.
	c = 27.4098(9) Å	γ = 90°.
Volume	3300.13(18) Å ³	

Z	8
Density (calculated)	1.241 Mg/m ³
Absorption coefficient	0.082 mm ⁻¹
F(000)	1312
Crystal size	0.42 x 0.32 x 0.15 mm ³
Theta range for data collection	2.61 to 25.13°.
Index ranges	-9<=h<=9, -17<=k<=17, -32<=l<=32
Reflections collected	38380
Independent reflections	5898 [R(int) = 0.0559]
Completeness to theta = 25.13°	99.8 %
Absorption correction	Semi-empirical from equivalents
Max. and min. transmission	1.00 and 0.857
Refinement method	Full-matrix least-squares on F ²
Data / restraints / parameters	5898 / 0 / 417
Goodness-of-fit on F ²	1.003
Final R indices [I>2sigma(I)]	R1 = 0.0422, wR2 = 0.0983
R indices (all data)	R1 = 0.0573, wR2 = 0.1059
Absolute structure parameter	-0.1(12)
Largest diff. peak and hole	0.341 and -0.204 e.Å ⁻³

4.5 $^1\text{H-NMR}$ and $^{13}\text{C-NMR}$ Spectra

Figure 4.6 $^1\text{H-NMR}$ Spectrum of 4.3a

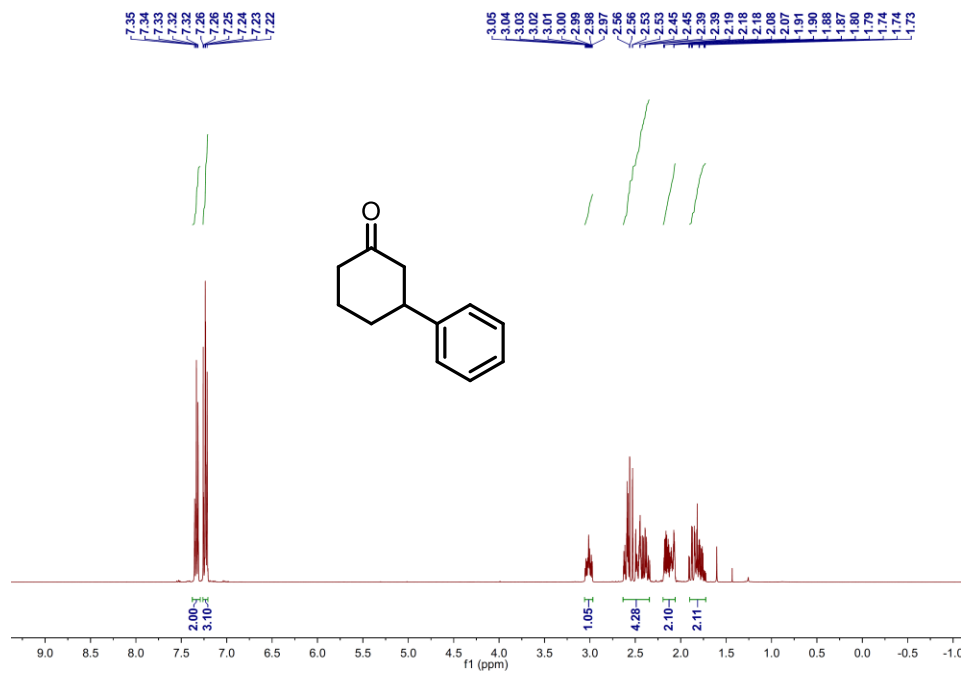


Figure 4.7 $^1\text{H-NMR}$ Spectrum of 4.3b

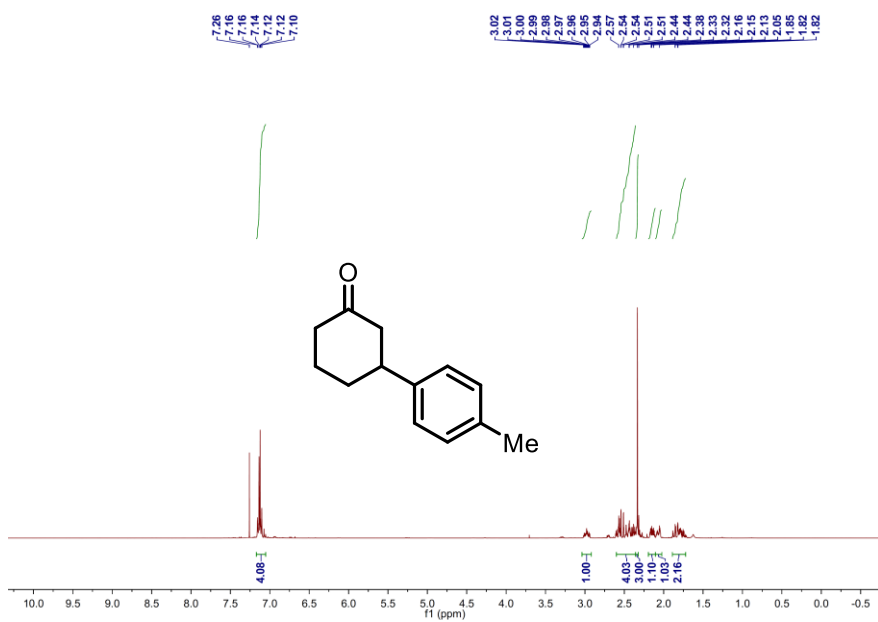


Figure 4.8 $^1\text{H-NMR}$ Spectrum of 4.3c

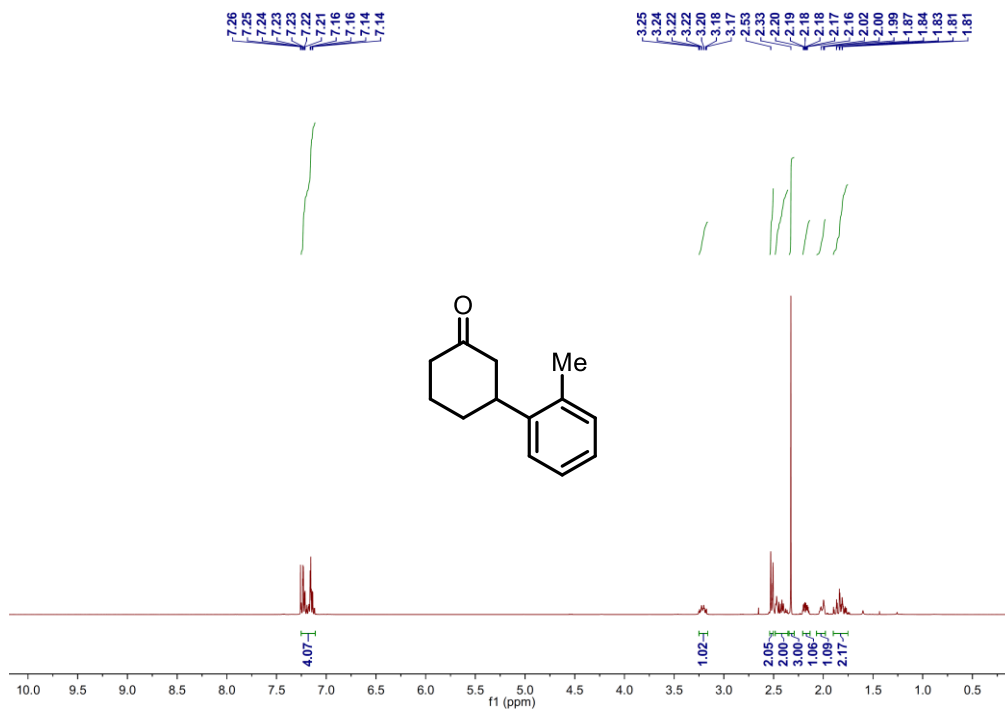


Figure 4.9 $^1\text{H-NMR}$ Spectrum of 4.3d

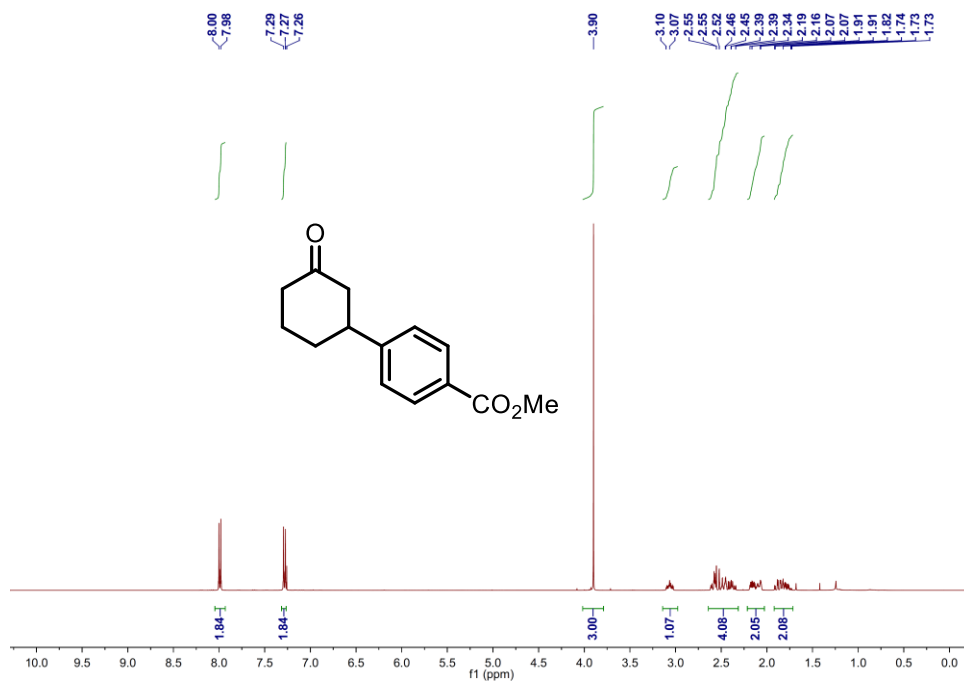


Figure 4.10 ¹H-NMR Spectrum of 4.3e

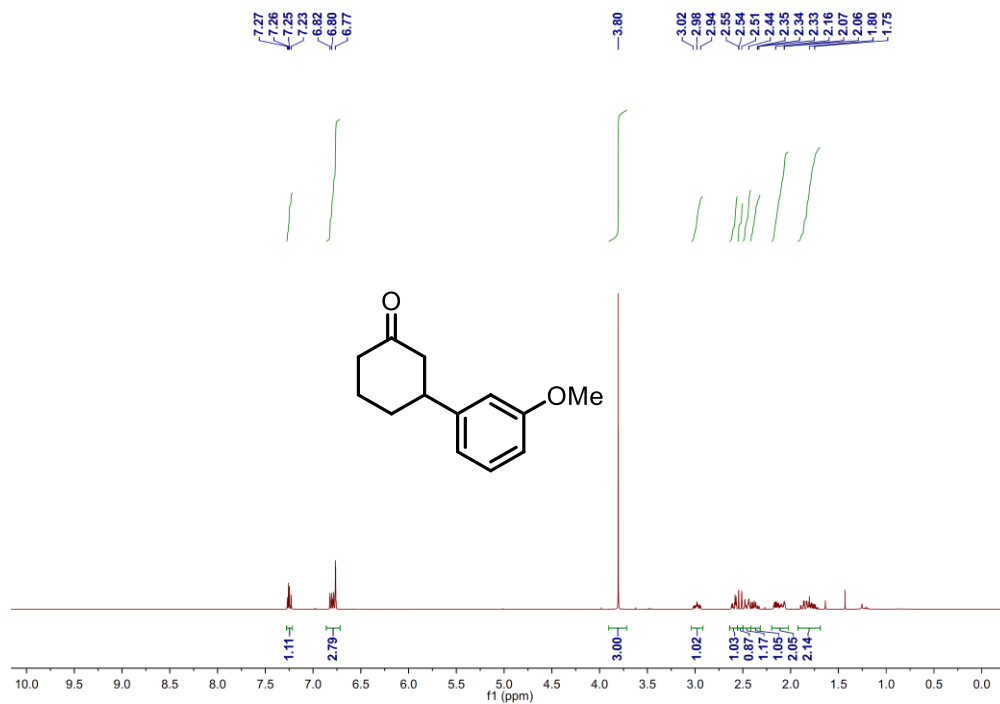


Figure 4.11 ¹H-NMR Spectrum of 4.3f

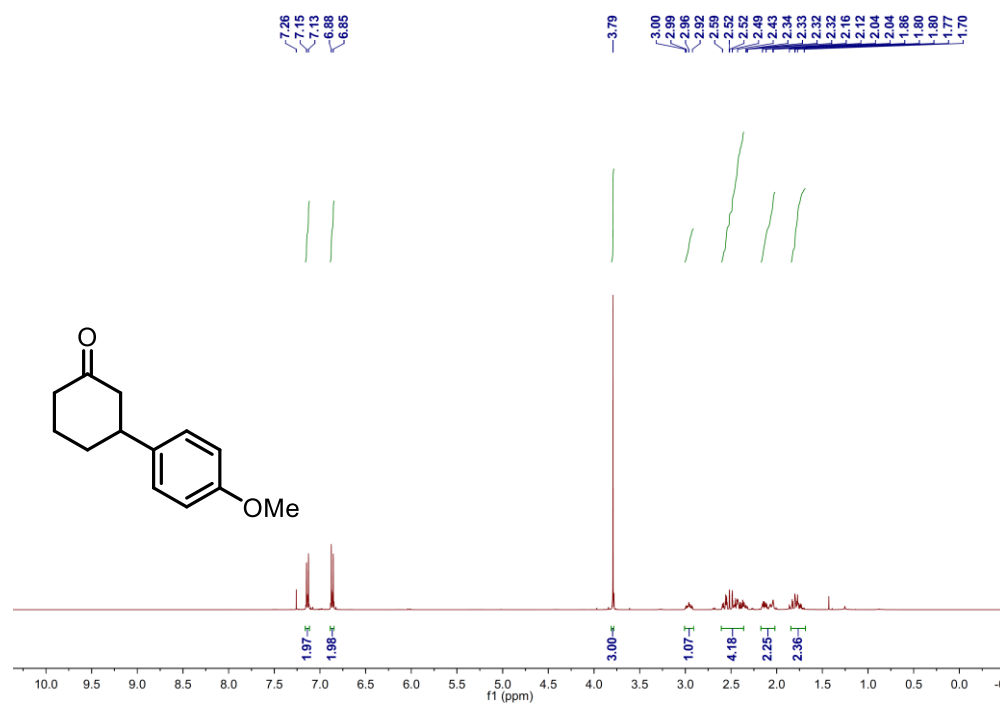


Figure 4.12 ¹H-NMR Spectrum of 4.3g

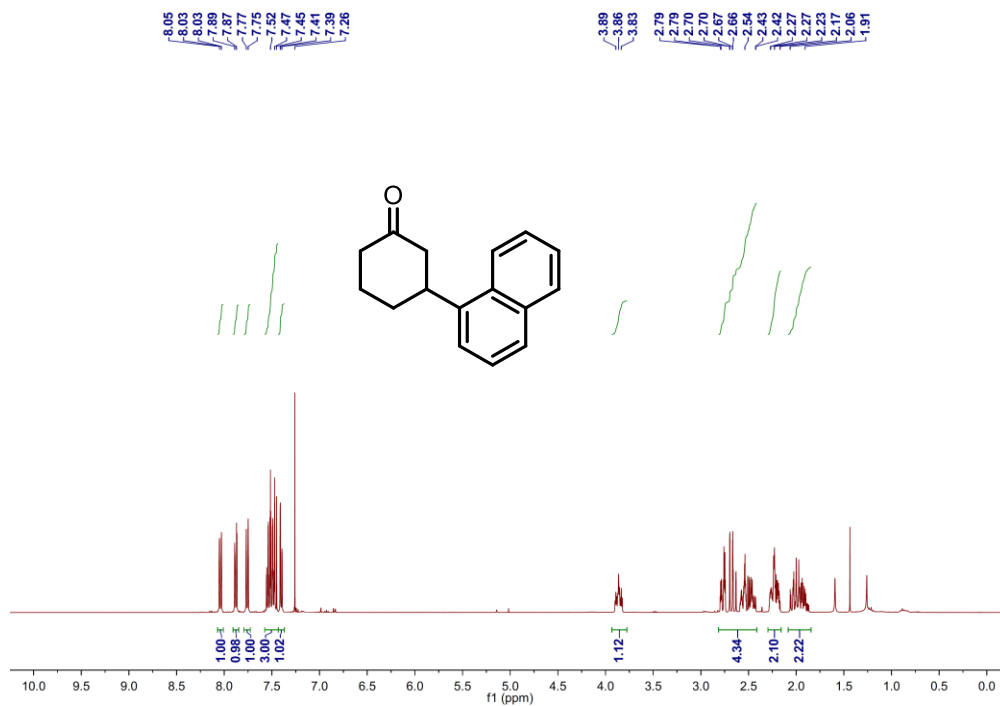


Figure 4.13 ¹H-NMR Spectrum of 4.3h

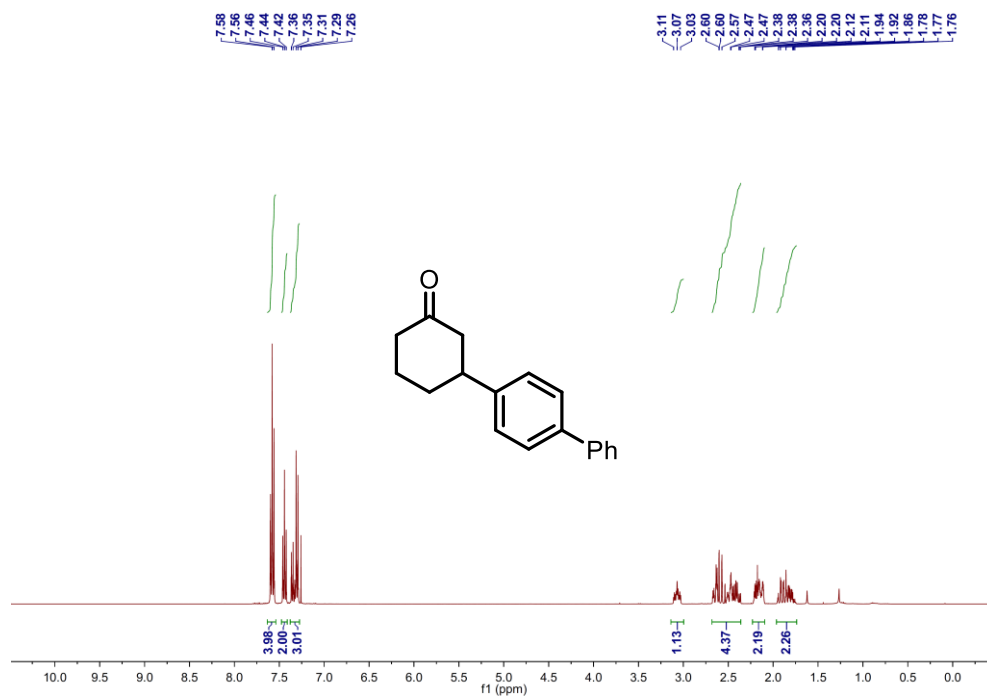


Figure 4.14 ^1H -NMR and ^{13}C -NMR Spectrum of 4.3i

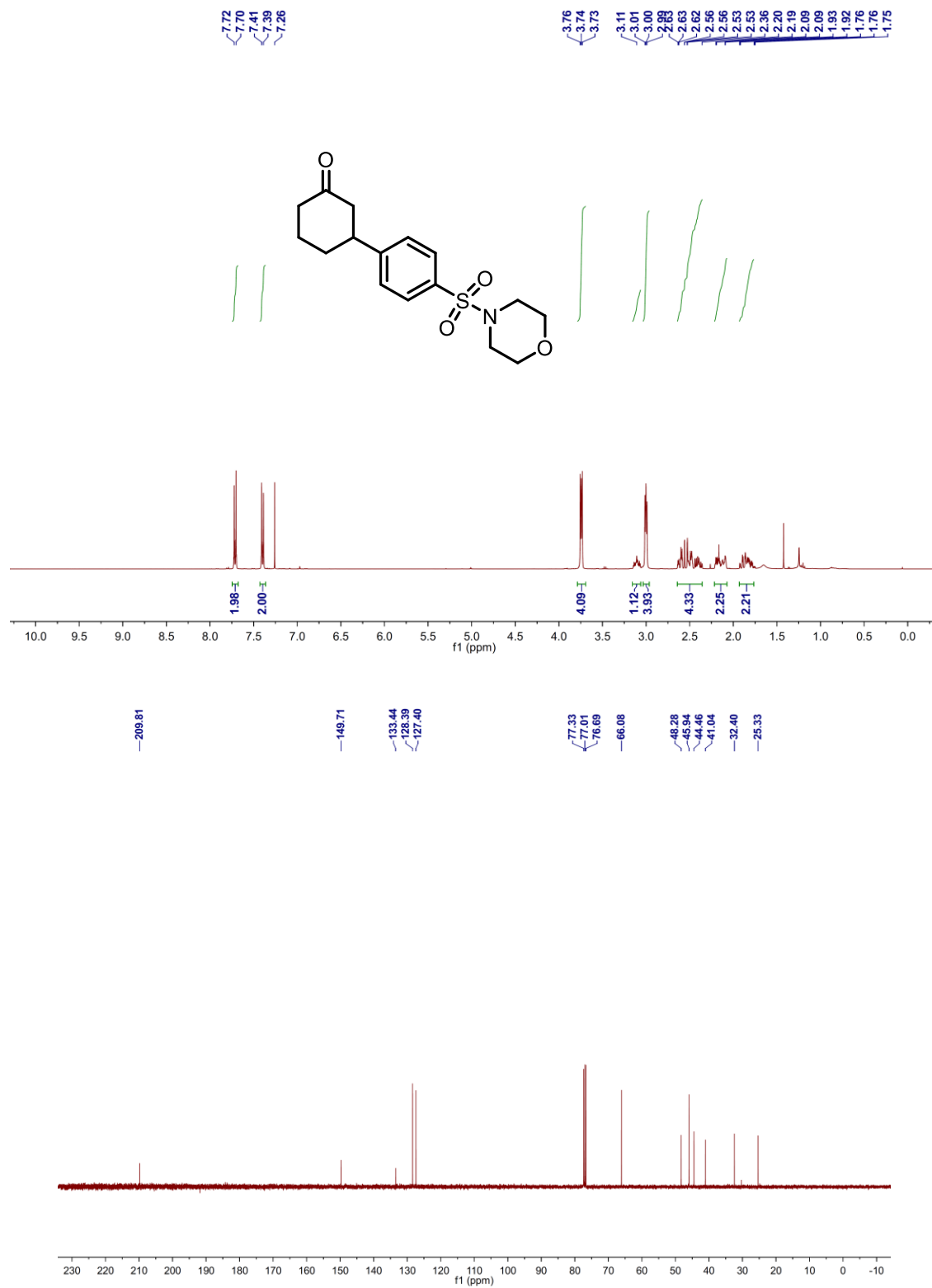


Figure 4.15 ¹H-NMR Spectrum of 4.3j

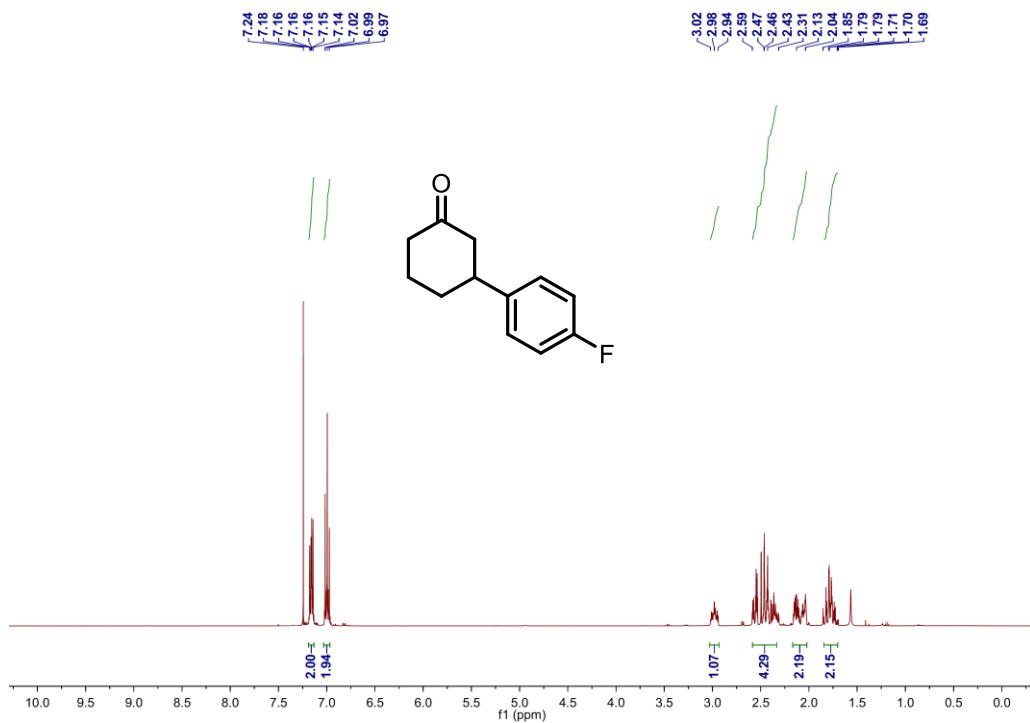


Figure 4.16 ¹H-NMR Spectrum of 4.3k

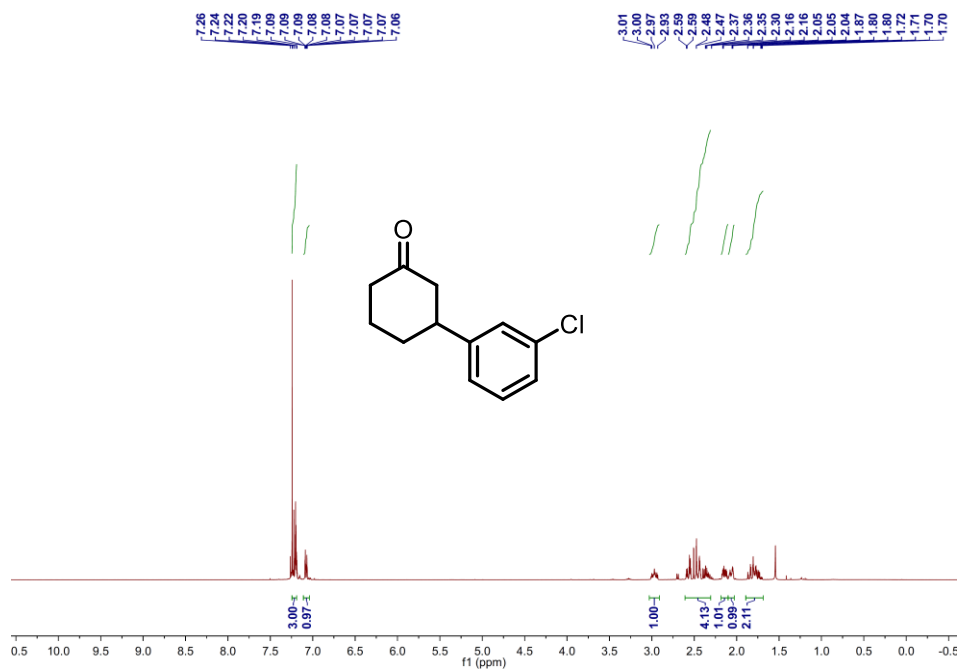


Figure 4.17 $^1\text{H-NMR}$ Spectrum of **4.31**

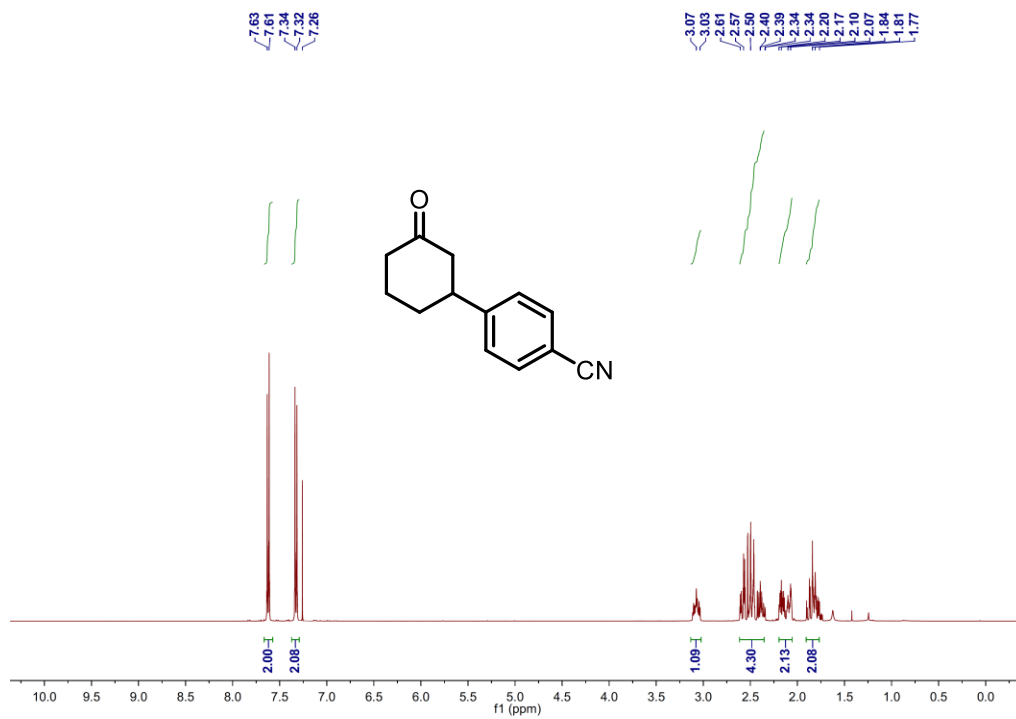


Figure 4.18 ^1H -NMR and ^{13}C -NMR Spectrum of 4.3m

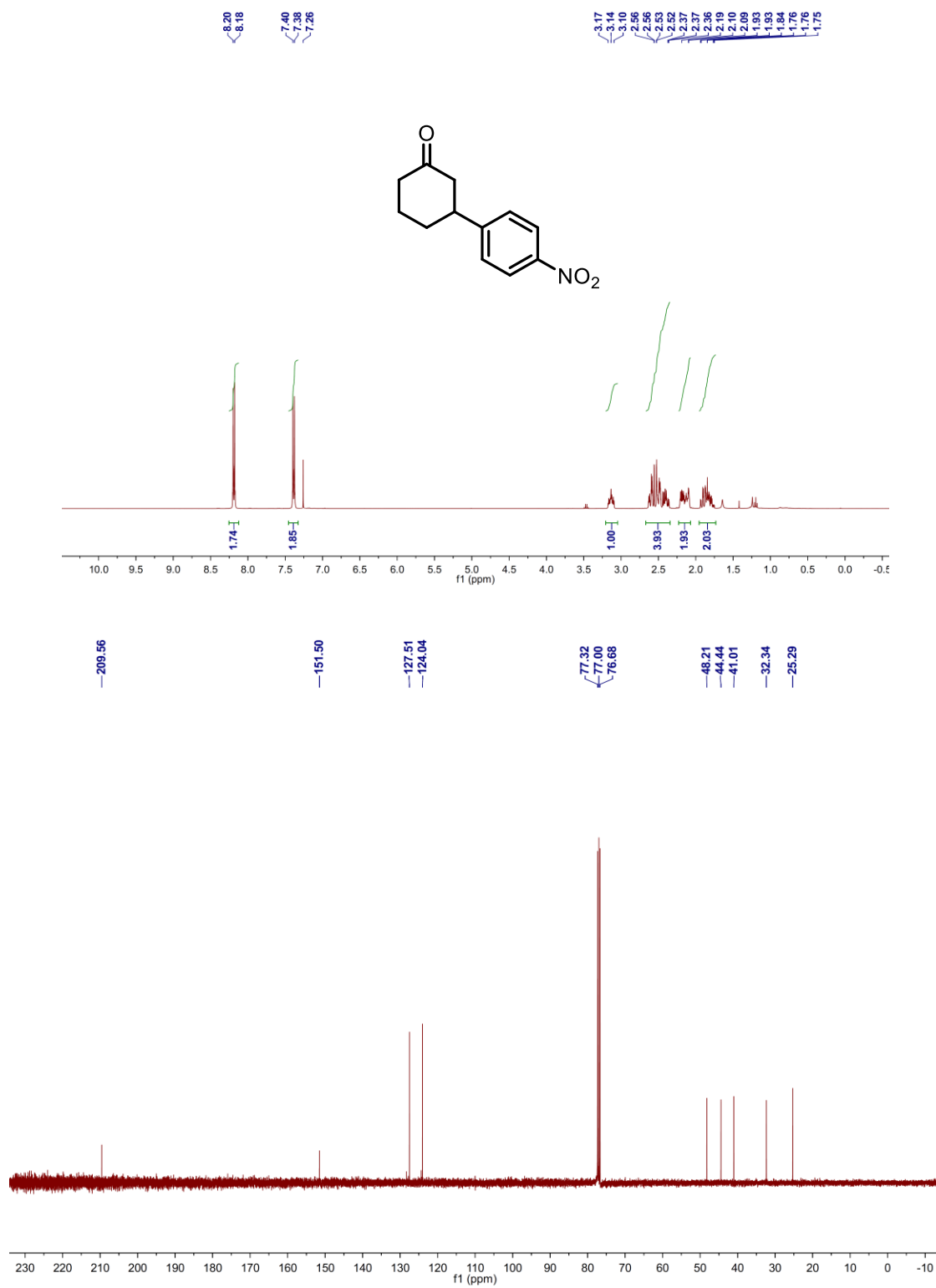


Figure 4.19 $^1\text{H-NMR}$ and $^{13}\text{C-NMR}$ Spectrum of 4.3n

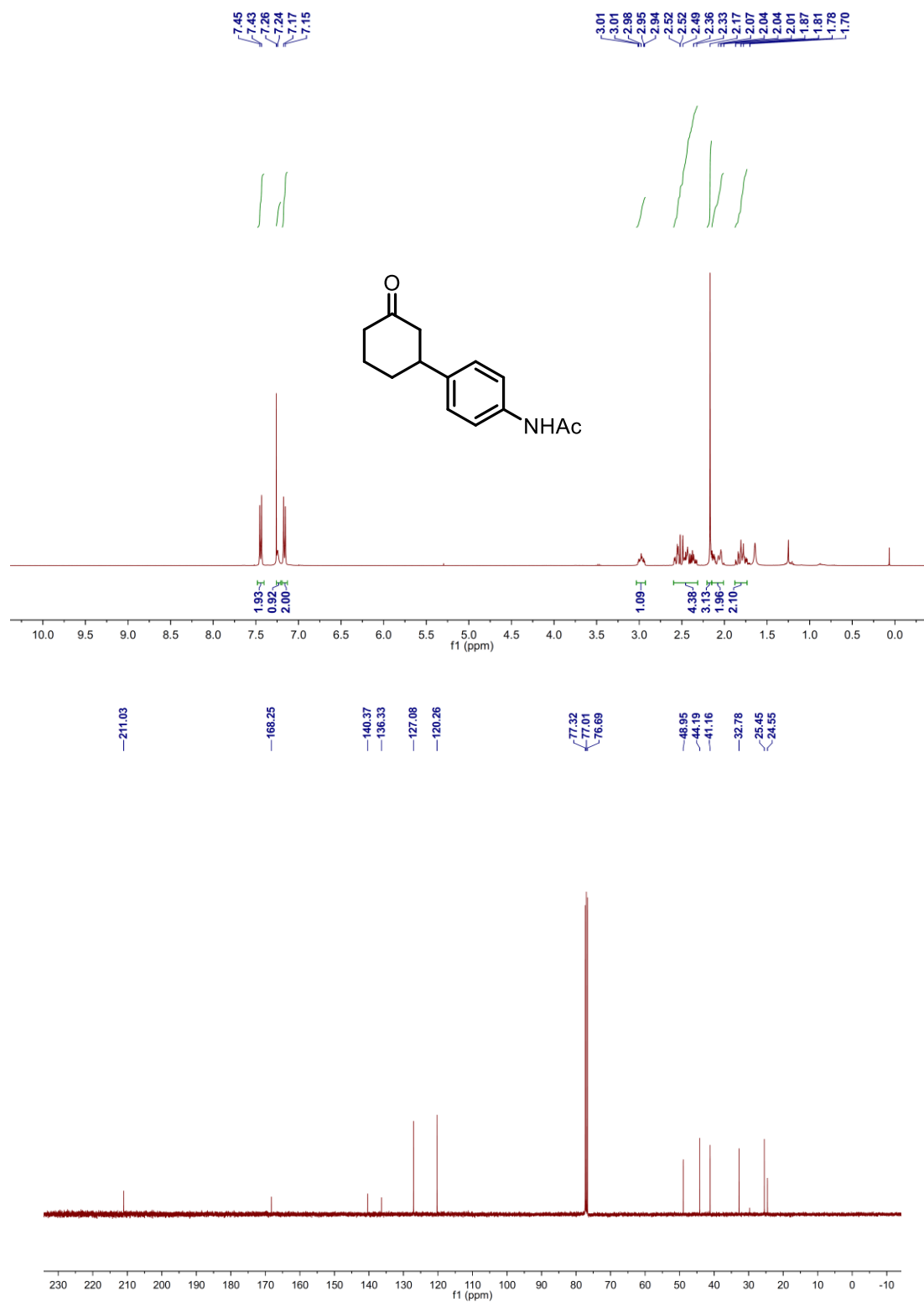


Figure 4.20 $^1\text{H-NMR}$ and $^{13}\text{C-NMR}$ Spectrum of 4.3o

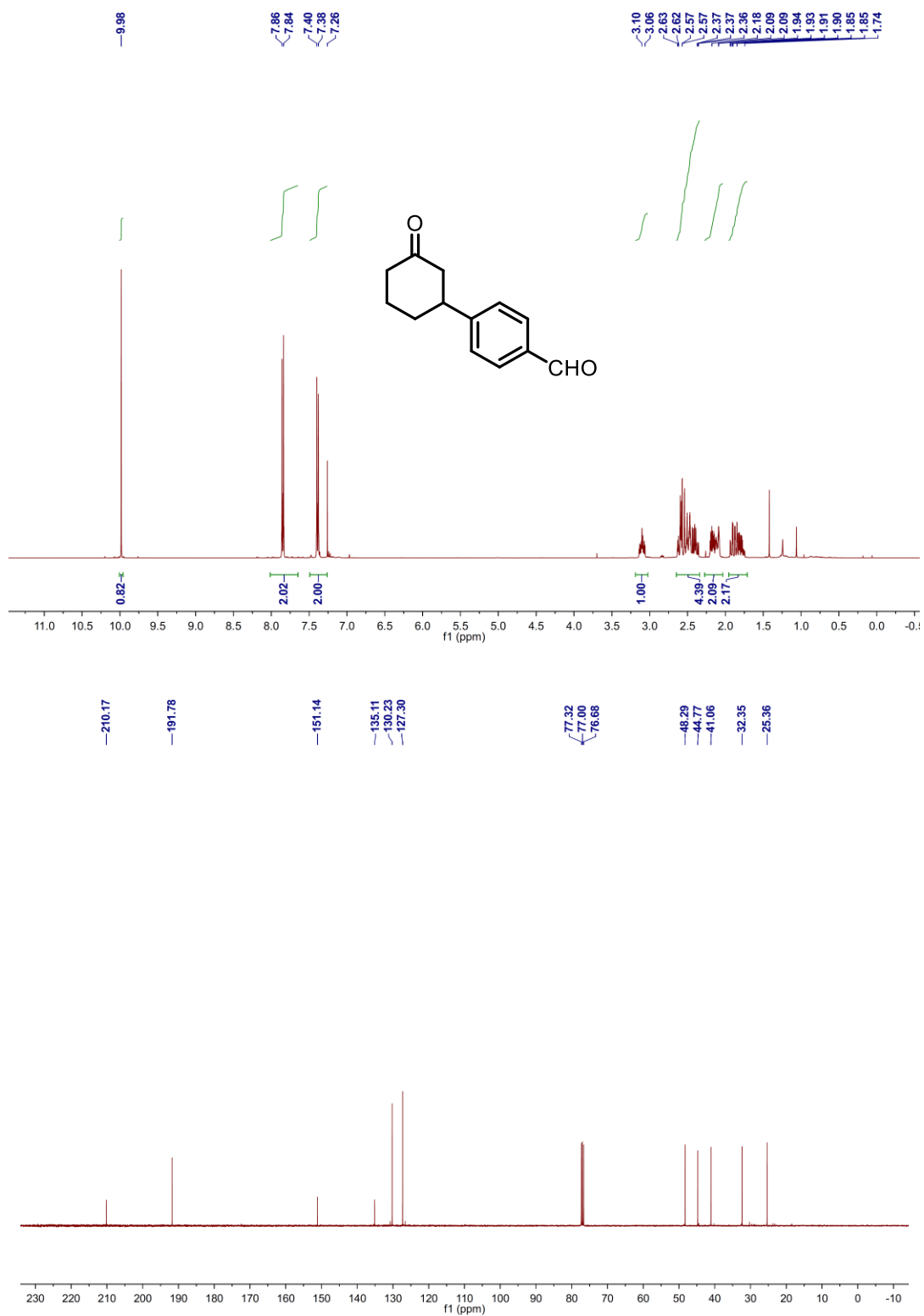


Figure 4.21 ¹H-NMR Spectrum of 4.3p

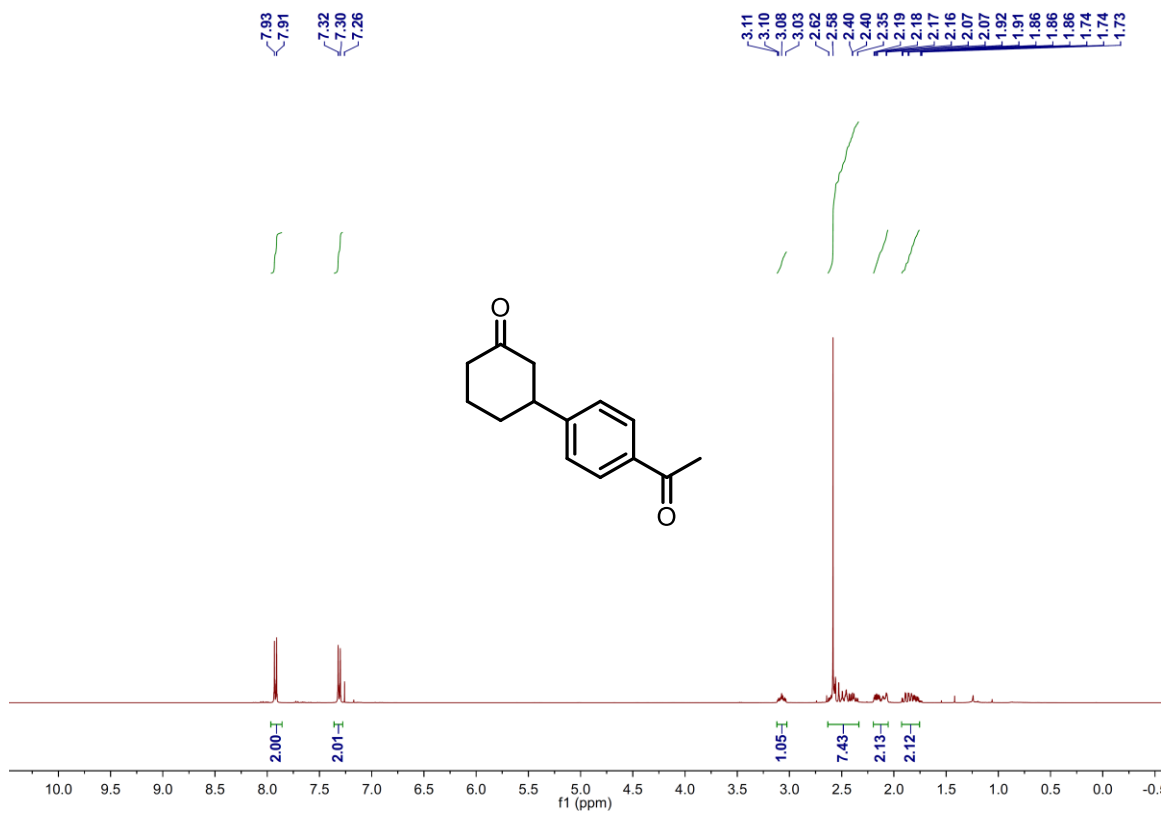


Figure 4.22 $^1\text{H-NMR}$ and $^{13}\text{C-NMR}$ Spectrum of 4.3q

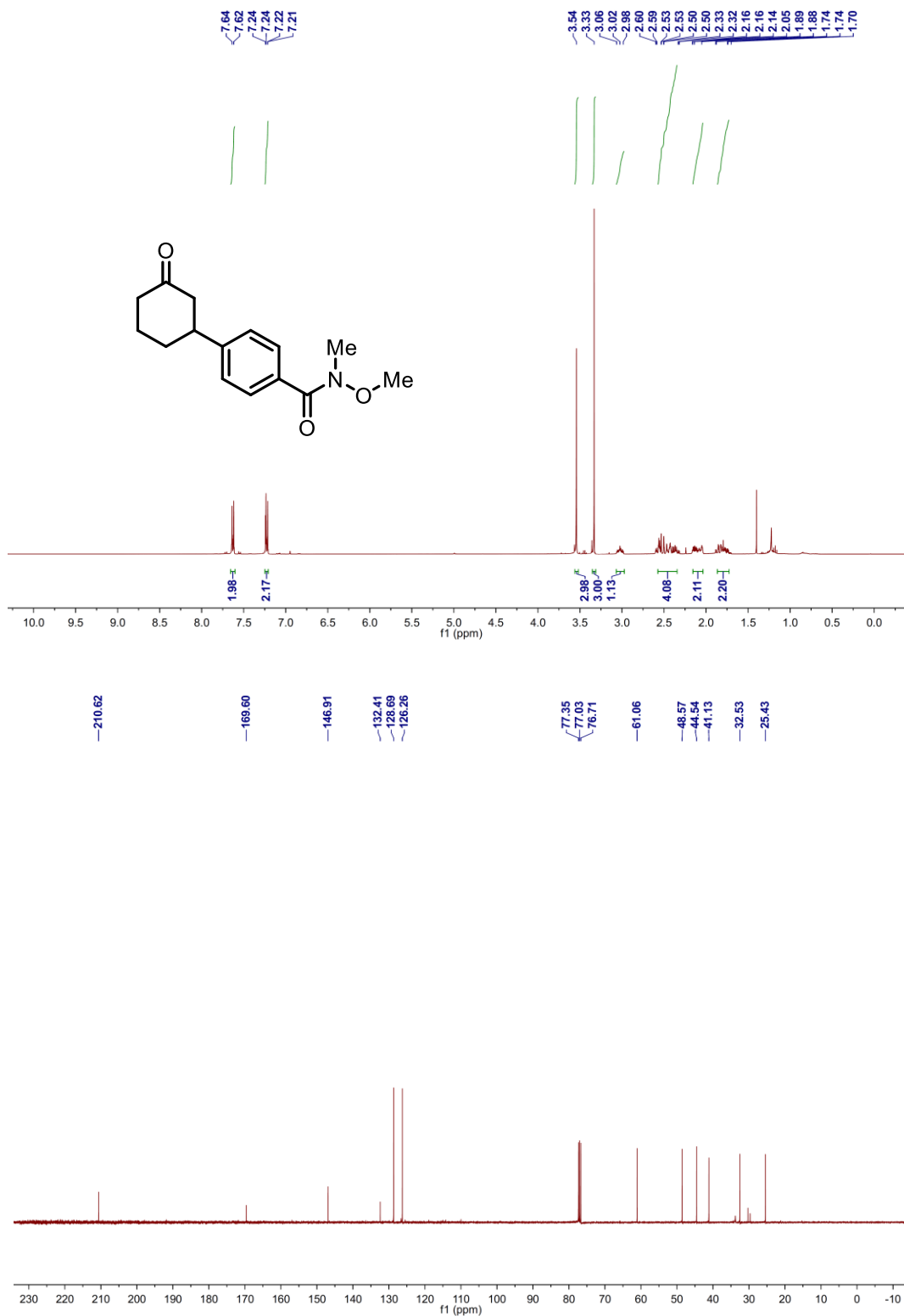


Figure 4.23 ¹H-NMR and ¹³C-NMR Spectrum of 4.3r

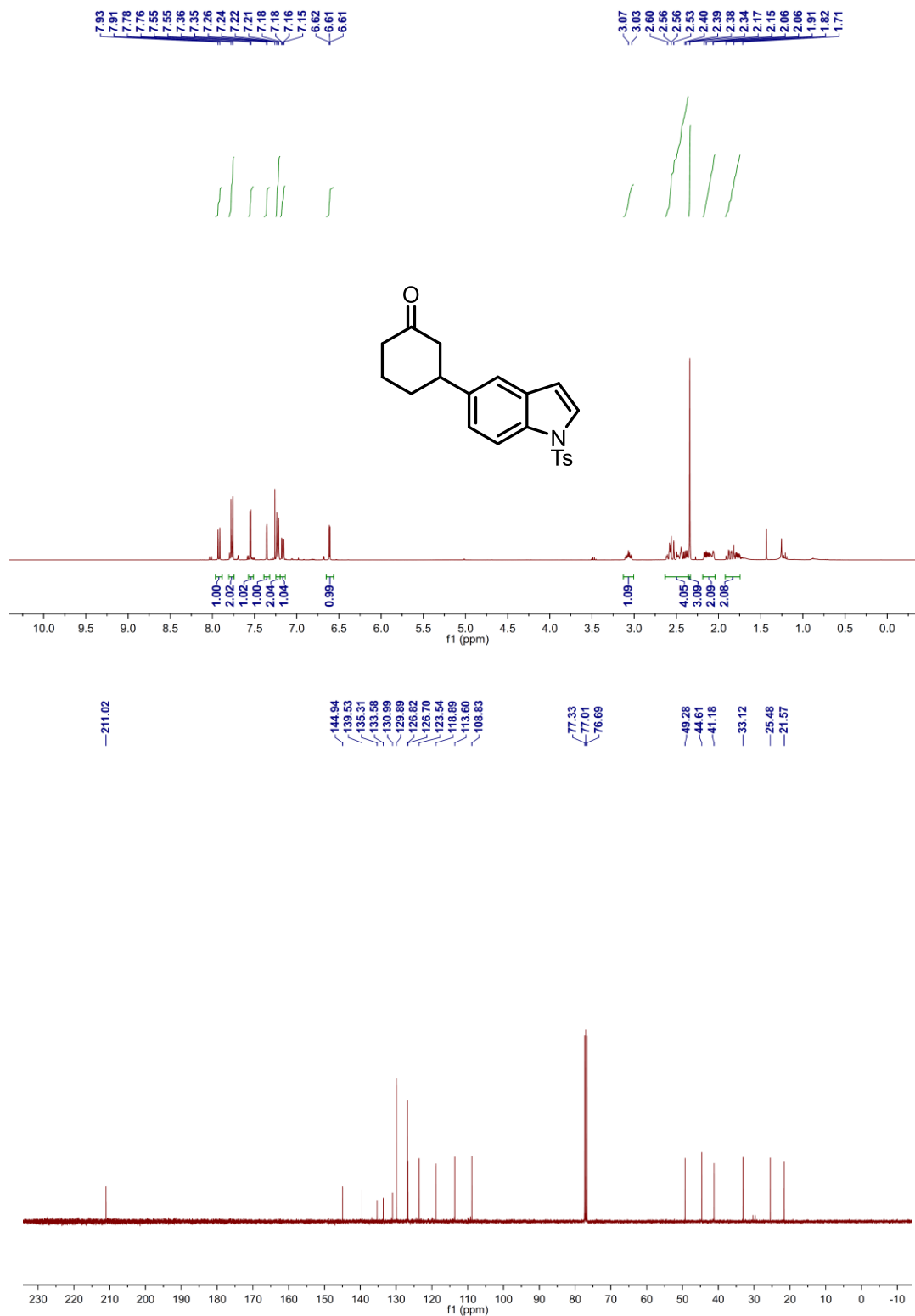


Figure 4.24 ¹H-NMR Spectrum of 4.3s

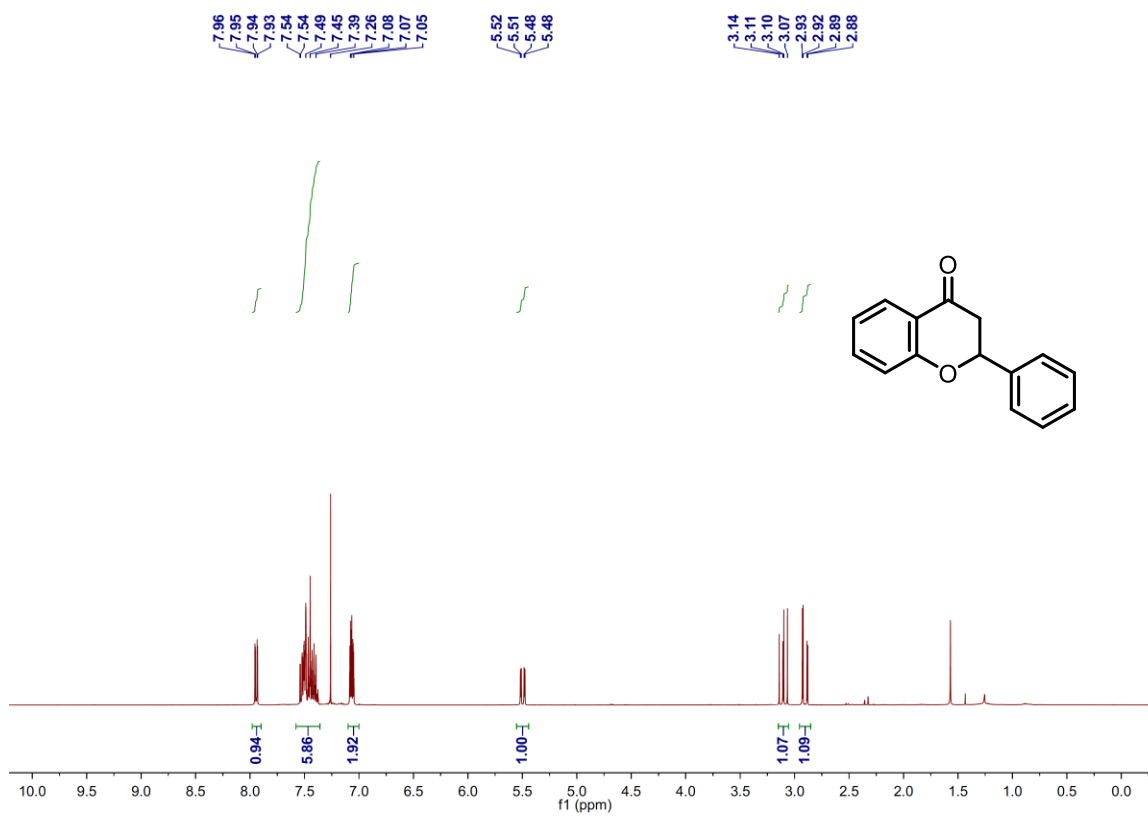


Figure 4.25 $^1\text{H-NMR}$ and $^{13}\text{C-NMR}$ Spectrum of 4.3t

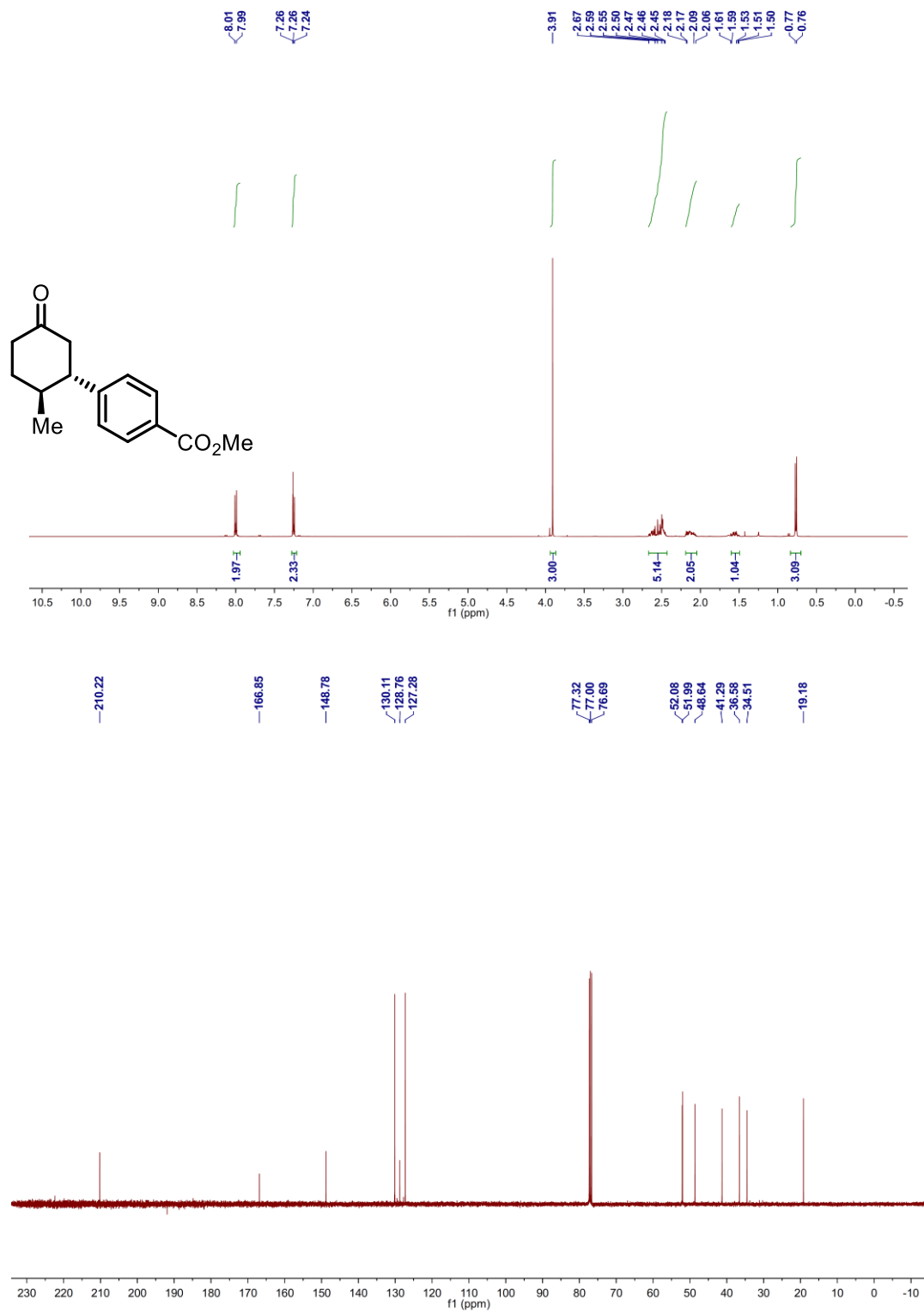


Figure 4.26 $^1\text{H-NMR}$ and $^{13}\text{C-NMR}$ Spectrum of 4.3u

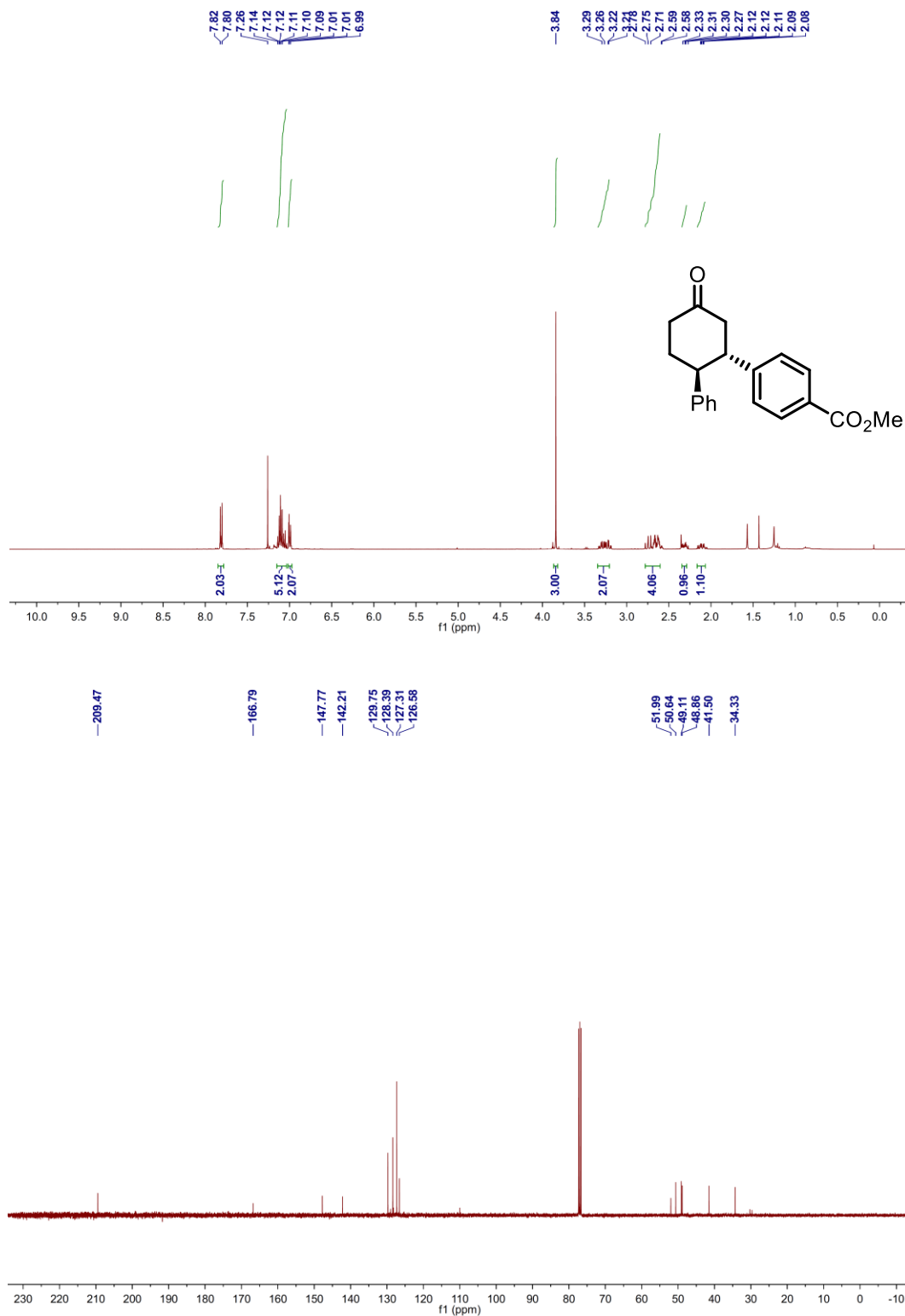


Figure 4.27 $^1\text{H-NMR}$ and $^{13}\text{C-NMR}$ Spectrum of 4.3v

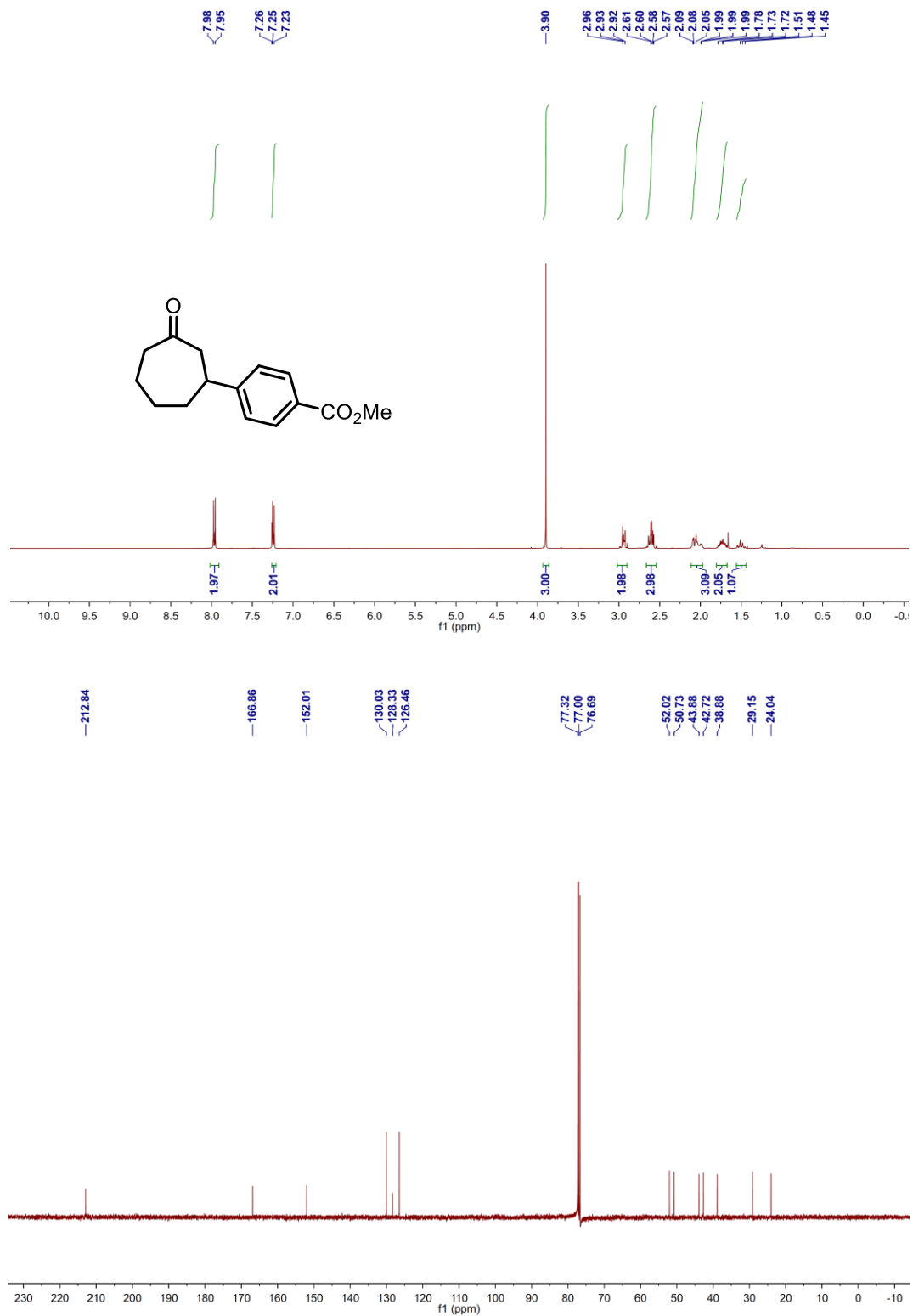


Figure 4.28 ^1H -NMR and ^{13}C -NMR Spectrum of 4.3w

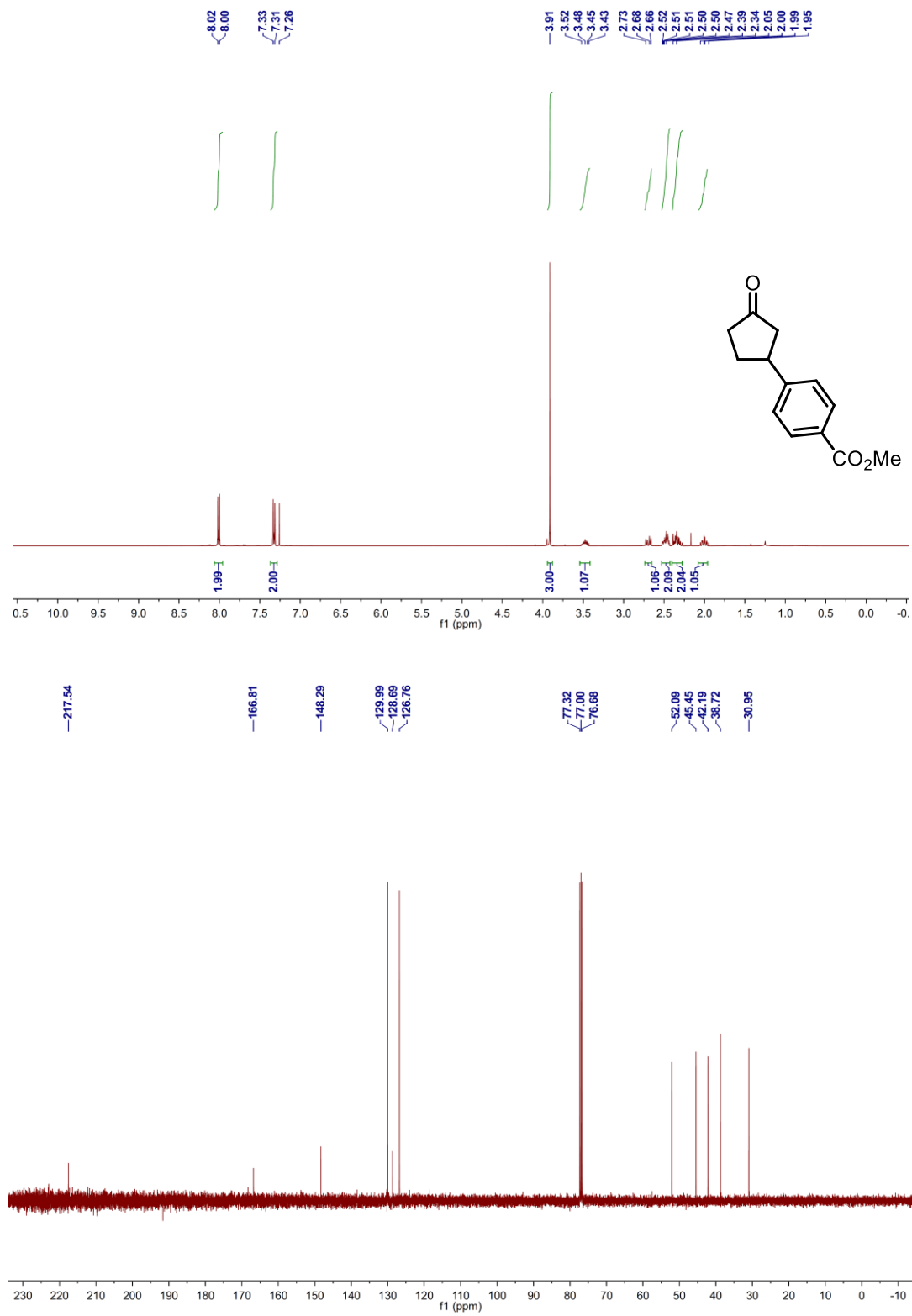


Figure 4.29 $^1\text{H-NMR}$ and $^{13}\text{C-NMR}$ Spectrum of 4.3x

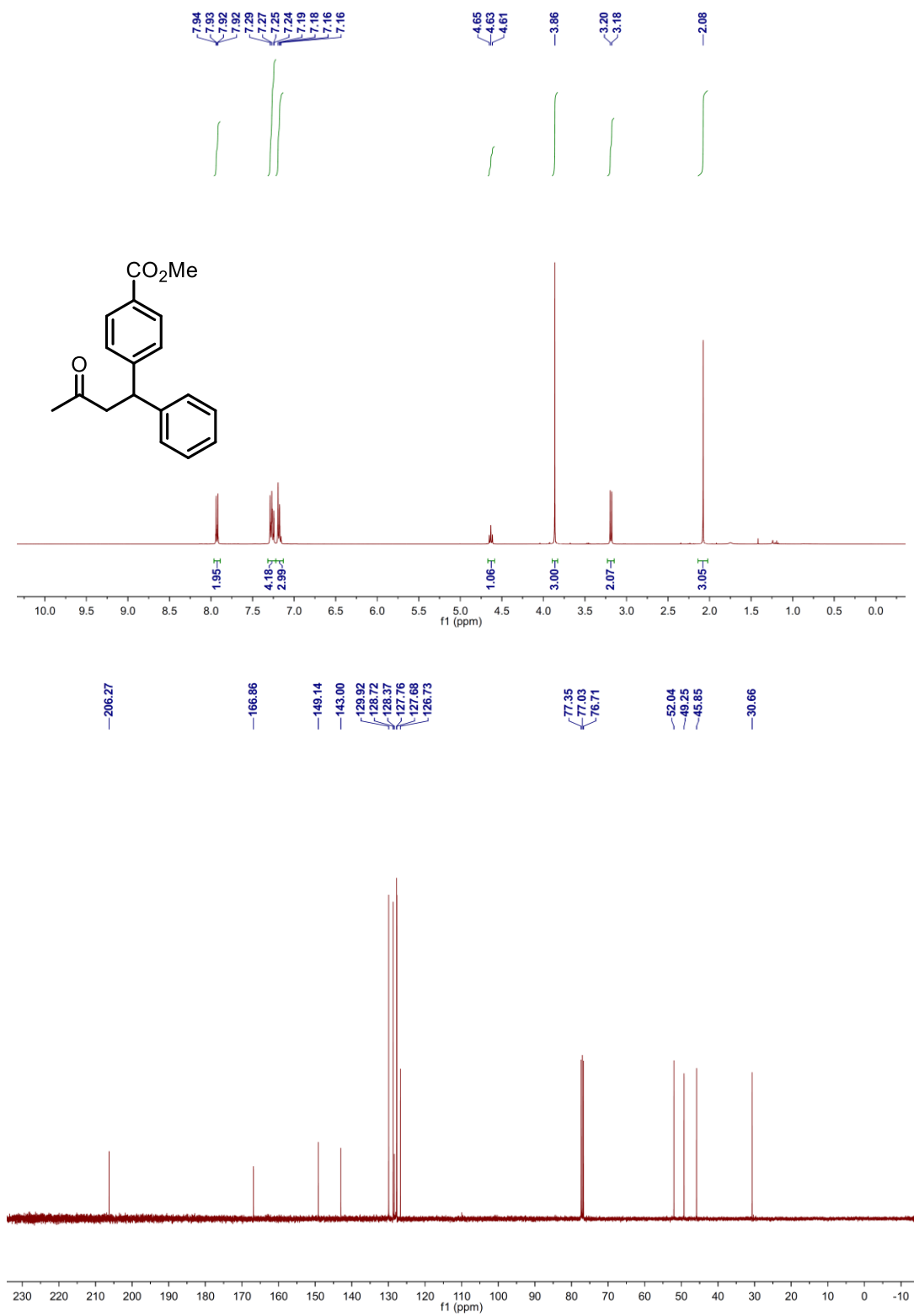


Figure 4.30 ¹H-NMR Spectrum of 4.3y-mono

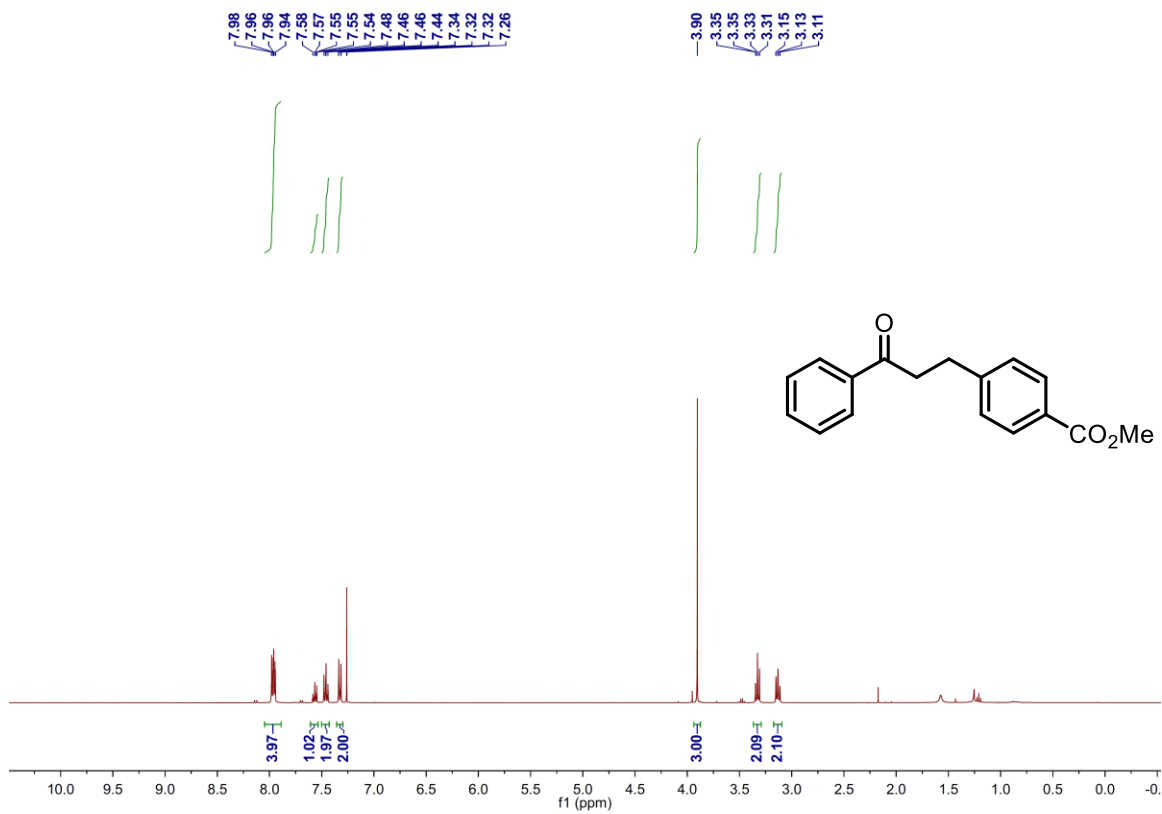


Figure 4.31 $^1\text{H-NMR}$ and $^{13}\text{C-NMR}$ Spectrum of 4.3y-di

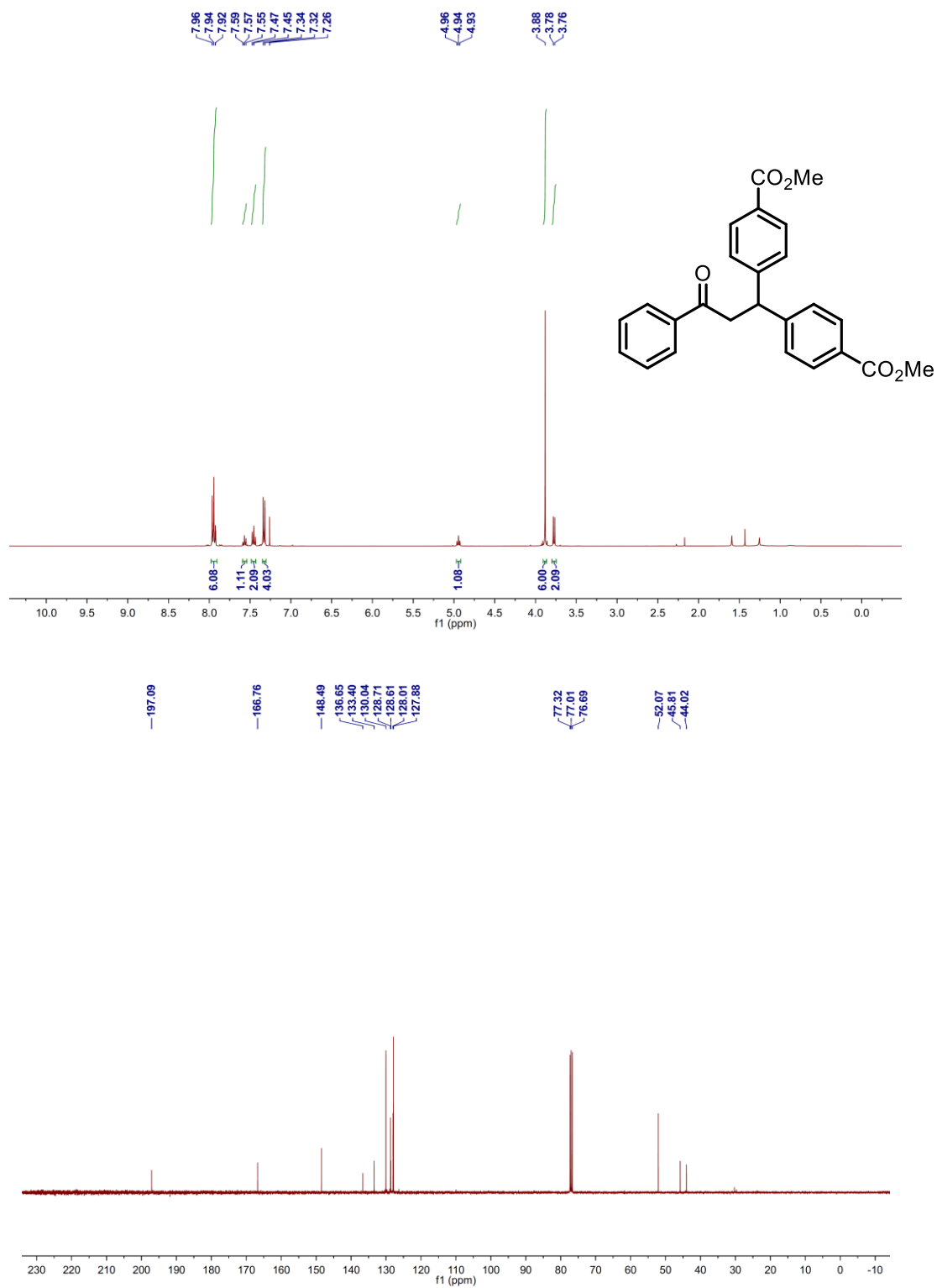


Figure 4.32 $^1\text{H-NMR}$ Spectrum of 4.3z

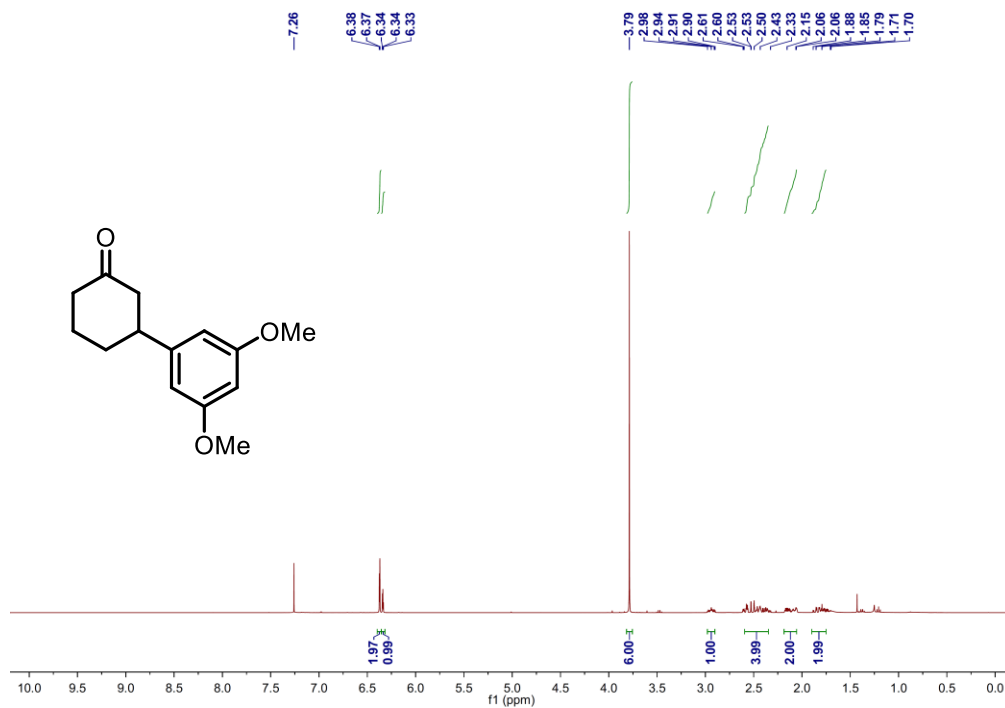
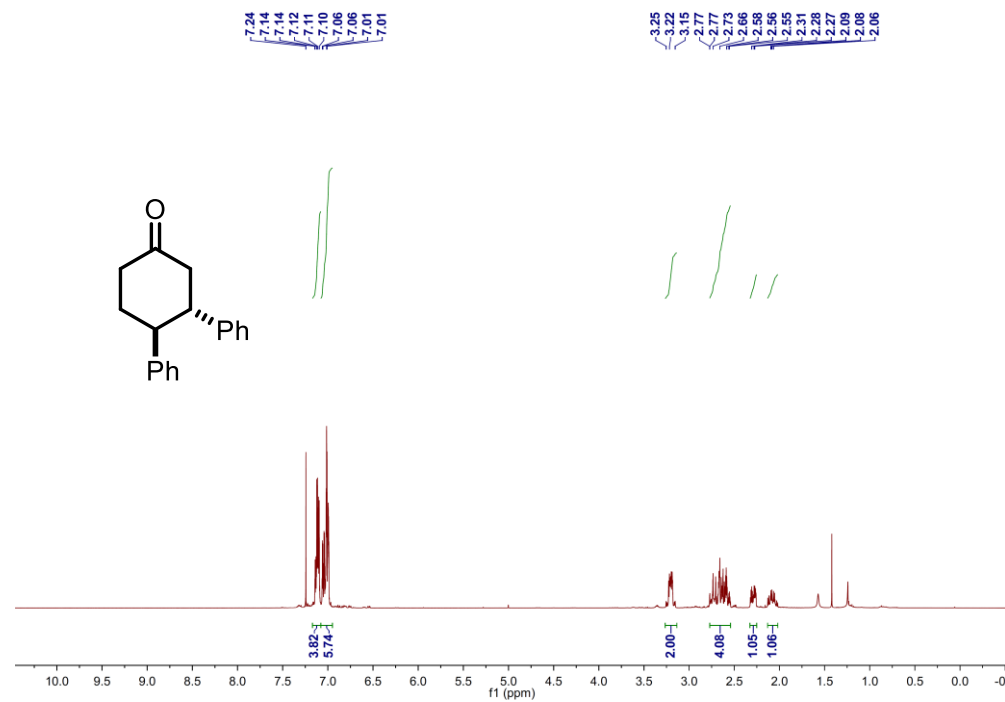


Figure 4.33 $^1\text{H-NMR}$ Spectrum of 4.20



4.6 References

1. For seminal works of the α -arylation of carbonyl compounds, see: (a) Kosugi, M.; Suzuki, M.; Hagiwara, I.; Goto, K.; Saitoh, K.; Migita, T. *Chem. Lett.* **1982**, 939. (b) Kosugi, M.; Hagiwara, I.; Sumiya, T.; Migita, T. *Bull. Chem. Soc. Jpn.* **1984**, *57*, 242. (c) Palucki, M.; Buchwald, S. L. J. *Am. Chem. Soc.* **1997**, *119*, 11108. (d) Hamann, B. C.; Hartwig, J. F. *J. Am. Chem. Soc.* **1997**, *119*, 12382. (e) Satoh, T.; Kawamura, Y.; Miura, M.; Nomura, M. *Angew. Chem., Int. Ed.* **1997**, *36*, 1740.
2. For recent reviews, see: (a) Johansson, C. C. C.; Colacot, T. J. *Angew. Chem., Int. Ed.* **2010**, *49*, 676. (b) Bellina, F.; Rossi, R. *Chem. Rev.* **2010**, *110*, 1082. (c) Culkin, D. A.; Hartwig, J. F. *Acc. Chem. Res.* **2003**, *36*, 234.
3. For representative examples, see: (a) Roth, G. N.; Chandra, A.; Nair, M. G. *J. Nat. Prod.* **1998**, *61*, 542. (b) Melvin, L. S.; Johnson, M. R.; Harbert, C. A.; Milne, G. M.; Weissman, A. *J. Med. Chem.* **1984**, *27*, 67.
4. Selected reviews on transition-metal-catalyzed conjugate addition: (a) Rossiter, B. E.; Swingle, N. M. *Chem. Rev.* **1992**, *92*, 771. (b) Gutnov, A. *Eur. J. Org. Chem.* **2008**, 4547. (c) Hayashi, T.; Yamasaki, K. *Chem. Rev.* **2003**, *103*, 2829.
5. Reviews of synthesis of α,β -unsaturated carbonyl compounds via dehydrogenation: (a) Buckle, D. R.; Pinto, I. L. In *Comprehensive Organic Synthesis*; Trost, B. M., Fleming, I., Eds.; Pergamon Press: Oxford, U.K., 1991; Vol. 7, pp 119-149. (b) Larock, R. C. In *Comprehensive Organic Transformations*; John Wiley & Sons: New York, 1999; pp 251-256.
6. For selected examples, see: (a) Itagaki, N.; Sugahara, T.; Iwabuchi, Y. *Org. Lett.* **2005**, *7*, 4181. (b) Zhang, Y.; Danishefsky, S. J. *J. Am. Chem. Soc.* **2010**, *132*, 9567
7. (a) Dugger, R. W.; Ragan, J. A.; Ripin, D. H. B. *Org. Process Res. Dev.* **2005**, *9*, 253. (b) Carey, J. S.; Laffan, D.; Thomson, C.; Williams, M. T. *Org. Biomol. Chem.* **2006**, *4*, 2337. (c) Caron, S.; Dugger, R. W.; Ruggeri, S. G.; Ragan, J. A.; Ripin, D. H. B. *Chem. Rev.* **2006**, *106*, 2943.
8. For selected examples, see: (a) Zaitsev, V. G.; Shabashov, D.; Daugulis, O. *J. Am. Chem. Soc.* **2005**, *127*, 13154; (b) Reddy, B. V. S.; Reddy, L. R.; Corey, E. J. *Org. Lett.* **2006**, *8*, 3391; (c) Shabashov, D.; Daugulis, O. *J. Am. Chem. Soc.* **2010**, *132*, 3965; (d) Feng, Y.; Wang, Y.; Landgraf, B.; Liu, S.; Chen, G. *Org. Lett.* **2010**, *12*, 3414; (e) Tran, L. D.; Daugulis, O. *Angew. Chem., Int. Ed.* **2012**, *51*, 5188; (f) Zhang, Q.; Chen, K.; Rao, W.; Zhang, Y.; Chen, F.-J. Shi, B.-F. *Angew. Chem., Int. Ed.* **2013**, *52*, 13588; (g) Pan, F.; Shen, P.-X.; Zhang, L.-S. Wang, X.; Shi, Z.-J. *Org. Lett.*, **2013**, *15*, 4758; (h) Wei, Y.; Tang, H.; Cong, X.; Rao, B.; Wu, C.; Zeng, X. *Org. Lett.*, **2014**, *16*, 2248; (i) Zhang, Q.; Yin, X.-S.; Zhao, S.; Fang, S.-L.; Shi, B.-F. *Chem. Commun.*, **2014**, *50*, 8353.

-
9. (a) Shang, R.; Ilies, L.; Matsumoto, A.; Nakamura, E. *J. Am. Chem. Soc.* **2013**, *135*, 6030. (b) Gu, Q.; Al Mamari, H. H.; Graczyk, K.; Diers, E.; Ackermann, L. *Angew. Chem., Int. Ed.* **2014**, *53*, 3868. (c) Aihara, Y.; Chatani, N. *J. Am. Chem. Soc.* **2014**, *136*, 901. (d) Li, M.; Dong, J.; Huang, X.; Li, K.; Wu, Q.; Song, F.; You, J. *Chem. Commun.* **2014**, *50*, 3944. (e) Iyanaga, M.; Aihara, Y.; Chatani, N. *J. Org. Chem.* **2014**, *79*, 11933.
10. (a) Wang, D.-H.; Wasa, M.; Giri, R.; Yu, J.-Q. *J. Am. Chem. Soc.* **2008**, *130*, 7190. (b) Wasa, M.; Engle, K. M.; Yu, J.-Q. *J. Am. Chem. Soc.* **2009**, *131*, 9886. (c) Wasa, M.; Engle, K. M.; Lin, D. W.; Yoo, E. J.; Yu, J.-Q. *J. Am. Chem. Soc.* **2011**, *133*, 19598. (d) Wasa, M.; Chan, K. S. L.; Zhang, X.-G.; He, J.; Miura, M.; Yu, J.-Q. *J. Am. Chem. Soc.* **2012**, *134*, 18570.
11. Jørgensen, M.; Lee, S.; Liu, X.; Wolkowski, J. P.; Hartwig, J. F. *J. Am. Chem. Soc.* **2002**, *124*, 12557.
12. (a) Renaudat, A.; Jean-Gérard, L.; Jazzar, R.; Kefalidis, C. E.; Clot, E.; Baudoin, O. *Angew. Chem. Int. Ed.* **2010**, *49*, 7261. (b) Larini, P.; Kefalidis, C. E.; Jazzar, R.; Renaudat, A.; Clot, E.; Baudoin, O. *Chem. Eur. J.* **2012**, *18*, 1932. (c) Aspin, S.; Goutierre, A.; Larini, P.; Jazzar, R.; Baudoin, O. *Angew. Chem. Int. Ed.* **2012**, *51*, 10808.
13. (a) Leskinen, M. V.; Yip, K.-T.; Valkonen, A.; Pihko, P. M. *J. Am. Chem. Soc.* **2012**, *134*, 5750. (b) Nimje, R. Y.; Leskinen, M. V.; Pihko, P. M. *Angew. Chem. Int. Ed.* **2013**, *52*, 4818. (c) Yip, K.-T.; Nimje, R. Y.; Leskinen, M. V.; Pihko, P. M. *Chem. Eur. J.* **2012**, *18*, 12590.
14. Pirnot, M. T.; Rankic, D. A.; Martin, D. B. C.; MacMillan, D. W. C. *Science* **2013**, *339*, 1593.
15. Theissen, R. J. *J. Org. Chem.* **1971**, *36*, 752.
16. (a) Muzart, J.; Pete, J. P. *J. Mol. Catal.* **1982**, *15*, 373. (b) Wenzel, T. T. *J. Chem. Soc., Chem. Commun.* **1989**, 932. (c) Park, Y. W.; Oh, H. H. *Bull. Korean Chem. Soc.* **1997**, *18*, 1123. (d) Shvo, Y.; Arisha, A. H. I. *J. Org. Chem.* **1998**, *63*, 5640. (e) Diao, T.; Stahl, S. S. *J. Am. Chem. Soc.* **2011**, *133*, 14566. (f) Diao, T.; Wadzinski, T. J.; Stahl, S. S. *Chem. Sci.* **2012**, *3*, 887. (g) Gao, W.; He, Z.; Qian, Y.; Zhao, J.; Huang, Y. *Chem. Sci.* **2012**, *3*, 883. (h) Diao, T.; Pun, D.; Stahl, S. S. *J. Am. Chem. Soc.* **2013**, *135*, 8205.
17. Hartwig, J. F. In *Organotransition Metal Chemistry: From Bonding to Catalysis*; University Science Books: Sausalito, 2010.
18. Izawa, Y.; Pun, D.; Stahl, S. S. *Science* **2011**, *333*, 209.
19. Gandeepan, P.; Rajamalli, P.; Cheng, C.-H. *ACS Catalysis* **2014**, *4*, 4485.
20. Schoenfeld, R. C., U.S. Patent 0136787, Jun 9, 2011.

-
21. Stephenson, T. A.; Morehouse, S. M.; Powell, A. R.; Heffer, J. P.; Wilkinson, G. J. *Chem. Soc.* **1965**, 3632.
22. Li, Q.; Dong, Z.; Yu, Z.-X. *Org. Lett.* **2011**, *13*, 1122.
23. Liu, C.-C.; Janmanchi, D.; Chen, C.-C.; Wu, H.-L. *Eur. J. Org. Chem.* **2012**, 2503.
24. Nakao, Y.; Chen, J.; Imanaka, H.; Hiyama, T.; Ichikawa, Y.; Duan, W.-L.; Shintani, R.; Hayashi, T. *J. Am. Chem. Soc.* **2007**, *129*, 9137.
25. Korenaga, T.; Osaki, K.; Maenishi, R.; Sakai, T. *Org. Lett.* **2009**, *11*, 2325.
26. Dubrovskiy, A. V.; Larock, R. C. *Org. Lett.* **2010**, *12*, 3117.
27. Colbon, P.; Ruan, J.; Purdie, M.; Mulholland, K.; Xiao, J. *Org. Lett.* **2011**, *13*, 5456.
28. Naeemi, Q.; Dindaroğlu, M.; Kranz, D. P.; Velder, J.; Schmalz, H.-G. *Eur. J. Org. Chem.* **2012**, 1179.

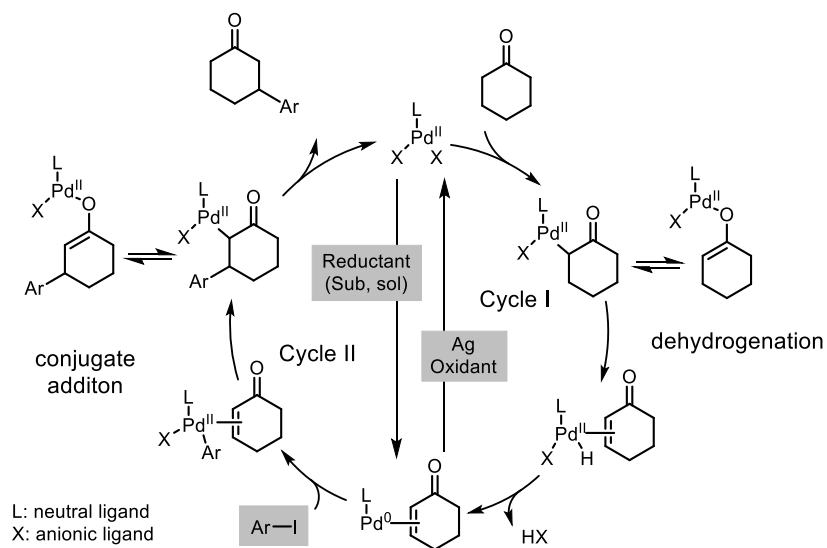
CHAPTER 5

Palladium-Catalyzed Direct β -Arylation of Ketones with Diaryliodonium Salts: A Stoichiometric Heavy Metal-Free and User-Friendly Approach

5.1 Introduction

In our previous study, the direct β -arylation of simple ketones with aryl iodides was achieved using $\text{Pd}(\text{TFA})_2/\text{P}(i\text{-Pr})_3$ as the precatalyst and AgTFA as the additive.¹ The role of the silver additive was proposed to extract iodide ligand on the palladium intermediate after the oxidative addition, and restore the active palladium dicarboxylate catalyst. Besides the high cost of silver salts that diminishes their applicability on a large scale, a major issue of using stoichiometric amount of silver salt is that it complicates the reaction mechanism due to the possibility of $\text{Ag}(\text{I})$ serving as potential oxidants for the $\text{Pd}(0)$ species. Thus, a mechanism containing two separate catalytic cycles (Pd -catalyzed desaturation and reductive Heck reaction), though less likely, cannot be easily ruled out (Scheme 5.1).

Scheme 5.1 An Alternative Mechanism Consisting of Two Separate Cycles



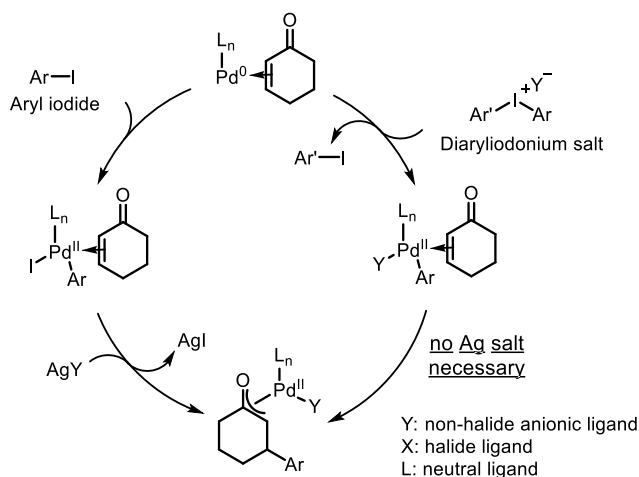
In the alternative ‘two-cycle’ mechanism, the stoichiometric Ag(I) salt is proposed to promote the palladium-catalyzed dehydrogenation by oxidizing Pd(0) intermediate to active Pd(II) catalyst (Cycle I). At the same time, a reductive Heck reaction proceeds with Pd(0) species and conjugate enone to give the β -arylation product and Pd(II) salt, which can be reduced by possible reductants in the reaction, such as excess ketones and solvent (i.e. 1,4-dioxane), to complete the catalytic cycle (Cycle II).

While our proposed redox cascade is a redox-neutral cycle, this ‘two-cycle’ mechanism requires both stoichiometric oxidant and reductant. Thus, the key to distinguish between these two mechanisms is to study the redox property of the reaction. However, as the terminal form of silver salt in the reaction is hard to identify and quantify, a study of the redox property of the current reaction conditions would be impractical. One direct approach to solve this issue is to find a non-redox-active salt that can also form insoluble metal-iodide salts under the reaction

conditions (*vide infra*, chapter 7). Therefore, a quantitative analysis of the organic components of the reaction mixture would suffice to elucidate the redox property. On the other hand, one indirect approach is to use aryl electrophiles that do not transfer a halide anion to palladium during the oxidative addition, thus avoiding the use of a halide scavenger at all.

Towards this end, we found the diaryliodonium salt may be a promising aryl source for the β -arylation without halide scavenger.² Unlike aryl iodides, the oxidative addition of diaryliodonium salts to Pd(0) transfers an aryl and a non-halide anion to the metal, and release an molecule of aryl iodide at the same time (Scheme 5.2).³ As a result, silver salt is not necessary to extract the iodide ligand and regenerate the active palladium catalyst any more.

Scheme 5.2 Use of Diaryliodonium Salt as the Aryl Source



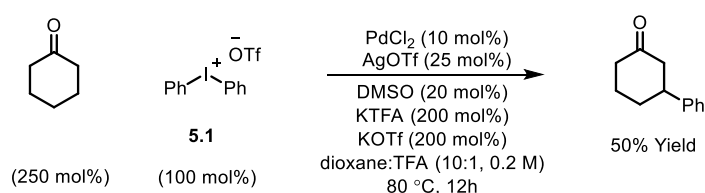
Besides the silver issue, the use of diaryliodonium salts would also address another limitation of our previous β -arylation conditions. The practicality of the reaction conditions is hampered by the use of the air-sensitive $P(i\text{-Pr})_3$ ligand, which necessitates air-free operations and highly purified reagents. As a more reactive aryl electrophile, the oxidative addition of

diaryliodonium salt with Pd(0) generally does not need the assistance of electron-rich phosphine ligand. Thus, new conditions that are tolerant of air should be expected for the β -arylation with diaryliodonium salts.

5.2 Results and Discussion

Our initial result indicated it is viable to use diaryliodonium salts as the aryl source for the β -arylation reaction. The reaction between cyclohexanone and diphenyliodonium triflate (**5.1**) afforded the desired β -aryl ketone in 50% yield using PdCl₂/AgOTf/DMSO as the precatalyst and KTFA/KOTf as additives in a mixed solvent of dioxane and trifluoroacetic acid. It should be noted that the role of catalytic amount of AgOTf in the conditions is proposed to react with PdCl₂ to form a cationic palladium precatalyst. Such an *in situ* generation of catalyst avoided the tedious preparation and handling of air- and moisture-sensitive Pd(OTf)₂.⁴

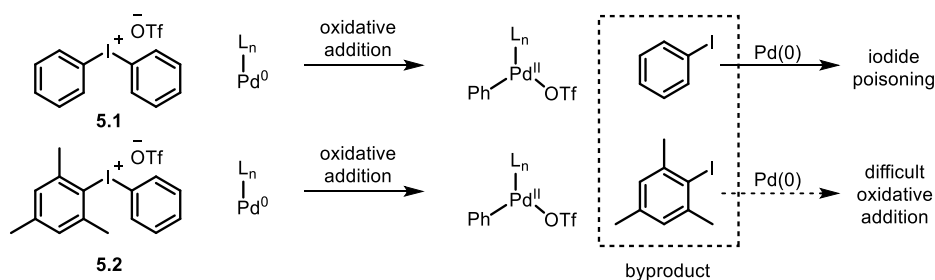
Scheme 5.3 β -Arylation of Cyclohexanone with Diphenyliodonium Triflate



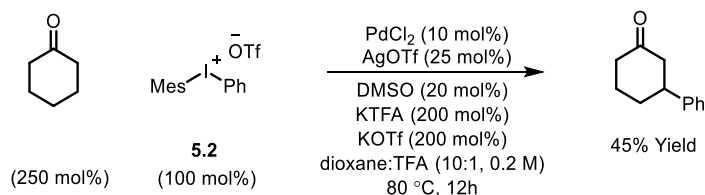
However, one concern about the use of diphenyliodonium salt is that it can act as two equivalents of aryl source, since the oxidative addition of the salt to Pd(0) will produce one molecule of iodobenzene as byproduct. Besides the complication of stoichiometry, the iodobenzene byproduct could potentially poison the palladium catalyst by undergoing oxidative

addition with Pd(0) intermediate in the reaction (Scheme 5.4). In order to avoid these issues, we switched to mesitylphenyliodonium salt as the aryl source. The use of bulky mesityl as one of the aryl groups is known to alleviate chemoselectivity issues, since the less sterically hindered aryl group would be transferred preferably.^{2c} In addition, iodomesitylene, the byproduct after the oxidative addition, would barely undergo oxidative addition with the Pd(0) intermediate, also due to its steric hindrance. As expected, the reactivity of β -arylation retained when mesitylphenyliodonium triflate was used in place of diphenyliodonium triflate (Scheme 5.5).

Scheme 5.4 Comparison between Diphenyliodonium and Mesitylphenyliodonium Salt

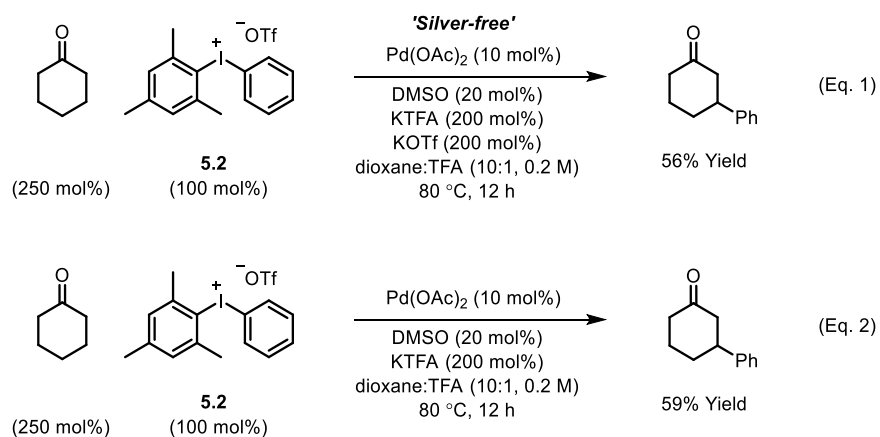


Scheme 5.5 β -Arylation of Cyclohexanone with Mesitylphenyliodonium Triflate

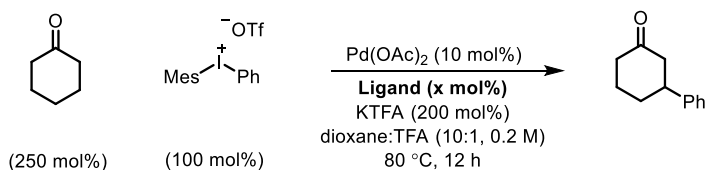


With mesitylphenyliodonium triflate (**5.2**) as the aryl source, the combination of PdCl₂ and AgOTf can be replaced with simple Pd(OAc)₂ with an increased yield (Scheme 5.6, Eq. 1), resulting in reaction conditions that are completely ‘silver-free’. We also found the KOTf salt is no longer necessary in the reaction, which led to simpler reaction conditions (Eq. 2).

Scheme 5.6 Simplified Reaction Conditions



Preliminary screening of ligands for the β -arylation reaction with diaryliodonium salts demonstrated that sulfur-based ligands are preferred, with sulfide ligands giving only slightly lower yields than corresponding sulfoxide ligands (Table 5.1). Among all the sulfoxide ligand screened, bidentate ligands are generally better than monodentate ones, and 1,2-bis(phenylsulfinyl)ethane (**5.3**), originally employed by White and coworkers for the allylic C–H activation,⁵ proved to be the best sulfoxide ligand (entry 11). Increasing the bite angle of the bis-sulfoxide ligand decreases the efficiency of the reaction while eliminating one carbon on the backbone of the ligand totally shut down the reaction. Replacing phenyl groups of the ligand with alkyl groups results in lower yields, and the use of electron-donating *tert*-butyl-substituted bis-sulfide ligand (entry 10) gave no β -arylation product, probably by inhibiting the dehydrogenation step.

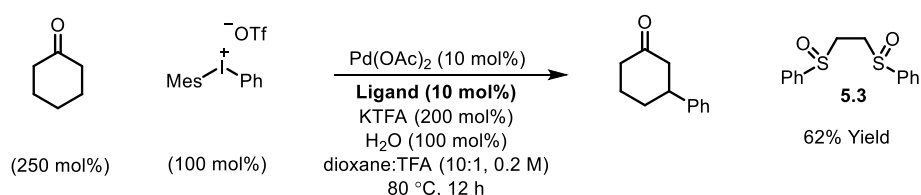
Table 5.1 Screening of Sulfide and Sulfoxide Ligands

Entry	Ligand (x mol%)	Yield	Entry	Ligand (x mol%)	Yield
1	(20)	56%	8	(10)	53%
2	(20)	47%	9	(10)	48%
3	(20)	45%	10	(10)	0%
4	(20)	48%	11	(10) 5.3 (20)	62% 61%
5	(20)	48%	12	(10)	59%
6	(20)	44%	13	(10)	0%
7	(20)	21%	14	(10)	55%

Based on the backbone of 1,2-bis(phenylsulfinyl)ethane (**5.3**), we modified the aryl substituents to examine their effects on the reaction efficiency (Table 5.2). However, alternating the electronic properties of the arenes seemed to have little effects on the reaction; ligands with either electron-donating or -withdrawing substituents gave comparable or lower yields than **5.3**. We also attempted to affect the reaction by increasing the steric hindrance of the sulfur ligand. However, the bis-sulfoxide ligand with *o*-tol groups (entry 10) afforded the product in a lower yield.

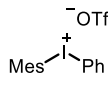
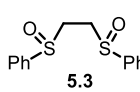
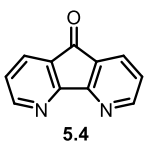
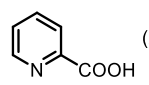
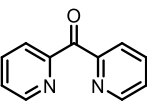
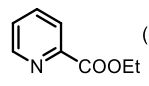
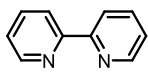
Performances of selected ligands other than sulfur-base ligands are depicted in Table 5.3. While phosphine-based ligands give lower yields than the sulfur-based ones, nitrogen-based ligands are detrimental to the reaction. However, reaction with 4,5-diazafluoren-9-one (**5.4**) gives slightly lower yield than **5.3**.⁶ Considering **5.3** and **5.4** ligands are both π -acids, it is reasonable to propose an electrophilic palladium center is essential for the reaction.

Table 5.2 Screening of Sulfide and Sulfoxide Ligands



Entry	Ligand (x mol%)	Yield	Entry	Ligand (x mol%)	Yield
1		42%	6		42%
2		59%	7		59%
3		62%	8		62%
4		61%	9		61%
5		63%	10		63%

Table 5.3 Screening of Non-sulfur-based Ligands

 (250 mol%)	 (100 mol%)	$\xrightarrow[\text{Ligand (x mol\%)}]{\text{Pd(OAc)}_2 \text{ (10 mol\%)}}$ KTFA (200 mol%) H ₂ O (100 mol%) dioxane:TFA (10:1, 0.2 M) 80 °C, 12 h	 (250 mol%)	 5.3 62% Yield			
Ligand (x mol%)		Yield		Ligand (x mol%)		Yield	
PPh ₃ (20)		32%		dtbpy (20)		0%	
P(OPh) ₃ (20)		22%		 5.4 (10)		56%	
 (20)		0%		 (10)		0%	
 (20)		0%		dppe (10)		3%	
 (10)		0%					

Finally, Several sulfilimine ligands were also synthesized, examined, and compared with sulfide and sulfoxide ligands for the β -arylation reaction. In general, sulfilimine ligands gave comparable or lower yields than their sulfoxide counterparts (Table 5.4). However, the bis-*N*-tosylsulfilimine ligand **5.5** turned out to be superior. This ligand can be easily prepared in one step from 1,2-bis(phenylthio)ethane and Chloramine-T (Scheme 5.7), and the *meso* and *racemic* ligand demonstrated nearly identical reactivity. Although sulfur-based ligands, such as sulfides and sulfoxides, are widely used,⁷ to the best of our knowledge, the family of bis-sulfilimines has not been previously employed as ligands for transition-metal catalysis. The reaction was found sensitive to the structure of the sulfilimine ligands. Monodentate sulfilimine ligands (**5.7-5.9**) and the bis-sulfilimine ligand with an elongated backbone (**5.10**) are found inferior to **5.5**. Compared

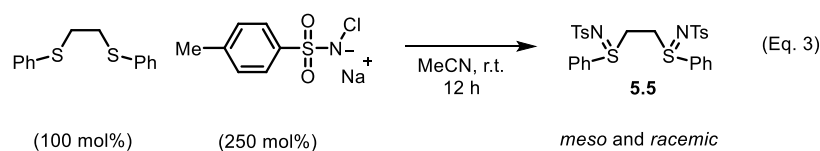
with corresponding bis-sulfide (**5.6**) and bis-sulfoxide ligands (**5.3**), as well as 4,5-diazafluoren-9-one (**5.4**), the new sulfilimine ligand gave the β -arylation product in a higher yield.

Table 5.4 Effects of Sulfilimine Ligands

(250 mol%) (100 mol%) Pd(OAc)₂ (10 mol%)
 Ligand (x mol%)
 KTFA (200 mol%)
 dioxane:TFA: H₂O (20:2:1)
 air, 80 °C, 12 h

Entry	Ligand (x mol%)	Yield	Entry	Ligand (x mol%)	Yield
1	 5.5	(10) 70%	5	 5.8	(20) 22%
2	 5.3	(10) 60%	6	 5.9	(20) 41%
3	 5.6	(10) 41%	7	 5.10	(10) 47%
4	 5.7	(20) 29%	8	 5.4	(10) 42%

Scheme 5.7 Synthesis of Bis-*N*-sulfilimine Ligand **5.5**



meso



racemic

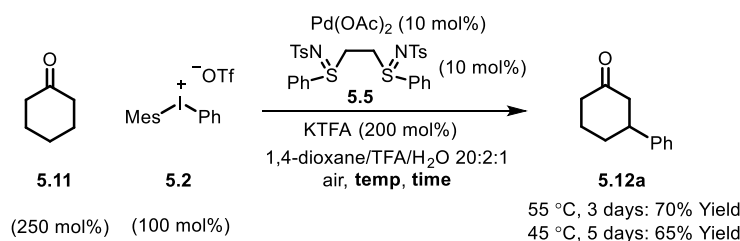
With the optimal ligand and conditions in hand, a set of control experiments were subsequently performed to gain deeper understanding of the reaction (Table 5.5). Common mesitylphenyliodonium salts with other counteranions are also suitable arylation reagents under the reaction conditions (entries 1 and 2). However, diphenyliodonium salt led to a greatly decreased yield (entry 3). As explained, the poor efficiency can be attributed to the iodobenzene (PhI) byproduct released during the reaction, since oxidative addition of iodobenzene to Pd(0) is facile, and the resulting iodide ligand would poison the palladium catalyst. Such a hypothesis was also supported by the marginal yield when **5.2** was directly replaced by PhI (entry 4). The reaction was completely terminated without the palladium catalyst, indicating its pivotal role in this tandem catalysis (entry 5). In addition, the reaction without any ligand only gave a trace amount of product **5.12a** (entry 6).

The combination of KTFA/TFA proved to be indispensable: the yield dropped significantly in the absence of one or both of the reagents (entries 7-9). It is likely that these two reagents act as a 'buffer pair' to control the acidity of the reaction medium. The strong acidity of TFA would facilitate the protonation of the palladium enolate to give the product. Nevertheless, triflic acid (HOTf) should be produced when **5.2** was consumed, which proved to be detrimental to the reaction (entry 10). Although TFA and KTFA can be replaced by other salts and acids, the yields dropped variably (entries 11-14). The addition of water was found important to promote the reaction, although the exact reason is unclear (entry 15, *vide infra*). In addition, this new β -arylation reaction proved to be robust and user-friendly: all the reagents can be added in one batch without glovebox or Schlenk techniques, and no inert atmosphere is necessary. And a control reaction that was fully degassed and run under nitrogen atmosphere gave a similar yield

(73%, entry 16), excluding the possibility of oxygen serving as a stoichiometric oxidant. The β -arylation reaction also proceeded smoothly with high mass balance when an equimolar amount of the two reactants was used (entry 17).

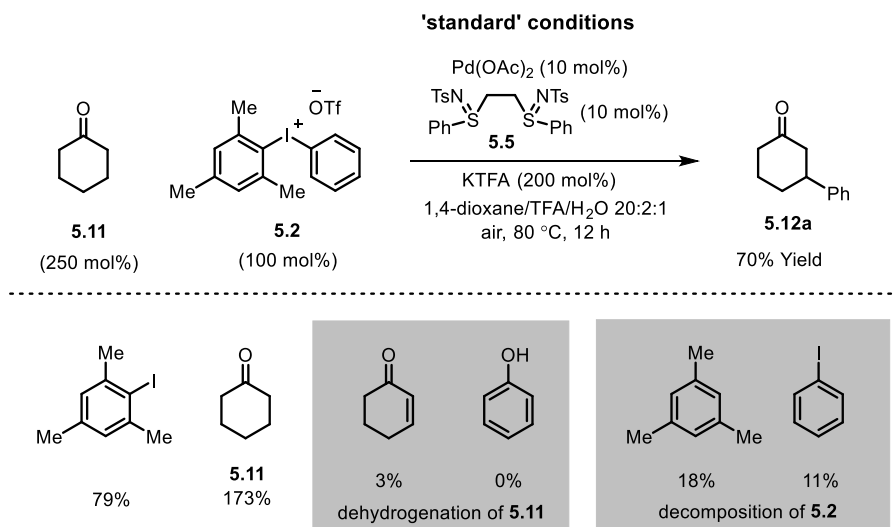
Furthermore, we also discovered that the reaction maintained its catalytic activity at lower temperatures, although a prolonged reaction time was required (Scheme 5.8).

Scheme 5.8 Reactions at Lower Temperature



As no redox-active additives were used in the new conditions, a clear analysis of the redox property of the β -arylation can be executed (Scheme 5.9). For the cyclohexanone starting material, while excess amount was necessary, a high recovery of unreacted ketone was observed, and there are minimum amount of cyclohexen-1-one and no phenol from the over-oxidation. On the side of Mesitylphenyliodonium salt, there are two major reaction pathways. Around three quarters of 5.2 participated in the β -arylation reaction to give desired β -aryl ketone, and iodomesitylene as the byproduct. Most of the remaining iodonium salt proceeded through a decomposition pathway to mesitylene and iodobenzene. Altogether, these data supported that the β -arylation reaction between cyclohexanone and mesitylphenyliodonium salt is indeed redox-neutral.

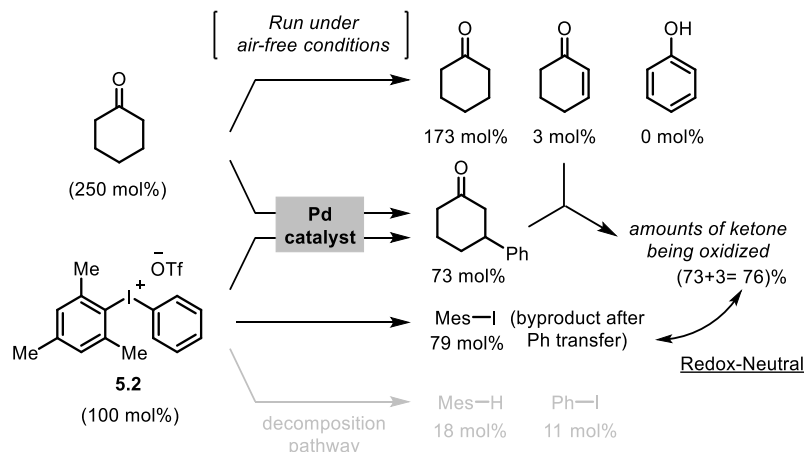
Table 5.5 Control Experiments^{a,b}



Entry	Variations from the 'standard' conditions	Yield of 5.12a (%)	5.11 (%)
1	[MesIPh]BF ₄ instead of 5.2	50	158
2	[MesIPh]TFA instead of 5.2	56	168
3	[Ph ₂]OTf instead of 5.2	36	199
4	PhI instead of 5.2	5	240
5	w/o Pd(OAc) ₂	0	244
6	w/o 5.5	8	235
7	w/o KTFa and TFA	13	128
8	w/o TFA	36	179
9	w/o KTFa	34	179
10	100 mol% HOTf instead of TFA	2	142
11	KOAc instead of KTFa	66	176
12	NaOAc instead of KTFa	59	167
13	HOAc instead of TFA	40	181
14	HFIP instead of TFA	43	195
15	w/o H ₂ O	47	176
16	N ₂ instead of air	73	170
17	5.11 : 5.2 = 1:1	48	47

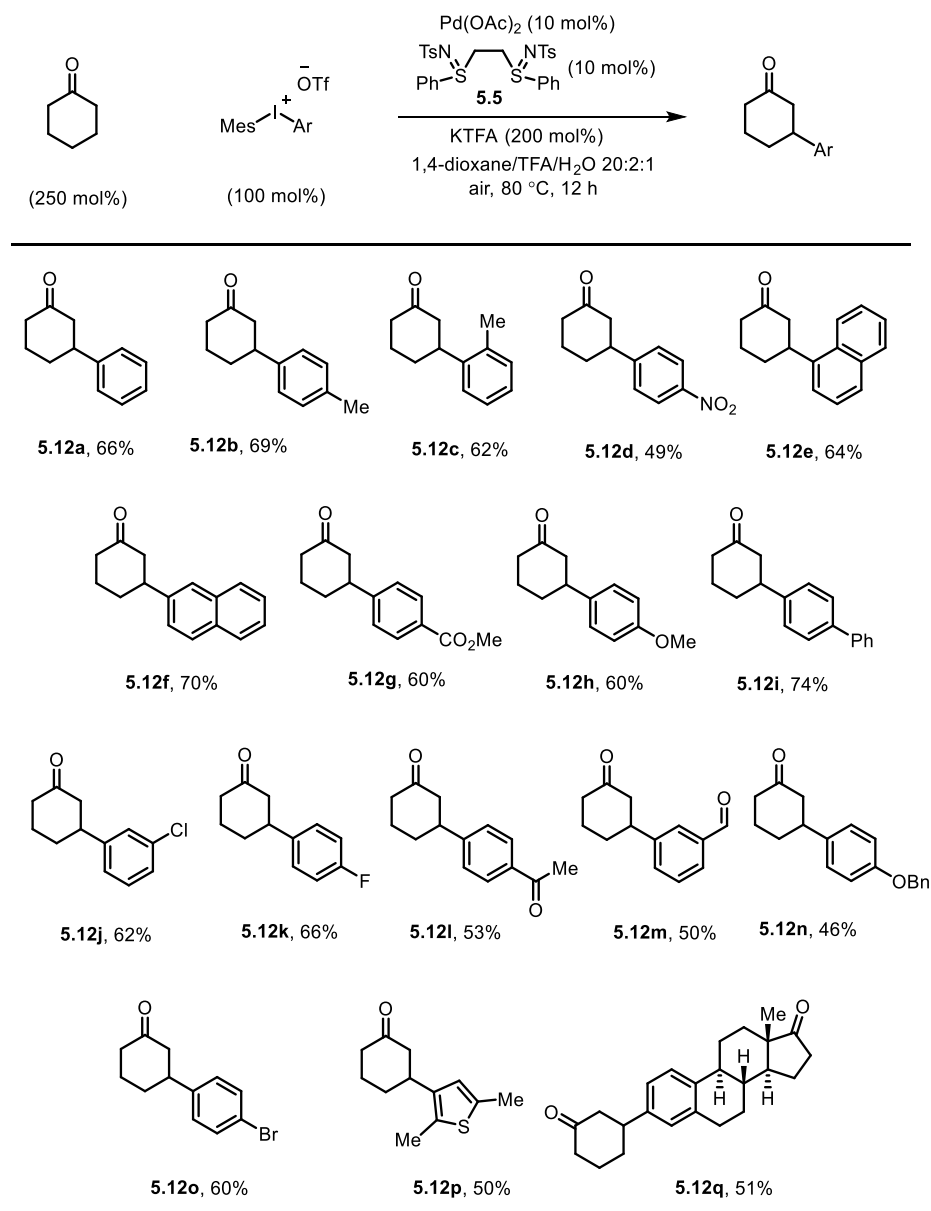
^aStandard conditions: mesitylphenyliodonium salt **5.2** (0.2 mmol), cyclohexanone (0.5 mmol), Pd(OAc)₂ (0.02 mmol), **5.5** (0.02 mmol, *d.r.*>20:1), KTFa (0.4 mmol), 1,4-dioxane (1 mL), TFA (100 μL), H₂O (50 μL), 80 °C, 12 h. ^bAll the yields were determined by GC using dodecane as the internal standard.

Scheme 5.9 Analysis of Redox Property



The optimized conditions were then adopted to examine the substrate scope of this β -arylation reaction (Table 5.6). Aryl groups with a wide span of electronic properties (electron-rich and -deficient) all participated to give the corresponding β -aryl ketones (**5.12a-b**, **5.12d**, **5.12f-i**, **5.12k**). The reaction is also compatible with various *para*-, *meta*- and *ortho*- substituents on the arenes (**5.12c**, **5.12e**, **5.12j**, **5.12m**). Base- and nucleophile-sensitive functional groups (those hard to survive under traditional conjugate addition conditions), such as methyl ketone (**5.12l**) and aldehyde (**5.12m**), remained intact in the reaction. Note that aryl bromide (**5.12o**), not compatible with our previous system, can be tolerated under these conditions, which serves as a handle for further derivatization through cross couplings. It is also encouraging to note that the diaryliodonium salt containing a thiophene moiety also reacted to give the arylation product (**5.12p**). A complex estrone-derived iodonium salt smoothly delivered the product (**5.12q**). In this case, the cyclohexanone ring was selectively arylated while the cyclopentanone motif of the estrone remained intact.

Table 5.6 Scope of Diaryliodonium Salts^a

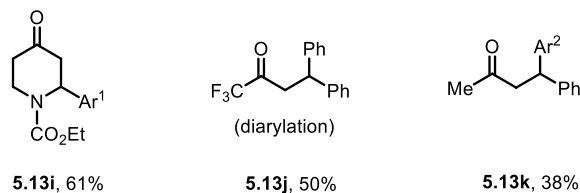
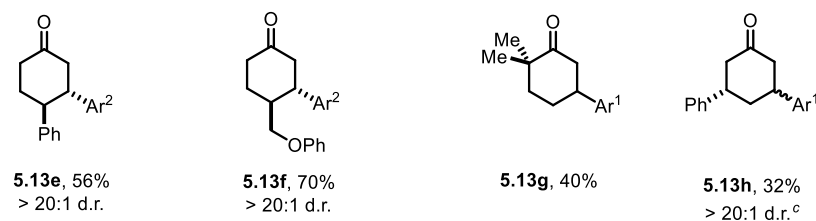
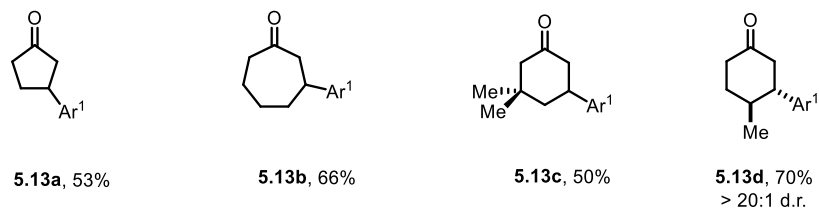
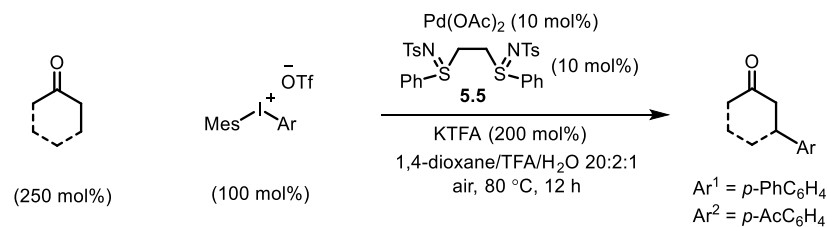


^aStandard conditions: mesitylphenyliodonium salt (0.4 mmol), cyclohexanone (1.0 mmol), Pd(OAc)₂ (0.04 mmol), **5.5** (0.04 mmol, *d.r.*>20:1 *racemic:meso*), KTFA (0.8 mmol), 1,4-dioxane (2 mL), TFA (200 μL), H₂O (100 μL), 80 °C, 12 h.

Moreover, the ketone scope was greatly improved with this new catalytic system (Table 5.7). Cyclic ketones with different ring-sizes were arylated in good yields (**5.13a**, **5.13b**). Unlike

our previous method, this new catalytic system enabled arylation of cyclohexanones containing α -, β -, or γ -substituents. For example, 3,3-dimethylcyclohexanone proved to be a suitable substrate (**5.13c**). Substituents at the C4 position yielded the *trans* products (**5.13d-f**) with excellent diastereoselectivity (>20:1). Sterically hindered 2,2-dimethylcyclohexanones were also compatible. Interestingly, when product **5.12a** was subjected to the reaction conditions, 3,3'-diarylcyclohexanone **5.13h** was formed with excellent site- and diastereoselectivity. The relatively lower yields with **5.13g** and **5.13h** can be attributed to the competing decomposition of the diaryliodonium salt. 4-Piperidinone derivatives, a class of important pharmaceutical intermediates, can also be β -arylated (**5.13i**). While linear ketones are more challenging substrates, they still hold great promises under the new reaction conditions. The use of trifluoromethyl ethyl ketone selectively afforded the diarylation product (**5.13j**), indicating that, after the aryl migratory insertion, the Pd(II)-enolate intermediate underwent a faster β -hydrogen elimination instead of protonation. Mono β -arylation was observed for 4-phenyl-butan-2-one (**5.13k**), and a considerable amount of the dehydrogenative β -arylation product was also formed.⁸

Table 5.7 Scope of Ketones^{a,b}

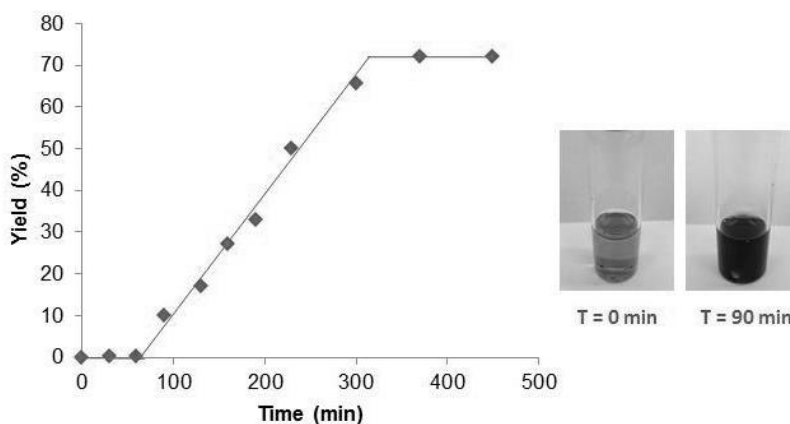


^aStandard conditions: mesitylphenyliodonium salt (0.4 mmol), ketone (1.0 mmol), Pd(OAc)₂ (0.04 mmol), **5.5** (0.04 mmol, *d.r.*>20:1 *racemic:meso*), KTFA (0.8 mmol), 1,4-dioxane (2 mL), TFA (200 μL), H₂O (100 μL), 80 °C, 12 h. ^bDiastereoselectivity determined by crude NMR. ^cWhile **5.13h** was isolated as a single diastereomer, attempts to determine the relative stereochemistry (*cis* or *trans*) were unsuccessful.

To gain a better understanding of the reaction, a set of kinetic studies was first performed, where gas chromatography was employed to monitor the reaction progress. Under the standard conditions, the β-arylation of cyclohexanone with mesitylphenyliodonium salt **5.2** exhibited an induction period (Figure 5.1). The length of the induction period for the standard reaction varies from 30 minutes to an hour, during which we observed an evident color change from yellow to

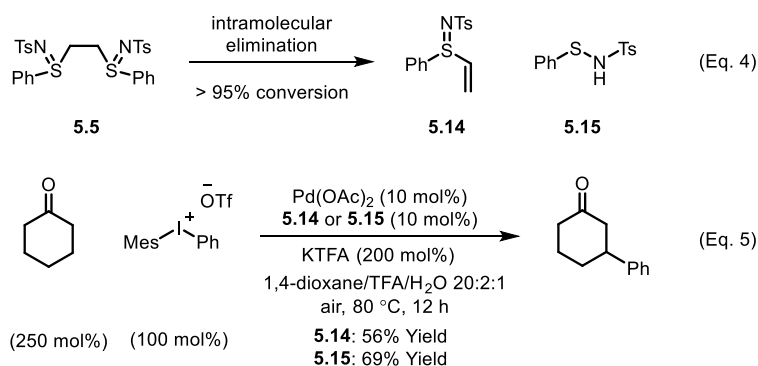
dark red. Accordingly, the initiation of the product formation was usually marked by the opaque dark red solution.

Figure 5.1 Kinetic Profile



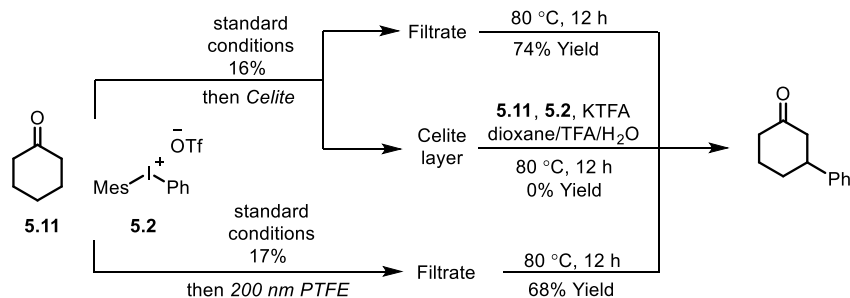
It was also observed that the induction period was accompanied with the pyrolysis of ligand **5.5**. At the reaction temperature, the thermal elimination of ligand **5.5** yielded an equimolar amount of phenyl vinyl sulfilimine **5.14** and *N*-phenylsulfanyl tosylamine **5.15** in more than 95% conversion (Scheme 5.10, Eq. 4).⁹ In addition, when used independently as the ligands, both ligands proved to be effective for the β -arylation reaction with **5.14** giving a higher yield (Eq. 5). However, the direct use of the ligands from the decomposition did not eliminate the induction period.

Scheme 5.10 Pyrolysis of Ligand 5.5



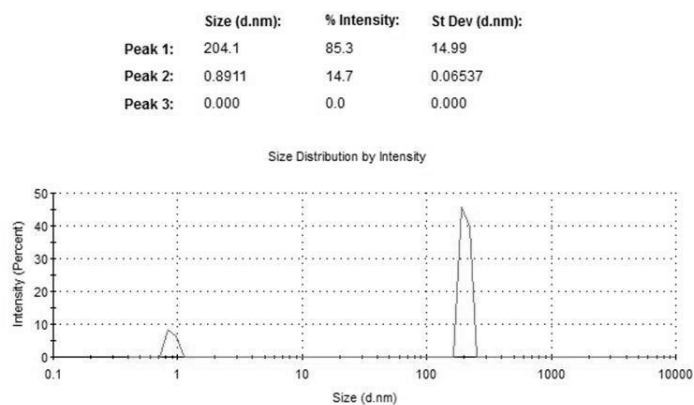
Based on the above information, we hypothesized that the induction period, as well as the formation of dark red opaque solution was likely attributed to the transformation of molecular palladium complexes to active catalysts in the form of a cluster.¹⁰ It is known that sulfur-based ligands like sulfide and sulfoxide, strong acids (e.g. TFA) and solvents of high dielectric constant (e.g. water) promote the formation and/or stabilize the palladium nanoparticles. Recently, Stahl and coworkers also presented evidence for the role of palladium nanoparticles in the dehydrogenation of cyclohexanones and cyclohexenones.¹¹ Here, we conducted a series of experiments to probe the involvement of palladium nanoparticles during the catalysis.¹²

Scheme 5.11 Hot Filtration Test



As the precipitation of palladium black was noted during and after the reaction, hot filtration test was first employed to distinguish between a soluble nanoparticle and a heterogeneous catalyst.¹³ Parallel reactions were set up under the reaction conditions and the conversion was monitored by gas chromatography (Scheme 5.11). When the reactions initiated and reached around 20% yield, the reaction mixtures were passed through either a short plug of Celite or a 200 nm PTFE filter to remove over-sized particles. Subsequently, heat was restored to the dark red filtrates obtained. Regarding the Celite layer, the heterogeneous filtrand was added to a reaction vessel with newly mixed substrates, additives and solvents, and the reaction was then run at 80 °C for 12 h. We observed that the filtrates from both the Celite and PTFE filtration showed comparable catalytic activity as the standard conditions. However, the filtrand from the Celite layer was catalytically inactive and failed to deliver any desired product. This hot filtration test suggested that the active palladium catalyst generated during the induction period sustained the solubility, and those heterogeneous species were not responsible for the transformation.

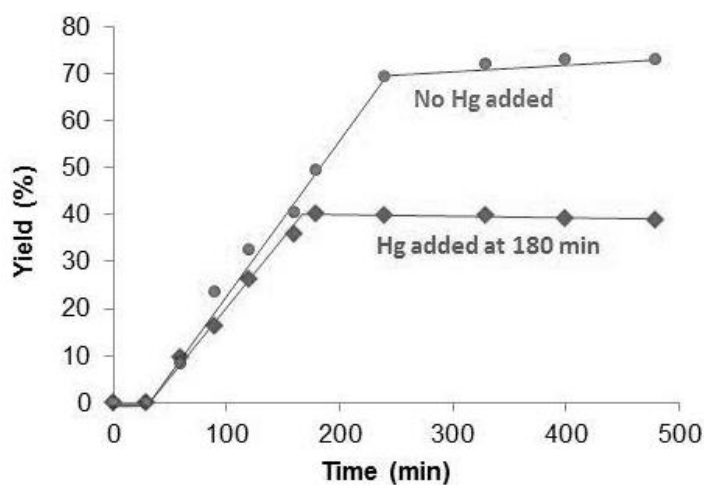
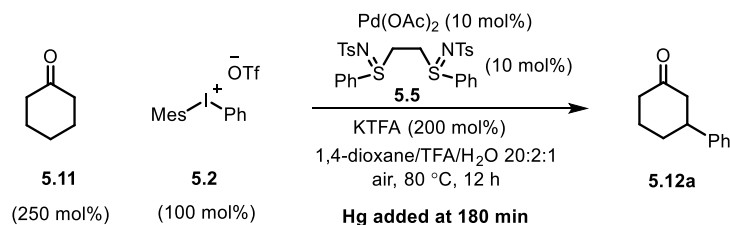
Figure 5.2 Dynamic Light Scattering Data



The formation of nanoparticle species was also evidenced by dynamic light scattering (DLS) experiments, a technique for measuring the size distribution of small particles.¹⁴ The DLS data obtained from the standard reaction showed the presence of particles with an average size of 0.9 and 204 nm at 90 min after the initiation (Figure 5.2).

A supplementary mercury poisoning test was also executed to support the presence of palladium nanoparticles.¹⁵ Molecular mercury is known to inhibit noble metal-nanoparticle-catalyzed reactions through amalgamation. Under our reaction conditions, when excessive amount of mercury was added during the middle of the reaction, a complete inhibition was observed (Scheme 5.12).

Scheme 5.12 Mercury Poisoning Test



5.3 Conclusion

In summary, we have developed a distinct catalytic system for the direct β -arylation of ketones with widely accessible diaryliodonium salts. Compared to our previous method using aryl halides, this new protocol possesses several advantages. First, it avoids the use of stoichiometric silver or copper promoters. Second, the conditions are much user friendly: both moisture and air can be tolerated. Third, the substrate scope is also extended to cyclic ketones with α , β , or γ -substituents. Finally, the catalytic system is able to sustain the reactivity under milder conditions (e.g. low temperatures). The unique catalytic system featured by the use of the bis-*N*-tosylsulfilimine ligand should have broad implications beyond the present work, and may inspire others to use similar systems to develop other transformations.

5.4 Experimental

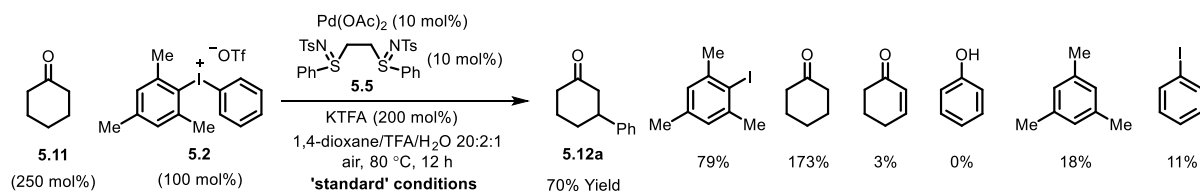
Unless stated otherwise, all reactions were run in vials sealed with PTFE lined caps, purchased from Qorpak. 1,4-Dioxane was distilled from Na and freeze-pump-thawed three times prior to use. Trifluoroacetic acid (TFA, 99%) and palladium acetate (98%) were purchased from Aldrich and used as received. Potassium trifluoroacetate (KTFA) was purchased from Oakwood Chemical and used as received. All commercially available substrates were used without further purification. Thin layer chromatography (TLC) analysis was run on silica gel plates purchased from EMD Chemical (silica gel 60, F254). Gas chromatography (GC) data was obtained from Agilent 7820A GC system, equipped with Agilent 19091J-413 column and a FID detector. GC yield of 3-phenyl cyclohexanone (**5.12a**) was determined using standard curves with dodecane as internal standard. Mass spectra were recorded on an Autospec or Agilent 6150. Accurate masses from high-resolution mass spectra were reported for the molecular ion $[M+Na]^+$, $[M]^+$ or $[M+H]^+$. 1H NMR and ^{13}C NMR spectra were recorded on a Varian Gemini (400 MHz for 1H , 100 MHz for ^{13}C). Chemical shifts are reported as parts per million (ppm) using residual solvent signals as internal standard ($CHCl_3$, $\delta = 7.26$ ppm for 1H NMR, $\delta = 77.00$ ppm for ^{13}C NMR, DMSO, $\delta = 40.45$ ppm for ^{13}C NMR). Data for 1H NMR were presented as following: chemical shifts (δ , ppm), multiplicity (br = broad, s = singlet, d = doublet, t = triplet, q = quartet, dd = doublet of doublets, tt = triplet of triplets, td = triplet of doublets, m = multiplet), coupling constant (Hz), and integration. The chemical shifts of peaks found were reported for ^{13}C NMR spectra. Infrared spectra were obtained from a Nicolet iS5 FTIR spectrometer. Dynamic light scattering experiments were performed on a Zetasizer Nano ZS instrument.

General procedure for reaction condition screening

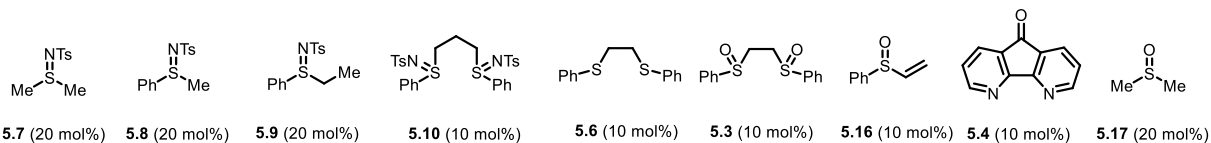
The reaction was run at a 0.2 mmol scale based on the limiting reagent. A 4 mL vial was charged with palladium salt, ligand, additives, cyclohexanones, mesitylphenyliodonium salt, 1 mL 1,4-dioxane and cosolvent. The vial was sealed with a PTFE lined cap and heated in a pie-block at 80 °C for 12 hours under stirring. Then the mixture was allowed to cool to room temperature. The reaction mixture was diluted with 1 mL ethyl acetate and appropriate amount of dodecane (~10 mg) was added as the internal standard. The mixture was stirred for an additional 5 min to fully mix. ~0.2 mL of the resulting mixture was filtered through a small plug of silica gel, eluted with diethyl ether. The filtrate was directly used for GC analysis.

GC instrument conditions: inlet temperature: 250 °C, detector temperature: 300 °C, hydrogen flow: 40 mL/min, air flow: 400 mL/min, column + makeup flow: 30 mL/min. Method: 50 °C hold for 0 min, followed by a temperature increase of 10°C/min to 280 °C, hold 0 min (total run time: 23 min). Yields of product and byproducts are calculated using standard curves with dodecane as the internal standard. Full details of the control reactions are listed below (Table 5.8).

Table 5.8 Full Details of the Control Reactions



entry	variations from the 'standard' conditions	yield of 5.12a (%)	5.11 (%)	iodomesitylene (%)	enone (%)	mesitylene (%)	iodobenzene (%)
1	[MesIPh]BF ₄ instead of 5.2	50	158	79	2	18	10
2	[MesIPh]TFA instead of 5.2	56	168	78	3	17	12
3	[Ph ₂]OTf instead of 5.2	36	199	--	0	--	50
4	PhI instead of 5.2	5	240	--	0	--	65
5	w/o Pd(OAc) ₂	0	244	9	0	1	3
6	w/o 5.5	8	235	33	1	7	6
7	other ligands instead of L1	listed below	--	--	--	--	--
8	w/o KTFA and TFA	13	128	73	0	10	9
9	w/o TFA	36	179	86	1	12	10
10	w/o KTFA	34	179	62	0	8	6
11	100 mol% HOTf instead of TFA	2	142	29	0	2	3
12	KOAc instead of KTFA	66	176	76	3	17	9
13	NaOAc instead of KTFA	59	167	72	3	16	8
14	HOAc instead of TFA	40	181	77	5	19	10
15	HFIP instead of TFA	43	195	82	2	16	10
16	w/o H ₂ O	47	176	71	7	15	11
17	N ₂ instead of air	73	170	80	2	18	11
18	5.2:5.11 = 1:1	48	47	68	0	15	10
19	5.7	29	212	52	2	15	10
20	5.8	22	212	58	1	13	12
21	5.9	41	194	64	4	18	13
22	5.10	47	187	66	3	17	9
23	5.6	41	178	74	9	19	20
24	5.3	60	164	81	4	20	15
25	5.16	44	199	71	1	15	13
26	5.4	42	173	71	7	18	20
27	5.17	36	169	62	1	22	12

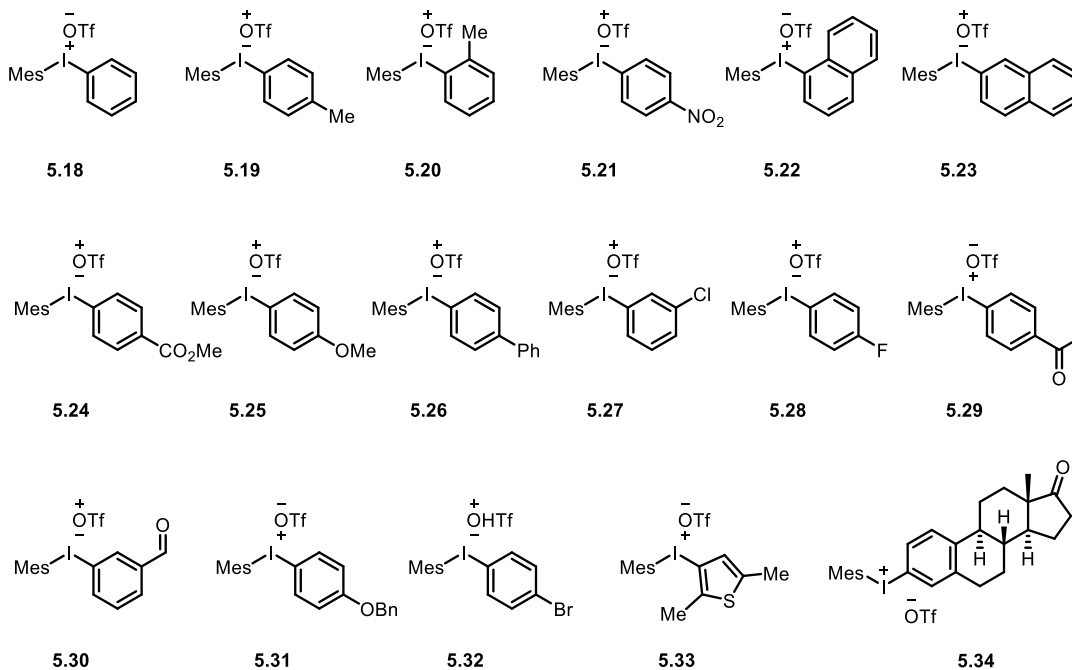
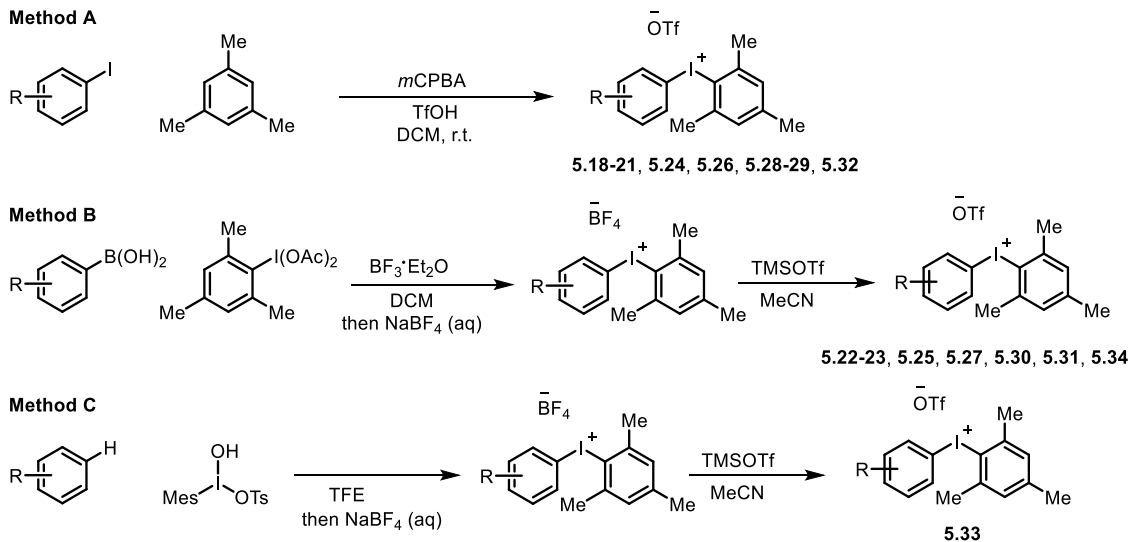


General Procedure for the β -Arylation of Ketones with Mesitylaryliodonium Salts

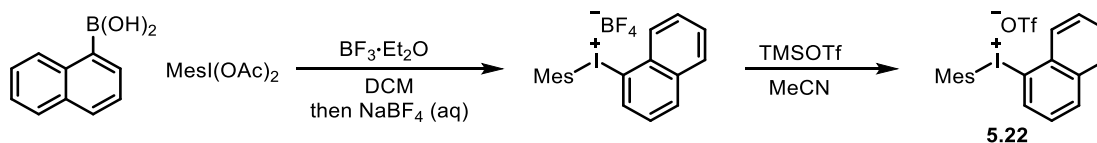
Unless stated otherwise, an 8 mL vial was charged with Pd(OAc)₂ (9.0 mg, 0.1 equiv.), KTFA (122 mg, 2.0 equiv.), Mesitylaryliodonium salt (0.4 mmol), **5.5** (24 mg, 0.1 equiv.), TFA (200 μ L), ketone (1.0 mmol, 2.5 equiv.), H₂O (100 μ L) and 1,4-dioxane (2 mL). The vial was sealed with a PTFE lined cap and heated in a pie-block at 80 °C for 12 hours under stirring. Then, the vial was allowed to cool to room temperature and the mixture was filtered through a small plug of silica gel, eluted with diethyl ether. The solvent was then removed *in vacuo* and flash column chromatography (hexane/ethyl acetate or DCM/methanol) of the residue gave the arylation product.

Synthesis of mesitylaryliodonium salts

Scheme 5.13 Methods for the Synthesis of Mesitylaryliodonium Salts

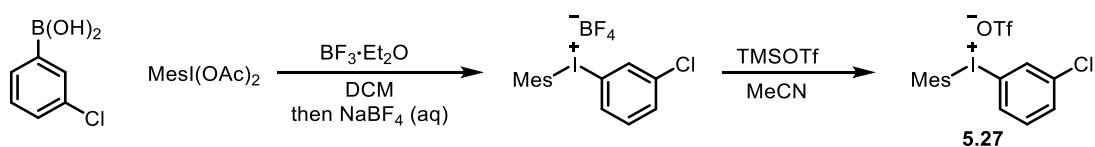


Detailed procedure for selected mesitylaryliodonium salts



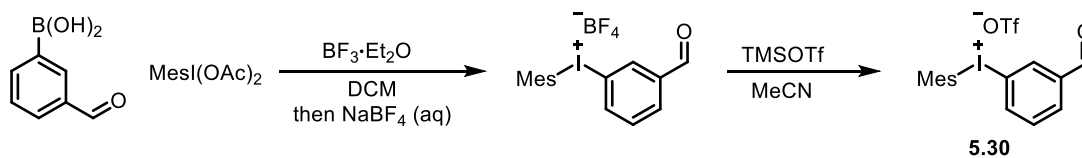
Mesityl(1-naphthyl)iodonium trifluoromethanesulfonate (5.22): A 250 mL round bottom flask was charged with naphthalene-1-boronic acid (860 mg, 5.0 mmol) and 50 mL DCM. The suspension was cooled to 0 °C using an ice bath. Boron trifluoride diethyl etherate (1.2 mL, 2.0 equiv.) was added to the mixture dropwise at 0 °C and the solution was stirred at the same temperature for 10 min. A solution of iodomesitylene diacetate (1.91 g, 1.05 equiv.) in 15 mL DCM was added to the flask dropwise at 0 °C. After the addition, the mixture was warmed to room temperature and stirred for 2 hr. The reaction was quenched by 100 mL saturated NaBF₄ solution and the bi-phase mixture was stirred vigorously for 30 min. The organic layer was separated and the aqueous extracted with DCM. The combined organic phase was washed with water and brine, dried and concentrated in vacuo. The residue was triturated with diethyl ether to give a white solid. The solid was filtered, washed with diethyl ether and dried to give mesityl(1-naphthyl)iodonium tetrafluoroborate (1.78 g, 77 % Yield). The tetrafluoroborate salt was dissolved in 20 mL acetonitrile and cooled to 0 °C. Trimethylsilyl trifluoromethanesulfonate (1.1 mL, 1.5 equiv.) was added to the solution dropwise at 0 °C. The mixture was warmed to room temperature and stirred overnight. The solvent was removed in vacuo and the residue triturated with diethyl ether. The suspension was stored at -20 °C for 2 hr and the solid was filtered and washed with diethyl ether to give mesityl(1-naphthyl)iodonium trifluoromethanesulfonate as a white solid (1.85 g, 92 % Yield). Mp. 175-177 °C. ¹H NMR (400 MHz, CDCl₃) δ 8.07 (d, *J* =

8.0 Hz, 1H), 7.98-7.92 (m, 2H), 7.81-7.74 (m, 2H), 7.71-7.67 (m, 1H), 7.42 (t, $J = 8.0$ Hz, 1H), 7.10 (s, 2H), 2.65 (s, 6H), 2.35 (s, 3H). ^{13}C NMR (100 MHz, CDCl_3) δ 144.62, 142.49, 135.11, 133.65, 133.31, 131.70, 130.74, 130.04, 129.46, 128.38, 127.54, 127.29, 120.88, 120.35 (q, $J_{\text{C-F}} = 319$ Hz), 113.41, 27.23, 21.06. ^{19}F NMR (376 MHz, CDCl_3) δ -78.32. IR (KBr, cm^{-1}) 1499, 1450, 1249, 1161, 1030, 912, 741. HRMS calcd $\text{C}_{19}\text{H}_{18}\text{I}^+ [\text{M}-\text{CF}_3\text{SO}_3]^+$: 373.04480. Found: 373.04470.



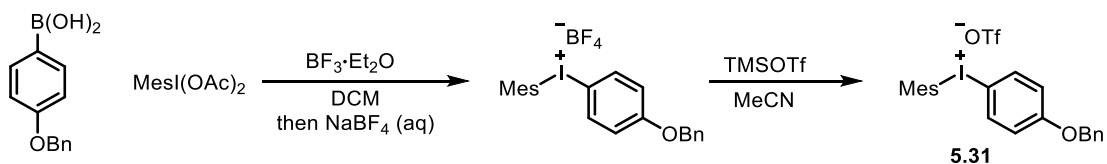
Mesityl(3-chlorophenyl)iodonium trifluoromethanesulfonate (5.27): A 250 mL round bottom flask was charged with 3-chlorophenylboronic acid (780 mg, 5.0 mmol) and 50 mL DCM. The suspension was cooled to 0 °C using an ice bath. Boron trifluoride diethyl etherate (1.2 mL, 2.0 equiv.) was added to the mixture dropwise at 0 °C and the solution was stirred at the same temperature for 10 min. A solution of iodomesitylene diacetate (1.91 g, 1.05 equiv.) in 15 mL DCM was added to the flask dropwise at 0 °C. After the addition, the mixture was warmed to room temperature and stirred for 2 hr. The reaction was quenched by 100 mL saturated NaBF_4 solution and the bi-phase mixture was stirred vigorously for 30 min. The organic layer was separated and the aqueous extracted with DCM. The combined organic phase was washed with water and brine, dried and concentrated in vacuo. The residue was triturated with diethyl ether to give a white solid. The solid was filtered, washed with diethyl ether and dried to give mesityl(3-chlorophenyl)iodonium tetrafluoroborate (1.18 g, 53 % Yield). The tetrafluoroborate salt was

dissolved in 20 mL acetonitrile and cooled to 0 °C. Trimethylsilyl trifluoromethanesulfonate (0.8 mL, 1.5 equiv.) was added to the solution dropwise at 0 °C. The mixture was warmed to room temperature and stirred overnight. The solvent was removed in vacuo and the residue triturated with diethyl ether. The suspension was stored at -20 °C for 2 hr and the solid was filtered and washed with diethyl ether to give mesityl(3-chlorophenyl)iodonium trifluoromethanesulfonate as a white solid (1.28 g, 95 % Yield). Mp. 187-189 °C. **¹H NMR** (400 MHz, CDCl₃) δ 7.63 (ddd, $J_1 = 8.1$ Hz, $J_2 = 1.8$ Hz, $J_3 = 0.9$ Hz, 1H), 7.60 (t, $J = 1.8$ Hz, 1H), 7.46 (ddd, $J_1 = 8.1$ Hz, $J_2 = 1.8$ Hz, $J_3 = 0.9$ Hz, 1H), 7.31 (t, $J = 8.1$ Hz, 1H), 7.09 (s, 2H), 2.61 (s, 6H), 2.34 (s, 3H). **¹³C NMR** (100 MHz, CDCl₃) δ 144.54, 142.47, 137.25, 132.61, 132.29, 132.02, 131.24, 130.36, 120.73, 120.09 (q, $J_{C-F} = 318$ Hz), 111.60, 27.10, 21.14. **¹⁹F NMR** (376 MHz, CDCl₃) δ -78.45. **IR** (KBr, cm⁻¹) 1558, 1250, 1165, 1030, 913, 744. **HRMS** calcd C₁₅H₁₅ClI⁺ [M-CF₃SO₃]⁺: 356.99015. Found: 356.99000.



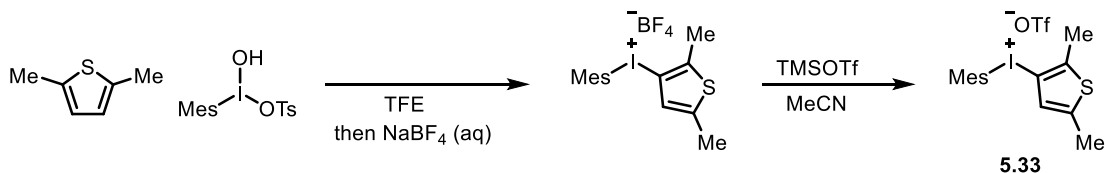
Mesityl(3-formylphenyl)iodonium trifluoromethanesulfonate (5.30): A 250 mL round bottom flask was charged with 3-formylphenylboronic acid (1.50 g, 10 mmol) and 100 mL DCM. The suspension was cooled to 0 °C using an ice bath. Boron trifluoride diethyl etherate (2.4 mL, 2.0 equiv.) was added to the mixture dropwise at 0 °C and the solution was stirred at the same temperature for 10 min. A solution of iodomesitylene diacetate (3.82 g, 1.05 equiv.) in 30 mL

DCM was added to the flask dropwise at 0 °C. After the addition, the mixture was warmed to room temperature and stirred for 2 hr. The reaction was quenched by 150 mL saturated NaBF₄ solution and the bi-phase mixture was stirred vigorously for 30 min. The organic layer was separated and the aqueous extracted with DCM. The combined organic phase was washed with water and brine, dried and concentrated in vacuo. The residue was triturated with diethyl ether to give a white solid. The solid was filtered, washed with diethyl ether and dried to give mesityl(3-formylphenyl)iodonium tetrafluoroborate (2.50 g, 57 % Yield). The tetrafluoroborate salt was dissolved in 30 mL acetonitrile and cooled to 0 °C. Trimethylsilyl trifluoromethanesulfonate (1.6 mL, 1.5 equiv.) was added to the solution dropwise at 0 °C. The mixture was warmed to room temperature and stirred overnight. The solvent was removed in vacuo and the residue triturated with diethyl ether. The suspension was stored at -20 °C for 2 hr and the solid was filtered and washed with diethyl ether to give mesityl(3-formylphenyl)iodonium trifluoromethanesulfonate as a white solid (2.42 g, 85 % Yield). Mp. 147-149 °C. ¹H NMR (400 MHz, CDCl₃) δ 9.93 (s, 1H), 8.20 (t, *J* = 1.6 Hz, 1H), 8.02-7.98 (m, 2H), 7.58 (t, *J* = 8.0 Hz, 1H), 7.11 (s, 2H), 2.64 (s, 6H), 2.36 (s, 3H). ¹³C NMR (100 MHz, DMSO) δ 192.60, 144.32, 142.66, 140.41, 139.40, 135.35, 133.58, 130.84, 123.52, 121.64 (q, *J*_{C-F} = 320 Hz), 116.09, 27.31, 21.49. ¹⁹F NMR (376 MHz, CDCl₃) δ -78.45. IR (KBr, cm⁻¹) 1708, 1701, 1588, 1451, 1271, 1241, 1187, 1029, 742. HRMS calcd C₁₆H₁₆IO⁺ [M-CF₃SO₃]⁺: 351.02400. Found: 351.02430.



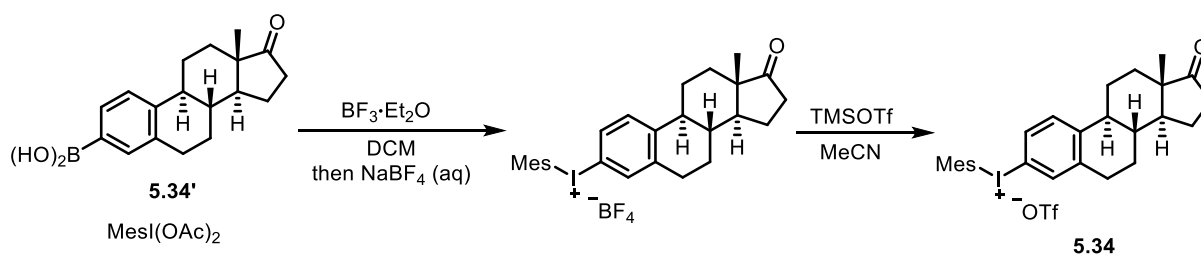
Mesityl(4-benzyloxyphenyl)iodonium trifluoromethanesulfonate (5.31): A 250 mL round bottom flask was charged with 4-benzyloxyphenylboronic acid (1.14 g, 5 mmol) and 50 mL DCM. The suspension was cooled to 0 °C using an ice bath. Boron trifluoride diethyl etherate (1.2 mL, 2.0 equiv.) was added to the mixture dropwise at 0 °C and the solution was stirred at the same temperature for 10 min. A solution of iodomesitylene diacetate (1.91 g, 1.05 equiv.) in 15 mL DCM was added to the flask dropwise at 0 °C. After the addition, the mixture was warmed to room temperature and stirred for 2 hr. The reaction was quenched by 100 mL saturated NaBF₄ solution and the bi-phase mixture was stirred vigorously for 30 min. The organic layer was separated and the aqueous extracted with DCM. The combined organic phase was washed with water and brine, dried and concentrated in vacuo. The residue was triturated with diethyl ether to give a white solid. The solid was filtered, washed with diethyl ether and dried to give mesityl(4-benzyloxyphenyl)iodonium tetrafluoroborate (2.12 g, 82 % Yield). The tetrafluoroborate salt was dissolved in 20 mL acetonitrile and cooled to 0 °C. Trimethylsilyl trifluoromethanesulfonate (1.1 mL, 1.5 equiv.) was added to the solution dropwise at 0 °C. The mixture was warmed to room temperature and stirred overnight. The solvent was removed in vacuo and the residue triturated with diethyl ether. The suspension was stored at -20 °C for 2 hr and the solid was filtered and washed with diethyl ether to give mesityl(4-benzyloxyphenyl)iodonium trifluoromethanesulfonate as a white solid (2.25 g, 95 % Yield). Mp. 166-169 °C. **¹H NMR** (400 MHz, CDCl₃) δ 7.66-7.62 (m, 2H), 7.41-7.32 (m, 5H), 7.08 (s, 2H), 7.00-6.96 (m, 2H), 5.05 (s, 2H), 2.64 (s, 6H), 2.34 (s, 3H). **¹³C NMR** (100 MHz, DMSO) δ 161.72, 143.81, 142.26, 137.53, 137.07, 130.62, 129.45, 129.06, 128.81, 124.05, 121.63 (q, J_{C-F} = 320 Hz), 119.21, 104.65, 70.61, 27.19, 21.44. **¹⁹F NMR** (376 MHz, CDCl₃) δ -78.34. **IR** (KBr,

cm⁻¹) 1572, 1485, 1246, 1180, 913, 748. **HRMS** calcd C₂₂H₂₂IO⁺ [M-CF₃SO₃]⁺: 429.07100.
Found: 429.07090.



Mesityl(2,5-dimethylthiophen-3-yl)iodonium trifluoromethanesulfonate (5.33): To a stirring solution of 2,5-dimethylthiophene (1.12 g, 10 mmol) in 40 mL trifluoroethanol (TFE) was added (hydroxy(tosyloxy)iodo)mesitylene (4.34 g, 1.0 equiv.). The mixture was stirred at room temperature and monitored by TLC. After 2,5-dimethylthiophene was consumed, the reaction was quenched by 150 mL saturated NaBF₄ solution and the mixture was stirred vigorously for 30 min. The mixture was extracted with DCM. The combined organic phase was washed with water and brine, dried and concentrated in vacuo. The residue was triturated with diethyl ether to give a white solid. The solid was filtered, washed with diethyl ether and dried to give mesityl(2,5-dimethylthiophen-3-yl)iodonium tetrafluoroborate (1.20 g, 27 % Yield). The tetrafluoroborate salt was dissolved in 20 mL acetonitrile and cooled to 0 °C. Trimethylsilyl trifluoromethanesulfonate (0.8 mL, 1.5 equiv.) was added to the solution dropwise at 0 °C. The mixture was warmed to room temperature and stirred overnight. The solvent was removed in vacuo and the residue triturated with diethyl ether. The suspension was stored at -20 °C for 2 hr and the solid was filtered and washed with diethyl ether to give mesityl(2,5-dimethylthiophen-3-yl)iodonium trifluoromethanesulfonate as a off-white solid (700 mg, 51 % Yield). Mp. 219-221

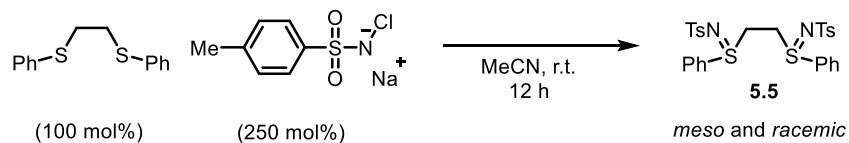
°C. **¹H NMR** (400 MHz, CDCl₃) δ 7.07 (s, 2H), 6.64-6.63 (m, 1H), 2.65 (s, 6H), 2.59 (s, 3H), 2.41 (s, 3H), 2.34 (s, 3H). **¹³C NMR** (100 MHz, CDCl₃) δ 144.47, 144.02, 142.29, 141.65, 130.41, 127.75, 121.70, 120.29 (q, *J*_{C-F} = 319 Hz), 94.68, 27.08, 21.02, 16.99, 15.42. **¹⁹F NMR** (376 MHz, CDCl₃) δ -78.36. **IR** (KBr, cm⁻¹) 1275, 1237, 1164, 1032, 913, 744. **HRMS** calcd C₁₅H₁₈IS⁺ [M-CF₃SO₃]⁺: 357.01680. Found: 357.01720.



5.34: A 250 mL round bottom flask was charged with boronic acid **5.34'** (1.67 g, 5.6 mmol) and 50 mL DCM. The suspension was cooled to 0 °C using an ice bath. Boron trifluoride diethyl etherate (1.2 mL, 2.0 equiv.) was added to the mixture dropwise at 0 °C and the solution was stirred at the same temperature for 10 min. A solution of iodomesitylene diacetate (2.14 g, 1.05 equiv.) in 15 mL DCM was added to the flask dropwise at 0 °C. After the addition, the mixture was warmed to room temperature and stirred for 2 hr. The reaction was quenched by 100 mL saturated NaBF₄ solution and the bi-phase mixture was stirred vigorously for 30 min. The organic layer was separated and the aqueous extracted with DCM. The combined organic phase was washed with water and brine, dried and concentrated in vacuo. The residue was triturated with diethyl ether to give a white solid. The solid was filtered, washed with diethyl ether and dried to give tetrafluoroborate salt (1.53 g, 47 % Yield). The tetrafluoroborate salt was dissolved

in 20 mL acetonitrile and cooled to 0 °C. Trimethylsilyl trifluoromethanesulfonate (0.75 mL, 1.5 equiv.) was added to the solution dropwise at 0 °C. The mixture was warmed to room temperature and stirred overnight. The solvent was removed in vacuo and the residue triturated with diethyl ether. The suspension was stored at -20 °C for 2 hr and the solid was filtered and washed with diethyl ether to give **S3q** as a white solid (1.43 g, 84 % Yield). Mp. 185-188 °C. **¹H NMR** (400 MHz, CDCl₃) δ 7.54 (s, 1H), 7.33-7.28 (m, 2H), 7.10 (s, 2H), 2.92-2.88 (m, 2H), 2.63 (s, 6H), 2.50 (dd, *J*₁ = 19 Hz, *J*₂ = 8.7 Hz, 1H), 2.35 (s, 3H), 2.33-2.26 (m, 2H), 2.19-1.94 (m, 4H), 1.67-1.37 (m, 6H), 0.88 (s, 3H). **¹³C NMR** (100 MHz, CDCl₃) δ 220.16, 144.56, 144.33, 142.44, 141.96, 133.59, 130.32, 129.82, 129.45, 120.30 (q, *J*_{C-F} = 320 Hz), 119.99, 108.45, 50.28, 47.73, 44.18, 37.33, 35.72, 31.34, 29.24, 27.17, 25.83, 25.34, 21.48, 21.10, 13.71. **¹⁹F NMR** (376 MHz, CDCl₃) δ -78.32. **IR** (KBr, cm⁻¹) 2931, 1736, 1250, 1162, 1028, 913, 743. **HRMS** calcd C₂₇H₃₂IO⁺ [M-CF₃SO₃]⁺: 499.14920. Found: 499.14900.

Synthesis and pyrolysis of ligand 5.5



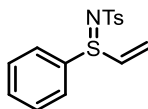
To a stirred solution of 1,2-bis(phenylthio)ethane (5.0 g, 20.3 mmol) in 80 mL of acetonitrile was added Chloramine-T trihydrate (14.3 g, 2.5 equiv.). The mixture was stirred overnight at room temperature and a large amount of white precipitate was observed. After the completion of the reaction, 120 mL of dichloromethane was added to the mixture. The white

precipitate was filtered off and the solvent was removed in vacuo to give a white solid. The residue was dissolved in about 400 mL of acetone. Brief heat can be used to facilitate the dissolution, but the ligand may decompose under elevated temperature (the ligand pyrolysis proceeds in above 95% conversion within 30 min at 80 °C). After the majority of the solid was dissolved, the mixture was filtered to remove the insoluble impurities when hot (The filtration step is important since the insoluble impurities were observed to hamper the β -arylation reactions). The filtrate was allowed to cool to room temperature and stand for 1 day to crystalize. The small white crystals were filtered and washed with cold acetone to give a mixture of *meso* and *racemic* ligands (5.87 g, 49% Yield). Among the two diastereomers, the *meso* ligand has worse solubility than the racemic ligand. Thus both ligands can be isolated as pure diastereomers by collecting the early or late portion of the crystalized solids.

5.5-meso: Mp. 165-168 °C. **¹H NMR** (400 MHz, CDCl₃) δ 7.64-7.53 (m, 14H), 7.09 (d, J = 8.0 Hz, 4H), 3.37-3.22 (m, 4H), 2.30 (s, 6H). **¹³C NMR** (100 MHz, CDCl₃) δ 142.09, 140.47, 132.97, 132.61, 130.29, 129.28, 126.12, 126.03, 46.17, 21.40. **IR** (KBr, cm⁻¹) 1305, 1293, 1145, 953, 913, 748. **HRMS** calcd C₂₈H₂₈N₂NaO₄S₄⁺ [M+Na]⁺: 607.08240. Found: 607.08230.

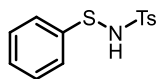
5.5-racemic: Mp. 141-143 °C. **¹H NMR** (400 MHz, CDCl₃) δ 7.86-7.84 (m, 4H), 7.79 (d, J = 8.0 Hz, 4H), 7.57-7.50 (m, 6H), 7.20 (d, J = 8.0 Hz, 4H), 3.92-3.83 (m, 2H), 3.32-3.22 (m, 2H), 2.34 (s, 6H). **¹³C NMR** (100 MHz, CDCl₃) δ 142.19, 140.30, 132.55, 132.23, 130.11,

129.39, 126.28, 126.12, 49.78, 21.39. **IR** (KBr, cm^{-1}) 3061, 2924, 1597, 1446, 1283, 1143, 1088, 968, 913, 747. **HRMS** calcd $\text{C}_{28}\text{H}_{28}\text{N}_2\text{NaO}_4\text{S}_4^+$ $[\text{M}+\text{Na}]^+$: 607.08240. Found: 607.08230.



5.14

N-Tosyl phenyl vinyl sulfilimine (5.14): White solid. Mp. 109-112 °C. $R_f = 0.5$ (DCM/MeOH = 20:1). **$^1\text{H NMR}$** (400 MHz, CDCl_3) δ 7.75 (d, $J = 8.0$ Hz, 2H), 7.65-7.63 (m, 2H), 7.56-7.47 (m, 3H), 7.17 (d, $J = 8.0$ Hz, 2H), 6.43-6.37 (m, 1H), 6.32-6.28 (m, 1H), 6.05-6.02 (m, 1H), 2.35 (s, 3H). **$^{13}\text{C NMR}$** (100 MHz, CDCl_3) δ 141.73, 141.31, 134.64, 133.14, 132.56, 130.01, 129.17, 126.97, 126.22, 125.99, 21.40. **IR** (KBr, cm^{-1}) 3055, 2924, 1723, 1446, 1282, 1142, 1089, 966, 750. **HRMS** calcd $\text{C}_{15}\text{H}_{16}\text{NO}_2\text{S}_2$ $[\text{M}+\text{H}]^+$: 306.0622. Found: 306.0625.



5.15

N-Phenylsulfanyl tosylamine (5.15): White solid. Mp. 101-104 °C. $R_f = 0.6$ (hexane/ethyl acetate = 2:1). **$^1\text{H NMR}$** (400 MHz, CDCl_3) δ 7.80-7.77 (m, 2H), 7.35-7.32 (m, 2H), 7.29-7.23 (m, 4H), 7.23-7.19 (m, 1H). 6.07-6.03 (m, 1H), 2.41 (s, 3H). **$^{13}\text{C NMR}$** (100 MHz, CDCl_3) δ 144.26, 137.23, 136.02, 129.62, 128.93, 127.72, 127.49, 126.11, 21.58. **IR** (KBr, cm^{-1})

1597, 1366, 1293, 1161, 1090, 913, 874, 743. **HRMS** calcd C₁₃H₁₃NO₂S₂ [M]⁺: 279.0388.
Found: 279.0387.

General procedure for kinetic measurement

An 8 mL vial or 10 mL round-bottom flask was charged with Pd(OAc)₂ (9.0 mg, 0.1 equiv.), KTFA (122 mg, 2.0 equiv.), Mesitylphenyliodonium salt (189 mg, 0.4 mmol), **5.5** (24 mg, 0.1 equiv.), TFA (200 μL), cyclohexanone (98 mg, 2.5 equiv.), H₂O (100 μL) and 1,4-dioxane (2 mL). Dodecane (~25 mg) was added to the reaction vial as the internal standard. The vial was sealed with a PTFE lined cap and heated in a pie-block at 80 °C (the round-bottom flask sealed with a rubber septum and heated in an oil-bath). Aliquots (~50 μL) were taken from the reaction mixture and directly passed through a small plug of silica gel (~400 mg), eluted with diethyl ether, to give ~10 mL solution. 1-2 mL of the solution was subsequently submitted to the gas chromatography.

General procedure for the hot filtration test

As the precipitation of palladium black was noted during and after the reaction, hot filtration tests were employed to distinguish between a soluble nanoparticle and a heterogeneous catalyst. Four parallel reactions were set up for the hot filtration test. To the 4 mL vial was charged with Pd(OAc)₂ (4.5 mg, 0.1 equiv.), KTFA (61 mg, 2.0 equiv.), Mesitylphenyliodonium salt (95 mg, 0.2 mmol), **5.5** (12 mg, 0.1 equiv.), TFA (100 μL), cyclohexanone (49 mg, 2.5

equiv.), H₂O (50 µL) and 1,4-dioxane (1 mL). Dodecane (~10 mg) was added to the reaction vial as the internal standard. The vial was sealed with a PTFE lined cap, heated in a pie-block at 80 °C, and monitored by gas chromatography when necessary.

Vial 1: This reaction was set up as the control reaction. The mixture was monitored at 90 min and 12 h using gas chromatography and the yields calculated.

Vial 2: This reaction was set up as the control reaction to investigate the effect of Celite on the reaction. The reaction was set up as described above. The mixture was monitored, and 100 mg Celite was added to the reaction at 90 min. The resulting mixture was kept stirring at 80 °C and monitored by gas chromatography at 12 h.

Vial 3: This reaction was set up as described above. The mixture was monitored at 90 min and 100 mg Celite was added to the reaction. After stirring for 1 min, the mixture was passed through a small plug of Celite (~100 mg) to a new vial (**Vial 3a**) when hot and the Celite plug was rinsed with ~200 µL of dioxane. The heat was restored to the new vial and reaction monitored at 110 min and 12 h. The remaining Celite layer was added to a new vial (**Vial 3b**) containing KTFA (61 mg, 2.0 equiv.), Mesitylphenyliodonium salt (95 mg, 0.2 mmol), TFA (100 µL), cyclohexanone (49 mg, 2.5 equiv.), H₂O (50 µL) and 1,4-dioxane (1 mL). The new vial was heated at 80 °C and monitored by gas chromatography at 110 min and 12 h.

Vial 4: This reaction was set up as described above. The mixture was monitored at 90 min and quickly passed through a PTFE 200 nm filter to a new vial when hot and the filter was rinsed with ~200 µL of dioxane. The heat was restored to the new vial and reaction monitored at 110 min and 12 h.

The yields obtained for different vials at different time point were summarized below (Table 5.9). These results suggested that the active palladium catalyst generated during the induction period sustained the solubility, and those heterogeneous species were not responsible for the transformation.

Table 5.9 Results of Hot Filtration Test

Yield (%)	Before filtration	After filtration	
	90 min	100 min	12 h
Vial 1	18	--	76
Vial 2	19	--	74
Vial 3a	16	22	74
Vial 3b		0	0
Vial 4	17	22	68

General procedure for the mercury poisoning test

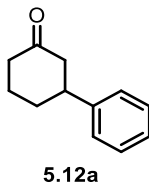
A supplementary mercury poisoning test was also executed to support the presence of palladium nanoparticles. Molecular mercury is known to inhibit noble metal-nanoparticle-catalyzed reactions through amalgamation. An 8 mL vial was charged with Pd(OAc)₂ (9.0 mg, 0.1 equiv.), KTFA (122 mg, 2.0 equiv.), Mesitylphenyliodonium salt (189 mg, 0.4 mmol), **5.5** (24 mg, 0.1 equiv.), TFA (200 μL), cyclohexanone (98 mg, 2.5 equiv.), H₂O (100 μL) and 1,4-dioxane (2 mL). Dodecane (~25 mg) was added to the reaction vial as the internal standard. The vial was sealed with a PTFE lined cap and heated in a pie-block at 80 °C. Aliquots (~50 μL) were taken from the reaction mixture and directly passed through a small plug of silica gel (~400 mg), eluted with diethyl ether, to give ~10 mL solution. 1-2 mL of the solution was subsequently

submitted to the gas chromatography. When the product formation initiated and the yield reached ~40%, 200 μL of mercury was added to the mixture via syringe. The resulting mixture was heated at 80 $^{\circ}\text{C}$ and monitored by gas chromatography. The kinetic data showed the product formation was inhibited with the addition of mercury.

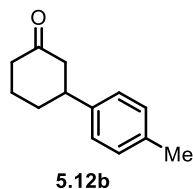
General procedure for dynamic light scattering (DLS) experiment

An 4 mL vial was charged with $\text{Pd}(\text{OAc})_2$ (4.5 mg, 0.1 equiv.), KTFA (61 mg, 2.0 equiv.), Mesitylphenyliodonium salt (95 mg, 0.2 mmol), **5.5** (12 mg, 0.1 equiv.), TFA (100 μL), cyclohexanone (49 mg, 2.5 equiv.), H_2O (50 μL) and 1,4-dioxane (1 mL). Dodecane (~10 mg) was added to the reaction vial as the internal standard. The vial was sealed with a PTFE lined cap and heated in a pie-block at 80 $^{\circ}\text{C}$. After the reaction has proceeded for 90 min, the mixture was allowed to cool to room temperature, and gas chromatography was used to confirm that the product formation had initiated. Subsequently, the reaction solution was directly used for the dynamic light scattering analysis using a Zetasizer Nano ZS instrument. The data was collected at 25 $^{\circ}\text{C}$ and the medium parameters were set according to the properties of 1,4-dioxane (dispersant refractive index: 1.420, viscosity: 1.1944 $\text{mPa}\cdot\text{s}$).

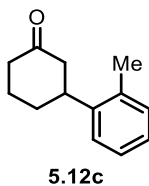
Characterization of products



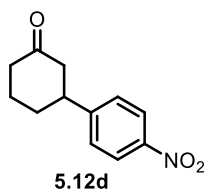
3-Phenylcyclohexan-1-one (5.12a): 66 % Yield. **¹H NMR** (400 MHz, CDCl₃) δ 7.36-7.21 (m, 2H), 7.26-7.22 (m, 3H), 3.06-2.98 (m, 1H), 2.60 (ddt, $J_1 = 14.0$ Hz, $J_2 = 4.6$ Hz, $J_3 = 1.9$ Hz, 1H), 2.53 (dd, $J_1 = 12.3$ Hz, $J_2 = 1.1$ Hz, 1H), 2.51-2.44 (m, 1H), 2.43-2.35 (m, 1H), 2.19-2.07 (m, 2H), 1.91-1.73 (m, 2H). **EI-MS** (m/z , relative intensity): 174 (M^+ , 90), 131 (80), 117 (100), 104 (78), 91 (50), 78 (40).



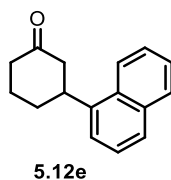
3-(p-Tolyl)cyclohexan-1-one (5.12b): 69 % Yield. **¹H NMR** (400 MHz, CDCl₃) δ 7.16-7.09 (m, 4H), 3.02-2.94 (m, 1H), 2.57 (ddt, $J_1 = 10.6$ Hz, $J_2 = 4.6$ Hz, $J_3 = 1.9$ Hz, 1H), 2.55-2.28 (m, 3H), 2.33 (s, 3H), 2.17-2.25 (m, 2H), 1.89-1.72 (m, 2H). **EI-MS** (m/z , relative intensity): 188 (M^+ , 65), 145 (40), 131 (100), 118 (46), 105 (20), 91 (30).



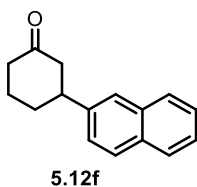
3-(*o*-Tolyl)cyclohexan-1-one (5.12c): 62 % Yield. $^1\text{H NMR}$ (400 MHz, CDCl_3) δ 7.25-7.12 (m, 4H), 3.26-3.19 (m, 1H), 2.53-2.37 (m, 4H), 2.33 (s, 3H), 2.22-2.15 (m, 1H), 2.05-2.00 (m, 1H), 1.90-1.76 (m, 2H). **EI-MS** (m/z , relative intensity): 188 (M^+ , 70), 145 (100), 131 (90), 117 (75), 105 (30), 91 (50).



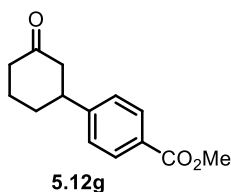
3-(4-Nitrophenyl)cyclohexan-1-one (5.12d): 49 % Yield. $^1\text{H NMR}$ (400 MHz, CDCl_3) δ 8.19 (d, $J = 8.8$ Hz, 2H), 7.39 (d, $J = 8.8$ Hz, 2H), 3.12 (tt, $J_1 = 11.7$ Hz, $J_2 = 3.9$ Hz, 1H), 2.64-2.37 (m, 4H), 2.21-2.10 (m, 2H), 1.94-1.70 (m, 2H). **EI-MS** (m/z , relative intensity): 219 (M^+ , 90), 176 (100), 163 (30), 115 (25), 91 (20), 77 (23).



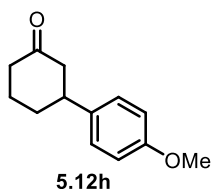
3-(Naphthalen-1-yl)cyclohexan-1-one (5.12e): 64 % Yield. $^1\text{H NMR}$ (400 MHz, CDCl_3) δ 8.04 (d, $J = 8.4$ Hz, 1H), 7.90-7.87 (m, 1H), 7.77 (d, $J = 8.4$ Hz, 1H), 7.56-7.46 (m, 3H), 7.40 (d, $J = 7.2$ Hz, 1H), 3.87 (ddd, $J_1 = 11.7$ Hz, $J_2 = 7.2$ Hz, $J_3 = 3.6$ Hz 1H), 2.81-2.77 (m, 1H), 2.71-2.65 (m, 1H), 2.61-2.55 (m, 1H), 2.52-2.44 (m, 1H), 2.29-2.18 (m, 2H), 2.06-1.85 (m, 2H). **EI-MS** (m/z , relative intensity): 224 (M^+ , 85), 181 (25), 167 (100), 153 (70), 141 (30), 128 (20).



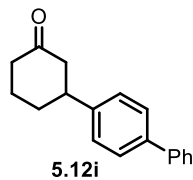
3-(Naphthalen-2-yl)cyclohexan-1-one (5.12f): 70 % Yield. $^1\text{H NMR}$ (400 MHz, CDCl_3) δ 7.83-7.81 (m, 3H), 7.65 (d, $J = 1.3$ Hz, 1H), 7.50-7.43 (m, 2H), 7.37 (dd, $J_1 = 8.6$ Hz, $J_2 = 1.8$ Hz, 1H), 3.19 (tdd, $J_1 = 11.4$ Hz, $J_2 = 5.2$ Hz, $J_3 = 3.3$ Hz 1H), 2.72-2.61 (m, 2H), 2.51 (dq, $J_1 = 14.3$ Hz, $J_2 = 3.2$ Hz, $J_3 = 1.6$ Hz, 1H), 2.47-2.33 (m, 1H), 2.22-2.16 (m, 2H), 2.06-1.92 (m, 1H), 1.89-1.77 (m, 1H). **EI-MS** (m/z , relative intensity): 224 (M^+ , 90), 181 (33), 167 (100), 154 (60), 141 (45), 128 (30), 115 (21).



Methyl 4-(3-oxocyclohexyl)benzoate (5.12g): 60 % Yield. $^1\text{H NMR}$ (400 MHz, CDCl_3) δ 7.99 (d, $J = 8.0$ Hz, 2H). 7.28 (d, $J = 8.0$ Hz, 2H), 3.90 (s, 3H), 3.10-3.03 (m, 1H), 2.59 (ddt, $J_1 = 14.1$ Hz, $J_2 = 4.9$ Hz, $J_3 = 1.9$ Hz, 1H), 2.57-2.53 (m, 1H), 2.52-2.45 (m, 1H), 2.44-2.35 (m, 1H), 2.19-2.07 (m, 2H), 1.91-1.73 (m, 2H). **EI-MS** (m/z , relative intensity): 232 (M^+ , 95), 201 (52), 189 (75), 145 (71), 131 (100), 91 (33), 77 (40).

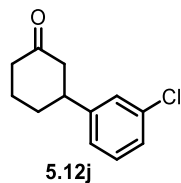


3-(4-Methoxyphenyl)cyclohexan-1-one (5.12h): 60 % Yield. $^1\text{H NMR}$ (400 MHz, CDCl_3) δ 7.16-7.12 (m, 2H), 6.89-6.85 (m, 2H), 3.80 (s, 3H), 2.95 (tt, $J_1 = 11.7$ Hz, $J_2 = 4.0$ Hz, 1H), 2.59 (ddt, $J_1 = 14.0$ Hz, $J_2 = 4.2$ Hz, $J_3 = 1.9$ Hz, 1H), 2.53-2.33 (m, 3H), 2.18-2.05 (m, 2H), 1.87-1.71 (m, 2H). **EI-MS** (m/z , relative intensity): 204 (M^+ , 55), 161 (30), 147 (100), 134 (35), 91 (30), 77 (20).

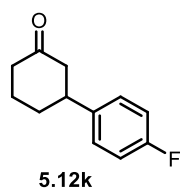


3-([1,1'-Biphenyl]-4-yl)cyclohexan-1-one (5.12i): 74 % Yield. $^1\text{H NMR}$ (400 MHz, CDCl_3) δ 7.61-7.56 (m, 4H), 7.47-7.43 (m, 2H), 7.34 (ddt, $J_1 = 6.6$ Hz, $J_2 = 5.2$ Hz, $J_3 = 1.3$ Hz,

1H), 7.32-7.30 (m, 2H), 3.12-3.04 (m, 1H), 2.69-2.64 (m, 1H), 2.62-2.55 (m, 1H), 2.54-2.35 (m, 2H), 2.22-2.12 (m, 2H), 1.95-1.76 (m, 2H). **EI-MS** (*m/z*, relative intensity): 250 (M^+ , 98), 207 (25), 193 (100), 178 (72), 165 (48), 152 (35), 115 (20).

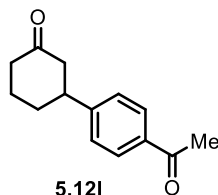


3-(3-Chlorophenyl)cyclohexan-1-one (5.12j): 62 % Yield. **$^1\text{H NMR}$** (400 MHz, CDCl_3) δ 7.28-7.20 (m, 3H), 7.07 (dt, $J_1 = 7.4$ Hz, $J_2 = 1.3$ Hz, 1H), 2.99 (tt, $J_1 = 11.9$ Hz, $J_2 = 3.9$ Hz, 1H), 2.62-2.56 (m, 1H), 2.53-2.27 (m, 3H), 2.19-2.13 (m, 1H), 2.10-2.06 (m, 1H), 1.88-1.71 (m, 2H). **EI-MS** (*m/z*, relative intensity): 208 (M^+ , 85), 165 (100), 151 (46), 138 (60), 115 (50), 103 (52), 77 (33).

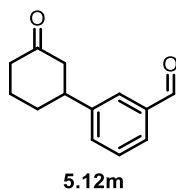


3-(4-Fluorophenyl)cyclohexan-1-one (5.12k): 66 % Yield. **$^1\text{H NMR}$** (400 MHz, CDCl_3) δ 7.19-7.16 (m, 2H), 7.03-6.99 (m, 2H), 3.00 (tt, $J_1 = 11.8$ Hz, $J_2 = 3.9$ Hz, 1H), 2.57 (ddt, $J_1 = 13.9$ Hz, $J_2 = 4.2$ Hz, $J_3 = 2.0$ Hz, 1H), 2.52-2.33 (m, 3H), 2.17-2.04 (m, 2H), 1.87-1.71 (m, 2H).

EI-MS (m/z , relative intensity): 192 (M^+ , 60), 149 (40), 135 (100), 122 (70), 109 (35), 96 (30), 70 (20).

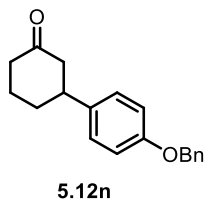


3-(4-Acetylphenyl)cyclohexan-1-one (5.12l): 53 % Yield. $^1\text{H NMR}$ (400 MHz, CDCl_3) δ 7.94-7.91 (m, 2H), 7.33-7.30 (m, 2H), 3.12-3.04 (m, 1H), 2.64-2.50 (m, 2H), 2.47 (dq, $J_1 = 11.0$ Hz, $J_2 = 3.3$ Hz, $J_3 = 1.7$ Hz, 1H), 2.42-2.32 (m, 1H), 2.59 (s, 3H), 2.20-2.13 (m, 1H), 2.12-2.07 (m, 1H), 1.93-1.74 (m, 2H). **EI-MS** (m/z , relative intensity): 216 (M^+ , 40), 201 (100), 173 (20), 145 (20), 131 (40), 115 (20), 77 (20).

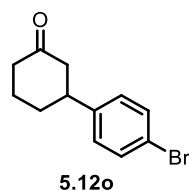


3-(3-Oxocyclohexyl)benzaldehyde (5.12m): 50 % Yield. Colorless oil. $R_f = 0.5$ (Hex/EA = 2:1). $^1\text{H NMR}$ (400 MHz, CDCl_3) δ 10.01 (s, 1H), 7.76-7.73 (m, 2H), 7.50-7.49 (m, 2H), 3.13-3.05 (m, 1H), 2.64-2.45 (m, 3H), 2.43-2.35 (m, 1H), 2.22-2.14 (m, 1H), 2.13-2.08 (m, 1H), 1.94-1.74 (m, 2H). $^{13}\text{C NMR}$ (100 MHz, CDCl_3) δ 210.22, 192.20, 145.34, 136.76, 132.94,

129.39, 128.70, 127.08, 48.59, 44.37, 41.04, 32.56, 25.39. **IR** (KBr, cm^{-1}) 2939, 2868, 1700, 1602, 1448, 1255, 1144, 913, 743. **HRMS** calcd $\text{C}_{13}\text{H}_{14}\text{O}_2$ $[\text{M}]^+$: 202.0994. Found: 202.0995.

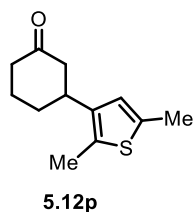


3-(4-(Benzyloxy)phenyl)cyclohexan-1-one (5.12n): 46 % Yield. White solid. Mp. 96-98 °C. $R_f = 0.4$ (Hex/EA = 5:1). **$^1\text{H NMR}$** (400 MHz, CDCl_3) δ 7.45-7.31 (m, 5H), 7.16-7.13 (m, 2H), 6.97-6.93 (m, 2H), 5.05 (s, 2H), 2.97 (tt, $J_1 = 11.8$ Hz, $J_2 = 3.9$ Hz, 1H), 2.61-2.56 (ddt, $J_1 = 13.9$ Hz, $J_2 = 4.2$ Hz, $J_3 = 1.9$ Hz, 1H), 2.53-2.44 (m, 2H), 2.41-2.33 (m, 1H), 2.17-2.11 (m, 1H), 2.09-2.05 (m, 1H), 1.87-1.71 (m, 2H). **$^{13}\text{C NMR}$** (100 MHz, CDCl_3) δ 211.39, 157.47, 136.98, 136.79, 128.56, 127.94, 127.49, 127.44, 114.91, 70.03, 49.19, 43.96, 41.15, 32.95, 25.47. **IR** (KBr, cm^{-1}) 3033, 2932, 2868, 1710, 1512, 1244, 913, 743. **HRMS** calcd $\text{C}_{19}\text{H}_{20}\text{O}_2$ $[\text{M}]^+$: 280.1463. Found: 280.1459.

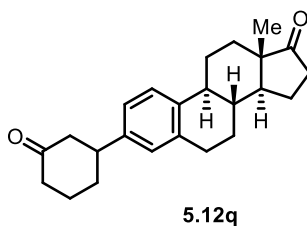


3-(4-Bromophenyl)cyclohexan-1-one (5.12o): 60 % Yield. **$^1\text{H NMR}$** (400 MHz, CDCl_3) δ 7.46-7.43 (m, 2H), 7.11-7.07 (m, 2H), 2.98 (tt, $J_1 = 11.7$ Hz, $J_2 = 3.9$ Hz, 1H), 2.61-2.56 (m,

1H), 2.52-2.45 (m, 2H), 2.42-2.34 (m, 1H), 2.18-2.12 (m, 1H), 2.08-2.04 (m, 1H), 1.90-1.70 (m, 2H). **EI-MS** (*m/z*, relative intensity): 252 (M^+ , 75), 254 (75), 209 (50), 211 (50), 195 (60), 197 (50), 182 (60), 184 (60), 116 (100), 103 (50), 77 (60).

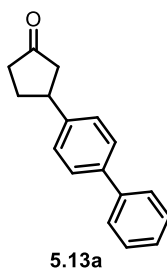


3-(2,5-Dimethylthiophen-3-yl)cyclohexan-1-one (5.12p): 50 % Yield. Yellow oil. R_f = 0.4 (Hex/EA = 5:1). **1H NMR** (400 MHz, $CDCl_3$) δ 6.54 (s, 1H), 3.04-2.96 (m, 1H), 2.46-2.31 (m, 4H), 2.40-2.39 (m, 3H), 2.28 (s, 3H), 2.16-2.10 (m, 1H), 1.98-1.93 (m, 1H), 1.79-1.68 (m, 2H). **^{13}C NMR** (100 MHz, $CDCl_3$) δ 211.01, 139.62, 135.88, 130.12, 123.61, 48.61, 41.25, 38.23, 32.19, 25.60, 15.22, 12.60. **IR** (KBr, cm^{-1}) 2937, 2863, 1713, 1447, 1221, 1145, 913, 742. **HRMS** calcd $C_{12}H_{16}OS$ [M] $^+$: 208.0922. Found: 208.0923.

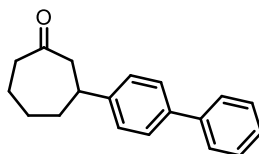


(8R,9S,13S,14S)-13-methyl-3-(3-oxocyclohexyl)-6,7,8,9,11,12,13,14,15,16-decahydro-17H-cyclopenta[a]phenanthren-17-one (5.12q): 51 % Yield as a mixture of two diastereomers.

White solid. Mp. 115-117 °C. $R_f = 0.3$ (Hex/EA = 5:1). $^1\text{H NMR}$ (400 MHz, CDCl_3) δ 7.27 (d, $J = 8.0$ Hz, 1H), 7.03-7.01 (m, 1H), 6.96 (s, 1H), 2.98-2.90 (m, 3H), 2.61-2.26 (m, 7H), 2.20-1.94 (m, 6H), 1.89-1.72 (m, 2H), 1.68-1.40 (m, 6H), 0.91 (s, 3H). $^{13}\text{C NMR}$ (100 MHz, CDCl_3) δ 221.02, 211.35, 141.85, 138.14, 136.73, 127.23, 127.20, 125.66, 123.96, 123.92, 50.44, 48.97, 48.95, 47.98, 44.32, 44.28, 41.17, 38.11, 35.83, 32.80, 31.54, 29.45, 26.49, 25.65, 25.59, 21.55, 13.82. **IR** (KBr, cm^{-1}) 2931, 2863, 1738, 1712, 1454, 1256, 1222, 1007, 913, 734. **HRMS** calcd $\text{C}_{24}\text{H}_{31}\text{O}_2$ $[\text{M}+\text{H}]^+$: 351.2324. Found: 351.2321.

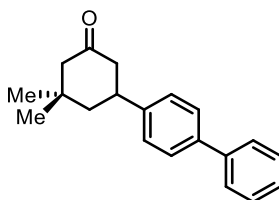


(3-([1,1'-Biphenyl]-4-yl)cyclopentan-1-one (5.13a): 53 % Yield. White solid. Mp. 120-122 °C. $R_f = 0.5$ (Hex/EA = 5:1). $^1\text{H NMR}$ (400 MHz, CDCl_3) δ 7.59-7.57 (m, 4H), 7.47-7.43 (m, 2H), 7.37-7.33 (m, 3H), 3.46 (ddd, $J_1 = 18.0$ Hz, $J_2 = 11.1$ Hz, $J_3 = 7.1$ Hz, 1H), 2.72 (dd, $J_1 = 18.3$ Hz, $J_2 = 7.3$ Hz, 1H), 2.54-2.43 (m, 2H), 2.43-2.29 (m, 2H), 2.10-1.98 (m, 1H). $^{13}\text{C NMR}$ (100 MHz, CDCl_3) δ 218.37, 142.07, 140.69, 139.72, 128.76, 127.37, 127.24, 127.14, 126.99, 45.81, 41.91, 38.88, 31.22. **IR** (KBr, cm^{-1}) 3031, 2975, 2895, 1737, 1488, 1403, 1135, 912, 843, 774. **HRMS** calcd $\text{C}_{17}\text{H}_{16}\text{O}$ $[\text{M}]^+$: 236.1201. Found: 236.1204.



5.13b

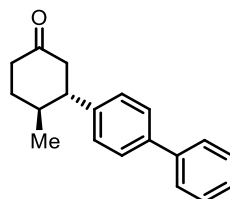
3-([1,1'-Biphenyl]-4-yl)cycloheptan-1-one (5.13b): 66 % Yield. White solid. Mp. 130-132 °C. $R_f = 0.4$ (Hex/EA = 5:1). $^1\text{H NMR}$ (400 MHz, CDCl_3) δ 7.59-7.52 (m, 4H), 7.45-7.41 (m, 2H), 7.35-7.31 (m, 1H), 7.27-7.25 (m, 2H). 2.98-2.92 (m, 2H), 2.73-2.60 (m, 3H), 2.15-1.98 (m, 3H), 1.83-1.69 (m, 2H), 1.57-1.48 (m, 1H). $^{13}\text{C NMR}$ (100 MHz, CDCl_3) δ 213.43, 145.95, 140.80, 139.30, 128.72, 127.35, 127.14, 126.98, 126.83, 51.21, 43.96, 42.40, 39.19, 29.23, 24.17. **IR** (KBr, cm^{-1}) 2932, 2869, 1692, 1395, 1142, 913, 744. **HRMS** calcd $\text{C}_{19}\text{H}_{20}\text{O}$ $[\text{M}]^+$: 264.1514. Found: 264.1513.



5.13c

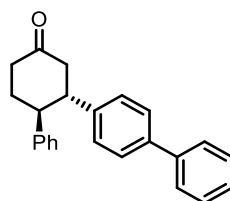
5-([1,1'-Biphenyl]-4-yl)-3,3-dimethylcyclohexan-1-one (5.13c): 50% Yield. Colorless oil. $R_f = 0.5$ (Hex/EA = 5:1). $^1\text{H NMR}$ (400 MHz, CDCl_3) δ 7.60-7.56 (m, 4H), 7.46-7.42 (m, 2H), 7.37-7.31 (m, 3H), 3.21 (tt, $J_1 = 12.4$ Hz, $J_2 = 4.5$ Hz, 1H) 2.62-2.57 (m, 1H), 2.52-2.45 (m, 1H), 2.37-2.33 (m, 1H), 2.21 (dt, $J_1 = 13.5$ Hz, $J_2 = 2.1$ Hz, 1H), 1.92-1.80 (m, 2H), 1.15 (s, 3H), 1.04 (s, 3H). $^{13}\text{C NMR}$ (100 MHz, CDCl_3) δ 211.01, 143.22, 140.72, 139.70, 128.74, 127.40, 127.21, 127.07, 127.00, 54.31, 48.15, 46.37, 40.04, 35.46, 32.17, 25.72. **IR** (KBr, cm^{-1}) 3028,

2957, 2869, 1710, 1487, 1142, 913, 762, 743. **HRMS** calcd C₂₀H₂₂O [M]⁺: 278.1671. Found: 278.1663.



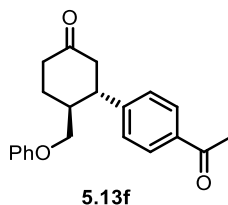
5.13d

3-([1,1'-Biphenyl]-4-yl)-4-methylcyclohexan-1-one (5.13d): 70% Yield. The relative stereochemistry was determined by X-ray crystallography. White solid. Mp. 107-109 °C. R_f = 0.5 (Hex/EA = 5:1). **¹H NMR** (400 MHz, CDCl₃) δ 7.61-7.55 (m, 4H), 7.46-7.42 (m, 2H), 7.37-7.33 (m, 1H), 7.26-7.24 (m, 2H), 2.62-2.46 (m, 5H), 2.21-2.05 (m, 2H), 1.62-1.52 (m, 1H), 0.83 (d, *J* = 6.4 Hz, 3H). **¹³C NMR** (100 MHz, CDCl₃) δ 210.92, 142.65, 140.72, 139.60, 128.73, 127.61, 127.38, 127.18, 126.96, 51.73, 49.09, 41.38, 36.74, 34.59, 19.32. **IR** (KBr, cm⁻¹) 3028, 2955, 2870, 1714, 1467, 1143, 913, 765, 743. **HRMS** calcd C₁₉H₂₀O [M]⁺: 264.1514. Found: 264.1510.

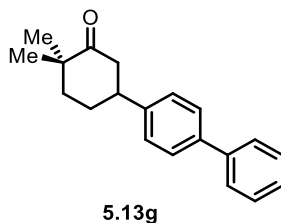


5.13e

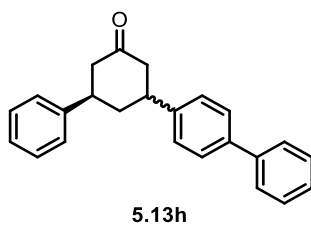
3-([1,1'-Biphenyl]-4-yl)-4-phenylcyclohexan-1-one (5.13e): 56% Yield. The relative stereochemistry was determined by X-ray crystallography. White solid. Mp. 132-134 °C. $R_f = 0.3$ (Hex/EA = 5:1). $^1\text{H NMR}$ (400 MHz, CDCl_3) δ 7.49-7.46 (m, 2H), 7.38-7.34 (m, 4H), 7.29-7.25 (m, 1H), 7.15-7.11 (m, 2H), 7.08-7.03 (m, 5H), 3.31-3.19 (m, 2H), 2.79-2.56 (m, 4H), 2.34-2.27 (m, 1H), 2.14-2.04 (m, 1H). $^{13}\text{C NMR}$ (100 MHz, CDCl_3) δ 210.12, 142.77, 141.66, 140.57, 139.16, 128.64, 128.30, 127.63, 127.45, 127.09, 126.99, 126.84, 126.38, 50.23, 49.39, 49.18, 41.57, 34.49. **IR** (KBr, cm^{-1}) 3028, 2928, 2870, 1716, 1487, 1142, 913, 742. **HRMS** calcd $\text{C}_{24}\text{H}_{22}\text{O}$ $[\text{M}]^+$: 326.1671. Found: 326.1668.



3-(4-Acetylphenyl)-4-(phoxymethyl)cyclohexan-1-one (5.13f): 70% Yield. The relative stereochemistry was determined by coupling constants. Yellow oil. $R_f = 0.3$ (Hex/EA = 2:1). $^1\text{H NMR}$ (400 MHz, CDCl_3) δ 7.90-7.88 (m, 2H), 7.32-7.30 (m, 2H), 7.22-7.18 (m, 2H), 6.91-6.87 (m, 1H), 6.72-6.68 (m, 2H), 3.72 (dd, $J_1 = 9.3$ Hz, $J_2 = 2.8$ Hz, 1H), 3.54 (dd, $J_1 = 9.3$ Hz, $J_2 = 6.1$ Hz, 1H), 3.14 (ddd, $J_1 = 12.6$ Hz, $J_2 = 11.5$ Hz, $J_3 = 4.5$ Hz, 1H), 2.68-2.53 (m, 4H), 2.56 (s, 3H), 2.48-2.33 (m, 2H), 1.97-1.86 (m, 1H). $^{13}\text{C NMR}$ (100 MHz, CDCl_3) δ 209.51, 197.61, 158.54, 147.76, 136.11, 129.40, 129.08, 127.41, 120.89, 114.26, 68.77, 48.19, 46.31, 41.73, 40.66, 29.19, 26.59. **IR** (KBr, cm^{-1}) 2923, 1716, 1682, 1606, 1496, 1269, 1245, 756. **HRMS** calcd $\text{C}_{21}\text{H}_{22}\text{O}_3\text{Na}$ $[\text{M}+\text{Na}]^+$: 345.14610. Found: 345.14620.

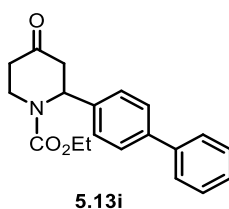


5-([1,1'-Biphenyl]-4-yl)-2,2-dimethylcyclohexan-1-one (5.13g): 40% Yield. White solid. Mp. 118-121 °C. $R_f = 0.7$ (Hex/EA = 5:1). $^1\text{H NMR}$ (400 MHz, CDCl_3) δ 7.60-7.55 (m, 4H), 7.46-7.42 (m, 2H), 7.36-7.30 (m, 3H), 3.08-3.00 (m, 1H), 2.81 (dd, $J_1 = 14.0$ Hz, $J_2 = 12.9$ Hz, 1H), 2.54 (ddd, $J_1 = 14.0$ Hz, $J_2 = 4.3$ Hz, $J_3 = 2.0$ Hz, 1H), 2.14-2.03 (m, 1H), 2.00-1.94 (m, 1H), 1.88 (dt, $J_1 = 13.8$ Hz, $J_2 = 3.6$ Hz, 1H), 1.76-1.69 (m, 1H), 1.28 (s, 3H), 1.14 (s, 3H). $^{13}\text{C NMR}$ (100 MHz, CDCl_3) δ 215.00, 143.45, 140.77, 139.61, 128.74, 127.35, 127.19, 127.01, 126.96, 45.18, 44.97, 44.55, 39.85, 29.23, 25.16, 25.15. **IR** (KBr, cm^{-1}) 3028, 2965, 2929, 1707, 1487, 1143, 913, 764, 742. **HRMS** calcd $\text{C}_{20}\text{H}_{22}\text{O}$ $[\text{M}]^+$: 278.1671. Found: 278.1673.

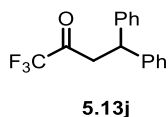


3-([1,1'-Biphenyl]-4-yl)-5-phenylcyclohexan-1-one (5.13h): 32% Yield as a single diastereomer. Attempts to determine the relative stereochemistry (*cis* or *trans*) were unsuccessful. Colorless oil. $R_f = 0.5$ (Hex/EA = 5:1). $^1\text{H NMR}$ (400 MHz, CDCl_3) δ 7.59-7.53 (m, 4H), 7.46-

7.42 (m, 2H), 7.36-7.31 (m, 3H), 7.27-7.20 (m, 5H), 3.42-3.34 (m, 2H), 2.83-2.71 (m, 4H), 2.38 (t, $J = 5.9$ Hz, 2H). ^{13}C NMR (100 MHz, CDCl_3) δ 211.20, 143.77, 142.84, 140.66, 139.47, 128.75, 128.62, 127.42, 127.28, 127.22, 127.00, 126.98, 126.57, 46.62, 46.55, 39.40, 38.86, 38.56. IR (KBr, cm^{-1}) 3028, 2923, 1710, 1487, 1275, 913, 764, 748. HRMS calcd $\text{C}_{24}\text{H}_{22}\text{O}$ $[\text{M}]^+$: 326.1671. Found: 326.1672.

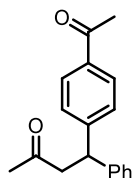


Ethyl 2-([1,1'-biphenyl]-4-yl)-4-oxopiperidine-1-carboxylate (5.13i): 61% Yield. ^1H NMR (400 MHz, CDCl_3) δ 7.56-7.53 (m, 4H), 7.44-7.40 (m, 2H), 7.35-7.31 (m, 3H), 5.86 (br, 1H), 4.30-4.21 (m, 3H), 3.22-3.15 (m, 1H), 3.04-2.99 (m, 1H), 2.88 (dd, $J_1 = 15.5$ Hz, $J_2 = 7.0$ Hz, 1H), 2.59-2.51 (m, 1H), 2.41-2.35 (m, 1H), 1.30 (t, $J = 7.1$ Hz, 3H). HRMS calcd $\text{C}_{20}\text{H}_{22}\text{NO}_3$ $[\text{M}+\text{H}]^+$: 324.15940. Found: 324.15950.



1,1,1-Trifluoro-4,4-diphenylbutan-2-one (5.13j): 50% Yield. ^1H NMR (400 MHz, CDCl_3) δ 7.31-7.26 (m, 4H), 7.23-7.18 (m, 6H), 4.65 (t, $J = 7.5$ Hz, 1H), 3.48 (dd, $J_1 = 7.5$ Hz, J_2

= 0.5 Hz, 2H). **EI-MS** (m/z , relative intensity): 278 (M^+ , 50), 209 (30), 167 (100), 152 (40), 103 (20), 77 (20).

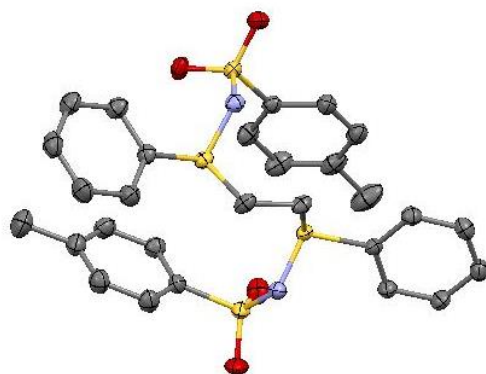


5.13k

4-(4-Acetylphenyl)-4-phenylbutan-2-one (5.13k): 38% Yield. $^1\text{H NMR}$ (400 MHz, CDCl_3) δ 7.87-7.84 (m, 2H), 7.32-7.25 (m, 4H), 7.20-7.16 (m, 3H), 4.64 (t, $J = 7.5$ Hz, 1H), 3.20 (d, $J = 7.5$ Hz, 2H), 2.54 (s, 3H), 2.09 (s, 3H). **EI-MS** (m/z , relative intensity): 266 (M^+ , 100), 251 (30), 223 (80), 209 (90), 165 (80).

X-ray data

Figure 5.3 Crystal Structure of *Racemic 5.5*



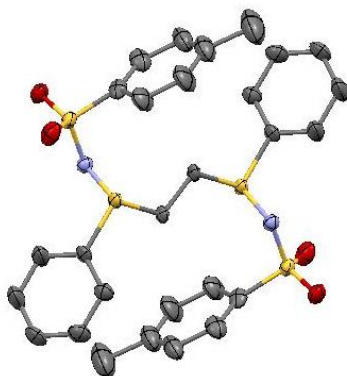
Empirical formula

$\text{C}_{28}\text{H}_{28}\text{N}_2\text{O}_4\text{S}_4$

Formula weight	584.76	
Temperature	100(2) K	
Wavelength	0.71073 Å	
Crystal system	Monoclinic	
Space group	I 2/a	
Unit cell dimensions	a = 15.181(6) Å	α = 90°.
	b = 15.559(5) Å	β = 105.016(18)°.
	c = 23.696(7) Å	γ = 90°.
Volume	5406(3) Å ³	
Z	8	
Density (calculated)	1.241 Mg/m ³	
Absorption coefficient	0.390 mm ⁻¹	
F(000)	2448.0	
Crystal size	0.73 x 0.27 x 0.20 mm ³	
Theta range for data collection	1.583 to 32.082°.	
Index ranges	-22 ≤ h ≤ 19, -22 ≤ k ≤ 23, -27 ≤ l ≤ 33	
Reflections collected	26405	
Independent reflections	7408 [R(int) = 0.0433]	
Completeness to theta = 32.082°	93.3 %	
Absorption correction	Multi-scan	
Max. and min. transmission	1.000 and 0.705	
Refinement method	Full-matrix least-squares on F ²	

Data / restraints / parameters	8824 / 0 / 345
Goodness-of-fit on F^2	1.065
Final R indices [$I > 2\sigma(I)$]	R1 = 0.0431, wR2 = 0.1080
R indices (all data)	R1 = 0.0521, wR2 = 0.1127
Largest diff. peak and hole	0.43 and -0.60 e.Å ⁻³

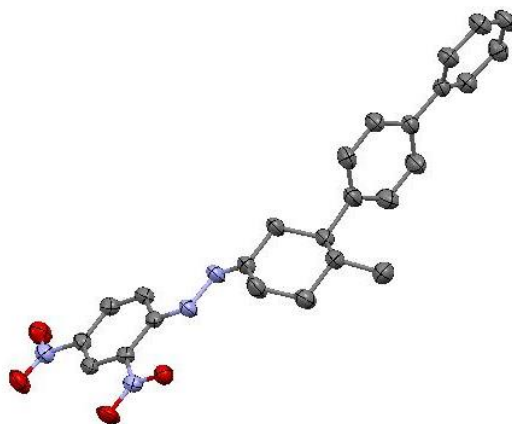
Figure 5.4 Crystal Structure of *Meso 5.5*



Empirical formula	C ₂₈ H ₂₈ N ₂ O ₄ S ₄
Formula weight	584.76
Temperature	133(2) K
Wavelength	0.71073 Å
Crystal system	Monoclinic
Space group	P 21/c
Unit cell dimensions	a = 6.5498(4) Å α = 90°.
	b = 20.4037(13) Å β = 100.469(3)°.

	$c = 11.0725(9) \text{ \AA}$	$\gamma = 90^\circ$.
Volume	1455.10(18) \AA^3	
Z	2	
Density (calculated)	1.335 Mg/m^3	
Absorption coefficient	0.362 mm^{-1}	
F(000)	612	
Crystal size	0.340 x 0.230 x 0.180 mm^3	
Theta range for data collection	3.317 to 27.498°.	
Index ranges	$-8 \leq h \leq 8, -26 \leq k \leq 26, -14 \leq l \leq 14$	
Reflections collected	20450	
Independent reflections	3345 [R(int) = 0.0550]	
Completeness to theta = 45.242°	99.8 %	
Absorption correction	Semi-empirical from equivalents	
Max. and min. transmission	1.000 and 0.848	
Refinement method	Full-matrix least-squares on F^2	
Data / restraints / parameters	3345 / 210 / 265	
Goodness-of-fit on F^2	1.023	
Final R indices [I > 2sigma(I)]	R1 = 0.0359, wR2 = 0.0833	
R indices (all data)	R1 = 0.0503, wR2 = 0.0935	
Largest diff. peak and hole	0.417 and -0.330 e.\AA^{-3}	

Figure 5.5 Crystal Structure of **5.13d/DNP Adduct**



Empirical formula	C ₂₅ H ₂₄ N ₄ O ₄
Formula weight	444.48
Temperature	100(2) K
Wavelength	1.5418 Å
Crystal system	Monoclinic
Space group	P 2 ₁ /c
Unit cell dimensions	a = 20.3743(10) Å α = 90°. b = 5.7348(4) Å β = 102.342(6)°. c = 19.2424(15) Å γ = 90°.
Volume	2196.4(3) Å ³
Z	4
Density (calculated)	1.344 Mg/m ³
Absorption coefficient	0.760 mm ⁻¹
F(000)	936

Crystal size	0.190 x 0.130 x 0.024 mm ³
Theta range for data collection	4.443 to 76.290°.
Index ranges	-25<=h<=25, -7<=k<=7, -23<=l<=23
Reflections collected	22364
Independent reflections	4531 [R(int) = 0.0248]
Completeness to theta = 67.680°	99.9 %
Absorption correction	Semi-empirical from equivalents
Max. and min. transmission	1.00 and 0.848
Refinement method	Full-matrix least-squares on F ²
Data / restraints / parameters	4531 / 57 / 327
Goodness-of-fit on F ²	1.058
Final R indices [I>2sigma(I)]	R1 = 0.0460, wR2 = 0.1146
R indices (all data)	R1 = 0.0500, wR2 = 0.1179
Largest diff. peak and hole	0.391 and -0.494 e.Å ⁻³

5.5 ^1H -NMR and ^{13}C -NMR Spectra

Figure 5.6 ^1H -NMR and ^{13}C -NMR Spectra of **5.22**

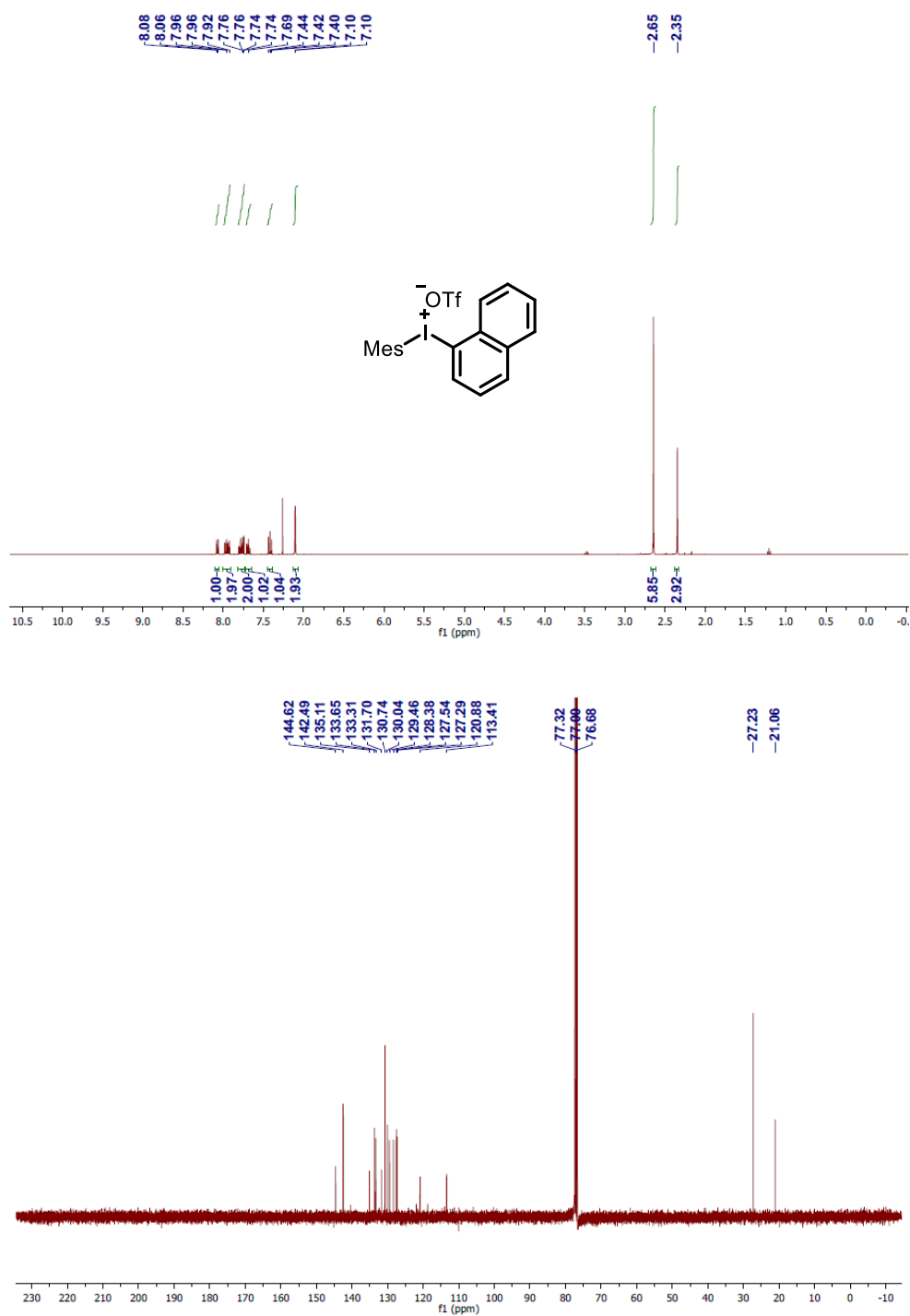


Figure 5.7 ^1H -NMR and ^{13}C -NMR Spectra of **5.27**

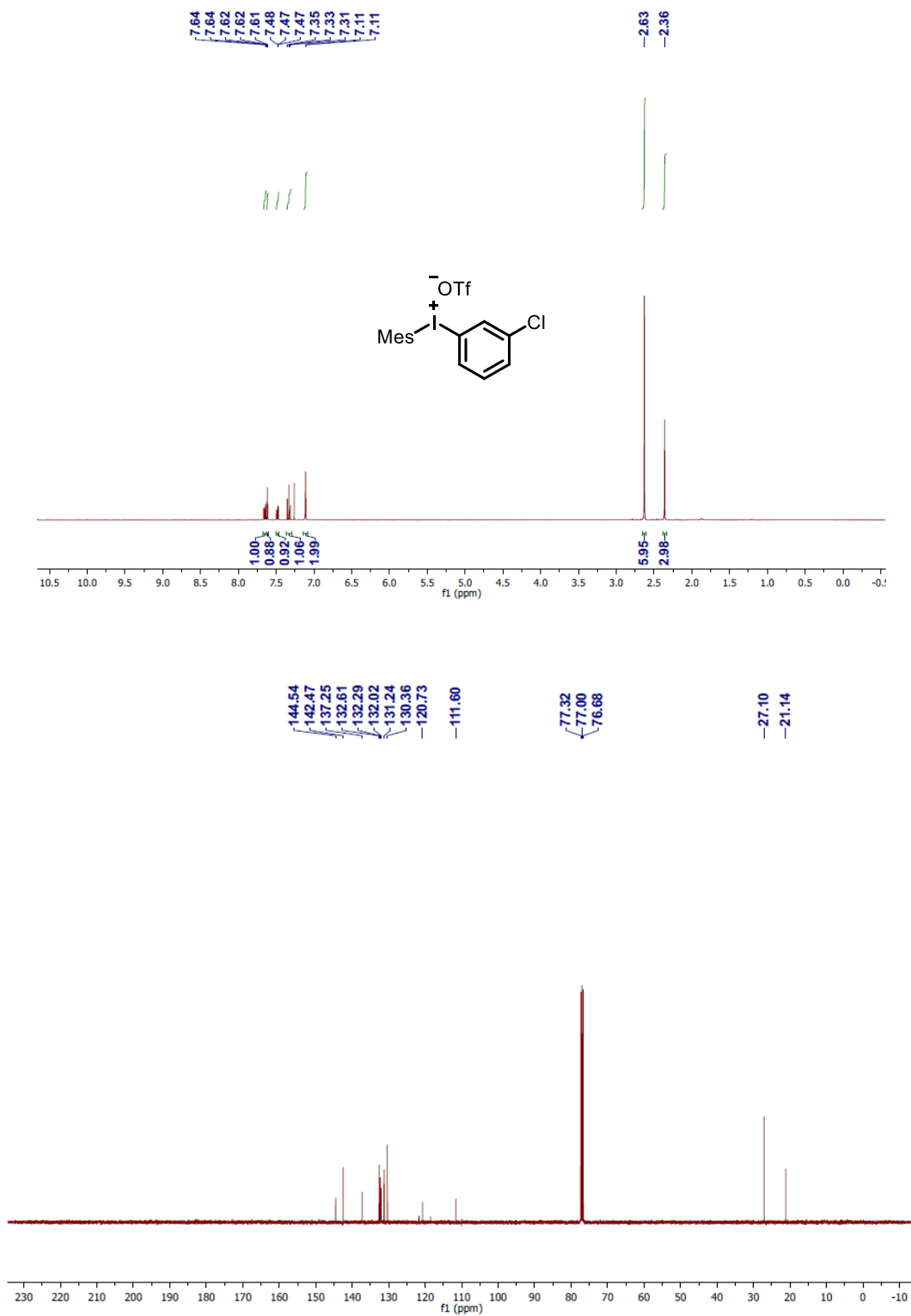


Figure 5.8 ^1H -NMR and ^{13}C -NMR Spectra of 5.30

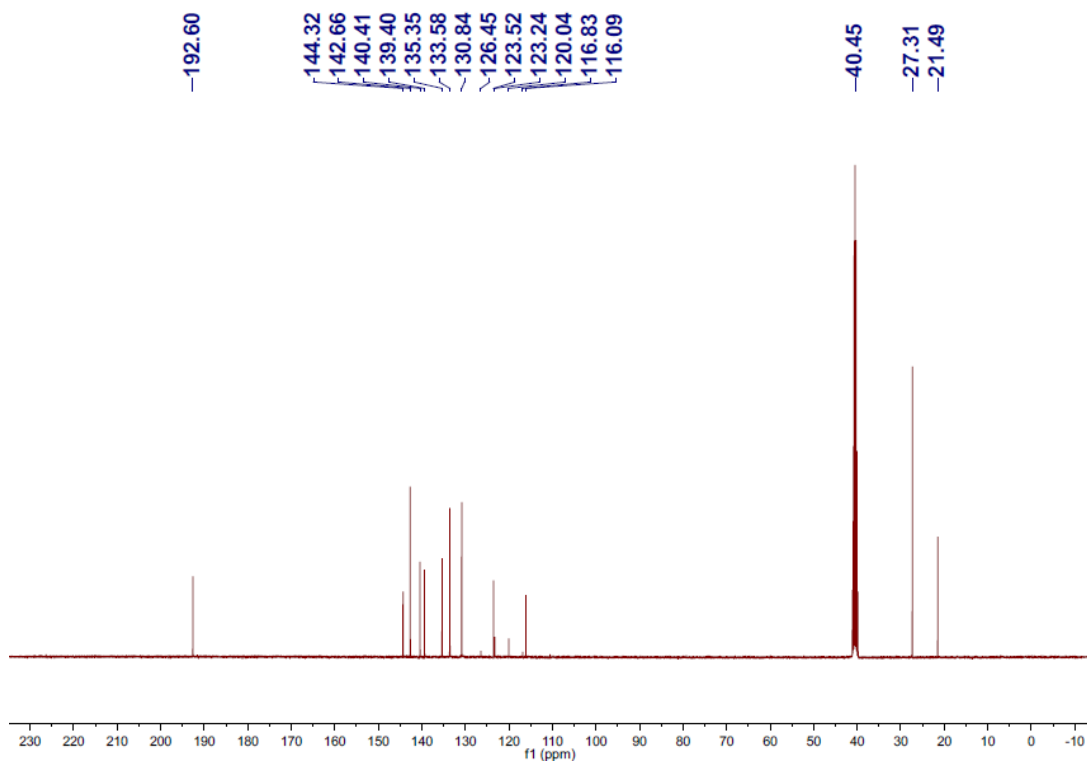
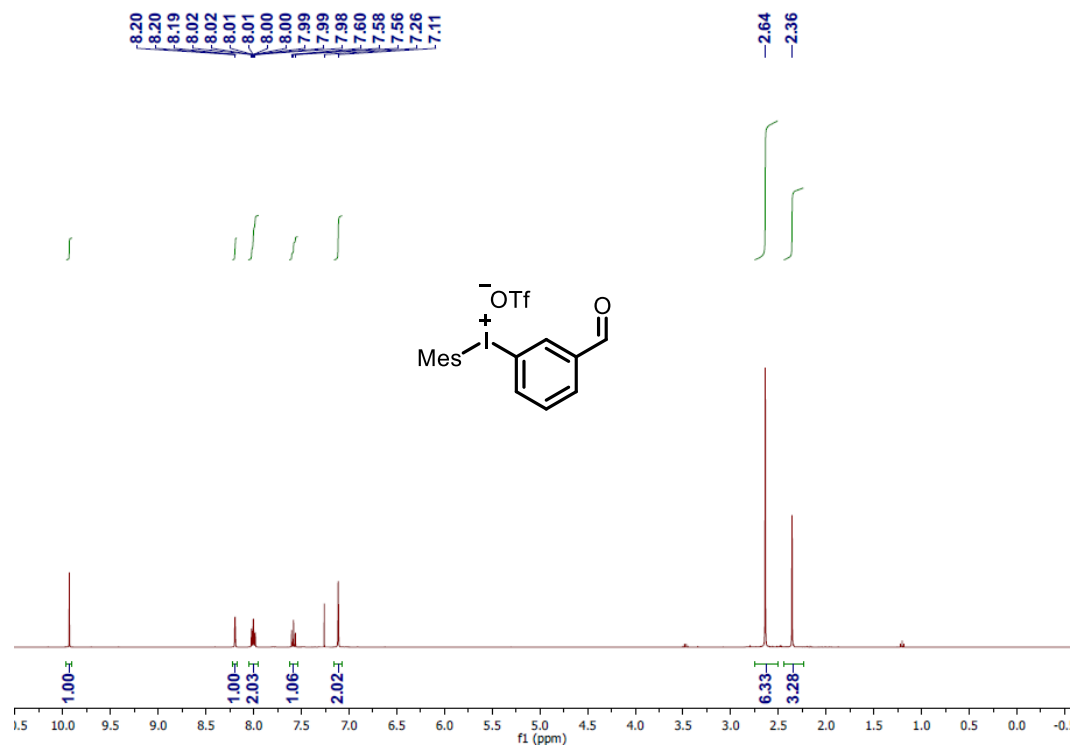


Figure 5.9 ^1H -NMR and ^{13}C -NMR Spectra of 5.31

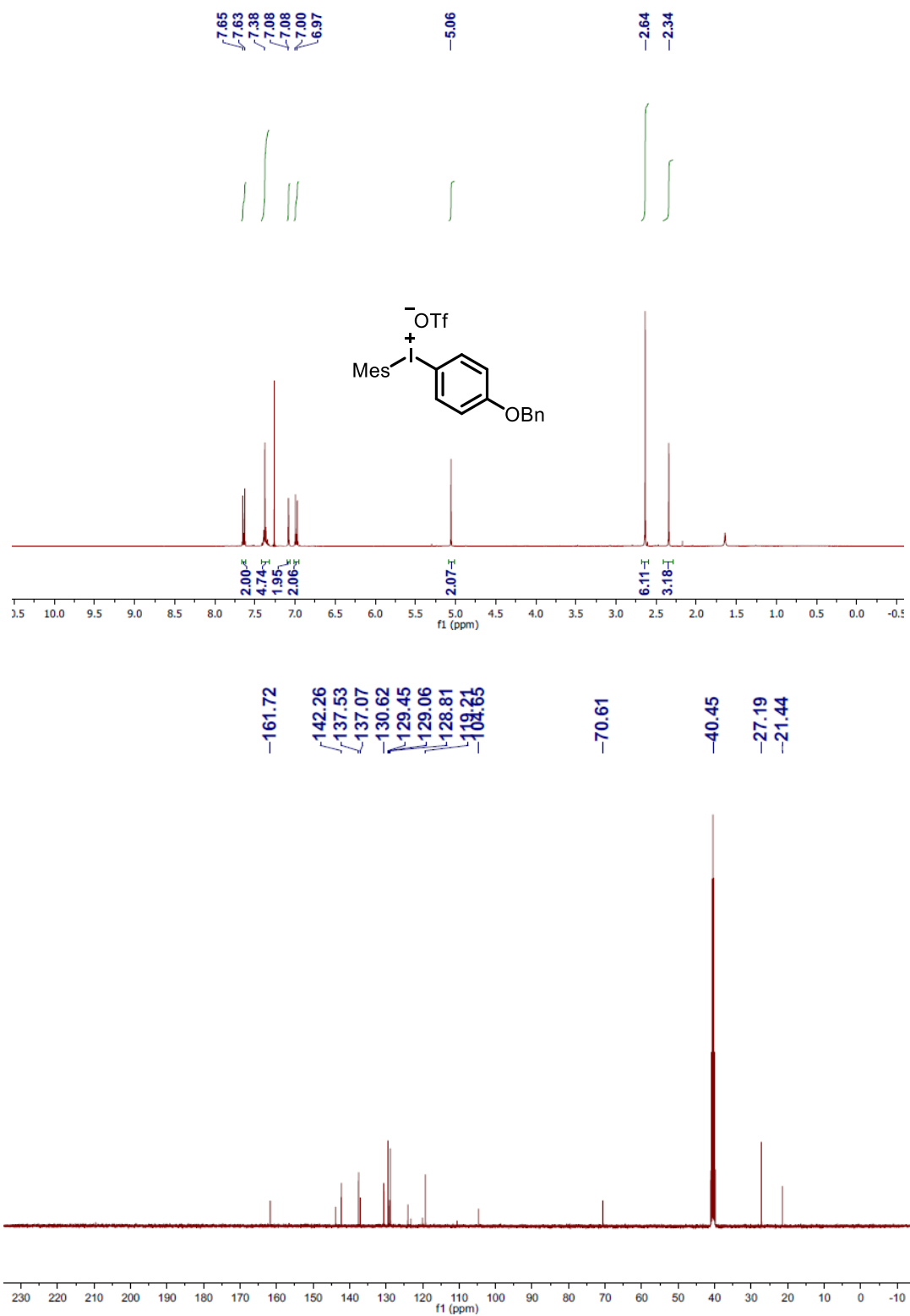


Figure 5.10 $^1\text{H-NMR}$ and $^{13}\text{C-NMR}$ Spectra of **5.33**

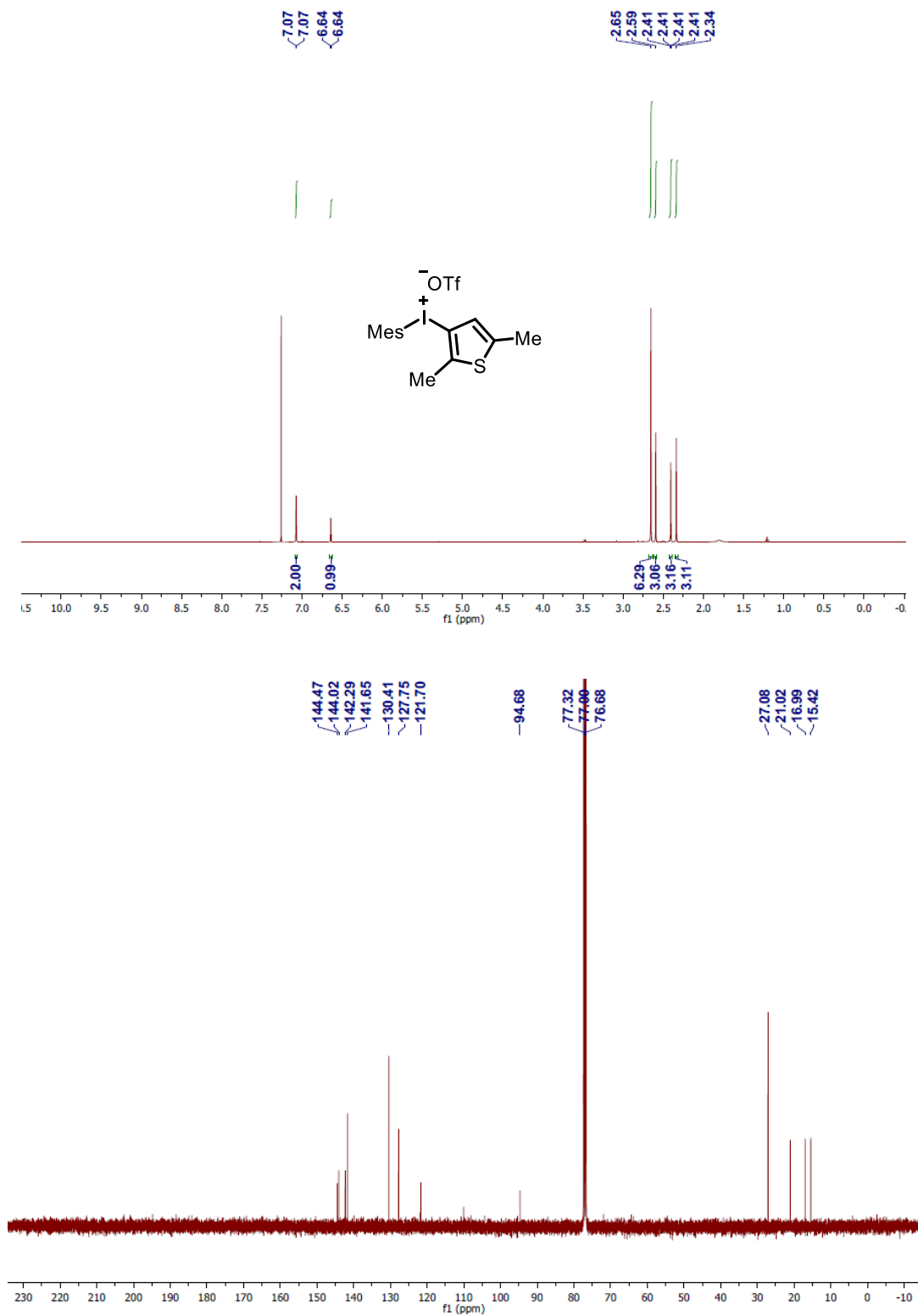


Figure 5.11 ¹H-NMR and ¹³C-NMR Spectra of 5.34

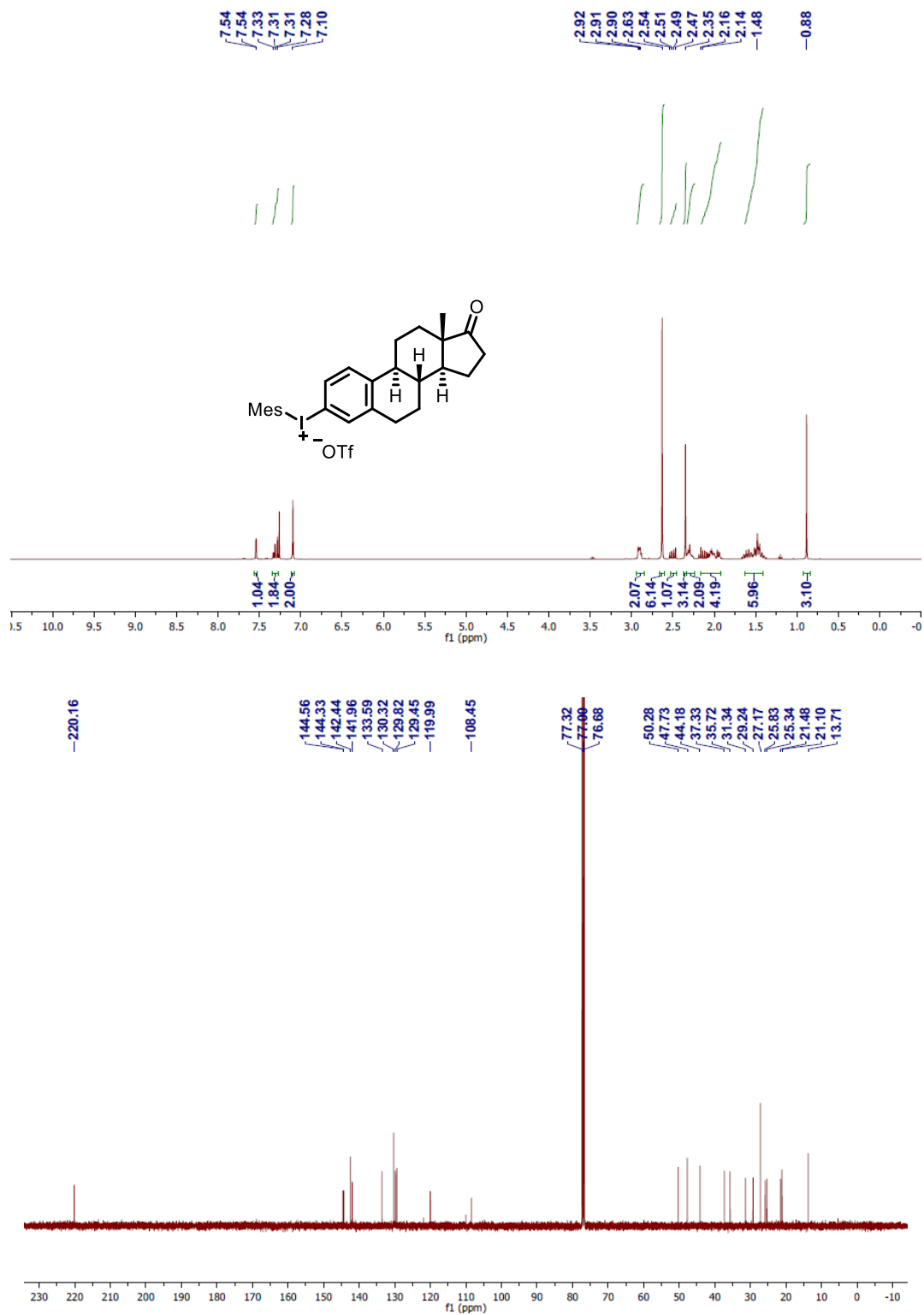


Figure 5.12 $^1\text{H-NMR}$ and $^{13}\text{C-NMR}$ Spectra of **5.5-meso**

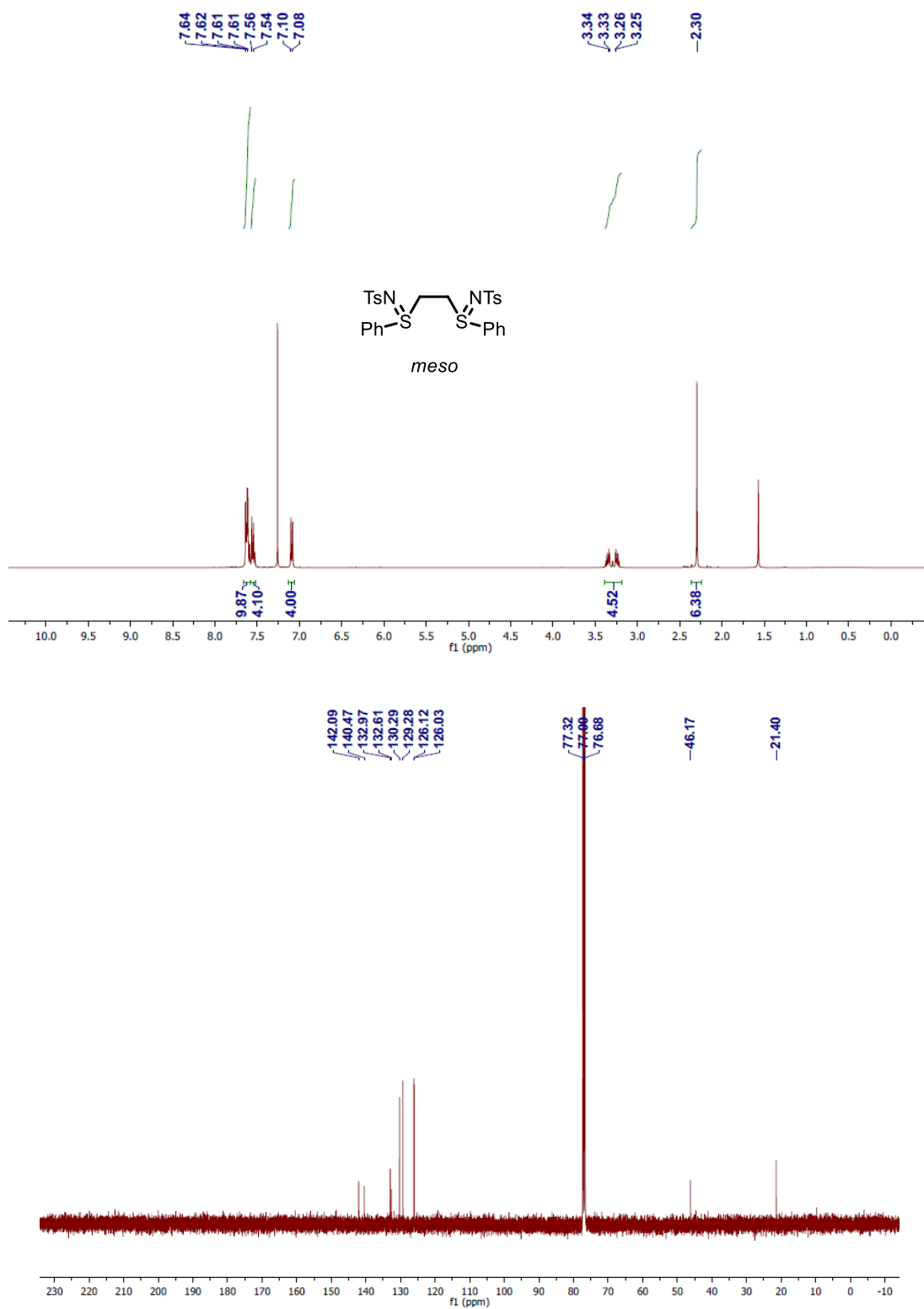


Figure 5.13 ^1H -NMR and ^{13}C -NMR Spectra of 5.5-*racemic*

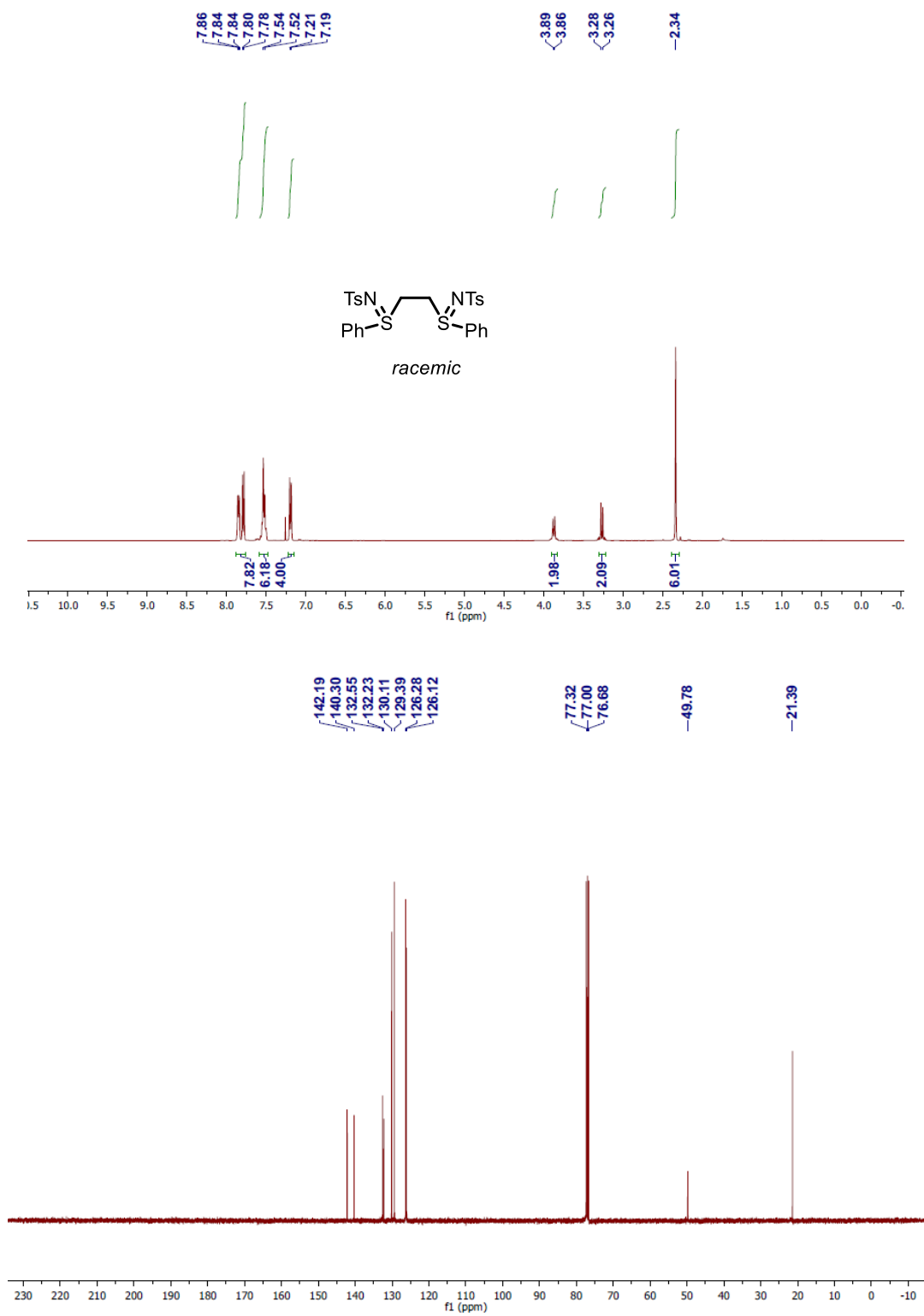


Figure 5.14 ^1H -NMR and ^{13}C -NMR Spectra of **5.14**

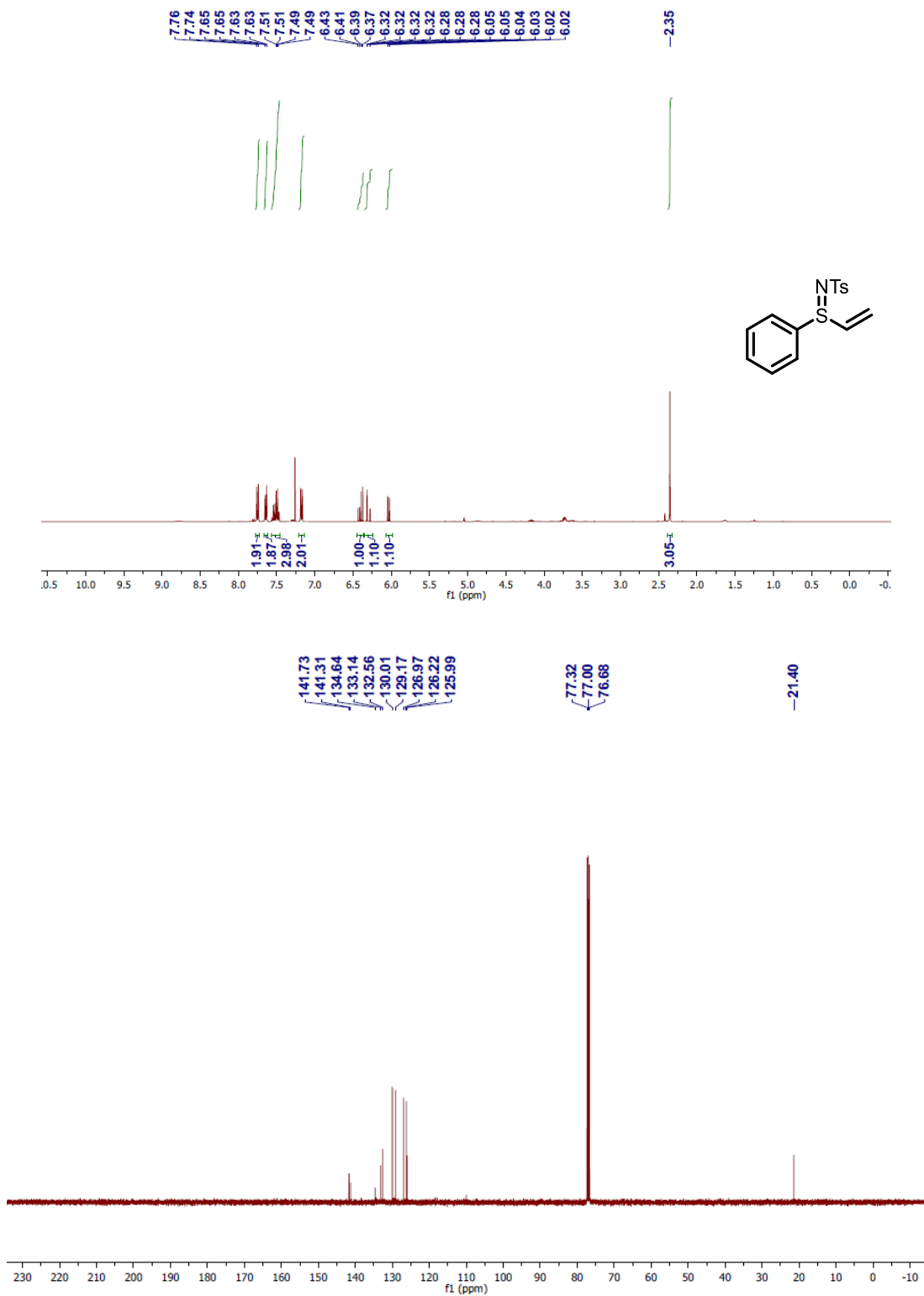


Figure 5.15 ^1H -NMR and ^{13}C -NMR Spectra of 5.15

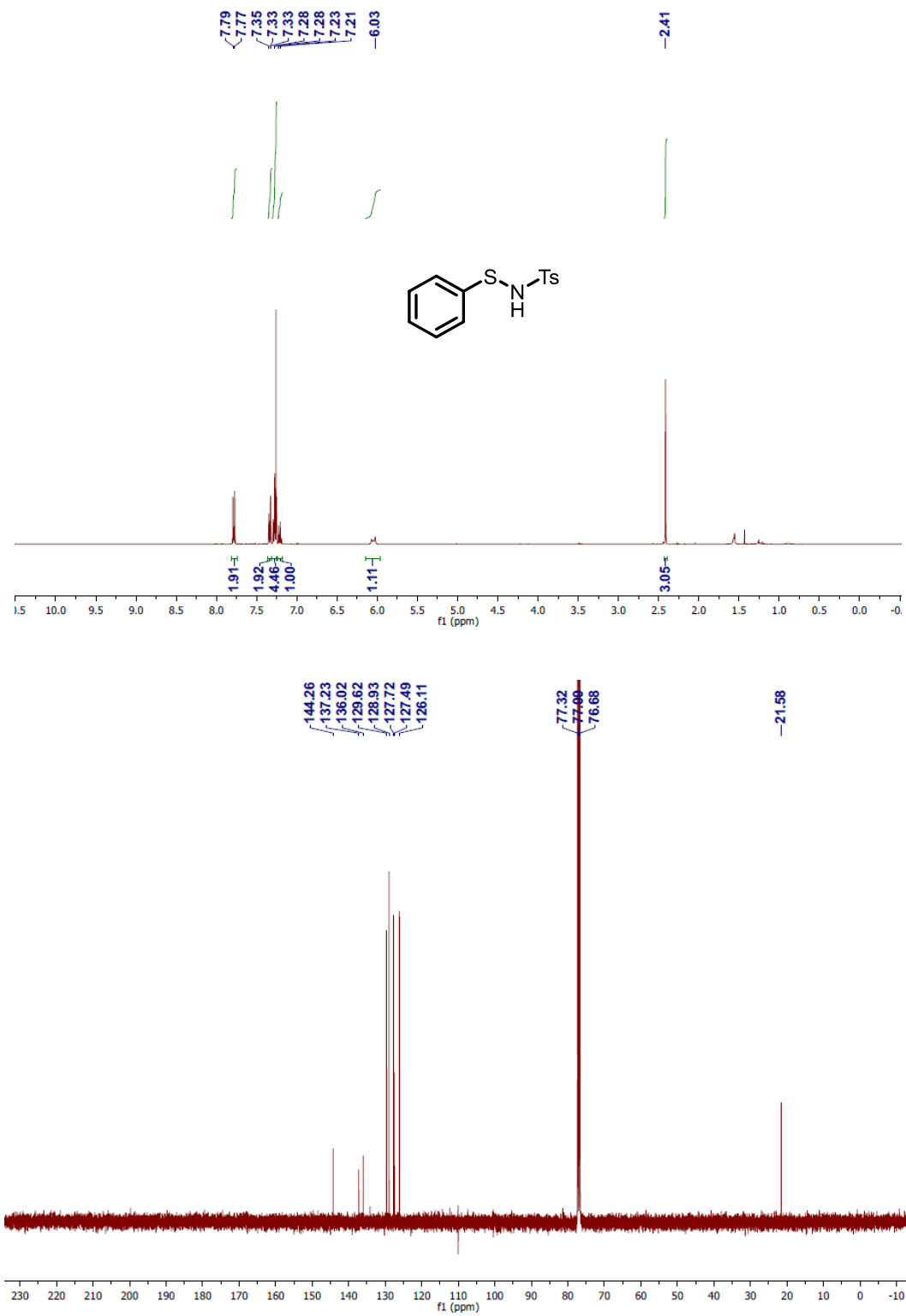


Figure 5.16 $^1\text{H-NMR}$ Spectrum of 5.12a

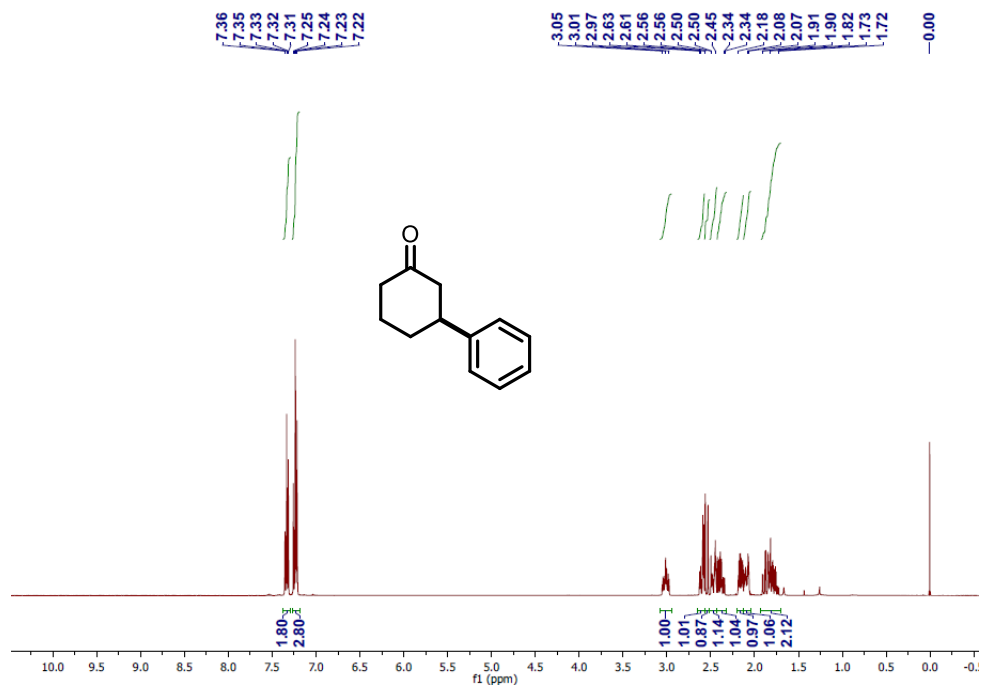


Figure 5.17 $^1\text{H-NMR}$ Spectrum of 5.12b

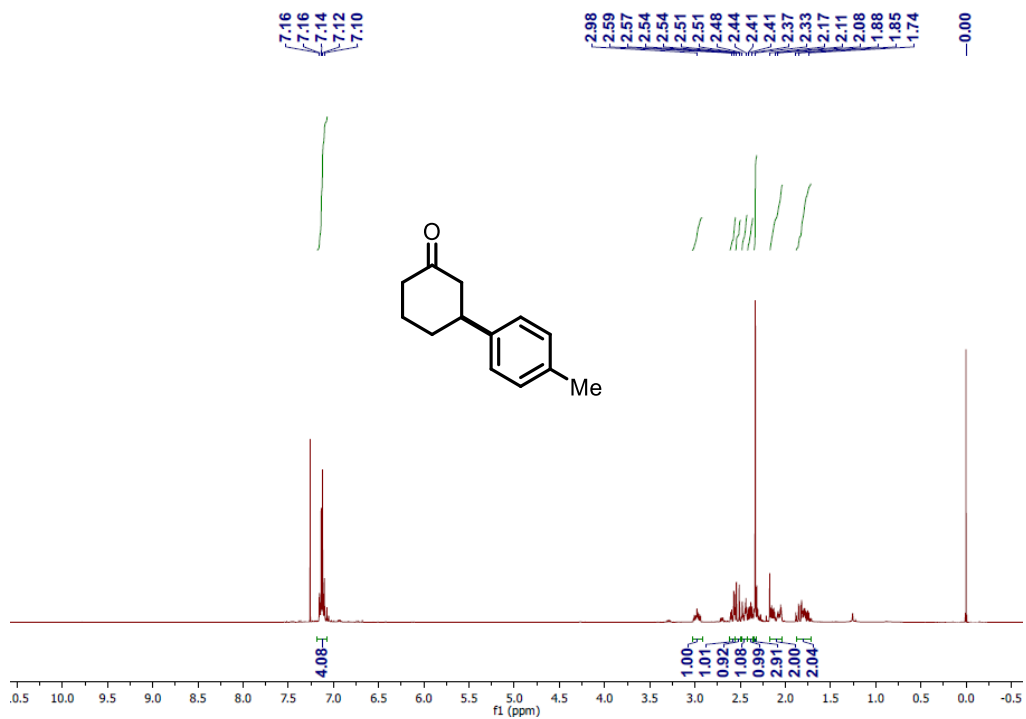


Figure 5.18 $^1\text{H-NMR}$ Spectrum of 5.12c

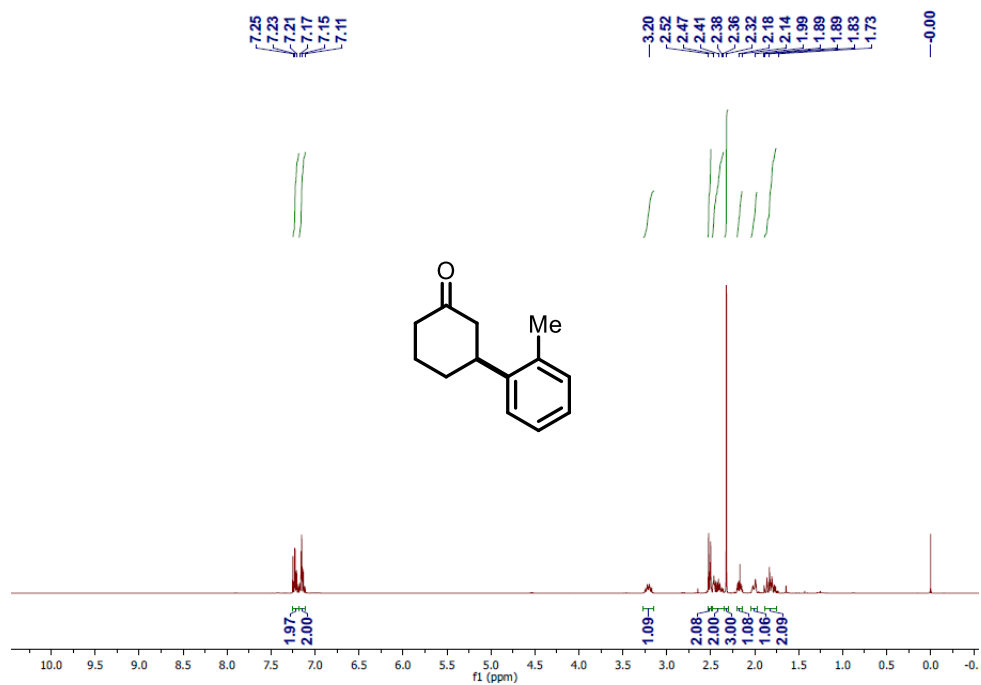


Figure 5.19 $^1\text{H-NMR}$ Spectrum of 5.12d

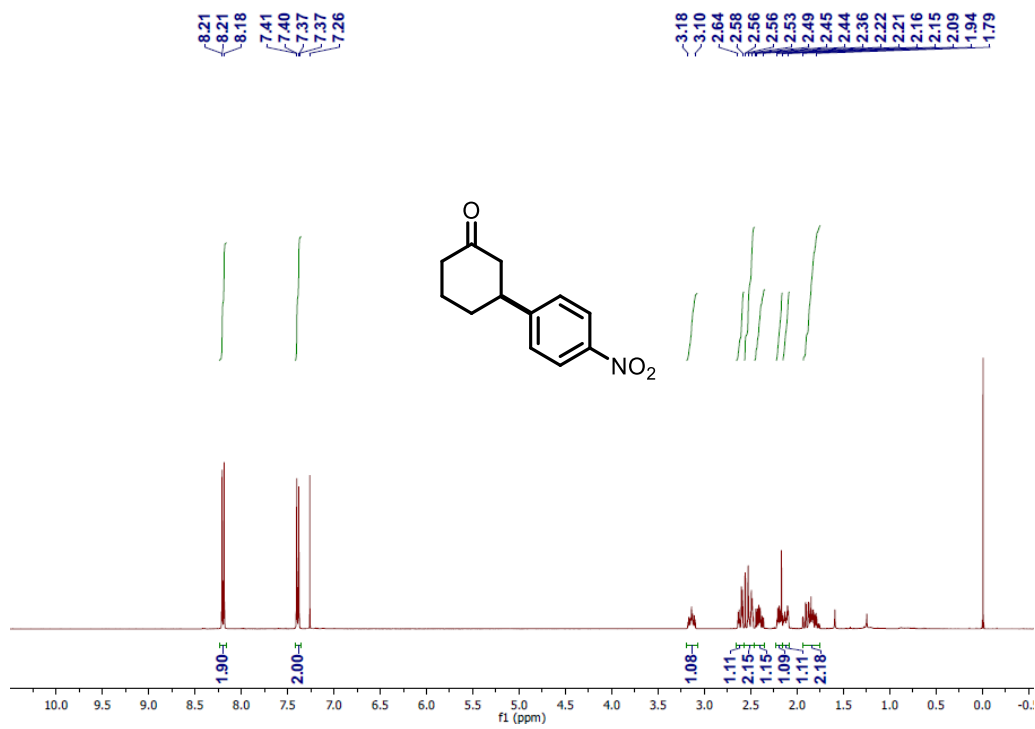


Figure 5.20 $^1\text{H-NMR}$ Spectrum of 5.12e

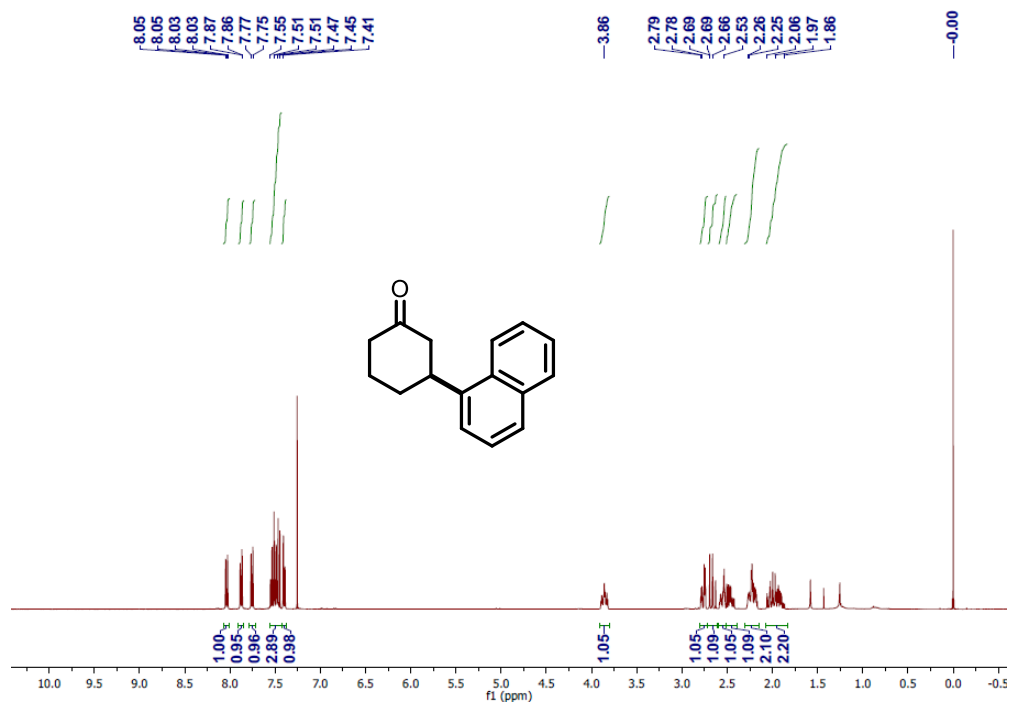


Figure 5.21 $^1\text{H-NMR}$ Spectrum of 5.12f

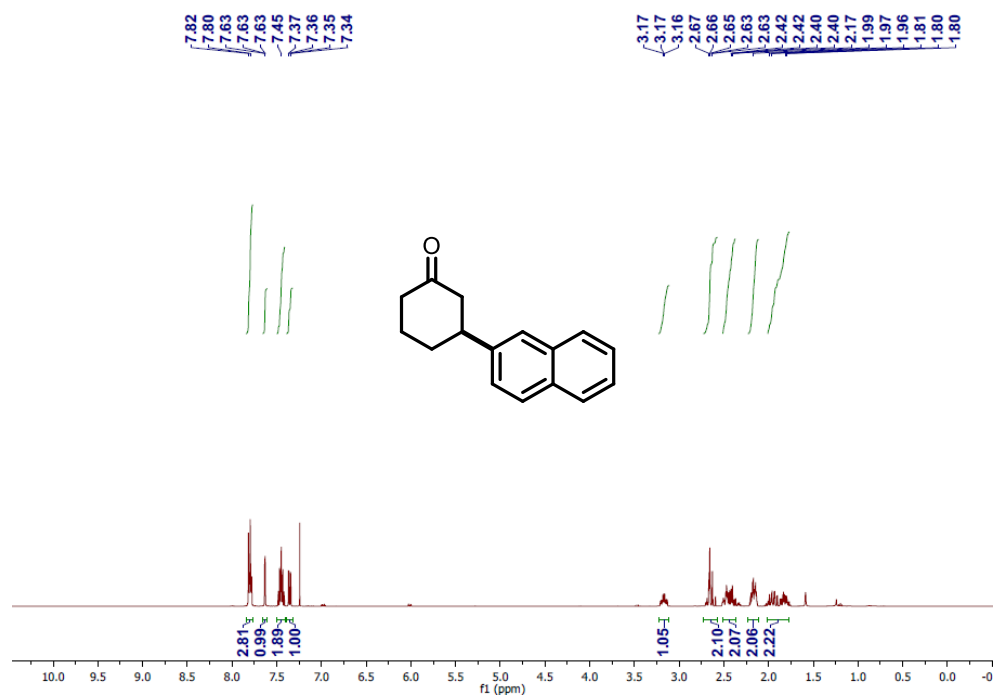


Figure 5.22 $^1\text{H-NMR}$ Spectrum of 5.12g

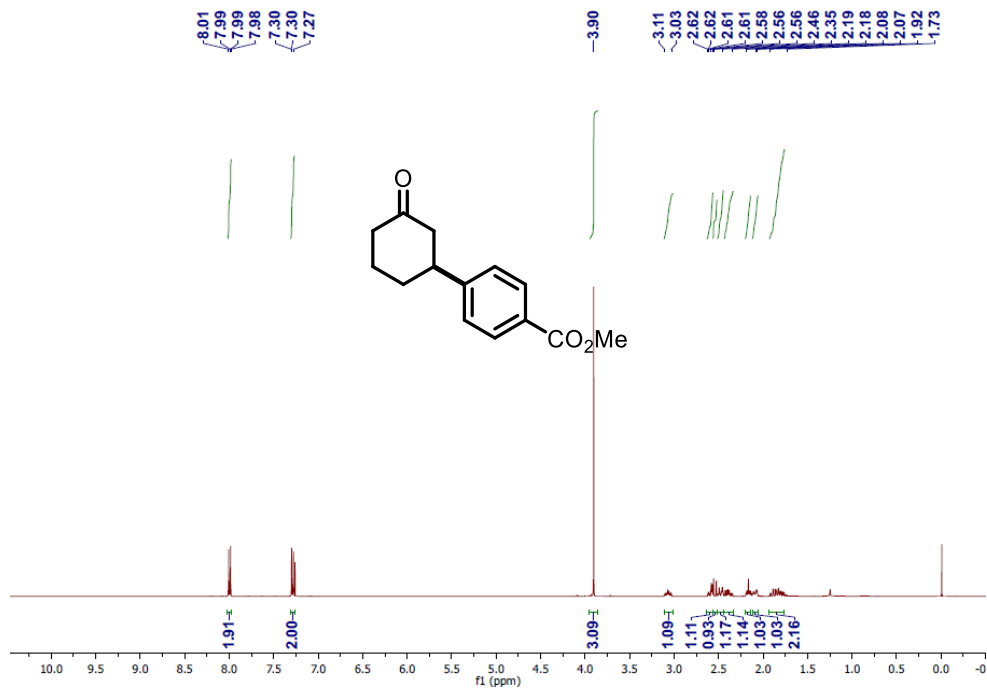


Figure 5.23 $^1\text{H-NMR}$ Spectrum of 5.12h

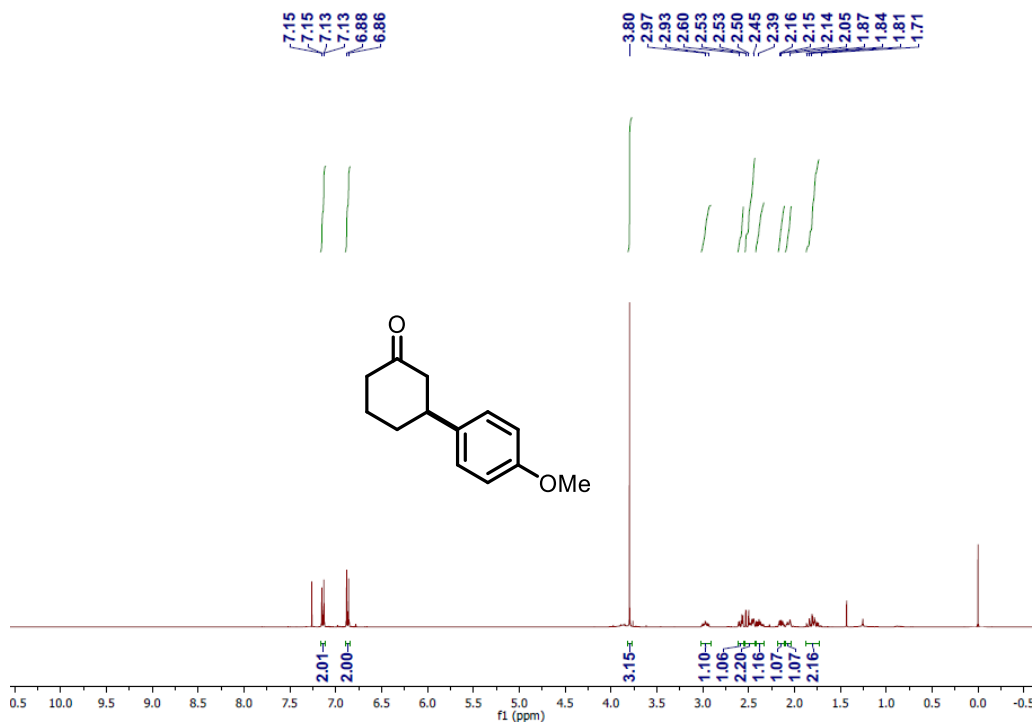


Figure 5.24 ¹H-NMR Spectrum of 5.12i

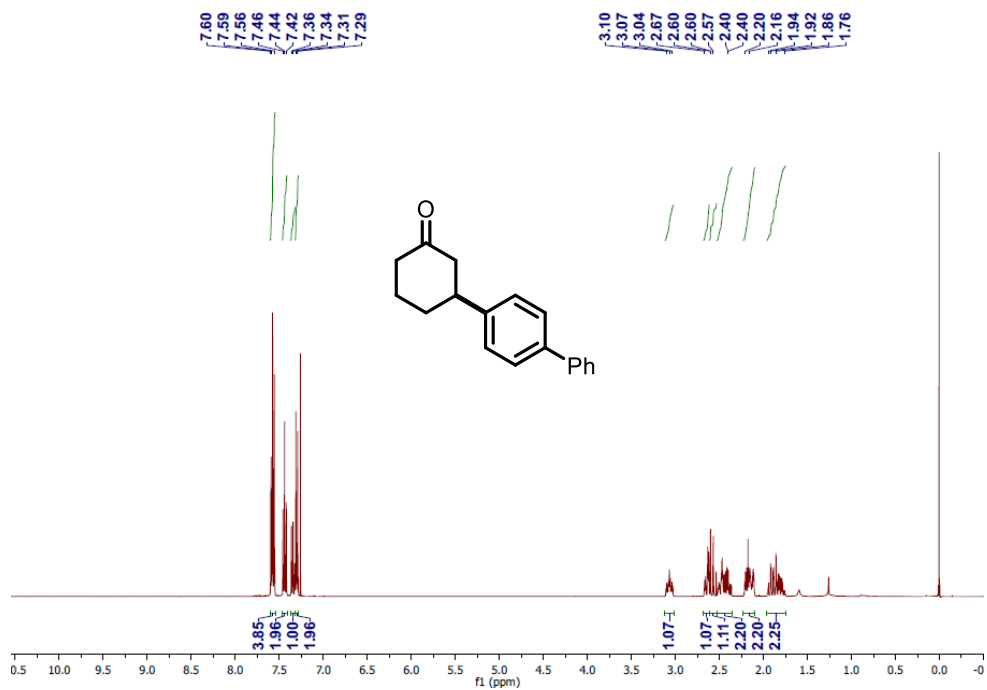


Figure 5.25 ¹H-NMR Spectrum of 5.12j

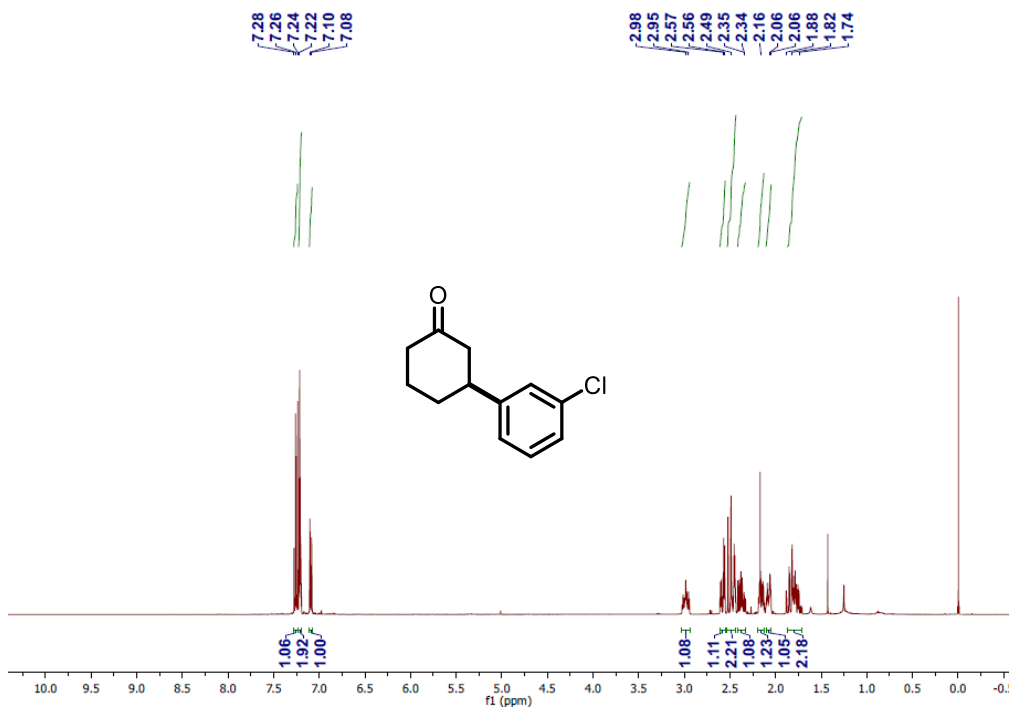


Figure 5.26 $^1\text{H-NMR}$ Spectrum of 5.12k

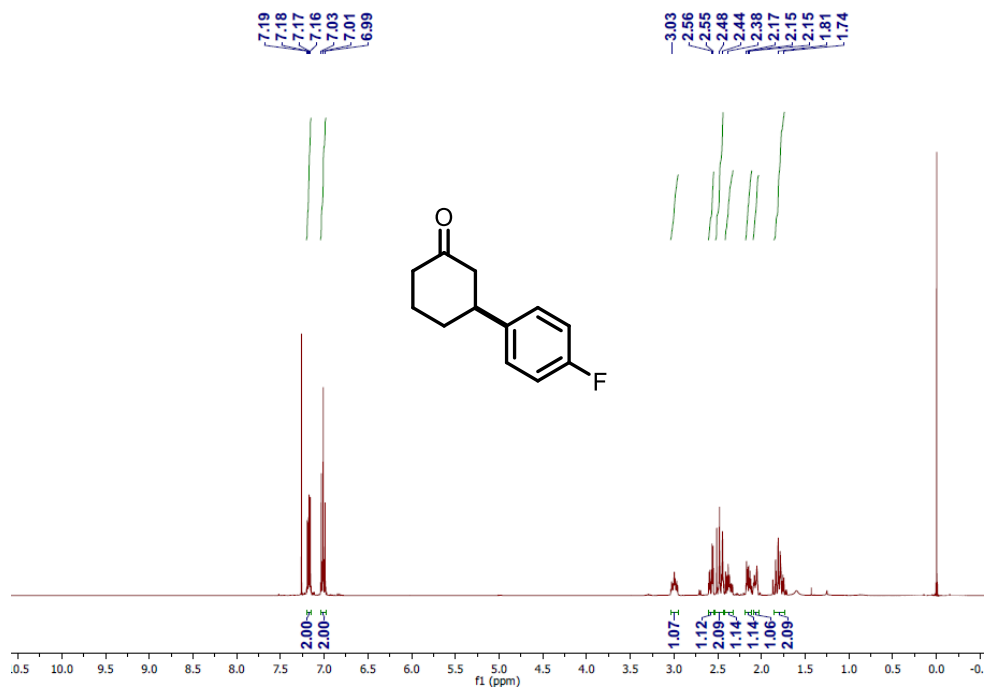


Figure 5.27 $^1\text{H-NMR}$ Spectrum of 5.12l

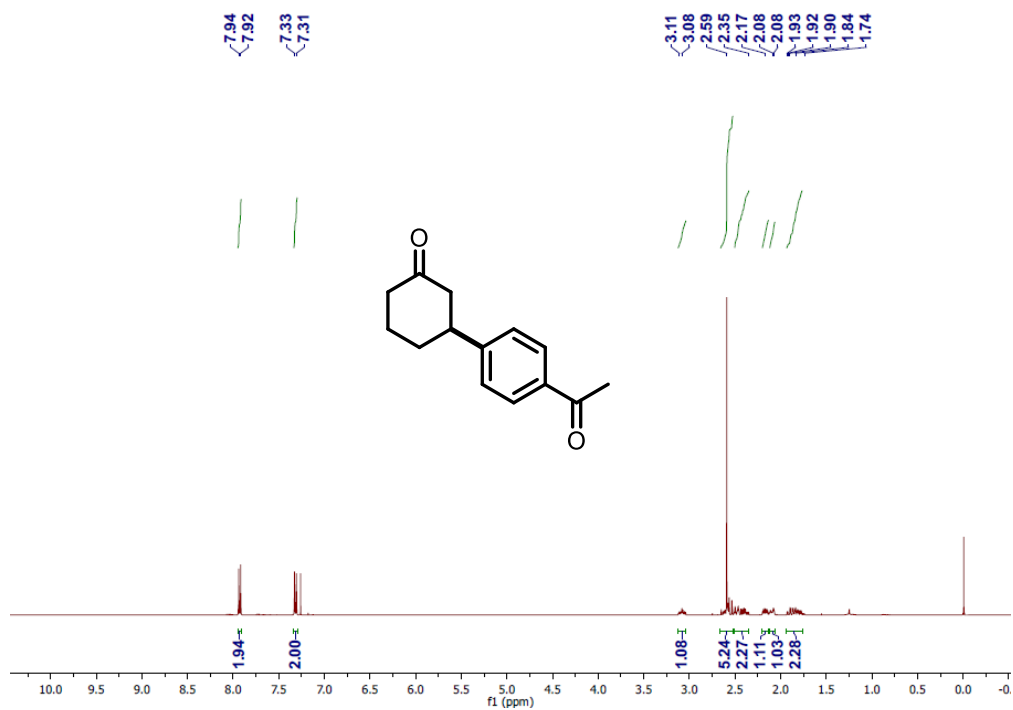


Figure 5.28 ¹H-NMR and ¹³C-NMR Spectrum of 5.12m

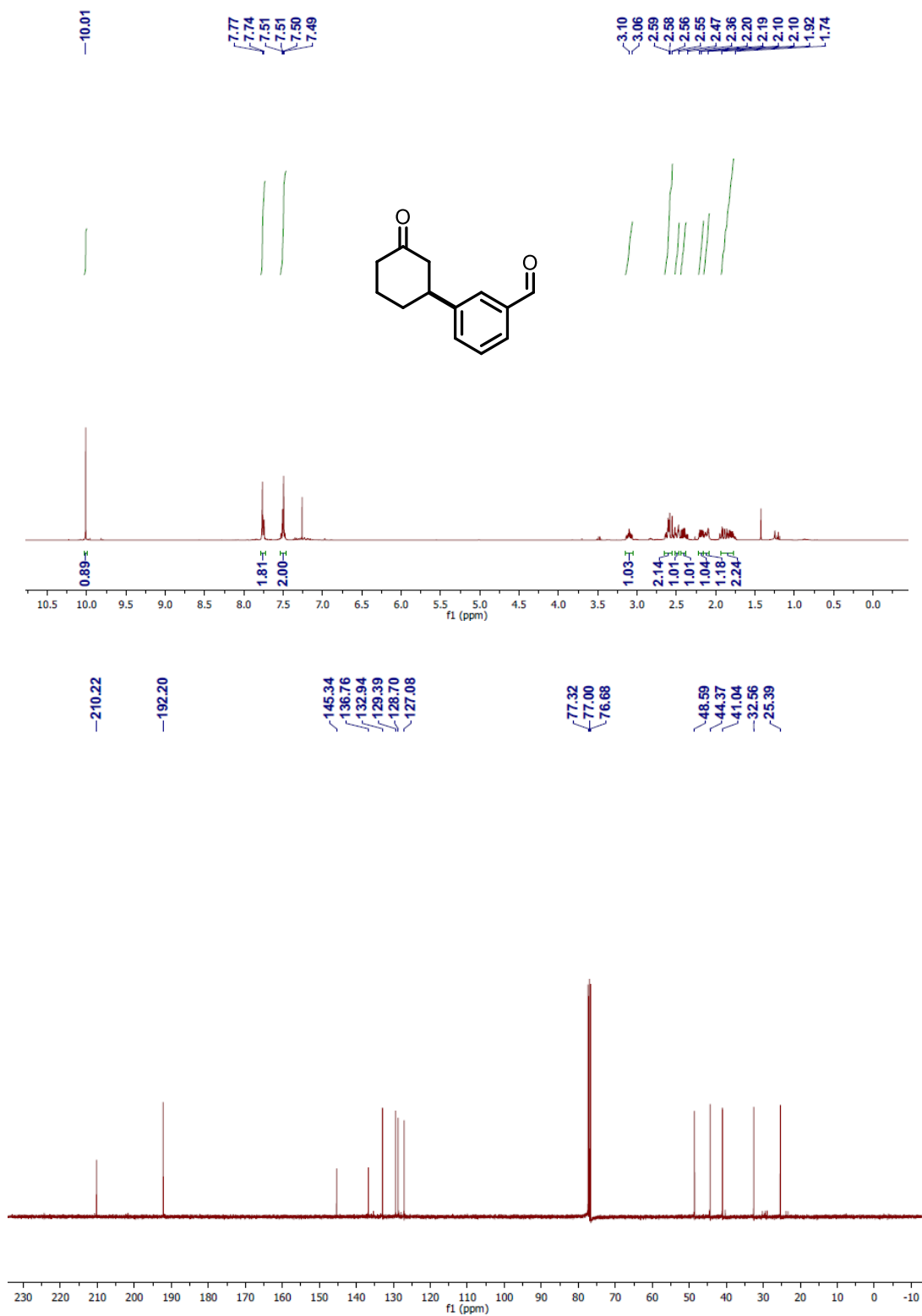


Figure 5.29 ^1H -NMR and ^{13}C -NMR Spectrum of 5.12n

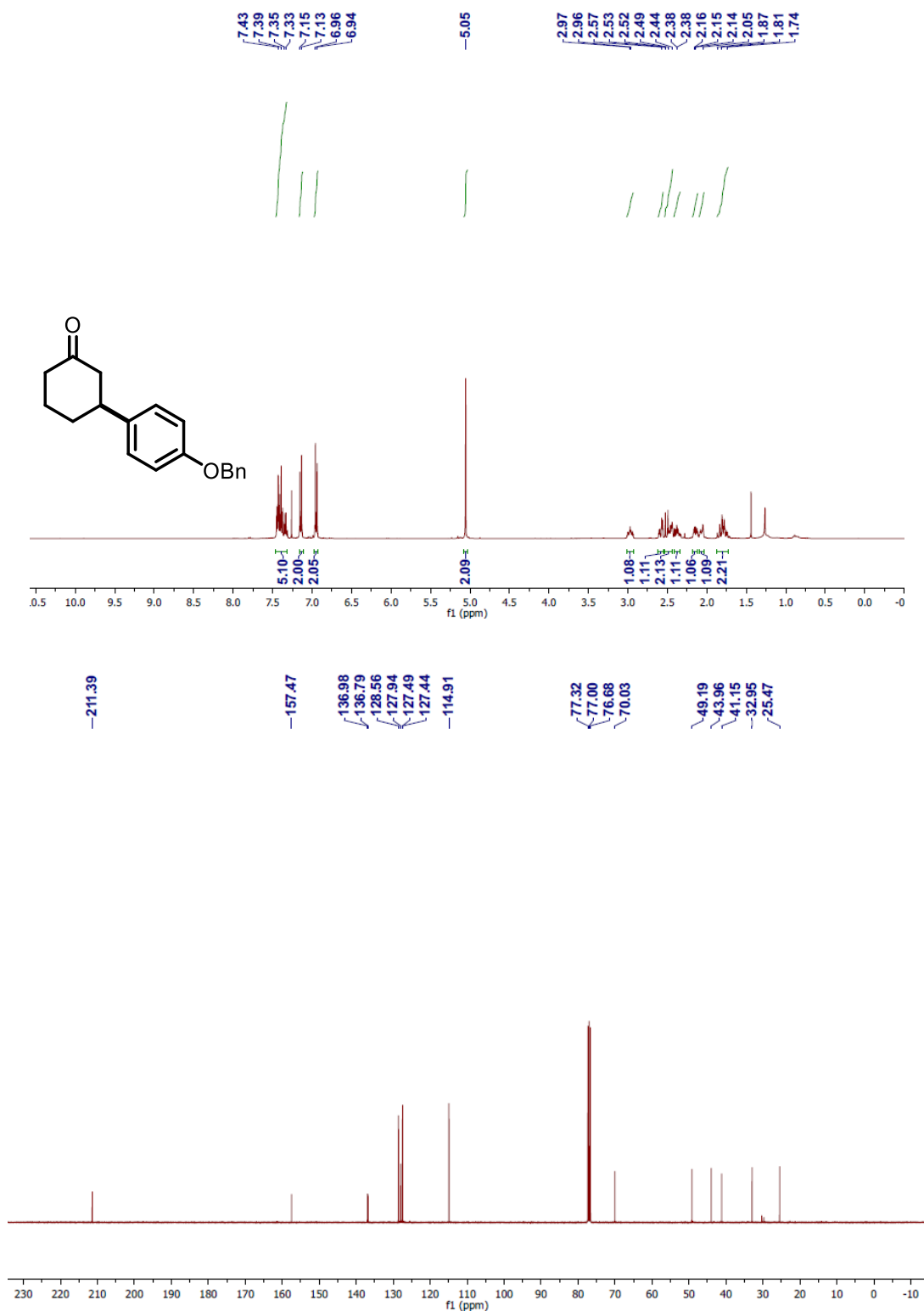


Figure 5.30 $^1\text{H-NMR}$ Spectrum of 5.12o

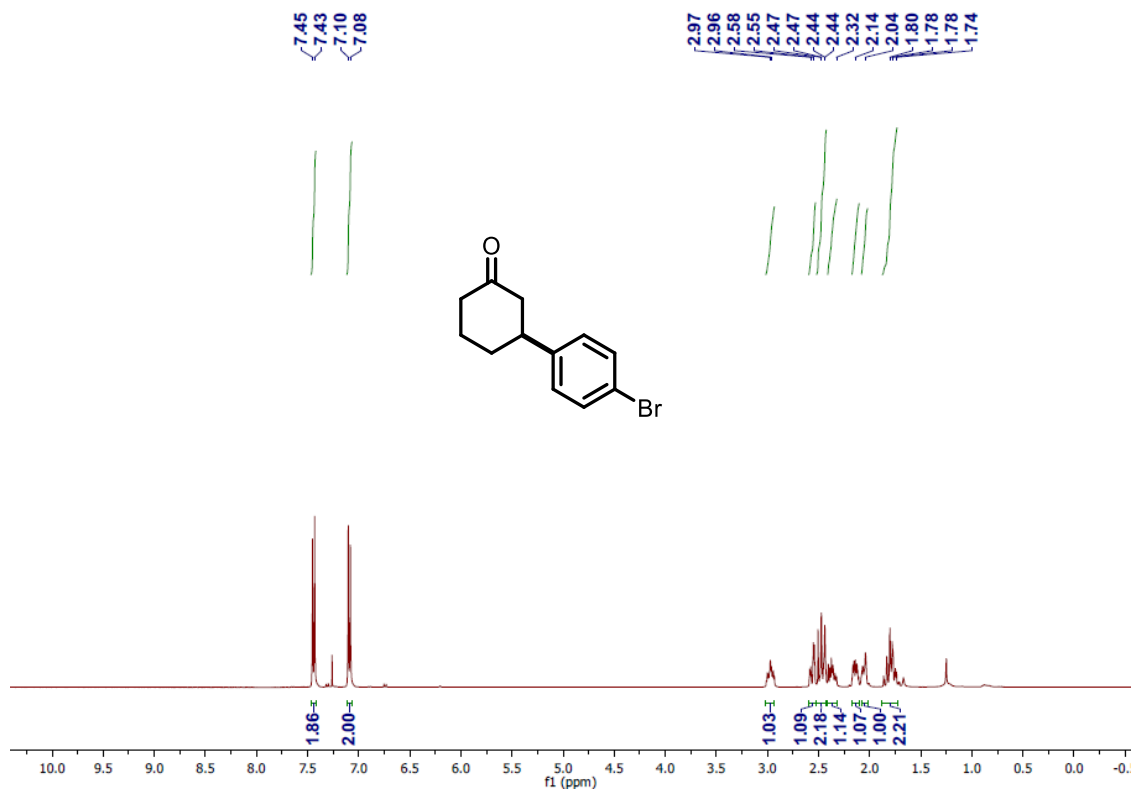


Figure 5.31 ^1H -NMR and ^{13}C -NMR Spectrum and of **5.12p**

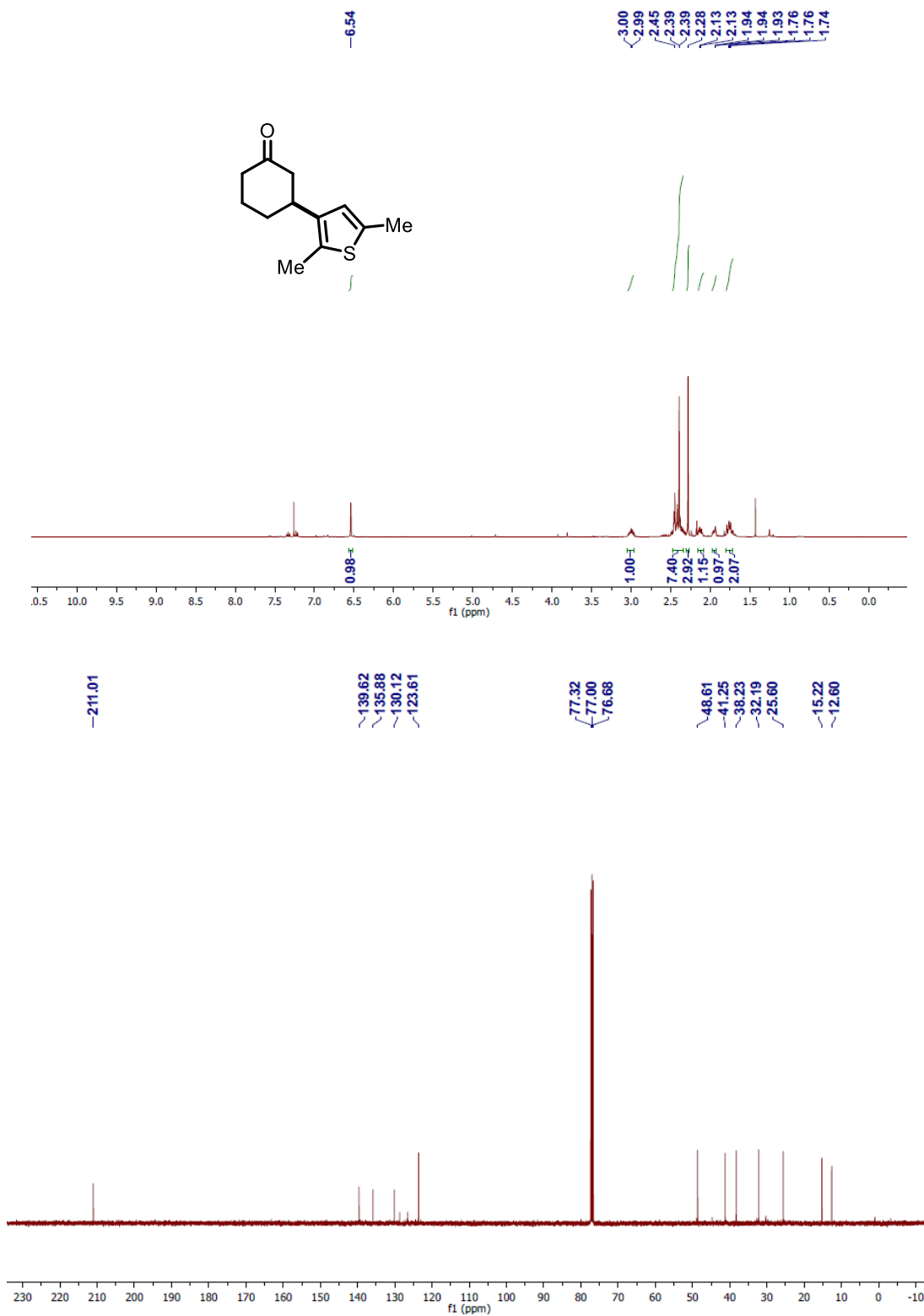


Figure 5.32 ^1H -NMR and ^{13}C -NMR Spectrum of 5.12q

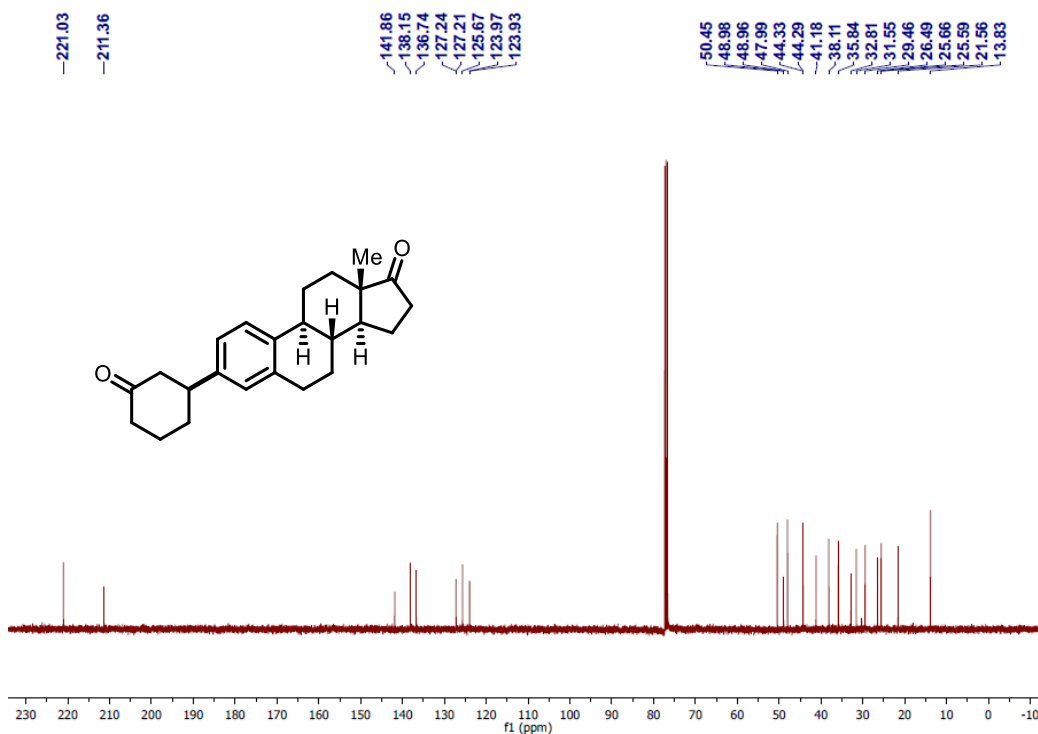
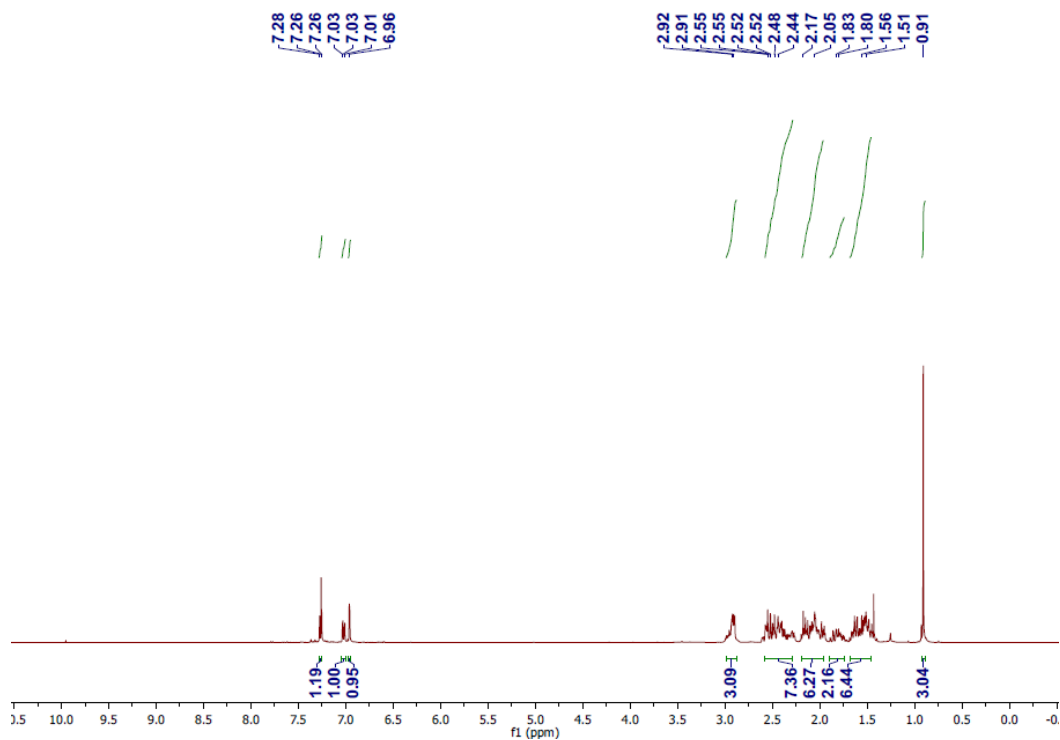


Figure 5.33 ^1H -NMR and ^{13}C -NMR Spectrum of 5.13a

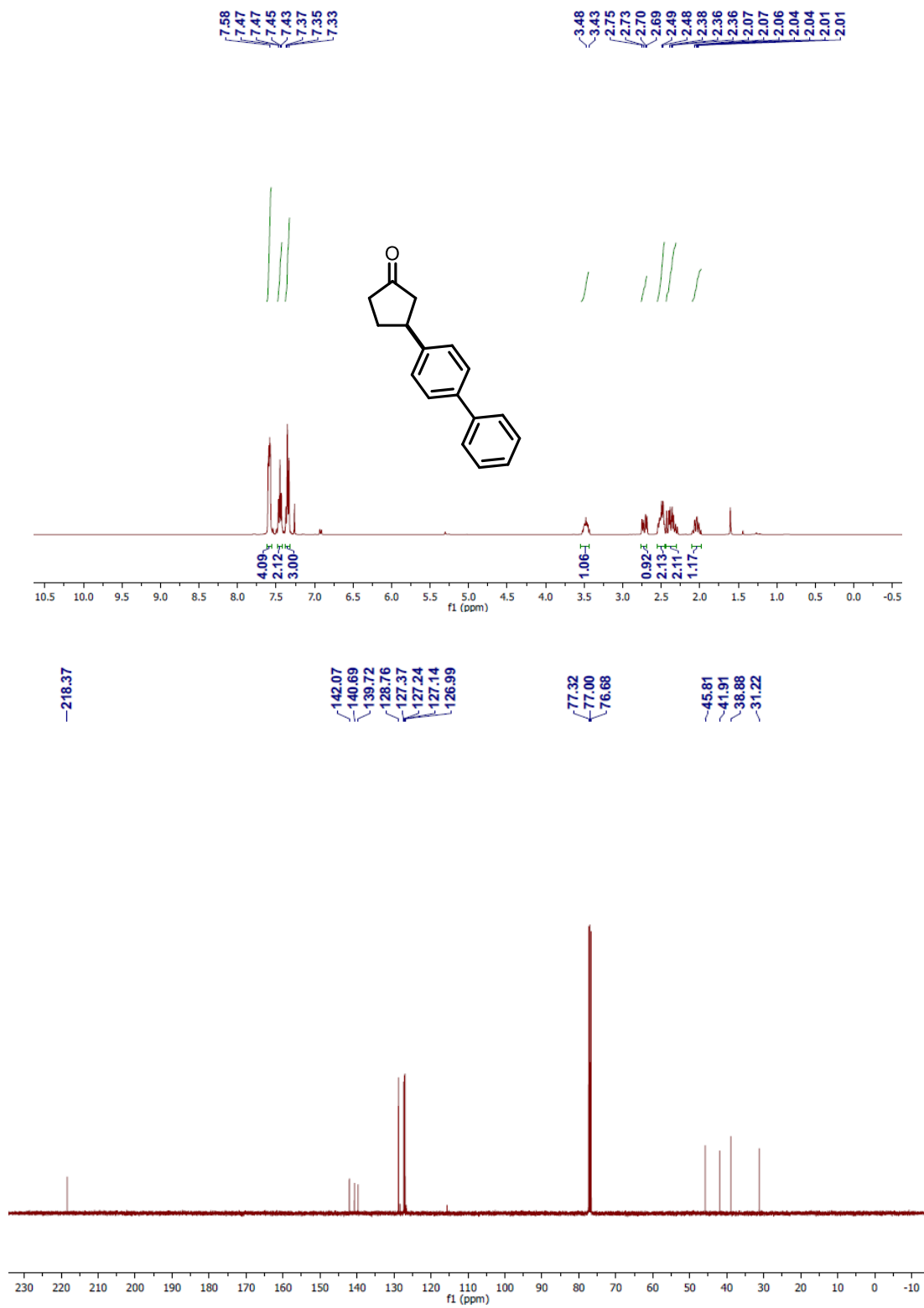


Figure 5.34 ^1H -NMR and ^{13}C -NMR Spectrum of **5.13b**

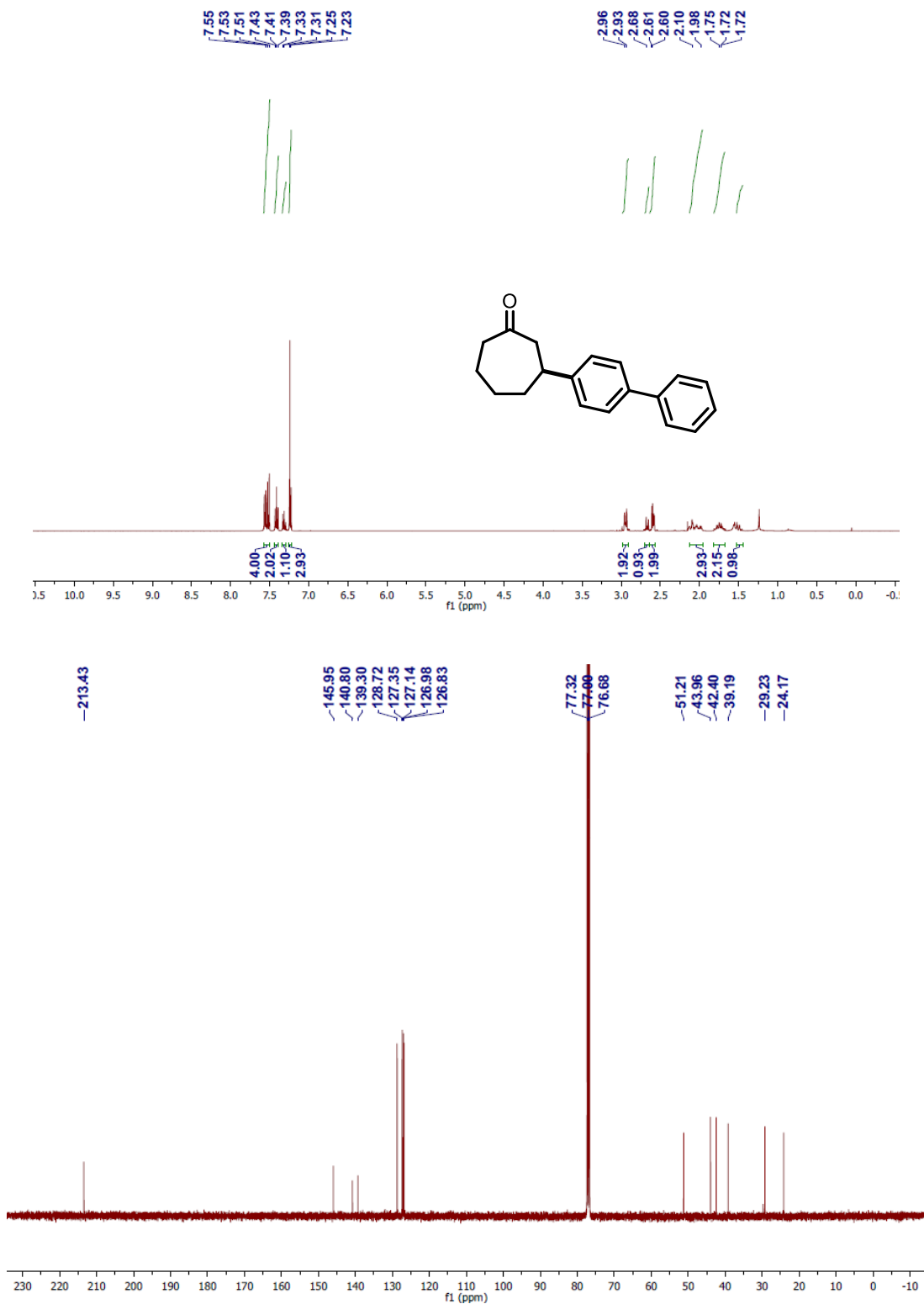


Figure 5.35 ^1H -NMR and ^{13}C -NMR Spectrum of **5.13c**

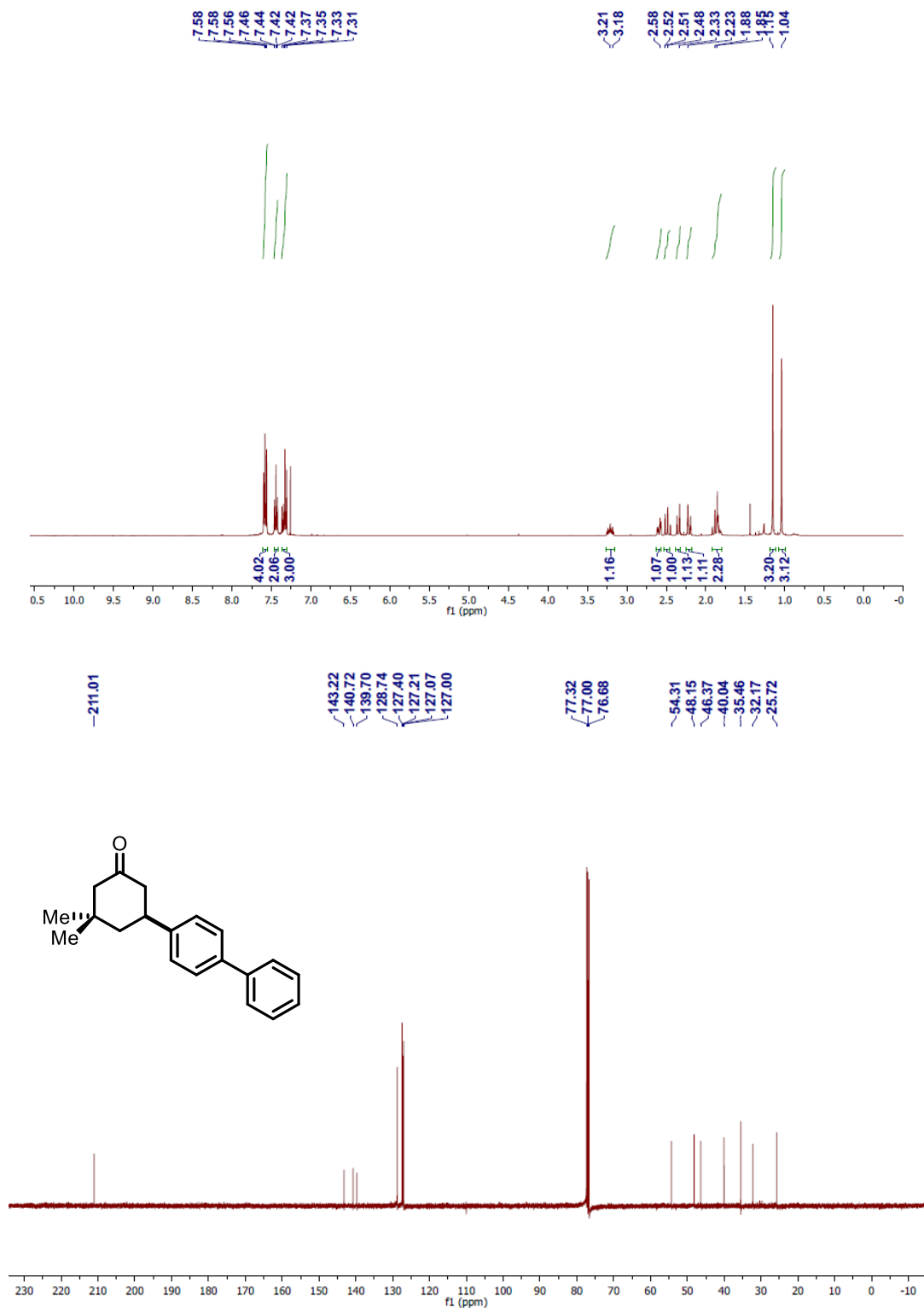


Figure 5.36 ^1H -NMR and ^{13}C -NMR Spectrum of 5.13d

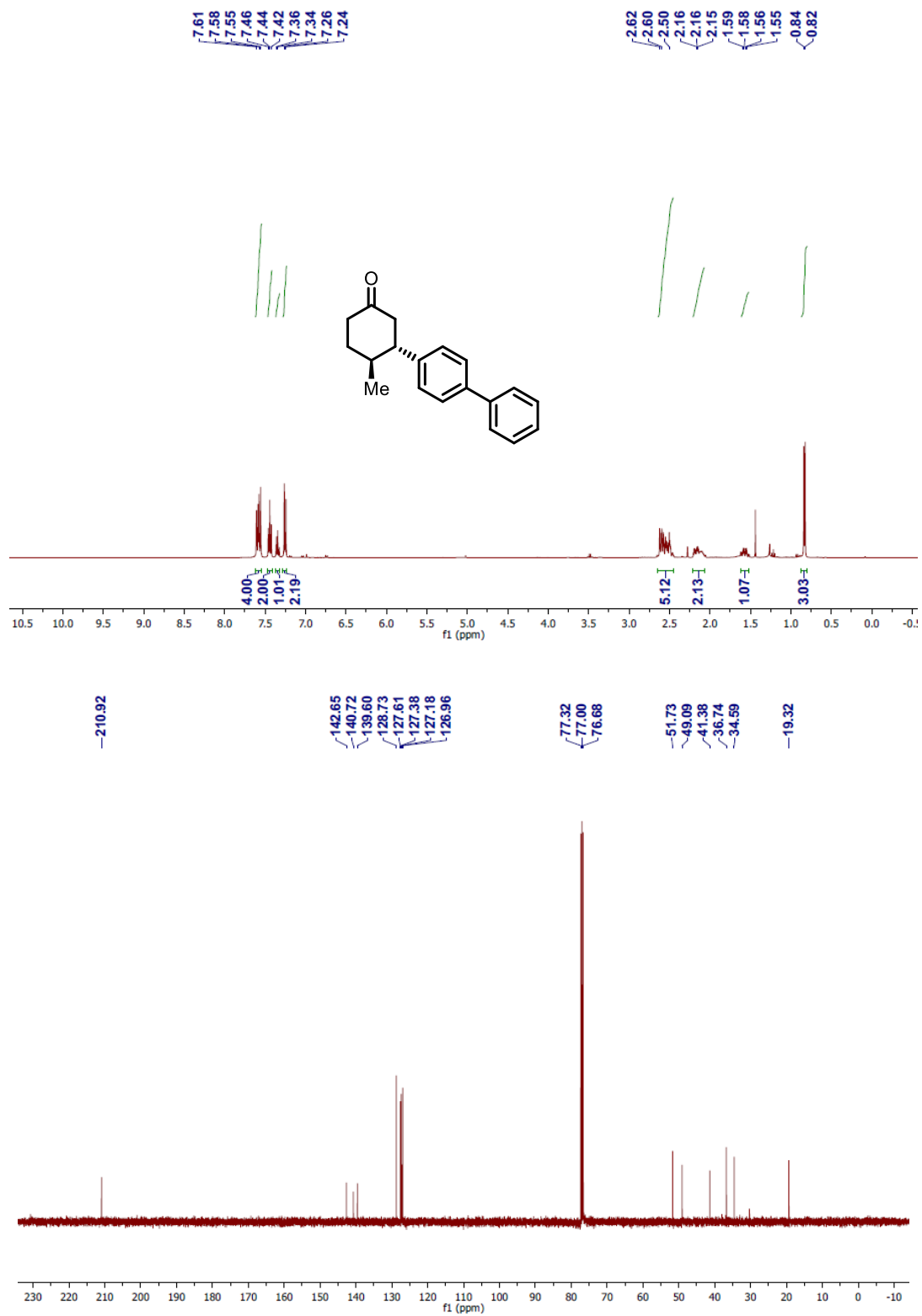


Figure 5.37 ¹H-NMR and ¹³C-NMR Spectrum of 5.13e

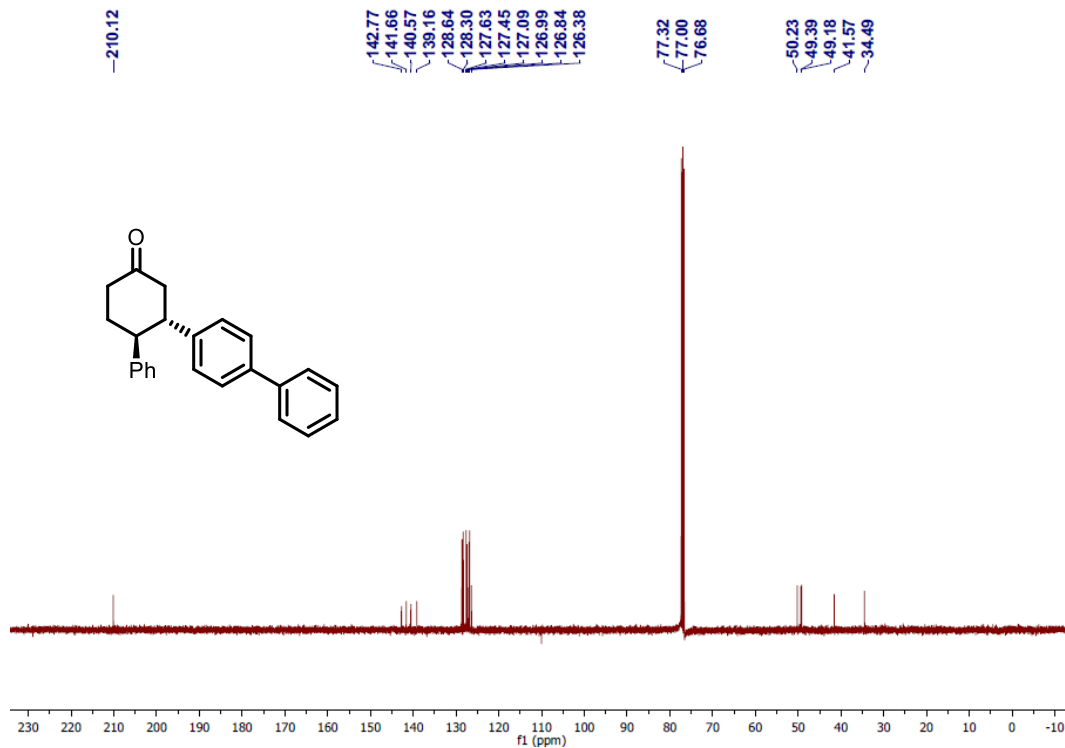
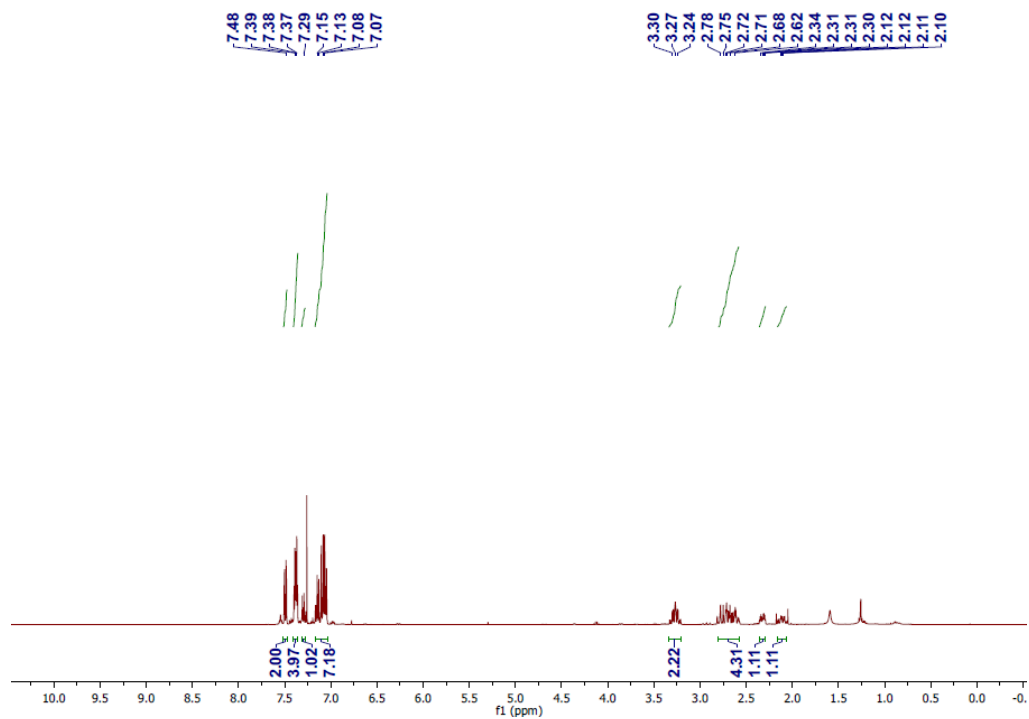


Figure 5.38 $^1\text{H-NMR}$ and $^{13}\text{C-NMR}$ Spectrum of **5.13f**

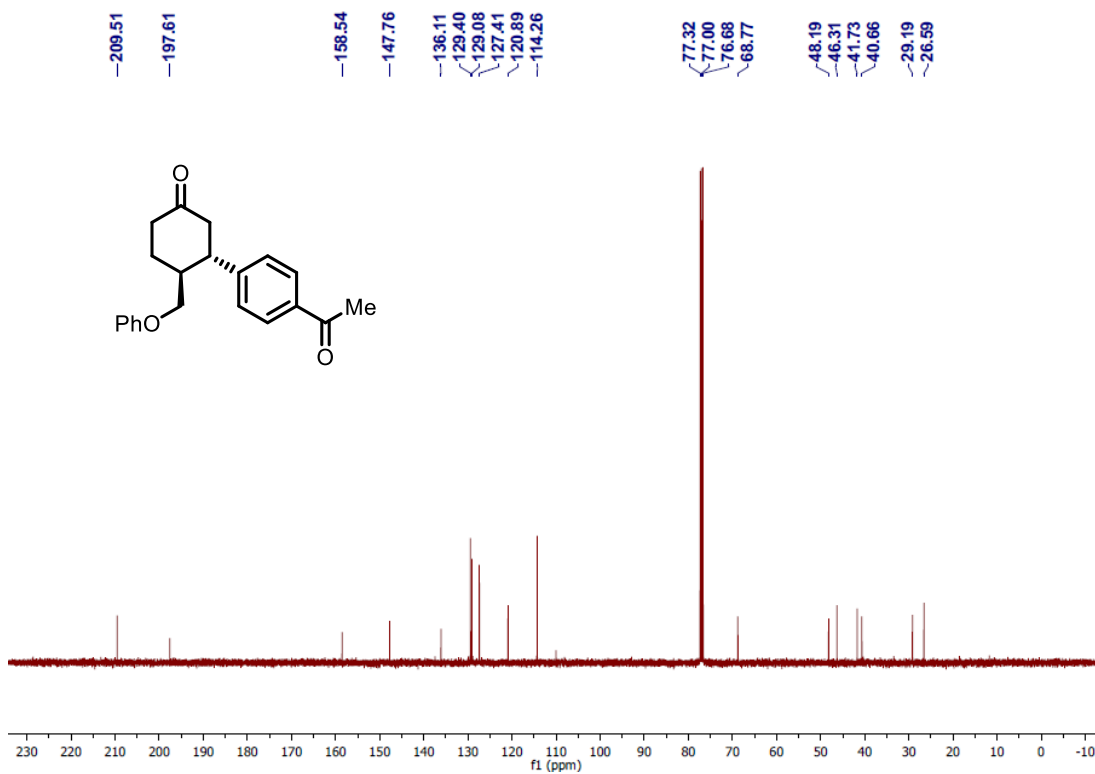
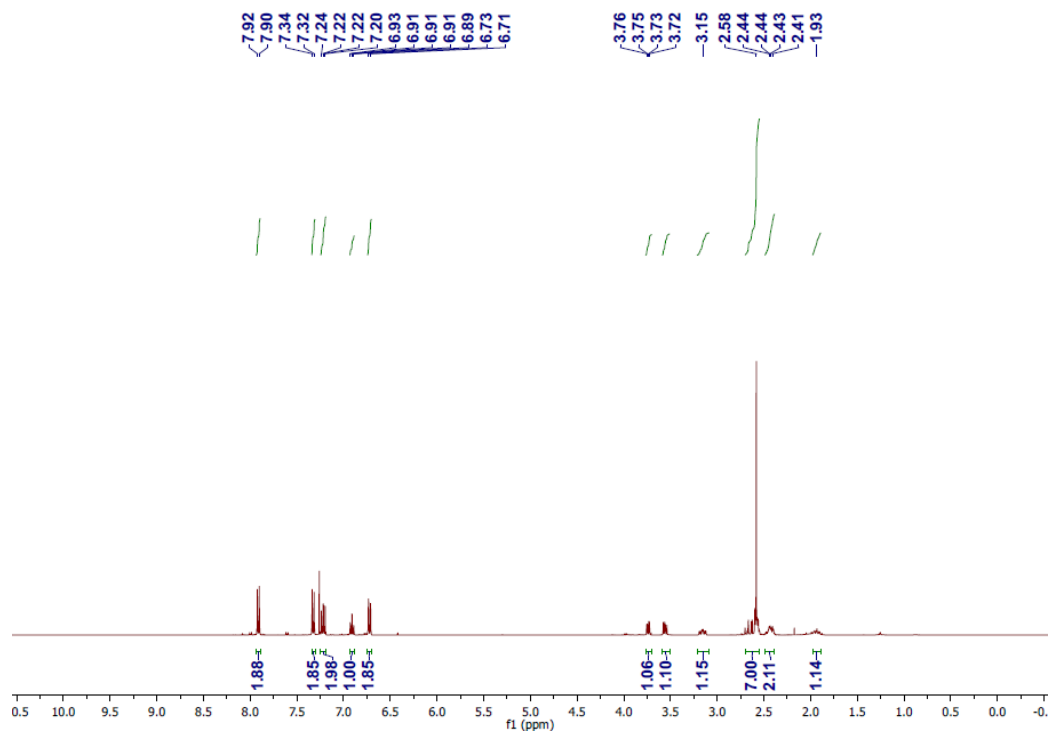


Figure 5.39 ^1H -NMR and ^{13}C -NMR Spectrum of 5.13g

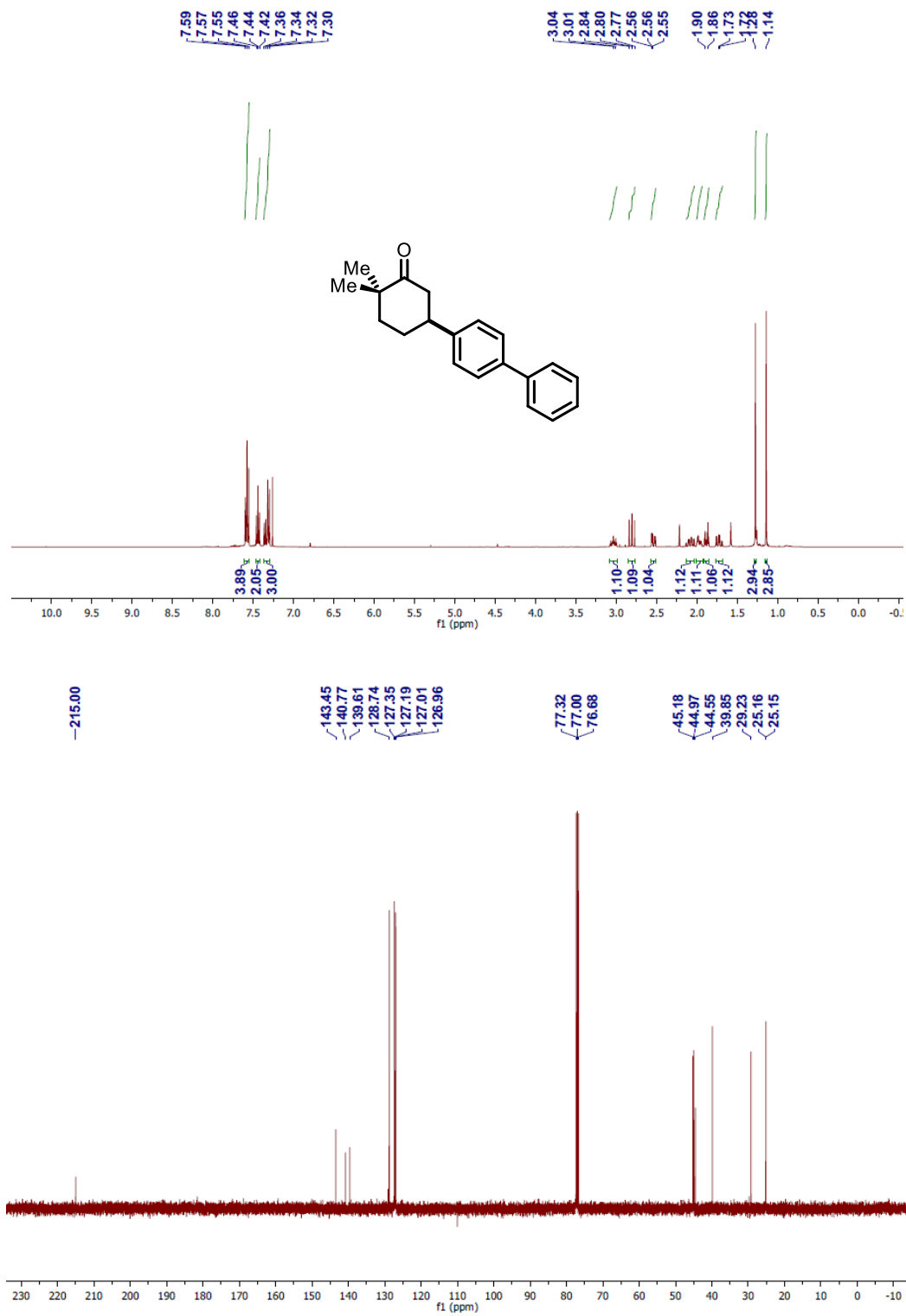


Figure 5.40 $^1\text{H-NMR}$ and $^{13}\text{C-NMR}$ Spectrum of **5.13h**

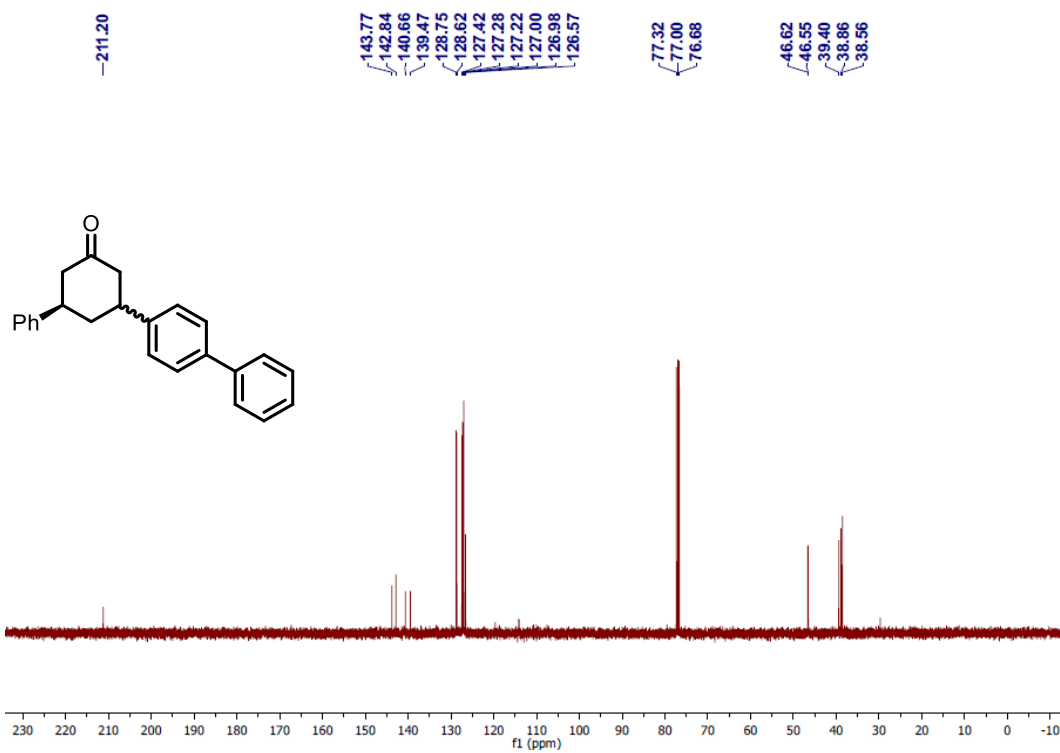
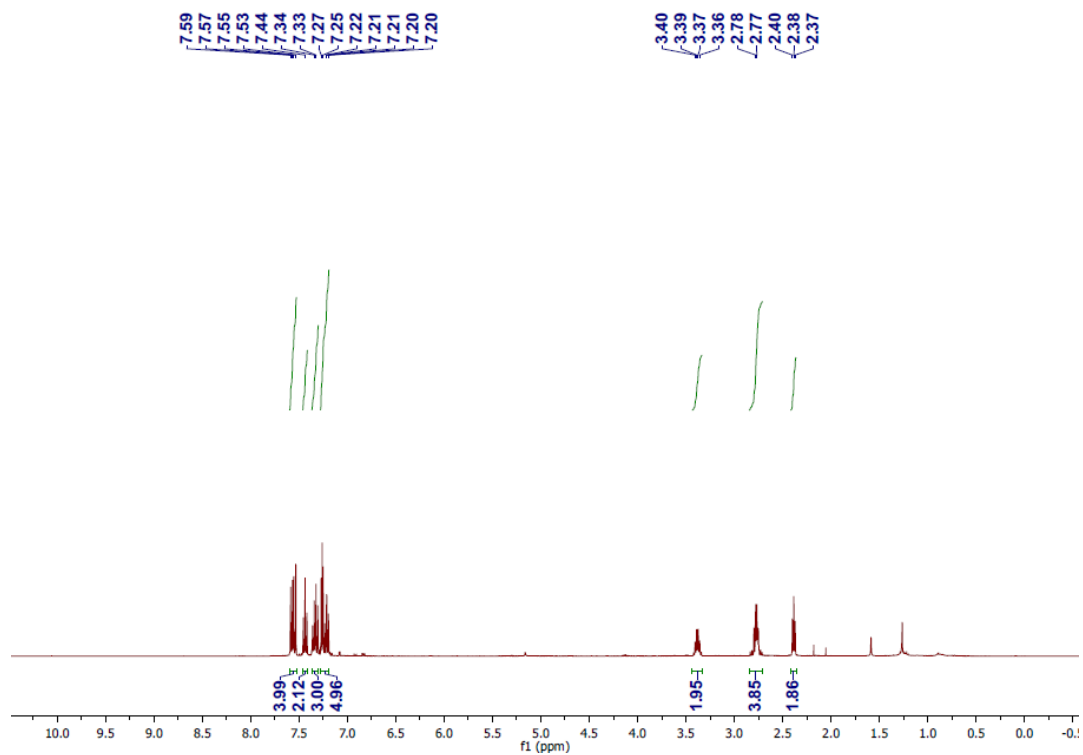


Figure 5.41 $^1\text{H-NMR}$ Spectrum of 5.13i

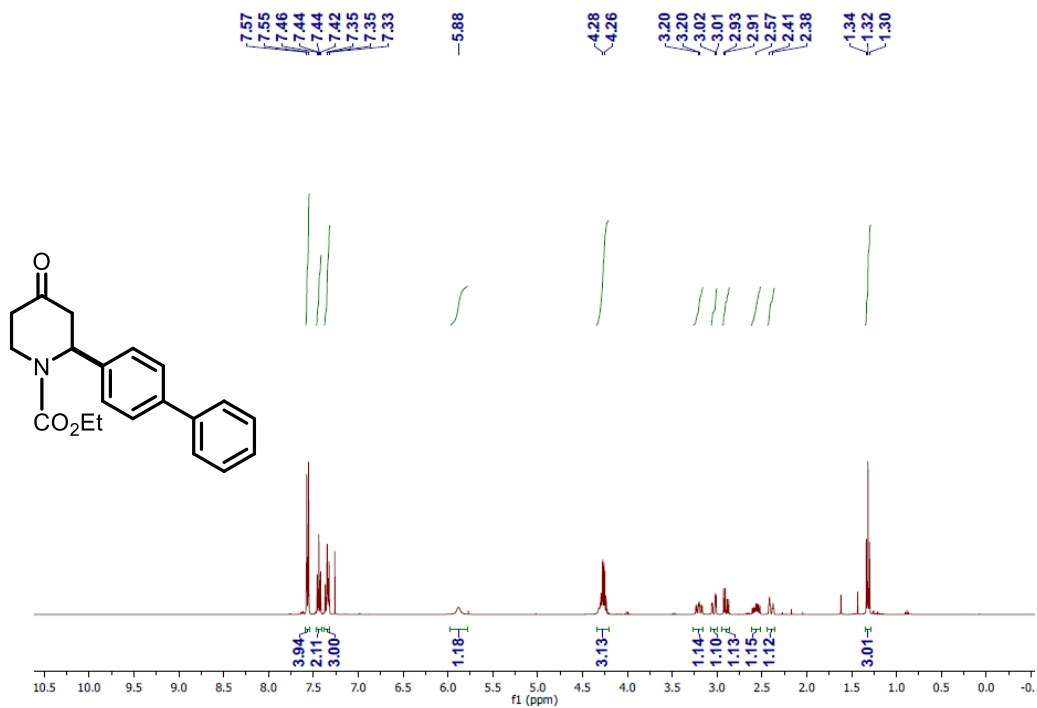


Figure 5.42 $^1\text{H-NMR}$ Spectrum of 5.13j

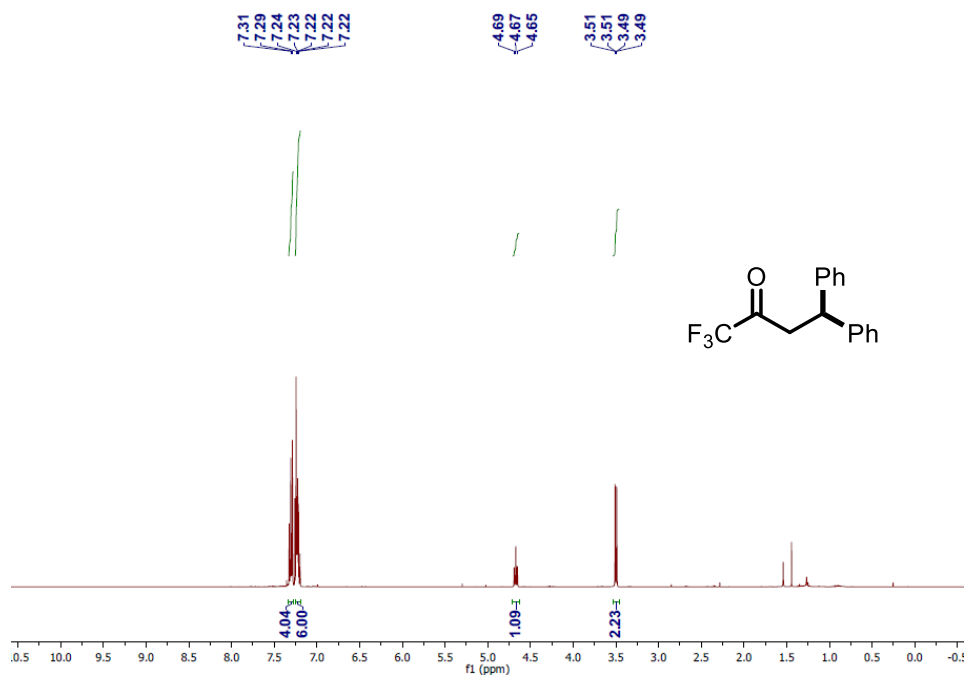
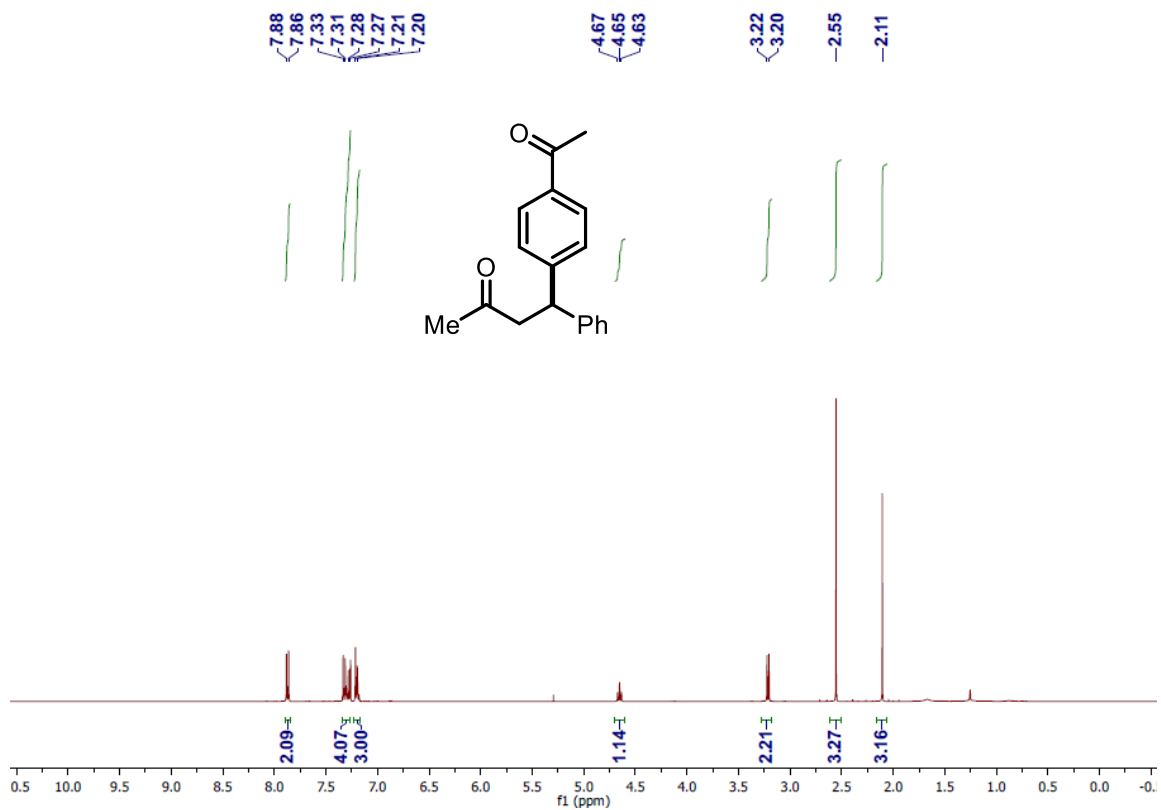


Figure 5.43 $^1\text{H-NMR}$ Spectrum of **5.13k**



5.6 References

1. Huang, Z.; Dong, G. *J. Am. Chem. Soc.* **2013**, *135*, 17747.
2. For recent reviews of the application of diaryliodonium salts in the arylation reactions, see: (a) Deprez, N. R.; Sanford, M. S. *Inorg. Chem.* **2007**, *46*, 1924. (b) Zhdankin, V. V.; Stang, P. J. *Chem. Rev.* **2008**, *108*, 5299. (c) Merritt, E. A.; Olofsson, B. *Angew. Chem., Int. Ed.* **2009**, *48*, 9052.
3. For recent references of the application of diaryliodonium salts in the C-H arylation reactions, see: (a) Kalyani, D.; Deprez, N. R.; Desai, L. V.; Sanford, M. S. *J. Am. Chem. Soc.* **2005**, *127*, 7330. (b) Daugulis, O.; Zaitsev, V. G. *Angew. Chem. Int. Ed.* **2005**, *44*, 4046. (c) Deprez, N. R.; Kalyani, D.; Krause, A.; Sanford, M. S. *J. Am. Chem. Soc.* **2006**, *128*, 4972. (d) Phipps, R. J.; Grimster, N. P.; Gaunt, M. J. *J. Am. Chem. Soc.* **2008**, *130*, 8172. (e) Phipps, R. J.; Gaunt, M. J. *Science* **2009**, *323*, 1593. (f) Deprez, N. R.; Sanford, M. S. *J. Am. Chem. Soc.* **2009**, *131*, 11234. (g) Aydin, J.; Larsson, J. M.; Selander, N.; Szabó, K. *J. Org. Lett.* **2009**, *11*, 2852. (h) Xiao, B.; Fu, Y.; Xu, J.; Gong, T.-J.; Dai, J.-J.; Yi, J.; Liu, L. *J. Am. Chem. Soc.* **2010**, *132*, 468. (i) Ciana, C.-L.; Phipps, R. J.; Brandt, J. R.; Meyer, F.-M.; Gaunt, M. J. *Angew. Chem. Int. Ed.* **2011**, *50*, 458. (j) Duong, H. A.; Gilligan, R. E.; Cooke, M. L.; Phipps, R. J.; Gaunt, M. J. *Angew. Chem. Int. Ed.* **2011**, *50*, 463. (k) Bigot, A.; Williamson, A. E.; Gaunt, M. J. *J. Am. Chem. Soc.* **2011**, *133*, 13778. (l) Harvey, J. S.; Simonovich, S. P.; Jamison, C. R.; MacMillan, D. W. C. *J. Am. Chem. Soc.* **2011**, *133*, 13782. (m) Allen, A. E.; MacMillan, D. W. C. *J. Am. Chem. Soc.* **2011**, *133*, 4260. (n) Phipps, R. J.; McMurray, L.; Ritter, S.; Duong, H. A.; Gaunt, M. J. *J. Am. Chem. Soc.* **2012**, *134*, 10773. (o) Toh, Q. Y.; McNally, A.; Vera, S.; Erdmann, N.; Gaunt, M. J. *J. Am. Chem. Soc.* **2013**, *135*, 3772. (p) Kieffer, M. E.; Chuang, K. V.; Reisman, S. E. *J. Am. Chem. Soc.* **2013**, *135*, 5557. (q) Wagner, A. M.; Hickman, A. J.; Sanford, M. S. *J. Am. Chem. Soc.* **2013**, *135*, 15710. (r) Zhang, F.; Das, S.; Walkinshaw, A. J.; Casitas, A.; Taylor, M.; Suero, M. G.; Gaunt, M. J. *J. Am. Chem. Soc.* **2014**, *136*, 8851.
4. Sheshenev, A. E.; Smith, A. M. R.; Hii, K. K. *Nature Protocols* **2012**, *7*, 1765.
5. For selected examples, see: (a) Chen, M. S.; White, M. C. *J. Am. Chem. Soc.* **2004**, *126*, 1346. (b) Delcamp, J. H.; White, M. C. *J. Am. Chem. Soc.* **2016**, *128*, 15076.
6. For an example of palladium-catalyzed dehydrogenation promoted by 4,5-diazafluoren-9-one, see: Diao, T.; Stahl, S. S. *J. Am. Chem. Soc.* **2011**, *133*, 14566.
7. For recent reviews of the application of sulfur-based ligands, see: (a) Fernandez, I.; Khiar, N. *Chem. Rev.* **2003**, *103*, 3651. (b) Pellissier, H. *Tetrahedron*, **2007**, *63*, 1297. (c) Mellah, M.; Voituriez, A.; Schulz, E. *Chem. Rev.* **2007**, *107*, 5133.
8. For a recent example of dehydrogenative β -arylation, see: Gandeepan, P.; Rajamalli, P.; Cheng, C.-H. *ACS Catal.* **2014**, *4*, 4485.

9. For a selected review of elimination of alkyl bis-*N*-tosylsulfilimine, see: Oae, S.; Furukawa, N. *Tetrahedron* **1977**, *33*, 2359.

10. For recent reviews on palladium nanoparticles, see: (a) Aiken III, J. D.; Finke, R. G. *J. Mol. Catal. A: Chem.* **1999**, *145*, 1. (b) Roucoux, A.; Schulz, J.; Patin, H. *Chem. Rev.* **2002**, *102*, 3757. (c) Astruc, D.; Lu, F.; Aranzaes, J. R. *Angew. Chem. Int. Ed.* **2005**, *44*, 7852. (d) Phan, N. T. S.; Van Der Sluys, M.; Jones, C. W. *Adv. Synth. Catal.* **2006**, *348*, 609. (e) Astruc, D. *Inorg. Chem.* **2007**, *46*, 1884. (f) Yan, N.; Xiao, C.; Kou, Y. *Coord. Chem. Rev.* **2010**, *254*, 1179.

11. Pun, D.; Diao, T.; Stahl, S. S. *J. Am. Chem. Soc.* **2013**, *135*, 8213.

12. For reviews of methods to distinguish metal-nanoparticle catalysis from single-molecule and heterogeneous catalysis, see: (a) Widegren, J. A.; Finke, R. G. *J. Mol. Catal. A: Chem.* **2003**, *198*, 317. (b) Crabtree, R. H. *Chem. Rev.* **2011**, *112*, 1536.

13. For examples of filtration tests, see: (a) Hamlin, J. E.; Hirai, K.; Millan, A.; Maitlis, P. M. *J. Mol. Catal.* **1980**, *7*, 543. (b) Sheldon, R. A.; Wallau, M.; Arends, I. W. C. E.; Schuchardt, U. *Acc. Chem. Res.* **1998**, *31*, 485. (c) Lempers, H. E. B.; Sheldon, R. A. *J. Catal.* **1998**, *175*, 62. (d) Biffis, A.; Zecca, M.; Basato, M. *Eur. J. Inorg. Chem.* **2001**, 1131. (e) Conlon, D. A.; Pipik, B.; Ferdinand, S.; LeBlond, C. R.; Sowa, J. R., Jr.; Izzo, B.; Collins, P.; Ho, G.-J.; Williams, M.; Shi, Y.-J.; Sun, Y. *Adv. Synth. Catal.* **2003**, *345*, 931. (f) Yu, K.; Sommer, W.; Weck, M.; Jones, C. W. *J. Catal.* **2004**, *226*, 101. (g) Gaikwad, A. V.; Holuigue, A.; Thathagar, M. B.; ten Elshof, J. E.; Rothenberg, G. *Chem. Eur. J.* **2007**, *13*, 6908.

14. For reviews and recent examples of DLS measurement of nanoparticle catalysis, see: (a) Bohren, C. F.; Huffman, D. R. *Absorption and Scattering of Light by Small Particles*, 1st ed.; John Wiley & Sons: New York, 1998. (b) Pecora, R. J. *Nanoparticle Res.* **2000**, *2*, 123. (c) Berne, B. J.; Pecora, R. *Dynamic Light Scattering (With Applications to Chemistry, Biology, and Physics)*, 2nd ed.; Dover: Mineola, NY, 2000. (d) Hintermair, U.; Hashmi, S. M.; Elimelech, M.; Crabtree, R. H. *J. Am. Chem. Soc.* **2012**, *134*, 9785.

15. For examples of mercury poisoning test, see: (a) Bayram, E.; Linehan, J. C.; Fulton, J. L.; Roberts, J. A. S.; Szymczak, N. K.; Smurthwaite, T. D.; Ozkar, S.; Balasubramanian, M.; Finke, R. G. *J. Am. Chem. Soc.* **2011**, *133*, 18889. (b) Yu, K.; Sommer, W.; Richardson, J. M.; Weck, M.; Jones, C. W. *Adv. Synth. Catal.* **2005**, *347*, 161. (c) Finney, E. E.; Finke, R. G. *Inorg. Chim. Acta* **2006**, *359*, 2879. (d) Weck, M.; Jones, C. W. *Inorg. Chem.* **2007**, *46*, 1865. (e) Jones, C. W. *Top. Catal.* **2010**, *53*, 942.

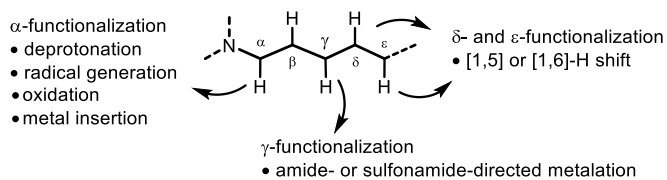
CHAPTER 6

Hydrazone-Based *exo*-Directing Groups for β -C–H Oxidation of Aliphatic Amines

6.1 Introduction

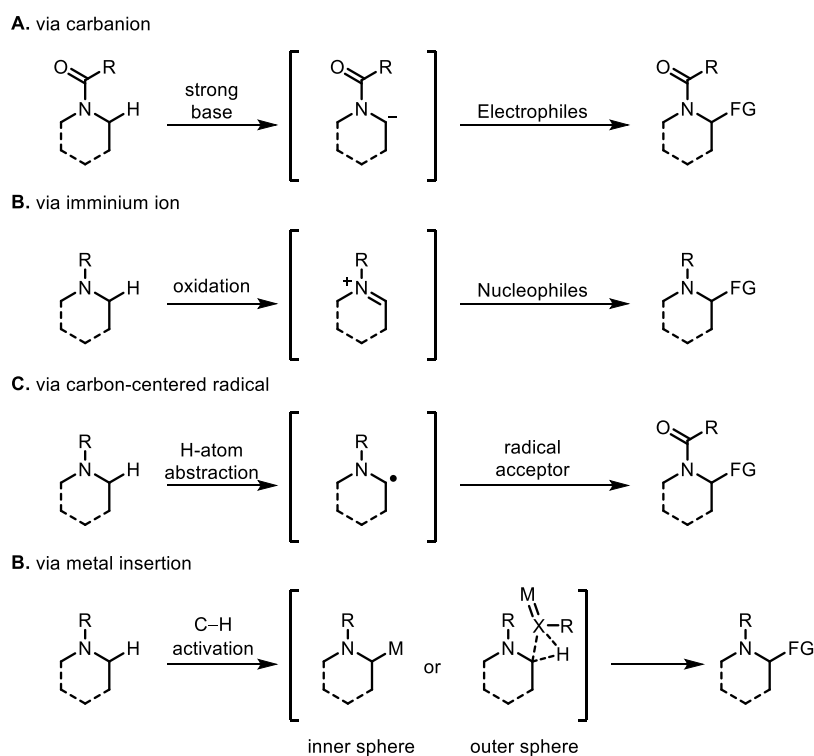
Site-selective C–H functionalization of aliphatic amines and protected amines, such as amides, carbamates, and sulfonamides, holds significant potential for pharmaceutical and agrochemical applications, as these motifs are ubiquitous in biologically important molecules.¹ Over the past several decades, a large number of new methods have emerged to transform C–H bonds at specific sites of aliphatic amines to a variety of functional groups (Figure 6.1).

Figure 6.1 Site-selective C–H Functionalization of Aliphatic Amines



It is known that α positions of aliphatic amines, inherently activated by the adjacent nitrogen atom, can be functionalized via a collection of reactive intermediates.² For example, the direct α -deprotonation of *N*-protected amine with a strong base gives a carbanion intermediate, which would subsequently react with a wide range of electrophiles to give α -substituted amines (Scheme 6.1A). On the other hand, the iminium ions from the oxidation of aliphatic amine can be coupled with a nucleophile (Scheme 6.1B). Carbon-centered radicals, generated from hydrogen atom abstraction, have been harnessed to functionalize the α positions of aliphatic amines (Scheme 6.1C). In addition, recent advances of transition metal mediated C–H activation have also inspired methodologies that proceed through metal insertions via inner or outer sphere mechanism (Scheme 6.1D).

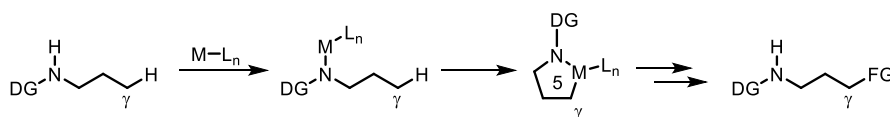
Scheme 6.1 α -C–H Functionalization of Aliphatic Amines



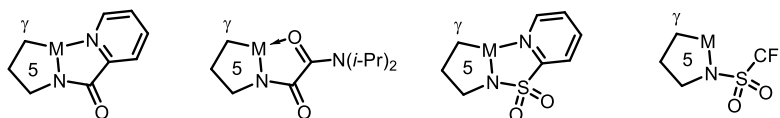
Amide/sulfonamide-based directing group strategies, pioneered by Daugulis, are often employed to activate the γ -C–H bonds of amine.³ In a general pathway, the acidic amide/sulfonamide is deprotonated and acts as an X-type ligand for the transition metal catalyst. The complexation with the directing group would then deliver the transition metal into the proximity of the γ position of the substrate, followed by the insertion of the metal into the C–H bond. The high site-selectivity of the γ -C–H bond in this case is attributed to the formation of kinetically favored five-membered ring metallacycle. In Daugulis' seminal work, a picolinamide-type directing group was used, which contains a pyridine moiety that acts as a secondary ligand for the metallacycle formation. For the past decade, a large collection of amide/sulfonamide directing groups, both bidentate and monodentate has been developed to enable the γ -C–H functionalization of aliphatic amines. These efforts have led to the expedited synthesis and late-stage functionalization of important amine derivatives (e.g. 1,3-amino alcohols⁴ and azetidines^{3c}).

Scheme 6.2 Directing Group Strategy for γ -C–H Functionalization of Amines

General pathway



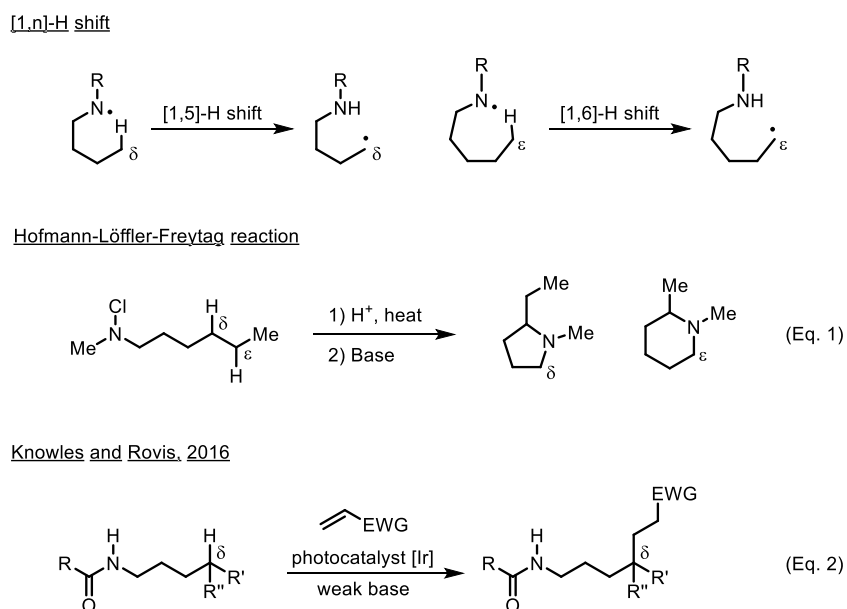
Selected examples of directing group



However, the directing group strategy is less capable of functionalizing remote δ - and ϵ -positions of aliphatic amines, probably due to the unfavorable formation of larger metallacycles. Instead, [1,5]- or [1,6]-H abstraction through generation of highly reactive nitrogen-centered

radicals has proved to be a general approach (Scheme 6.3).⁵ This pathway is exemplified by the classical Hofmann-Löffler-Freytag reaction, where a nitrogen-centered radical is generated through the homolysis of the N–X (X: halogen), followed by a [1,5]- or [1,6]-H shift to give a carbon-centered radical at the δ or ϵ position (Eq. 1). It is noteworthy that recent advances in photoredox catalysis have enabled the use of simple amide as the substrate for the remote δ -functionalization (Eq. 2).⁶

Scheme 6.3 Functionalization of δ - or ϵ -C–H Bond of Amines via Hydrogen Shift

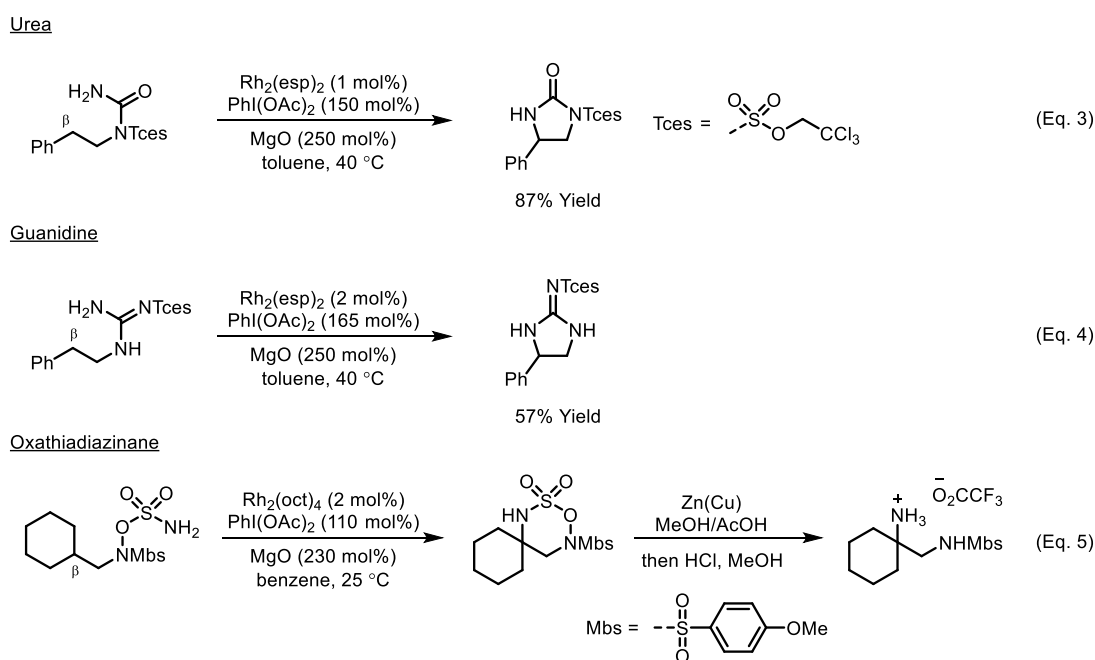


Despite all these advances of C–H functionalization of aliphatic amines, methods that can site-selectively functionalize unactivated β -C–H bonds of amines, by comparison, remain underdeveloped.

In 2006, Du Bois and coworkers reported a rhodium-catalyzed intramolecular C–H amination via nitrene insertion to form masked 1,2-diamines (Scheme 6.4).⁷ Urea (Eq. 3) and

guanidine (Eq. 4) moieties were used as the linkage, as well as the amine source, to facilitate the site-selective insertion of rhodium nitrene into the β -C–H bond via an out sphere mechanism. In 2008, the same group extended this methodology to the construction of oxathiadiazinane motifs (Eq. 5).⁸ It was demonstrated the oxathiadiazinane structures can be readily converted to 1,2-diamine derivatives under reductive conditions, an advantage over previous amination, as the hydrolysis of ureas and guanidines often requires forcing conditions.

Scheme 6.4 Site-selective Nitrene Insertion for the Synthesis of 1,2-Diamine Derivatives

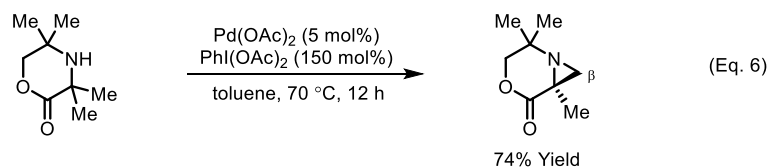


In 2014, Gaunt and coworkers disclosed a novel free amine-directed β -functionalization (Scheme 6.5).⁹ In their proposed mechanism, the aliphatic amine acts as an L-type ligand for the palladium catalyst and facilitates the formation of a strained four-membered palladacycle. Based on the oxidant and/or electrophiles employed in the reaction, a wide range of functionalization was achieved via the putative palladacycle, including aziridination (Eq. 6), acetoxylation (Eq. 7),

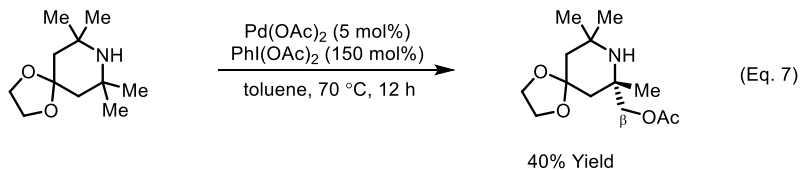
and arylation¹⁰ (Eq. 8). For all these functionalization, the use of sterically hindered secondary amines appears to be important, proposedly to inhibit the formation of catalytically inactive bis-amine palladium complexes.

Scheme 6.5 Free Amine-directed β -C–H Functionalization of Strained Secondary Amines

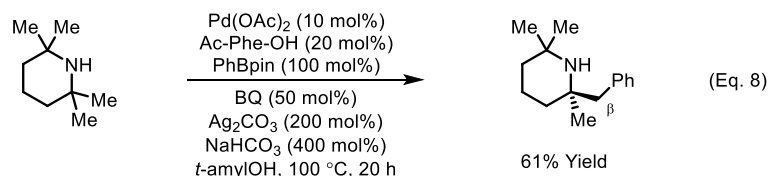
Aziridination



Acetoxylation



Arylation

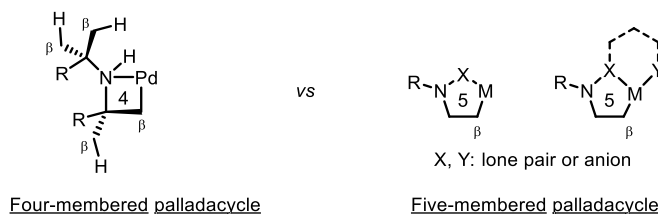


Considering the significance of site-selective C–H functionalization of amines and the limited number of methods available for the β positions, we envisioned a new directing group strategy for the β -C–H functionalization of aliphatic amine would be potentially useful for synthesizing and modifying amine derivatives of interest, as well as complement the chemistry of nitrene insertion and free amine-directed palladation.

6.2 Results and Discussion

Our guideline for the design of new directing group for the β -C–H bond of amines is based on the kinetically favored formation of five-membered metallacycle. Thus, in order to meet the criteria of ring size, a directing group must be built on the amine nitrogen and the adjacent atom should be able to coordinate to the metal catalyst with a lone pair or as an anion under the reaction conditions. Compared with the proposed four-membered palladacycle by Gaunt,⁹ while the installation and removal of directing groups need additional steps, our proposed metallacycle is much less strained, which in turn would potentially result in less restriction on the amine structures, such as the need of strained amines and multiple β sites present (Figure 6.2).

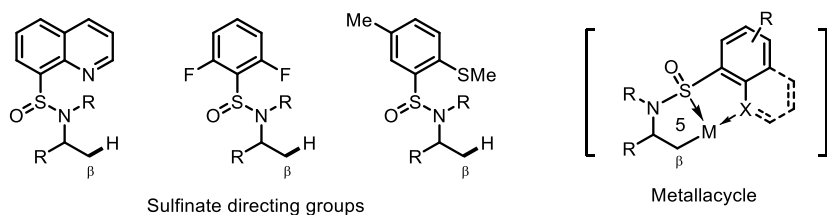
Figure 6.2 Four-membered and Five-membered Metallacycle



Based on the design, we first turned our attention to the sulfinate amide as a potential directing group. One advantage of the sulfinate amides is their easy accessibility from corresponding aliphatic amine through transamidation. In our proposal, the lone pair of the sulfur atom may be used to coordinate to the transition metal to direct the C–H cleavage. The electron-withdrawing nature of the sulfoxide group also diminished the Lewis basicity of the nitrogen atom, preventing its coordination to the metal catalyst. We also designed to attach a secondary coordinating moiety, such as 8-quinolyl, *ortho*-fluoride phenyl, or *ortho*-methylsulfide phenyl, to

the sulfinate structure, in the hope of stabilizing and facilitate the formation of the metallacycle through chelation (Figure 6.3).

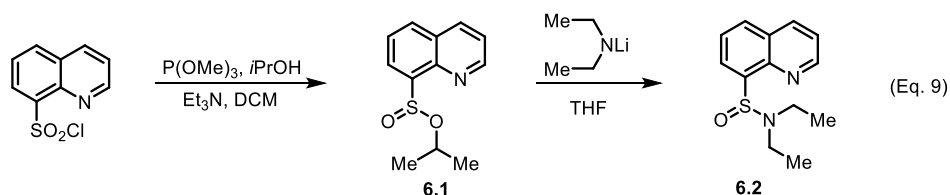
Figure 6.3 Sulfinate Amide Directing Groups



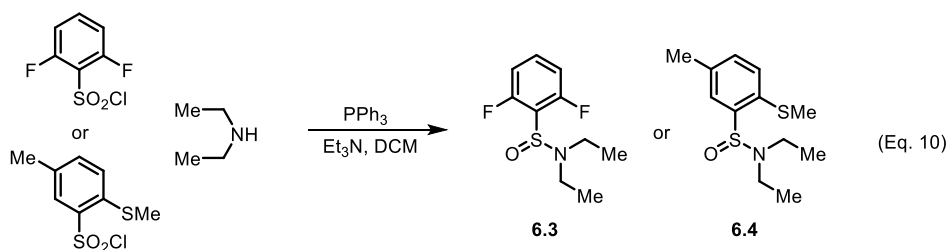
The synthesis of the standard sulfinate amide substrate turned out to be facile (Scheme 6.6). The transamidation between sulfinate ester **6.1** and lithium diethylamide successfully gave the sulfinate amide **6.2** (Eq. 9). The sulfinate ester **6.1** can be directly synthesized on a gram scale from commercially available 8-quinoline sulfonyl chlorides and isopropyl alcohol under reductive conditions. The sulfinate directing group can also be installed through a reductive sulfination method. In this case, free amines can be directly sulfinated with aryl sulfonyl chloride using PPh_3 as the reductant (Eq. 10).

Scheme 6.6 Synthesis of Sulfinato Amide

Transamidation

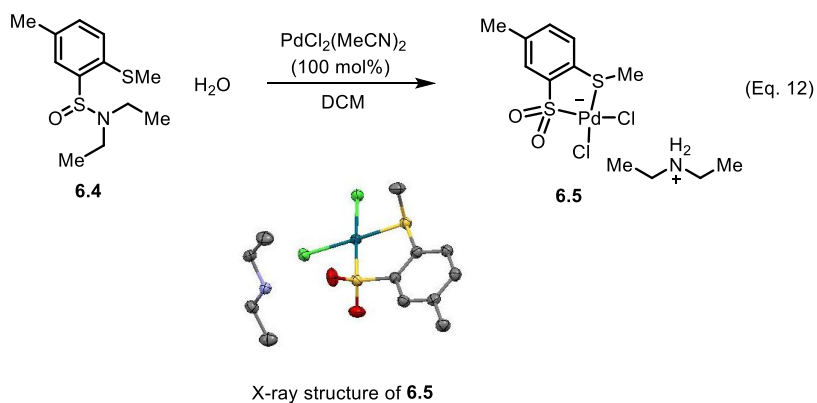
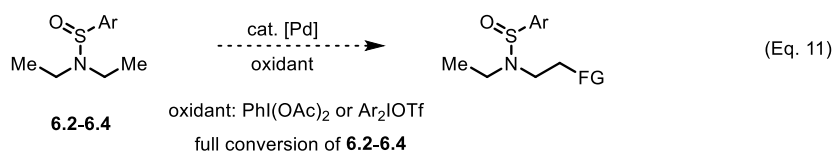


Reductive sulfination



Our attempts to use the new directing group for the palladium-catalyzed C–H oxidation were unsuccessful. When sulfinato amide substrates (**6.2-6.4**) were subjected to the palladium catalyst and stoichiometric amount of oxidant, such as (diacetoxyiodo)benzene and diaryliodonium salts, a full conversion was often observed but no C–H functionalization product can be identified (Scheme 6.7, Eq. 11). We proposed the high conversion is likely due to the instability of the substrate, especially the labile S–N bond. When sulfinato amide **6.4** was stirred with an equal amount of Pd(MeCN)₂Cl₂, a crystal was isolated and identified as a Pd(II) complex by X-ray crystallography. Complex **6.5** consists of an anionic Pd(II) complex and a protonated diethylamine (Eq. 12). This structure indicated the hydrolysis of **6.4** proceeded with adventitious water in the solvent to cleave the S–N bond in the sulfinato amide, possibly facilitated by the palladium salt as a Lewis acid.

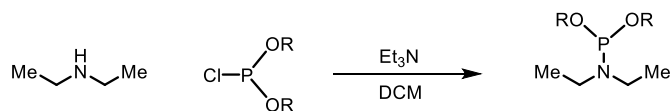
Scheme 6.7 Decomposition of Sulfinat Amide



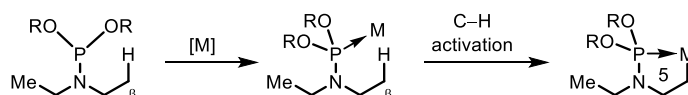
Phosphoramidite-based directing group is another potential solution for the β -C–H functionalization of aliphatic amines. It is well established that phosphoramidites can be synthesized from corresponding amine and chlorophosphite in a facile manner (Scheme 6.8). We proposed that the strong Lewis basicity of phosphine atom in the phosphoramidite could promote its complexation with transition metal catalysts, and subsequent activation of the β -C–H bond to form a five-membered metallacycle.

Scheme 6.8 Potential Phosphoramidite-based Directing Group

Synthesis of phosphoramidite

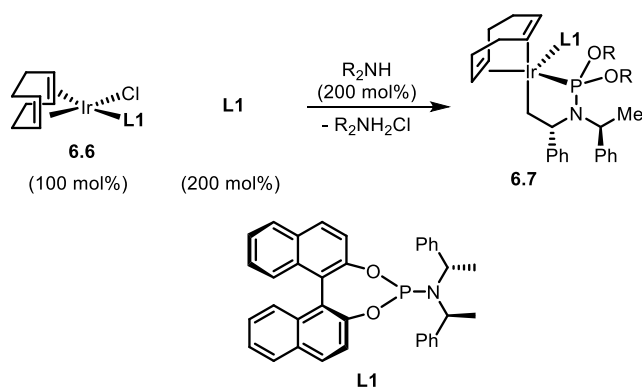


Proposed metallacycle formation



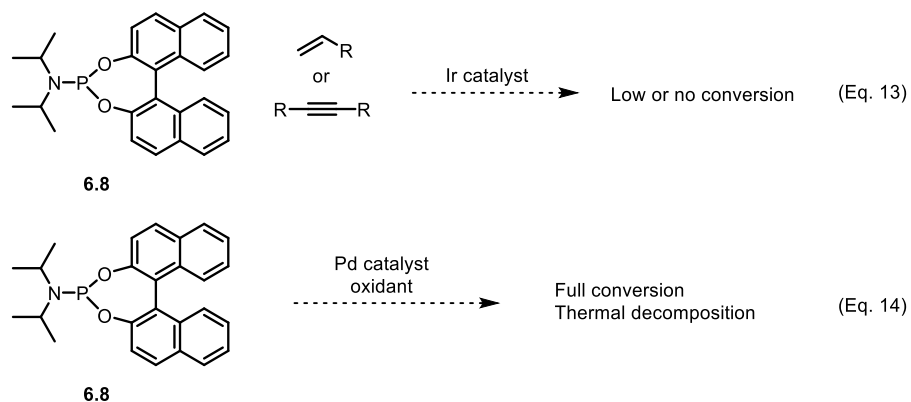
Our hypothesis is supported by Hartwig's discovery of a cyclometallated phosphoramidite complex **6.7** during his study of the activated catalyst of the iridium-catalyzed allylic substitution (Scheme 6.9).¹¹ The authors proposed that, from the starting complex **6.6** and an amine substrate, **6.7** is generated through a sequence of C–H activation at the methyl group by the iridium, reductive elimination of amine hydrochloride, and coordination of a second phosphoramidite ligand **L1**.

Scheme 6.9 Hartwig's Discovery of a Metallated Iridium-Phosphoramidite Complex



For the development of catalytic β -C–H functionalization based on this metallacycle intermediate, we first set out to examine whether the C–H activation event can be coupled with a further migratory insertion of alkenes or alkynes into the Ir–C bond (Scheme 6.10). However, when phosphoramidite **6.8** was reacted with alkenes or alkynes using catalytic amount of iridium/rhodium catalyst, no or low conversion is often observed. On the other hand, when the substrate was submitted to oxidative conditions using palladium catalyst, full conversion was obtained, and a new polar spot on the TLC. Nevertheless, control experiments showed the unidentified polar product may be generated through thermal decomposition of the phosphoramidite starting material.

Scheme 6.10 Attempts for Catalytic β -C–H Functionalization of Phosphoramidite

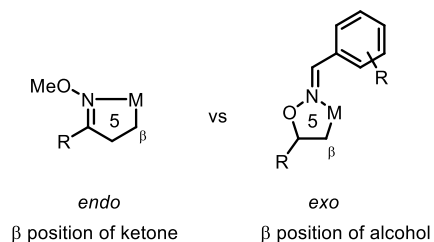


Next we switched the direction of our search of directing group to the hydrazone-based structures. Our focus on the hydrazone-based directing groups was inspired by our group's previous work on the oxime-directed C–H functionalization. The oxime-based directing groups can be viewed as mask alcohols and direct the palladation to the β positions of the alcohols (Scheme 6.11). In the postulated and isolated metallacycle intermediate¹², the C=N double bond

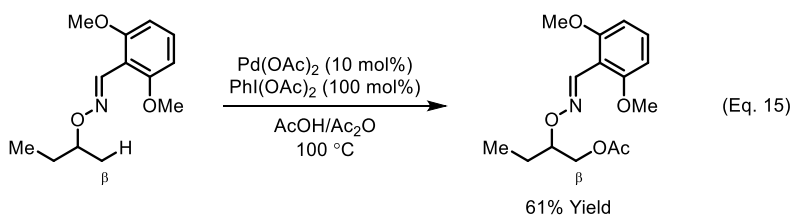
of the directing group is *exo* to the metallacycle, a distinct feature from the *endo* metallacycle proposed for previous oxime-directed alkyl C–H activation pioneered by Sanford¹³ and coworkers. Based on the directing mode, our group has achieved a wide range of β -C–H oxidation reactions of masked alcohols, including acetoxylation (Eq. 15),¹⁴ tosyloxylation (Eq. 16),¹⁵ and intramolecular ether formation¹⁶ (Eq. 17).

Scheme 6.11 Oxime-based *exo* Directing Group

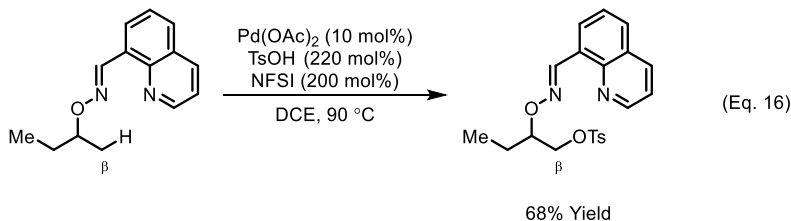
exo vs *endo* directing group



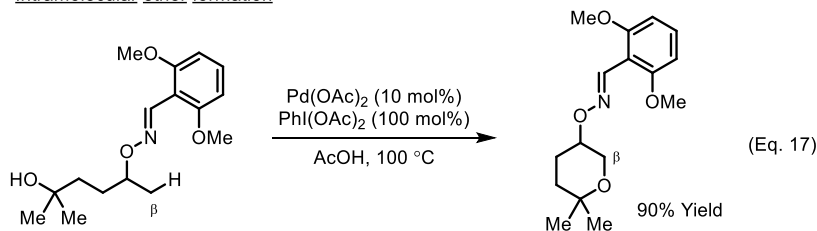
Acetoxylation



Tosyloxylation



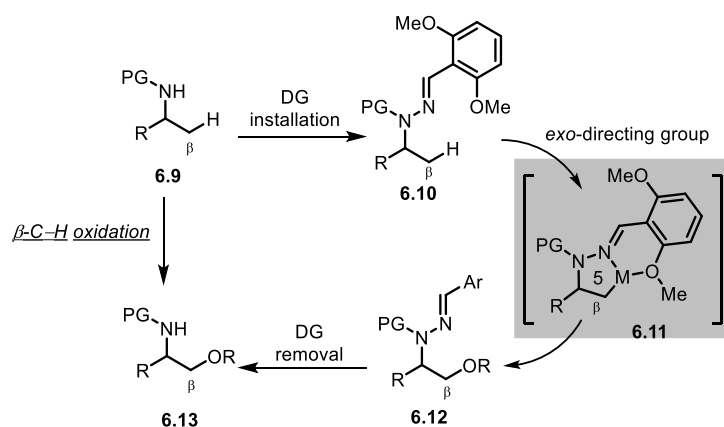
Intramolecular ether formation



We envisioned that this *exo*-directing strategy could be extended to the β -oxidation of amines through development of a new hydrazone-based directing group (Scheme 6.12). It was anticipated that the hydrazone (**6.10**), prepared from the corresponding mono-protected primary amine (**6.9**), would direct metalation at the primary β -position through forming a five-membered *exo*-metallacycle (**6.11**), which should lead to β -functionalized amines. The use of 2,6-

dimethoxyaryl as the hydrazone substituent should prevent *endo*-metalation and stabilize the metallacycle. However, the challenges associated with this strategy are two-fold: 1) compared to alcohols, amines are generally more coordinating and susceptible to oxidation; thus, to enable the desired site-selectivity, choosing an appropriate amine protecting group becomes important. 2) Efficient installation and chemoselective removal of the hydrazone directing group through forming and breaking an N–N bond is non-trivial.¹⁷

Scheme 6.12 Proposed Hydrazone-based Directing Group Strategy

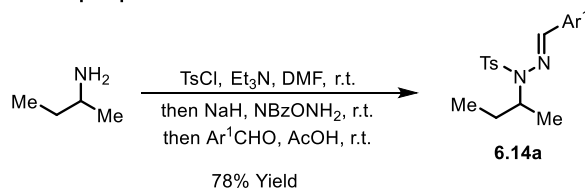


To test the feasibility of the proposed strategy, a practical directing group installation method was first sought. Gratifyingly, when NBzONH₂ was employed as the electrophilic amination reagent,¹⁸ sec-butylamine was protected and aminated to give a Ts-protected hydrazine intermediate, which upon condensation with 2,6-dimethoxybenzaldehyde (Ar¹CHO) provided hydrazone **6.14a** in 78% yield as a single *E* isomer (Scheme 6.13A). Both NBzONH₂ and Ar¹CHO are commercially available and can be prepared in bulk.¹⁹ In addition to this ‘one-pot’ procedure, hydrazone **6.14a** can also be prepared via a convenient ‘chromatography-free’ protocol from the corresponding sulfonamide (Scheme 6.13B). This protocol is also general

to other sulfonamide substrates (*vide infra*), and can be operated on a multi-gram scale without need of chromatography or isolation of the hydrazone intermediate.

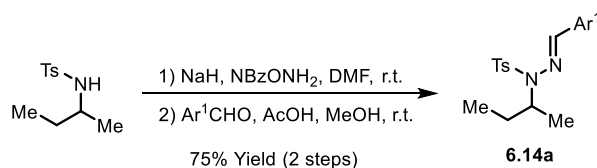
Scheme 6.13 Synthesis of Hydrazone Substrate

A. 'One-pot' procedure

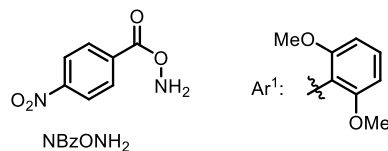


- same flask, same solvent
- sequential addition of reagents
- no interim isolation or work-up

B. 'Filter and wash'/chromatography-free procedure



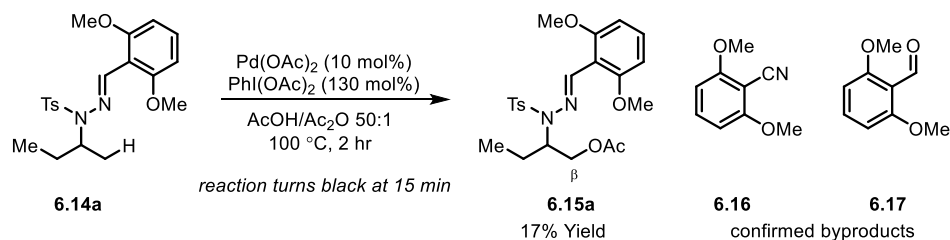
- multi-gram scale synthesis
- no chromatography
- direct precipitation
- 'filter and wash' purification



With the hydrazone substrate in hand, the palladium-catalyzed acetoxylation was initially tested to examine the reactivity and site-selectivity of the proposed functionalization reaction (Scheme 6.14). The acetoxylation of the β -C–H bond of the substrate proceeded in 17% yield with palladium acetate as the catalyst and (diacetoxyiodo)benzene as the stoichiometric oxidant. We also confirmed two major byproducts from the reaction: aryl nitrile (**6.16**) from the elimination of the directing group and aryl aldehyde (**6.17**) from the hydrolysis. In addition,

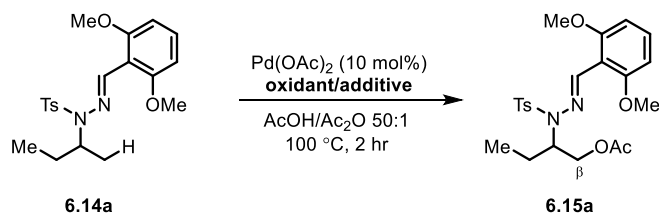
under the initial reaction conditions, the palladium black appeared in just 15 min and considerable amount of starting materials remained.

Scheme 6.14 Initial Attempts for β -Acetoxylation Reaction



Further optimization of oxidants and additives demonstrated that the addition of one equivalent of lithium acetate is beneficial to the yield (Table 6.1, entry 4). We proposed lithium acetate promoted the acetoxylation reaction probably by accelerating the reductive elimination step through a S_N2 mechanism.²⁰ The use of salts with other cation and anion turned out to be inferior to lithium acetate. However, there is still considerable amount of remaining substrates, as well as aldehyde from hydrolysis with the addition of lithium acetate.

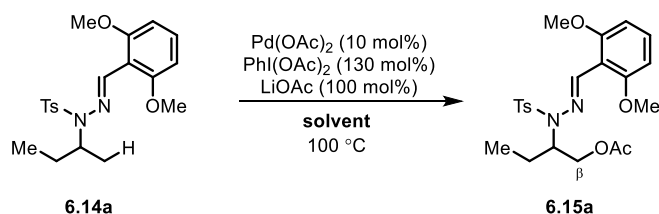
Table 6.1 Beneficial Effect of Lithium Acetate



Entry	Conditions	Product (%)	6.14a (%)	Aldehyde (%)
1	PhI(OAc) ₂ (130)	17	28	24
2	PhI(OAc) ₂ (200)	16	14	17
3	PhI(OAc) ₂ (300)	13	--	10
4	PhI(OAc)₂ (130)+LiOAc (100)	37	27	32
5	K ₂ S ₂ O ₈ (130)	23	15	18

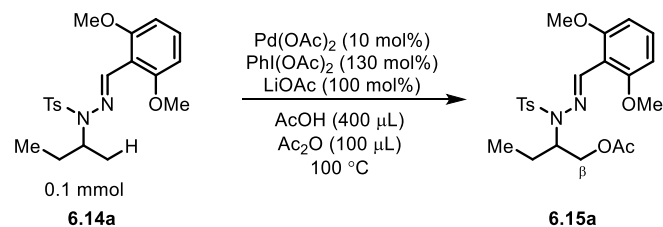
Control experiments showed that when small amount of water was added to the reaction, the β -acetoxylation reaction was completely inhibited, and the aldehyde from the hydrolysis was generated in a large amount (Table 6.2, entry 1). Thus, we envisioned that the strict elimination of water from the reaction might inhibit the hydrolysis and increase the yield of the β -acetoxylation. Indeed, when we increase the percentage of acetic anhydride in the mixed solvent, the aldehyde formation could be contained to near 10% (entry 3). We also observed that the addition of external aldehyde (**6.17**) contributed to the reaction (entry 4), probably because it might react with the hydrazine from the hydrolysis to give back the starting material.

Table 6.2 Inhibition of Aldehyde Formation from Hydrolysis



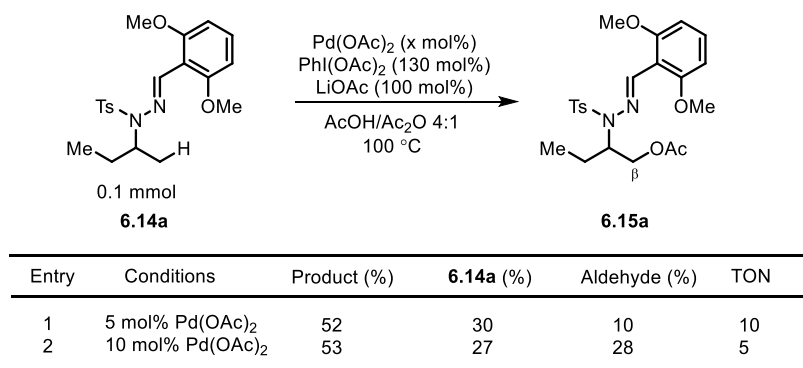
Entry	Conditions	Product (%)	6.14a (%)	Aldehyde (%)
1	AcOH/H ₂ O 50:1	0	0	77
2	AcOH/Ac ₂ O 9:1	47	23	20
3	AcOH/Ac ₂ O 4:1	51	27	11
4	AcOH/Ac ₂ O 4:1 + ArCHO (7.17 , 20 mol%)	53	27	28

Besides these improvements, we also discovered that a lower reaction temperature (Table 6.3, entry 2), or a more dilute concentration (entry 5) could further increase the efficiency of the acetoxylation reaction. We postulated that the low temperature of the reaction may slow down the decomposition of (diacetoxyiodo)benzene and the dilute concentration of the reaction may elongate the catalyst life time.

Table 6.3 Effects of Reaction Temperature and Concentration

Entry	Conditions	Product (%)	6.14a (%)	Aldehyde (%)
1	as above	53	27	28
2	90 °C	51	24	11
3	110 °C	48	25	18
4	AcOH (200 μL)/Ac ₂ O (50 μL)	46	28	9
5	AcOH (800 μL)/Ac ₂ O (200 μL)	58	20	18

Another interesting finding during the optimization is that when only 5 mol% of the palladium catalyst was used under the reaction conditions, 52% yield could be reached (Table 6.4, entry 1). Compared with the reaction with 10 mol% of catalyst (entry 2), while the yield are similar, the turnover number of the catalyst is much higher. This observation indicated that higher concentration of the catalyst may not be desired for the reaction, probably due to the faster decomposition. On the other hand, portionwise addition of 10 mol% palladium catalyst may be beneficial, as it keeps the palladium concentration low to disfavor decomposition; meanwhile a higher conversion could be accessed because of the overall larger amount of the catalyst. In addition, portionwise addition of (diacetoxyiodo)benzene should also benefit the reaction, as it decomposes under the reaction as well.

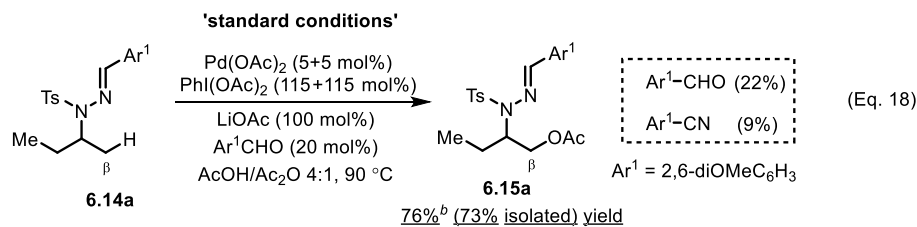
Table 6.4 Comparison between Low and High Loading of Palladium Catalyst

Eventually, when we combined all the improvements we have discovered during the reaction optimization and further increase the overall amount of oxidant, we were glad to find the desired product could be isolated in 73% yield with a 76% NMR yield (Table 6.5, Eq. 18). Under the optimized reaction condition, the hydrolysis of the substrate turned out to be minimal, and the aryl nitrile byproduct from the elimination was isolated in 9% yield.

To understand the role of each reactant, control experiments were conducted (Table 6.5). As expected, palladium played a pivotal role in this reaction (entry 1). While 230 mol% of PhI(OAc)_2 proved to be optimal, the yield only dropped marginally with 130 mol% of the oxidant (entry 2). On the other hand, other common oxidants, including KPS and NFSI, were less effective (entries 3-5). Acetate additives were found to facilitate the acetoxylation (entries 6-9). As discussed before (*vide supra*, Table 6.2), aldehyde **6.17** and nitrile **6.16** were identified as the major by-products, presumably from the hydrolysis and elimination of the DG, which was supported by the detrimental effect of added water (entry 12). Thus, additional **6.17** and Ac_2O were intentionally employed to suppress hydrolysis of the hydrazone DG, as the extra aldehyde would disfavour the hydrolysis equilibrium, whereas Ac_2O can remove adventitious water.

However, the use of molecular sieve as desiccant instead of **6.17** and Ac₂O was ineffective (entry 13). Finally, DCE can be used as a co-solvent (entry 14), and the ‘one-portion addition’ procedure slightly decreased the yield (entry 15).

Table 6.5 Control Experiments^a

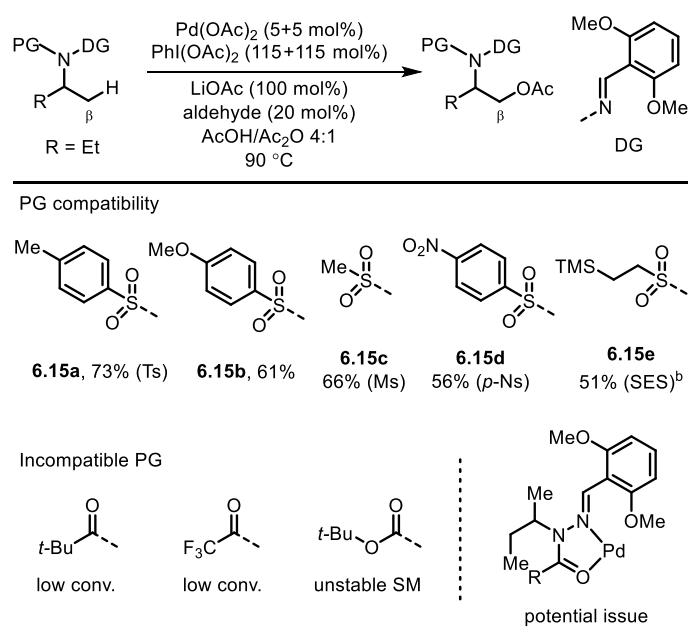


entry	variations from the 'standard conditions'	Yield ^b (%)	Conv. ^b (%)
1	w/o Pd(OAc) ₂	--	10
2	130 mol% instead of 230 mol% PhI(OAc) ₂	64	85
3	NFSI instead of PhI(OAc) ₂	23	86
4	KPS instead of PhI(OAc) ₂	26	100
5	200 mol% KPS and 20 mol% PhI(OAc) ₂ instead of PhI(OAc) ₂	24	100
6	w/o LiOAc	42	100
7	LiCl instead of LiOAc	39	84
8	NaOAc instead of LiOAc	69	100
9	KOAc instead of LiOAc	68	100
10	w/o Ar ¹ CHO ^c	64	100
11	w/o Ac ₂ O	38	93
12	H ₂ O instead of Ac ₂ O	--	100
13	100 mg 4Å MS instead of Ar ¹ CHO and Ac ₂ O ^d	70	90
14	DCE:AcOH:Ac ₂ O 4:4:1 instead of AcOH:Ac ₂ O	70	90
15	one portion addition of Pd(OAc) ₂ and oxidant	66	100

^aThe reactions were run on a 0.1 mmol scale in 1.0 mL solvent. ^bNMR yields determined using 1,1,1,2-tetrachloroethane as the internal standard. ^cAr¹CHO was recovered in 11% yield when no extra Ar¹CHO was added. ^da mixed solvent of DCE and AcOH (1:1) was used.

The optimized conditions were then employed to examine the scope of the β -acetoxylation reaction (Table 6.6). We found a wide panel of sulfonyl protecting groups is compatible with the β -oxidation protocol (**6.15a-e**), including nosyl (**6.15d**) and SES²¹ (**6.15e**) groups that are known to be readily removed under mild conditions. Nevertheless, substrates with amide or carbamate PGs gave low conversion, probably due to complexation of the carbonyl to the Pd catalyst that inhibits the cyclometallation step.

Table 6.6 Compatibility of Different Protecting Groups^a

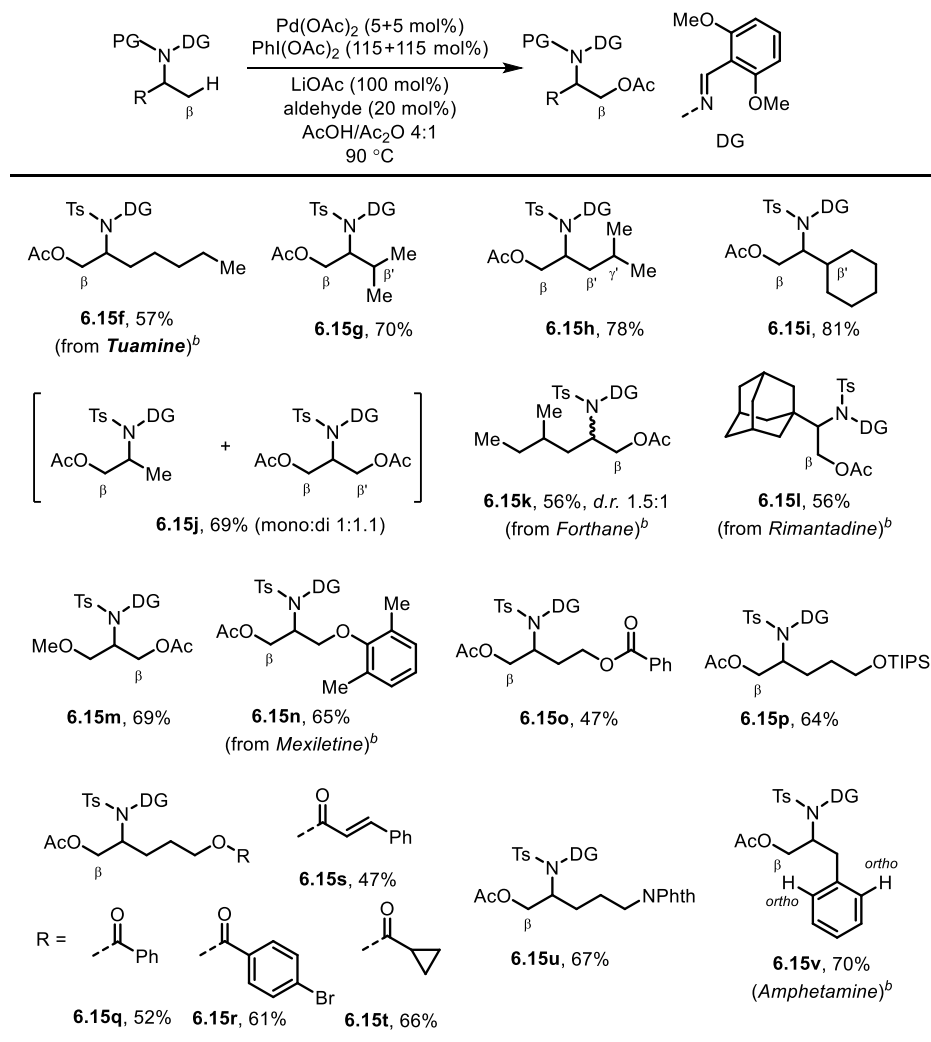


^aThe reactions were run on a 0.15 mmol scale. ^b400 mol% PhI(OAc)₂ was used.

Substrates with various alkyl scaffolds (Table 6.7, **6.15f-6.15k**) afforded the desired acetoxylation products in good yields. Branching at β' or γ' positions did not affect the reactivity, in which the oxidation occurred site-selectively at the less sterically hindered primary β position. The amine substrates can be directly derived from a number of approved drugs, such as Rimantidine (**6.15l**), Forthane (**6.15k**), Mexiletine (**6.15n**), and Amphetamine (**6.15v**), in simple

operations without chromatography. In particular, the hydrazone derived from Rimantidine that contains an adjacent and sterically demanding adamantyl group also smoothly gave the product (**6.15l**). Slower reactions were observed for substrates with adjacent coordinating groups, e.g. esters (**6.15o**) and ethers (**6.15m** and **6.15n**); nevertheless, moderate to good yields were obtained after an elongated reaction time. Several common and versatile functional groups, including cyclopropane (**6.15t**), aryl bromide (**6.15r**), electron-deficient olefin (**6.15s**), phthalimide (**6.15u**) and silyl ether (**6.15p**), were also tolerated. It is worth noting that, for the Amphetamine-derived substrate (**6.15v**), the C(*sp*³)-H bond was selectively acetoxyated over the more reactive *ortho*-aryl C-H bond, which represents a distinct feature from the amide- and oxime-directed reactions.²²

Table 6.7 Substrate Scope^a

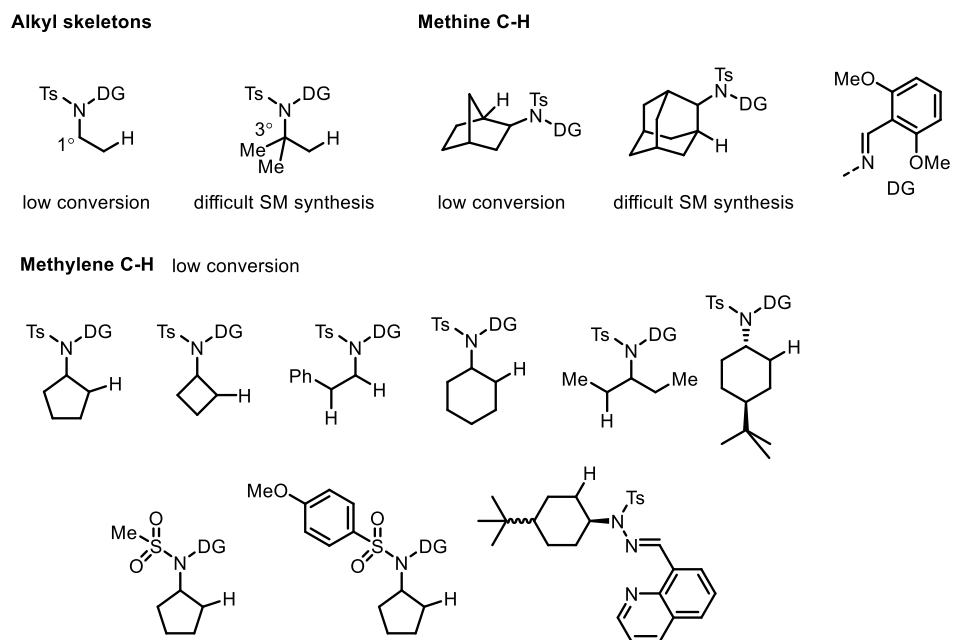


^aThe reactions were run on a 0.15 mmol scale. ^bDrug from which the substrate was directly derived from.

The limitation of this β -acetoxylation protocol was also probed (Figure 6.4). For the alkyl skeletons, both examples of amine with primary and tertiary carbon attached failed, due to low conversion and difficulty of substrate synthesis, respectively. Attempts to activate methine C–H bonds were also unsuccessful. For the challenging methylene C–H activation, a wide range of alkyl skeletons was tested and the major issue turned out to be the low or no conversion. Either elevating the reaction temperature or addition of various additives failed to solve the problem.

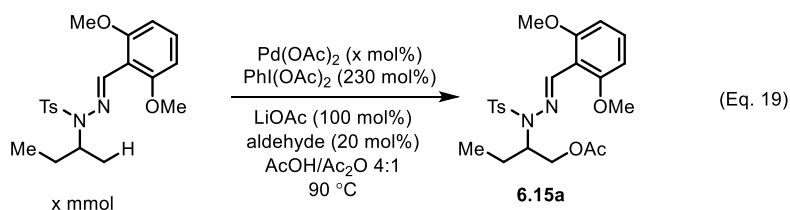
We also attempt to switch to different protecting groups and directing groups, but few positive results were obtained.

Figure 6.4 Selected Unsuccessful Substrates



We were delighted to find the acetoxylation reaction can be scaled up with a reduced amount of palladium catalyst (Scheme 6.15, Eq. 19). Especially, gram-scale syntheses of **6.15a** can be promoted using as little as 2 mol% of Pd(OAc)₂ catalyst, without significant decrease in yield.

Scheme 6.15 Scaled up β -Acetoxylation Reaction

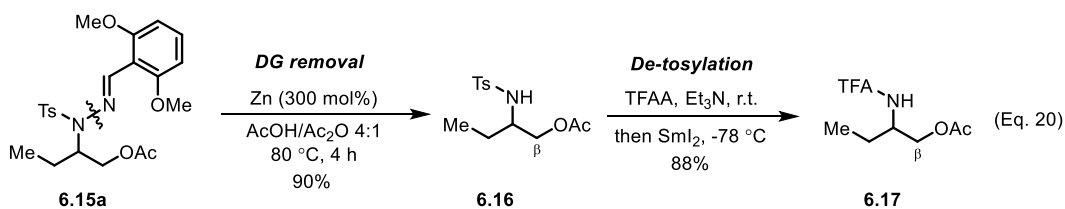


1 mmol (5 mol% Pd)	72%, 320 mg
4 mmol (5 mol% Pd)	71%, <u>1.27 g</u>
4 mmol (<u>2 mol% Pd</u>)	56%, <u>1.01 g</u>

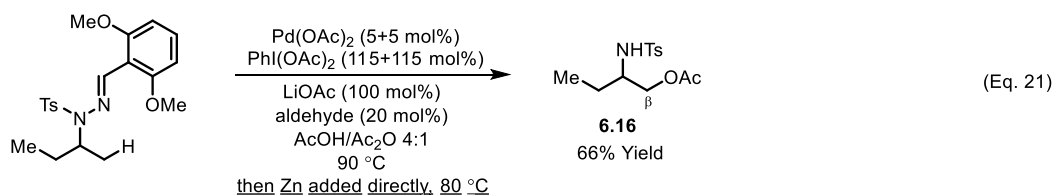
The hydrazone-based directing group can be efficiently removed to give β -acetoxy protected amine **6.16** through the cleavage of N–N bond with zinc powder (Scheme 6.16). This cleavage was compatible with the acidic medium of β -acetoxylation. Thus, a convenient one-pot acetoxylation/directing group removal sequence was accomplished, simply by adding zinc to the reaction mixture after the completion of acetoxylation (Eq. 21). Furthermore, the tosyl-protected primary amine in **6.16** could be further modified through the conversion to trifluoroacetamide **6.17**, where the tosyl protecting group was removed with SmI_2 under mild conditions.²³

Scheme 6.16 Removal of Protecting and Directing Group

A. DG and PG removal

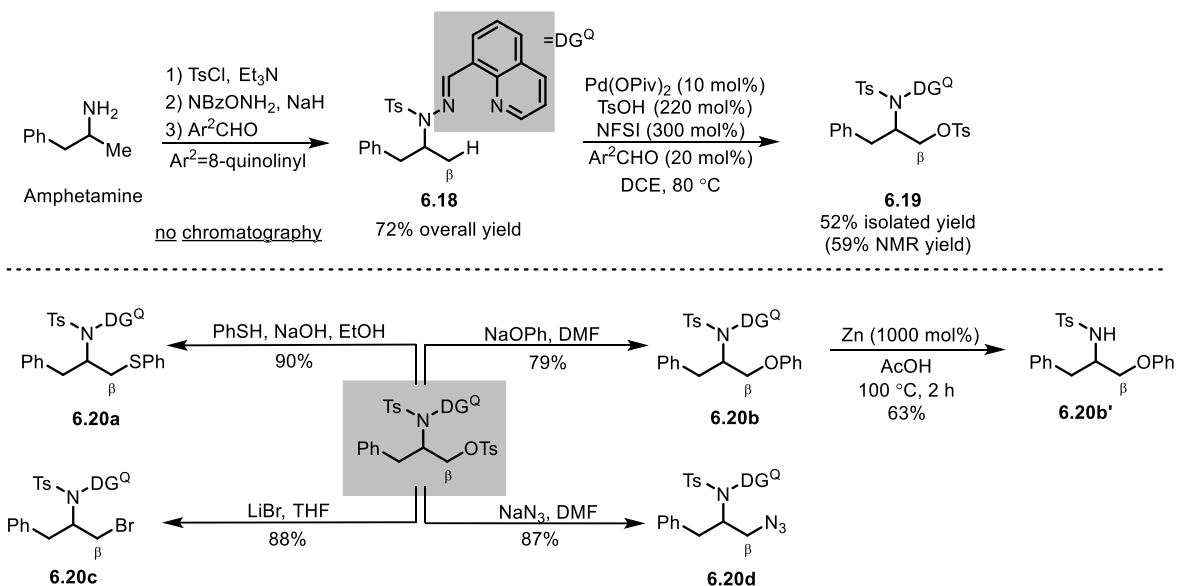


B. One-pot acetoxylation/DG removal



More recently, a $\beta\text{-C}(sp^3)\text{-H}$ sulfonyloxylation/ S_N2 approach was developed for the diverse functionalization of masked alcohols.¹⁵ Thus, it was expected that a similar strategy could be adopted for late-stage diversification of aliphatic amines using a hydrazone-based directing group, which in turn should expedite analogue preparation. Indeed, starting with Amphetamine, a chromatography-free three-step sequence afforded hydrazone **6.18** in 72% yield, wherein a quinoline-based directing group (DG^Q) was employed (Scheme 6.17). After a slight modification of the previously reported sulfonyloxylation conditions, the desired β -tosyloxylation product (**6.19**) was isolated in 52% yield. As expected, sulfonate **6.19** can be rapidly derivatized via S_N2 reactions to introduce various FGs, including sulfide, ether, bromide, and azide (**6.20a-d**) at the terminal position. Moreover, the quinoline-based directing group can also be removed smoothly with zinc in acetic acid.

Scheme 6.17 A β -tosyloxylation Strategy to Access Amphetamine Derivatives

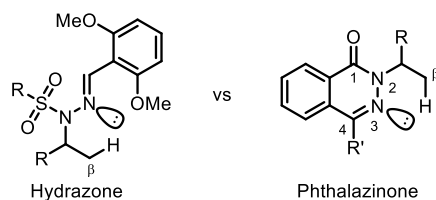


Despite the success of this β -oxidation strategy, we are fully aware of the limitation of the current protocol. First, to access the substrate of β -oxidation, the protecting group and directing group have to be installed separately through a three-step sequence. Second, the palladium-catalyzed β -oxidation reaction is limited to primary amines with a secondary carbon. Third, only primary methyl C–H bonds can be activated. In addition, the necessity of using sulfonamide protecting groups diminishes the synthetic utility of the method, since sulfonamide protecting groups are often hard to remove. Considering all these limitation above, we aimed to developing a new type of directing group that can address these issues.

We focus our attention on the structure of phthalazinone, a bicyclic aromatic heterocycle (Figure 6.5). In the six-membered aromatic ring system of phthalazinone, the N2 offers its lone pair for the aromaticity and can be seen as protected as the amide form. On the other hand, N3

and C4 participate in the π -system with a π bond. Thus, the remaining lone pair of N3 can act as a Lewis base and coordinate with transition metal through the lone pair.

Figure 6.5 Comparison between Hydrazone and Phthalazinone



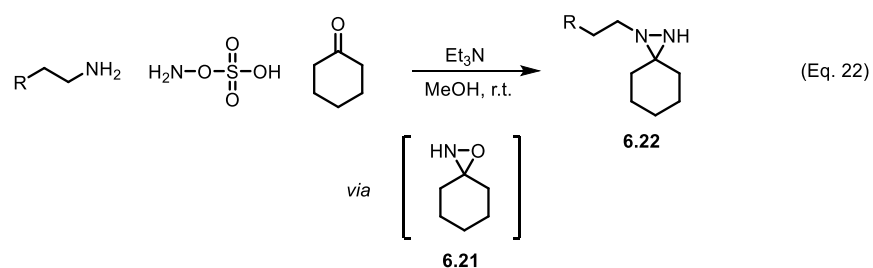
Compared to the structure of hydrazone-based directing group, the C1 carbonyl can be viewed as a protecting group for the N2, preventing it from complexing with metal catalyst. The N3, on other hand, could direct the transition metal to site-selectively activate the β -C–H bond of the alkyl chain on N2. A advantageous feature of phthalazinone, compared with hydrazone, is that the ‘protecting group’ and ‘directing group’ are incorporated in a single aromatic heterocycle. And due to the aromaticity, common side reaction for hydrazone, such as elimination and hydrolysis, would be hard to proceed for the phthalazinone-based directing group, which should in turn result in a higher efficiency for the β -functionalization reaction.

Nevertheless, an important issue of the phthalazinone-based directing group is its convenient synthesis from alkyl amine. We have successfully developed a two-step synthesis for the hydrazine synthesis from alkyl amine and subsequent condensation between the hydrazine and methyl 2-formylbenzoate to give the phthalazinone ring (Scheme 6.18). In the step of hydrazine synthesis, the hydroxylamine-*O*-sulfonic acid is proposed to react with cyclohexanone to give an oxaziridine intermediate **6.21** (Eq. 22).²⁴ Subsequently, alkyl amine reacts with the electrophilic oxaziridine to give diaziridine **6.22** as a hydrazine equivalent. In the second step,

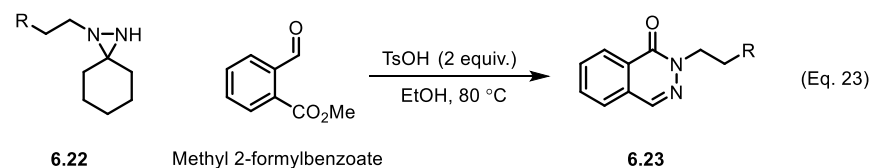
with stoichiometric amount of strong acid, the diaziridine would readily cyclize with methyl 2-formylbenzoate to give the phthalazinone **6.23** (Eq. 23).

Scheme 6.16 Synthesis of Phthalazinones from Alkyl Amines

Step 1: synthesis of hydrazone equivalent

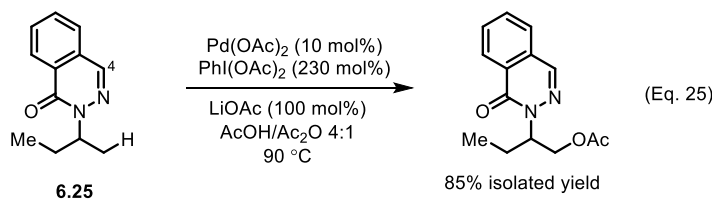
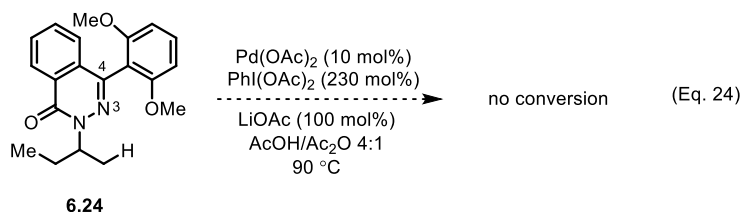


Step 2: Condensation



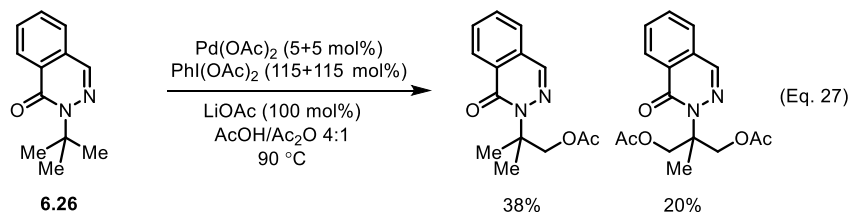
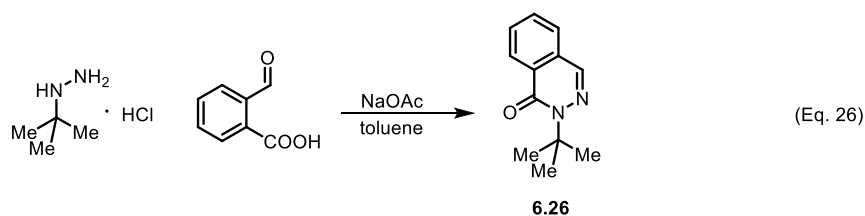
To test our hypothesis for the β -functionalization, we first synthesized phthalazinone **6.24** containing a 2,6-dimethoxybenzene moiety (Scheme 6.17). However, once submitted to the optimized acetoxylation conditions, no conversion was observed for the substrate (Eq. 24). We proposed that the inertness of **6.24** may result from the steric hindrance around N3 imposed by the 2,6-dimethoxybenzene moiety. Thus, phthalazinone substrate **6.25** without C4 substituents was synthesized and submitted to the acetoxylation reaction. To our delight, the acetoxylation proceeded in high efficiency and afforded the product in 85% yield (Eq. 25). The high efficiency is probably due to the enhanced stability of the directing group compared with previous hydrazone substrate, which may inhibit the possible side reactions such as elimination to nitrile and hydrolysis to aldehyde.

Scheme 6.17 β -Acetoxylation Using Phthalazinone-based Directing Group



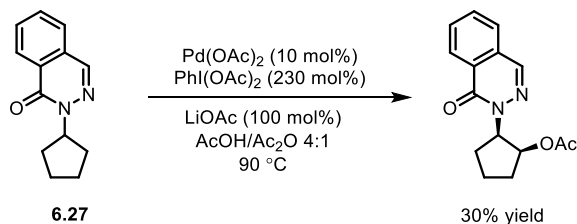
To further test the capability of this template, we synthesized the phthalazinone **6.26** with a *tert*-butyl alkyl chain, a challenging substrate to access using our previous strategy (*vide supra*, Scheme 6.13) probably due to the sterics of the Ts protecting group. The reaction between *tert*-butyl hydrazine and phthalaldehydic acid proceeded smoothly to give **6.26** (Scheme 6.18, Eq. 26). And the acetoxylation of **6.26** under previously optimized conditions gave both mono- and di-acetoxylation products in good yields (Eq. 27).

Scheme 6.18 β -Acetoxylation of *tert*-Butyl Substituted Phthalazinone



We also tested the reactivity of methylene C–H activation using this new template. To our surprise, the reaction of phthalazinone substrate with a cyclopentyl group (**6.27**) gave the methylene C–H acetoxylation product in 30% yield as a single *cis* diastereomer.

Scheme 6.19 β -Acetoxylation of Cyclopentyl Substituted Phthalazinone



6.3 Conclusion

In summary, a hydrazone-based directing group strategy is developed to realize the β -C–H functionalization of aliphatic amines. A number of key features can be noted: first, from common primary amines, an efficient ‘chromatography-free’ or ‘one-pot’ procedure were made available to install the directing group; second, through forming a hydrazone-directed *exo*-palladacycle, the β -C–H oxidation occurred site- and chemoselectively; finally, the directing groups can be easily removed either in a separate step or through a one-pot acetoxylation/reduction sequence. Considering the critical role of nitrogen-containing aliphatics in pharmaceutical and agrochemical research, this hydrazone-based approach should offer new strategies to synthesize functionalized amines. A phthalazinone-based directing group strategy has also been briefly investigated. Compared with hydrazone-based directing groups, the new strategy demonstrated a broader scope for the β -acetoxylation reaction. Especially, it enables the

functionalization of β -methylene C–H bonds. Studies to improve the β -oxidation reaction of aliphatic amines based on the phthalizinone directin group, as well as extend the strategy to introduce other functional groups at the β positions, such as C–C bond and C–X (X: halogen) formation, are currently underway in our lab.

6.4 Experimental

Unless stated otherwise, all reactions were run under air atmosphere and solvents were used as received. Tetrahydrofuran (THF) were distilled from Na prior to use. 1,2-Dichloroethane (DCE) and dimethylformamide (DMF) were distilled from CaH₂. Palladium acetate and palladium pivalate were obtained from Johnson Matthey and used without purification. Iodobenzene diacetate, lithium acetate, 2,6-dimethoxybenzaldehyde, 8-formyl quinoline, anhydrous *p*-toluenesulfonic acid and other reagents were purchased from commercial vendors and used without further purification unless stated otherwise. Thin layer chromatography (TLC) was run on silica gel plates purchased from EMD Chemical (silica gel 60, F254). ¹H NMR and ¹³C NMR spectra were obtained on a Varian Gemini (400 MHz for ¹H, 100 MHz for ¹³C, 376 MHz for ¹⁹F). Chemical shifts are reported as parts per million (ppm) with residual solvent signals as internal standard (CHCl₃, δ = 7.26 ppm for ¹H NMR, δ = 77.00 ppm for ¹³C NMR). Data for ¹H NMR were presented as following: chemical shifts (δ, ppm), multiplicity (br = broad, s = singlet, d = doublet, t = triplet, q = quartet, dd = doublet of doublets, tt = triplet of triplets, td = triplet of doublets, m = multiplet), coupling constant (Hz), and integration. Mass spectra were recorded on an Autospec or Agilent 6150. Accurate masses from high-resolution mass spectra were reported for the molecular ion [M+Na]⁺, [M]⁺ or [M+H]⁺. Infrared (IR) spectra were obtained from a Nicolet iS5 FTIR spectrometer and the data presented as per centimeter (cm⁻¹).

General procedure for reaction condition screening

Reactions for condition screening were run on 0.10 mmol scale (0.10 M) based on the substrate. All reactions were carried out in vials sealed with PTFE lined caps, purchased from Qorpak. To a 4-mL vial were added palladium salt, oxidant, additives, hydrazone substrate, and solvents. The vial was sealed and heated in a pie-block at 90 °C under stirring. The conversion was monitored by TLC analysis of aliquots. For protocols with portionwise addition, the vial was removed from the pie-block and allowed to cool to room temperature. A new portion of palladium catalyst and oxidant was then added and the vial was sealed again and heated. The completion of the acetoxylation reaction was marked by either the full conversion of hydrazone or appearance of palladium black. The vial was removed from the heat and allowed to cool to room temperature. The reaction mixture was diluted with 1 mL diethyl ether and passed through a small plug of silica gel, eluted with diethyl ether. The solvent was removed under vacuo (the removal of acetic anhydride requires higher temperature or vacuum). 1,1,2,2-Tetrachloroethane (~7 mg) was added as the internal standard and the sample was submitted for NMR analysis.

General procedure for the ‘one-pot’ protection/amination/condensation sequence

To a round bottom flask were added *sec*-butylamine (73 mg, 1.0 equiv. 1.0 mmol), triethylamine (202 mg, 2.0 equiv.), and 25 mL dry DMF. *p*-Toluenesulfonyl chloride (191 mg, 1.0 equiv.) was added to the flask portionwise. The resulting solution was stirred at room temperature and monitored by TLC. After the *p*-Toluenesulfonyl chloride was fully consumed, NaH (60%, 120 mg, 3.0 equiv.) was added to the mixture at room temperature portionwise.

When the gas ceased to evolve, NBzONH₂ (200 mg, 1.1 equiv.) was added to the suspension portionwise at room temperature. The mixture became dark when NBzONH₂ was first added and gradually turned orange along the amination. After 30 min, 2,6-dimethoxybenzaldehyde (166 mg, 1.0 equiv.) was added to the flask in one portion, followed by 5 mL AcOH. The reaction mixture turned yellow once AcOH was added, and the mixture was stirred at room temperature for 1 hr, monitored by TLC.

The reaction mixture was poured into 100 mL water and extracted with diethyl ether (5×30 mL). The combined ether layer was washed with saturated NaHCO₃ solution (2×50 mL), water (2×50 mL), and brine (50 mL). The organics were dried with MgSO₄ and concentrated under vacuum to a yellow oil. Flash column chromatography (hexane/EtOAc 20:1 to 2:1) of the residue gave **6.14a** as a white solid (304 mg, 78% yield).

General procedure for the ‘chromatography-free’ amination/condensation sequence

Protection: A round bottom flask was charged with aliphatic amine (1.0 equiv.) or amine hydrochloride, triethylamine (2.0 equiv. or 3.0 equiv. if amine hydrochloride was used) and DCM (0.2 M). The mixture was cooled to 0°C with an ice bath and sulfonyl chloride (1.0 equiv.) was added portionwise/dropwise. The reaction mixture was allowed to warm to room temperature and monitored with TLC. Upon the completion of sulfonylation, 1N HCl was added and the mixture stirred for 5 min. The organic layer was separated and aqueous extracted with DCM. The organics were combined, washed with water and brine, dried with MgSO₄, and

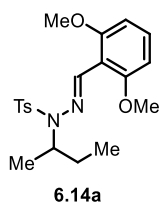
filtered. The solvent was removed in vacuo to give mono-protected amine, which was used for the following step without further purification.

Amination: A round bottom flask was charged with NaH (60%, 1.2 equiv.) and dry DMF (0.1 M). To this stirring mixture was added protected amine portionwise. The mixture was stirred at room temperature until the gas ceases to evolve. Subsequently, NBzONH₂ (1.1 equiv.) was added to the mixture portionwise under stirring at room temperature. The reaction mixture turned dark when NBzONH₂ was added, and gradually changed to orange during the amination. The thickening of the reaction to a gel was also observed. After the addition, the reaction was further stirred at room temperature for 15 min. The mixture was poured into water and extracted with diethyl ether for 3 times. The organics were combined and washed with water (to remove residual DMF) and brine, dried and concentrated to give the crude hydrazine. The hydrazine was directly used for the condensation without further purification.

Note: 1) In most cases, hydrazine has almost the same R_f as the mono-protected amine. However, hydrazines have obvious blue stains with PMA upon heating. 2) The hydrazine intermediate gradually decomposes under air at room temperature. Expedient work-up is recommended.

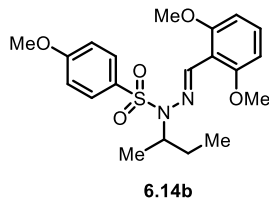
Condensation: Hydrazine (1.0 equiv.) was dissolved in MeOH (1.0 M) under stirring at room temperature. To this mixture was added 2,6-dimethoxybenzaldehyde (1.0 equiv.) in one portion. Catalytic acetic acid (5-10%) was added to the mixture. The reaction was stirred at room temperature and monitored by TLC. In most cases, white precipitation was observed and the reaction mixture solidified upon completion of the condensation. The resulting solid was filtered,

washed with mixed solvent (hexane/EtOAc 10:1), and dried to give the hydrazone substrate in its pure form. When the product is an oil and the precipitation didn't occur, the mixture was concentrated under vacuum. Subsequent flash chromatography of the residue (hexane/EtOAc) afforded the hydrazone substrate.



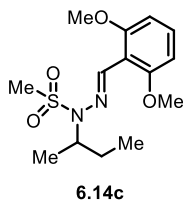
(E)-N-(*sec*-butyl)-N'-(2,6-dimethoxybenzylidene)-4-methylbenzenesulfonylhydrazone

(6.14a): Synthesized from *sec*-butyl amine and *p*-toluenesulfonyl chloride following the general procedure (75% yield over three steps). White solid. Mp. 116-119 °C. $R_f = 0.7$ (hexane/EtOAc 1:1). **$^1\text{H NMR}$** (400 MHz, CDCl_3) δ 8.83 (s, 1H), 7.86-7.83 (m, 2H), 7.32-7.26 (m, 3H), 6.57 (d, $J = 8.4$ Hz, 2H), 4.19-4.11 (m, 1H), 3.84 (s, 6H), 2.41 (s, 3H), 1.61-1.38 (m, 2H), 0.93 (t, $J = 7.4$ Hz, 3H), 0.92 (d, $J = 6.6$ Hz, 3H). **$^{13}\text{C NMR}$** (100 MHz, CDCl_3) δ 159.72, 157.69, 143.19, 136.85, 131.94, 129.14, 128.27, 111.65, 104.19, 58.43, 56.09, 28.65, 21.57, 16.68, 11.02. **IR** (KBr, cm^{-1}) 2966, 1596, 1472, 1257, 1113, 779. **HRMS** calcd $\text{C}_{20}\text{H}_{26}\text{N}_2\text{O}_4\text{SNa}^+$ $[\text{M}+\text{Na}]^+$: 413.15050. Found: 413.15120.



(E)-N-(sec-butyl)-N'-(2,6-dimethoxybenzylidene)-4-

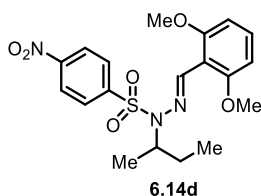
methoxybenzenesulfonylhydrazide (6.14b): Synthesized from *sec*-butyl amine and *p*-methoxybenzenesulfonyl chloride following the general procedure (72% yield over three steps). White solid. Mp. 104-106 °C. $R_f = 0.7$ (hexane/EtOAc 1:1). **$^1\text{H NMR}$** (400 MHz, CDCl_3) δ 8.82 (s, 1H), 7.91-7.87 (m, 2H), 7.30 (t, $J = 8.4$ Hz, 1H), 6.96-6.92 (m, 2H), 6.57 (d, $J = 8.4$ Hz, 2H), 4.18-4.10 (m, 1H), 3.86 (s, 3H), 3.84 (s, 6H), 1.61-1.38 (m, 2H), 0.94-0.91 (m, 6H). **$^{13}\text{C NMR}$** (100 MHz, CDCl_3) δ 162.81, 159.65, 157.62, 131.74, 131.56, 130.33, 113.67, 111.79, 104.22, 58.39, 56.09, 55.51, 28.69, 16.70, 11.06. **IR** (KBr, cm^{-1}) 2971, 1596, 1472, 1259, 1066, 750. **HRMS** calcd $\text{C}_{20}\text{H}_{26}\text{N}_2\text{O}_5\text{SNa}^+$ $[\text{M}+\text{Na}]^+$: 429.14550. Found: 429.14590.



(E)-N-(sec-butyl)-N'-(2,6-dimethoxybenzylidene)methanesulfonylhydrazide (6.14c):

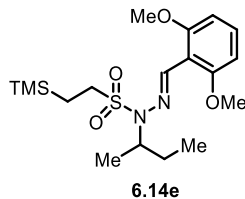
Synthesized from *sec*-butyl amine and methanesulfonyl chloride following the general procedure (64% yield over three steps). Colorless oil. $R_f = 0.7$ (hexane/EtOAc 1:1). **$^1\text{H NMR}$** (400 MHz, CDCl_3) δ 8.70 (s, 1H), 7.31 (t, $J = 8.4$ Hz, 1H), 6.57 (d, $J = 8.4$ Hz, 2H), 4.22-4.13 (m, 1H), 3.84

(s, 6H), 3.01 (s, 3H), 1.79-1.68 (m, 1H), 1.62-1.51 (m, 1H), 1.34 (d, $J = 6.7$ Hz, 3H), 0.97 (t, $J = 7.4$ Hz, 3H). ^{13}C NMR (100 MHz, CDCl_3) δ 159.51, 155.92, 131.81, 111.59, 104.15, 57.98, 56.11, 37.59, 28.29, 17.13, 11.13. IR (KBr, cm^{-1}) 2970, 1596, 1473, 1334, 1257, 1113, 743. HRMS calcd $\text{C}_{14}\text{H}_{22}\text{N}_2\text{O}_4\text{SNa}^+$ $[\text{M}+\text{Na}]^+$: 337.11920. Found: 337.11920.

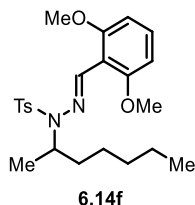


(E)-4-(1-(*sec*-butyl)-2-(2,6-dimethoxybenzylidene)hydrazinyl)-3-

nitrobenzenesulfonic acid (6.14d): Synthesized from *sec*-butyl amine and *p*-nitrobenzenesulfonyl chloride following the general procedure (48% yield over three steps). Yellow solid. Mp. 119-121 °C. $R_f = 0.7$ (hexane/EtOAc 1:1). ^1H NMR (400 MHz, CDCl_3) δ 8.87 (s, 1H), 8.34-8.31 (m, 2H), 8.19-8.16 (m, 2H), 7.36 (t, $J = 8.4$ Hz, 1H), 6.60 (d, $J = 8.4$ Hz, 2H), 4.19-4.11 (m, 1H), 3.87 (s, 6H), 1.56-1.41 (m, 2H), 0.92 (t, $J = 7.3$ Hz, 3H), 0.91 (d, $J = 6.7$ Hz, 3H). ^{13}C NMR (100 MHz, CDCl_3) δ 160.93, 159.87, 145.73, 132.62, 129.53, 123.62, 110.94, 104.16, 58.81, 56.13, 28.51, 16.60, 10.97. IR (KBr, cm^{-1}) 2971, 1597, 1530, 1473, 1349, 1258, 1113, 750. HRMS calcd $\text{C}_{19}\text{H}_{23}\text{N}_3\text{O}_6\text{SNa}^+$ $[\text{M}+\text{Na}]^+$: 444.12000. Found: 444.12030.

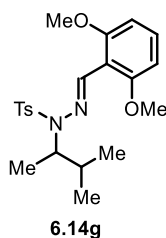


(E)-N-(*sec*-butyl)-N'-(2,6-dimethoxybenzylidene)-2-(trimethylsilyl)ethane-1-sulfonohydrazide (6.14e): Synthesized from *sec*-butyl amine and 2-(Trimethylsilyl)ethanesulfonyl chloride following the general procedure (55% yield over three steps). Colorless oil. $R_f = 0.7$ (hexane/EtOAc 2:1). $^1\text{H NMR}$ (400 MHz, CDCl_3) δ 8.59 (s, 1H), 7.30-7.25 (m, 1H), 6.56 (d, $J = 8.4$, Hz, 2H), 4.29-4.20 (m, 1H), 3.83 (s, 6H), 3.26-3.07 (m, 2H), 1.85-1.74 (m, 1H), 1.66-1.55 (m, 1H), 1.37 (d, $J = 6.7$ Hz, 3H), 1.12-1.07 (m, 2H), 0.98 (t, $J = 7.4$ Hz, 3H), 0.05-0.03 (m, 9H). $^{13}\text{C NMR}$ (100 MHz, CDCl_3) δ 159.29, 149.98, 131.23, 111.91, 104.13, 57.22, 56.08, 47.25, 28.46, 18.11, 11.30, 9.74, -1.98. **IR** (KBr, cm^{-1}) 2955, 1596, 1472, 1334, 1255, 1114, 839. **HRMS** calcd $\text{C}_{18}\text{H}_{33}\text{N}_2\text{O}_4\text{SSi}^+$ $[\text{M}+\text{H}]^+$: 401.19250. Found: 401.19330.

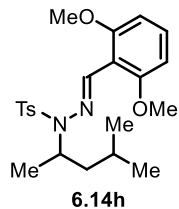


(E)-N'-(2,6-dimethoxybenzylidene)-N-(heptan-2-yl)-4-methylbenzenesulfonohydrazide (6.14f): Synthesized from 2-aminoheptane and *p*-toluenesulfonyl chloride following the general procedure (68% yield over three steps). Light yellow oil. $R_f = 0.7$ (hexane/EtOAc 1:1). $^1\text{H NMR}$ (400 MHz, CDCl_3) δ 8.82 (s, 1H), 7.86-7.83

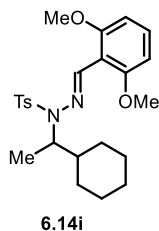
(m, 2H), 7.32-7.26 (m, 3H), 6.57 (d, $J = 8.4$ Hz, 2H), 4.27-4.18 (m, 1H), 3.84 (s, 6H), 2.41 (s, 3H), 1.55-1.46 (m, 1H), 1.42-1.16 (m, 7H), 0.91 (d, $J = 6.6$ Hz, 3H), 0.87 (t, $J = 7.0$ Hz, 3H). ^{13}C NMR (100 MHz, CDCl_3) δ 159.70, 158.10, 143.17, 136.90, 131.90, 129.12, 128.29, 111.67, 104.17, 56.84, 56.06, 35.51, 31.59, 25.95, 22.51, 21.55, 17.00, 14.04. IR (KBr, cm^{-1}) 2932, 1597, 1472, 1257, 1114, 780. HRMS calcd $\text{C}_{23}\text{H}_{32}\text{N}_2\text{O}_4\text{SNa}^+$ $[\text{M}+\text{Na}]^+$: 455.19750. Found: 455.19780.



(E)-N'-(2,6-dimethoxybenzylidene)-4-methyl-N-(3-methylbutan-2-yl)benzenesulfonohydrazide (6.14g): Synthesized from 2-amino-3-methylbutane and *p*-toluenesulfonyl chloride following the general procedure (65% yield over three steps). White solid. Mp. 99-102 °C. $R_f = 0.7$ (hexane/EtOAc 1:1). ^1H NMR (400 MHz, CDCl_3) δ 8.80 (s, 1H), 7.84-7.81 (m, 2H), 7.31-7.25 (m, 3H), 6.57 (d, $J = 8.4$ Hz, 2H), 3.94-3.87 (m, 1H), 3.83 (s, 6H), 2.41 (s, 3H), 1.83-1.71 (m, 1H), 1.02 (d, $J = 6.6$ Hz, 3H), 0.93 (d, $J = 6.7$ Hz, 3H), 0.88 (d, $J = 6.7$ Hz, 3H). ^{13}C NMR (100 MHz, CDCl_3) δ 159.59, 155.55, 143.13, 136.88, 131.55, 129.13, 128.24, 111.96, 104.23, 62.47, 56.08, 33.59, 21.57, 20.20, 19.75, 14.17. IR (KBr, cm^{-1}) 2934, 1597, 1473, 1260, 1115, 750. HRMS calcd $\text{C}_{21}\text{H}_{28}\text{N}_2\text{O}_4\text{SNa}^+$ $[\text{M}+\text{Na}]^+$: 427.16620. Found: 427.16670.

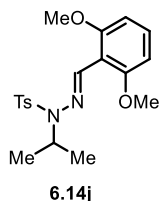


(E)-N'-(2,6-dimethoxybenzylidene)-4-methyl-N-(4-methylpentan-2-yl)benzenesulfonohydrazide (6.14h): Synthesized from 4-amino-2-methylpentane and *p*-toluenesulfonyl chloride following the general procedure (70% yield over three steps). White solid. Mp. 137-140 °C. $R_f = 0.7$ (hexane/EtOAc 1:1). $^1\text{H NMR}$ (400 MHz, CDCl_3) δ 8.83 (s, 1H), 7.87-7.84 (m, 2H), 7.33-7.26 (m, 3H), 6.58 (d, $J = 8.4$ Hz, 2H), 4.39-4.31 (m, 1H), 3.85 (s, 6H), 2.41 (s, 3H), 1.82-1.72 (m, 1H), 1.48 (ddd, $J_1 = 14.1$ Hz, $J_2 = 8.9$ Hz, $J_3 = 5.4$ Hz, 1H), 1.14 (ddd, $J_1 = 14.1$ Hz, $J_2 = 8.4$ Hz, $J_3 = 5.7$ Hz, 1H), 0.95 (d, $J = 6.6$ Hz, 3H), 0.88 (d, $J = 6.7$ Hz, 3H), 0.87 (d, $J = 6.7$ Hz, 3H). $^{13}\text{C NMR}$ (100 MHz, CDCl_3) δ 159.63, 158.80, 143.15, 137.01, 131.79, 129.12, 128.35, 111.78, 104.18, 56.06, 54.66, 44.73, 24.49, 22.93, 22.17, 21.58, 16.91. **IR** (KBr, cm^{-1}) 2937, 1597, 1471, 1257, 1114, 780. **HRMS** calcd $\text{C}_{22}\text{H}_{30}\text{N}_2\text{O}_4\text{SNa}^+$ $[\text{M}+\text{Na}]^+$: 441.18180. Found: 441.18230.



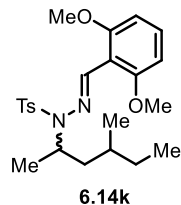
(E)-N-(1-cyclohexylethyl)-N'-(2,6-dimethoxybenzylidene)-4-methylbenzenesulfonohydrazide (6.14i): Synthesized from 1-cyclohexylethylamine and *p*-

toluenesulfonyl chloride following the general procedure (61% yield over three steps). White solid. Mp. 107-110 °C. $R_f = 0.7$ (hexane/EtOAc 1:1). **¹H NMR** (400 MHz, CDCl₃) δ 8.74 (s, 1H), 7.85-7.82 (m, 2H), 7.30-7.25 (m, 3H), 6.57 (d, $J = 8.4$ Hz, 2H), 4.00 (dq, $J_1 = 9.1$ Hz, $J_2 = 6.7$ Hz, 1H), 3.83 (s, 6H), 2.41 (s, 3H), 2.02-1.98 (m, 1H), 1.76-1.73 (m, 3H), 1.63-1.62 (m, 1H), 1.50-1.42 (m, 1H), 1.21-0.95 (m, 5H), 0.89 (d, $J = 6.7$ Hz, 3H). **¹³C NMR** (100 MHz, CDCl₃) δ 159.49, 154.41, 143.10, 136.96, 131.41, 129.12, 128.22, 112.05, 104.23, 61.29, 56.08, 42.69, 30.18, 30.15, 26.43, 26.29, 26.13, 21.57, 14.07. **IR** (KBr, cm⁻¹) 2930, 1596, 1472, 1257, 1114, 751. **HRMS** calcd C₂₄H₃₂N₂O₄SNa⁺ [M+Na]⁺: 467.19750. Found: 467.19770.

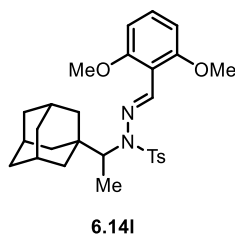


(E)-N'-(2,6-dimethoxybenzylidene)-N-isopropyl-4-methylbenzenesulfonylhydrazide

(6.14j): Synthesized from isopropylamine and *p*-toluenesulfonyl chloride following the general procedure (78% yield over three steps). White solid. Mp. 105-107 °C. $R_f = 0.7$ (hexane/EtOAc 1:1). **¹H NMR** (400 MHz, CDCl₃) δ 8.87 (s, 1H), 7.86-7.83 (m, 2H), 7.34-7.26 (m, 3H), 6.58 (d, $J = 8.5$ Hz, 2H), 4.40 (hept, $J = 6.7$ Hz, 1H), 3.85 (s, 6H), 2.42 (s, 3H), 1.03 (d, $J = 6.7$ Hz, 6H). **¹³C NMR** (100 MHz, CDCl₃) δ 159.74, 159.54, 143.19, 136.56, 131.97, 129.10, 128.35, 111.57, 104.16, 56.05, 52.62, 21.53, 20.22. **IR** (KBr, cm⁻¹) 2976, 1597, 1472, 1257, 1113, 750. **HRMS** calcd C₁₉H₂₄N₂O₄SNa⁺ [M+Na]⁺: 399.13490. Found: 399.13550.

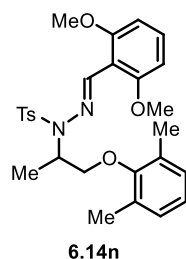


(E)-N'-(2,6-dimethoxybenzylidene)-4-methyl-N-(4-methylhexan-2-yl)benzenesulfonohydrazide (6.14k): Synthesized from Forthane hydrochloride and *p*-toluenesulfonyl chloride following the general procedure (77% yield over three steps, *d.r.* 1.5:1). White solid. Mp. 110-114 °C. $R_f = 0.7$ (hexane/EtOAc 1:1). $^1\text{H NMR}$ (400 MHz, CDCl_3) 8.84 (s, 0.6H), 8.82 (s, 0.4H), 7.87-7.84 (m, 2H), 7.33-7.26 (m, 3H), 6.58 (d, $J = 8.4$ Hz, 2H), 4.40-4.32 (m, 1H), 3.84 (s, 6H), 2.41 (s, 3H), 1.64-0.99 (m, 5H), 0.96 (d, $J = 6.4$ Hz, 1.8H), 0.90 (d, $J = 6.6$ Hz, 1.2H), 0.87-0.82 (m, 6H). $^{13}\text{C NMR}$ (100 MHz, CDCl_3) δ 159.68, 159.63, 158.40, 143.14, 143.11, 137.08, 131.86, 131.75, 129.11, 128.34, 111.72, 104.18, 104.15, 56.05, 56.01, 54.68, 54.32, 42.75, 42.40, 30.78, 30.67, 29.94, 28.94, 21.57, 19.16, 18.98, 16.92, 16.84, 11.35, 11.05. **IR** (KBr, cm^{-1}) 2968, 1597, 1472, 1258, 1114, 750. **HRMS** calcd $\text{C}_{23}\text{H}_{32}\text{N}_2\text{O}_4\text{SNa}^+$ $[\text{M}+\text{Na}]^+$: 455.19750. Found: 455.19780.



N-(1-((3*r*,5*r*,7*r*)-adamantan-1-yl)ethyl)-N'-(*E*)-2,6-dimethoxybenzylidene)-4-methylbenzenesulfonohydrazide (6.14l): Synthesized from Rimantadine hydrochloride and *p*-

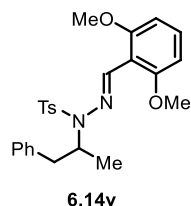
toluenesulfonyl chloride following the general procedure (44% yield over three steps). White solid. Mp. 155-158 °C. $R_f = 0.4$ (hexane/EtOAc 3:1). **$^1\text{H NMR}$** (400 MHz, CDCl_3) δ 9.03 (s, 1H), 7.79-7.76 (m, 2H), 7.32-7.25 (m, 3H), 6.57 (d, $J = 8.4$ Hz, 2H), 3.83 (s, 6H), 3.76 (q, $J = 6.9$ Hz, 1H), 2.41 (s, 3H), 1.97-1.96 (m, 3H), 1.69-1.57 (m, 12H), 0.74 (d, $J = 6.9$ Hz, 3H). **$^{13}\text{C NMR}$** (100 MHz, CDCl_3) δ 159.60, 159.41, 143.15, 136.49, 131.56, 129.15, 128.22, 112.18, 104.21, 64.99, 56.03, 39.26, 37.72, 37.15, 28.66, 21.57, 9.66. **IR** (KBr, cm^{-1}) 2972, 1596, 1471, 1256, 1112, 1066, 751. **HRMS** calcd $\text{C}_{28}\text{H}_{36}\text{N}_2\text{O}_4\text{SNa}^+ [\text{M}+\text{Na}]^+$: 519.22880. Found: 519.22880.



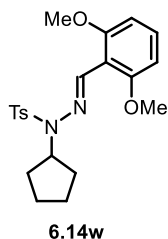
(E)-N'-(2,6-dimethoxybenzylidene)-N-(1-(2,6-dimethylphenoxy)propan-2-yl)-4-methylbenzenesulfonohydrazide (6.14n): Synthesized from Mexiletine hydrochloride and *p*-toluenesulfonyl chloride following the general procedure (78% yield over three steps). White solid. Mp. 144-146 °C. $R_f = 0.8$ (hexane/EtOAc 1:1). **$^1\text{H NMR}$** (400 MHz, CDCl_3) δ 8.92 (s, 1H), 7.90-7.86 (m, 2H), 7.32-7.25 (m, 3H), 6.97-6.94 (m, 2H), 6.88 (dd, $J_1 = 8.3$ Hz, $J_2 = 6.4$ Hz, 1H), 6.56 (d, $J = 8.4$ Hz, 2H), 4.75-4.67 (m, 1H), 3.81 (s, 6H), 3.80 (dd, $J_1 = 9.2$ Hz, $J_2 = 7.0$ Hz, 1H), 3.67 (dd, $J_1 = 9.2$ Hz, $J_2 = 5.8$ Hz, 1H), 2.41 (s, 3H), 2.19 (s, 6H), 1.20 (d, $J = 6.7$ Hz, 3H). **$^{13}\text{C NMR}$** (100 MHz, CDCl_3) δ 159.70, 157.22, 155.49, 143.45, 136.57, 131.86, 130.93, 129.20, 128.66, 128.40, 123.67, 111.58, 104.08, 73.85, 56.42, 55.98, 55.95, 21.56, 16.23, 15.04. **IR** (KBr,

cm⁻¹) 2938, 1597, 1472, 1257, 1114, 779. **HRMS** calcd C₂₇H₃₂N₂O₅SNa⁺ [M+Na]⁺: 519.19240.

Found: 519.19320.

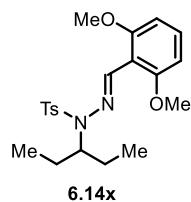


(E)-N'-(2,6-dimethoxybenzylidene)-4-methyl-N-(1-phenylpropan-2-yl)benzenesulfonohydrazide (6.14v): Synthesized from Amphetamine and *p*-toluenesulfonyl chloride following the general procedure (70% yield over three steps). White solid. Mp. 170-173 °C. *R_f* = 0.7 (hexane/EtOAc 1:1). **¹H NMR** (400 MHz, CDCl₃) δ 8.82 (s, 1H), 7.75-7.72 (m, 2H), 7.32 (t, *J* = 8.4 Hz, 1H), 7.28-7.16 (m, 7H), 6.60 (d, *J* = 8.4 Hz, 2H), 4.61-4.52 (m, 1H), 3.87 (s, 6H), 2.88 (dd, *J*₁ = 13.5 Hz, *J*₂ = 6.6 Hz, 1H), 2.68 (dd, *J*₁ = 13.5 Hz, *J*₂ = 8.2 Hz, 1H), 2.39 (s, 3H), 1.04 (d, *J* = 6.6 Hz, 3H). **¹³C NMR** (100 MHz, CDCl₃) δ 159.65, 157.45, 143.27, 139.19, 136.91, 131.80, 129.36, 129.19, 128.26, 128.20, 126.08, 111.76, 104.17, 58.28, 56.05, 41.36, 21.54, 17.36. **IR** (KBr, cm⁻¹) 2938, 1597, 1472, 1257, 1114, 743. **HRMS** calcd C₂₅H₂₈N₂O₄SNa⁺ [M+Na]⁺: 475.16620. Found: 475.16620.



(E)-N-cyclopentyl-N'-(2,6-dimethoxybenzylidene)-4-methylbenzenesulfonohydrazide

(6.14w): Synthesized from cyclopentylamine and *p*-toluenesulfonyl chloride following the general procedure (68% yield over three steps). White solid. Mp. 143-145 °C. $R_f = 0.7$ (hexane/EtOAc 1:1). $^1\text{H NMR}$ (400 MHz, CDCl_3) δ 8.96 (s, 1H), 7.82 (d, $J = 8.2$ Hz, 2H), 7.33 (t, $J = 8.4$ Hz, 1H), 7.28-7.26 (m, 2H), 6.58 (d, $J = 8.4$ Hz, 2H), 4.36-4.28 (m, 1H), 3.85 (s, 6H), 2.42 (s, 3H), 1.62-1.53 (m, 6H), 1.41-1.35 (m, 2H). $^{13}\text{C NMR}$ (100 MHz, CDCl_3) δ 161.74, 159.91, 143.34, 135.51, 132.24, 129.07, 128.69, 111.37, 104.11, 61.88, 56.04, 29.34, 24.24, 21.58. **IR** (KBr, cm^{-1}) 2956, 1597, 1472, 1258, 1115, 913, 743. **HRMS** calcd $\text{C}_{21}\text{H}_{26}\text{N}_2\text{O}_4\text{SNa}^+$ $[\text{M}+\text{Na}]^+$: 425.15050. Found: 425.15060.



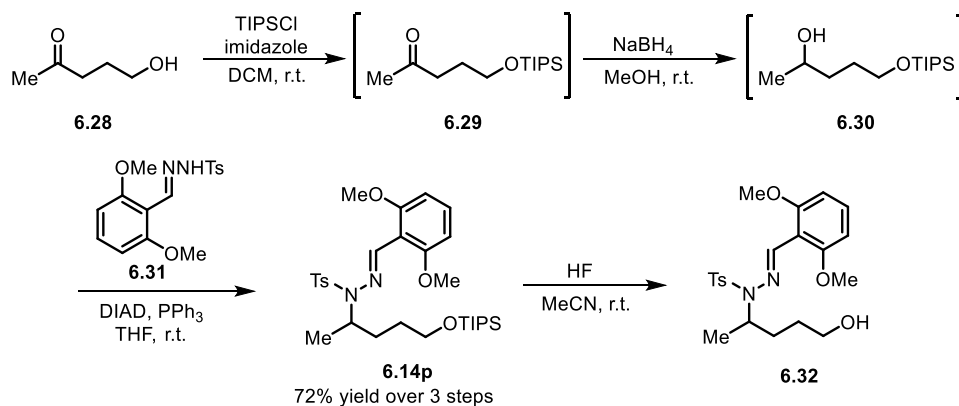
(E)-N'-(2,6-dimethoxybenzylidene)-4-methyl-N-(pentan-3-

yl)benzenesulfonohydrazide (6.14x): Synthesized from 3-pentylamine and *p*-toluenesulfonyl chloride following the general procedure (72% yield over three steps). White solid. Mp. 135-137 °C. $R_f = 0.7$ (hexane/EtOAc 1:1). $^1\text{H NMR}$ (400 MHz, CDCl_3) δ 8.71 (s, 1H), 7.86 (d, $J = 8.3$ Hz, 2H), 7.29-7.25 (m, 3H), 6.55 (d, $J = 8.3$ Hz, 2H), 4.05-3.98 (m, 1H), 3.82 (s, 6H), 2.41 (s, 3H), 1.59-1.44 (m, 4H), 0.86 (t, $J = 7.4$ Hz, 6H). $^{13}\text{C NMR}$ (100 MHz, CDCl_3) δ 159.43, 152.43, 143.12, 137.03, 131.32, 129.03, 128.24, 111.95, 104.16, 64.64, 56.03, 25.44, 21.55, 11.39. **IR**

(KBr, cm^{-1}) 2967, 1597, 1471, 1257, 1114, 913, 747. **HRMS** calcd $\text{C}_{21}\text{H}_{28}\text{N}_2\text{O}_4\text{SNa}^+$ $[\text{M}+\text{Na}]^+$: 427.16620. Found: 427.16630.

General procedure for synthesis of hydrazone substrates used for functional group tolerance test

Scheme 6.20 Substrate Synthesis for Functional Group Tolerance Test



TIPS Protection: To a 250 mL round bottom flask were added 5-hydroxy-2-pentanone (**6.28**, 1.0 equiv., 40 mmol, 4.08 g), imidazole (1.5 equiv., 60 mmol, 4.08 g), and 40 mL DCM. To this reaction mixture was added TIPSCl (1.2 equiv., 48 mmol, 9.26 g) in 20 mL DCM dropwise. The reaction was stirred at room temperature overnight. The reaction was quenched with 50 mL water and stirred for 10 min. The organic layer was separated and the aqueous extracted with DCM (3×30 mL). The combined organics were washed with water and brine, dried, filtered, and concentrated to give **6.29** as a colorless oil (10.01 g, 97% yield). **6.29** was directly used for the next step without further purification.

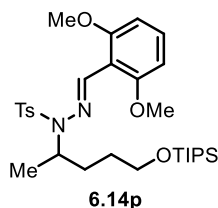
Reduction: To a 500 mL round bottom flask were added **6.29** (1.0 equiv., 33.0 mmol, 8.51 g) and 150 mL MeOH. To this stirring reaction mixture was added NaBH₄ (1.0 equiv., 33.0 mmol, 1.25 g) portionwise. The reaction was stirred at room temperature, monitored by TLC. Upon the completion of the reduction, most methanol was evaporated under vacuum. 50 mL water was added to the residue, followed by 1N HCl to make the solution acidic. The mixture was extracted with Et₂O (3×30 mL). The combined ethereal layer was washed with water and brine, dried, filtered, and concentrated to give **6.30** as a colorless oil (7.29 g, 85% yield). **6.30** was directly used for the next step without further purification.

Synthesis of 6.31: To a 100 mL round bottom flask were added *p*-toluenesulfonyl hydrazide (1.0 equiv., 30 mmol, 5.58 g) and 30 mL toluene. The mixture was heated to 40 °C using an oil bath. Subsequently, 2,6-dimethoxybenzaldehyde (1.0 equiv., 30 mmol, 4.98 g) and a catalytic amount of *p*-toluenesulfonic acid (~10 mg) were added to the suspension. The reaction was heated at the same temperature and monitored by TLC. When the starting materials were fully consumed, the solid in the suspension was filtered, washed with a mixed solvent (hexane/EtOAc 8:1), and dried to give pure **6.31** (10.00 g, quantitative yield).

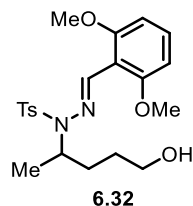
Mitsunobu reaction: A 250 mL round bottom flask was charged with PPh₃ (2.0 equiv., 22.6 mmol, 5.92 g) and 70 mL THF. To this mixture at room temperature was added diisopropyl azodicarboxylate (DIAD, 1.8 equiv., 20.3 mmol, 4.0 mL) dropwise to give an orange solution. The mixture was stirred at room temperature for 20 min (in some cases, the adduct of PPh₃ and DIAD would precipitate out). A solution of **6.30** (1.25 equiv., 14.1 mmol, 3.67 g) and **6.31** (1.0 equiv., 11.3 mmol, 3.77 g) in 50 mL THF was added to the flask dropwise. The resulting mixture was further stirred at room temperature, monitored by TLC. Upon the completion of the reaction,

the solution was concentrated under vacuum. Direct flash column chromatography (hexane/EtOAc 20:1 to 1:1) of the residue gave hydrazone **6.14p** as a colorless oil (5.69 g, 87% yield).

Deprotection: To a 100 mL round bottom flask were added **6.14p** (1.0 equiv., 5.0 mmol, 2.88 g) and 20 mL MeCN. Hydrofluoric acid (48% w/w, 5 mL) was added dropwise to the mixture. The reaction was stirred at room temperature overnight. 25 mL of 1N NaOH was added to quench the reaction and the mixture was extracted with EtOAc (3×30 mL). The combined organics were washed with water and brine, dried, filtered, and concentrated to give **6.32** (2.05 g, 98% yield) as a white solid. **6.32** was used for the next step without further purification.

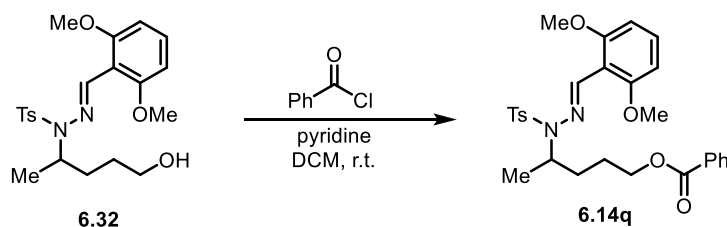


(E)-N'-(2,6-dimethoxybenzylidene)-4-methyl-N-(5-((triisopropylsilyl)oxy)pentan-2-yl)benzenesulfonohydrazide (6.14p): Colorless oil. $R_f = 0.8$ (hexane/EtOAc 1:1). $^1\text{H NMR}$ (400 MHz, CDCl_3) δ 8.83 (s, 1H), 7.85-7.82 (m, 2H), 7.32-7.25 (m, 3H), 6.57 (d, $J = 8.4$ Hz, 2H), 4.29-4.21 (m, 1H), 3.83 (s, 6H), 3.71-3.60 (m, 2H), 2.41 (s, 3H), 1.69-1.49 (m, 4H), 1.09-1.00 (m, 21H), 0.93 (d, $J = 6.6$ Hz, 3H). $^{13}\text{C NMR}$ (100 MHz, CDCl_3) δ 159.69, 158.03, 143.16, 136.90, 131.77, 129.14, 128.30, 111.75, 104.15, 63.09, 56.63, 56.04, 31.94, 29.78, 21.57, 18.01, 17.05, 11.96. **IR** (KBr, cm^{-1}) 2942, 1597, 1471, 1257, 1114, 882. **HRMS** calcd $\text{C}_{30}\text{H}_{48}\text{N}_2\text{O}_5\text{SSiNa}^+$ $[\text{M}+\text{Na}]^+$: 599.29450. Found: 599.29630.



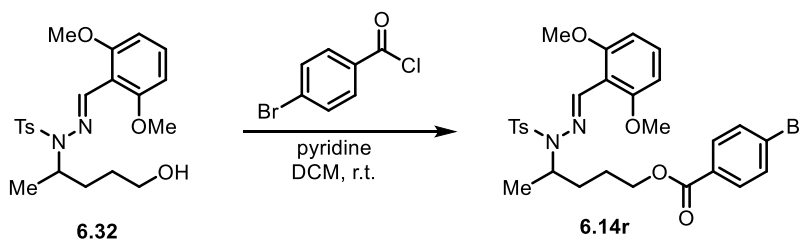
(E)-N'-(2,6-dimethoxybenzylidene)-N-(5-hydroxypentan-2-yl)-4-

methylbenzenesulfonohydrazide (6.32): White solid. Mp. 145-147 °C. $R_f = 0.4$ (hexane/EtOAc 1:1). $^1\text{H NMR}$ (400 MHz, CDCl_3) δ 8.85 (s, 1H), 7.85-7.82 (m, 2H), 7.33-7.27 (m, 3H), 6.57 (d, $J = 8.5$ Hz, 2H), 4.32-4.23 (m, 1H), 3.84 (s, 6H), 3.64 (t, $J = 6.2$ Hz, 2H), 2.42 (s, 3H), 1.71-1.44 (m, 4H), 1.40 (br, 1H), 0.92 (d, $J = 6.6$ Hz, 3H). $^{13}\text{C NMR}$ (100 MHz, CDCl_3) δ 159.70, 158.36, 143.40, 136.65, 132.14, 129.22, 128.25, 111.49, 104.18, 62.61, 56.59, 56.10, 31.69, 29.38, 21.57, 17.19. **IR** (KBr, cm^{-1}) 3546, 2939, 1597, 1472, 1257, 1113, 781. **HRMS** calcd $\text{C}_{21}\text{H}_{28}\text{N}_2\text{O}_5\text{SNa}^+$ $[\text{M}+\text{Na}]^+$: 443.16110. Found: 443.16210.



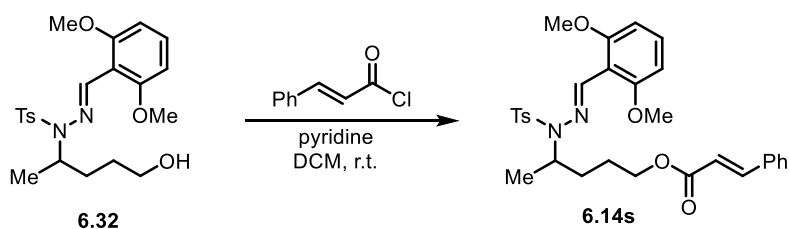
To a 50 mL round bottom flask were added **6.32** (1.0 equiv., 1.0 mmol, 420 mg), pyridine (2.5 equiv., 2.5 mmol, 200 mg), and 10 mL DCM. To this mixture was added benzoyl chloride (1.5 equiv., 1.5 mmol, 0.17 mL) dropwise at room temperature. The reaction was stirred at room temperature for 2 hrs, monitored by TLC. Upon the completion of the acylation reaction, the

reaction mixture was diluted with 20 mL 1N NaOH. The organic layer was separated and the aqueous extracted with DCM (3×20 mL). The combined organics were washed subsequently with 1N HCl (2×20 mL), water, and brine. The resulting solution was dried, filtered, and concentrated. The residue was purified by flash column chromatography (hexane/EtOAc 20:1 to 2:1) to give **6.14q** as a yellow oil (356 mg, 68% yield). $R_f = 0.7$ (hexane/EtOAc 1:1). $^1\text{H NMR}$ (400 MHz, CDCl_3) δ 8.90 (s, 1H), 8.02-7.99 (m, 2H), 7.85-7.82 (m, 2H), 7.55-7.50 (m, 1H), 7.40-7.36 (m, 2H), 7.33-7.25 (m, 3H), 6.56 (d, $J = 8.4$ Hz, 2H), 4.35-4.26 (m, 3H), 3.81 (s, 6H), 2.39 (s, 3H), 2.00-1.79 (m, 2H), 1.73-1.63 (m, 1H), 1.58-1.50 (m, 1H), 0.94 (d, $J = 6.6$ Hz, 3H). $^{13}\text{C NMR}$ (100 MHz, CDCl_3) δ 166.54, 159.64, 158.61, 143.33, 136.67, 132.70, 131.94, 130.32, 129.45, 129.17, 128.20, 111.50, 104.09, 64.76, 56.39, 55.98, 32.02, 25.54, 21.51, 17.00. **IR** (KBr, cm^{-1}) 2941, 1716, 1597, 1472, 1257, 1114, 714. **HRMS** calcd $\text{C}_{28}\text{H}_{32}\text{N}_2\text{O}_6\text{SNa}^+$ $[\text{M}+\text{Na}]^+$: 547.18730. Found: 547.18810.



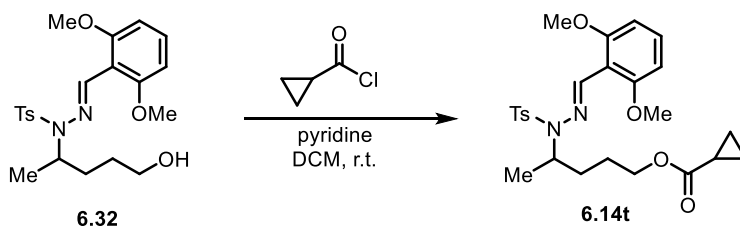
To a 25 mL round bottom flask were added **6.32** (1.0 equiv., 0.7 mmol, 294 mg), pyridine (2.0 equiv., 1.4 mmol, 110 mg), and 7 mL DCM. To this mixture was added *p*-bromobenzoyl chloride (1.4 equiv., 1.0 mmol, 219 mg) portionwise at room temperature. The reaction was stirred at room temperature for 4 hrs, monitored by TLC. Upon the completion of the acylation

reaction, the reaction mixture was diluted with 20 mL 1N NaOH. The organic layer was separated and the aqueous extracted with DCM (3×20 mL). The combined organics were washed subsequently with 1N HCl (2×20 mL), water, and brine. The resulting solution was dried, filtered, and concentrated. The residue was purified by flash column chromatography (hexane/EtOAc 20:1 to 2:1) to give **6.14r** as a colorless oil (329 mg, 78% yield). $R_f = 0.8$ (hexane/EtOAc = 1:1). **$^1\text{H NMR}$** (400 MHz, CDCl_3) δ 8.89 (s, 1H), 7.87-7.81 (m, 4H), 7.52-7.48 (m, 2H), 7.34-7.25 (m, 3H), 6.57 (d, $J = 8.3$ Hz, 2H), 4.32-4.26 (m, 3H), 3.81 (s, 6H), 2.41 (s, 3H), 2.00-1.78 (m, 2H), 1.72-1.62 (m, 1H), 1.59-1.46 (m, 1H), 0.92 (d, $J = 6.6$ Hz, 3H). **$^{13}\text{C NMR}$** (100 MHz, CDCl_3) δ 165.85, 159.68, 158.60, 143.38, 136.73, 131.97, 131.57, 131.05, 129.27, 129.22, 128.25, 127.82, 111.56, 104.14, 65.06, 56.37, 56.03, 32.07, 25.51, 21.58, 17.00. **IR** (KBr, cm^{-1}) 2940, 1719, 1594, 1471, 1257, 1114, 757. **HRMS** calcd $\text{C}_{28}\text{H}_{32}\text{BrN}_2\text{O}_6\text{SNa}^+$ $[\text{M}+\text{H}]^+$: 603.11590. Found: 603.11630.



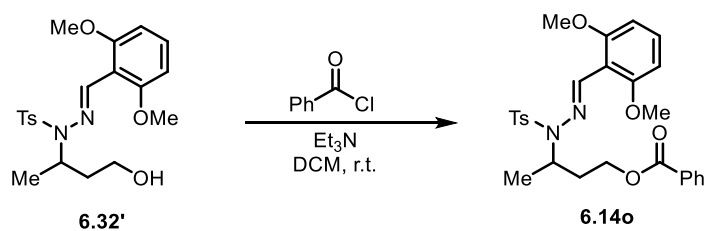
To a 25 mL round bottom flask were added **6.32** (1.0 equiv., 1.0 mmol, 420 mg), pyridine (2.5 equiv., 2.5 mmol, 200 mg), and 10 mL DCM. To this mixture was added cinnamoyl chloride (1.5 equiv., 1.5 mmol, 250 mg) portionwise at room temperature. The reaction was stirred at room temperature for 3 hrs, monitored by TLC. Upon the completion of the acylation reaction, the reaction mixture was diluted with 20 mL 1N NaOH. The organic layer was separated and the

aqueous extracted with DCM (3×20 mL). The combined organics were washed subsequently with 1N HCl (2×20 mL), water, and brine. The resulting solution was dried, filtered, and concentrated. The residue was purified by flash column chromatography (hexane/EtOAc 20:1 to 2:1) to give **6.14s** as a colorless oil (313 mg, 69% yield). $R_f = 0.6$ (hexane/EtOAc = 1:1). $^1\text{H NMR}$ (400 MHz, CDCl_3) δ 8.88 (s, 1H), 7.84-7.81 (m, 2H), 7.64 (d, $J = 16.0$ Hz, 1H), 7.46-7.43 (m, 2H), 7.34-7.30 (m, 3H), 7.28-7.23 (m, 3H), 6.52 (d, $J = 8.5$ Hz, 2H), 6.39 (d, $J = 16.0$ Hz, 1H), 4.32-4.24 (m, 1H), 4.18 (t, $J = 6.5$ Hz, 2H), 3.78 (s, 6H), 2.36 (s, 3H), 1.92-1.72 (m, 2H), 1.67-1.57 (m, 1H), 1.54-1.45 (m, 1H), 0.91 (d, $J = 6.6$ Hz, 3H). $^{13}\text{C NMR}$ (100 MHz, CDCl_3) δ 166.71, 159.42, 158.30, 144.30, 143.19, 136.48, 134.10, 131.81, 130.00, 129.01, 128.62, 128.02, 127.77, 117.93, 111.27, 103.94, 64.14, 56.18, 55.80, 31.82, 25.33, 21.32, 16.79. **IR** (KBr, cm^{-1}) 2941, 1713, 1597, 1472, 1341, 1257, 1114, 733. **HRMS** calcd $\text{C}_{30}\text{H}_{34}\text{N}_2\text{O}_6\text{SNa}^+$ $[\text{M}+\text{Na}]^+$: 573.20300. Found: 573.20350.



To a 25 mL round bottom flask were added **6.32** (1.0 equiv., 1.0 mmol, 420 mg), pyridine (2.5 equiv., 2.5 mmol, 200 mg), and 10 mL DCM. To this mixture was added cyclopropanecarbonyl chloride (1.5 equiv., 1.5 mmol, 157 mg) dropwise at room temperature. The reaction was stirred at room temperature for 3 hrs, monitored by TLC. Upon the completion of the acylation reaction, the reaction mixture was diluted with 20 mL 1N NaOH. The organic

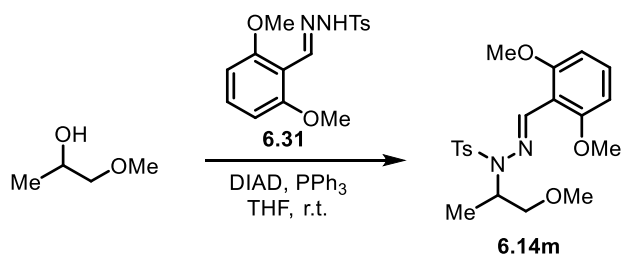
layer was separated and the aqueous extracted with DCM (3×20 mL). The combined organics were washed subsequently with 1N HCl (2×20 mL), water, and brine. The resulting solution was dried, filtered, and concentrated. The residue was purified by flash column chromatography (hexane/EtOAc 20:1 to 2:1) to give **6.14t** as a colorless oil (231 mg, 58% yield). $R_f = 0.7$ (hexane/EtOAc = 1:1). $^1\text{H NMR}$ (400 MHz, CDCl_3) δ 8.86 (s, 1H), 7.84-7.81 (m, 2H), 7.33-7.26 (m, 3H), 6.57 (d, $J = 8.4$ Hz, 2H), 4.29-4.21 (m, 1H), 4.09-4.00 (m, 2H), 3.84 (s, 6H), 2.41 (s, 3H), 1.84-1.65 (m, 2H), 1.62-1.41 (m, 3H), 0.98-0.94 (m, 2H), 0.91 (d, $J = 6.6$ Hz, 3H), 0.84-0.79 (m, 2H). $^{13}\text{C NMR}$ (100 MHz, CDCl_3) δ 174.90, 159.69, 158.63, 143.35, 136.70, 132.01, 129.20, 128.25, 111.56, 104.13, 64.31, 56.41, 56.05, 31.95, 25.50, 21.57, 16.96, 12.85, 8.28. **IR** (KBr, cm^{-1}) 2941, 1724, 1596, 1473, 1257, 1114, 743. **HRMS** calcd $\text{C}_{25}\text{H}_{32}\text{N}_2\text{O}_6\text{SNa}^+$ $[\text{M}+\text{Na}]^+$: 511.18730. Found: 511.18820.



To a 25 mL round bottom flask were added **6.32'** (1.0 equiv., 1.48 mmol, 600 mg, prepared using a similar procedure as above), triethylamine (3.0 equiv., 4.44 mmol, 0.62 mL), and 10 mL DCM. To this mixture was added benzoyl chloride (1.1 equiv., 1.62 mmol, 0.2 mL) dropwise at room temperature. The reaction was stirred at room temperature for 4 hrs, monitored by TLC. Upon the completion of the acylation reaction, the reaction mixture was diluted with 30 mL 1N NaOH. The organic layer was separated and the aqueous extracted with DCM (3×30 mL).

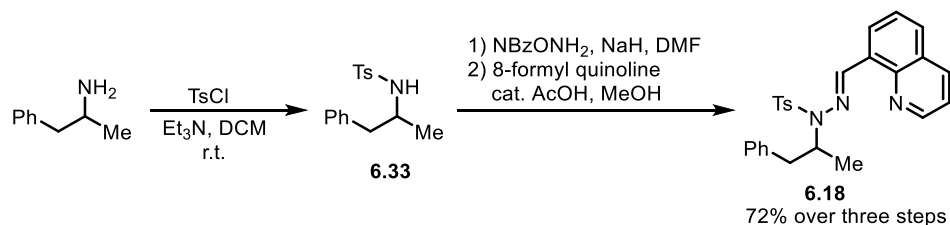
and the aqueous extracted with DCM (3×30 mL). The combined organics were washed subsequently with 1N HCl (2×20 mL), water, and brine. The resulting solution was dried, filtered, and concentrated to give the crude protected alcohol (784 mg, 91% yield).

To an 8 mL vial were added NaH (60%, 1.0 equiv., 1.1 mmol, 45 mg) and 3 mL dry DMF. Phthalimide (1.0 equiv., 1.1 mmol, 164 mg) in 1 mL DMF was added to the mixture dropwise. The vial was sealed with a PTFE lined cap and heated in a pie block at 70 °C for 1 hr. The vial was cooled to room temperature, and Ts-protected alcohol (1.0 equiv., 1.1 mmol, 640 mg) in 1 mL DMF was added dropwise. The reaction mixture was heated in a pie block at 100 °C overnight. The mixture was poured into 20 mL water and extracted with EtOAc (3×20 mL). The combined organics were washed with water and brine, dried, filtered and concentrated. Flash column chromatography (hexane/EtOAc 20:1 to 2:1) of the residue gave **6.14u** as a colorless oil (331 mg, 54% yield). $R_f = 0.7$ (hexane/EtOAc = 1:1). **¹H NMR** (400 MHz, CDCl₃) δ 8.85 (s, 1H), 7.83-7.78 (m, 4H), 7.68 (dd, $J_1 = 5.4$ Hz, $J_2 = 3.1$ Hz, 2H), 7.31-7.25 (m, 3H), 6.55 (d, $J = 8.4$ Hz, 2H), 4.32-4.24 (m, 1H), 3.83 (s, 6H), 3.74-3.60 (m, 2H), 2.39 (s, 3H), 1.86-1.69 (m, 2H), 1.61-1.51 (m, 1H), 1.43-1.35 (m, 1H), 0.89 (d, $J = 6.6$ Hz, 3H). **¹³C NMR** (100 MHz, CDCl₃) δ 168.31, 159.67, 158.80, 143.29, 136.69, 133.76, 132.12, 131.84, 129.19, 128.27, 123.05, 111.64, 104.12, 56.21, 56.04, 37.63, 32.61, 25.44, 21.55, 16.99. **IR** (KBr, cm⁻¹) 2939, 1774, 1712, 1596, 1471, 1257, 1114, 722. **HRMS** calcd C₂₉H₃₁N₃O₆SNa⁺ [M+Na]⁺: 572.18260. Found: 572.18320.



Due to the purchase restriction on 1-methoxy-2-propylamine, hydrazone substrate **6.14m** was synthesized using a Mitsunobu reaction: A 50 mL round bottom flask was charged with PPh₃ (2.0 equiv., 3.0 mmol, 786 mg) and 7 mL THF. To this mixture at room temperature was added diisopropyl azodicarboxylate (DIAD, 1.8 equiv., 2.7 mmol, 0.56 mL) dropwise to give an orange solution. The mixture was stirred at room temperature for 20 min (in some cases, the adduct of PPh₃ and DIAD would precipitate out). A solution of 1-methoxy-2-propanol (1.5 equiv., 2.25 mmol, 203 mg) and **6.31** (1.0 equiv., 1.5 mmol, 501 mg) in 7 mL THF was added to the flask dropwise. The resulting mixture was further stirred at room temperature, monitored by TLC. Upon the completion of the reaction, the solution was concentrated under vacuum. Direct flash column chromatography (hexane/EtOAc 20:1 to 1:1) of the residual oil gave **6.14m** as a white solid (469 mg, 77% yield). $R_f = 0.6$ (hexane/EtOAc = 1:1). Mp. 156-158 °C. ¹H NMR (400 MHz, CDCl₃) δ 8.85 (s, 1H), 7.88-7.84 (m, 2H), 7.32-7.26 (m, 3H), 6.57 (d, $J = 8.4$ Hz, 2H), 4.47 (h, $J = 6.7$ Hz, 1H), 3.84 (s, 6H), 3.44 (dd, $J_1 = 9.9$ Hz, $J_2 = 6.5$ Hz, 1H), 3.29 (dd, $J_1 = 9.9$ Hz, $J_2 = 6.7$ Hz, 1H), 3.28 (s, 3H), 2.42 (s, 3H), 0.98 (d, $J = 6.7$ Hz, 3H). ¹³C NMR (100 MHz, CDCl₃) δ 159.69, 157.42, 143.34, 136.67, 131.83, 129.14, 128.40, 111.67, 104.16, 74.94, 58.63, 56.04, 55.60, 21.59, 14.46. IR (KBr, cm⁻¹) 2936, 1596, 1475, 1257, 1114, 781. HRMS calcd C₂₀H₂₆N₂O₅SNa⁺ [M+Na]⁺: 429.14550. Found: 429.14600.

Procedure for synthesis of hydrazone substrates for β -tosyloxylation



To a 100 mL round bottom flask was added Amphetamine (1.0 equiv., 7.6 mmol, 1.03 g) and 35 mL DCM. To this mixture was added *p*-toluenesulfonyl chloride (1.0 equiv., 7.6 mmol, 1.45 g) portionwise at 0°C. The reaction mixture was allowed to warm to room temperature and stirred overnight. 50 mL 1N HCl was added to the mixture and stirred for 10 min. The organic layer was separated and the aqueous extracted with DCM (3×30 mL). The combined organics were washed with water and brine, dried, filtered, and concentrated to give **6.33** as a white solid (quantitative yield). **6.33** was used for the next step without further purification.

A 100 mL round bottom flask was charged with NaH (60%, 1.2 equiv., 270 mg) and 28 mL dry DMF. To this stirring mixture was added **6.33** (1.0 equiv., 5.7 mmol, 1.65 g) portionwise. The mixture was stirred at room temperature until the gas ceases to evolve. Subsequently, NBzONH₂ (1.1 equiv., 6.3 mmol, 1.14 g) was added to the mixture portionwise under stirring at room temperature. The reaction mixture turned dark when NBzONH₂ was added, and gradually changed to orange during the amination. The thickening of the reaction to a gel was also observed. After the addition, the reaction was further stirred at room temperature for 15 min. The mixture was poured into water and extracted with diethyl ether (3×30 mL). The organics were combined and washed with water (3×80 mL) and brine, dried and concentrated to give crude hydrazine. The hydrazine was directly used for the condensation without further purification.

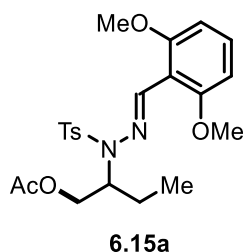
The hydrazine was dissolved in 4 mL MeOH under stirring at room temperature. To this mixture was added 8-formylquinoline (1.0 equiv., 5.7 mmol, 895 mg) in one portion. Three drops of acetic acid was added to the mixture. The reaction was stirred at room temperature. After 30 min, a light yellow precipitation was observed and the reaction mixture solidified. The resulting solid was filtered, washed with mixed solvent (hexane/ EtOAc 8:1), and dried to give hydrazone **6.18** as a light yellow solid (1.81 g, 72% yield over two steps). $R_f = 0.7$ (hexane/EtOAc = 1:1). Mp. 99-103 °C. **¹H NMR** (400 MHz, CDCl₃) δ 9.81 (s, 1H), 8.99 (dd, $J_1 = 4.3$ Hz, $J_2 = 1.8$ Hz, 1H), 8.36 (dd, $J_1 = 7.3$ Hz, $J_2 = 1.4$ Hz, 1H), 8.18 (dd, $J_1 = 8.3$ Hz, $J_2 = 1.8$ Hz, 1H), 7.89 (dd, $J_1 = 8.2$ Hz, $J_2 = 1.5$ Hz, 1H), 7.70-7.66 (m, 2H), 7.61 (t, $J = 7.7$ Hz, 1H), 7.45 (dd, $J_1 = 8.3$ Hz, $J_2 = 4.2$ Hz, 1H), 7.30-7.20 (m, 7H), 4.86-4.77 (m, 1H), 3.11 (dd, $J_1 = 13.5$ Hz, $J_2 = 6.9$ Hz, 1H), 2.89 (dd, $J_1 = 13.5$ Hz, $J_2 = 8.0$ Hz, 1H), 2.37 (s, 3H), 1.26 (d, $J = 6.6$ Hz, 3H). **¹³C NMR** (100 MHz, CDCl₃) δ 150.16, 143.64, 138.96, 136.35, 136.12, 131.95, 129.91, 129.44, 129.39, 128.40, 128.20, 128.08, 126.32, 126.27, 125.96, 121.39, 58.57, 41.77, 21.53, 18.21. **IR** (KBr, cm⁻¹) 3029, 2932, 1596, 1496, 1347, 1162, 913, 747. **HRMS** calcd C₂₆H₂₆N₃O₂S⁺ [M+H]⁺: 444.17400. Found: 444.17520.

General procedures and characterization data for the β-oxidation

General procedure for β-acetoxylation

Unless stated otherwise, a 4 mL vial was charged with Pd(OAc)₂ (5 mol%, 0.0075 mmol, 1.7 mg), PhI(OAc)₂ (115 mmol%, 0.18 mmol, 57 mg), LiOAc (1.0 equiv., 0.15 mmol, 10 mg), 2,6-dimethoxybenzaldehyde (20 mol%, 0.03 mmol, 5 mg) and hydrazone substrate (1.0 equiv.,

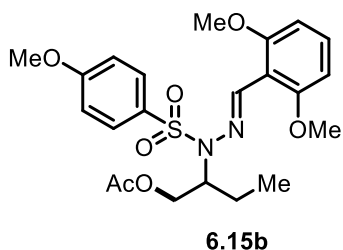
0.15 mmol). To the mixture was added 1.2 mL AcOH and 0.3 mL Ac₂O. The vial was sealed with a PTFE lined cap and heated in a pie block at 90°C. The acetoxylation reaction was monitored by TLC. When the formation of palladium black was observed, the vial was removed from the pie block and allowed to cool to room temperature. Another portion of Pd(OAc)₂ (5 mol%, 0.0075 mmol, 1.7 mg) and PhI(OAc)₂ (115 mmol%, 0.18 mmol, 57 mg) was added to the reaction. The vial was sealed and heated in a pie at 90°C again. In most cases, the previous palladium black disappeared and the mixture stayed orange. When TLC indicated the hydrazone was fully consumed or palladium black was observed again. The reaction was cooled to room temperature and passed through a small plug of silica gel, eluted with Et₂O. The solvent was removed under vacuum. Flash column chromatography (hexane/EtOAc, gradient elution) of the residue gave the acetoxylation product.



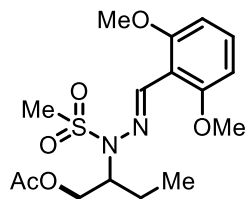
(E)-2-(2-(2,6-dimethoxybenzylidene)-1-tosylhydrazinyl)butyl acetate (6.15a):

Synthesized from **6.14a** following the general procedure (reaction time: 4 hrs). 73% Yield. Yellow oil. $R_f = 0.6$ (hexane/EtOAc 1:1). ¹H NMR (400 MHz, CDCl₃) δ 8.78 (s, 1H), 7.87-7.84 (m, 2H), 7.29-7.25 (m, 3H), 6.54 (d, $J = 8.4$ Hz, 2H), 4.42-4.35 (m, 1H), 4.14 (dd, $J_1 = 11.3$ Hz, $J_2 = 5.3$ Hz, 1H), 4.07 (dd, $J_1 = 11.3$ Hz, $J_2 = 7.5$ Hz, 1H), 3.81 (s, 6H), 2.41 (s, 3H), 1.97 (s, 3H),

1.61-1.54 (m, 2H), 0.93 (t, $J = 7.4$ Hz, 3H). ^{13}C NMR (100 MHz, CDCl_3) δ 170.84, 159.48, 152.69, 143.56, 136.72, 131.52, 129.22, 128.27, 111.70, 104.04, 64.64, 61.07, 55.94, 23.39, 21.56, 20.86, 10.75. IR (KBr, cm^{-1}) 2967, 1741, 1596, 1474, 1257, 1114, 912, 780. HRMS calcd $\text{C}_{22}\text{H}_{29}\text{N}_2\text{O}_6\text{S}^+$ $[\text{M}+\text{H}]^+$: 449.17410. Found: 449.17440.



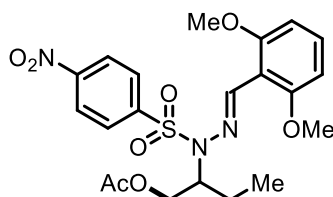
(E)-2-(2-(2,6-dimethoxybenzylidene)-1-((4-methoxyphenyl)sulfonyl)hydrazinyl)butyl acetate (6.15b): Synthesized from **6.14b** following the general procedure (reaction time: 6 hrs). 61% Yield. Colorless oil. $R_f = 0.4$ (hexane/EtOAc 2:1) ^1H NMR (400 MHz, CDCl_3) δ 8.77 (s, 1H), 7.92-7.89 (m, 2H), 7.27 (t, $J = 8.4$ Hz, 1H), 6.96-6.93 (m, 2H), 6.54 (d, $J = 8.4$ Hz, 2H), 4.41-4.34 (m, 1H), 4.14 (dd, $J_1 = 11.3$ Hz, $J_2 = 5.4$ Hz, 1H), 4.07 (dd, $J_1 = 11.3$ Hz, $J_2 = 7.4$ Hz, 1H), 3.85 (s, 3H), 3.80 (s, 6H), 1.99 (s, 3H), 1.62-1.54 (m, 2H), 0.93 (t, $J = 7.4$ Hz, 3H). ^{13}C NMR (100 MHz, CDCl_3) δ 170.83, 163.03, 159.46, 152.60, 131.49, 131.24, 130.38, 113.76, 111.72, 104.04, 64.71, 61.04, 55.94, 55.55, 23.37, 20.91, 10.77. IR (KBr, cm^{-1}) 2939, 1741, 1596, 1473, 1257, 1114, 835. HRMS calcd $\text{C}_{22}\text{H}_{28}\text{N}_2\text{O}_7\text{SNa}^+$ $[\text{M}+\text{Na}]^+$: 487.15090. Found: 487.15360.



6.15c

(E)-2-(2-(2,6-dimethoxybenzylidene)-1-(methylsulfonyl)hydrazinyl)butyl acetate

(6.15c): Synthesized from **6.14c** following the general procedure (reaction time: 5 hrs). 66% Yield. Yellow oil. $R_f = 0.6$ (hexane/EtOAc 1:1) $^1\text{H NMR}$ (400 MHz, CDCl_3) δ 8.77 (s, 1H), 7.30 (t, $J = 8.4$ Hz, 1H), 6.57 (d, $J = 8.4$ Hz, 2H), 4.43 (dd, $J_1 = 11.0$ Hz, $J_2 = 8.5$ Hz, 1H), 4.38-4.31 (m, 1H), 4.23 (dd, $J_1 = 11.0$ Hz, $J_2 = 3.9$ Hz, 1H), 3.83 (s, 6H), 3.10 (s, 3H), 2.06 (s, 3H), 1.74-1.56 (m, 2H), 1.02 (t, $J = 7.4$ Hz, 3H). $^{13}\text{C NMR}$ (100 MHz, CDCl_3) δ 170.61, 159.43, 152.24, 131.70, 111.58, 104.01, 64.39, 61.05, 56.01, 37.40, 23.52, 20.95, 10.60. **IR** (KBr, cm^{-1}) 2937, 1743, 1596, 1473, 1257, 1114, 913, 744. **HRMS** calcd $\text{C}_{16}\text{H}_{24}\text{N}_2\text{O}_6\text{SNa}^+$ $[\text{M}+\text{Na}]^+$: 395.12470. Found: 395.12490.

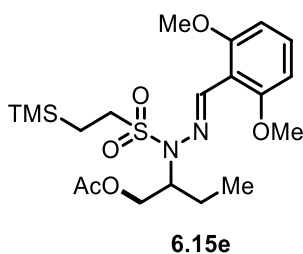


6.15d

(E)-2-(2-(2,6-dimethoxybenzylidene)-1-((4-nitrophenyl)sulfonyl)hydrazinyl)butyl

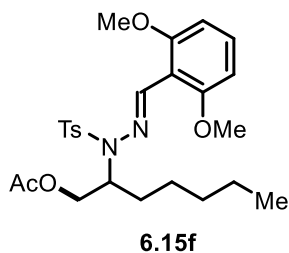
acetate (6.15d): Synthesized from **6.14d** following the general procedure (reaction time: 6 hrs). 56% Yield. Yellow oil. $R_f = 0.6$ (hexane/EtOAc 1:1) $^1\text{H NMR}$ (400 MHz, CDCl_3) δ 8.84 (s, 1H),

8.35-8.31 (m, 2H), 8.20-8.16 (m, 2H), 7.34 (t, $J = 8.4$ Hz, 1H), 6.58 (d, $J = 8.4$ Hz, 2H), 4.38-4.31 (m, 1H), 4.11 (dd, $J_1 = 11.5$ Hz, $J_2 = 5.4$ Hz, 1H), 4.06 (dd, $J_1 = 11.5$ Hz, $J_2 = 7.3$ Hz, 1H), 3.84 (s, 6H), 1.94 (s, 3H), 1.66-1.47 (m, 2H), 0.91 (t, $J = 7.4$ Hz, 3H). ^{13}C NMR (100 MHz, CDCl_3) δ 170.57, 159.75, 157.65, 150.06, 145.38, 132.56, 129.57, 123.69, 110.78, 104.03, 64.10, 61.38, 56.03, 23.19, 20.79, 10.75. IR (KBr, cm^{-1}) 2938, 1742, 1597, 1531, 1474, 1349, 1258, 1114, 913, 743. HRMS calcd $\text{C}_{21}\text{H}_{25}\text{N}_3\text{O}_8\text{SNa}^+$ $[\text{M}+\text{Na}]^+$: 502.12550. Found: 502.12600.

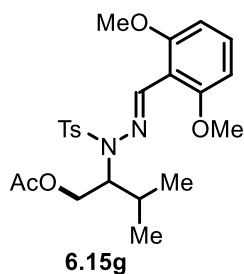


(*E*)-2-(2-(2,6-dimethoxybenzylidene)-1-((2-

(trimethylsilyl)ethyl)sulfonyl)hydrazinyl)butyl acetate (6.15e): Synthesized from **6.14e** following the general procedure with 4.0 equiv. of $\text{PhI}(\text{OAc})_2$ (reaction time: 10 hrs). 51% Yield. Colorless oil. $R_f = 0.8$ (hexane/EtOAc 2:1) ^1H NMR (400 MHz, CDCl_3) δ 8.63 (s, 1H), 7.27 (t, $J = 8.4$ Hz, 1H), 6.56 (d, $J = 8.4$ Hz, 2H), 4.40-4.33 (m, 2H), 4.29-4.23 (m, 1H), 3.82 (s, 6H), 3.26-3.18 (m, 2H), 2.06 (s, 3H), 1.80-1.72 (m, 1H), 1.71-1.61 (m, 1H), 1.19-1.10 (m, 2H), 1.02 (t, $J = 7.4$ Hz, 3H), 0.05 (s, 9H). ^{13}C NMR (100 MHz, CDCl_3) δ 170.71, 159.20, 147.44, 131.14, 111.95, 104.02, 64.72, 60.51, 55.98, 47.44, 23.63, 21.02, 10.73, 9.70, -1.96. IR (KBr, cm^{-1}) 2954, 1745, 1596, 1472, 1336, 1255, 1114, 844. HRMS calcd $\text{C}_{20}\text{H}_{34}\text{N}_2\text{O}_6\text{SSiNa}^+$ $[\text{M}+\text{Na}]^+$: 481.17990. Found: 481.18030.

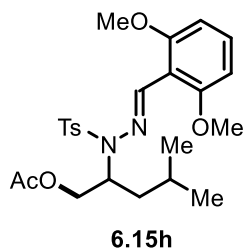


(E)-2-(2-(2,6-dimethoxybenzylidene)-1-tosylhydrazinyl)heptyl (6.15f): Synthesized from **6.14f** following the general procedure (reaction time: 7 hrs). 57% Yield. Colorless oil. $R_f = 0.7$ (hexane/EtOAc 1:1). $^1\text{H NMR}$ (400 MHz, CDCl_3) δ 8.78 (s, 1H), 7.87-7.85 (m, 2H), 7.30-7.25 (m, 3H), 6.55 (d, $J = 8.4$ Hz, 2H), 4.47-4.40 (m, 1H), 4.12 (dd, $J_1 = 11.3$ Hz, $J_2 = 5.3$ Hz, 1H), 4.05 (dd, $J_1 = 11.3$ Hz, $J_2 = 7.5$ Hz, 1H), 3.81 (s, 6H), 2.41 (s, 3H), 1.97 (s, 3H), 1.55-1.43 (m, 2H), 1.36-1.18 (m, 6H), 0.87-0.83 (m, 3H). $^{13}\text{C NMR}$ (100 MHz, CDCl_3) δ 170.85, 159.51, 153.34, 143.54, 136.76, 131.55, 129.21, 128.29, 111.72, 104.04, 64.80, 59.61, 55.94, 31.58, 30.10, 25.72, 22.43, 21.55, 20.87, 14.00. **IR** (KBr, cm^{-1}) 2931, 1740, 1597, 1472, 1257, 1115, 913, 744. **HRMS** calcd $\text{C}_{25}\text{H}_{34}\text{N}_2\text{O}_6\text{SNa}^+$ $[\text{M}+\text{Na}]^+$: 513.20300. Found: 513.20350.



(E)-2-(2-(2,6-dimethoxybenzylidene)-1-tosylhydrazinyl)-3-methylbutyl acetate

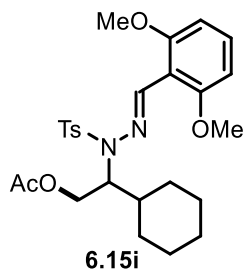
(6.15g): Synthesized from **6.14g** following the general procedure (reaction time: 6 hrs). 70% Yield. Colorless oil. $R_f = 0.6$ (hexane/EtOAc 1:1). $^1\text{H NMR}$ (400 MHz, CDCl_3) δ 8.76 (s, 1H), 7.88-7.85 (m, 2H), 7.28-7.23 (m, 3H), 6.53 (d, $J = 8.4$ Hz, 2H), 4.28-4.22 (m, 2H), 4.19-4.13 (m, 1H), 3.79 (s, 6H), 2.41 (s, 3H), 2.06-1.96 (m, 1H), 1.88 (s, 3H), 1.06 (d, $J = 6.8$ Hz, 3H), 0.99 (d, $J = 6.8$ Hz, 3H). $^{13}\text{C NMR}$ (100 MHz, CDCl_3) δ 170.74, 159.39, 149.68, 143.52, 136.67, 131.24, 129.13, 128.41, 111.87, 104.01, 64.86, 63.36, 55.89, 30.33, 21.54, 20.81, 19.80, 19.77. **IR** (KBr, cm^{-1}) 2964, 1741, 1597, 1472, 1257, 1114, 913, 748. **HRMS** calcd $\text{C}_{23}\text{H}_{30}\text{N}_2\text{O}_6\text{SNa}^+$ $[\text{M}+\text{Na}]^+$: 485.17170. Found: 485.17230.



(E)-2-(2-(2,6-dimethoxybenzylidene)-1-tosylhydrazinyl)-4-methylpentyl acetate

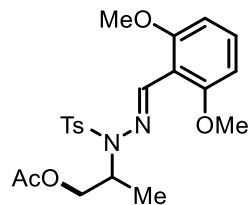
(6.15h): Synthesized from **6.14h** following the general procedure (reaction time: 5 hrs). 78% Yield. Colorless oil. $R_f = 0.8$ (hexane/EtOAc 1:1). $^1\text{H NMR}$ (400 MHz, CDCl_3) δ 8.77 (s, 1H), 7.88-7.85 (m, 2H), 7.30-7.25 (m, 3H), 6.55 (d, $J = 8.4$ Hz, 2H), 4.59-4.52 (m, 1H), 4.09 (dd, $J_1 = 11.3$ Hz, $J_2 = 5.5$ Hz, 1H), 4.02 (dd, $J_1 = 11.3$ Hz, $J_2 = 7.3$ Hz, 1H), 3.81 (s, 6H), 2.41 (s, 3H), 1.97 (s, 3H), 1.79-1.69 (m, 1H), 1.57-1.50 (m, 1H), 1.32-1.25 (m, 1H), 0.96 (d, $J = 6.6$ Hz, 3H), 0.89 (d, $J = 6.7$ Hz, 3H). $^{13}\text{C NMR}$ (100 MHz, CDCl_3) δ 170.81, 159.46, 153.67, 143.53, 136.80,

131.55, 129.21, 128.31, 111.69, 104.02, 64.77, 57.59, 55.93, 39.29, 24.42, 23.10, 22.07, 21.55, 20.86. **IR** (KBr, cm^{-1}) 2958, 1741, 1597, 1472, 1257, 1114, 913, 744. **HRMS** calcd $\text{C}_{24}\text{H}_{32}\text{N}_2\text{O}_6\text{SNa}^+$ $[\text{M}+\text{Na}]^+$: 499.18730. Found: 499.18820.

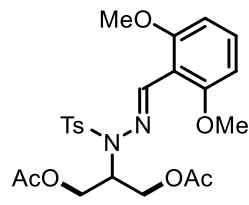


(E)-2-cyclohexyl-2-(2-(2,6-dimethoxybenzylidene)-1-tosylhydrazinyl)ethyl acetate

(6.15i): Synthesized from **6.14i** following the general procedure (reaction time: 5 hrs). 81% Yield. Colorless oil. $R_f = 0.8$ (hexane/EtOAc 1:1). **$^1\text{H NMR}$** (400 MHz, CDCl_3) δ 8.70 (s, 1H), 7.88-7.85 (m, 2H), 7.28-7.23 (m, 3H), 6.53 (d, $J = 8.4$ Hz, 2H), 4.34-4.25 (m, 2H), 4.20-4.15 (m, 1H), 3.79 (s, 6H), 2.41 (s, 3H), 1.87 (s, 3H), 1.84-1.64 (m, 6H), 1.26-1.09 (m, 5H). **$^{13}\text{C NMR}$** (100 MHz, CDCl_3) δ 170.76, 159.32, 148.55, 143.49, 136.73, 131.12, 129.11, 128.42, 111.98, 104.02, 64.10, 63.29, 55.90, 39.62, 30.30, 29.69, 26.28, 26.21, 26.19, 21.54, 20.82. **IR** (KBr, cm^{-1}) 2929, 1741, 1596, 1472, 1257, 1114, 913, 744. **HRMS** calcd $\text{C}_{26}\text{H}_{34}\text{N}_2\text{O}_6\text{SNa}^+$ $[\text{M}+\text{Na}]^+$: 525.20300. Found: 525.20350.



6.15j-mono



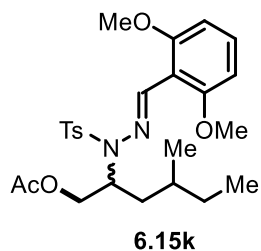
6.15j-di

(E)-2-(2-(2,6-dimethoxybenzylidene)-1-tosylhydrazinyl)propyl acetate (6.15j-mono):

Synthesized from **6.14i** following the general procedure (reaction time: 8 hrs). 33% Yield. Light yellow oil. $R_f = 0.6$ (hexane/EtOAc 1:1). $^1\text{H NMR}$ (400 MHz, CDCl_3) δ 8.87 (s, 1H), 7.85-7.82 (m, 2H), 7.32-7.27 (m, 3H), 6.56 (d, $J = 8.4$ Hz, 2H), 4.54 (h, $J = 6.7$ Hz, 1H), 4.05-4.03 (m, 2H), 3.83 (s, 6H), 2.42 (s, 3H), 2.03 (s, 3H), 1.01 (d, $J = 6.7$ Hz, 3H). $^{13}\text{C NMR}$ (100 MHz, CDCl_3) δ 170.88, 159.68, 157.38, 143.58, 136.53, 131.93, 129.29, 128.25, 111.52, 104.08, 65.91, 56.00, 55.13, 21.58, 20.88, 14.33. **IR** (KBr, cm^{-1}) 2971, 1740, 1597, 1473, 1259, 1113, 913, 747. **HRMS** calcd $\text{C}_{21}\text{H}_{26}\text{N}_2\text{O}_6\text{SNa}^+$ $[\text{M}+\text{Na}]^+$: 457.14040. Found: 457.14090.

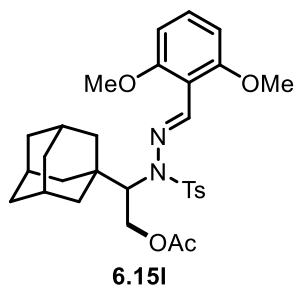
(E)-2-(2-(2,6-dimethoxybenzylidene)-1-tosylhydrazinyl)propane-1,3-diyl diacetate (6.15j-di):

Synthesized from **6.14i** following the general procedure (reaction time: 8 hrs). 36% Yield. Yellow oil. $R_f = 0.5$ (hexane/EtOAc 1:1). $^1\text{H NMR}$ (400 MHz, CDCl_3) δ 8.84 (s, 1H), 7.86-7.83 (m, 2H), 7.31-7.26 (m, 3H), 6.54 (d, $J = 8.4$ Hz, 2H), 4.72 (tt, $J_1 = 7.2$ Hz, $J_2 = 5.7$ Hz, 1H), 4.21 (dd, $J_1 = 11.4$ Hz, $J_2 = 5.7$ Hz, 2H), 4.12 (dd, $J_1 = 11.4$ Hz, $J_2 = 7.2$ Hz, 2H), 3.81 (s, 6H), 2.42 (s, 3H), 2.00 (s, 6H). $^{13}\text{C NMR}$ (100 MHz, CDCl_3) δ 170.65, 159.63, 154.31, 143.96, 136.21, 131.90, 129.39, 128.30, 111.31, 103.94, 62.34, 57.98, 55.92, 21.59, 20.77. **IR** (KBr, cm^{-1}) 2938, 1743, 1597, 1473, 1257, 1114, 913, 744. **HRMS** calcd $\text{C}_{23}\text{H}_{28}\text{N}_2\text{O}_8\text{SNa}^+$ $[\text{M}+\text{Na}]^+$: 515.14590. Found: 515.14650.



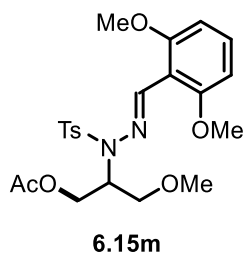
(E)-2-(2-(2,6-dimethoxybenzylidene)-1-tosylhydrazinyl)-4-methylhexyl acetate

(6.15k): Synthesized from **6.14k** as an inseparable mixture of two diastereomers (*d.r.* 1.5:1) following the general procedure (reaction time: 8 hrs). 56% Yield. Colorless oil. $R_f = 0.8$ (hexane/EtOAc 1:1). $^1\text{H NMR}$ (400 MHz, CDCl_3) δ 8.79 (s, 0.6H), 8.77 (s, 0.4H), 7.89-7.85 (m, 2H), 7.30-7.25 (m, 3H), 6.54 (d, $J = 8.4$ Hz, 2H), 4.59-4.52 (m, 1H), 4.12-3.97 (m, 2H), 3.81 (s, 6H), 2.41 (s, 3H), 1.97 (s, 1.2H), 1.95 (s, 1.8H), 1.71-1.64 (m, 0.6H), 1.57-1.36 (m, 2H), 1.31-1.09 (m, 2.4H), 0.96 (d, $J = 6.5$ Hz, 1.8H), 0.88-0.81 (m, 4.2H). $^{13}\text{C NMR}$ (100 MHz, CDCl_3) δ 170.86, 170.76, 159.52, 159.47, 154.56, 153.79, 143.51, 136.84, 131.64, 131.55, 129.22, 129.20, 128.33, 128.30, 111.71, 111.61, 104.03, 104.00, 64.87, 64.64, 57.54, 57.34, 55.94, 55.90, 37.28, 37.09, 30.67, 30.57, 29.96, 28.77, 21.56, 20.87, 20.85, 19.37, 18.89, 11.28, 10.93. **IR** (KBr, cm^{-1}) 2960, 1742, 1597, 1472, 1257, 1114, 912, 780. **HRMS** calcd $\text{C}_{25}\text{H}_{34}\text{N}_2\text{O}_6\text{SNa}^+$ $[\text{M}+\text{Na}]^+$: 513.20300. Found: 513.20360.



2-((3*R*,5*R*,7*R*)-Adamantan-1-yl)-2-((*E*)-2,6-dimethoxybenzylidene)-1-

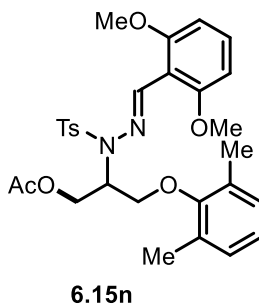
tosylhydrazinyl)ethyl acetate (6.15l): Synthesized from **6.14l** following the general procedure (reaction time: 10 hrs). 56% Yield. Colorless oil. $R_f = 0.7$ (hexane/EtOAc 1:1). **$^1\text{H NMR}$** (400 MHz, CDCl_3) δ 8.89 (s, 1H), 7.88-7.85 (m, 2H), 7.26-7.22 (m, 3H), 6.52 (d, $J = 8.4$ Hz, 2H), 4.39 (dd, $J_1 = 11.7$ Hz, $J_2 = 7.8$ Hz, 1H), 4.33 (dd, $J_1 = 11.7$ Hz, $J_2 = 4.1$ Hz, 1H), 4.16 (dd, $J_1 = 7.8$ Hz, $J_2 = 4.1$ Hz, 1H), 3.78 (s, 6H), 2.39 (s, 3H), 2.00-1.98 (m, 3H), 1.83-1.79 (m, 6H), 1.71-1.59 (m, 9H). **$^{13}\text{C NMR}$** (100 MHz, CDCl_3) δ 170.76, 159.30, 148.72, 143.53, 136.39, 131.02, 129.01, 128.74, 111.97, 103.85, 68.01, 61.64, 55.74, 39.31, 37.27, 36.89, 28.52, 21.52, 20.84. **IR** (KBr, cm^{-1}) 2902, 1739, 1596, 1472, 1258, 1114, 913, 747. **HRMS** calcd $\text{C}_{30}\text{H}_{38}\text{N}_2\text{O}_6\text{SNa}^+$ $[\text{M}+\text{Na}]^+$: 577.23430. Found: 577.23490.



(*E*)-2-(2-(2,6-dimethoxybenzylidene)-1-tosylhydrazinyl)-3-methoxypropyl acetate

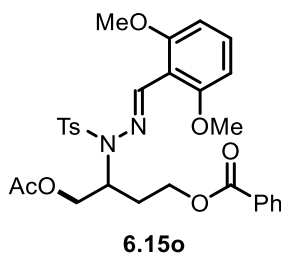
(6.15m): Synthesized from **6.14m** following the general procedure (reaction time: 9 hrs). 69%

Yield. Light yellow oil. $R_f = 0.6$ (hexane/EtOAc 1:1). $^1\text{H NMR}$ (400 MHz, CDCl_3) δ 8.81 (s, 1H), 7.88-7.85 (m, 2H), 7.30-7.26 (m, 3H), 6.54 (d, $J = 8.4$ Hz, 2H), 4.69-4.62 (m, 1H), 4.23 (dd, $J_1 = 11.4$ Hz, $J_2 = 4.9$ Hz, 1H), 4.15 (dd, $J_1 = 11.4$ Hz, $J_2 = 7.8$ Hz, 1H), 3.81 (s, 6H), 3.49-3.41 (m, 2H), 3.24 (s, 3H), 2.42 (s, 3H), 1.98 (s, 3H). $^{13}\text{C NMR}$ (100 MHz, CDCl_3) δ 170.77, 159.57, 154.31, 143.66, 136.38, 131.75, 129.20, 128.42, 111.51, 104.02, 70.87, 62.73, 58.76, 58.65, 55.94, 21.57, 20.80. **IR** (KBr, cm^{-1}) 2932, 1742, 1597, 1476, 1257, 1114, 913, 747. **HRMS** calcd $\text{C}_{22}\text{H}_{28}\text{N}_2\text{O}_7\text{SNa}^+$ $[\text{M}+\text{Na}]^+$: 487.15090. Found: 487.15180.



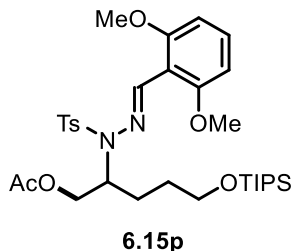
(*E*)-2-(2-(2,6-dimethoxybenzylidene)-1-tosylhydrazinyl)-3-(2,6-dimethylphenoxy)propyl acetate (6.15n): Synthesized from **6.14n** following the general procedure (reaction time: 8 hrs). 65% Yield. Colorless oil. $R_f = 0.7$ (hexane/EtOAc 1:1). $^1\text{H NMR}$ (400 MHz, CDCl_3) δ 8.90 (s, 1H), 7.90-7.87 (m, 2H), 7.31-7.23 (m, 3H), 6.96-6.94 (m, 2H), 6.88 (dd, $J_1 = 8.5$ Hz, $J_2 = 6.2$ Hz, 1H), 6.54 (d, $J = 8.4$ Hz, 2H), 4.89-4.83 (m, 1H), 4.47 (dd, $J_1 = 11.3$ Hz, $J_2 = 4.8$ Hz, 1H), 4.31 (dd, $J_1 = 11.3$ Hz, $J_2 = 7.5$ Hz, 1H), 3.89-3.85 (m, 1H), 3.81-3.77 (m, 1H), 3.79 (s, 6H), 2.40 (s, 3H), 2.14 (s, 6H), 2.01 (s, 3H). $^{13}\text{C NMR}$ (100 MHz, CDCl_3) δ 170.73, 159.65, 155.42, 155.25, 143.75, 136.21, 131.88, 130.83, 129.28, 128.72, 128.41, 123.86, 111.37, 103.96, 69.65, 62.59, 59.24, 55.91, 55.88, 21.55, 20.81, 16.13. **IR** (KBr,

cm⁻¹) 2969, 1742, 1597, 1473, 1257, 1113, 912, 747. **HRMS** calcd C₂₉H₃₄N₂O₇SNa⁺ [M+Na]⁺: 577.19790. Found: 577.19850.

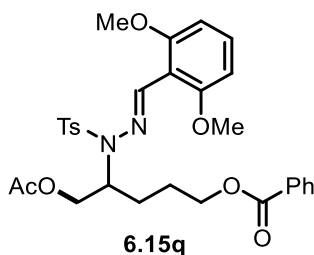


(E)-4-acetoxy-3-(2-(2,6-dimethoxybenzylidene)-1-tosylhydrazinyl)butyl benzoate

(6.15o): Synthesized from **6.14o** following the general procedure (reaction time: 10 hrs). 47% Yield. Colorless oil. R_f = 0.6 (hexane/EtOAc 1:1). ¹H NMR (400 MHz, CDCl₃) δ 8.86 (s, 1H), 8.09-8.06 (m, 2H), 7.84-7.81 (m, 2H), 7.58-7.54 (m, 1H), 7.47-7.42 (m, 2H), 7.28 (t, J = 8.4 Hz, 1H), 7.22-7.19 (m, 2H), 6.55 (d, J = 8.4 Hz, 2H), 4.79-4.72 (m, 1H), 4.41 (dt, J₁ = 11.1 Hz, J₂ = 5.5 Hz, 1H), 4.25-4.19 (m, 2H), 4.15 (dd, J₁ = 11.3 Hz, J₂ = 7.2 Hz, 1H), 3.81 (s, 6H), 2.37 (s, 3H), 2.07-2.02 (m, 2H), 2.01 (s, 3H). ¹³C NMR (100 MHz, CDCl₃) δ 170.75, 166.33, 159.55, 153.58, 143.88, 136.31, 132.87, 131.77, 130.23, 129.59, 129.36, 128.34, 128.17, 111.46, 103.95, 64.83, 61.56, 56.50, 55.91, 29.29, 21.54, 20.85. **IR** (KBr, cm⁻¹) 2927, 1742, 1719, 1597, 1474, 1257, 1114, 913, 743. **HRMS** calcd C₂₉H₃₂N₂O₈SNa⁺ [M+Na]⁺: 591.17720. Found: 591.17760.

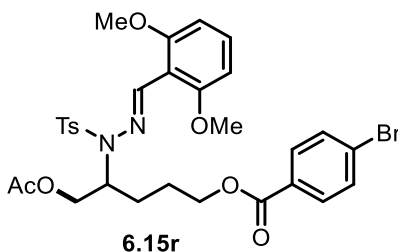


(E)-N'-(2,6-dimethoxybenzylidene)-4-methyl-N-(5-((triisopropylsilyl)oxy)pentan-2-yl)benzenesulfonohydrazide (6.15p): Synthesized from **6.14p** following the general procedure (reaction time: 6 hrs). 64% Yield. Colorless oil. $R_f = 0.8$ (hexane/EtOAc 1:1). $^1\text{H NMR}$ (400 MHz, CDCl_3) δ 8.80 (s, 1H), 7.87-7.83 (m, 2H), 7.29-7.25 (m, 3H), 6.54 (d, $J = 8.4$ Hz, 2H), 4.50-4.44 (m, 1H), 4.13 (dd, $J_1 = 11.3$ Hz, $J_2 = 5.6$ Hz, 1H), 4.06 (dd, $J_1 = 11.3$ Hz, $J_2 = 7.2$ Hz, 1H), 3.80 (s, 6H), 3.70-3.58 (m, 2H), 2.41 (s, 3H), 1.96 (s, 3H), 1.74-1.55 (m, 4H), 1.07-0.99 (m, 21H). $^{13}\text{C NMR}$ (100 MHz, CDCl_3) δ 170.79, 159.53, 153.32, 143.55, 136.68, 131.57, 129.23, 128.29, 111.65, 103.98, 64.81, 62.84, 59.39, 55.89, 29.44, 26.64, 21.55, 20.84, 17.99, 11.93. **IR** (KBr , cm^{-1}) 2943, 1744, 1597, 1472, 1257, 1115, 780. **HRMS** calcd $\text{C}_{32}\text{H}_{50}\text{N}_2\text{O}_7\text{SSi}^+$ $[\text{M}+\text{H}]^+$: 635.31810. Found: 635.32070.



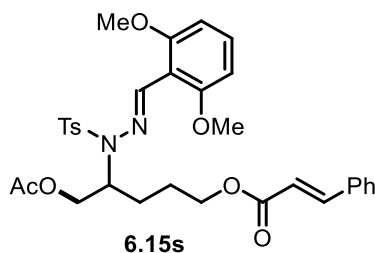
(E)-5-acetoxy-4-(2-(2,6-dimethoxybenzylidene)-1-tosylhydrazinyl)pentyl benzoate (6.15q): Synthesized from **6.14q** following the general procedure (reaction time: 8 hrs). 52%

Yield. Colorless oil. $R_f = 0.8$ (hexane/EtOAc 1:1). $^1\text{H NMR}$ (400 MHz, CDCl_3) δ 8.86 (s, 1H), 8.01-7.98 (m, 2H), 7.87-7.84 (m, 2H), 7.55-7.51 (m, 1H), 7.41-7.36 (m, 2H), 7.31-7.25 (m, 3H), 6.54 (d, $J = 8.4$ Hz, 2H), 4.54-4.47 (m, 1H), 4.29 (t, $J = 6.4$ Hz, 2H), 4.13 (dd, $J_1 = 11.3$ Hz, $J_2 = 5.8$ Hz, 1H), 4.04 (dd, $J_1 = 11.3$ Hz, $J_2 = 6.9$ Hz, 1H), 3.79 (s, 6H), 2.39 (s, 3H), 1.95 (s, 3H), 1.92-1.78 (m, 2H), 1.74-1.68 (m, 2H). $^{13}\text{C NMR}$ (100 MHz, CDCl_3) δ 170.72, 166.53, 159.57, 154.04, 143.78, 136.48, 132.79, 131.75, 130.30, 129.51, 129.32, 128.26, 111.50, 103.99, 64.77, 64.56, 59.17, 55.91, 26.85, 25.27, 21.55, 20.82. **IR** (KBr, cm^{-1}) 2942, 1741, 1718, 1597, 1472, 1257, 1114, 913, 744. **HRMS** calcd $\text{C}_{30}\text{H}_{34}\text{N}_2\text{O}_8\text{SNa}^+$ $[\text{M}+\text{Na}]^+$: 605.19280. Found: 605.19350.

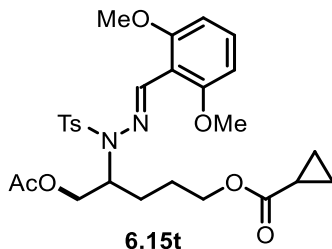


(E)-5-acetoxy-4-(2-(2,6-dimethoxybenzylidene)-1-tosylhydrazinyl)pentyl 4-bromobenzoate (6.15r): Synthesized from **6.14r** following the general procedure (reaction time: 6 hrs). 61% Yield. Colorless oil. $R_f = 0.4$ (hexane/EtOAc 2:1). $^1\text{H NMR}$ (400 MHz, CDCl_3) δ 8.85 (s, 1H), 7.86-7.83 (m, 4H), 7.51-7.48 (m, 2H), 7.31-7.26 (m, 3H), 6.54 (d, $J = 8.4$ Hz, 2H), 4.53-4.47 (m, 1H), 4.29 (t, $J = 6.3$ Hz, 2H), 4.13 (dd, $J_1 = 11.3$ Hz, $J_2 = 5.9$ Hz, 1H), 4.04 (dd, $J_1 = 11.3$ Hz, $J_2 = 6.9$ Hz, 1H), 3.78 (s, 6H), 2.40 (s, 3H), 1.95 (s, 3H), 1.93-1.64 (m, 4H). $^{13}\text{C NMR}$ (100 MHz, CDCl_3) δ 170.69, 165.78, 159.54, 153.77, 143.81, 136.46, 131.80, 131.60, 131.03, 129.31, 129.17, 128.24, 127.87, 111.44, 103.99, 64.81, 59.13, 55.95, 55.88, 26.86, 25.18,

21.59, 20.84. **IR** (KBr, cm^{-1}) 2958, 1741, 1720, 1595, 1473, 1257, 1114, 913. **HRMS** calcd $\text{C}_{30}\text{H}_{34}\text{BrN}_2\text{O}_8\text{S}^+$ $[\text{M}+\text{H}]^+$: 661.12140. Found: 661.12370.

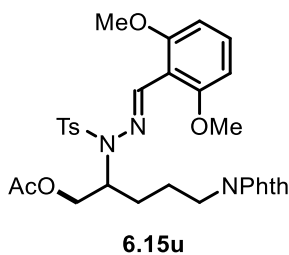


5-Acetoxy-4-(2-((*E*)-2,6-dimethoxybenzylidene)-1-tosylhydrazinyl)pentyl cinnamate (6.15s): Synthesized from **6.14s** following the general procedure (reaction time: 8 hrs). 47% Yield. Colorless oil. $R_f = 0.3$ (hexane/EtOAc 3:1). **$^1\text{H NMR}$** (400 MHz, CDCl_3) δ 8.84 (s, 1H), 7.87-7.83 (m, 2H), 7.66 (d, $J = 16.0$ Hz, 1H), 7.51-7.47 (m, 2H), 7.39-7.36 (m, 3H), 7.31-7.26 (m, 3H), 6.54 (d, $J = 8.4$ Hz, 2H), 6.40 (d, $J = 16.0$ Hz, 1H), 4.53-4.47 (m, 1H), 4.17 (td, $J_1 = 6.4$ Hz, $J_2 = 1.1$ Hz, 2H), 4.13 (dd, $J_1 = 11.3$ Hz, $J_2 = 5.7$ Hz, 1H), 4.05 (dd, $J_1 = 11.3$ Hz, $J_2 = 7.0$ Hz, 1H), 3.81 (s, 6H), 2.41 (s, 3H), 1.96 (s, 3H), 1.88-1.73 (m, 2H), 1.72-1.64 (m, 2H). **$^{13}\text{C NMR}$** (100 MHz, CDCl_3) δ 170.74, 166.95, 159.55, 153.86, 144.63, 143.77, 136.51, 134.39, 131.73, 130.21, 129.32, 128.84, 128.28, 128.04, 118.10, 111.52, 104.00, 64.76, 64.23, 59.19, 55.94, 26.90, 25.25, 21.59, 20.85. **IR** (KBr, cm^{-1}) 2940, 1740, 1711, 1596, 1472, 1257, 1163, 1114, 913. **HRMS** calcd $\text{C}_{32}\text{H}_{36}\text{N}_2\text{O}_8\text{SNa}^+$ $[\text{M}+\text{H}]^+$: 631.20850. Found: 631.20900.



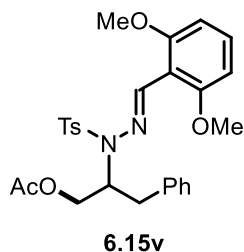
(E)-5-acetoxy-4-(2-(2,6-dimethoxybenzylidene)-1-tosylhydrazinyl)pentyl

cyclopropanecarboxylate (6.15t): Synthesized from **6.14t** following the general procedure (reaction time: 8 hrs). 66% Yield. Colorless oil. $R_f = 0.3$ (hexane/EtOAc 3:1). $^1\text{H NMR}$ (400 MHz, CDCl_3) δ 8.82 (s, 1H), 7.86-7.83 (m, 2H), 7.30-7.26 (m, 3H), 6.54 (d, $J = 8.4$ Hz, 2H), 4.49-4.43 (m, 1H), 4.11 (dd, $J_1 = 11.3$ Hz, $J_2 = 5.7$ Hz, 1H), 4.08-3.98 (m, 3H), 3.81 (s, 6H), 2.41 (s, 3H), 1.96 (s, 3H), 1.79-1.66 (m, 2H), 1.65-1.53 (m, 3H), 0.98-0.94 (m, 2H), 0.88-0.79 (m, 2H). $^{13}\text{C NMR}$ (100 MHz, CDCl_3) δ 174.84, 170.71, 159.52, 153.73, 143.74, 136.50, 131.71, 129.30, 128.26, 111.52, 103.98, 64.73, 64.09, 59.15, 55.93, 26.81, 25.21, 21.57, 20.83, 12.83, 8.31. **IR** (KBr, cm^{-1}) 2946, 1740, 1725, 1597, 1473, 1257, 1114, 912, 739. **HRMS** calcd $\text{C}_{27}\text{H}_{34}\text{N}_2\text{O}_8\text{SNa}^+ [\text{M}+\text{Na}]^+$: 569.19280. Found: 569.19360.



(E)-2-(2-(2,6-dimethoxybenzylidene)-1-tosylhydrazinyl)-5-(1,3-dioxisoindolin-2-yl)pentyl acetate (6.15u): Synthesized from **6.14u** following the general procedure (reaction

time: 7 hrs). 67% Yield. Colorless oil. $R_f = 0.6$ (hexane/EtOAc 1:1). $^1\text{H NMR}$ (400 MHz, CDCl_3) δ 8.81 (s, 1H), 7.85-7.82 (m, 2H), 7.81 (dd, $J_1 = 5.5$ Hz, $J_2 = 3.0$ Hz, 2H), 7.69 (dd, $J_1 = 5.5$ Hz, $J_2 = 3.0$ Hz, 2H), 7.29-7.24 (m, 3H), 6.52 (d, $J = 8.4$ Hz, 2H), 4.50-4.44 (m, 1H), 4.06 (dd, $J_1 = 11.3$ Hz, $J_2 = 5.8$ Hz, 1H), 4.00 (dd, $J_1 = 11.3$ Hz, $J_2 = 6.9$ Hz, 1H), 3.80 (s, 6H), 3.72-3.58 (m, 2H), 2.37 (s, 3H), 1.94 (s, 3H), 1.80-1.68 (m, 2H), 1.63-1.48 (m, 2H). $^{13}\text{C NMR}$ (100 MHz, CDCl_3) δ 170.71, 168.24, 159.55, 154.30, 143.70, 136.43, 133.80, 132.07, 131.68, 129.28, 128.28, 123.07, 111.49, 103.96, 64.75, 58.93, 55.92, 37.52, 27.43, 25.11, 21.51, 20.82. **IR** (KBr, cm^{-1}) 2940, 1740, 1713, 1597, 1471, 1257, 1114, 912, 722. **HRMS** calcd $\text{C}_{31}\text{H}_{33}\text{N}_3\text{O}_8\text{SNa}^+$ $[\text{M}+\text{Na}]^+$: 630.18810. Found: 630.18850.

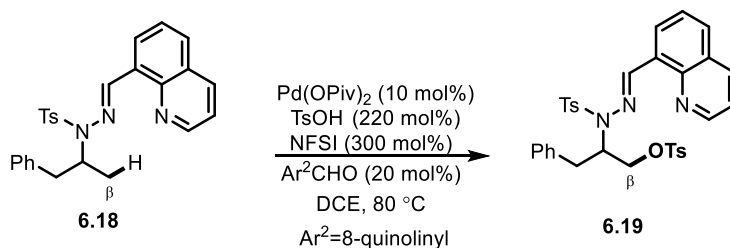


(E)-2-(2-(2,6-dimethoxybenzylidene)-1-tosylhydrazinyl)-3-phenylpropyl acetate

(6.15v): Synthesized from **6.14v** following the general procedure (reaction time: 5 hrs). 70% Yield. Colorless oil. $R_f = 0.7$ (hexane/EtOAc 1:1). $^1\text{H NMR}$ (400 MHz, CDCl_3) δ 8.68 (s, 1H), 7.51-7.48 (m, 2H), 7.31-7.14 (m, 8H), 6.57 (d, $J = 8.4$ Hz, 2H), 4.86-4.79 (m, 1H), 4.22-4.16 (m, 2H), 3.84 (s, 6H), 2.93 (dd, $J_1 = 13.8$ Hz, $J_2 = 8.0$ Hz, 1H), 2.85 (dd, $J_1 = 13.8$ Hz, $J_2 = 7.0$ Hz, 1H), 2.37 (s, 3H), 2.00 (s, 3H). $^{13}\text{C NMR}$ (100 MHz, CDCl_3) δ 170.94, 159.45, 151.35, 143.48, 138.18, 136.84, 131.42, 129.48, 129.28, 128.50, 128.09, 126.38, 111.86, 104.06, 64.22, 61.13,

55.97, 36.00, 21.54, 20.87. **IR** (KBr, cm^{-1}) 2941, 1742, 1596, 1472, 1257, 1114, 751. **HRMS** calcd $\text{C}_{27}\text{H}_{30}\text{N}_2\text{O}_6\text{SNa}^+$ $[\text{M}+\text{Na}]^+$: 533.17170. Found: 533.17230.

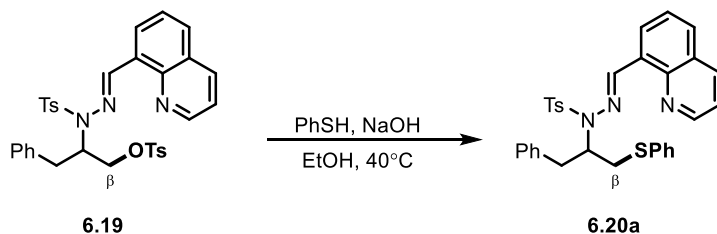
General procedure for β -tosyloxylation



To an 8 mL vial was charged with $\text{Pd}(\text{OPiv})_2$ (10 mol%, 0.04 mmol, 12.4 mg), *N*-fluorobenzenesulfonimide (NFSI, 3.0 equiv., 1.2 mmol, 378 mg), 8-formylquinoline (20 mol%, 0.08 mmol, 13 mg) and hydrazone substrate **6.18** (1.0 equiv., 0.4 mmol, 177 mg). The vial was transferred to the glovebox. Anhydrous *p*-toluenesulfonic acid (2.2 equiv., 0.88 mmol, 151 mg) and 4 mL DCE were added to the vial. The vial was sealed with a PTFE lined cap, transferred out of the glovebox, and heated in a pie block at 80°C overnight. The reaction mixture was allowed to cool to room temperature. 360 mg Na_2CO_3 and 15 mg 1,10-phenanthroline were added and the mixture stirred for 36 hrs. The resulting mixture was passed through a small plug of Celite, eluted with Et_2O to give a dark red solution. The solvent was removed under vacuum and flash column chromatography of the residue (hexane/EtOAc 20:1 to 1:1) yielded the tosyloxylation product **6.19** as a colorless oil (127 mg, 52% yield). $R_f = 0.5$ (hexane/EtOAc 2:1). **^1H NMR** (400 MHz, CDCl_3) δ 9.66 (s, 1H), 9.00 (dd, $J_1 = 4.1$ Hz, $J_2 = 1.8$ Hz, 1H), 8.17 (dd, $J_1 = 8.3$ Hz, $J_2 = 1.8$ Hz, 1H), 7.97 (dd, $J_1 = 7.3$ Hz, $J_2 = 1.4$ Hz, 1H), 7.86 (dd, $J_1 = 8.1$ Hz, $J_2 = 1.4$

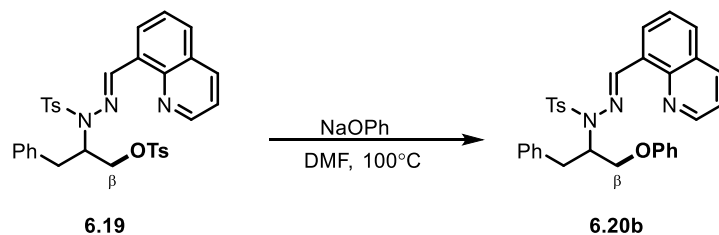
Hz, 1H), 7.72-7.68 (m, 2H), 7.54-7.49 (m, 3H), 7.47 (dd, $J_1 = 8.3$ Hz, $J_2 = 4.2$ Hz, 1H), 7.26-7.20 (m, 5H), 7.17-7.14 (m, 2H), 6.95-6.93 (m, 2H), 5.06-4.99 (m, 1H), 4.24 (dd, $J_1 = 10.0$ Hz, $J_2 = 7.9$ Hz, 1H), 4.19 (dd, $J_1 = 10.0$ Hz, $J_2 = 4.9$ Hz, 1H), 3.04-2.93 (m, 2H), 2.36 (s, 3H), 1.94 (s, 3H). ^{13}C NMR (100 MHz, CDCl_3) δ 150.18, 146.64, 146.06, 144.44, 144.16, 136.97, 135.94, 135.67, 132.16, 131.83, 129.64, 129.55, 129.47, 129.42, 128.67, 128.55, 128.16, 127.95, 126.78, 126.16, 125.23, 121.43, 69.40, 61.14, 36.82, 21.57, 21.14. IR (KBr, cm^{-1}) 2924, 1596, 1496, 1361, 1176, 1161, 981, 793. HRMS calcd $\text{C}_{33}\text{H}_{32}\text{N}_3\text{O}_5\text{S}_2^+$ $[\text{M}+\text{H}]^+$: 614.17780. Found: 614.17990.

Procedures for the derivatization of 6.19 via $\text{S}_{\text{N}}2$ reactions



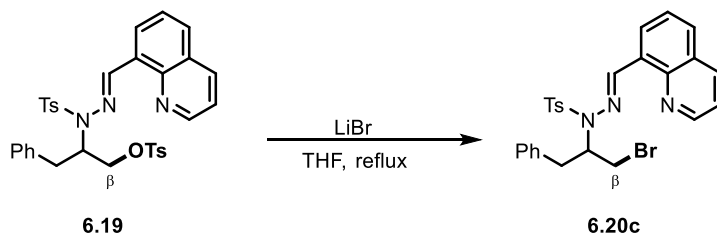
To a 4 mL vial was added PhSH (3.3 equiv., 0.1 mmol, 11 mg), NaOH (3.3 equiv., 0.1 mmol, 4 mg) and 0.5 mL EtOH. The vial was sealed with a PTFE lined cap and heated in a pie block at 40°C for 1 hr. The vial was cooled to room temperature and hydrazone **6.19** (1.0 equiv., 0.03 mmol, 18 mg) was added to the mixture. The vial was sealed and heated at 40°C again overnight. The reaction mixture was cooled to room temperature and solvent removed under vacuum. Flash column chromatography of the residue (hexane/EtOAc 30:1 to 2:1) afforded **6.20a** as a colorless oil (14.9 mg, 90% yield). $R_f = 0.7$ (hexane/EtOAc 2:1). ^1H NMR (400 MHz,

CDCl₃) δ 9.78 (s, 1H), 8.96 (dd, $J_1 = 4.1$ Hz, $J_2 = 1.8$ Hz, 1H), 8.28 (dd, $J_1 = 7.3$ Hz, $J_2 = 1.4$ Hz, 1H), 8.16 (dd, $J_1 = 8.3$ Hz, $J_2 = 1.8$ Hz, 1H), 7.87 (dd, $J_1 = 8.1$ Hz, $J_2 = 1.5$ Hz, 1H), 7.61-7.53 (m, 3H), 7.44 (dd, $J_1 = 8.3$ Hz, $J_2 = 4.2$ Hz, 1H), 7.32-7.29 (m, 2H), 7.27-7.21 (m, 5H), 7.19-7.14 (m, 3H), 7.13-7.11 (m, 2H), 4.87-4.80 (m, 1H), 3.37-3.24 (m, 3H), 3.11 (dd, $J_1 = 13.8$ Hz, $J_2 = 8.1$ Hz, 1H), 2.34 (s, 3H). ¹³C NMR (100 MHz, CDCl₃) δ 150.17, 148.38, 146.23, 143.78, 138.43, 136.09, 135.94, 135.74, 132.08, 129.78, 129.68, 129.51, 129.42, 128.91, 128.51, 128.23, 128.19, 126.39, 126.24, 126.21, 125.59, 121.38, 62.52, 38.72, 37.16, 21.55. IR (KBr, cm⁻¹) 2924, 1596, 1496, 1351, 1159, 913. HRMS calcd C₃₂H₃₀N₃O₂S₂⁺ [M+H]⁺: 552.17740. Found: 552.17960.



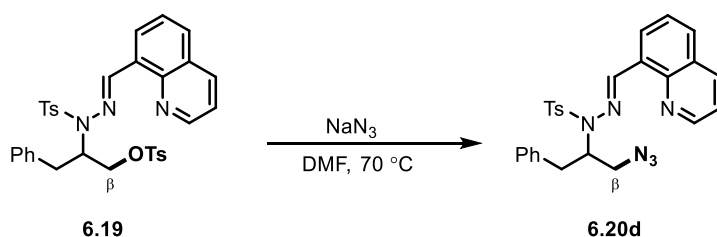
To a 4 mL vial was added NaOPh (4.0 equiv., 0.12 mmol, 14 mg), hydrazone **6.19** (1.0 equiv., 0.03 mmol, 18 mg) and 0.5 mL DMF. The vial was sealed and heated in a pie block at 100°C for 4 hrs. The reaction mixture was cooled to room temperature and diluted with 10 mL water. The mixture was extracted with DCM (3×10 mL). The combined organics were washed with water (3×10 mL) and brine, dried, filtered, and concentrated under vacuum. Flash column chromatography of the residue (hexane/EtOAc 30:1 to 2:1) afforded **6.20b** as a colorless oil (12.7 mg, 79% yield). $R_f = 0.6$ (hexane/EtOAc 2:1). ¹H NMR (400 MHz, CDCl₃) δ 9.81 (s, 1H), 8.95 (dd, $J_1 = 4.1$ Hz, $J_2 = 1.8$ Hz, 1H), 8.26 (dd, $J_1 = 7.2$ Hz, $J_2 = 1.5$ Hz, 1H), 8.15 (dd, $J_1 = 8.3$

Hz, $J_2 = 1.6$ Hz, 1H), 7.85 (dd, $J_1 = 8.2$ Hz, $J_2 = 1.4$ Hz, 1H), 7.70-7.66 (m, 2H), 7.59-7.55 (m, 1H), 7.43 (dd, $J_1 = 8.3$ Hz, $J_2 = 4.2$ Hz, 1H), 7.27-7.21 (m, 7H), 7.17-7.14 (m, 2H), 6.93-6.89 (m, 1H), 6.86-6.82 (m, 2H), 5.19-5.12 (m, 1H), 4.32 (dd, $J_1 = 9.7$ Hz, $J_2 = 6.7$ Hz, 1H), 4.16 (dd, $J_1 = 9.7$ Hz, $J_2 = 5.6$ Hz, 1H), 3.24 (dd, $J_1 = 13.8$ Hz, $J_2 = 6.9$ Hz, 1H), 3.16 (dd, $J_1 = 13.8$ Hz, $J_2 = 8.0$ Hz, 1H), 2.34 (s, 3H). ^{13}C NMR (100 MHz, CDCl_3) δ 158.44, 150.11, 147.43, 146.22, 143.77, 138.15, 136.08, 135.93, 132.15, 129.65, 129.55, 129.41, 129.32, 128.56, 128.36, 128.18, 126.49, 126.24, 125.49, 121.36, 120.85, 114.68, 68.39, 62.01, 36.93, 21.54. IR (KBr, cm^{-1}) 2972, 1598, 1496, 1242, 1160, 1048, 913. HRMS calcd $\text{C}_{32}\text{H}_{30}\text{N}_3\text{O}_3\text{S}^+$ $[\text{M}+\text{H}]^+$: 536.20020. Found: 536.20260.



To a 4 mL vial was added LiBr (5.0 equiv., 0.15 mmol, 13 mg), hydrazone **6.19** (1.0 equiv., 0.03 mmol, 18 mg) and 0.5 mL THF. The vial was sealed and heated at reflux for 48 hrs. The reaction mixture was cooled to room temperature and concentrated under vacuum. Flash column chromatography of the residue (hexane/EtOAc 20:1 to 2:1) afforded **6.20c** as a colorless oil (13.7 mg, 88% yield). $R_f = 0.6$ (hexane/EtOAc 2:1). ^1H NMR (400 MHz, CDCl_3) δ 9.85 (s, 1H), 8.98 (dd, $J_1 = 4.2$ Hz, $J_2 = 1.8$ Hz, 1H), 8.27 (dd, $J_1 = 7.3$ Hz, $J_2 = 1.4$ Hz, 1H), 8.16 (dd, $J_1 = 8.3$ Hz, $J_2 = 1.8$ Hz, 1H), 7.88 (dd, $J_1 = 8.1$ Hz, $J_2 = 1.5$ Hz, 1H), 7.67-7.63 (m, 2H), 7.60-7.56 (m, 1H), 7.45 (dd, $J_1 = 8.3$ Hz, $J_2 = 4.2$ Hz, 1H), 7.29-7.18 (m, 7H), 4.98-4.91 (m, 1H), 3.66 (dd,

$J_1 = 10.5$ Hz, $J_2 = 6.7$ Hz, 1H), 3.61 (dd, $J_1 = 10.5$ Hz, $J_2 = 6.6$ Hz, 1H), 3.26 (dd, $J_1 = 13.9$ Hz, $J_2 = 6.5$ Hz, 1H), 3.12 (dd, $J_1 = 13.9$ Hz, $J_2 = 7.9$ Hz, 1H), 2.36 (s, 3H). ^{13}C NMR (100 MHz, CDCl_3) δ 150.23, 149.35, 145.97, 144.08, 137.77, 135.88, 135.83, 131.83, 129.99, 129.54, 129.48, 128.62, 128.28, 128.21, 126.61, 126.22, 125.68, 121.44, 63.99, 38.21, 34.13, 21.54. IR (KBr, cm^{-1}) 2924, 1595, 1496, 1351, 1161, 913. HRMS calcd $\text{C}_{26}\text{H}_{25}\text{BrN}_3\text{O}_2\text{S}^+$ $[\text{M}+\text{H}]^+$: 544.06650. Found: 544.06660.

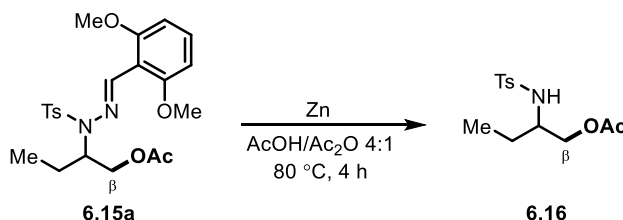


To a 4 mL vial was added NaN_3 (5.0 equiv., 0.15 mmol, 10 mg), hydrazone **6.19** (1.0 equiv., 0.03 mmol, 18 mg) and 0.5 mL DMF. The vial was sealed and heated in a pie block at 70°C for 24 hrs. The reaction mixture was cooled to room temperature and diluted with 10 mL water. The mixture was extracted with DCM (3×10 mL). The combined organics were washed with water (3×10 mL) and brine, dried, filtered, and concentrated under vacuum. Flash column chromatography of the residue (hexane/EtOAc 35:1 to 2:1) afforded **6.20d** as a colorless oil (12.6 mg, 87% yield). $R_f = 0.7$ (hexane/EtOAc 2:1). ^1H NMR (400 MHz, CDCl_3) δ 9.91 (s, 1H), 8.98 (dd, $J_1 = 4.2$ Hz, $J_2 = 1.8$ Hz, 1H), 8.29 (dd, $J_1 = 7.2$ Hz, $J_2 = 1.5$ Hz, 1H), 8.17 (dd, $J_1 = 8.4$ Hz, $J_2 = 1.9$ Hz, 1H), 7.89 (dd, $J_1 = 8.2$ Hz, $J_2 = 1.4$ Hz, 1H), 7.70-7.67 (m, 2H), 7.61-7.57 (m, 1H), 7.45 (dd, $J_1 = 8.3$ Hz, $J_2 = 4.2$ Hz, 1H), 7.30-7.19 (m, 7H), 4.86-4.79 (m, 1H), 3.68 (dd, $J_1 = 12.6$ Hz, $J_2 = 8.2$ Hz, 1H), 3.44 (dd, $J_1 = 12.6$ Hz, $J_2 = 5.1$ Hz, 1H), 3.09-2.98 (m, 2H), 2.36 (s,

3H). ^{13}C NMR (100 MHz, CDCl_3) δ 150.29, 149.72, 146.37, 144.09, 137.67, 135.96, 135.84, 131.89, 130.05, 129.55, 129.44, 128.66, 128.27, 128.22, 126.66, 126.22, 125.65, 121.46, 62.34, 53.05, 37.81, 21.58. IR (KBr, cm^{-1}) 2924, 2100, 1496, 1354, 1160, 913. HRMS calcd $\text{C}_{26}\text{H}_{25}\text{N}_6\text{O}_2\text{S}^+$ $[\text{M}+\text{H}]^+$: 485.17540. Found: 485.17740.

Procedures for the directing group and protecting group removal

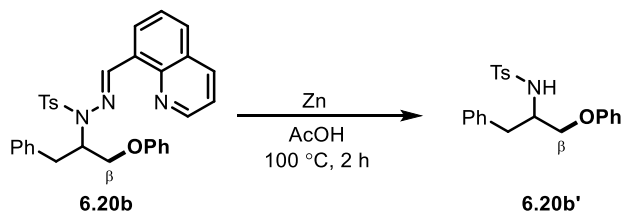
Procedure for removal of 2,6-dimethoxyphenyl-based directing group



To a 4 mL vial was added **6.15a** (1.0 equiv., 0.05 mmol, 22 mg), 0.8 mL AcOH, and 0.2 mL Ac_2O . Zn powder (3.0 equiv., 0.15 mmol, 10 mg) was added to the mixture. The vial was sealed with a PTFE lined cap and heated in a pie block at 80°C for 4 hrs. The reaction mixture was cooled to room temperature and passed through a small plug of silica gel. The filtrate was concentrated under vacuum and purified by flash column chromatography (hexane/EtOAc 20:1 to 2:1) to give **6.16** as a colorless oil (12.8 mg, 90% yield). $R_f = 0.7$ (hexane/EtOAc 1:1). ^1H NMR (400 MHz, CDCl_3) δ 7.77-7.74 (m, 2H), 7.31-7.28 (m, 2H), 4.67 (d, $J = 8.5$ Hz, 1H), 4.00 (dd, $J_1 = 11.5$ Hz, $J_2 = 5.5$ Hz, 1H), 3.88 (dd, $J_1 = 11.5$ Hz, $J_2 = 4.3$ Hz, 1H), 3.44-3.36 (m, 1H), 2.42 (s, 3H), 1.93 (s, 3H), 1.56-1.41 (m, 2H), 0.82 (t, $J = 7.5$ Hz, 3H). ^{13}C NMR (100 MHz, CDCl_3) δ 170.82, 143.39, 138.02, 129.65, 126.97, 65.38, 54.24, 25.45, 21.51, 20.63, 9.95. IR

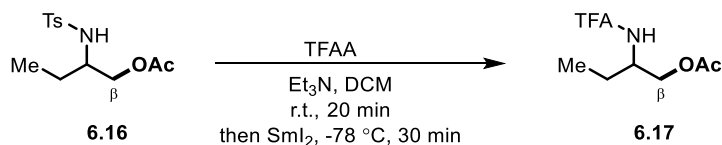
(KBr, cm^{-1}) 3285, 2970, 1743, 1329, 1162, 1094, 816. **HRMS** calcd $\text{C}_{13}\text{H}_{19}\text{NO}_4\text{SNa}^+$ $[\text{M}+\text{Na}]^+$: 308.09270. Found: 308.09320.

Procedure for removal of quinoline-based directing group



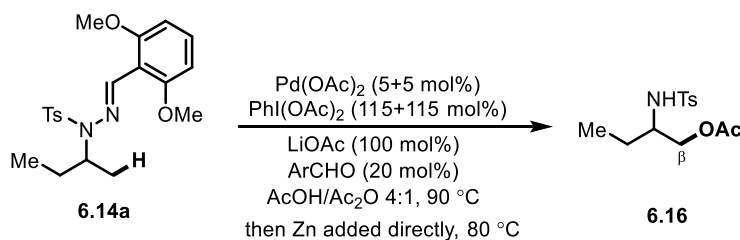
To a 4 mL vial was added **6.20b** (1.0 equiv., 0.05 mmol, 27 mg) and 2.0 mL AcOH. Zn powder (10 equiv., 0.5 mmol, 32 mg) was added to the mixture. The vial was sealed with a PTFE lined cap and heated in a pie block at 100°C for 2 hrs. The reaction mixture was cooled to room temperature and passed through a small plug of silica gel. The filtrate was concentrated under vacuum and purified by flash column chromatography (hexane/EtOAc 20:1 to 2:1) to give **6.20b'** as a colorless oil (12.0 mg, 63% yield). $R_f = 0.5$ (hexane/EtOAc 1:1). **$^1\text{H NMR}$** (400 MHz, CDCl_3) δ 7.65 (d, $J = 8.3$ Hz, 2H), 7.26-7.24 (m, 2H), 7.21-7.18 (m, 5H), 7.06-7.02 (m, 2H), 6.98-6.94 (m, 1H), 6.78-6.76 (m, 2H), 4.89 (d, $J = 7.7$ Hz, 1H), 3.87-3.83 (m, 1H), 3.79-3.72 (m, 2H), 3.00-2.86 (m, 2H), 2.39 (s, 3H). **$^{13}\text{C NMR}$** (100 MHz, CDCl_3) δ 158.02, 143.32, 137.34, 136.61, 129.64, 129.47, 129.33, 128.65, 126.93, 126.73, 121.24, 114.39, 67.53, 54.12, 38.19, 21.49. **IR** (KBr, cm^{-1}) 3282, 2927, 1599, 1496, 1329, 1244, 1160, 913, 748. **HRMS** calcd $\text{C}_{22}\text{H}_{23}\text{NO}_3\text{SNa}^+$ $[\text{M}+\text{Na}]^+$: 404.12910. Found: 404.13060.

Procedure for switch of *p*-toluenesulfonyl protecting group



To a 50 mL Schlenk tube were added **6.16** (1.0 equiv., 0.2 mmol, 56 mg), triethylamine (2.0 equiv., 0.4 mmol, 60 μ L), and 3 mL DCM. Trifluoroacetic anhydride (TFAA, 2.0 equiv., 0.4 mmol, 60 μ L) was added to this mixture. The reaction was stirred at room temperature for 20 min. The solvent was removed under vacuum and the residue was diluted with 2 mL THF. The Schlenk tube was purged evacuated and refilled with N₂ for three times. The solution was cooled to -78°C and 10 mL 0.1 M SmI₂ THF (5.0 equiv.) solution was added dropwise to the reaction mixture. The reaction was stirred at the same temperature for 30 min. Several drops of methanol were added to quench the reaction, where the deep blue color disappeared. The reaction mixture was passed through a plug of silica gel, eluted with EtOAc, and the filtrate was concentrated under vacuum. Flash column chromatography of the residue gave **6.17** as a white solid (40.0 mg, 88% yield). Mp. 68-70 °C. *R_f* = 0.8 (DCM/MeOH 20:1). **¹H NMR** (400 MHz, CDCl₃) δ 6.43 (br, 1H), 4.24-4.10 (m, 3H) 2.09 (s, 3H), 1.71-1.52 (m, 2H), 0.98 (t, *J* = 7.5 Hz, 3H). **¹³C NMR** (100 MHz, CDCl₃) δ 171.19, 157.08 (q, *J* = 37.0 Hz), 115.76 (q, *J* = 288.0 Hz), 64.73, 51.03, 24.12, 20.67, 10.10. **¹⁹F NMR** (376 MHz, CDCl₃) δ -76.00 (s, 3F). **IR** (KBr, cm⁻¹) 3318, 2972, 1747, 1715, 1556, 1183, 913. **HRMS** calcd C₈H₁₂F₃NO₃Na⁺ [*M*+Na]⁺: 250.06610. Found: 250.06610.

Procedure for one-pot acetoxylation/directing group removal



A 4 mL vial was charged with $\text{Pd}(\text{OAc})_2$ (5 mol%, 0.005 mmol, 1.2 mg), $\text{PhI}(\text{OAc})_2$ (115 mmol%, 0.115 mmol, 37 mg), LiOAc (1.0 equiv., 0.10 mmol, 6.6 mg), 2,6-dimethoxybenzaldehyde (20 mol%, 0.02 mmol, 3.3 mg) and hydrazone substrate **6.14a** (1.0 equiv., 0.10 mmol, 39 mg). To the mixture was added 0.8 mL AcOH and 0.2 mL Ac_2O . The vial was sealed with a PTFE lined cap and heated in a pie block at 90°C. The acetoxylation reaction was monitored by TLC. When the formation of palladium black was observed, the vial was removed from the pie block and allowed to cool to room temperature. Another portion of $\text{Pd}(\text{OAc})_2$ (5 mol%, 0.005 mmol, 1.2 mg) and $\text{PhI}(\text{OAc})_2$ (115 mmol%, 0.115 mmol, 37 mg) was added to the reaction. The vial was sealed and heated in a pie block at 90°C again. When TLC indicated the hydrazone was fully consumed, the reaction was cooled to room temperature and Zn powder (3.0 equiv., 0.30 mmol, 20 mg) was added. The vial was sealed again and heated in a pie block at 80°C for 3 hrs. The reaction was cooled to room temperature and passed through a small plug of silica gel. The solvent was removed under vacuum. Flash column chromatography (hexane/ EtOAc 20:1 to 2:1) of the residue gave **6.16** as a colorless oil (18.8 mg, 66% yield).

6.5 ^1H -NMR and ^{13}C -NMR Spectra

Figure 6.6 ^1H -NMR and ^{13}C -NMR Spectrum of **6.14a**

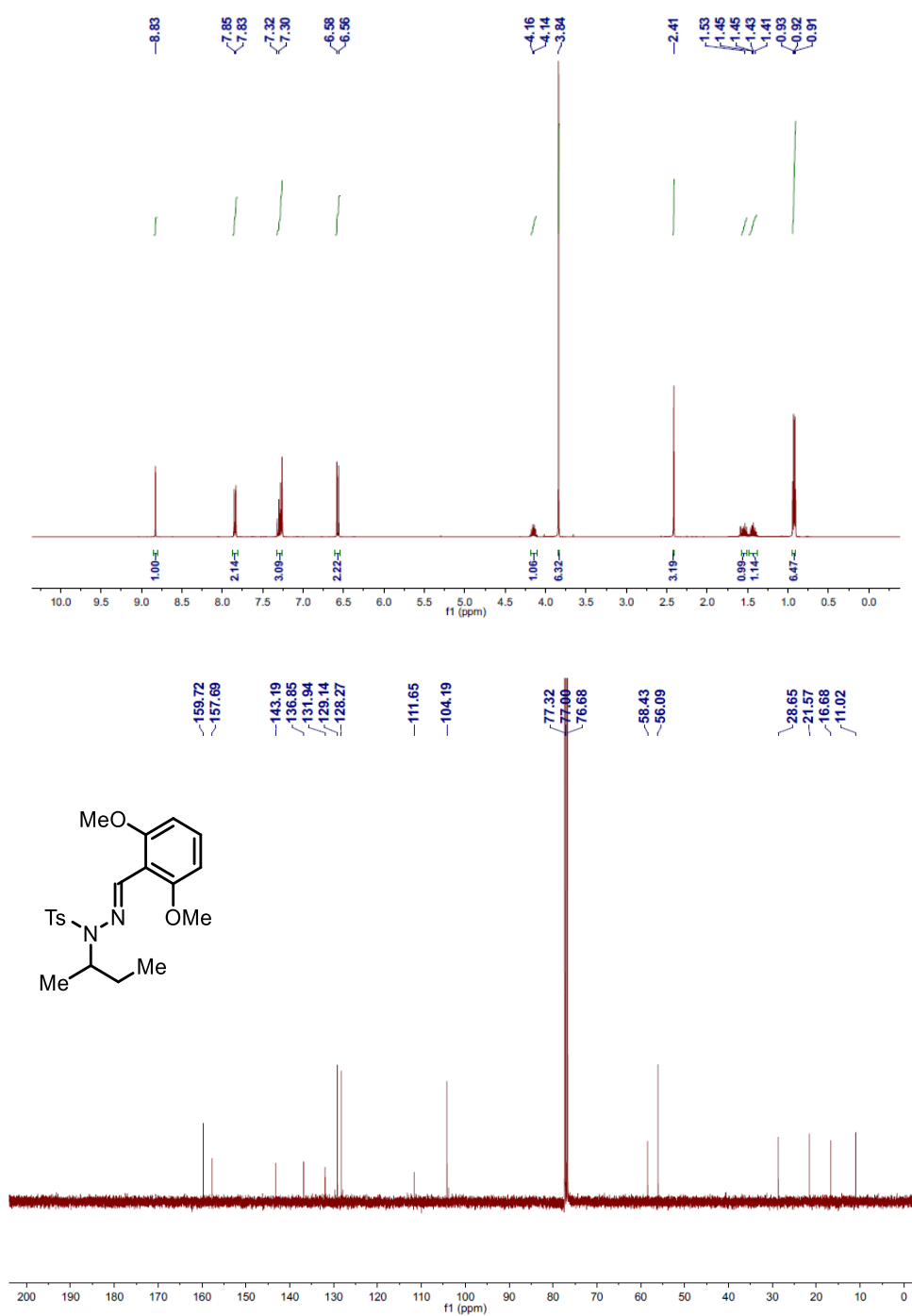


Figure 6.7 $^1\text{H-NMR}$ and $^{13}\text{C-NMR}$ Spectrum of **6.14b**

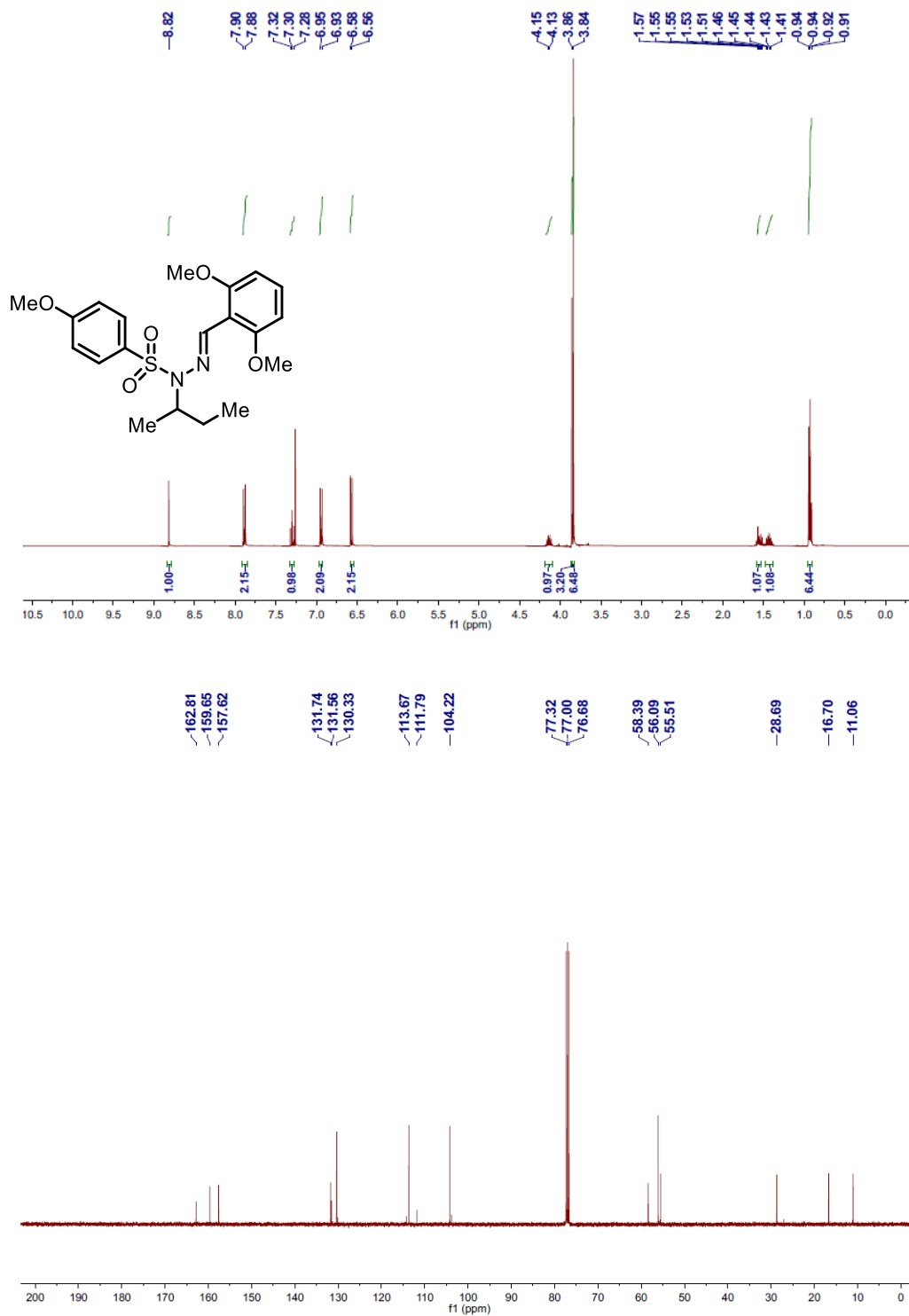


Figure 6.8 $^1\text{H-NMR}$ and $^{13}\text{C-NMR}$ Spectrum of **6.14c**

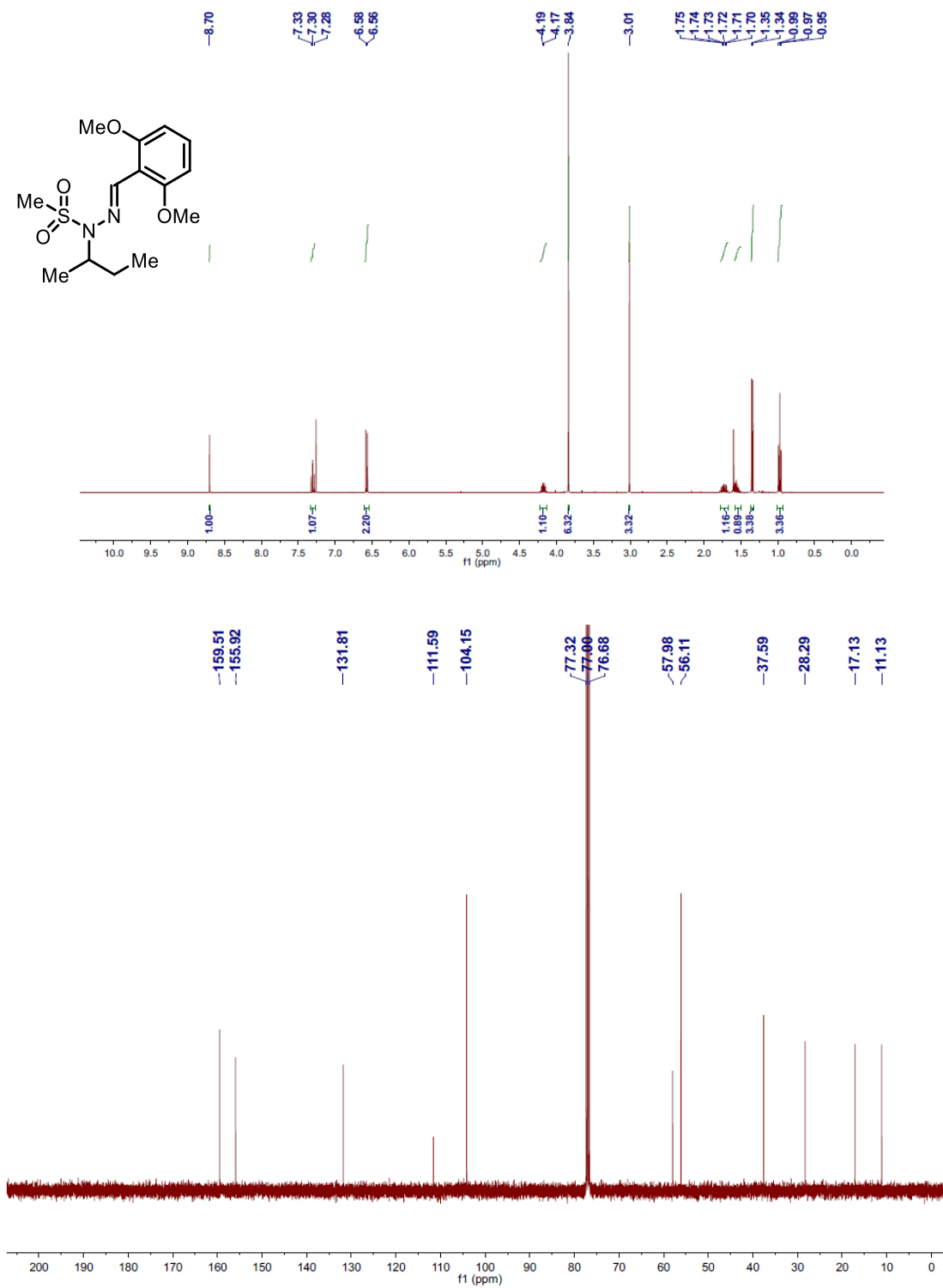


Figure 6.9 $^1\text{H-NMR}$ and $^{13}\text{C-NMR}$ Spectrum of 6.14d

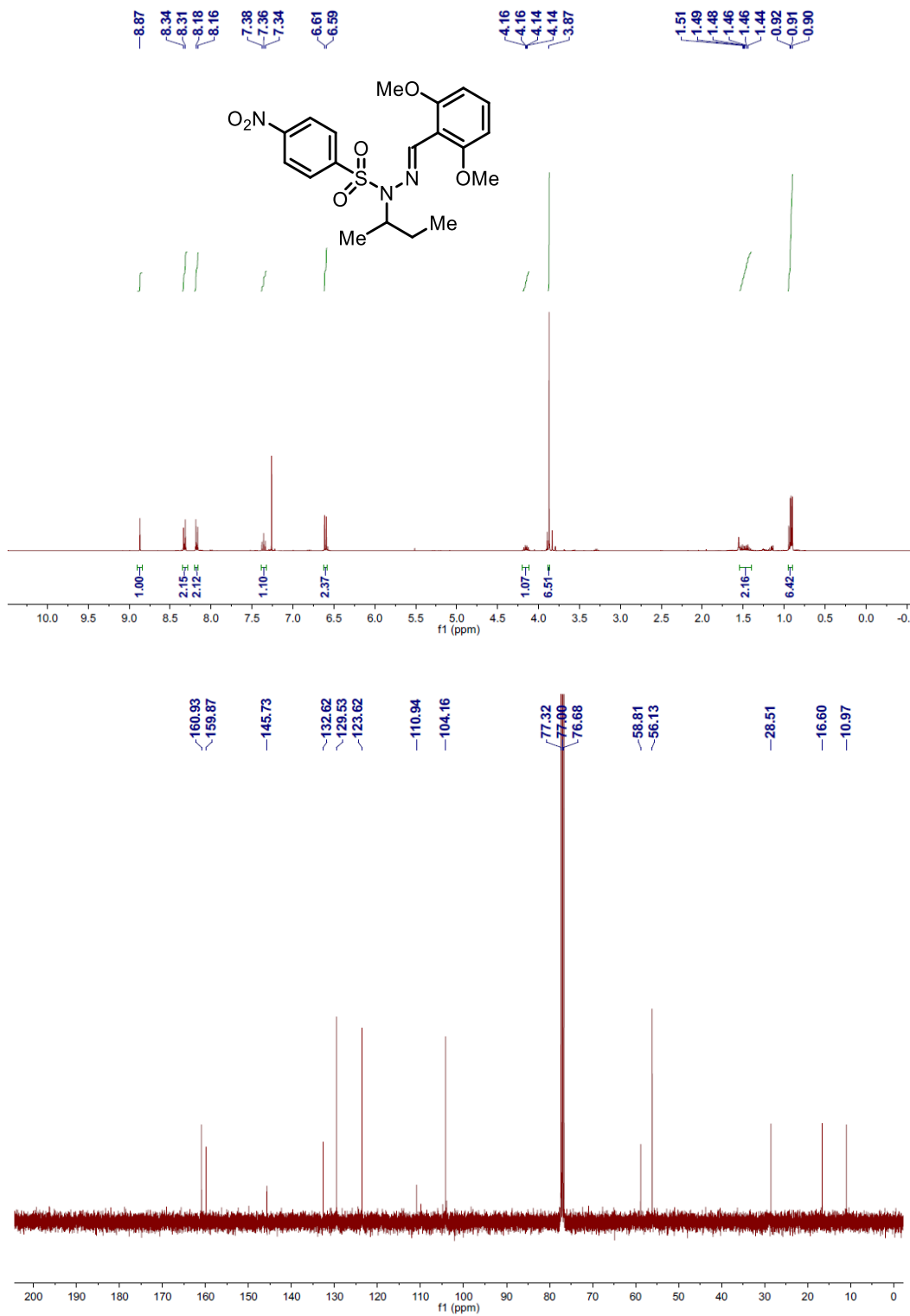


Figure 6.10 ^1H -NMR and ^{13}C -NMR Spectrum of **6.14e**

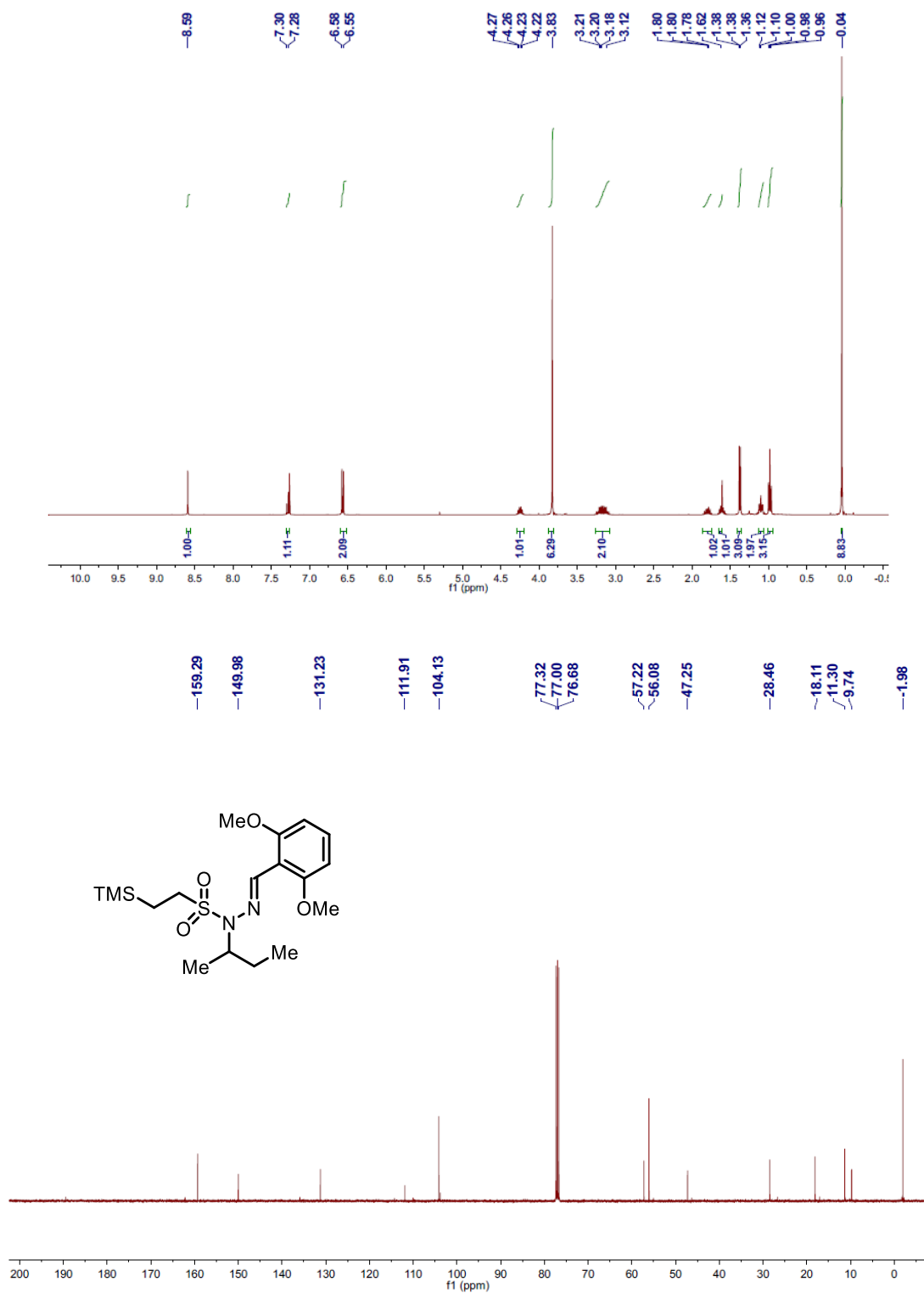


Figure 6.11 ^1H -NMR and ^{13}C -NMR Spectrum of 6.14f

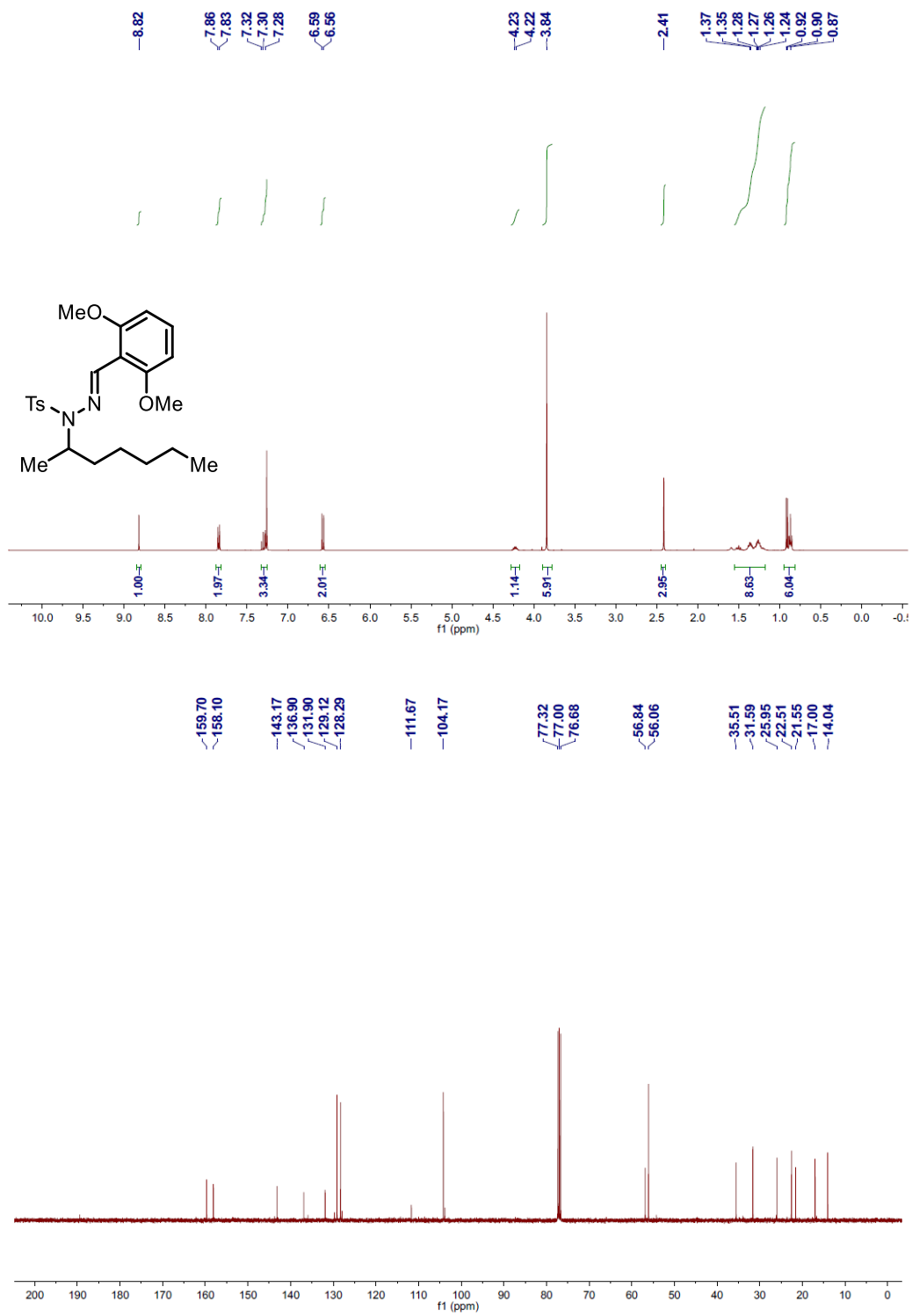


Figure 6.12 ^1H -NMR and ^{13}C -NMR Spectrum of 6.14g

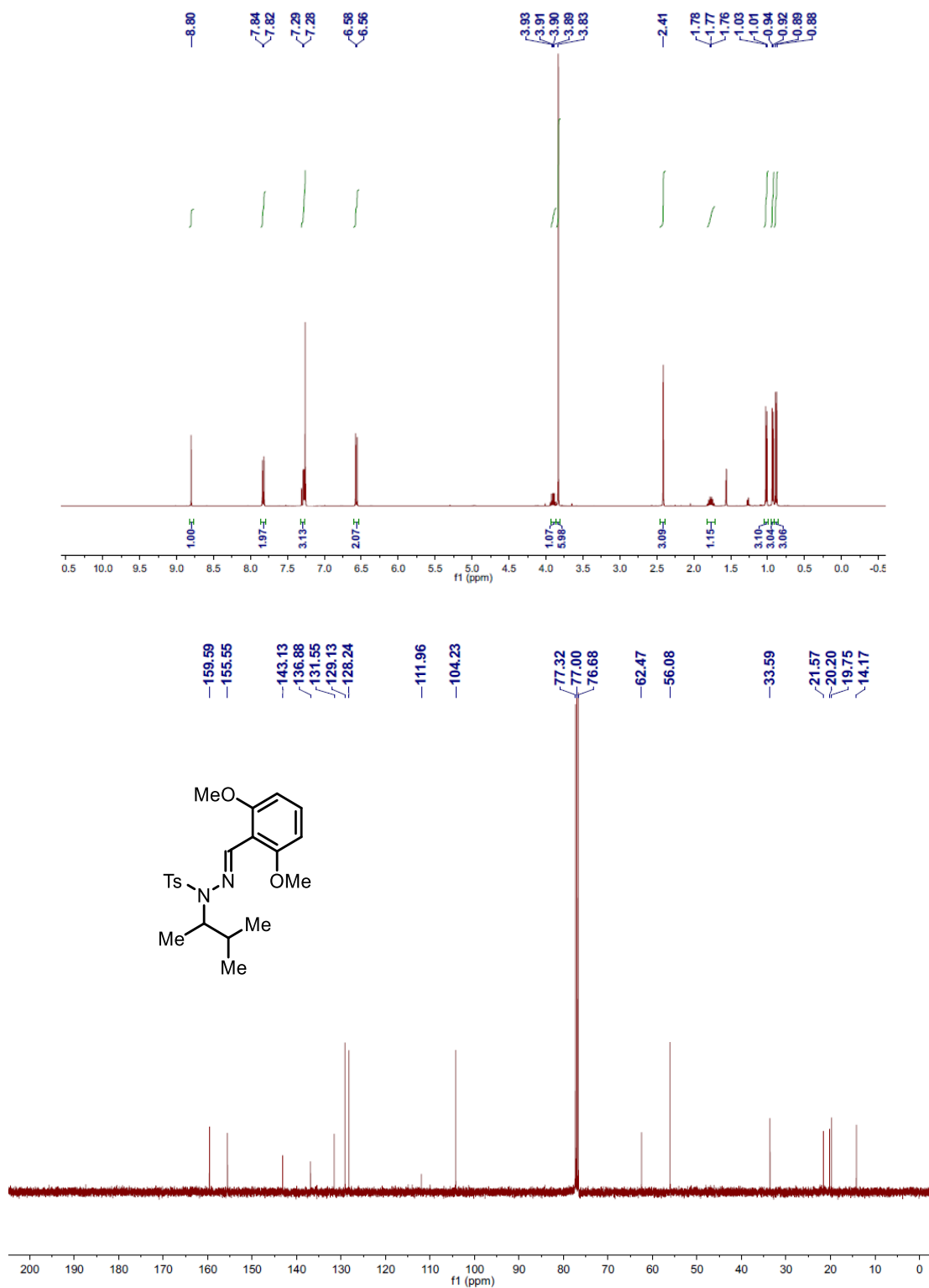


Figure 6.13 ¹H-NMR and ¹³C-NMR Spectrum of 6.14h

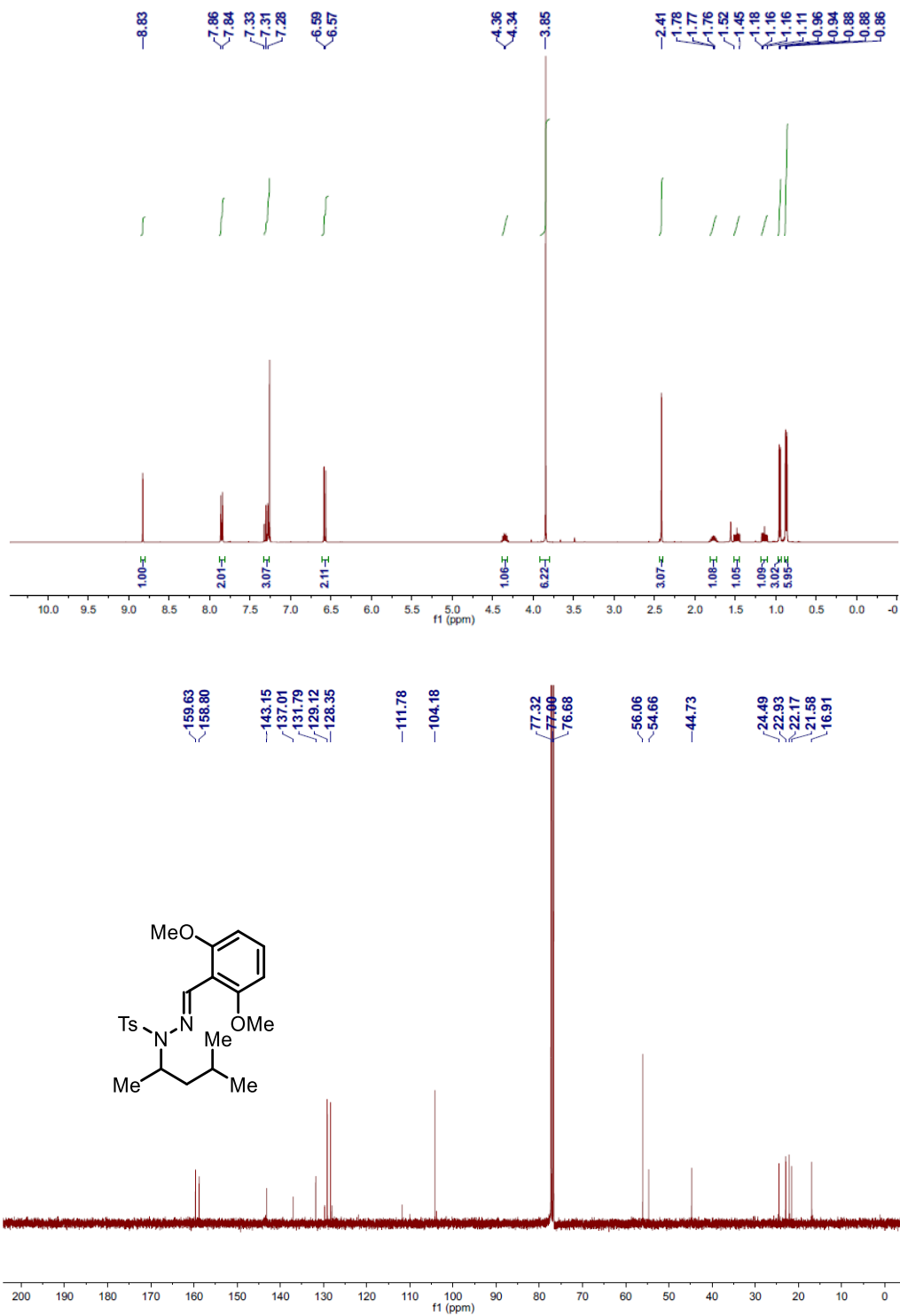


Figure 6.14 ¹H-NMR and ¹³C-NMR Spectrum of 6.14i

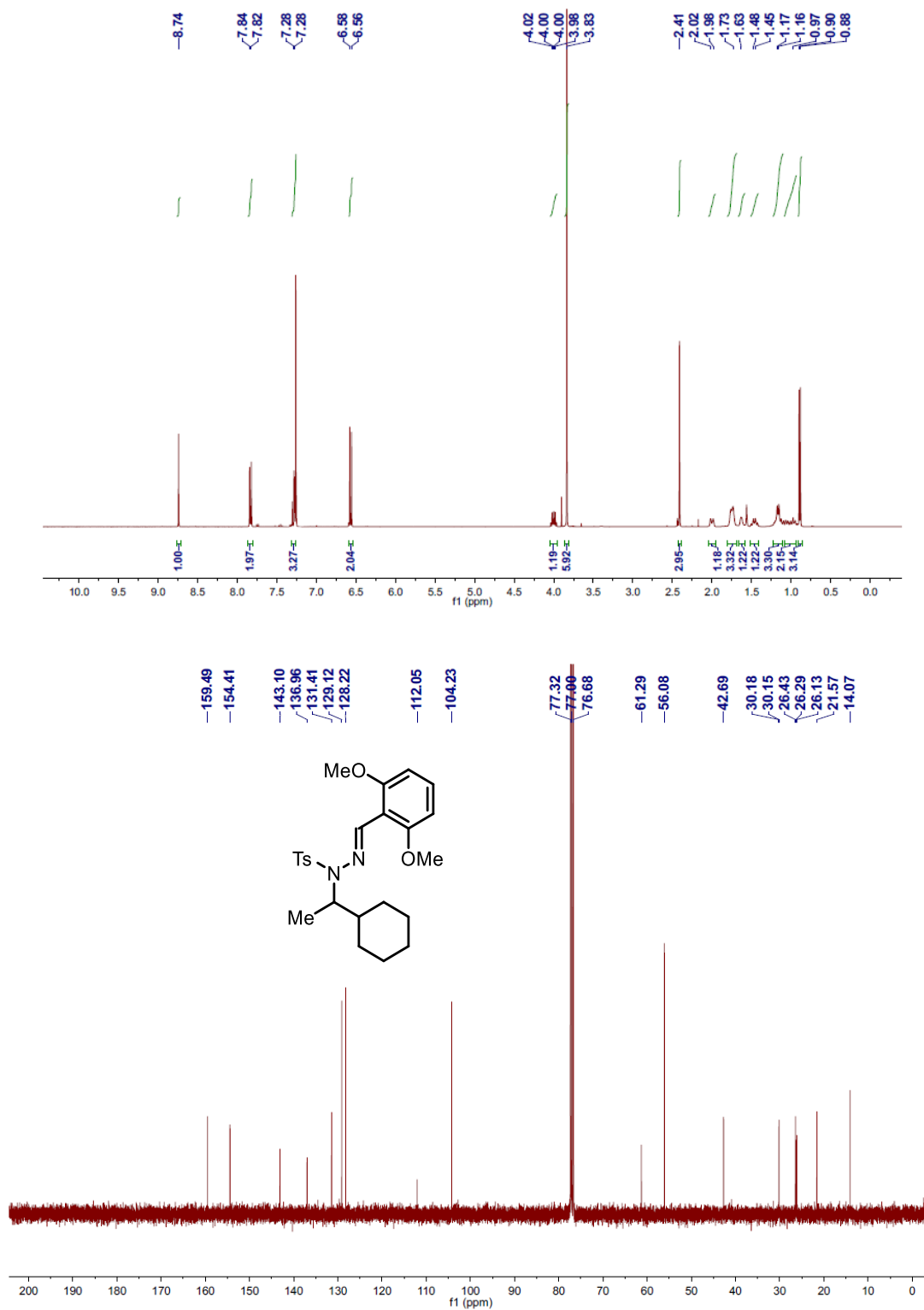


Figure 6.15 ^1H -NMR and ^{13}C -NMR Spectrum of 6.14j

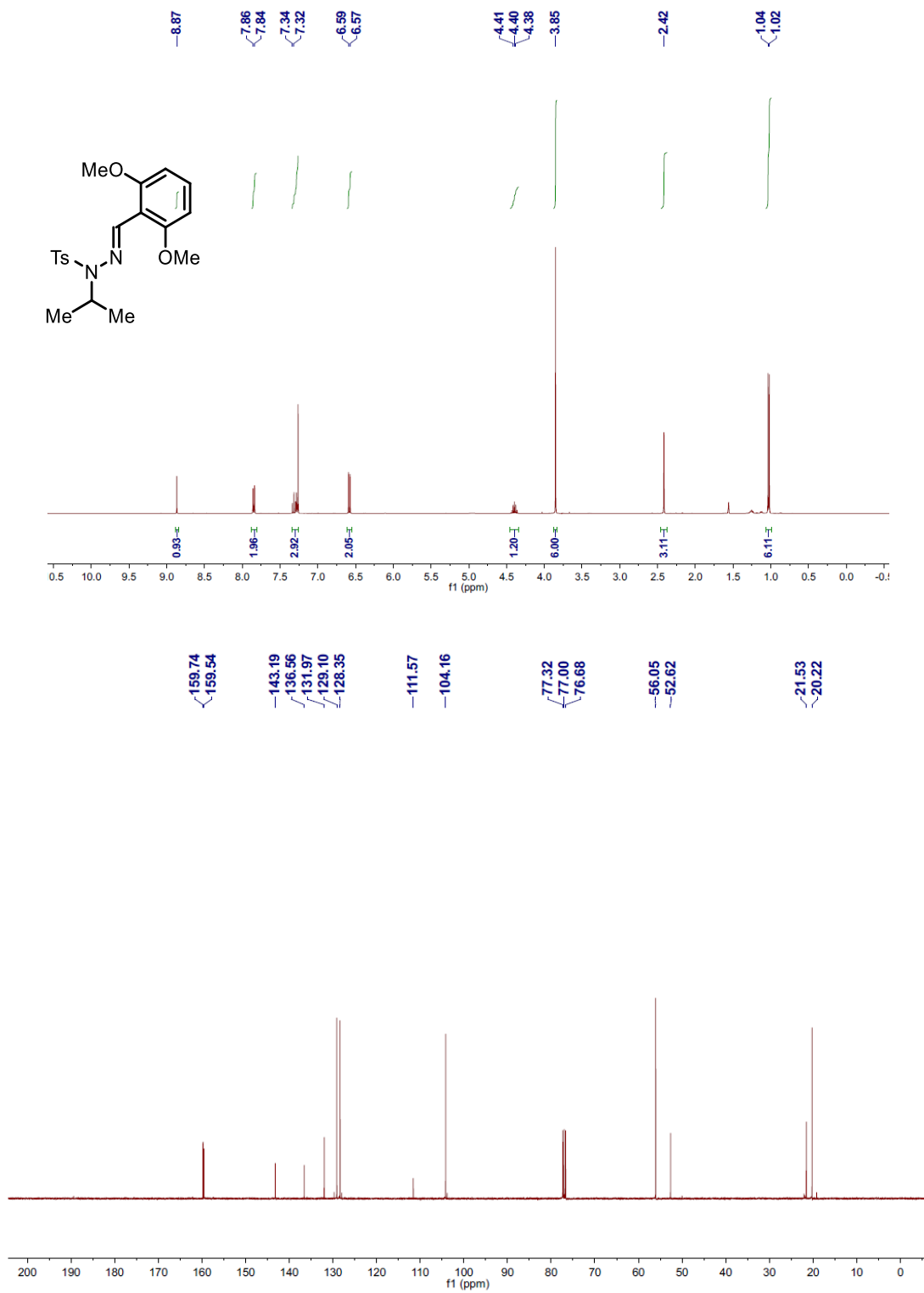


Figure 6.16 ¹H-NMR and ¹³C-NMR Spectrum of 6.14k

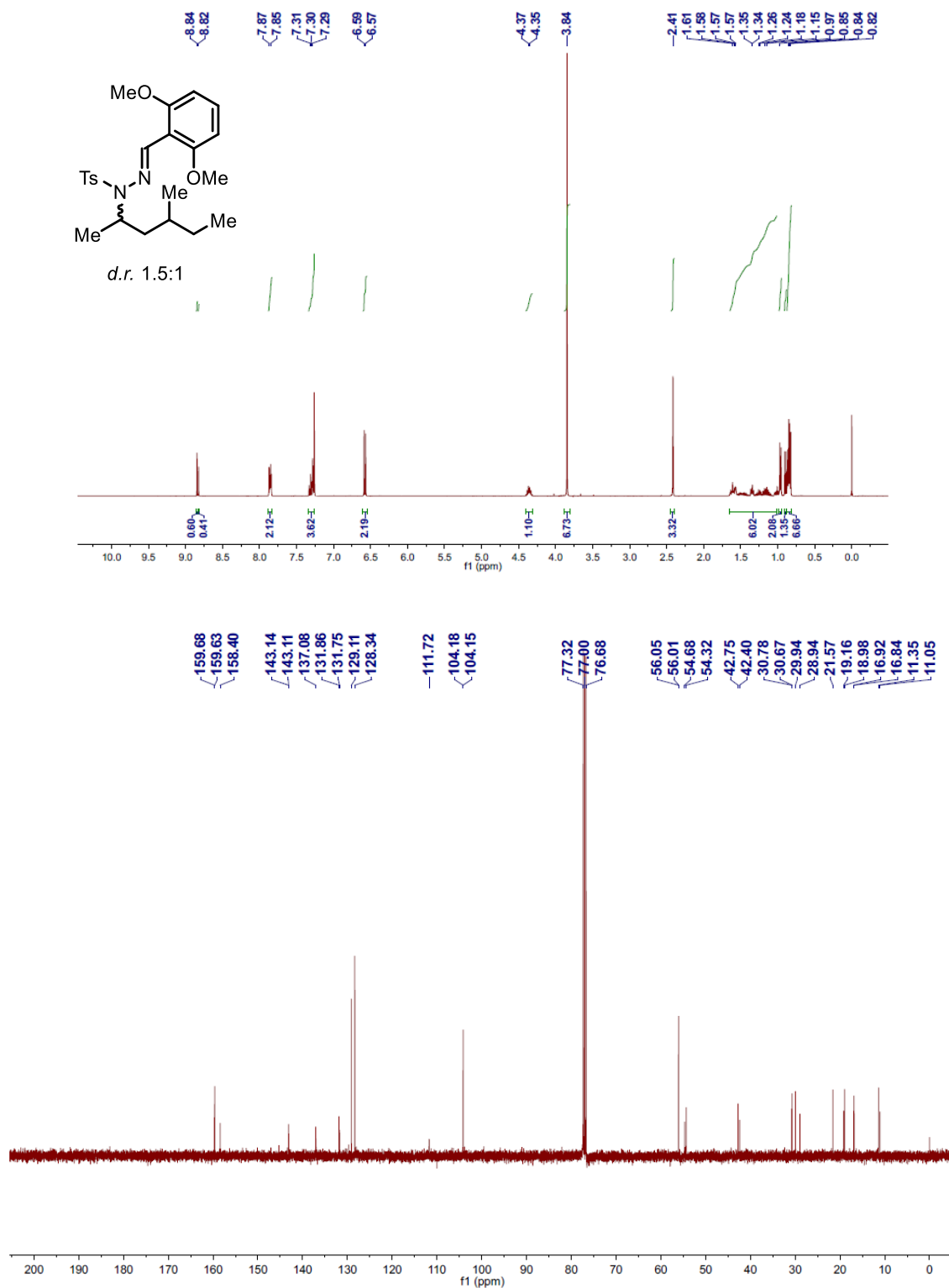


Figure 6.17 ¹H-NMR and ¹³C-NMR Spectrum of 6.14I

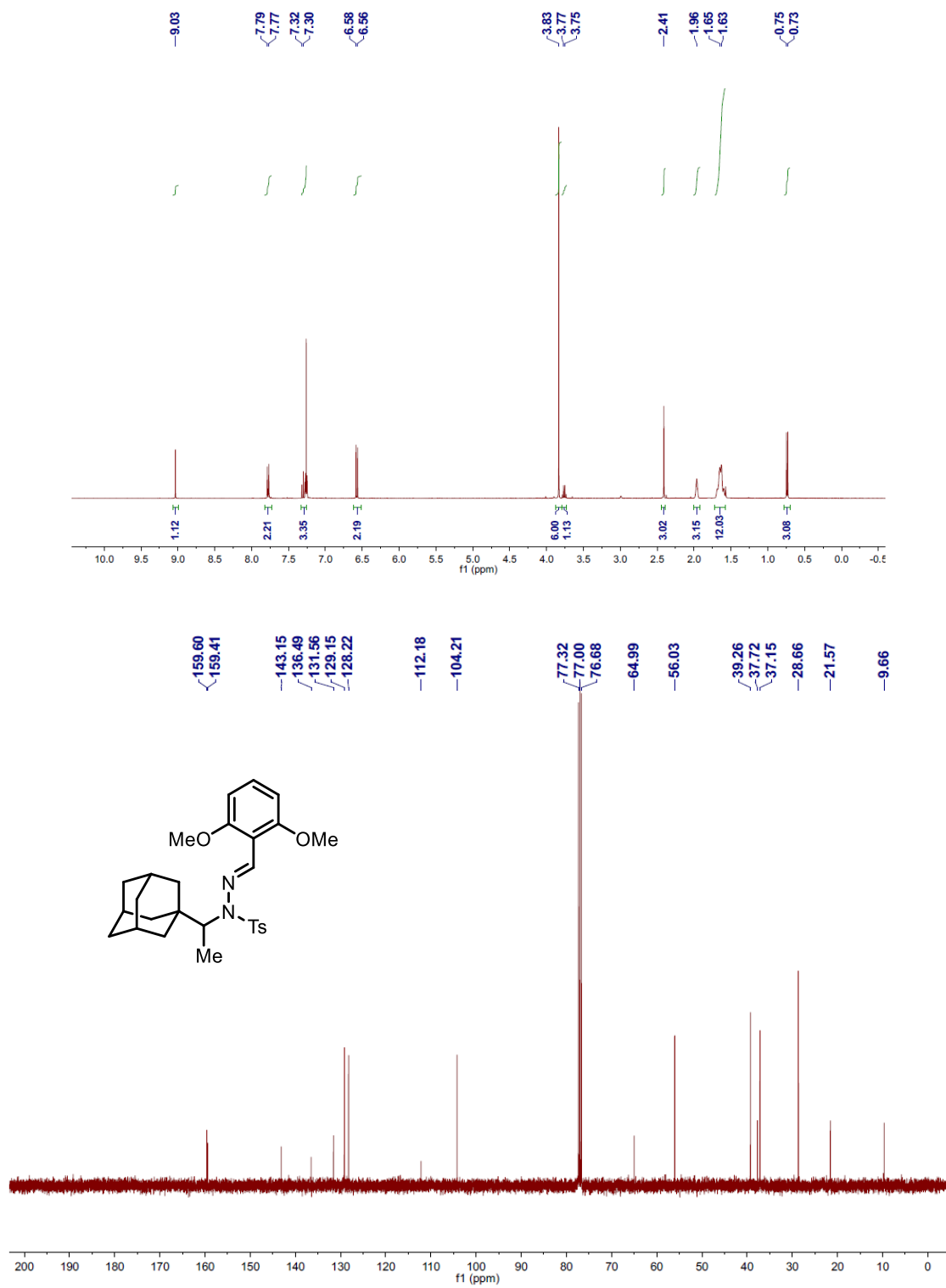


Figure 6.18 ^1H -NMR and ^{13}C -NMR Spectrum of 6.14m

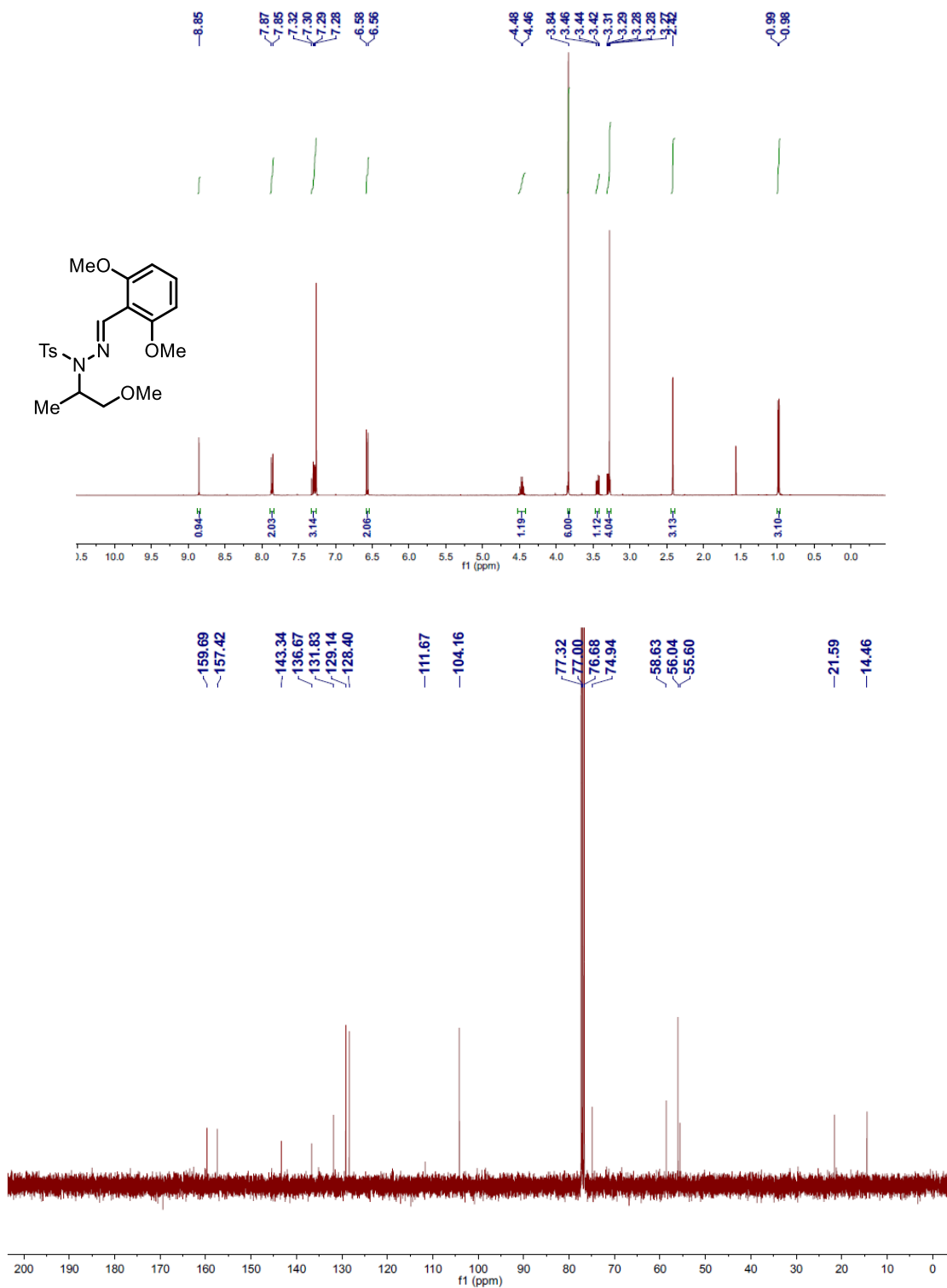


Figure 6.19 ^1H -NMR and ^{13}C -NMR Spectrum of 6.14n

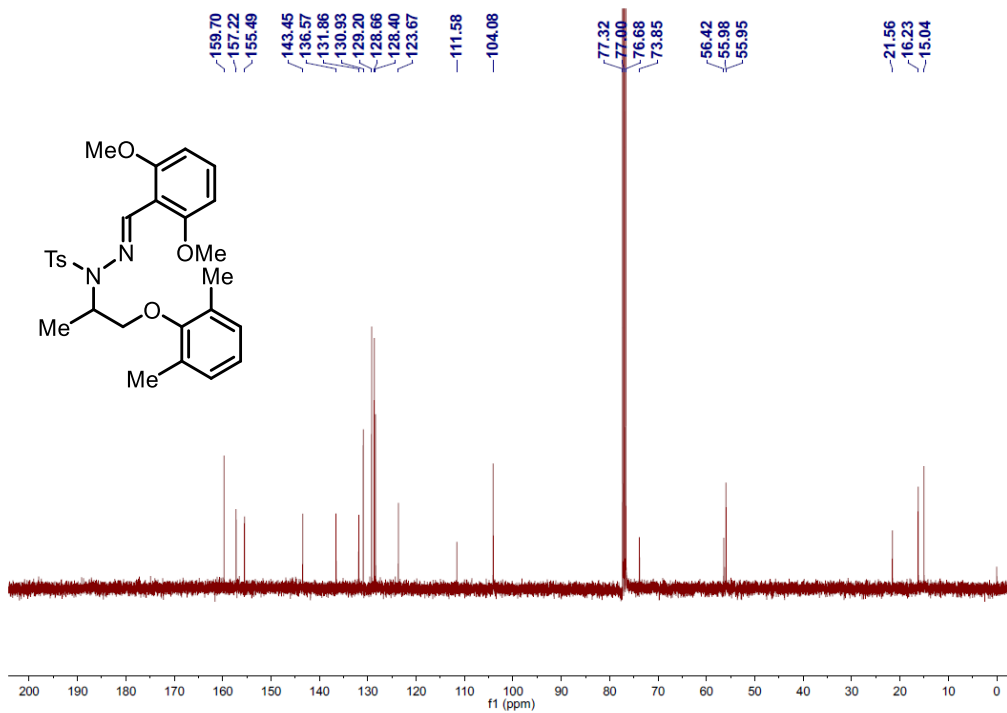
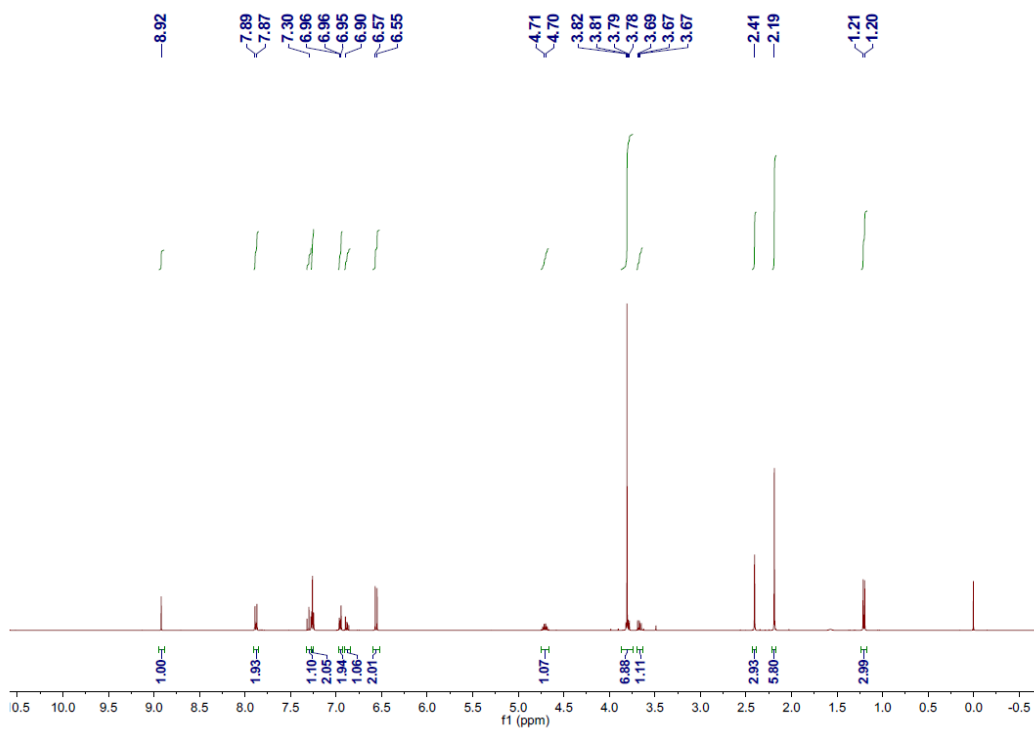


Figure 6.20 ^1H -NMR and ^{13}C -NMR Spectrum of 6.14o

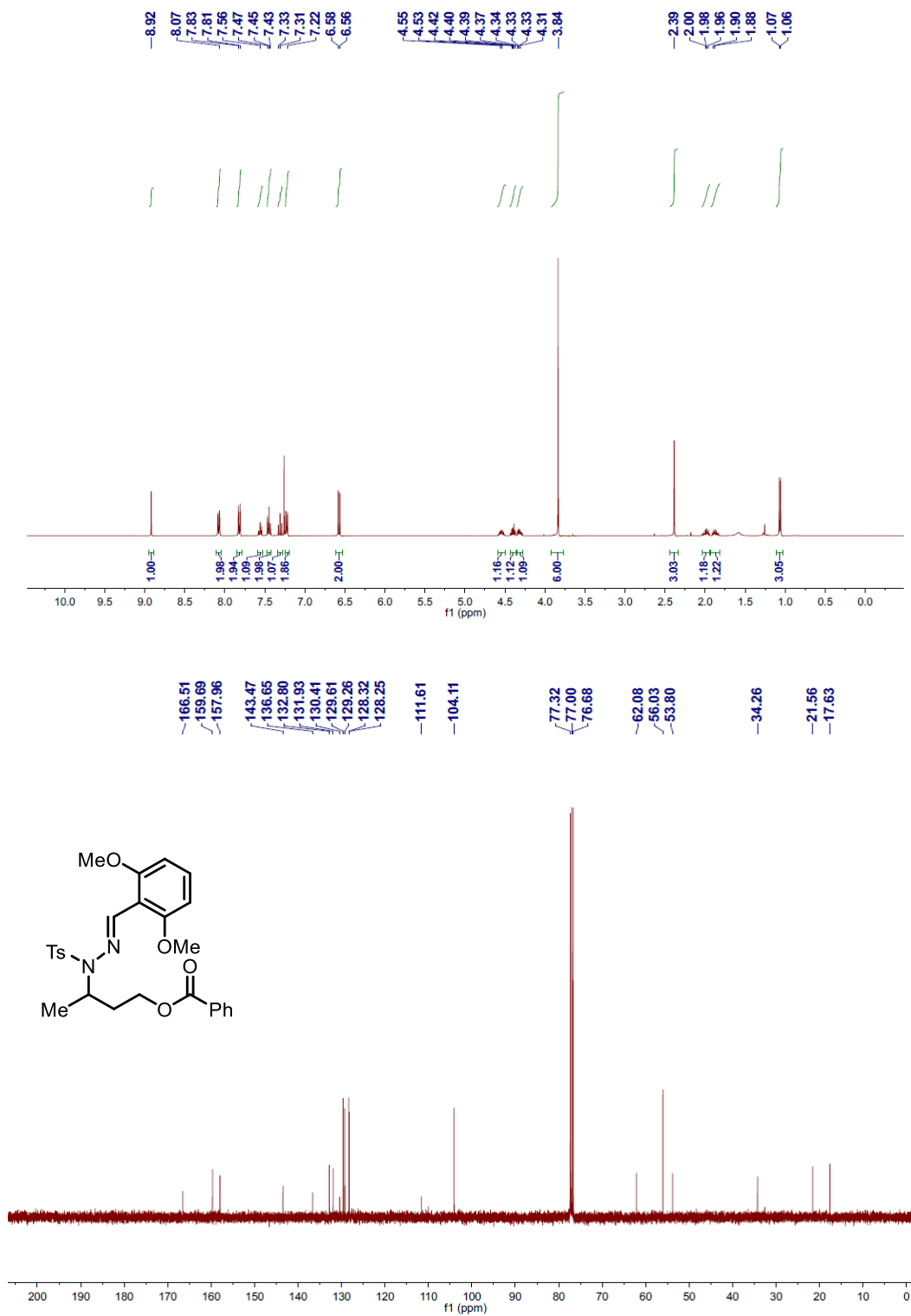


Figure 6.22 ¹H-NMR and ¹³C-NMR Spectrum of 6.14q

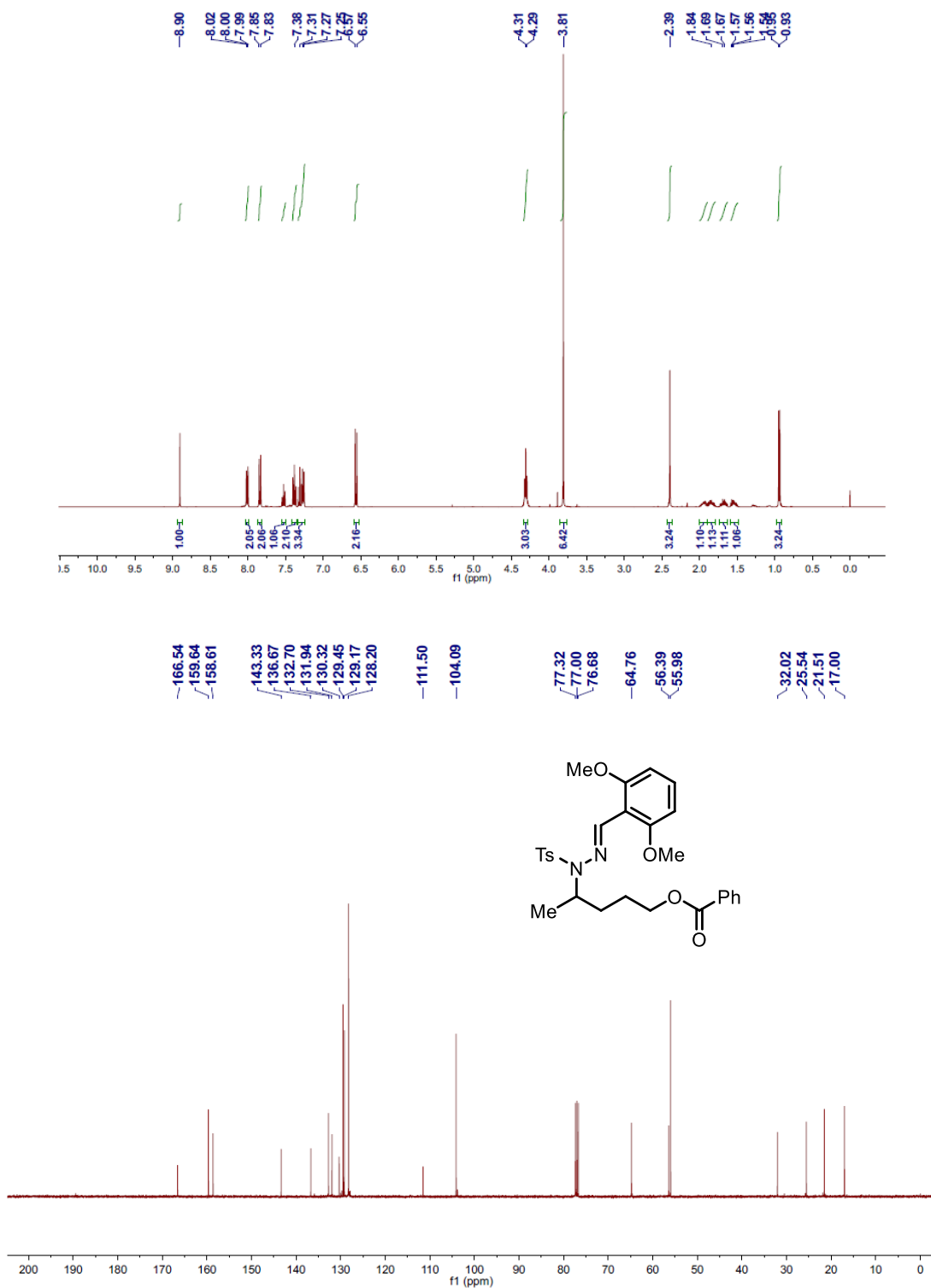


Figure 6.23 ^1H -NMR and ^{13}C -NMR Spectrum of **6.14r**

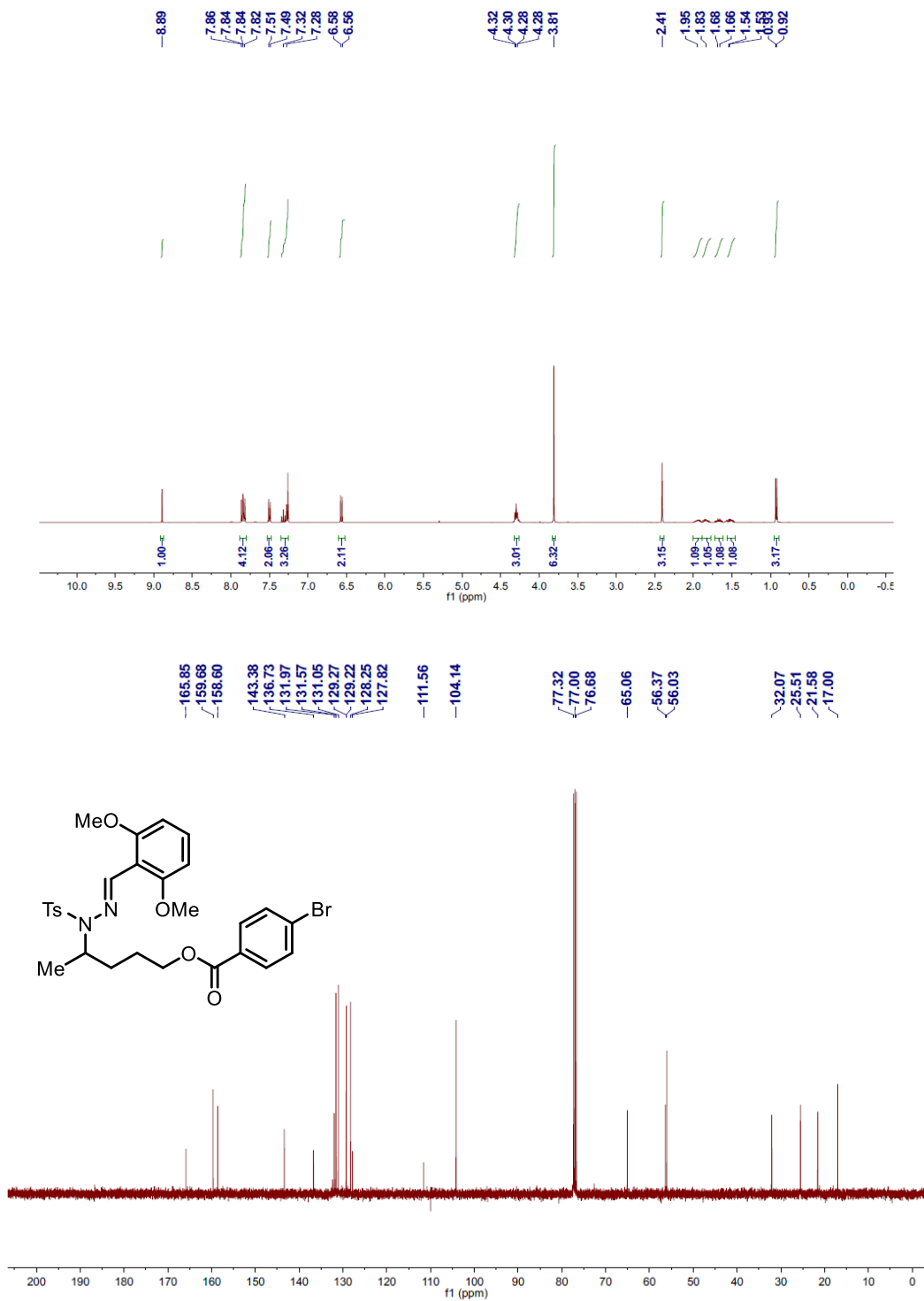


Figure 6.25 ^1H -NMR and ^{13}C -NMR Spectrum of 6.14t

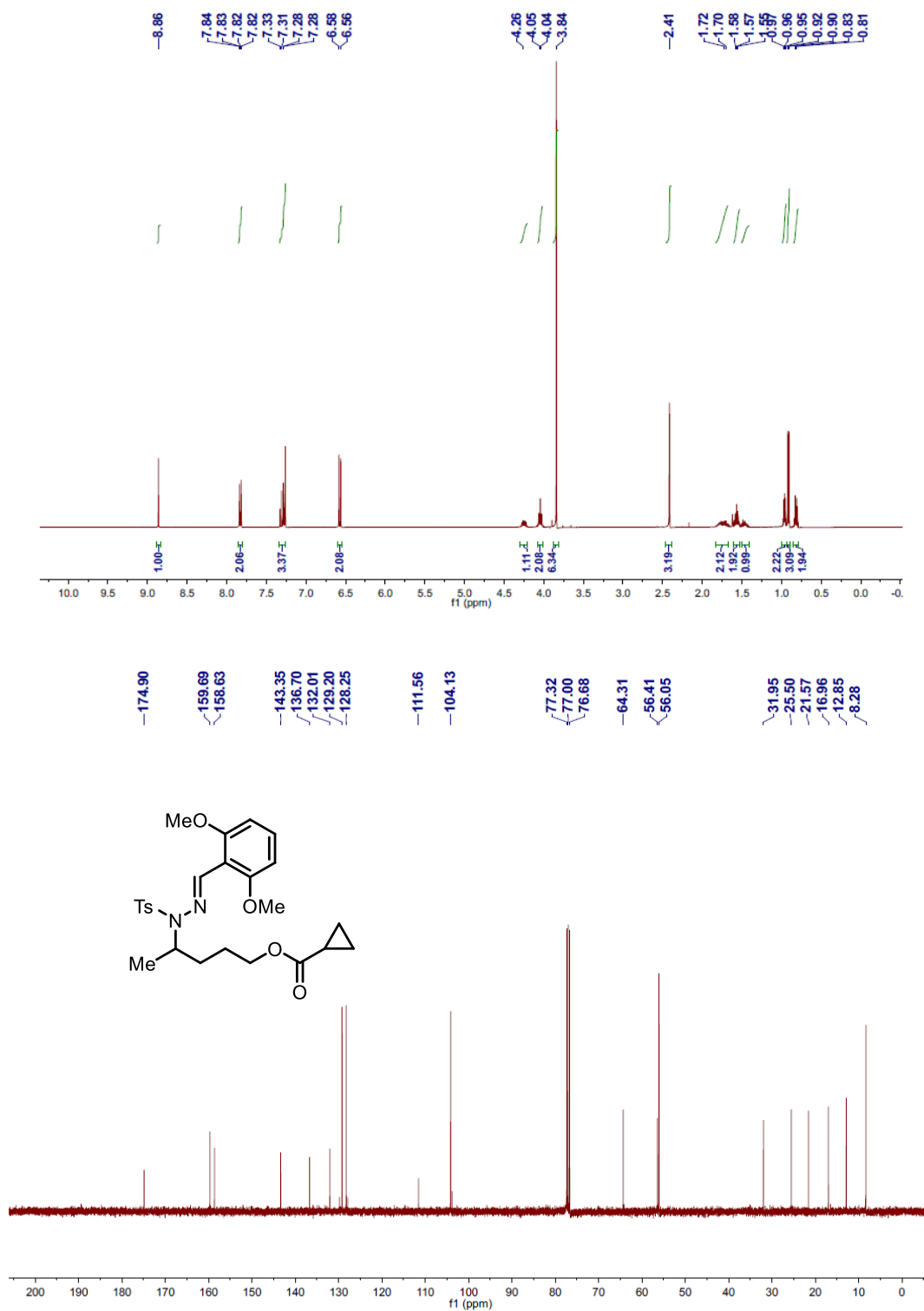


Figure 6.26 ^1H -NMR and ^{13}C -NMR Spectrum of 6.14u

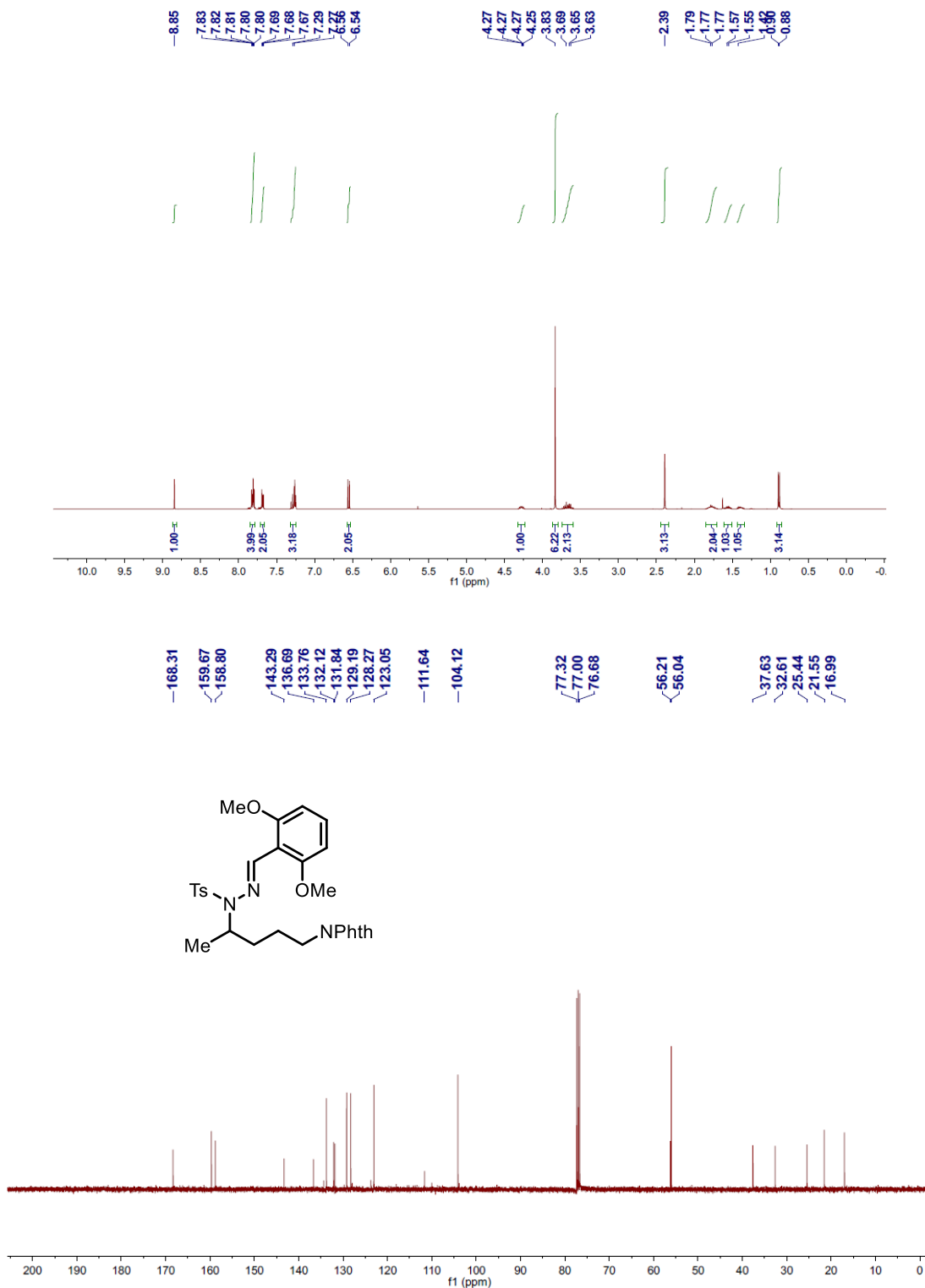


Figure 6.27 ^1H -NMR and ^{13}C -NMR Spectrum of 6.14v

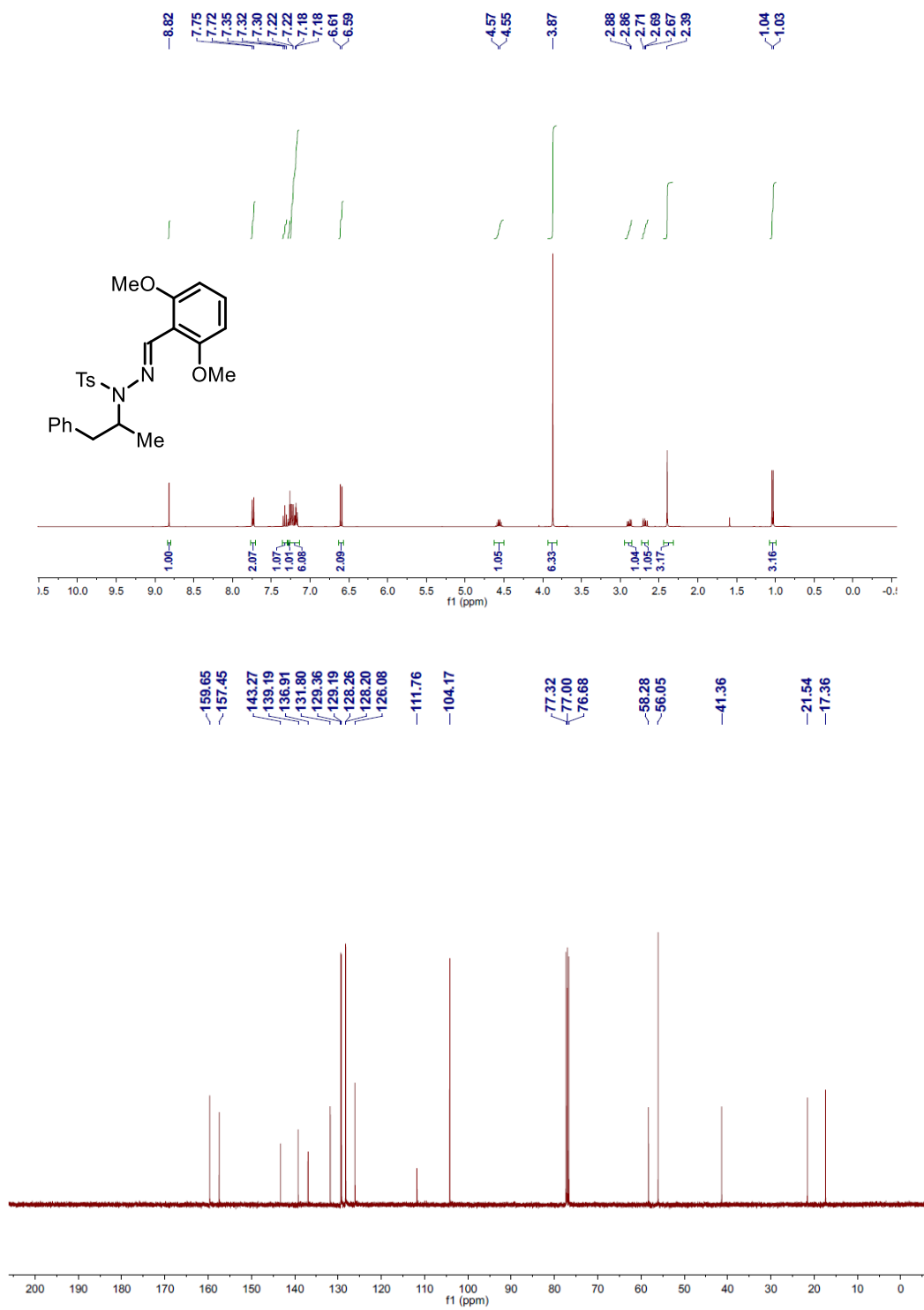


Figure 6.28 $^1\text{H-NMR}$ and $^{13}\text{C-NMR}$ Spectrum of **6.32**

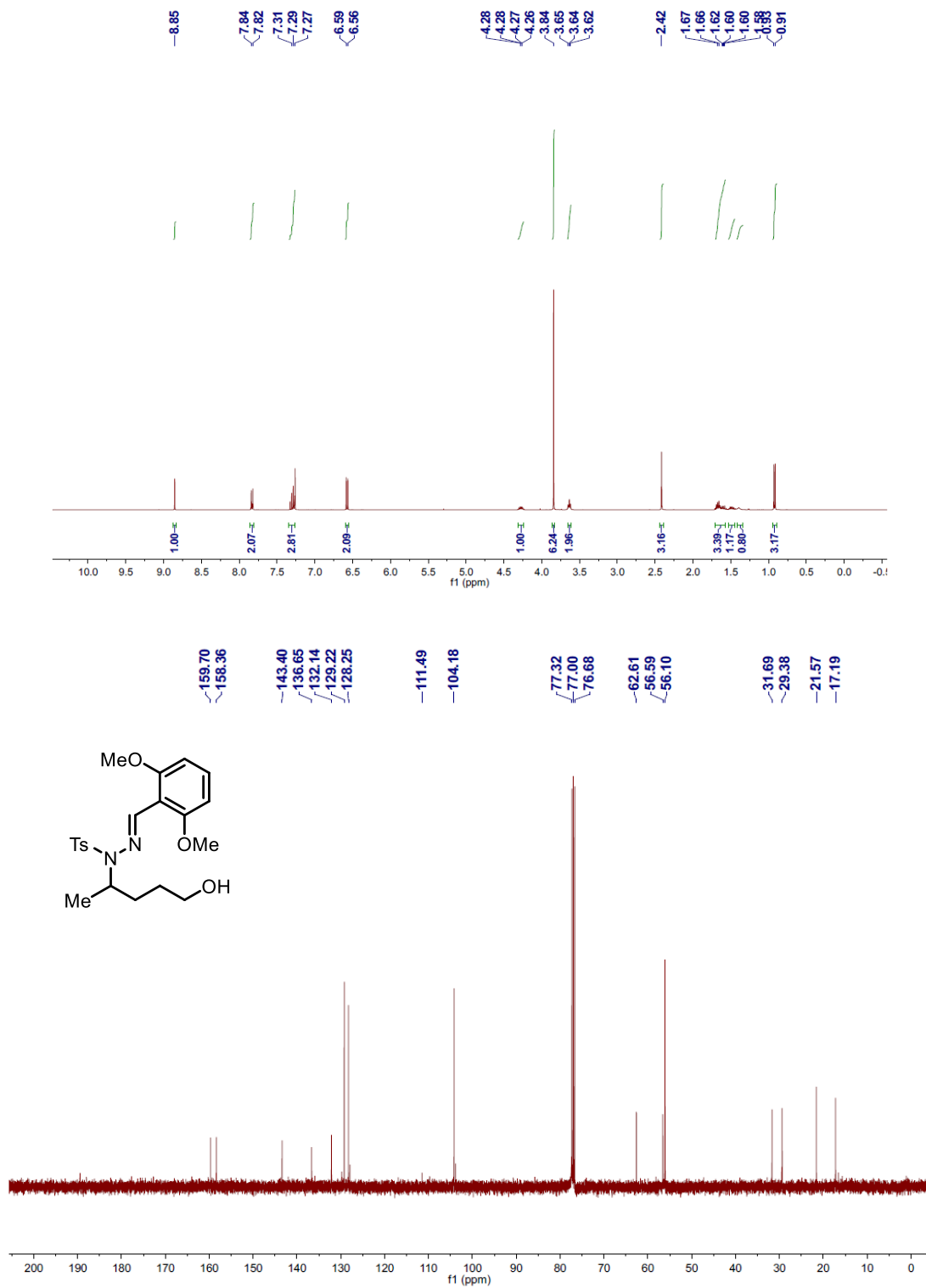


Figure 6.29 $^1\text{H-NMR}$ and $^{13}\text{C-NMR}$ Spectrum of 6.18

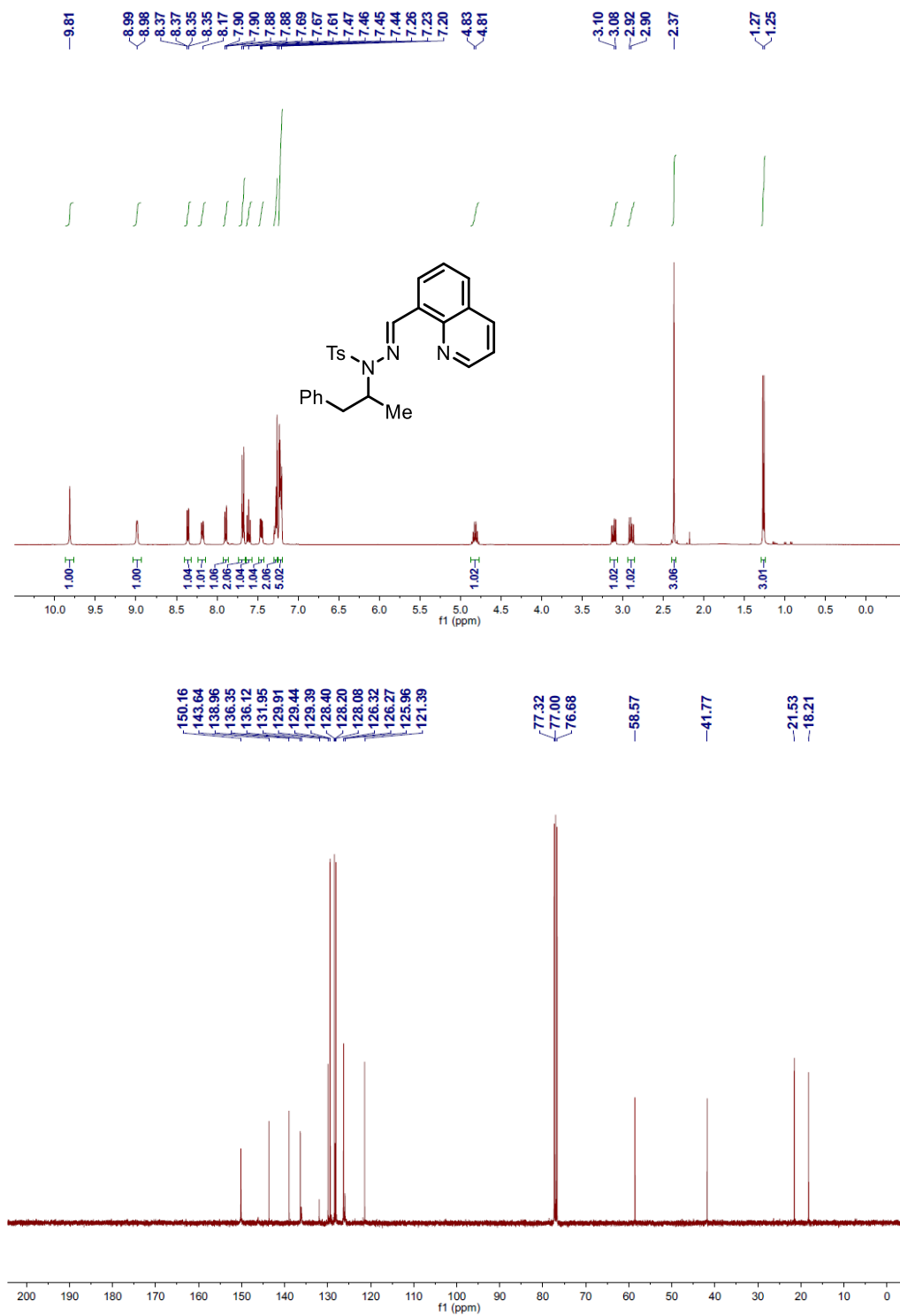


Figure 6.30 ^1H -NMR and ^{13}C -NMR Spectrum of 6.15a

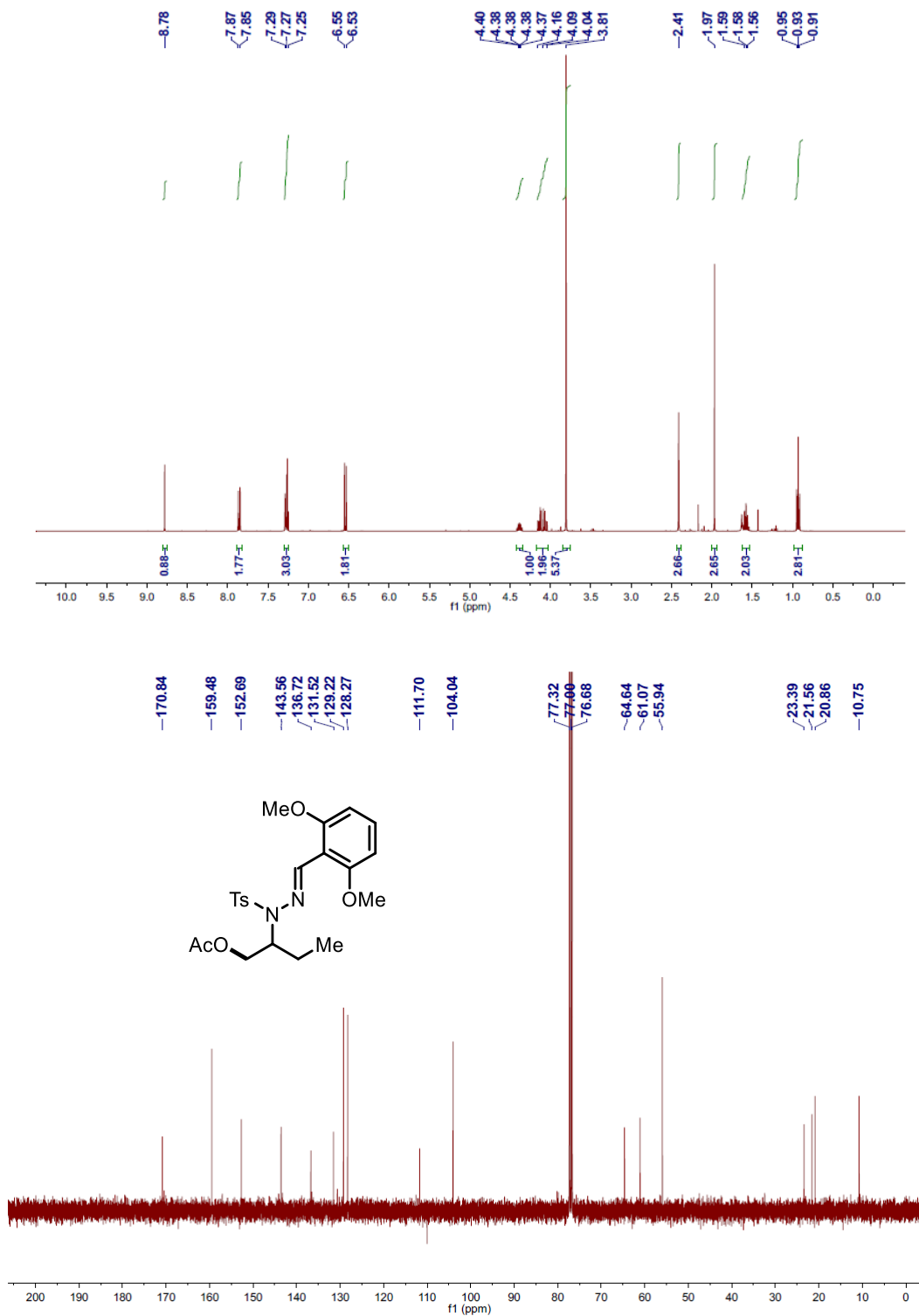


Figure 6.31 ^1H -NMR and ^{13}C -NMR Spectrum of 6.15b

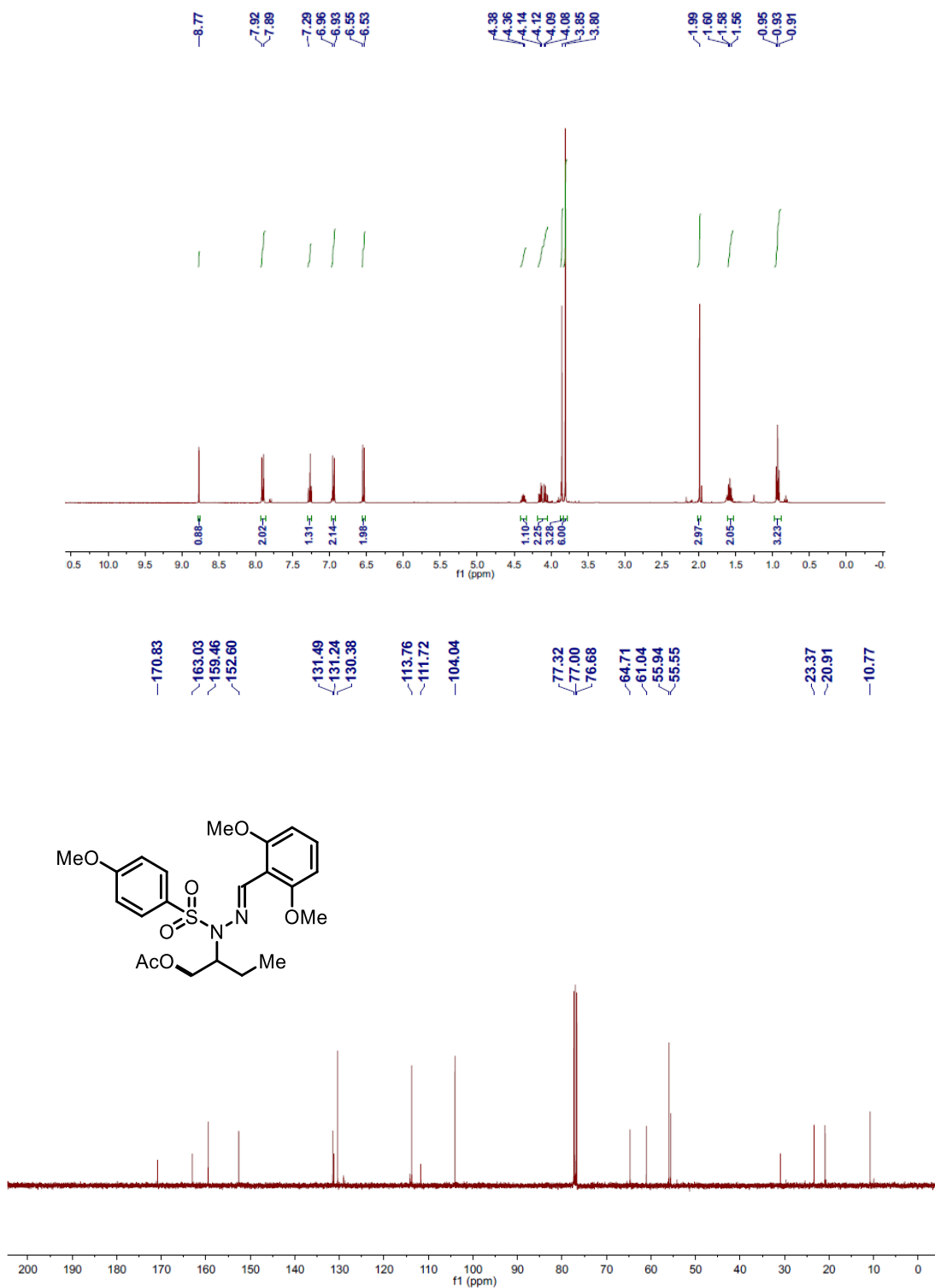


Figure 6.32 ^1H -NMR and ^{13}C -NMR Spectrum of **6.15c**

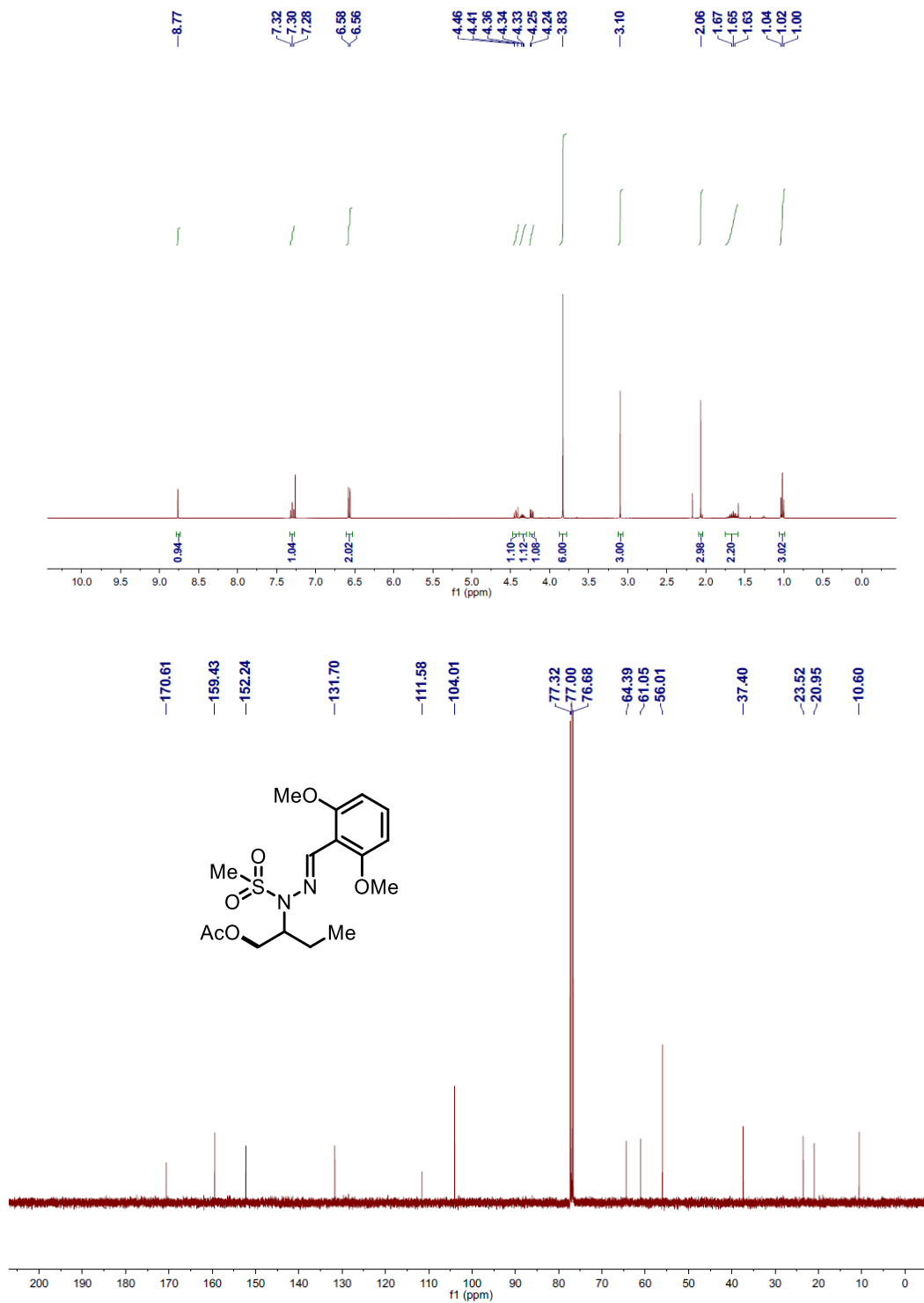


Figure 6.33 ^1H -NMR and ^{13}C -NMR Spectrum of 6.15d

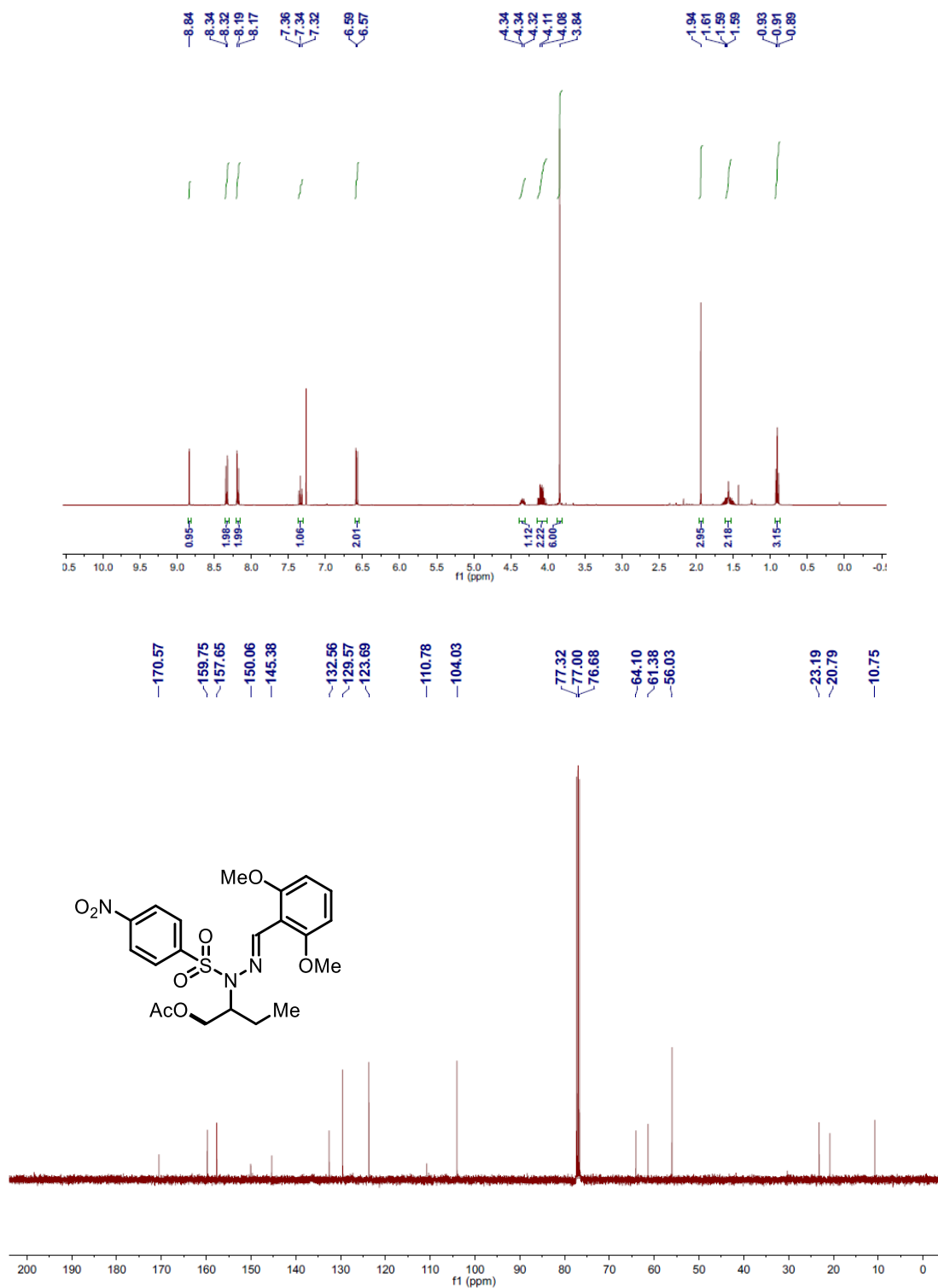


Figure 6.34 ^1H -NMR and ^{13}C -NMR Spectrum of **6.15e**

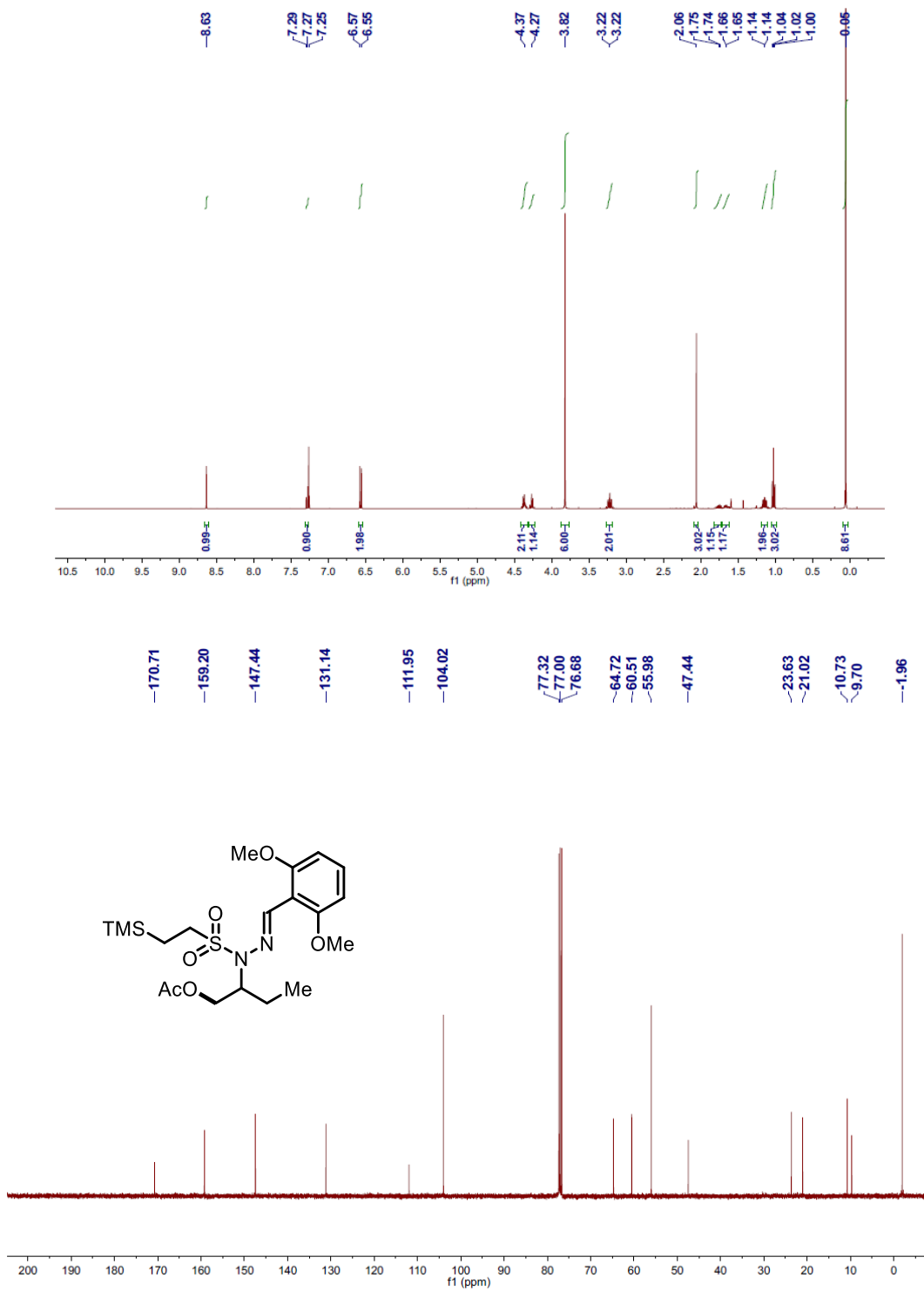


Figure 6.35 ^1H -NMR and ^{13}C -NMR Spectrum of **6.15f**

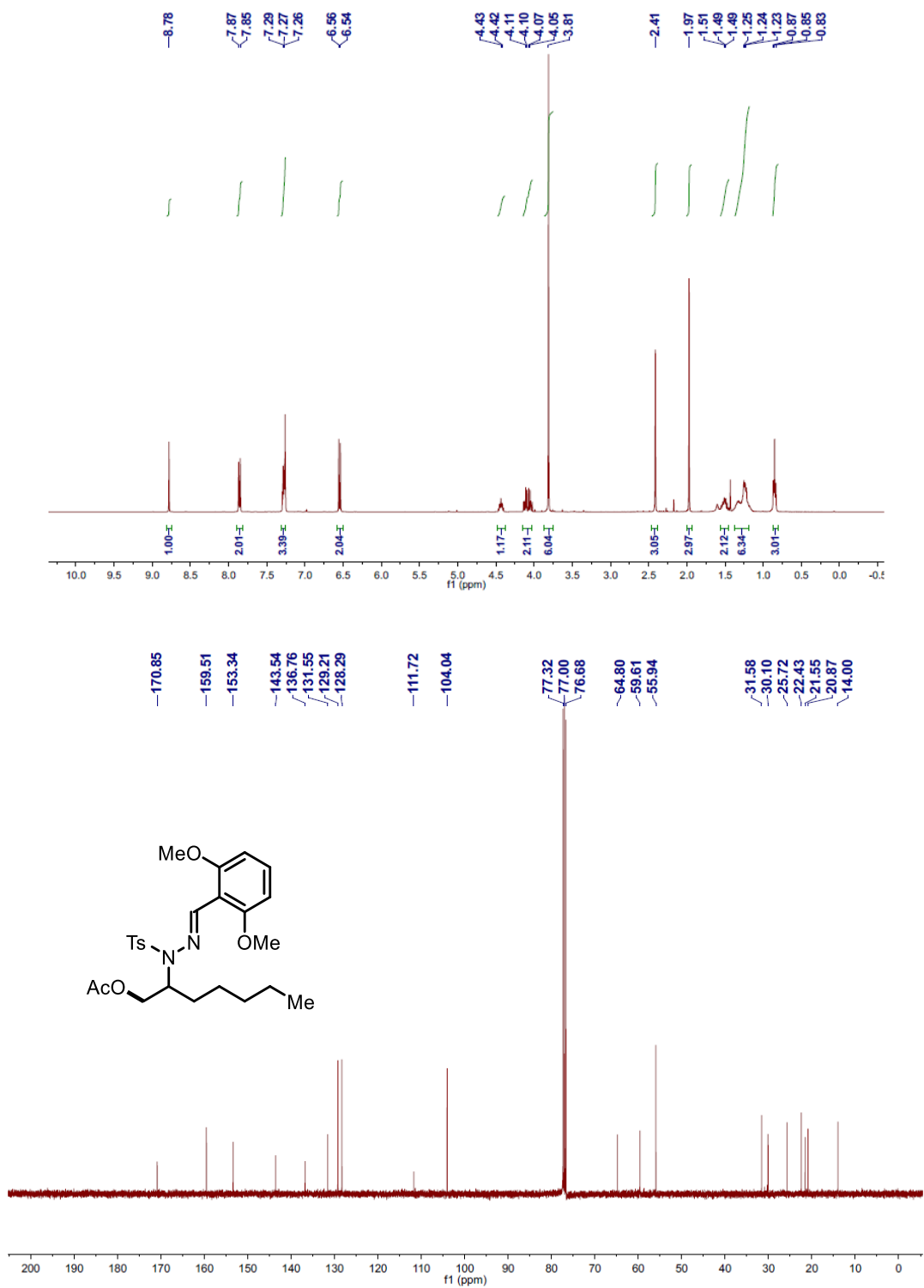


Figure 6.36 ^1H -NMR and ^{13}C -NMR Spectrum of 6.15g

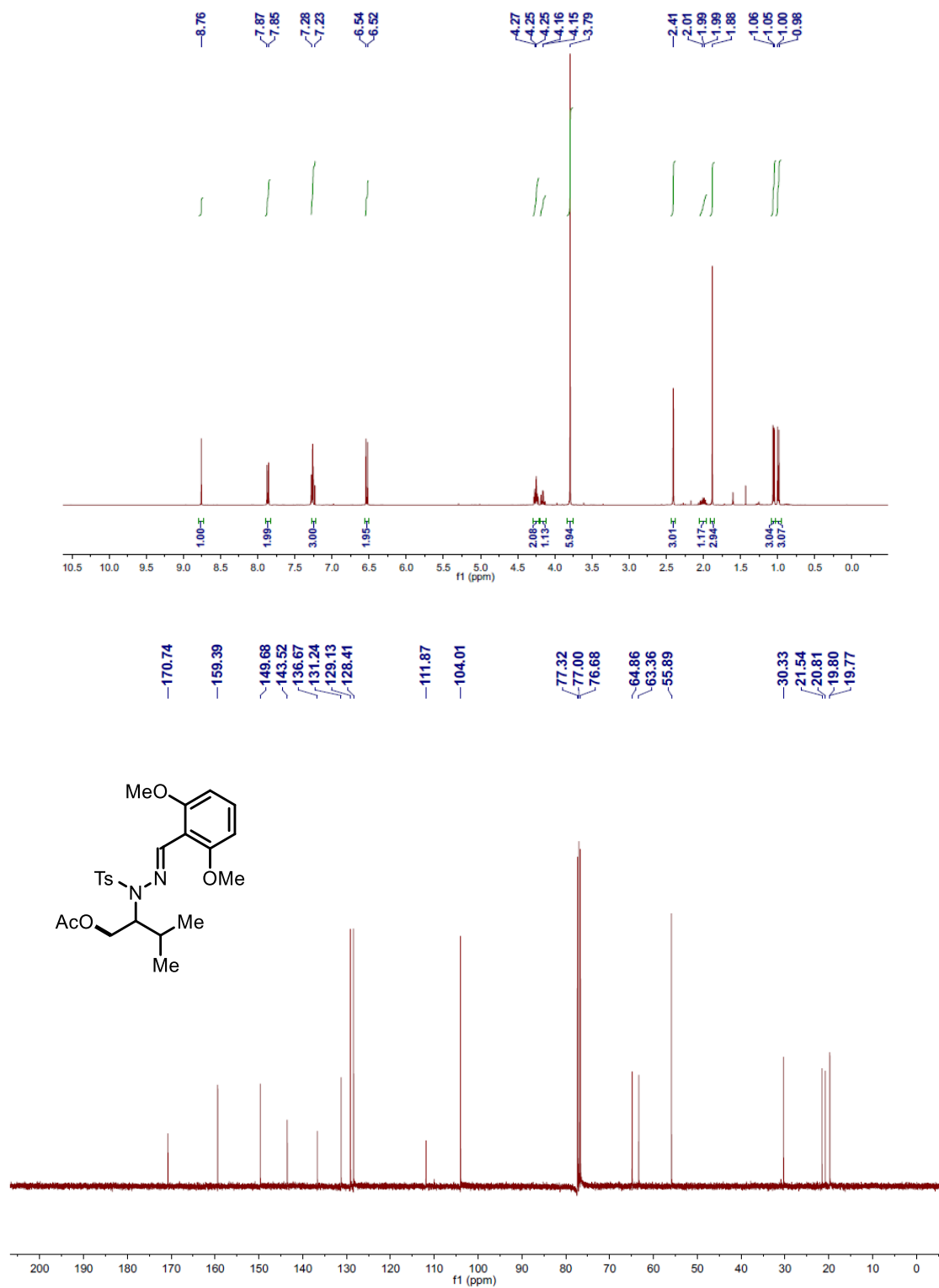


Figure 6.37 ¹H-NMR and ¹³C-NMR Spectrum of 6.15h

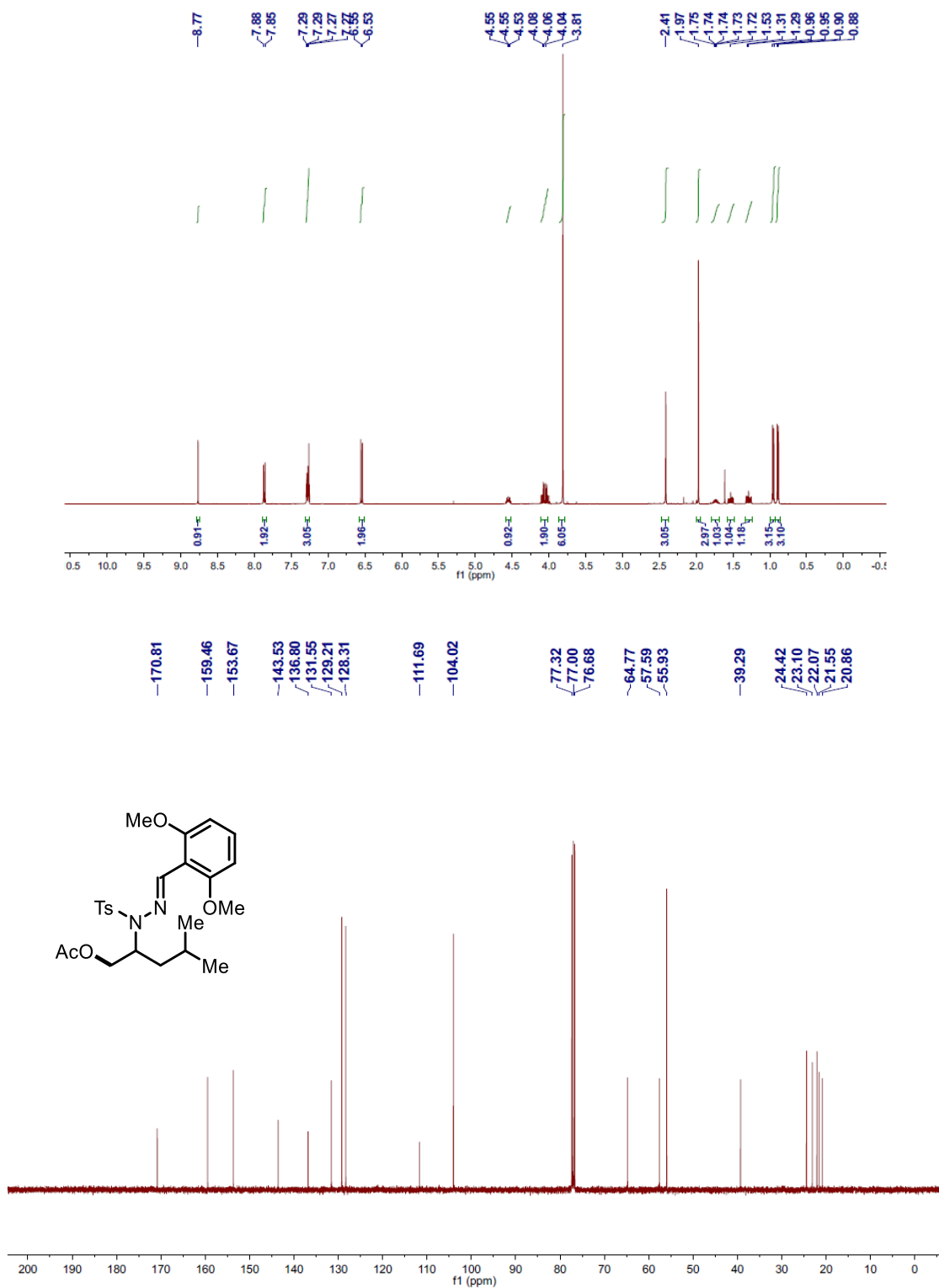


Figure 6.38 ¹H-NMR and ¹³C-NMR Spectrum of 6.15i

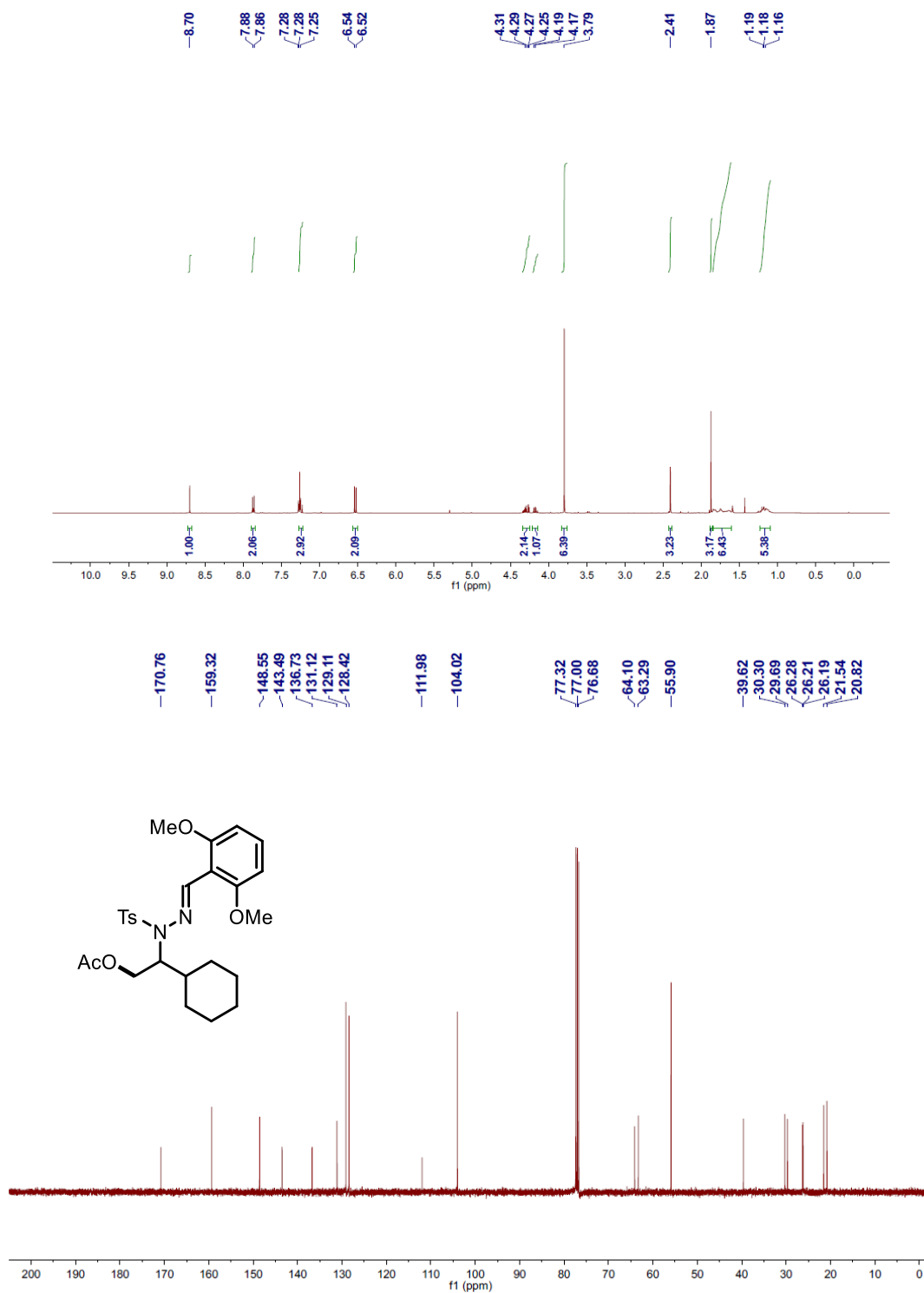


Figure 6.39 $^1\text{H-NMR}$ and $^{13}\text{C-NMR}$ Spectrum of 6.15j-mono

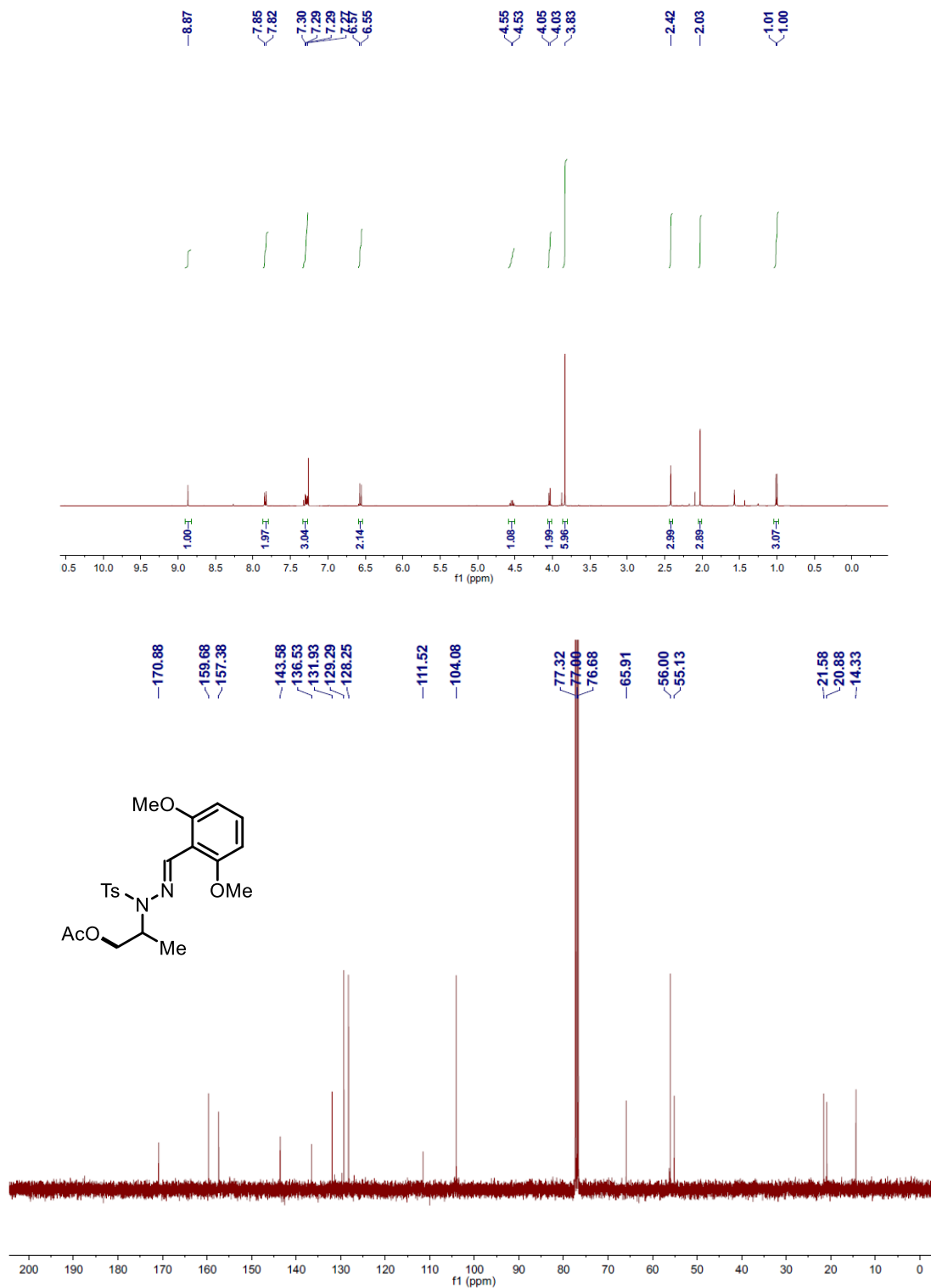


Figure 6.40 ^1H -NMR and ^{13}C -NMR Spectrum of 6.15j-di

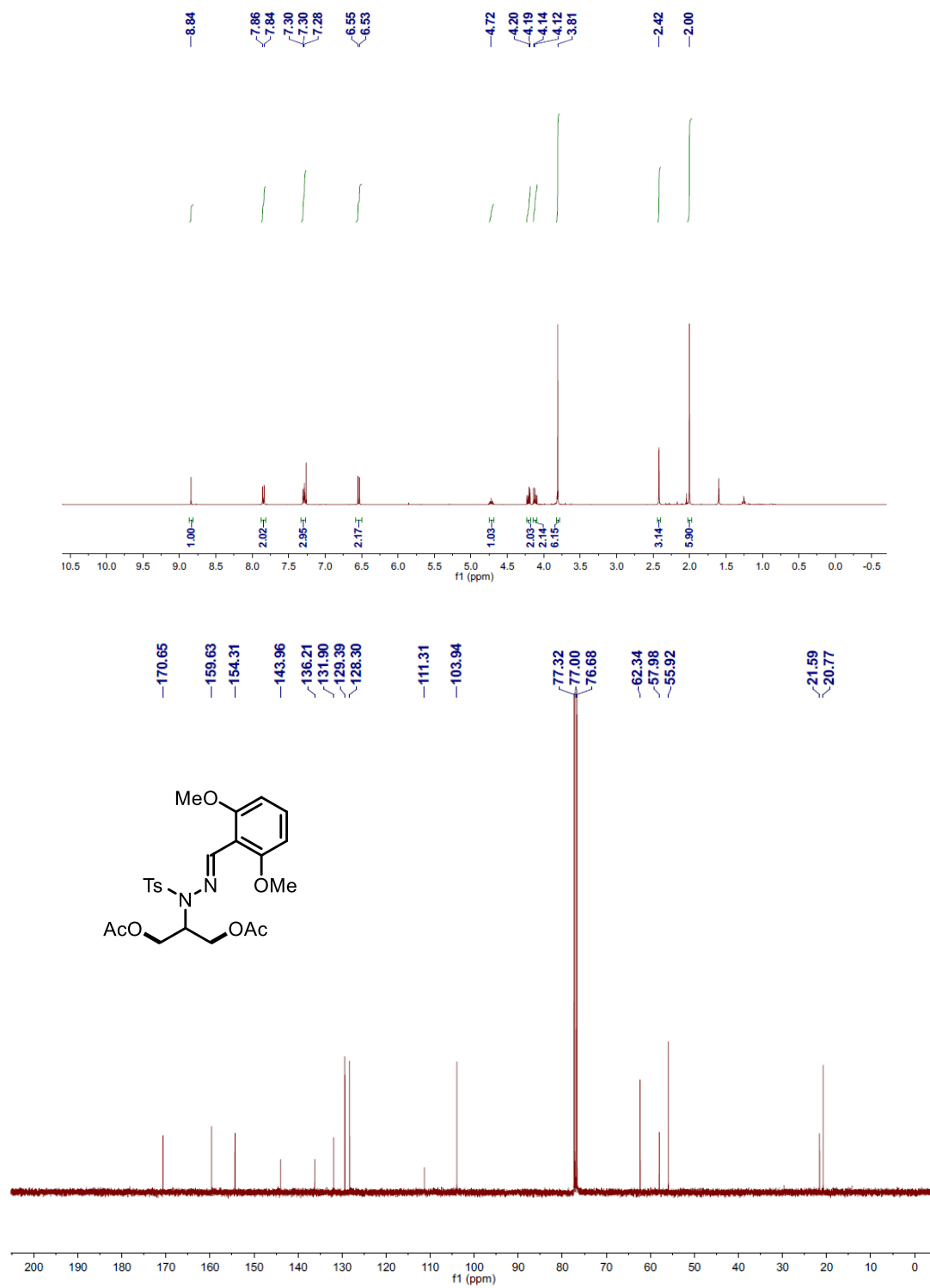
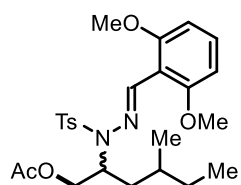
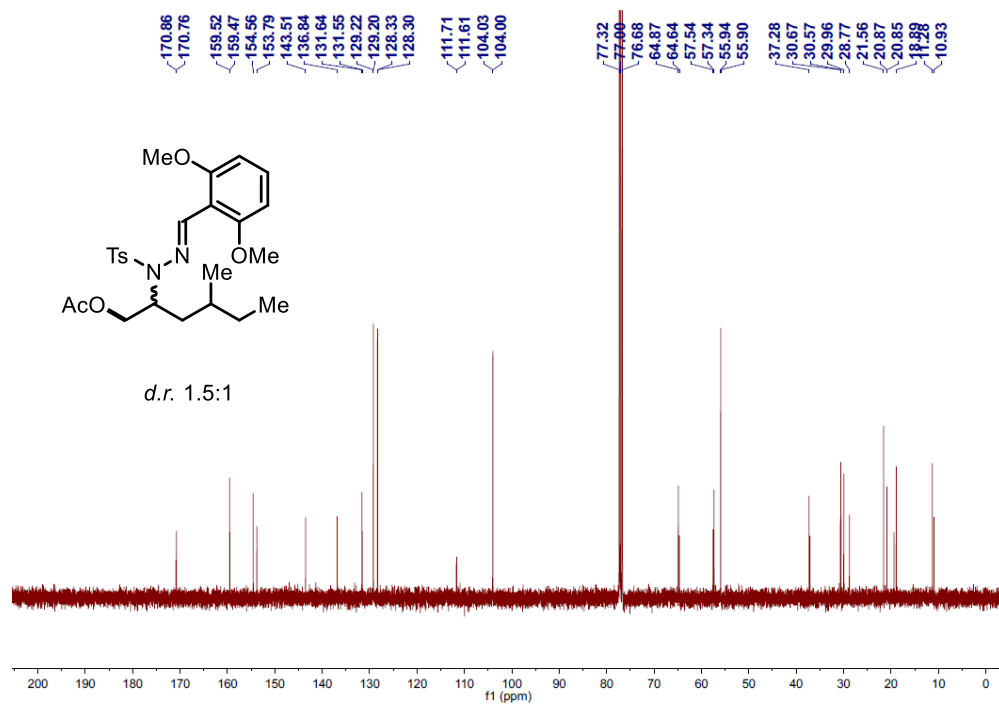
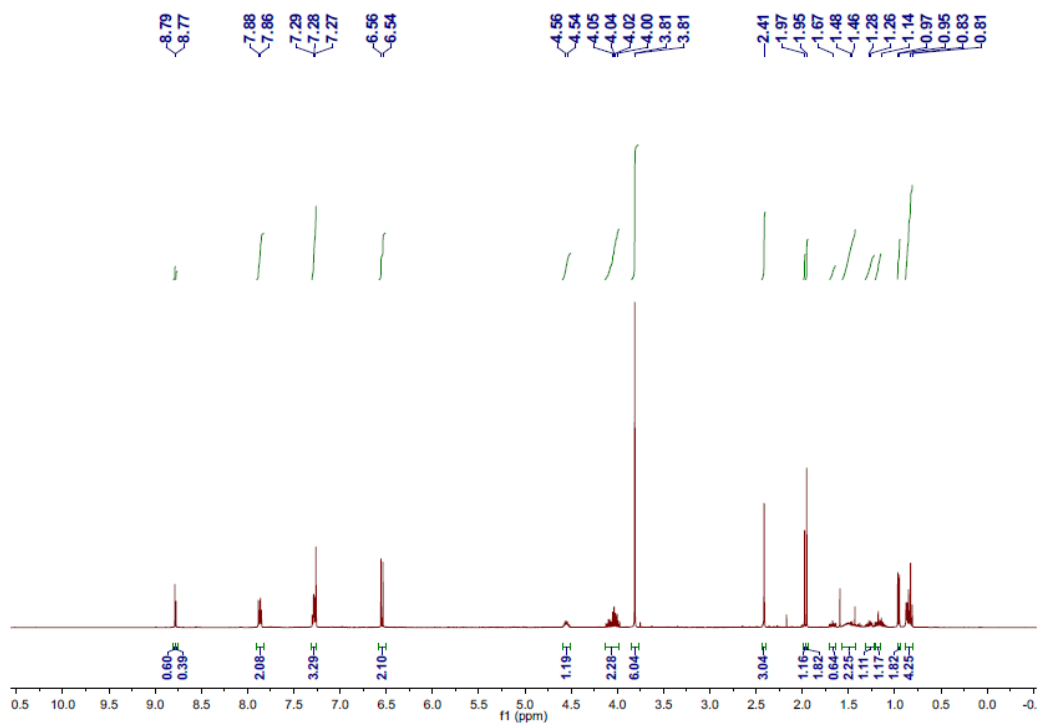


Figure 6.41 ^1H -NMR and ^{13}C -NMR Spectrum of **6.15k**



d.r. 1.5:1

Figure 6.42 $^1\text{H-NMR}$ and $^{13}\text{C-NMR}$ Spectrum of **6.151**

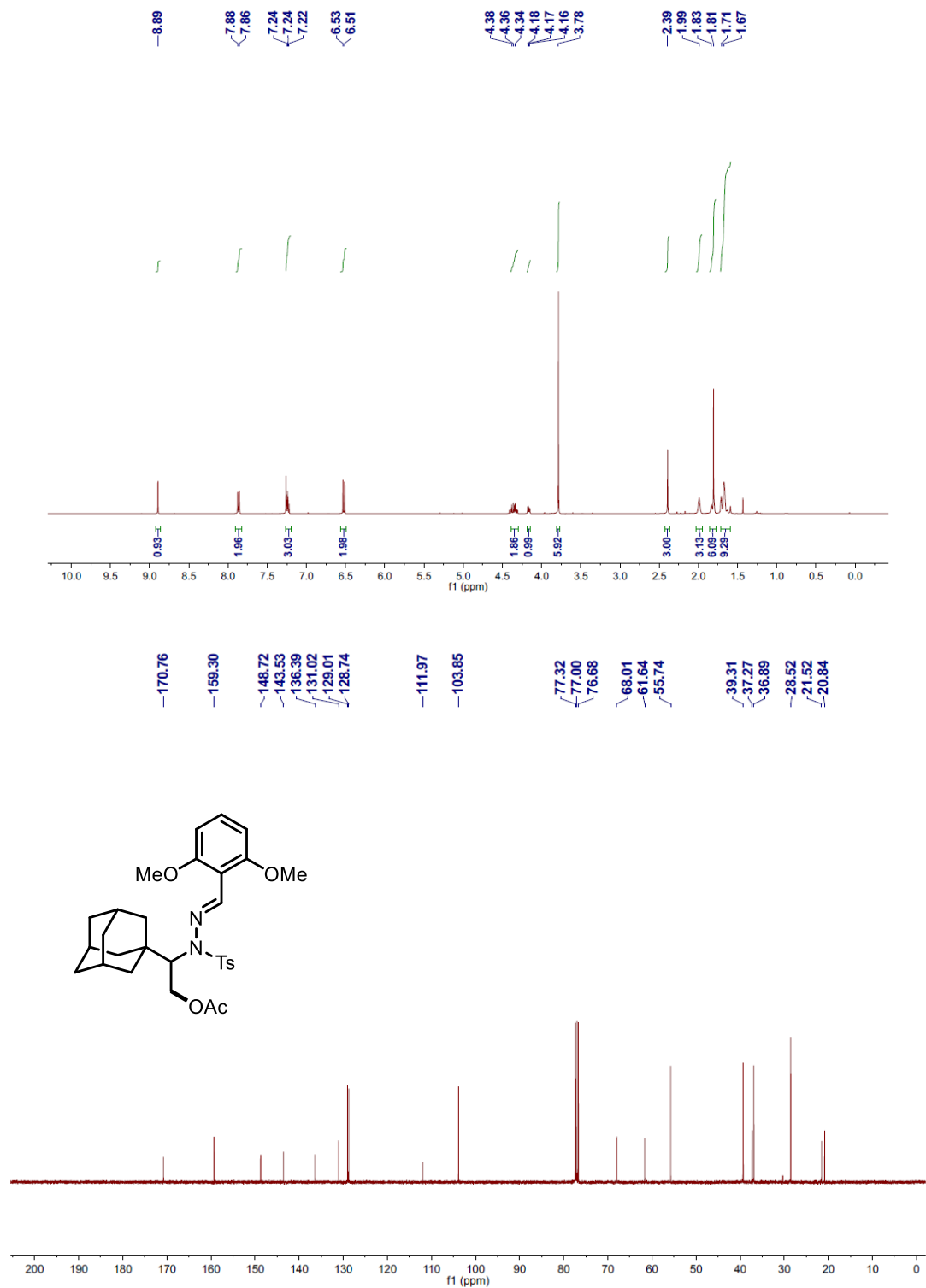


Figure 6.43 $^1\text{H-NMR}$ and $^{13}\text{C-NMR}$ Spectrum of **6.15m**

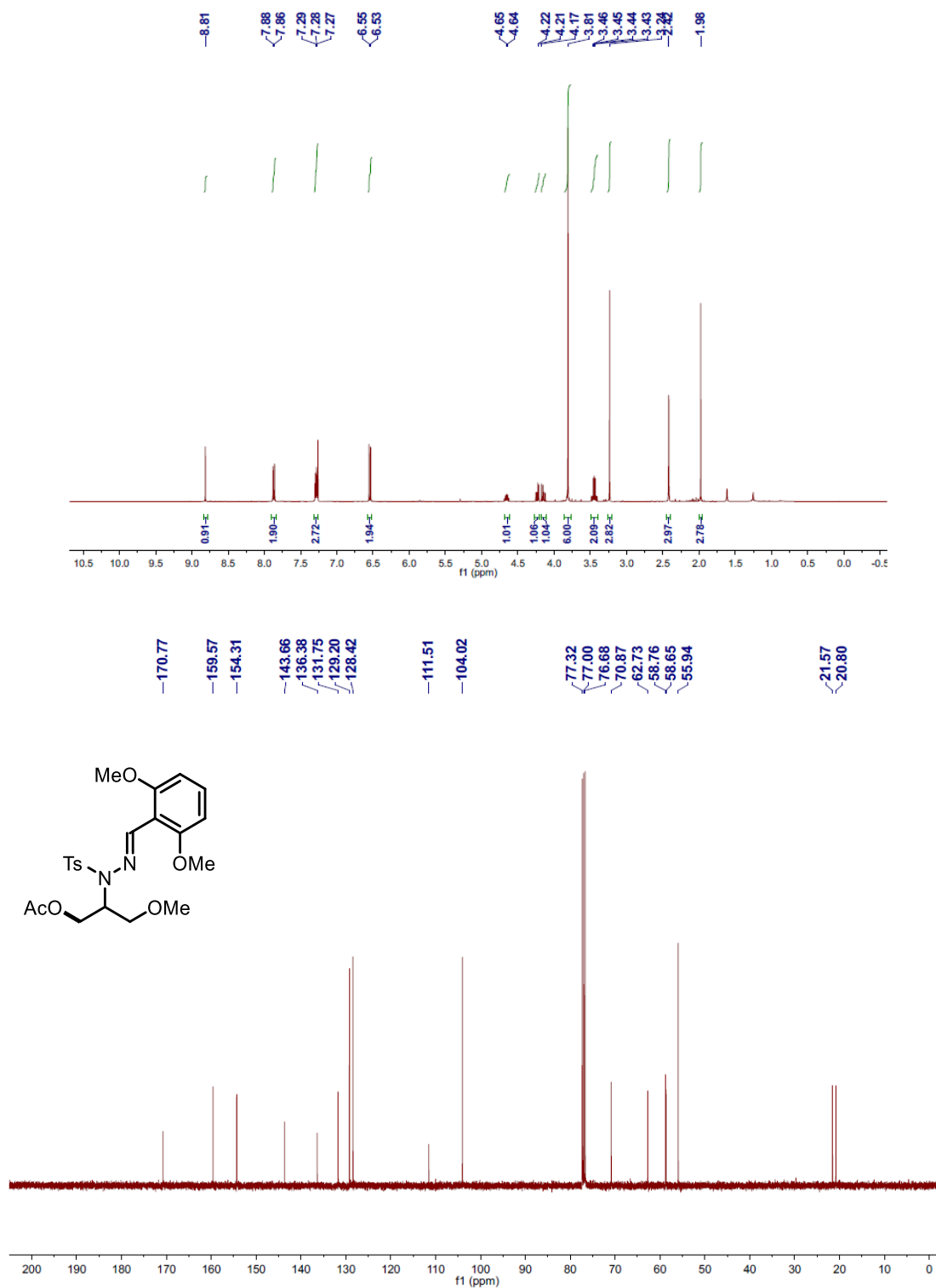


Figure 6.44 ¹H-NMR and ¹³C-NMR Spectrum of 6.15n

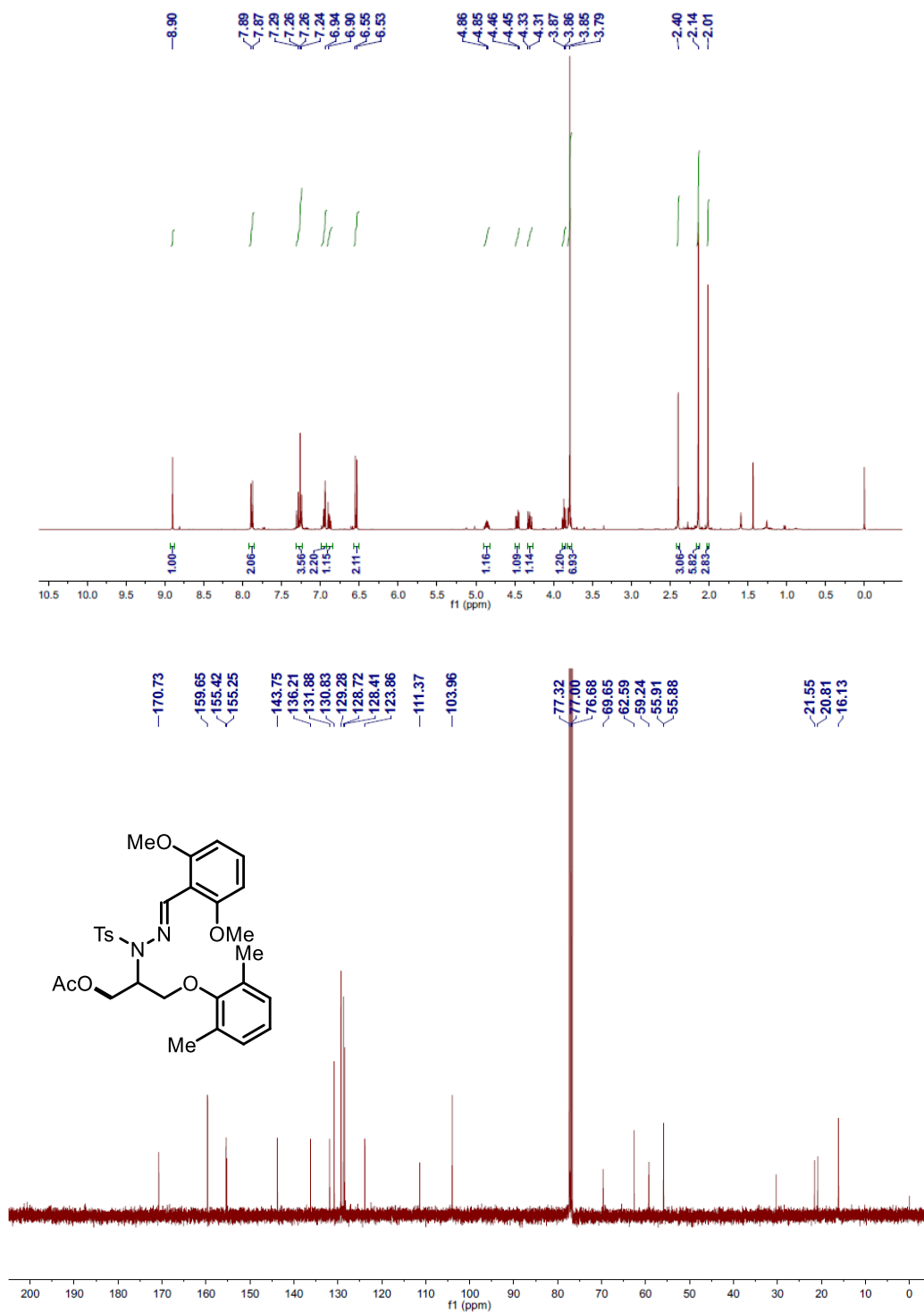


Figure 6.45 ¹H-NMR and ¹³C-NMR Spectrum of 6.15o

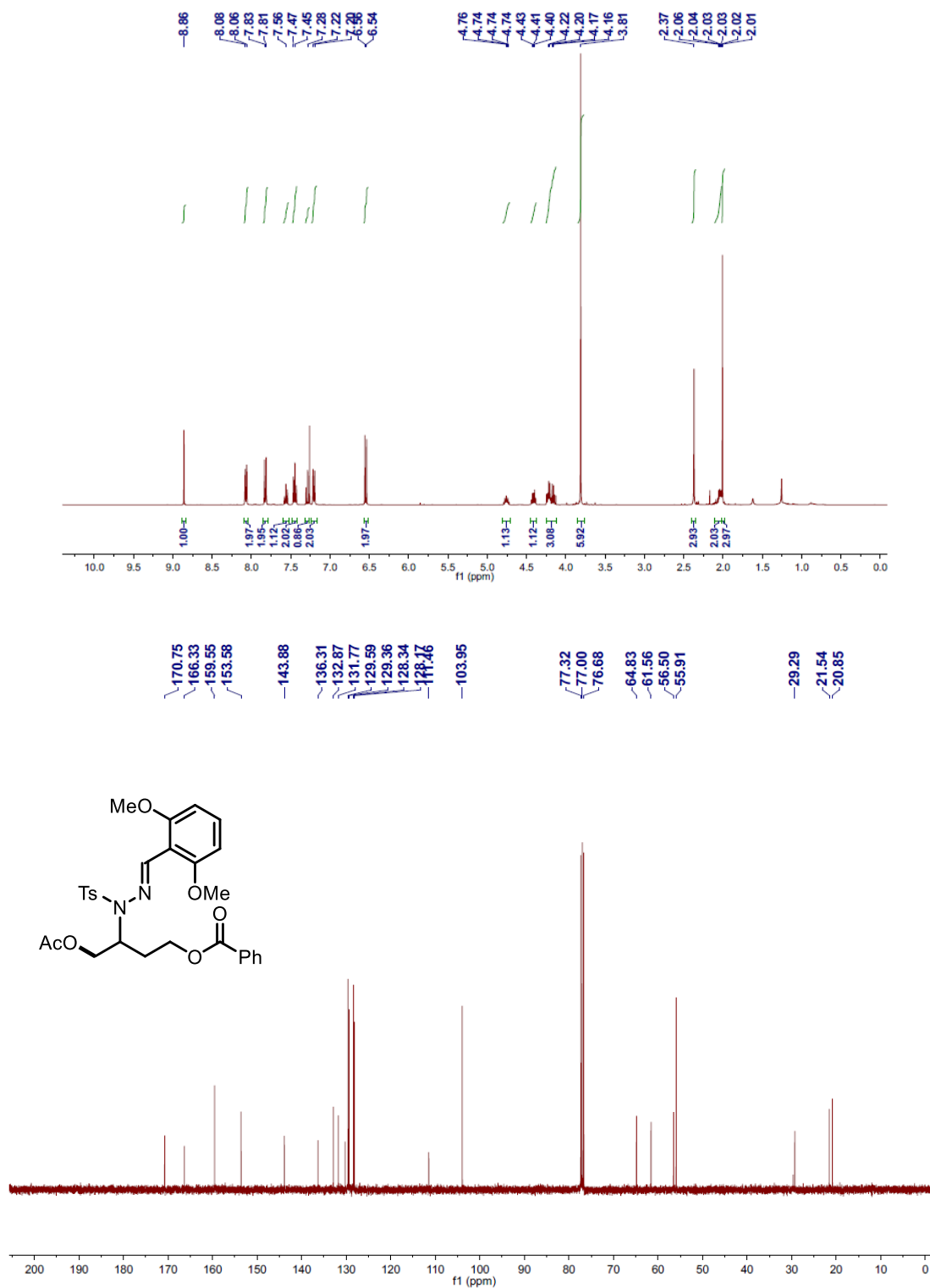


Figure 6.47 ¹H-NMR and ¹³C-NMR Spectrum of 6.15q

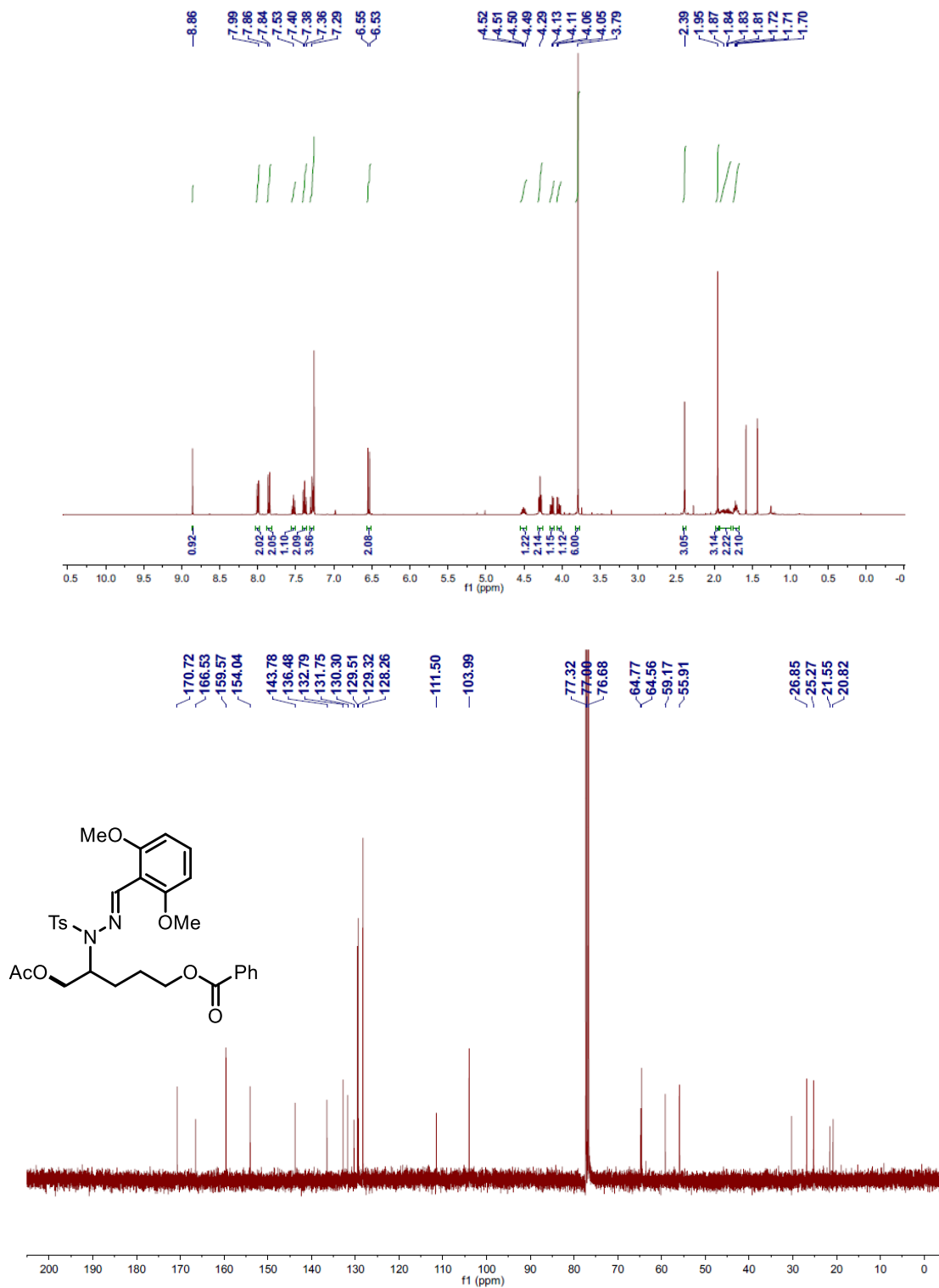


Figure 6.48 ^1H -NMR and ^{13}C -NMR Spectrum of **6.15r**

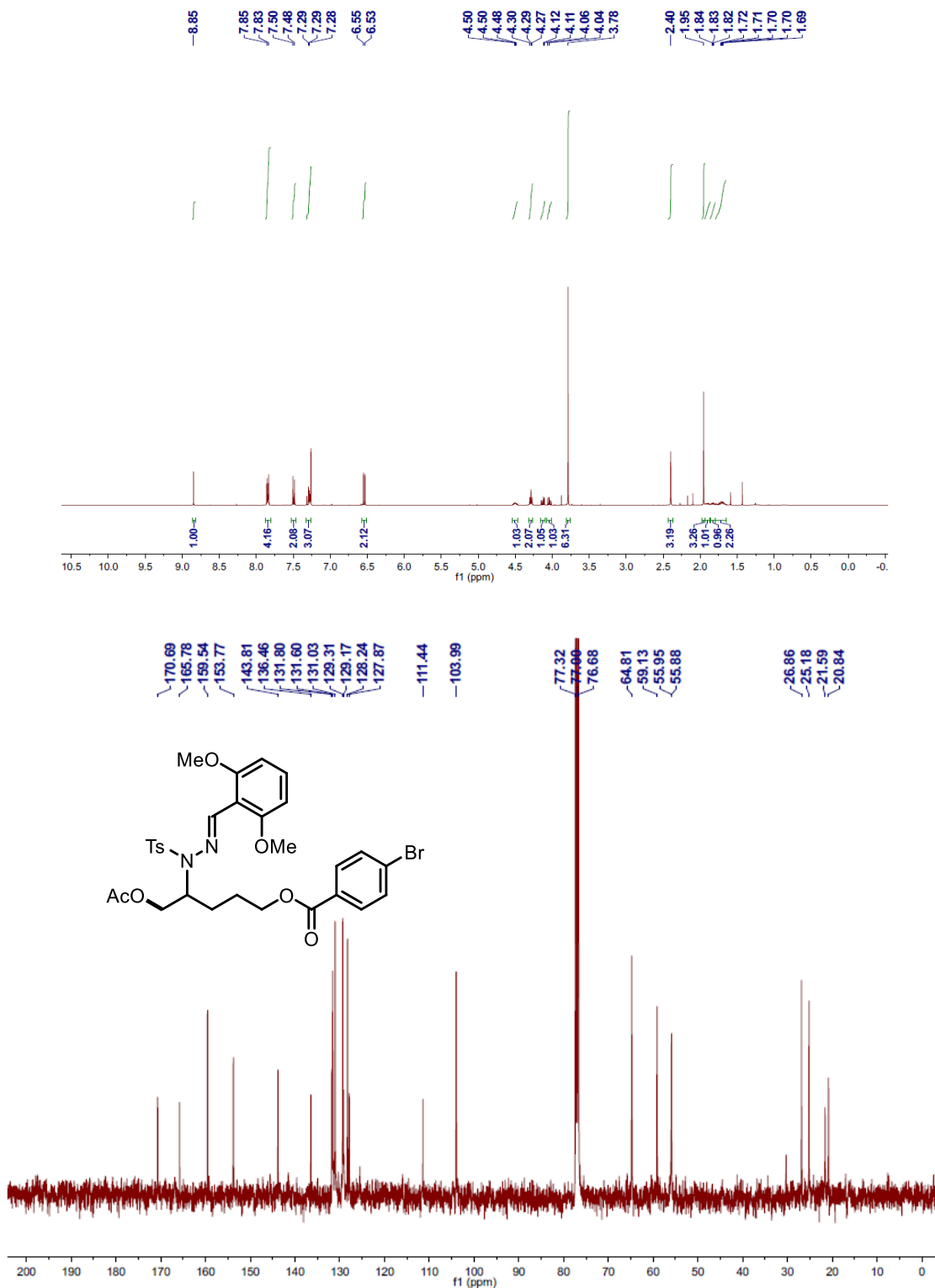


Figure 6.49 ^1H -NMR and ^{13}C -NMR Spectrum of **6.15s**

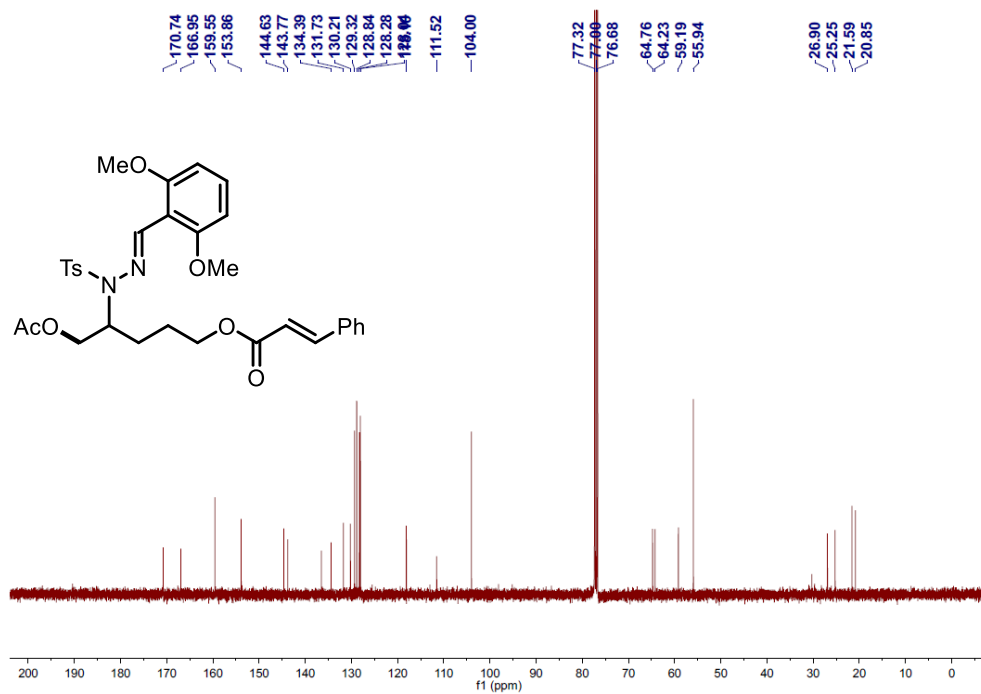
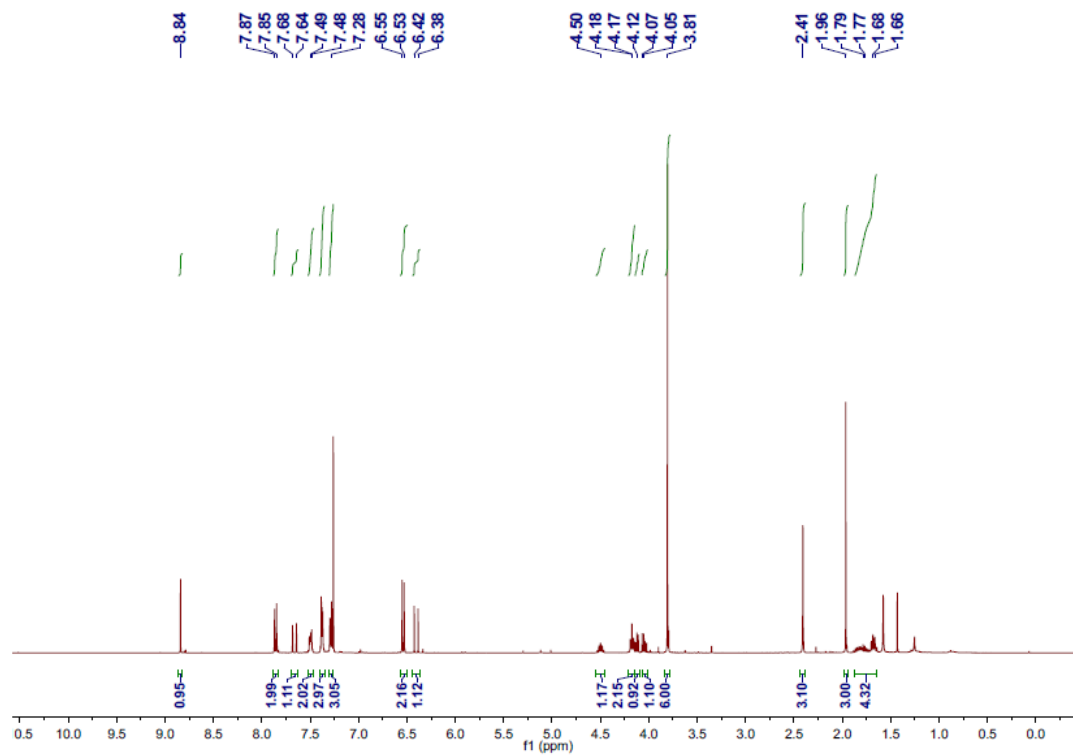


Figure 6.50 ¹H-NMR and ¹³C-NMR Spectrum of 6.15t

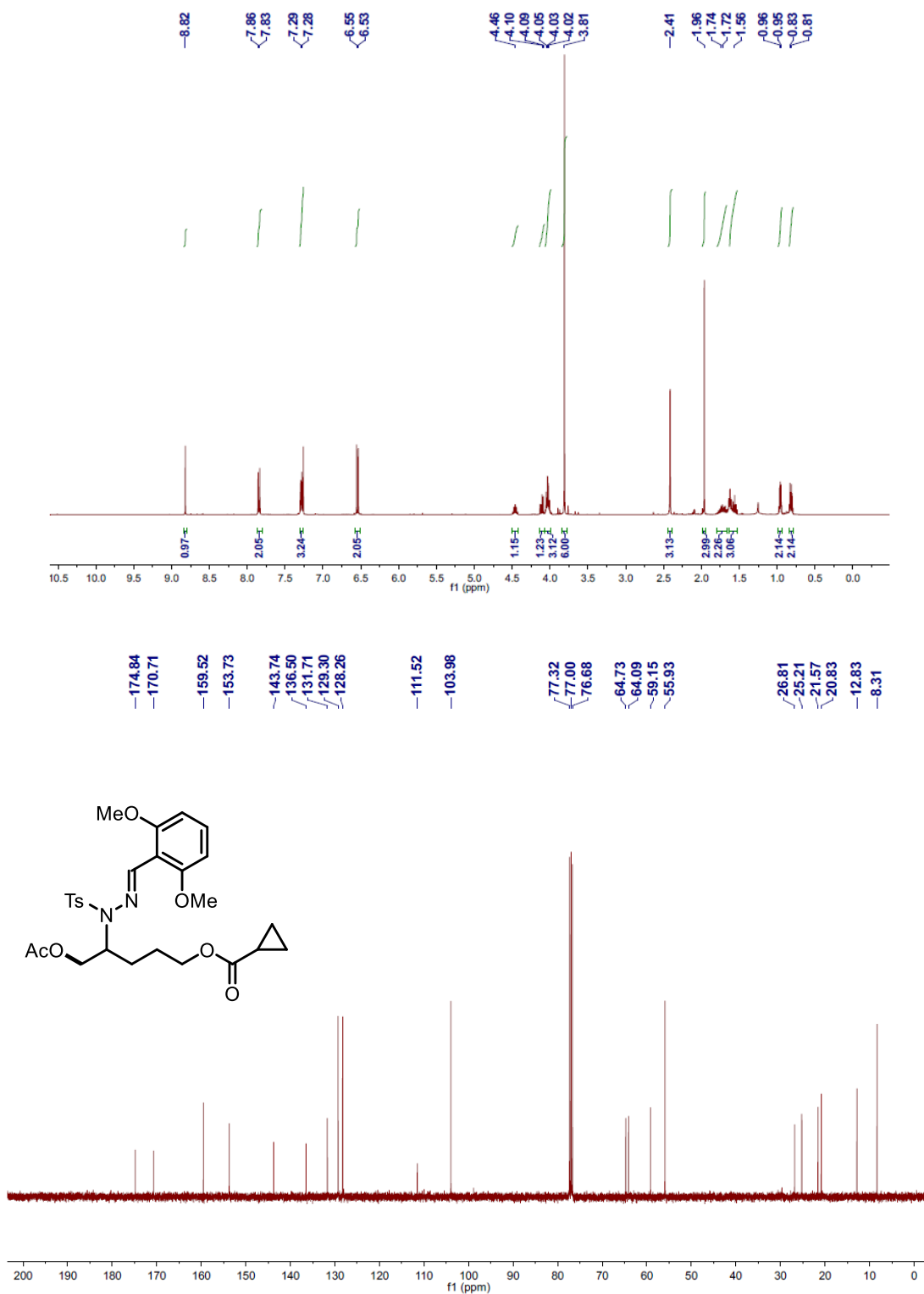


Figure 6.51 ^1H -NMR and ^{13}C -NMR Spectrum of 6.15u

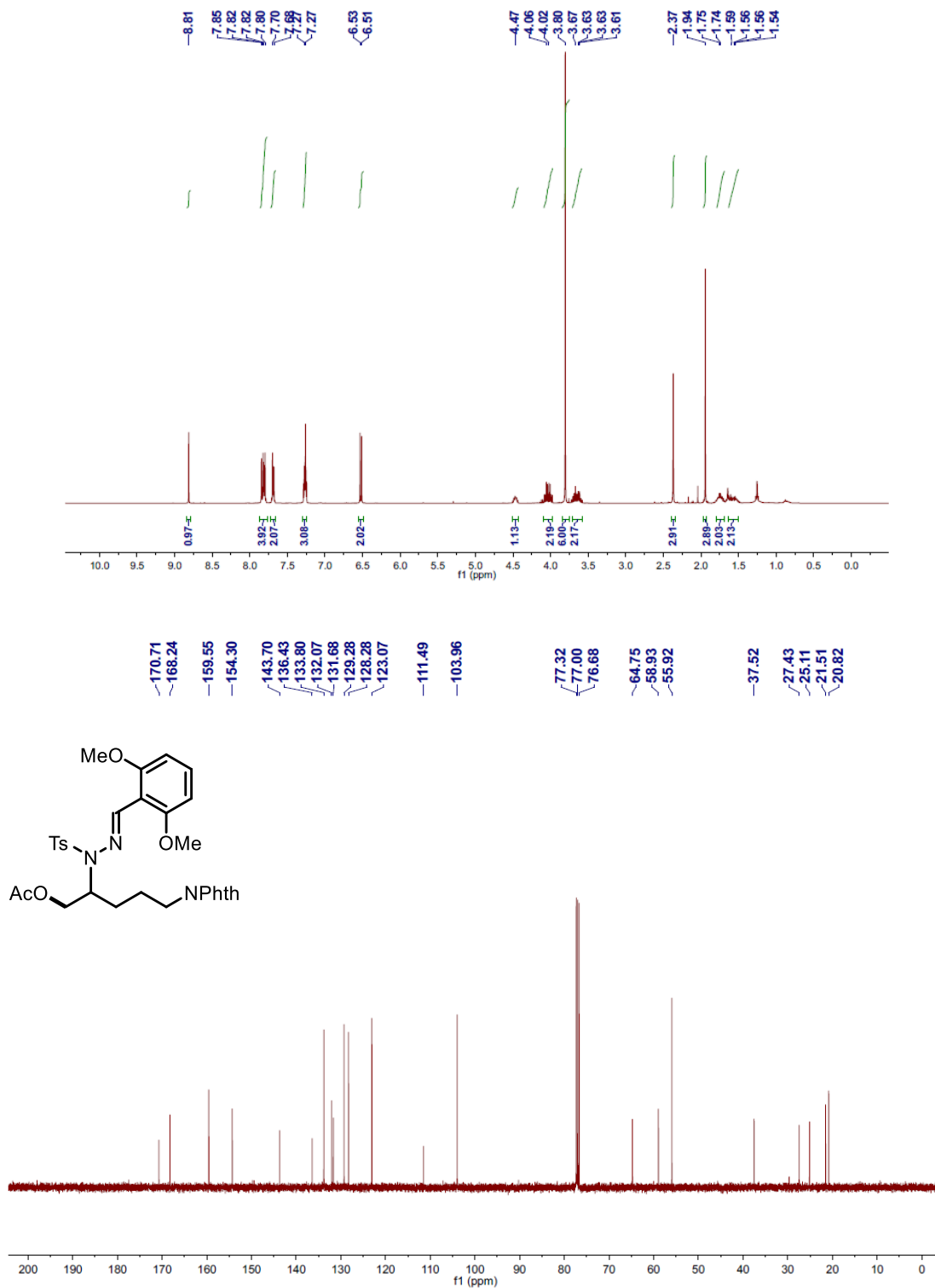


Figure 6.52 ^1H -NMR and ^{13}C -NMR Spectrum of **6.15v**

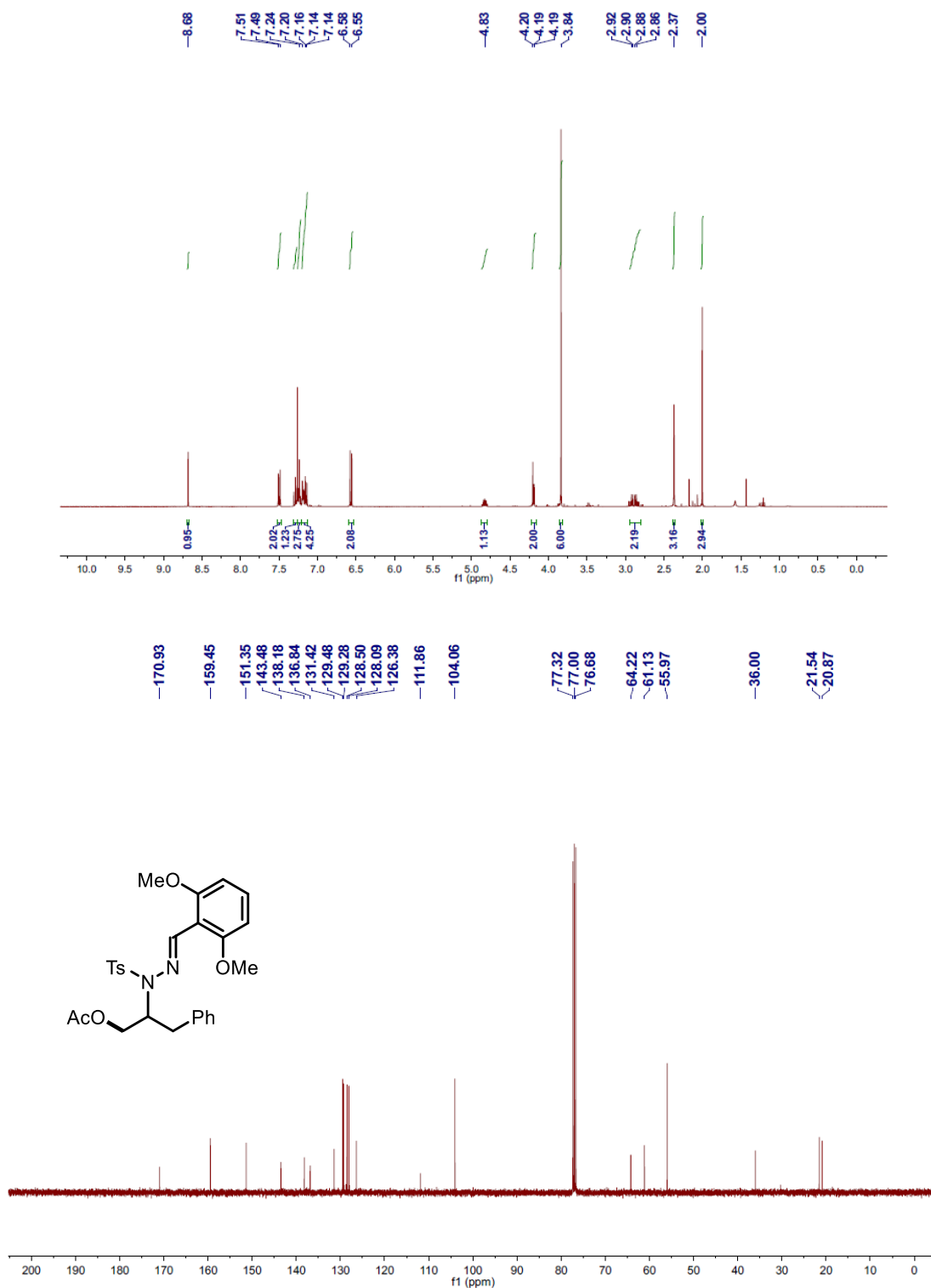


Figure 6.53 ¹H-NMR and ¹³C-NMR Spectrum of 6.19

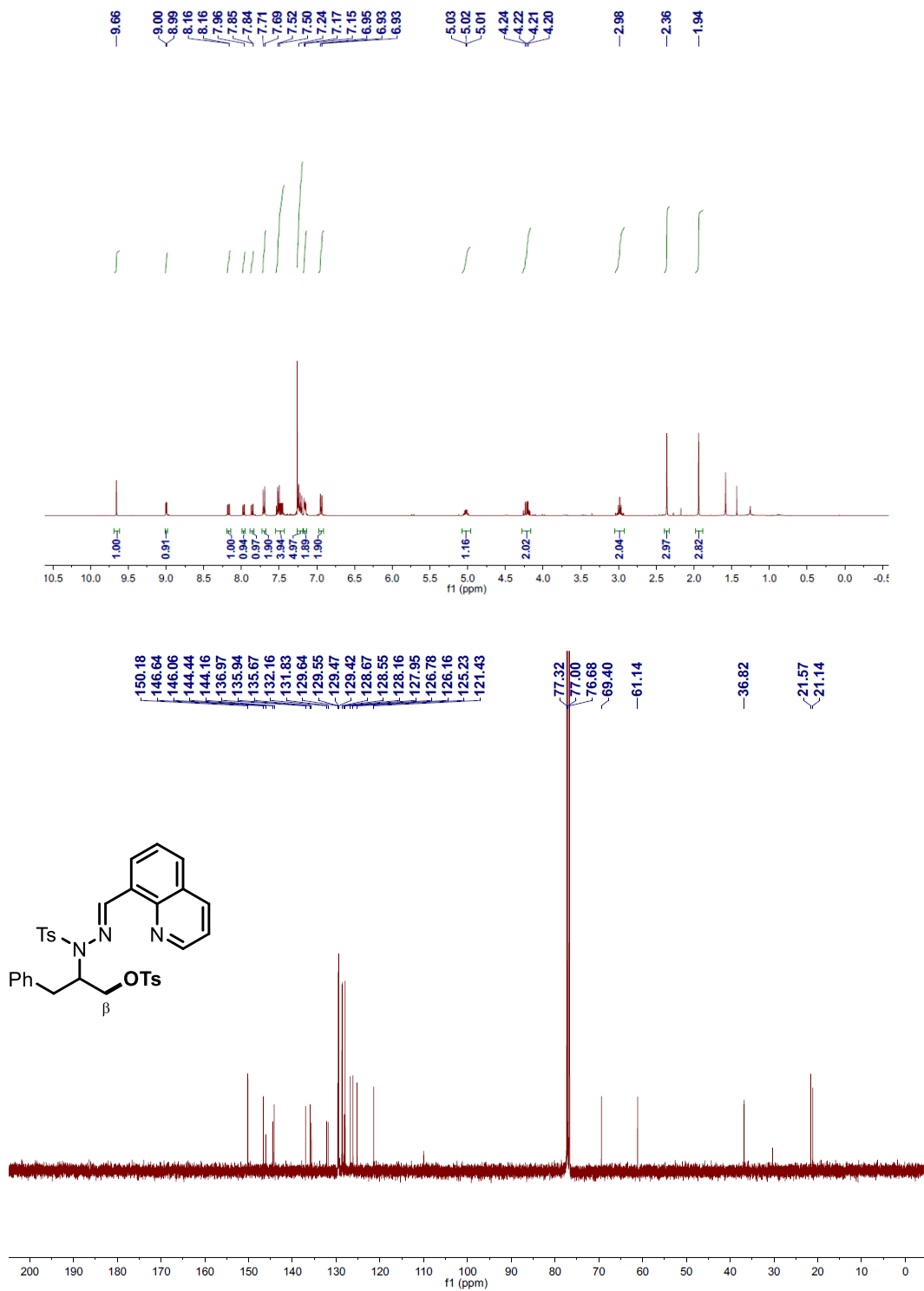


Figure 6.54 ^1H -NMR and ^{13}C -NMR Spectrum of 6.20a

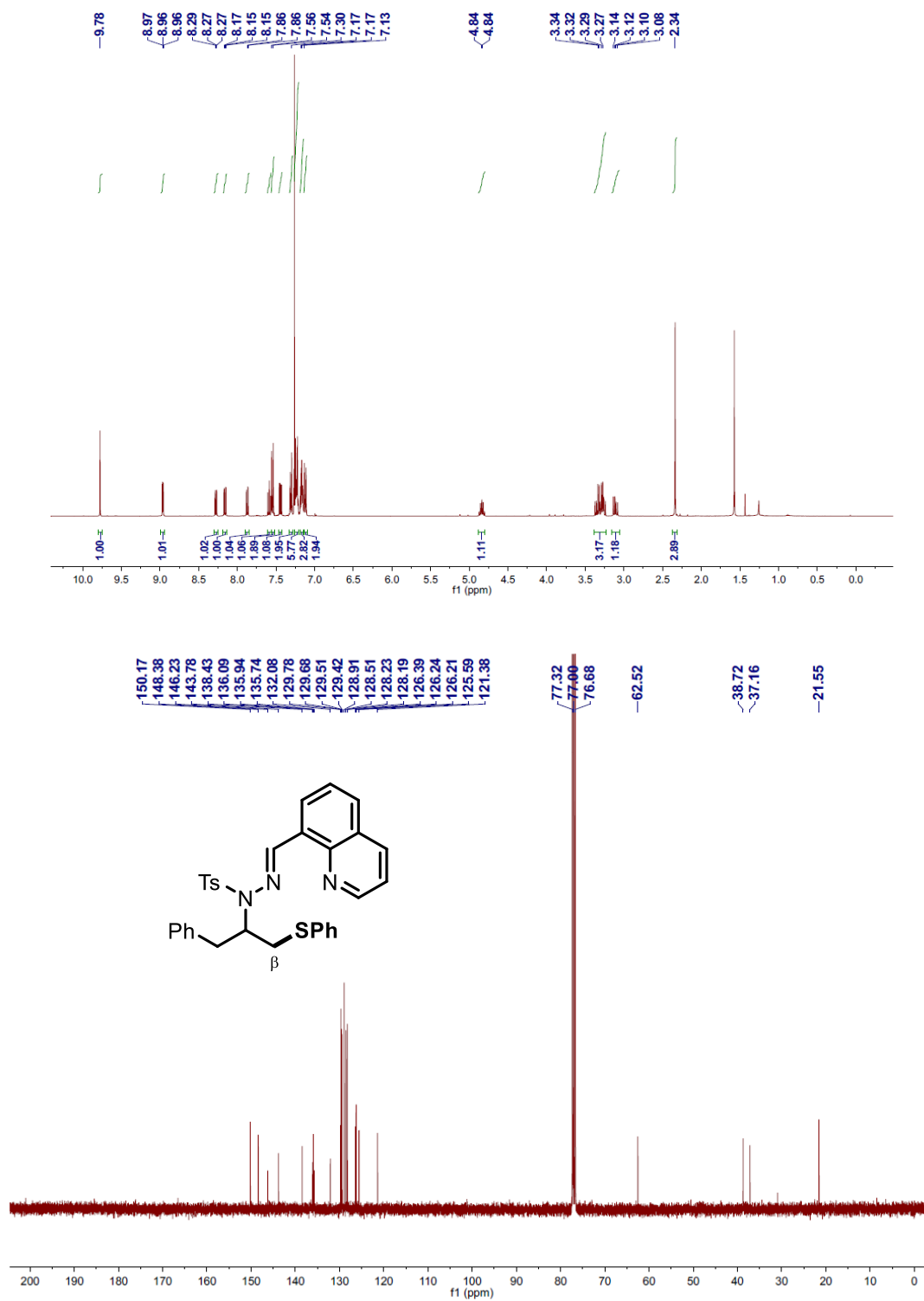


Figure 6.55 ¹H-NMR and ¹³C-NMR Spectrum of 6.20b

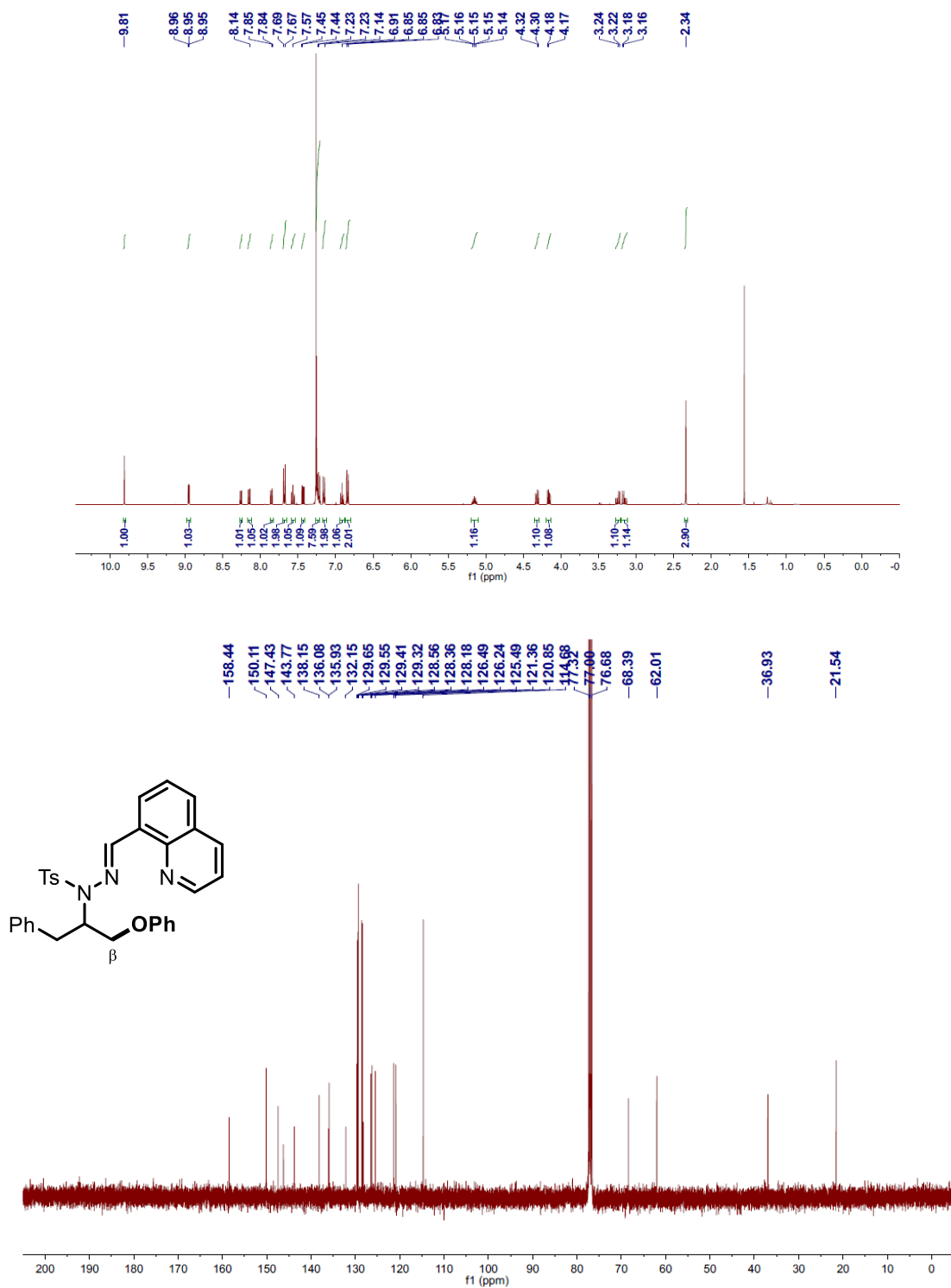


Figure 6.56 ^1H -NMR and ^{13}C -NMR Spectrum of 6.20c

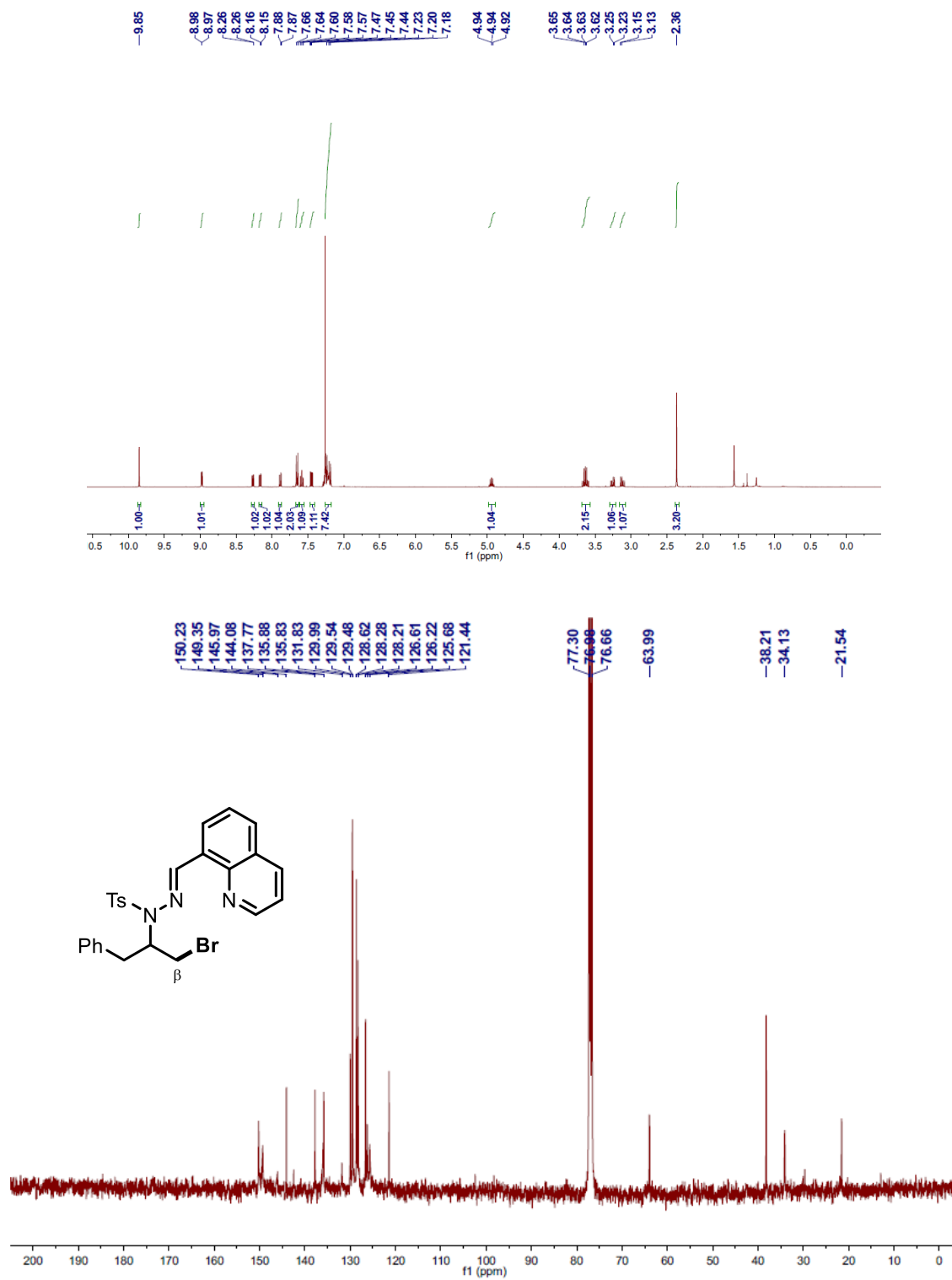


Figure 6.57 ¹H-NMR and ¹³C-NMR Spectrum of 6.20d

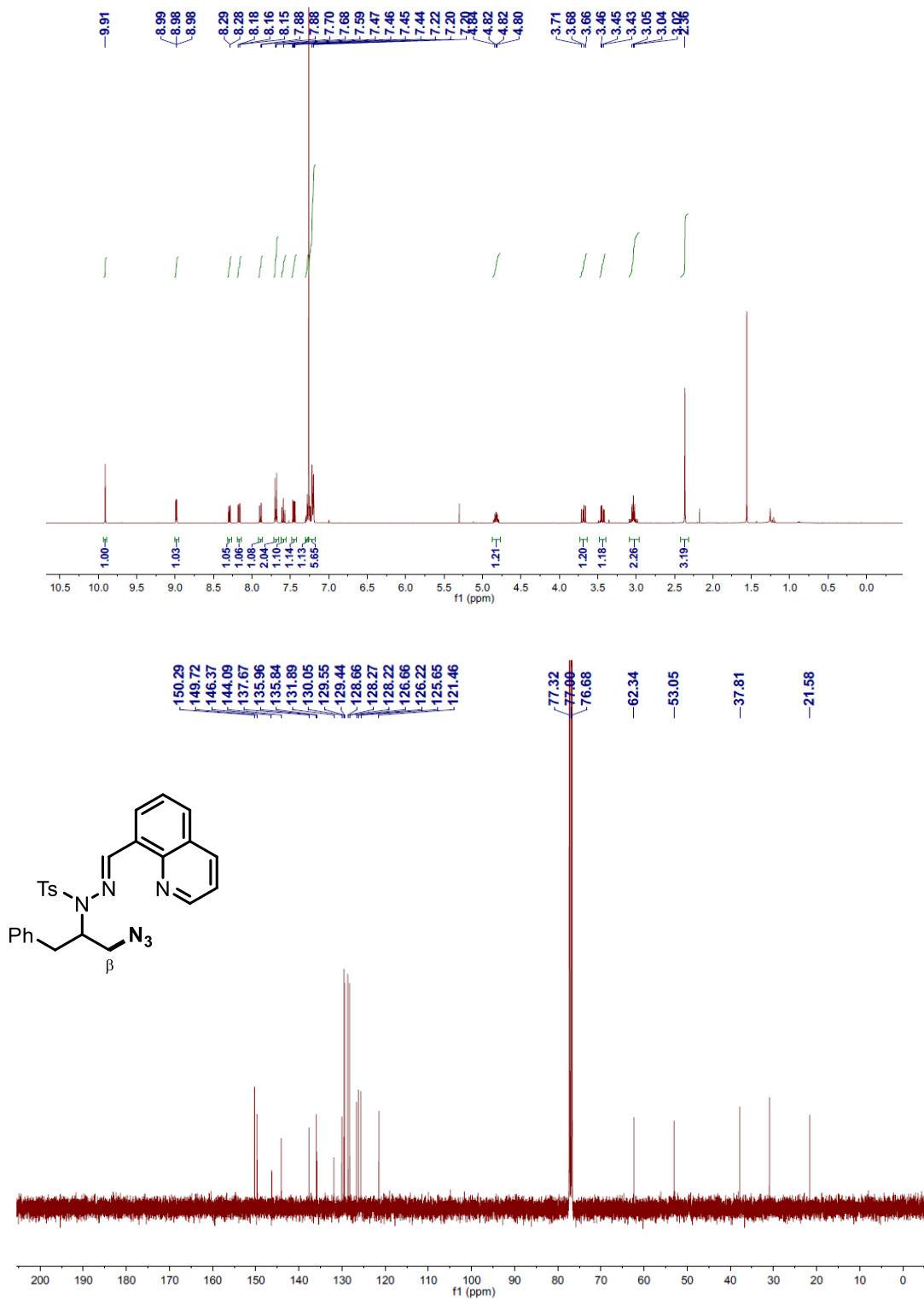


Figure 6.58 $^1\text{H-NMR}$ and $^{13}\text{C-NMR}$ Spectrum of 6.16

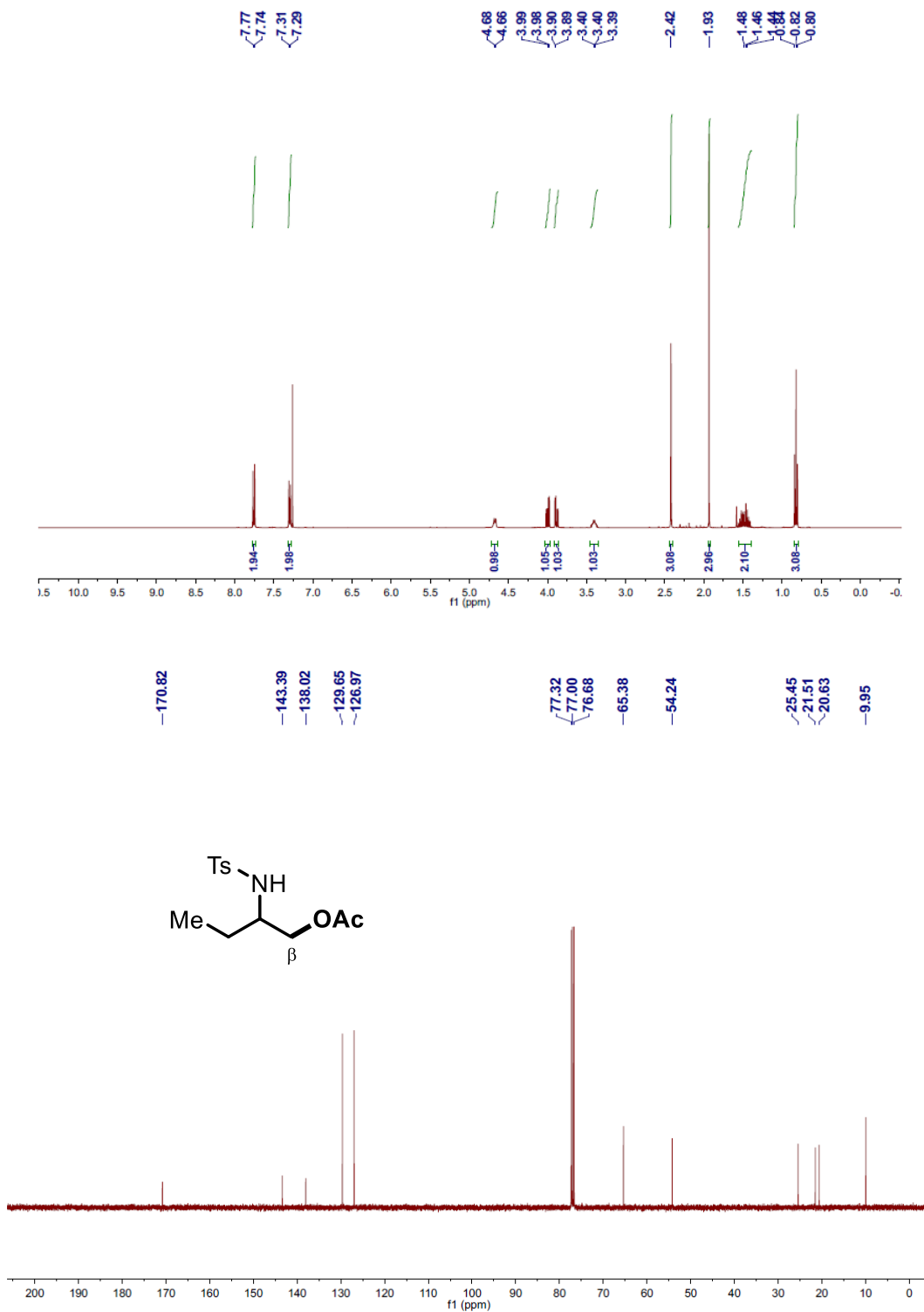


Figure 6.59 ¹H-NMR and ¹³C-NMR Spectrum of 6.20b'

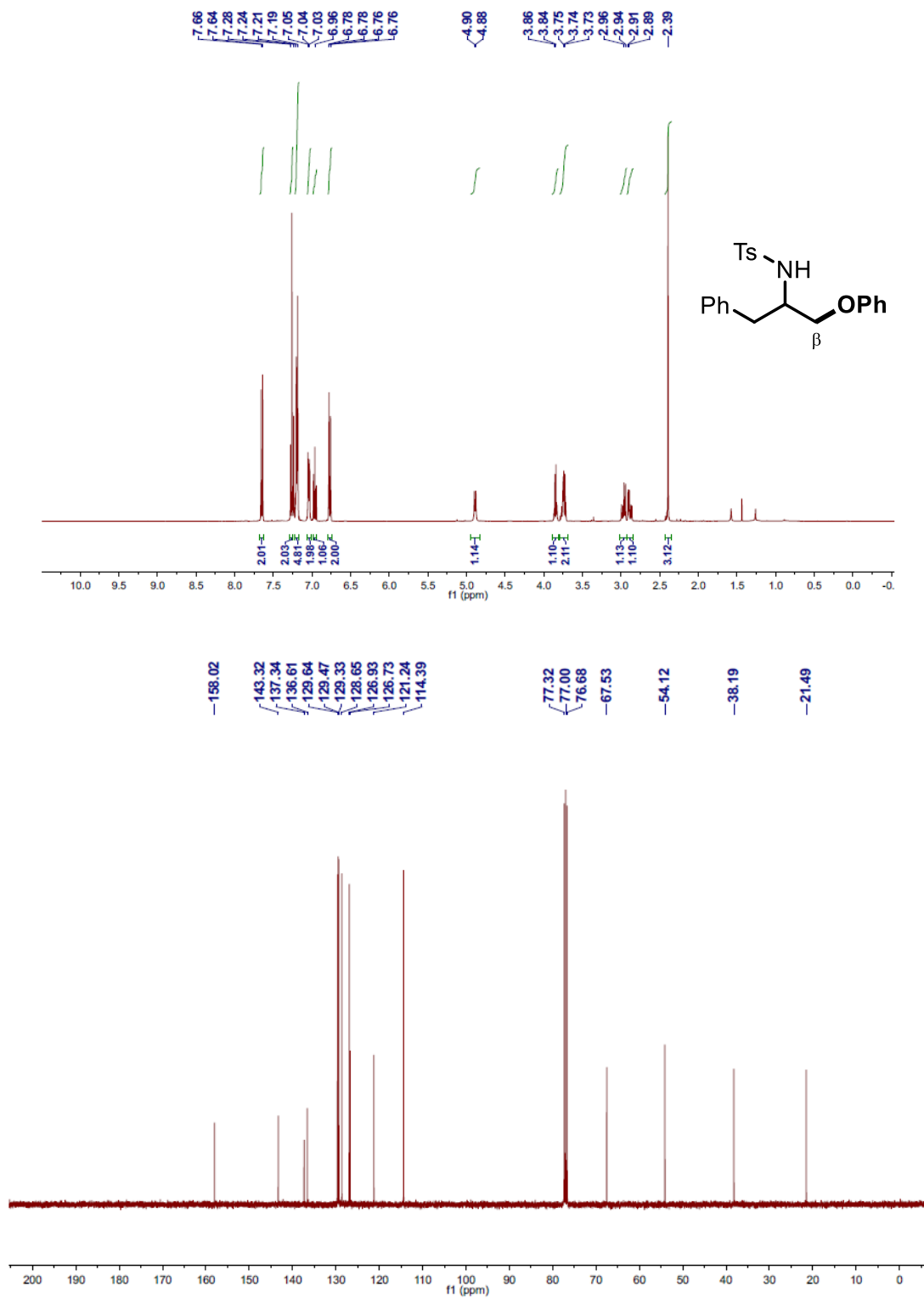
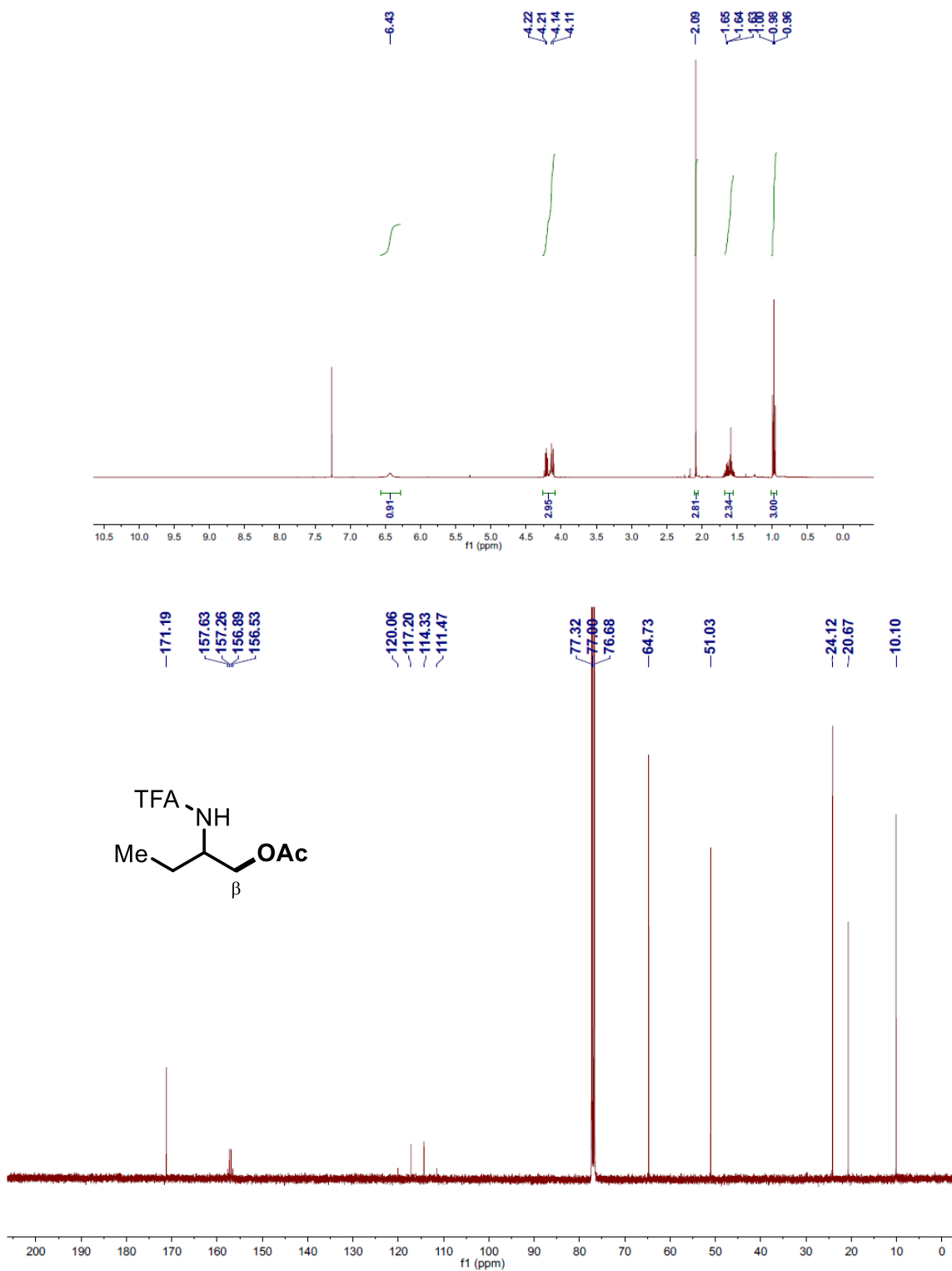


Figure 6.60 $^1\text{H-NMR}$ and $^{13}\text{C-NMR}$ Spectrum of 6.17



6.6 References

1. Vitaku, E.; Smith, D. T.; Njardarson, J. T. *J. Med. Chem.* **2014**, *57*, 10257.
2. For recent reviews, see: (a) Campos, K. R. *Chem. Soc. Rev.* **2007**, *36*, 1069. (b) Mitchell, E. A.; Pesciulli, A.; Lefevre, N.; Meerpoel, L.; Maes, B. U. W. *Chem. Eur. J.* **2012**, *18*, 10092. (c) Prier, C. K.; Rankic, D. A.; MacMillan, D. W. C. *Chem. Rev.* **2013**, *113*, 5322.
3. For seminal and recent examples, see: (a) Zaitsev, V. G.; Shabashov, D.; Daugulis, O. *J. Am. Chem. Soc.* **2005**, *127*, 13154. (b) He, G.; Chen, G. *Angew. Chem. Int. Ed.* **2011**, *50*, 5192. (c) He, G.; Zhao, Y.; Zhang, S.; Lu, C.; Chen, G. *J. Am. Chem. Soc.* **2012**, *134*, 3. (d) Nadres, E. T.; Daugulis, O. *J. Am. Chem. Soc.* **2012**, *134*, 7. (e) Zhang, S.; He, G.; Zhao, Y.; Wright, K.; Nack, W. A.; Chen, G.; *J. Am. Chem. Soc.* **2012**, *134*, 7313. (f) Zhang, S.-Y.; He, G.; Nack, W. A.; Zhao, Y.; Li, Q.; Chen, G. *J. Am. Chem. Soc.* **2013**, *135*, 2124. (g) Rodriguez, N.; Romero-Revilla, J. A.; Fernandez-Ibanez, M. A.; Carretero, J. C. *Chem. Sci.* **2013**, *4*, 175. (h) Fan, M.; Ma, D. *Angew. Chem. Int. Ed.* **2013**, *52*, 12152. (i) Ye, X.; He, Z.; Ahmed, T.; Weise, K.; Akhmedov, N. G.; Petersen, J. L.; Shi, X. *Chem. Sci.* **2013**, *4*, 3712. (j) Ling, P.-X.; Fang, S.-L.; Yin, X.-S.; Chen, K.; Sun, B.-Z.; Shi, B.-F. *Chem. Eur. J.* **2015**, *21*, 17503. (k) Zhang, L.-S.; Chen, G.; Wang, X.; Guo, Q.-Y.; Zhang, X.-S.; Pan, F.; Chen, K.; Shi, Z.-J. *Angew. Chem. Int. Ed.* **2014**, *53*, 3899. (l) Chan, K. S. L.; Wasa, M.; Chu, L.; Laforteza, B. N.; Miura, M.; Yu, J.-Q. *Nat. Chem.* **2014**, *6*, 146.
4. Li, Q.; Zhang, S.-Y.; He, G.; Nack, W. A.; Chen, G. *Adv. Synth. Catal.* **2014**, 356, 1544.
5. For recent examples, see: (a) Reddy, L. R.; Reddy, B. V. S.; Corey, E. J. *Org. Lett.* **2006**, *8*, 2819. (b) Francisco, C. G.; Herrera, A. J.; Martin, A.; Perez-Martin, I.; Suarez, E. *Tetrahedron Lett.* **2007**, *48*, 6384. (c) Fan, R.; Pu, D.; Wen, F.; Wu, J. *J. Org. Chem.* **2007**, *72*, 8994. (d) Chen, K.; Richter, J. M.; Baran, P. S. *J. Am. Chem. Soc.* **2008**, *130*, 7247. (e) Liu, T.; Mei, T.-S.; Yu, J.-Q. *J. Am. Chem. Soc.* **2015**, *137*, 5871.
6. (a) Choi, G. J.; Zhu, Q.; Miller, D. C.; Gu, C. J.; Knowles, R. R. *Nature* **2016**, *539*, 268. (b) Chu, J. C.K.; Rovis, T. *Nature* **2016**, *539*, 272.
7. Kim, M.; Mulcahy, J. V.; Espino, C. G.; Du Bois, J. *Org. Lett.* **2006**, *8*, 1073.
8. Olson, D. E.; Du Bois, J. *J. Am. Chem. Soc.* **2008**, *130*, 11248.
9. McNally, A.; Haffemayer, B.; Collins, B. S. L.; Gaunt, M. J. *Nature* **2014**, *510*, 129.
10. He, C.; Gaunt, M. J. *Angew. Chem. Int. Ed.* **2015**, *54*, 15840.
11. Kiener, C. A.; Shu, C.; Incarvito, C.; Hartwig, J. F. **2003**, *125*, 14272.

-
12. Ren, Z.; Dong, G. *Organometallics* **2016**, *35*, 1057.
13. (a) Desai, L. V.; Hull, K. L.; Sanford, M. S. *J. Am. Chem. Soc.* **2004**, *126*, 9542. (b) Neufeldt, S. R.; Sanford, M. S. *Org. Lett.* **2010**, *12*, 532.
14. (a) Ren, Z.; Mo, F.; Dong, G. *J. Am. Chem. Soc.* **2012**, *134*, 16991. (b) Ren, Z.; Schulz, J. E.; Dong, G. *Org. Lett.* **2015**, *17*, 2696.
15. Xu, Y.; Yan, G.; Ren, Z.; Dong, G. *Nat. Chem.* **2015**, *7*, 829.
16. Thompson, S. J.; Thach, D.; Dong, G. *J. Am. Chem. Soc.* **2015**, *137*, 11586.
17. For reviews of electrophilic amination, see: (a) Tamura, Y.; Minamikaw, J.; Ikeda, M. *Synthesis* **1977**, *1*. (b) Erdik, E. *Tetrahedron* **2004**, *60*, 8747.
18. (a) Marmer, W. N.; Marerker, G. *J. Org. Chem.* **1972**, *37*, 3520. (b) Shen, Y.; Friestad, G. K. *J. Org. Chem.* **2002**, *67*, 6236.
19. For a kilogram-scale synthesis of NBzONH₂, see: Shi, Z.; Kiau, S.; Lobben, P.; Hynes, J.; Wu, H.; Parlanti, L.; Discordia, R. P.; Doubleday, W.; Leftheris, K.; Dyckman, A. J.; Wroblewski, S. T.; Dambalas, K.; Tummala, S.; Leung, S. S. W.; Lo, E. T. *Org. Process Res. Dev.* **2012**, *10*, 1618.
20. For representative studies of S_N2-type reductive elimination on Pd(IV) intermediates, see: (a) Liu, G.; Stahl, S. S. *J. Am. Chem. Soc.* **2006**, *128*, 7179; (b) Racowski, J. M.; Gary, J. B.; Sanford, M. S. *Angew. Chem. Int. Ed.* **2012**, *51*, 3412; (c) Camasso, N. M.; Pérez-Temprano, M. H.; Sanford, M. S. *J. Am. Chem. Soc.* **2014**, *136*, 12771.
21. The SES protecting group can be readily removed using fluoride salts under mild conditions, see: Ribière, P.; Declerck, V.; Martinez, J.; Lamaty, F. *Chem. Rev.* **2006**, *106*, 2249.
22. (a) Nack, W. A.; He, G.; Zhang, S.-Y.; Lu, C.; Chen, G. *Org. Lett.* **2013**, *15*, 3440. (b) Guo, K.; Chen, X.; Guan, M.; Zhao, Y. *Org. Lett.* **2015**, *17*, 1802.
23. Moussa, Z.; Romo, D. *Synlett.* **2006**, 3294.
24. Capretto, D. A.; Brouwer, C.; Poor, C. B.; He, C. *Org. Lett.* **2011**, *13*, 5842.

CHAPTER 7

Further Exploration of Palladium-Catalyzed Direct β -Arylation of Ketones

7.1 Stoichiometric Heavy Metal-Free β -Arylation of Ketones with Aryl Iodides

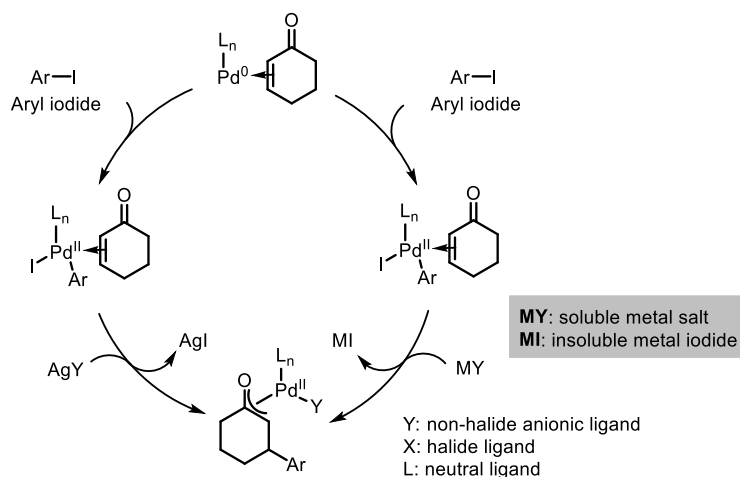
7.1.1 Introduction

There is no denying that there is still a long way before making this β -arylation reaction a truly practical methodology. One major direction we are pursuing is to avoid the use of stoichiometric amount of heavy metal additives (i.e. silver or copper salt). In our original β -arylation conditions with aryl iodides, these heavy metal salts are essential for extracting iodide ligands from the palladium intermediate and restoring the active catalysts. However, as these salts can both serve as an oxidant for the Pd(0) species, the reaction mechanism is thus complicated by the possibility of a ‘two-cycle’ pathway, where both stoichiometric oxidant (heavy metal salts) and reductant (excess ketone or solvent) are involved (*vide supra*, Scheme 5.1).

The strategy outlined in Chapter 6 offered an indirect solution to avoid the use of silver salts and elucidate the redox property of the β -arylation reaction by using mesitylaryliodonium salt as the aryl source. The key to the success is that the oxidative addition of mesitylaryliodonium salt to Pd(0) transfers an aryl group and a non-halide ligand (i.e. trifluoromethanesulfonate), and the iodide is released in the form of iodomesitylene, an inert aryl electrophile (*vide supra*, Scheme 5.2). Thus, as iodide is never transferred to the palladium intermediate, iodide scavenger is no longer necessary. Without redox-active additives, the analysis of the optimized conditions indicated the β -arylation with mesitylaryliodonium salt is indeed redox-neutral (*vide supra*, Scheme 5.9).

A direct solution to eliminate the use of stoichiometric silver salts for the arylation with iodides, on the other hand, is to replace the silver salts with cheap and non-redox-active metal salts that can form insoluble metal halides under the reaction conditions (Scheme 7.1). The key of the success of this strategy is a significant difference in solubility between the metal salt additive and the resulting metal iodide. In addition, when the metal salt undergoes the salt metathesis with the palladium intermediate after the oxidative addition, it also transfers an anionic ligand to the palladium. Thus, in order to restore the active palladium catalyst for the dehydrogenation step, a metal salt with acetate-type ligands should be necessary.

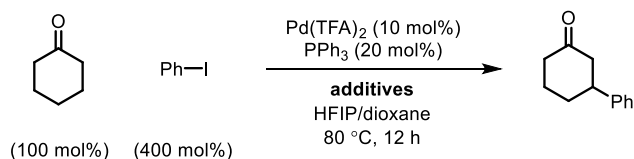
Scheme 7.1 Use of Non-redox-active Salts as the Iodide Scavenger



7.1.2 Results and Discussion

We first attempted to directly replace the silver salts in our previous β -arylation conditions with a wide range of metal additives with acetate-type anions (Table 7.1). However, when Pd(TFA)₂ and PPh₃ were used as the precatalyst, these salts turned out to be ineffective for the β -arylation reaction, and only lead trifluoroacetate gave the desired product in a low yield.

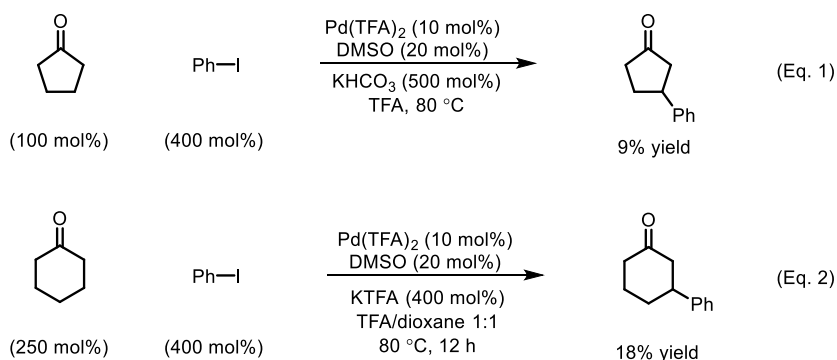
Table 7.1 Replacement of Silver Salts in Previous Conditions



Additives (mol%)	Yield (%)	Conversion (%)
NaOAc (300)	0%	0%
KOAc (300)	0%	0%
Pb(TFA) ₂ (150)	7%	11%
LiOAc (150)	0%	0%
KTFA (200)	0%	5%
CsTFA (200)	0%	15%
LiTFA (200)	0%	2%

We then switched our attention to an early entry of conditions that was capable of giving the β -arylation product without silver additive (*vide supra*, Scheme 4.9). By using potassium bicarbonate instead of silver salt, the β -arylation reaction of cyclopentanone could still afford the product in 9% yield. Considering the fact that potassium bicarbonate can readily react with TFA in the conditions, we assumed the active promoter is KTFA. Starting from these particular conditions, we further improved the reaction by employing a mixed solvent consisting of trifluoroacetic acid and dioxane. An extensive optimization of ligands also demonstrated that DMSO is a supreme ligand for the new reaction.¹ Therefore, the reaction of cyclohexanone and iodobenzene could afford the desired β -arylation product in 18% yield, by using 400 mol% of KTFA as the promoter, DMSO as the ligand and TFA/dioxane as the mix-solvent (Scheme 7.2, Eq. 2).

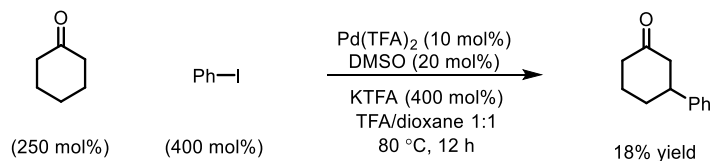
Scheme 7.2 Early Results Using KTFA as Iodide Scavenger



A brief kinetic profile was also obtained during the condition optimization (Scheme 7.3). The preliminary reaction conditions turned out to be very chemoselective, with few byproducts formed. Especially, no phenols from the over-oxidation, as well as enone, were observed throughout the course of the reaction. While the yield ceased to increase at around 20%, the

conversion of iodobenzene was also low, meaning a brsm (based on recovered starting material) yield. It was also observed that the reaction turned black when the yield ceased to increase, probably due to the deactivation of palladium catalyst to palladium black.

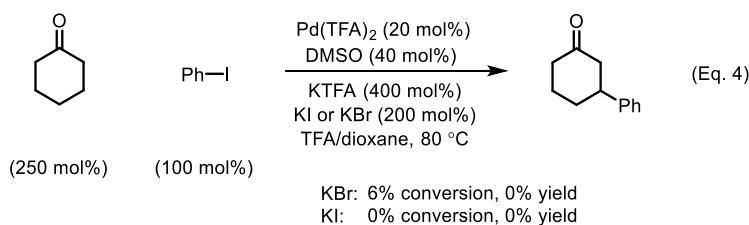
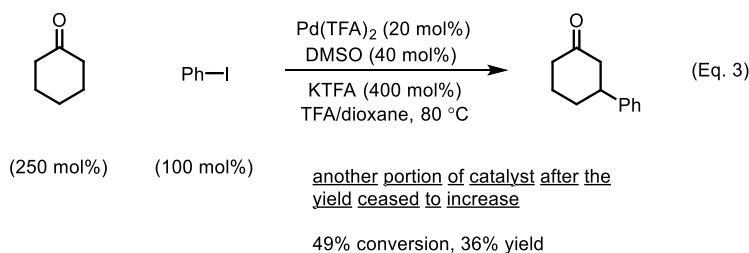
Scheme 7.3 Kinetic Profile of Early Reaction Conditions



Time	Yield (%)	PhI conversion (%)
0 min	0	0
3 min	1	8
8 min	3	9
16 min	5	8
25 min	7	10
40 min	7	10
120 min	14	19
180 min	16	17
210 min	16	17
265 min	16	17
300 min	16	17
330 min	15	17
450 min	17	18

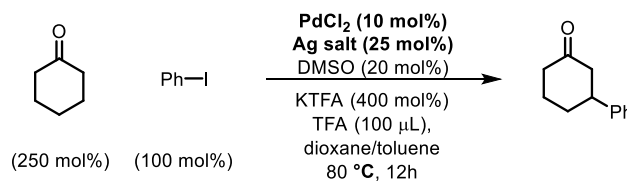
Another observation also indicated the deactivation of catalyst is the limiting factor of the reaction (Scheme 7.4). After the kinetic study was done, we added another portion of Pd(TFA)₂ and DMSO ligand and let it further react overnight. The GC analysis of the resulting mixture showed that the yield of the reaction doubled, which supported our hypothesis that the reaction ceased because of the loss of active palladium catalyst (Eq. 3). On the other hand, it is also observed the addition of 200 mol% of KBr or KI salt completely inhibited the product formation (Eq. 4). This implied that the abstraction of iodide by the potassium salt is not sufficient and/or the solubility of KI is not bad enough under the reaction conditions, which may contribute to the catalyst deactivation.

Scheme 7.4 Kinetic Profile of Early Reaction Conditions



Generally, there are two solutions to solve the issue of catalyst deactivation. The first is to elongate the lifetime of catalyst, and the second is to increase the reactivity of catalyst to make it undergo more catalytic cycles before the deactivation takes place.

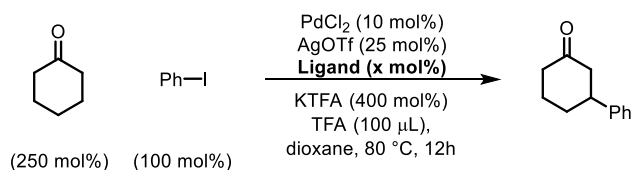
In our case, we did find that modifying the palladium catalyst could double the TON. By using the combinations of catalytic palladium dichloride and different silver salts, the yield of the reaction can be increased to near 40% (Table 7.2). Among all the silver salts screened, silver triflate gave the best result. Compared with palladium trifluoroacetate, we proposed the *in situ* formed palladium triflate has more cationic characters, which may favor the palladium enolate formation by facilitating the initial coordination of the weakly Lewis basic ketone carbonyl to the palladium catalyst.

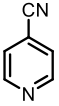
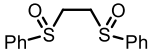
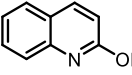
Table 7.2 Combination of Catalytic PdCl₂ and Silver Salts as Precatalysts

Ag salt (mol%)	Yield (%)	Conversion (%)
AgOTs	28	36
AgOTf	36	46
AgBF ₄	29	37
AgSbF ₆	31	39
AgPF ₆	29	44
AgNTf ₂	28	31
AgTFA	28	34

With the new palladium precatalyst, we set out to screen different types of ligands (Table 7.3). The new stoichiometric heavy metal-free conditions demonstrated a distinct preference for ligands compared with previous conditions using stoichiometric amount of silver salts (*vide supra*, Table 4.1). While P(*i*-Pr)₃ was the best ligand for the previous conditions, phosphine-based ligands (e.g. triarylphosphine, trialkylphosphine, and phosphite) generally gave low yield for the new conditions. Pyridine-based ligands didn't deliver the β-arylation product in high efficiency either. Instead, sulfur-based ligands turned out to superior, with monodentate sulfoxide ligands outperforming their bidentate and sulfide counterparts. Eventually, simple DMSO was selected as the ligand for the following screening study.

Table 7.3 Selected Screening of Ligands

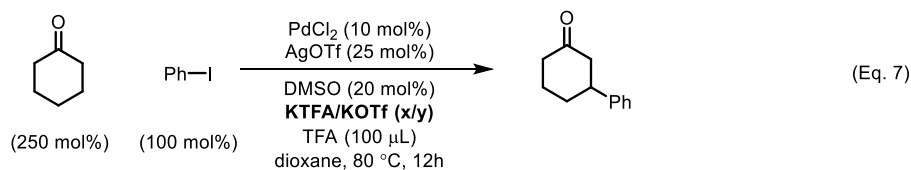
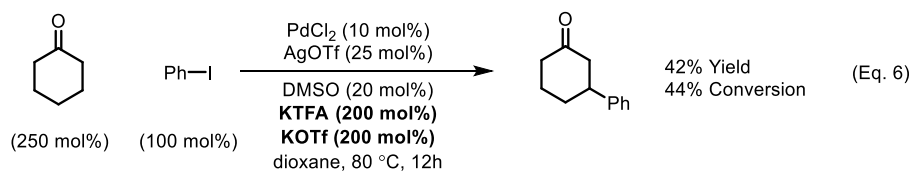
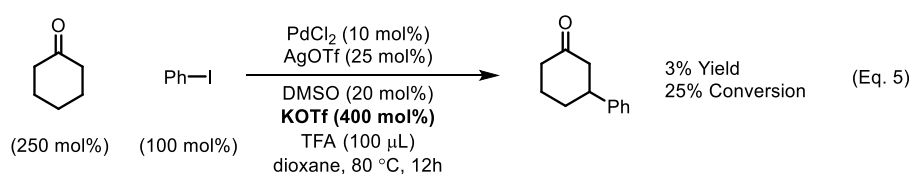


Ligands	Yield(%)	Conversion(%)
 (20)	8	19
DMSO (20)	37	47
 (20)	29	41
 (10)	26	27
 (20)	0	10
 (20)	0	0
 (20)	22	23
PPh_3 (20)	7	33
$\text{P}(p\text{-OMeC}_6\text{H}_4)_3$ (20)	7	27
$\text{P}(\text{C}_6\text{F}_5)_3$ (20)	8	32
$\text{P}(3,5\text{-diCF}_3\text{-C}_6\text{H}_3)_3$ (20)	1	18
PCy_3 (20)	0	14
dppb (10)	0	7
$\text{P}(\text{OCH}_2\text{CF}_3)_3$ (20)	10	35

After *in situ* generated palladium triflate was established as a superior catalyst, it was reasonable to postulate that potassium triflate might be a better promoter than potassium trifluoroacetate. However, to our surprise, the reaction was significantly inhibited when KOTf was used in place of KTFA (Scheme 7.5, Eq. 5). We proposed that the disastrous effect might be

attributed to the strong triflate acid that was released during the reaction. And interestingly, when an equal molar mixture of KTFA and KOTf was used as promoters, the yield slightly increase compared with using merely KTFA (Eq. 6). Regarding this observation, we hypothesized that KOTf might also act as a promoter to extract iodide from palladium, and at the same time maintain the cationic property of the palladium catalyst by transferring triflate anion. However, to prevent the reaction medium from becoming too acidic, KTFA is still needed to react with generated triflate acid to give relatively weak trifluoroacetate acid. In another word, the KTFA/TFA in the reaction conditions acted as a buffer system to keep the reaction acidity from going too high. In addition, a micro-tuning of the reaction conditions showed that changing the ratio between two potassium salts could slightly increase the yield (Eq. 7).

Scheme 7.5 Effects of a Mixture of KTFA and KOTf as the Additive



Salt (mol%)	Yield(%)	Conv.(%)
KTFA/KOTf (300/100)	43	46
KTFA/KOTf (100/300)	33	41
KTFA/KOTf (350/50)	39	42

The better performance of the mixture of KTFA and KOTf prompted us to carry out a detailed screening of salts with weakly coordinating anions (Table 7.4). While most of anions, including *p*-toluenesulfonic, hexafluorophosphate, and triflate, could afford the β -arylation product, sodium tetrafluoroborate turned out to be better in terms of yield. In addition, replacement of KTFA with other trifluoroacetate salts results in a lower reactivity.

Table 7.4 Screening of Salt Combination

Reaction scheme: Cyclohexanone (250 mol%) + Ph-I (100 mol%) $\xrightarrow[\text{salt combination, dioxane/TFA 10:1, 80 }^\circ\text{C}]{\text{PdCl}_2 (10 \text{ mol\%}), \text{AgOTf} (25 \text{ mol\%}), \text{DMSO} (20 \text{ mol\%})}$ 2-phenylcyclohexanone

	Yield (%)	PhI conversion (%)	ketone consumed (/250 mol%)
KTFA (300) and:			
KH ₂ PO ₄ (100)	42	57	60
K ₂ HPO ₄ (100)	41	55	50
NaOTf (100)	32	61	87
NaBF₄ (100)	43	46	50
NaOTs (100)	30	54	74
NaPF ₆ (100)	31	57	75
NH ₄ BF ₄ (100)	21	50	59
NH ₄ PF ₆ (100)	18	44	62
MeSO ₂ Na (100)	8	17	33
PhSO ₂ Na (100)	13	35	60
CF ₃ SO ₂ Na (100)	29	45	70
KOTf (100) and:			
CsTFA (300)	28	51	69
Zn(TFA) ₂ (300)	25	57	43
Zn(TFA) ₂ (100) withKTFA (200)	39	59	37

Control experiments aiming to compare the effects of KOTf and NaBF₄ showed the latter led to a high efficiency for the β -arylation reaction. Considering the beneficial role of the tetrafluoroborate anion, we moved forward to replace the triflate anion in the catalytic silver salt. However, use of silver tetrafluoroborate did not benefit the reaction compared with silver triflate.

We proposed the use of silver triflate is necessary for an efficient abstraction of chloride ligand of PdCl₂ and initiation of the reaction. On the other hand, during the course of the β-arylation, tetrafluoroborate anion is a better choice to replace the iodide ligand after the oxidative addition.

One of the concerns during our optimization is the efficient generation of the active palladium catalyst. We proposed that the palladium would undergo a ligand exchange with the silver salt and complexation with DMSO to become a ligated and cationic palladium catalyst. However, as we often observed that the non-ligated palladium chloride took a long time to dissolve in the mixed solvent, the formation of the active palladium catalyst may not be complete under the reaction conditions. Thus, the effective catalyst loading could be lower than the amount of added palladium chloride. To address this concern, we have synthesized the DMSO-ligated palladium chloride, it proved to be a better precatalyst than the combination of palladium chloride and DMSO (Scheme 7.6). Later, using the new palladium catalyst, a systematic screening of the amount of KTFA and NaBF₄ additive showed a 3:2 mixture of these two salts in a total amount of 500 mol% is optimal for the β-arylation reaction (Table 7.5).

Scheme 7.6 Use of Ligated Palladium Chloride as Precatalyst

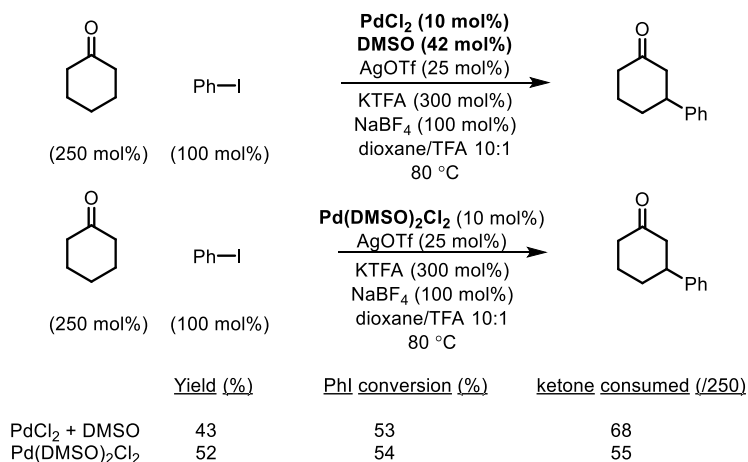
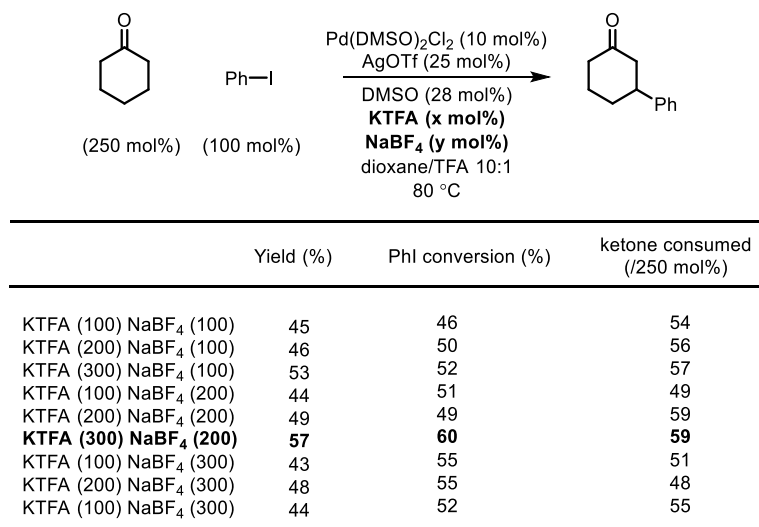


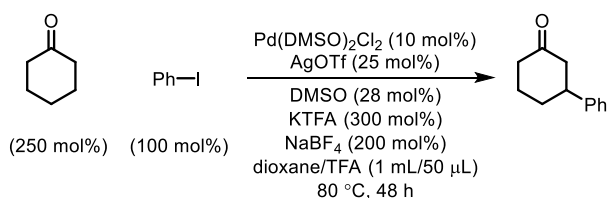
Table 7.5 Screening of the Amount and Ratio of Salt Additives



As mentioned above (*vide supra*, Scheme 7.4), the addition of a second portion of palladium catalyst and ligand would further increase the conversion and yield of the β -arylation. This observation implied that the deactivated palladium species (i.e. palladium black) wouldn't interfere with the new added palladium catalyst. In addition, the rate of the deactivation of active catalyst is often positively correlated to the concentration of palladium species. Thus we

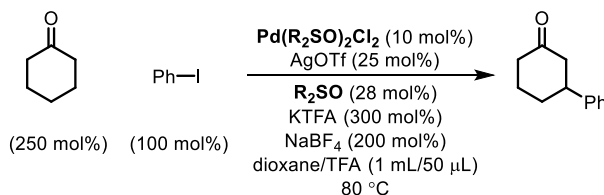
anticipated that a portionwise addition of the catalyst and reagent would benefit the reaction by maintaining a low concentration of the palladium intermediates. Indeed, when the precatalyst, ligand and salt additives were added to the reactant in two portions, the yield and conversion can be both boosted (Table 7.6, entry 1 and 2). While an even higher yield can be obtained using a four-portion addition method, the applicability of method may be hampered by the complicated reaction set-up and addition procedure (entry 3).

Table 7.6 Portion-wise Addition of Catalyst and Additives



Entry	[Pd]	[Ag]	DMSO	KTFA	NaBF ₄	solvent	Yield (%)	PhI conversion (%)	ketone consumed (/250)
1	1	1	1	1	1	1 mL	53	58	59
2	2	2	2	2	2	1 mL	61	62	68
3	4	4	4	1	4	1 mL	68	71	76

Table 7.7 Effects of Pd(Ph₂SO)₂Cl₂ as Precatalyst



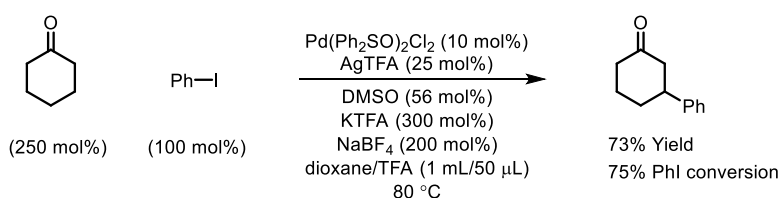
Entry	Pd precatalyst	additional ligand	Yield (%)	PhI conversion (%)	ketone consumed (/250)
1	Pd(Ph ₂ SO) ₂ Cl ₂	DMSO	65	70	90
2	Pd(Ph ₂ SO) ₂ Cl ₂	none	54	56	75
3	Pd(Ph ₂ SO) ₂ Cl ₂	PhSOPh	44	50	67
4	Pd(DMSO) ₂ Cl ₂	PhSOPh	52	61	90

Another improvement of the optimization was achieved when Pd(Ph₂SO)₂Cl₂ was used as the precatalyst instead of the DMSO-ligated palladium chloride. A set of detailed control

experiments was executed to compare the performance between DMSO and diphenylsulfoxide (Table 7.7). It was discovered that the best result was obtained when Pd(Ph₂SO)₂Cl₂ and additional DMSO ligand were employed in combination (entry 1). Pd(Ph₂SO)₂Cl₂ without any additional ligands led to a drop in the yield (entry 2). On the other hand, when diphenylsulfoxide was used in its free form with either Pd(Ph₂SO)₂Cl₂ or Pd(DMSO)₂Cl₂, the yields are not as good (entry 3 and 4). Based on these results, we hypothesized the better performance of Pd(Ph₂SO)₂Cl₂ may be due to a faster initiation of the reaction or generation of the active catalyst, and a mixture of DMSO and Ph₂SO is important to maintain the reactivity during the course of the reaction.

At the late stage of the optimization, we found the silver triflate additive can be replaced with silver trifluoroacetate, leading to a better yield of the reaction, as well as simplified conditions, where two types of anion (instead of three types when silver triflate was used) operate together to deliver the β-arylation product (Scheme 7.7). In addition, further increasing the amount of additional DMSO ligand proved to be beneficial to the reaction outcome.

Scheme 7.7 Optimized Stoichiometric Heavy Metal-Free Conditions with Aryl Iodides



7.2 β -Arylation of Ketones with Aryl Bromides

7.2.1 Introduction

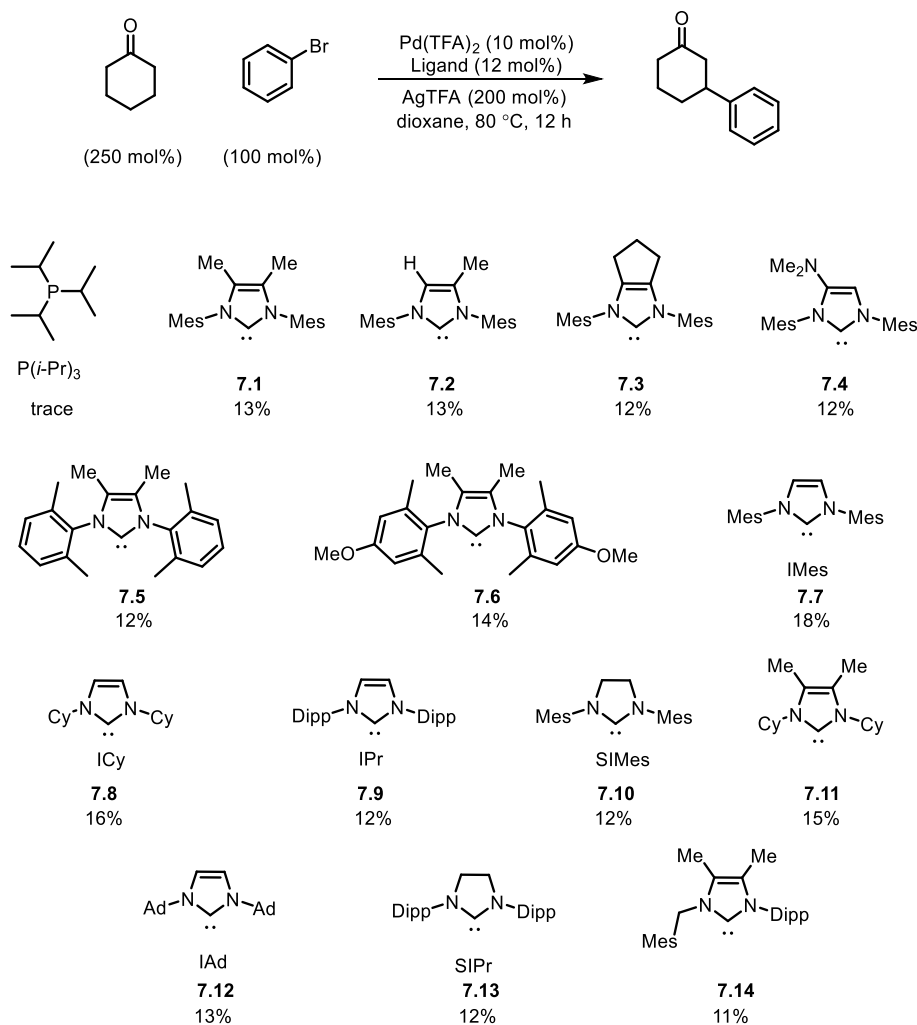
As mentioned in Chapter 4 (*vide supra*, Scheme 4.14), the use of more available and cheaper aryl bromides replace aryl iodides as the aryl source for the β -arylation reaction is highly sought after. However, the major obstacle to achieving this goal is the slower oxidative addition of aryl bromides compared with iodides.² Without a rapid oxidative addition, the resting Pd(0) intermediate is prone to decomposition to palladium black through aggregation in the absence of excess ligands. It was found that addition of more phosphine ligands inhibited the ketone desaturation step likely by blocking the coordination site for β -H elimination. The use of bidentate phosphine ligand may increase rate of oxidative addition of Pd(0) and prevent decomposition. However, they are not effective for the ketone dehydrogenation step. Thus, the key to address the challenge of using ArBr as the coupling partner is to find a suitable ligand that can stabilize the Pd(0) intermediate but meanwhile not interfere with the desaturation step.

We hypothesized that instead of using monodentate phosphine ligands, bulky *N*-heterocyclic carbene (NHC) ligands are known to promote efficient oxidative addition of Pd(0) with ArBr, ArOTf and even ArCl due to their strong σ -donating ability.³ Comparing with trialkylphosphines, NHC ligands (e.g. IMes) also have stronger π -interactions with electron-rich metals and possess an umbrella shape, thus can better stabilize Pd(0) species. In addition, NHC ligands holds a strong “trans effect”, which should aid the final protonation of the Pd(II)-enolate.⁴

7.2.2 Results and Discussion

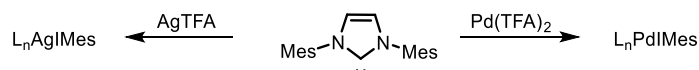
To test the hypothesis, we first screened free NHC ligands with a wide range of steric and electronic properties by directly replacing $P(i\text{-Pr})_3$ in our previous conditions. As we proposed, compared with $P(i\text{-Pr})_3$, all these NHC ligands demonstrated superior reactivity for the β -arylation with bromobenzene (Scheme 7.8). However, the difference among these ligands is not dramatic, with IMes (**7.7**) and ICy (**7.8**), two unsaturated NHC ligands, being the best candidates.

Scheme 7.8 Preliminary Screening of Various Free NHC Ligands



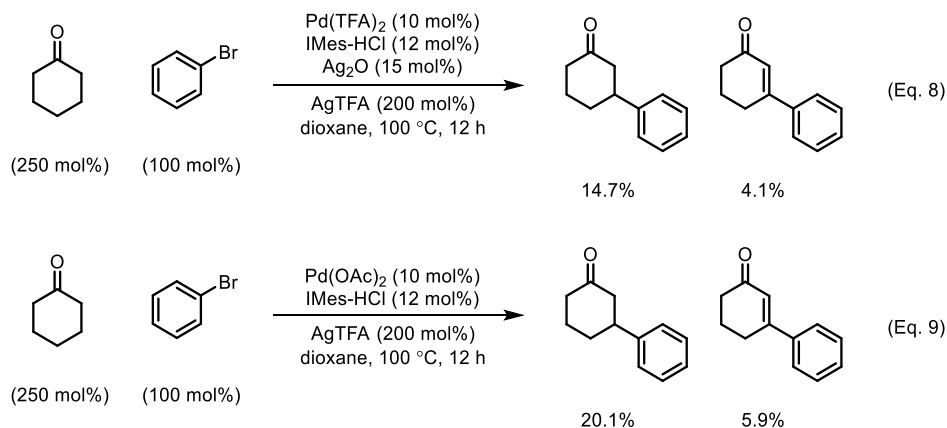
A concern regarding the use of free NHC ligand under the reaction conditions is the selectivity of its complexation with metals. As a stoichiometric amount of silver salt is employed for the β -arylation reaction, it may compete with the palladium catalyst for the NHC ligand (Scheme 7.9). Also due to the strong metal-NHC bond and large amount of silver, the formed silver-NHC complex may not be able to exchange the ligand back to the palladium catalyst. It is also known that high concentration of free NHC ligand tends to facilitate the side reaction of dimerization, if the complexation with the metal catalyst is not fast enough. To address this issue, we have tested several methods for the generation of active Pd-NHC catalyst other than the direct of free NHC ligands (Scheme 7.10).

Scheme 7.9 Competing Complexation with NHC ligand of Palladium and Silver Salt



We first attempted to use the combination of NHC hydrochloride salt and silver oxide. It is well established that the reaction between these two can *in situ* generate a Ag-NHC complex and subsequently transfer the NHC ligand to other metal catalyst, thus avoiding a high concentration of free NHC ligands. However, probably due to the large amount of silver salts present, this method of catalyst generation did not improve the efficiency of the β -arylation reaction (Eq. 8). By using the IMes hydrochloride salt, we also tried to replace Pd(TFA)₂ with more basic Pd(OAc)₂, which could deprotonate the IMes salt and form Pd-NHC complex *in situ*. The advantage of this method is a good selectivity, as AgTFA would not compete with Pd(OAc)₂ due to the lower basicity of trifluoroacetate anion. However, only a slight improvement in the yield was observed with this method (Eq. 9).

Scheme 7.10 *In Situ* Generation of Pd-NHC Catalyst



We hypothesized that a reliable solution for the catalyst generation is to use a palladium precatalyst that is already complexed with NHC ligands. Thus, three types of IMes-ligated palladium catalysts with different anions were synthesized and submitted the reaction conditions. These precatalysts turned out to be outstanding and delivered the β -arylation product in over 30% yield (Table 7.8).

Table 7.8 Effects of IMes-ligated Palladium Precatalyst

catalyst (x mol%)	Yield (%)	By-product (%)
[IMesPdCl ₂] ₂ (5)	31.3	9.2
[IMesPd(OAc) ₂] ₂ (5)	30.0	6.8
[IMesPd(TFA) ₂] ₂ (5)	30.7	8.1

Detailed analysis of the reaction mixture showed only around 40% of bromobenzene was consumed under the reaction condition. This is a distinct feature from reactions with

iodobenzene, where a full conversion was often observed. Again, as we explained previously, the low conversion also supported the premature deactivation of the palladium catalyst due to the difficult oxidative additive. While umbrella-shape IMes ligand could prevent Pd(0) from aggregation, we proposed a secondary ligand could further help stabilize the palladium center through the occupation of vacant coordination site. This strategy has been demonstrated in prior literatures, where PEPPSI-type palladium complex with both an NHC and pyridine-type ligand showed high stability in the coupling reactions. However, the secondary ligand should not be strongly coordinating, as it needs to be readily replaced by ketone substrate for the dehydrogenation step.

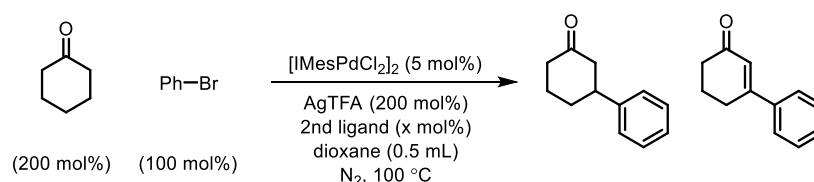
Table 7.9 Examination of PEPPSI-type Ligands

Reaction scheme: Cyclohexanone (200 mol%) + Ph-Br (100 mol%) $\xrightarrow[\text{AgTFA (200 mol\%), dioxane (0.5 mL), N}_2, 100\text{ }^\circ\text{C}]{\text{catalyst}}$ 2-phenylcyclohexanone + 2-phenylcyclohex-2-enone

Catalyst (x mol%)	Yield (%)	By-product (%)
[IMesPdCl ₂] ₂ (5)	25.7	6.9
 (10)	30.6	3.8
 (10)	26.7	14.3

Based on these hypotheses, we first tested two PEPPSI-type⁵ Pd-NHC complexes for the reaction, which indeed gave better results compared with [IMesPdCl₂]₂ (Table 7.9). A large collection of ligands, including phosphines, phosphites, amines, and sulfides, was also screened as an additional ligand for [IMesPdCl₂]₂ (Table 7.10). Nevertheless, while some of these ligands could afford the β-arylation product in a higher yield, no significant improvement was obtained.

Table 7.10 Screening of a Secondary Ligand



Ligand (x mol%)	Yield (%)	By-product (%)
as above	25.4	4.5
(10)		
Ar = <i>p</i> -OMeC ₆ H ₄	9.7	0.2
Ar = <i>p</i> -FC ₆ H ₄	10.0	0.3
(10)	14.6	2.8
P(OPh) ₃	28.0	4.6
(50)	22.3	1.5
(50)	26.6	4.5
Pt-Bu ₃	26.5	4.0
pyridine	16.8	1.7
pyridine	trace	trace
(25)	19.2	2.5
(25)	15.6	1.7

We also tried to further stabilize the Pd(0) intermediate using bidentate NHC ligands. First, a bis-NHC ligand (**7.15**) was employed in combination with Pd(OAc)₂. However, the β-arylation reaction was completely inhibited, probably due to the large steric hindrance, or strong electron-donating property that prevents the palladium catalyst from dehydrogenating the ketone (Table 7.11). On the other hand, when NHC ligands with a carboxylic acid (**7.16**) or amide (**7.17**) side chain were used, the reactivity of arylation can be maintained. However, no improvement in terms of yield was observed compared with simple IMes ligand.

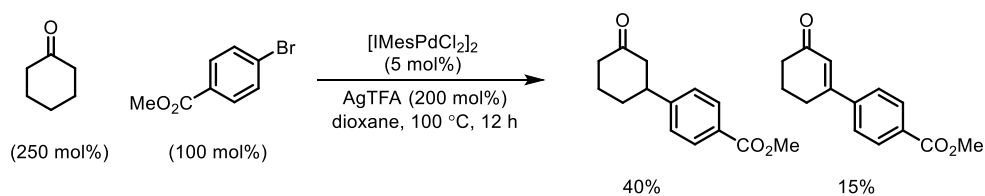
Table 7.11 Effects of Bidentate NHC Ligands

(250 mol%) (100 mol%)

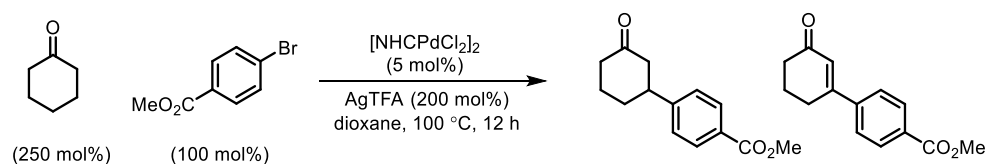
NHC ligand	Yield (%)	By-product (%)
<p>7.15</p>	0.0	0.0
<p>7.16</p>	9.4	0.0
<p>7.17</p>	27.6	2.7

It is noteworthy that under the reaction conditions with NHC ligands, the preference of the β -arylation reaction for electron-deficient aryl halides is still obvious: when methyl 4-iodobenzoate was subjected to the reaction, a higher yield was obtained (Scheme 7.11, which is consistent with our hypothesis that oxidative addition is the main obstacle).

Scheme 7.11 Reaction with Methyl 4-Iodobenzoate under Conditions with IMes Ligand



The latest improvement for the reaction conditions was achieved when a set of NHC-ligated palladium chloride precatalyst was synthesized and tested (Table 7.12). It can be concluded from the results that catalysts with saturated NHC ligands (SIMes and SIPr) are not suitable for the reaction. As NHC ligands with saturated backbones are more electron-donating than their unsaturated counterparts, we proposed this might lead to palladium centers that are too electron-rich for the dehydrogenation. On the other hand, increasing the steric of the NHC ligands by replacing mesityl with adamantyl group also lowered the yield to a large extent. And ICy was found to outperform IMes ligand for the reaction, giving the highest yield so far for the β -arylation with bromobenzene.

Table 7.12 Reaction with Different NHC-ligated Palladium Precatalysts

Precatalyst	Yield (%)	conversion of ArBr (%)	ketone (out of 250%) consumed	Enone (%)
[IMesPdCl ₂] ₂	42	68	79	14
[SIMesPdCl ₂] ₂	27	52	80	16
[SIPrPdCl ₂] ₂	22	54	60	9
[IAdPdCl ₂] ₂	20	33	42	5
[ICyPdCl ₂] ₂	45	80	84	2

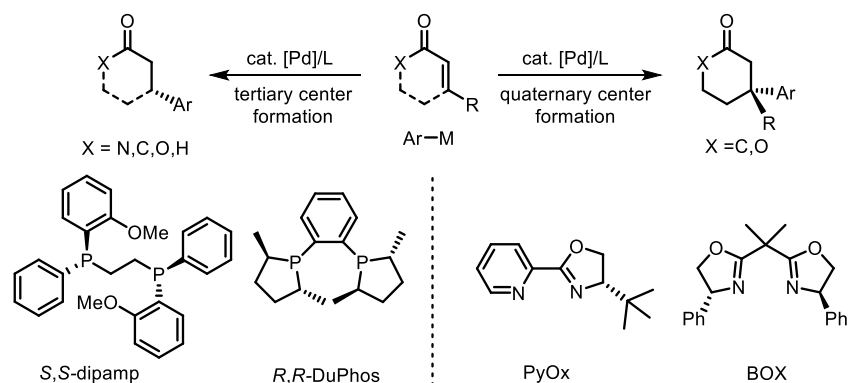
7.3 Enantioselective β -Arylation of Ketones

7.3.1 Introduction

One of the major directions of the β -arylation project is to develop an enantioselective version of the reaction that can directly introduce a chiral center at the β positions of the simple ketones. With respect to the proposed asymmetric β -arylation reaction, the chirality of the product is generated in the step of migratory insertion between the Pd–aryl species and the enone. This is also the enantio-determining step in the palladium-catalyzed asymmetric conjugate addition reaction between metal-based aryl nucleophiles and enones. C_2 -symmetric bidentate phosphine ligands, such as ChiralPhos⁶ and DuPhos⁷, have been employed in the palladium-catalyzed asymmetric conjugate addition reactions using both acyclic and cyclic enones to forge chiral tertiary centers effectively (Scheme 7.12). Recently, Stoltz⁸ and Minnaard⁹ independently

discovered that oxazoline-based ligands are efficient to construct chiral quaternary centers on cyclic ketones and lactones.

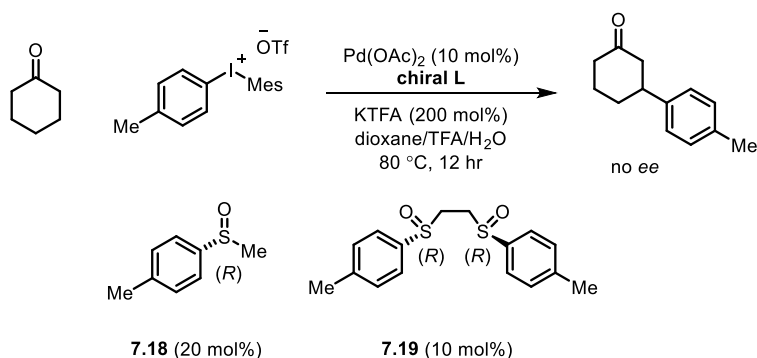
Scheme 7.12 Palladium-Catalyzed Asymmetric Conjugate Addition



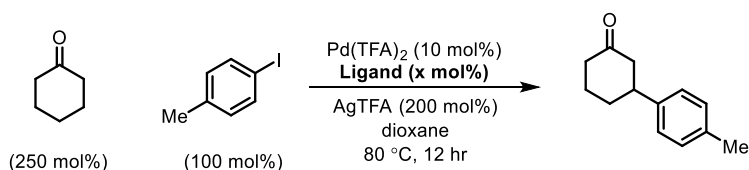
7.3.2 Results and Discussion

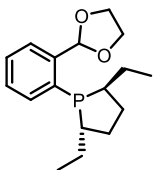
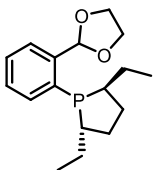
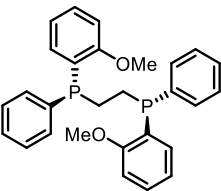
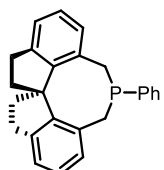
At the initial stage of developing enantioselective β -arylation reaction, both generations of conditions were modified to investigate whether enantioinduction can be achieved. Considering chiral sulfur-based ligands are easily accessible, we first turn to the heavy-metal-free conditions (*vide supra*, Chapter 5). Both monodentate and bidentate sulfoxide ligands (**7.18** and **7.19**) were synthesized using established methods. However, when these ligands were submitted to the β -arylation conditions with mesitylaryliodonium salts, racemic arylation products were isolated (Scheme 7.13). Given the fact that our reaction conditions are proposed to involve active palladium nanoparticles, the enantioinduction using small molecule chiral ligands might not be effective.

Scheme 7.13 Attempts for Enantioselective β -arylation with Diaryliodonium Salts



While monodentate phosphine ligands did promote the β -arylation reaction with aryl iodides (*vide supra*, Chapter 4), there are several difficulties regarding employing their chiral counterparts for the enantioselective reaction. First, chiral and electron-rich monodentate phosphines are generally tedious to synthesize and often require strictly anaerobic conditions. Second, in many cases, the asymmetric induction imposed by monodentate phosphines is moderate. On the other hand, bidentate chiral phosphines are widely utilized in transition metal catalyzed enantioselective transformations. However, the rigid configuration as well as the need of two coordinating sites has been shown to be detrimental to the β -arylation reaction (*vide supra*, Table 4.1). In accordance with our expectation, examination of several chiral mono- and bidentate phosphine ligands has demonstrated that they are indeed not suitable for the enantioselective β -arylation reaction (Table 7.13).

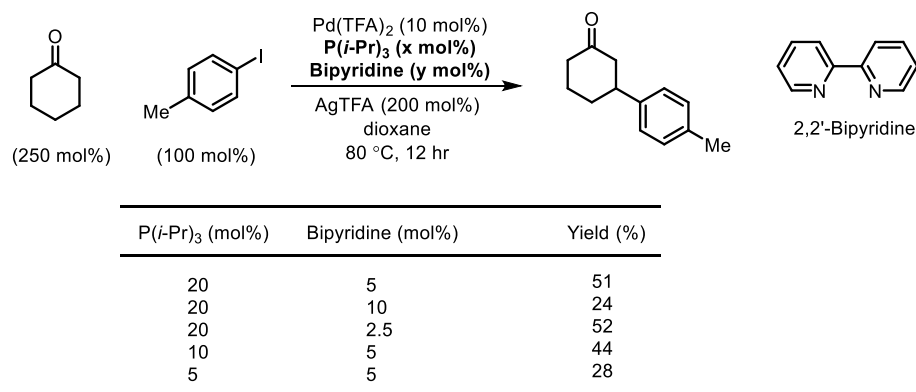
Table 7.13 Investigation of Chiral Phosphine Ligands

Ligand (mol%)	Yield (%)	ee (%)
 (10)	8.0	-6
 (20)	9.5	-4
 (10)	2.9	31
 P-Ph	8.0	n/a

It is known that chiral diamine ligands are capable of promoting the palladium-catalyzed asymmetric conjugate addition. However, little information was available regarding whether this type of ligand is compatible with our palladium-catalyzed redox cascade. Thus, in order to test whether they can be employed to achieve enantioselective β -arylation reaction, we first set out to examine the outcome of the non-asymmetric version when symmetric diamine ligands are added. To our delight, when 2,2'-bipyridine was added as an additional ligand to the β -arylation conditions with triisopropylphosphine, the arylated product can be isolated in a good yield (Table 7.14). Additional reactions also demonstrated that the β -arylation reaction still proceeds

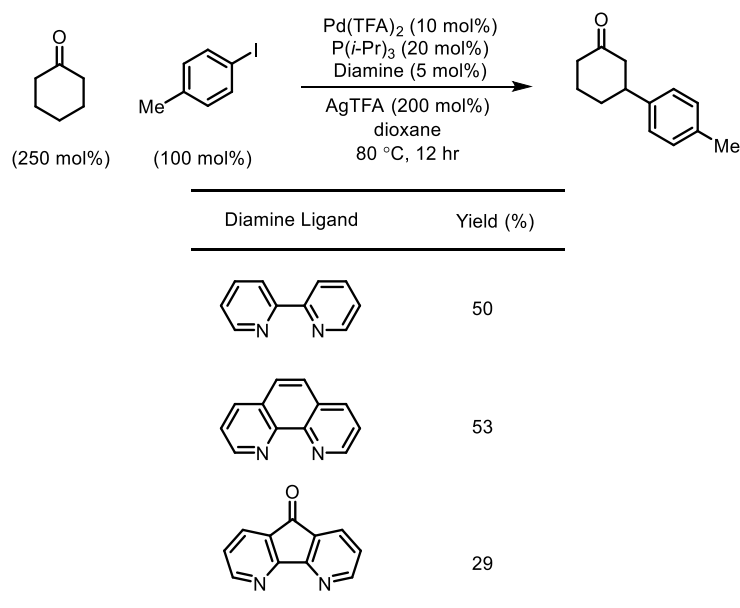
smoothly when the amount of either of these two ligands is varied. These information showed us that the diamine ligand is compatible with the arylation conditions.

Table 7.14 Effects of 2,2'-Bipyridine as An Additional Ligand



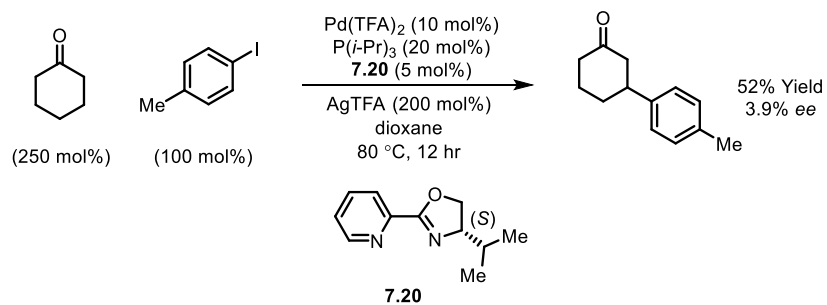
Several diamine ligands with similar structures are also tested (Table 7.15). While 1,10-phenanthroline as co-ligand afforded similar yield as bipyridine, the use of 4,5-Diazafluoren-9-one significantly lowered the yield. Considering this ligand is known to facilitate the palladium-catalyzed dehydrogenation of ketones, we believed the lowered efficiency may be attributed to the poor performance of the ligand at the conjugate addition stage. Thus, in another word, the enhanced reactivity when 2,2'-bipyridine was added as the co-ligand might indicate it promotes the palladium-catalyzed conjugate addition. As the enantio-determining step in the direct β -arylation is the conjugate addition, these results implied that a chiral diamine ligand may be used to affect the enantioselectivity.

Table 7.15 Effects of Related Achiral Diamine Ligands



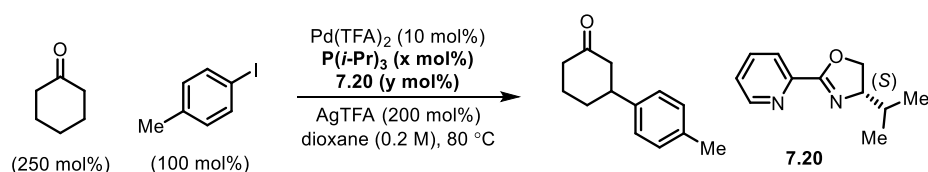
To our delight, a slight enantioinduction was observed when (*S*)-*i*Pr-Pyox (**7.20**) was used as the co-ligand in the β -arylation reaction (Scheme 7.14). On the other hand, the chiral sulfoxide ligand (**7.18** and **7.19**) tested previously gave racemic products.

Scheme 7.14 Preliminary Results with Chiral Pyox-type Ligand



However, the enantioselectivity failed to further increase when (*S*)-*i*Pr-Pyox was used in a small amount as a co-ligand: *ee* remained under 5% when 5 mol% of the ligand was added (Table 7.16). Fortunately, when the equivalence of **7.20** ligand was increased to above 10 mol%, the enantioselectivity also increased considerably (entry 5-10). Later, it was also discovered that Pyox ligand can promote the enantioselective β -arylation reaction without the addition of trisopropylphosphine as the co-ligand (entry 5).

Table 7.16 Effects of Different Amount of Pyox-type Ligand

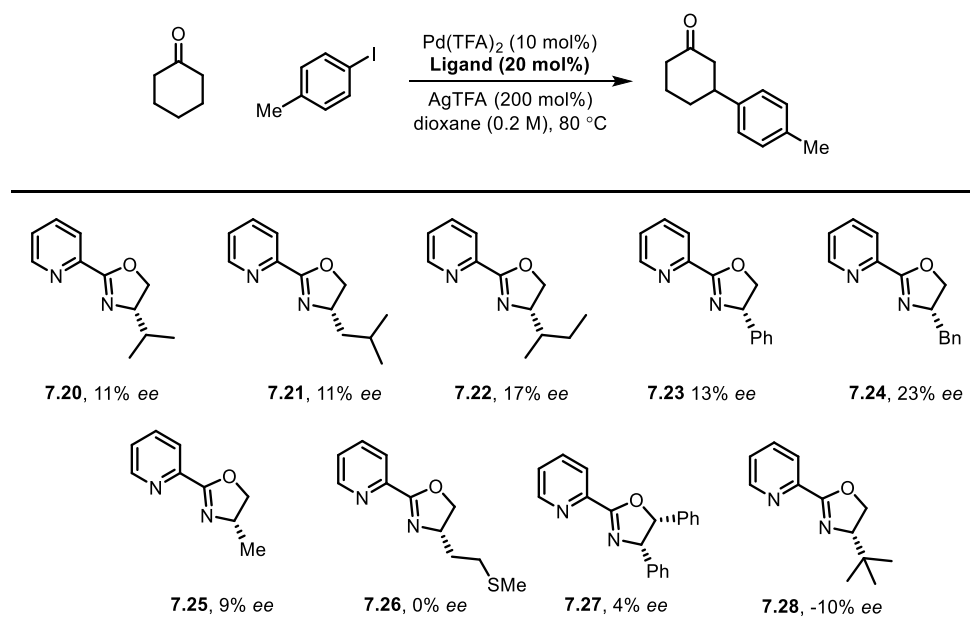


entry	$\text{P}(\textit{i}\text{-Pr})_3$ (mol%)	7.20 (mol%)	<i>ee</i> (%)	Yield (%)
1	0	5	0.0	n/a
2	5	5	2.0	n/a
3	10	5	1.1	n/a
4	20	5	1.3	n/a
5	0	10	9.0	50
6	5	10	1.5	53
7	10	10	9.6	54
8	20	10	9.9	60
9	10	15	12.3	n/a
10	10	20	11.6	n/a

With the success of (*S*)-*i*Pr-Pyox ligand (**7.20**), a variety of Pyox-type ligands were synthesized for the exploration of enantioselective β -arylation (Scheme 7.15). Among all the ligands that are derived from natural amino alcohols, the phenylalaninol-derived ligand **7.24** proved to be the best, giving the β -arylation product in 23% *ee*. Probably due to the poisoning effect of the thiomethyl group, methioninol-derived **7.26** failed to give any enantioinduction. In addition, Pyox ligand with a 2,3-*cis*-substitution pattern on the oxazoline ring (i.e. **7.27**) gave a low *ee*. It is worthy of mentioning that when a sterically demanding *tert*-butyl group was

introduced on the Pyox ligand (**7.28**), the enantioselectivity was reversed, possibly due to the change of transition state.

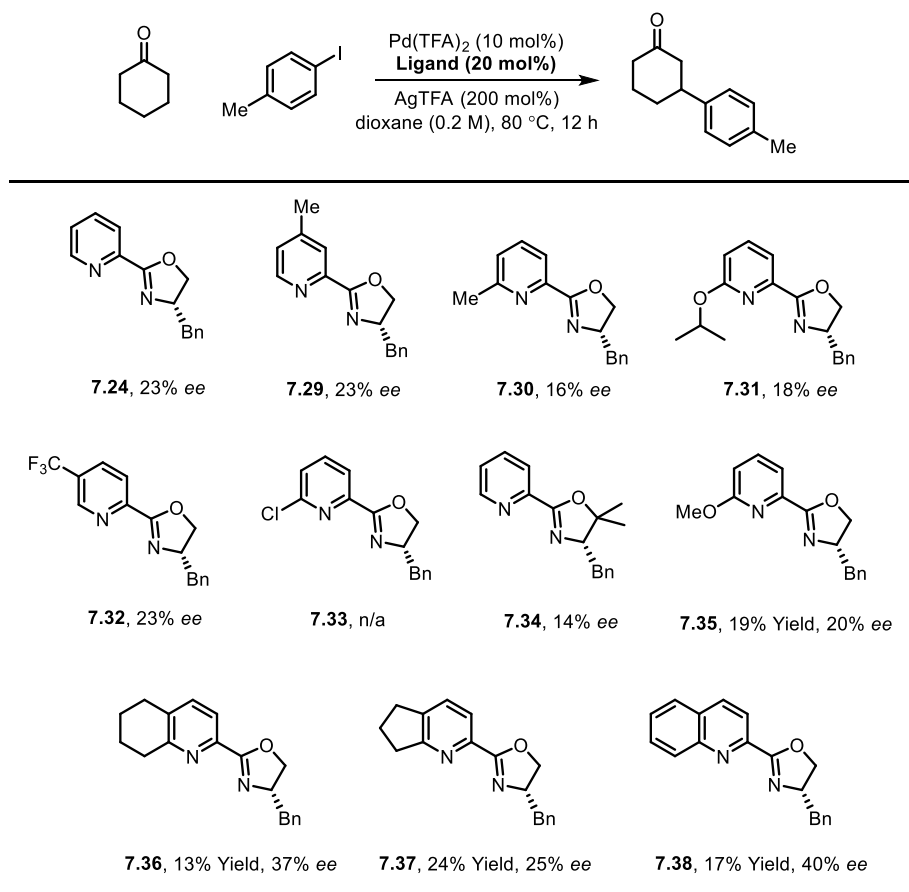
Scheme 7.15 Performance of Different Pyox-type Ligands



Given the result that benzyl-substituted Pyox ligand **7.24** gave the best enantioselectivity, we further attempted to optimize the structure of the ligand backbone (Scheme 7.16). A *para*-methyl (**7.29**), as well as *meta*-trifluoromethyl (**7.32**) substitution on the pyridine ring turned out to have little influence on the outcome of the reaction, while 2-methyl pyridine moiety suppressed the enantioinduction, resulting in a lowered *ee*. 2-chloropyridine motif, on the other hand, did not give any β -arylation product, probably due to the liability of the C–Cl bond. A blocked 5-position of the Pyox ligand (**7.34**) also decreased the enantioselectivity of the arylation reaction. We were pleased to find when a quinoline-based ligand (**7.38**) was used, the *ee* can be improved to 40%. A similar ligand derived from tetrahydroquinoline (**7.36**) also led to an

increased enantioselectivity. However, when a cyclopentane was fused with the pyridine ring (**7.37**), the enantioselectivity dropped back to 25%, indicating the important role of the sterics near the pyridine ring.

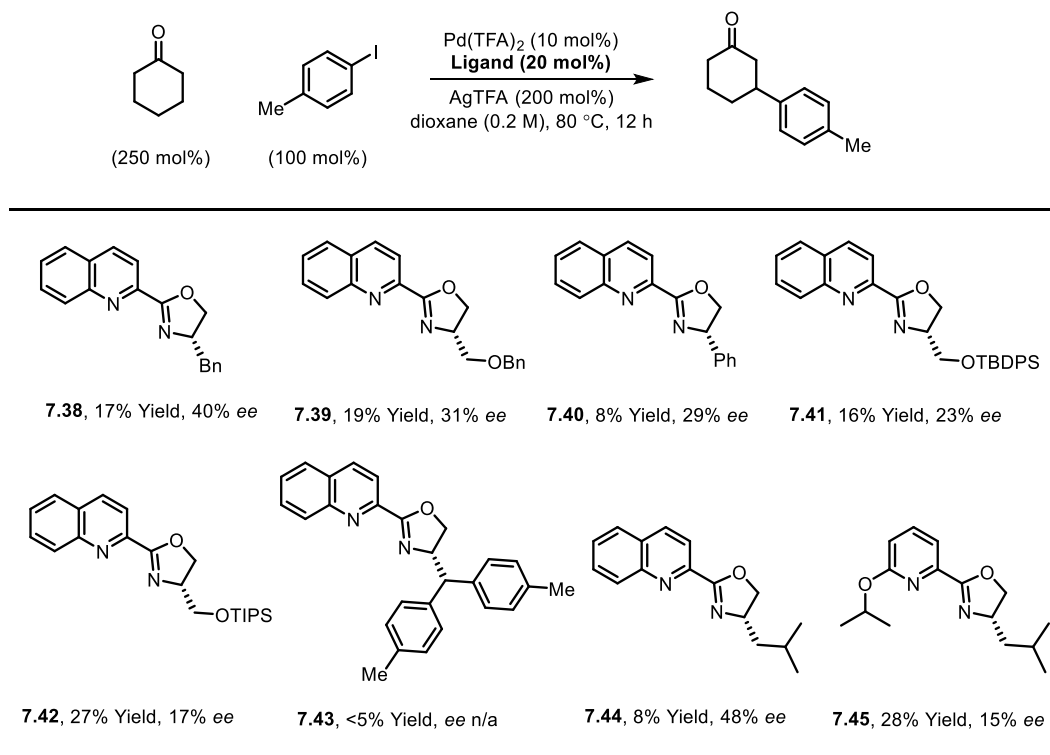
Scheme 7.16 Performance of Pyox-type Ligands with Benzyl Side Chain



After we learned that the Quinox ligand backbone is crucial to the enantioselectivity, we further optimized the structure of the ligand by changing the pendent motif on the oxazoline ring (Scheme 7.17). Ligands with a range of sterics were tested, demonstrating that *i*Bu-Quinox ligand **7.44** is the best ligand so far, giving the β -arylation product in 48% *ee*. However, the yield

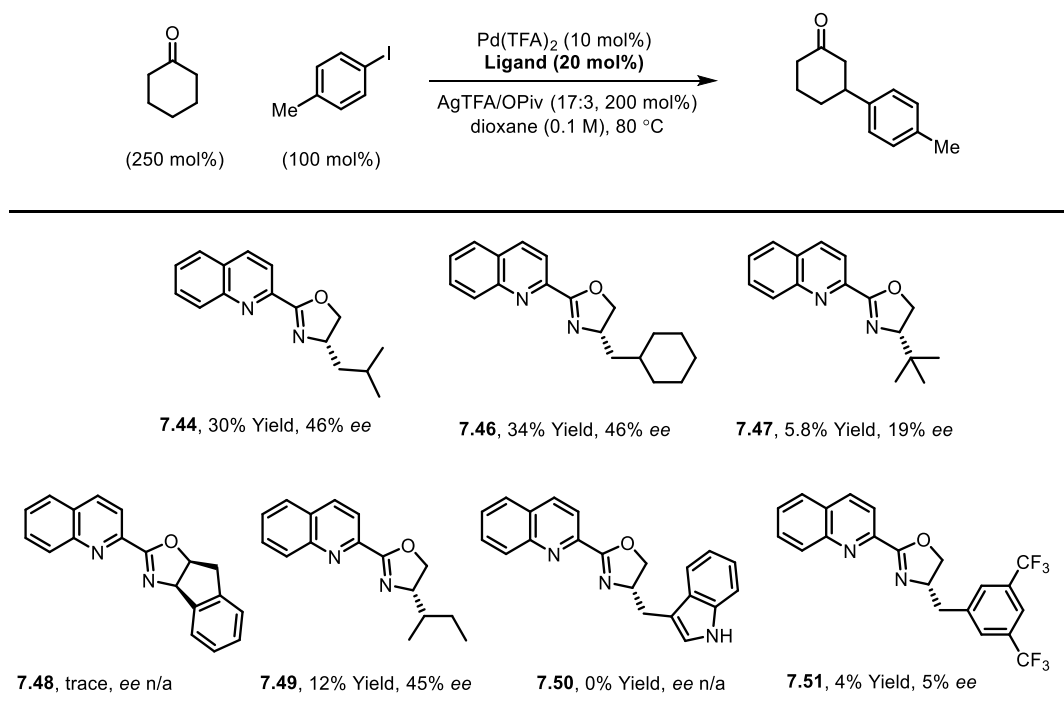
of the reaction dropped to 8% accordingly. Further attempts to maintain both good yield and enantioselectivity by changing the quinoline moiety (**7.45**) were unsuccessful.

Scheme 7.17 Screening of Quinox-type Ligands



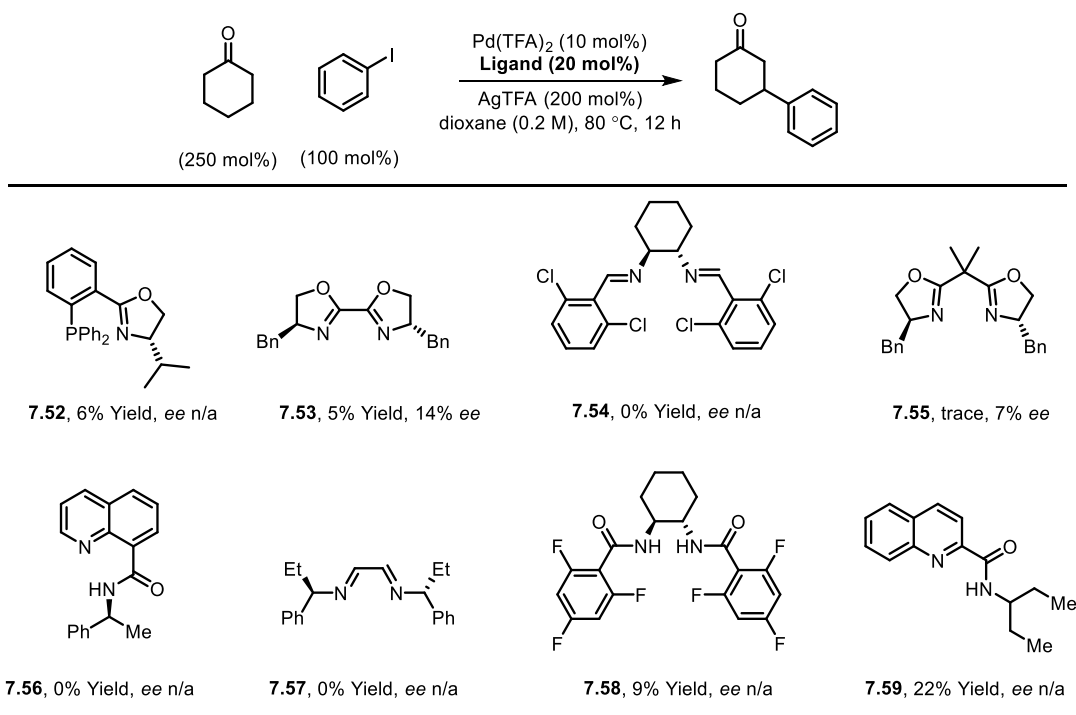
Before we continued to optimize the ligand structure for improving the enantioselectivity, we found that by diluting the reaction, the enantioselectivity of the reaction using **7.44** can be increased to over 50%, albeit with decreased yield. On the other hand, a mixture of silver pivalate and silver trifluoroacetate was shown to increase the yield of the arylation while only slightly decreasing the enantioselectivity. With the new modified reaction conditions, a new set of Quinox-type ligands were synthesized and tested (Scheme 7.18). However, these ligands all gave similar or inferior results compared with **7.44**.

Scheme 7.18 Screening of Quinox-type Ligands (Continued)



Besides Pyox and Quinox-type ligands, a wide range of other types of ligands were also synthesized and tested for the β -arylation reaction (Scheme 7.19). Phox-type ligand (**7.52**), a hybrid of phosphine and oxazoline ligand, gave a very low yield. The Box-type ligand, a privileged class of chiral ligands (**7.53** and **7.55**) for transition-metal catalysis, is not as competitive as Pyox/Quinox ligands and gave the β -arylation product in low yields. Bis-amide (**7.58**) is also tested, although it gave the arylation product in low yield. Bis-imine (**7.54** and **7.57**) ligands, on the other hand, didn't give the desired product. Ligands with both pyridine and amide moiety are also synthesized. While **7.56** failed to afford the β -arylation product, **7.59** turned out to be compatible with the palladium-catalyzed redox cascade. Chiral derivatives of this ligand should be promising for the enantioselective reaction.

Scheme 7.19 Screening of Other Types of Ligands



By using *i*Bu-Quinox **7.44** as the optimized ligand, we set out to investigate the effect of additives to the enantioselectivity and efficiency of the reaction. The initial results are summarized in Table 7.17. Compared with standard conditions, the addition of inorganic base in general lowered the yield of the arylation enantioselectivity. This can be attributed to the introduction of different counteranions for the palladium catalyst. However, the enantioselectivity of the arylation was affected little. Especially, when NaHCO₃ was used as the additive, the *ee* of the reaction can be boosted to 67%. Considering the arylation conditions generate trifluoroacetic acid during the course of the reaction, which may protonate the basic Quinox ligand. Thus, a possible explanation of the increased *ee* is that NaHCO₃ may neutralize the generated strong acid and keep the ligand from protonation. The superiority of NaHCO₃ also lies in the fact that the neutralization product is carbonic acid, which is difficult to interfere with

the palladium catalyst due to its easy decomposition into gaseous CO₂. On the other hand, the addition of strong trifluoroacetic acid could significantly increase the yield of the reaction. Proposedly, strong proton source could promote the final protonation of palladium enolate. Another possibility is the protonation of the *N*-based ligand would result in a faster dehydrogenation step by offering more coordination sites. However, the addition of trifluoroacetic acid also led to the erosion of enantioselectivity of the β-arylation reaction. Fortunately, weaker acids, such as acetic acid and benzoic acid, did not damage the *ee* while slightly increased the yield.

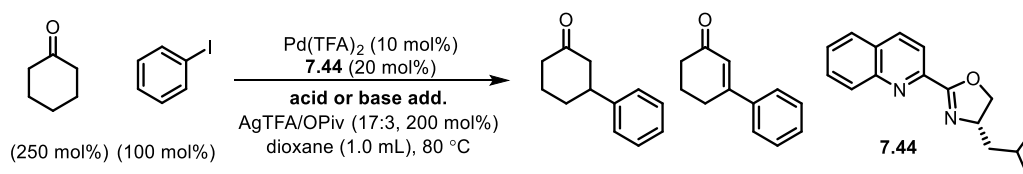
Table 7.17 Effects of Acid or Base Additives

	Additive	Yield (%)	ee (%)
<u>Basic additive:</u>	NaTFA (200 mol%)	3	52
	NaOAc (100 mol%)	1.4	54
	NaHCO₃ (100 mol%)	1.2	67
	KOPiv (100 mol%)	15	37
	K ₃ PO ₄ (100 mol%)	trace	63
	K ₂ HPO ₄ (100 mol%)	5.1	52
	KH ₂ PO ₄ (100 mol%)	3.4	59
<u>Acidic additive:</u>	TFA (50 μL)	47	8
	TFA (25 μL)	27	20
	TFA (10 μL)	17	29
	AcOH (200 mol%)	4.1	55
	PivOH (200 mol%)	6.9	53
	AdCOOH (200 mol%)	9.3	n/a
	MesCOOH (200 mol%)	8.6	52
	PhCOOH (200 mol%)	7.1	55
	<i>p</i> -OMeC ₆ H ₄ COOH (200 mol%)	7.1	52
	<i>p</i> -NO ₂ C ₆ H ₄ COOH (200 mol%)	5.5	52

During the condition optimization, we were also able to identify the major byproduct of the reaction as the dehydrogenative β-arylation product. We rationalize that after the conjugate

addition step, the resulting palladium enolate species could undergo a π - σ - π isomerization, followed by β -hydride elimination to give the by product. Subsequently, a detailed analysis of the effects of acid/base additives was carried out by quantifying the yield for both the product and byproduct, as well as the conversion of iodobenzene (Table 7.18). The analysis showed that the beneficial effect of trifluoroacetic acid for the yield is probably due to the inhibition of dehydrogenative byproduct (entry 2). Similar effects can be observed for other acid additives, including pivalic acid and benzoic acid, of which the byproduct is afforded in under 10% yield. On the other hand, the base additive gave significant amount of dehydrogenative byproduct because of the slow protonation step.

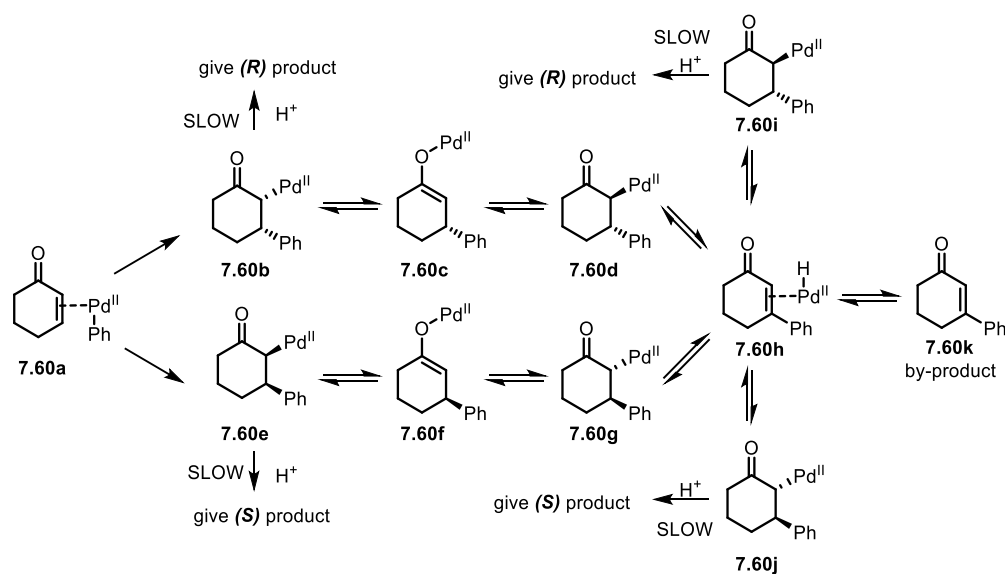
Table 7.18 Detailed Analysis of Reactions with Acid or Base Additives



Entry	Additive (mol%)	Yield (%)	ee (%)	Byproduct (%)	Conversion (%)
1	none	33	40	35	100
2	TFA (10 μL)	31	26	7.6	87
3	PivOH (20)	4.6	54	7.2	66
4	PivOH (50)	6.8	56	16	65
5	PivOH (100)	1.8	48	5.2	72
6	PivOH (150)	2.5	52	5.6	71
7	PivOH (200)	1.7	55	5.5	58
8	AdCOOH (200)	9.1	53	6.4	74
9	PhCOOH (200)	--	33	--	--
10	NaHCO_3 (100)	9.6	51	32	100
11	K_2HPO_4 (100)	16	40	9	80
12	KH_2PO_4 (100)	26	40	25	100
13	$\text{Zn}(\text{TFA})_2$ (30)	5.9	45	26	63
14	$\text{Cu}(\text{TFA})_2$ (30)	18	38	14	78

Our hypotheses were supported by a preliminary DFT computation, which demonstrated the protonation of the Pd(II)-enolate to give the β -arylation product is indeed the most difficult step in the reaction.¹⁰ The computation study also indicated that after the initial migratory insertion of Pd-Ar species, the resulting Pd(II)-enolates (**7.60b** and **7.60e**) are prone to undergo a π - σ - π isomerization to pose the palladium on the other side of the enolate. The β -hydride elimination of resulting enolates (**7.60d** and **7.60g**) is facile to give **7.60h**, which upon dissociation of the palladium, would release the byproduct **7.60k**. Another complication of the reaction is that intermediate **7.60h** could further undergo a Pd-H migratory insertion, also an enantio-determining step for the reaction. Thus, due to the high activation barrier for the final protonation step, all these Pd(II)-enolate intermediates are proposed to be in an equilibrium with each other. And such an equilibrium should erode the enantioselectivity established at the initial step of Pd-Ar migratory insertion.

Scheme 7.20 Reaction Pathways by Computation



7.4 Conclusion

In summary, we have developed new conditions for the palladium-catalyzed direct β -arylation of ketones with aryl iodides that avoid the use of stoichiometric heavy metal as the additive. Instead, a combination of KTFA and NaBF₄ was employed to act as the iodide scavenger and restore the active palladium catalyst. It is also worthy of noting that the catalytic amount of silver salt in the conditions was proposed to extract the chloride ligand on the palladium precatalyst and initiate the arylation reaction.

We have also explored the possibility of using cheaper and more available aryl bromides as the aryl source for the palladium-catalyzed β -arylation reaction. It was figured out that the main obstacle to this goal is the slow oxidative addition of aryl bromides to Pd(0) intermediate. We discovered that an NHC-ligated palladium precatalyst, [IMesPdCl₂]₂, could significantly boost the reactivity of aryl bromides towards the β -arylation reaction.

In addition, attempts to develop an enantioselective version of the palladium-catalyzed β -arylation reaction have been made. While chiral bidentate phosphine ligands are not compatible with the reaction, Pyox and Quinox-type ligands were found to induce a moderate degree of enantioselectivity. However, based on the mechanistic studies and DFT computation, further improvement on the yield and enantioselectivity was hampered by the slow protonation of the palladium enolate after the conjugate addition, which led to the loss of chirality via enolate isomerization and subsequent β -hydride elimination to give the over-oxidation product.

7.5 Experimental

Typical procedure for stoichiometric heavy metal-free β -arylation with aryl iodides

A 4 mL vial was charged with Pd(Ph₂SO)₂Cl₂ (5.8 mg, 0.010 mmol, 5 mol%), AgTFA (5.5 mg, 0.013 mmol, 12.5 mol%), DMSO (4.4 mg, 0.056 mmol, 28 mol%), KTFA (90 mg, 0.60 mmol, 300 mol%), and KOTf (22 mg, 0.20 mmol, 100 mol%). A stir-bar was added to the vial and the vial was sealed with a PTFE lined cap, and transferred to a glove-box filled with nitrogen. The vial was then opened in the glove-box and 1.0 mL of 1,4-dioxane was added, followed by cyclohexanone (49 mg, 0.50 mmol, 250 mol%), iodobenzene (41 mg, 0.20 mmol, 100 mol%), and 50 μ L of trifluoroacetic acid. The vial was sealed again, transferred out of the glove-box, and heated at 80 °C for 12 hours under stirring. Subsequently, the reaction was cooled to room temperature and the vial opened. Another portion of Pd(Ph₂SO)₂Cl₂ (5.8 mg, 0.010 mmol, 5 mol%), AgTFA (5.5 mg, 0.013 mmol, 12.5 mol%), DMSO (4.4 mg, 0.056 mmol, 28 mol%), and KOTf (22 mg, 0.20 mmol, 100 mol%) was added. And the vial was sealed again with a new PTFE lined cap, and heated at 80 °C for another 12 hours under stirring. Then the mixture was allowed to cool to room temperature. Appropriate amount of dodecane (~10 mg) was added to the reaction mixture as internal standard and the mixture was stirred for an additional 5 min to fully mix. ~0.3 mL of the resulting mixture was filtered through a small plug of silica gel, eluted with diethyl ether. The filtrate was directly used for GC analysis.

GC instrument conditions: inlet temperature: 250 °C, detector temperature: 300 °C, hydrogen flow: 40 mL/min, air flow: 400 mL/min. Method: 50 °C hold for 0 min, followed by a temperature increase of 10°C/min to 210 °C, hold 0 min (total run time: 16 min). Retention times

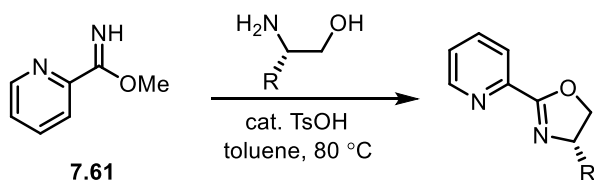
were as follows: cyclohexanone (3.9), iodobenzene (5.7), dodecane (7.99) and 3-phenylcyclohexanone (12.54).

Typical procedure for β -arylation with aryl bromides

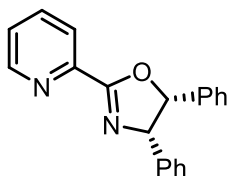
A 4 mL vial was charged with [IMesPdCl₂]₂ (4.8 mg, 0.005 mmol, 5 mol%), AgTFA (44 mg, 0.20 mmol, 200 mol%), and a stir-bar. The vial was sealed with a PTFE lined cap, and transferred to a glove-box filled with nitrogen. The vial was then opened in the glove-box and 0.5 mL of 1,4-dioxane was added, followed by cyclohexanone (24.5 mg, 0.25 mmol, 250 mol%) and bromobenzene (15.7 mg, 0.10 mmol, 100 mol%). The vial was sealed again, transferred out of the glove-box, and heated at 100 °C for 12 hours under stirring. The mixture was allowed to cool to room temperature. Appropriate amount of dodecane (~10 mg) was added to the reaction mixture as internal standard and the mixture was stirred for an additional 5 min to fully mix. ~0.3 mL of the resulting mixture was filtered through a small plug of silica gel, eluted with diethyl ether. The filtrate was directly used for GC analysis.

Procedures for the synthesis of Pyox-type ligands

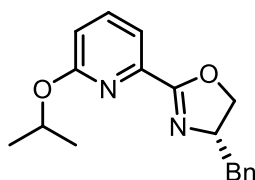
Method A



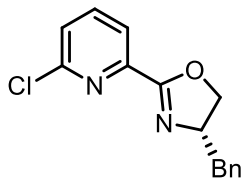
To a 100 mL round bottom flask were added imidate **7.61** (1.0 equiv.), chiral amino alcohol (0.96 equiv.), catalytic amount of *p*-toluenesulfonic acid (5 mol%), and toluene (0.2 M). The mixture was stirred at 80 °C for 3 hrs, monitored by TLC. Once completed, the reaction was cooled to room temperature, and quenched with saturated NaHCO₃ solution. The organic layer was separated and the aqueous layer extracted with EtOAc. The organics were combined, washed with water and brine, dried, and filtered. The solvent was removed in vacuo and the residue was submitted to flash column chromatography to yield the desired Pyox-type ligand. The ¹H-NMR data of selected ligands was shown below.



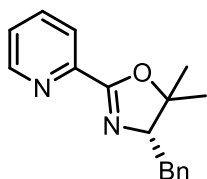
7.27, ¹H-NMR (500 MHz, CDCl₃) δ 8.83 (dd, *J* = 4.8, 0.7 Hz, 1H), 8.32 (d, *J* = 7.9 Hz, 1H), 7.88 (td, *J* = 7.8, 1.7 Hz, 1H), 7.49 (ddd, *J* = 7.6, 4.8, 1.1 Hz, 1H), 7.05-7.03 (m, 6H), 6.99-6.95 (m, 4H), 6.14 (d, *J* = 10.3 Hz, 1H), 5.84 (d, *J* = 10.3 Hz, 1H).



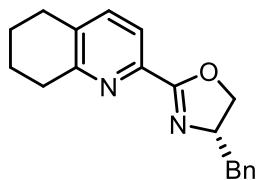
7.31, ¹H-NMR (500 MHz, CDCl₃) δ 7.63-7.57 (m, 2H), 7.32-7.29 (m, 2H), 7.26-7.22 (m, 3H), 6.78 (dd, *J* = 7.9, 1.1 Hz, 1H), 5.47 (hept, *J* = 6.2 Hz, 1H), 4.63 (tdd, *J* = 9.3, 7.5, 4.9 Hz, 1H), 4.39 (t, *J* = 9.0 Hz, 1H), 4.20 (dd, *J* = 8.4, 7.5 Hz, 1H), 3.29 (dd, *J* = 13.7, 4.8 Hz, 1H), 2.74 (dd, *J* = 13.7, 9.2 Hz, 1H), 1.35 (dd, *J* = 6.1, 4.7 Hz, 6H).



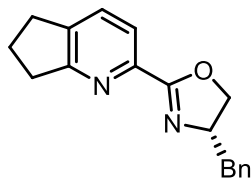
7.33, ¹H-NMR (500 MHz, CDCl₃) δ 8.00 (d, *J* = 7.6 Hz, 1H), 7.75 (t, *J* = 7.8 Hz, 1H), 7.45 (d, *J* = 8.0 Hz, 1H), 7.33-7.30 (m, 2H), 7.26-7.24 (m, 2H), 4.65 (ddd, *J* = 16.9, 9.2, 5.2 Hz, 1H), 4.45 (t, *J* = 9.1 Hz, 1H), 4.24 (t, *J* = 8.2 Hz, 1H), 3.28 (dd, *J* = 13.8, 5.1 Hz, 1H), 2.75 (dd, *J* = 13.8, 9.0 Hz, 1H).



7.34, ¹H-NMR (500 MHz, CDCl₃) δ 8.77 (d, *J* = 4.4 Hz, 1H), 8.25-8.17 (m, 1H), 7.83 (t, *J* = 7.4 Hz, 1H), 7.44-7.42 (m, 1H), 7.36-7.35 (m, 3H), 7.26-7.25 (m, 2H), 4.33-4.30 (m, 1H), 3.30-3.27 (m, 1H), 2.90 (dd, *J* = 14.2, 8.0 Hz, 1H), 1.47 (s, 6H).

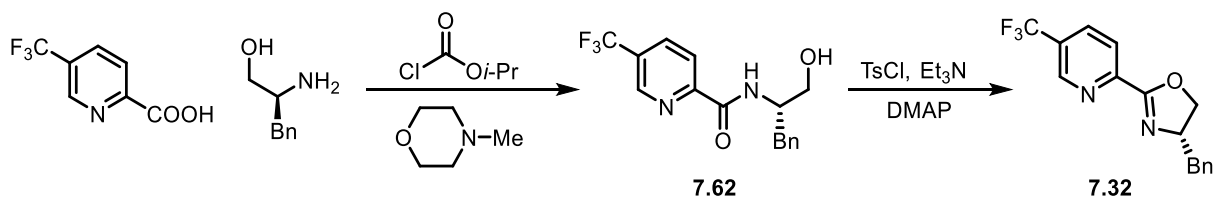


7.36, ¹H NMR (500 MHz, CDCl₃) δ 7.83 (d, *J* = 7.9 Hz, 1H), 7.45 (d, *J* = 7.9 Hz, 1H), 7.32 (t, *J* = 7.5 Hz, 2H), 7.28-7.22 (m, 3H), 4.64 (td, *J* = 14.2, 9.1 Hz, 1H), 4.43 (t, *J* = 9.0 Hz, 1H), 4.23 (t, *J* = 8.1 Hz, 1H), 3.32 (dd, *J* = 13.7, 4.8 Hz, 1H), 3.02 (t, *J* = 6.4 Hz, 2H), 2.83 (t, *J* = 6.2 Hz, 2H), 2.75 (dd, *J* = 13.7, 9.4 Hz, 1H), 1.92 (dt, *J* = 10.3, 5.3 Hz, 2H), 1.86-1.81 (m, 2H).



7.37, $^1\text{H NMR}$ (500 MHz, CDCl_3) δ 7.83 (d, $J = 7.8$ Hz, 1H), 7.57 (d, $J = 7.8$ Hz, 1H), 7.31 (t, $J = 7.4$ Hz, 2H), 7.26-7.23 (m, 3H), 4.63 (ddd, $J = 17.0, 9.3, 4.9$ Hz, 1H), 4.42 (t, $J = 9.0$ Hz, 1H), 4.23 – 4.18 (m, 1H), 3.32 (dd, $J = 13.8, 4.9$ Hz, 1H), 3.09 (t, $J = 7.7$ Hz, 2H), 2.98 (t, $J = 7.5$ Hz, 2H), 2.73 (dd, $J = 13.8, 9.4$ Hz, 1H), 2.15 (p, $J = 7.6$ Hz, 2H).

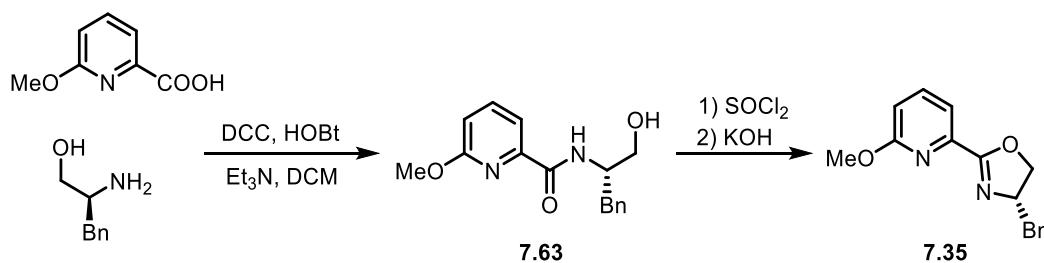
Method B



To a 100 mL round bottom flask were added 5-(trifluoromethyl)picolinic acid (3.0 mmol, 471 mg), *N*-methylmorpholine (4.5 mmol, 0.5 mL), and 25 mL DCM. The mixture was cooled to 0 °C, and isopropyl chloroformate (1.0 M, 3.5 mL) was added dropwise to the solution. The mixture was stirred at 0 °C for 30min. Then a solution of phenylalaninol (3.6 mmol, 544 mg) and *N*-methylmorpholine (4.5 mmol, 0.5 mL) in 10 mL DCM was added. The resulting mixture was stirred overnight and then diluted with DCM. The solution was washed with 1N HCl, water and brine. The solvent was removed in vacuo and the residue submitted to flash column chromatography to give **7.62**.

To a 100 mL round bottom flask were added intermediate **7.62** (2.0 mmol, 652 mg), TsCl (3.0 mmol, 573 mg), DMAP (0.20 mmol, 24 mg), triethylamine (8.0 mmol, 1.1 mL), and 25 mL DCM. The mixture was stirred at room temperature for 3 hours and refluxed overnight. The reaction was quenched with saturated NaHCO₃ solution, and the organic layer separated. The organics were washed with water and brine, dried, filtered and concentrated. Flash column chromatography gave **7.32**.

7.32, ¹H NMR (500 MHz, CDCl₃) δ 8.96 (s, 1H), 8.19 (d, *J* = 8.2 Hz, 1H), 8.04 (dd, *J* = 8.2, 2.1 Hz, 1H), 7.31 (dd, *J* = 9.8, 5.0 Hz, 2H), 7.27-7.22 (m, 3H), 4.70 (ddd, *J* = 16.9, 9.0, 5.3 Hz, 1H), 4.53-4.43 (m, 1H), 4.30-4.24 (m, 1H), 3.29 (dd, *J* = 13.8, 5.2 Hz, 1H), 2.80 (dd, *J* = 13.8, 8.8 Hz, 1H).



To a 100 mL round bottom flask were added 6-(methoxy)picolinic acid (6.0 mmol, 918 mg) and 50 mL DCM. To the flask were added DCC (6.6 mmol, 1.36 g) and HOBT (6.6 mmol, 891 mg) at 0°C. The mixture was warmed to room temperature and stirred for 1 hr. Phenylalaninol (7.2 mmol, 1.09 g) was then added and the mixture was stirred at room temperature overnight. The precipitate was filtered off and washed with DCM. The resulting

filtrate was concentrated in vacuo. The residue submitted to flash column chromatography to give **7.63**.

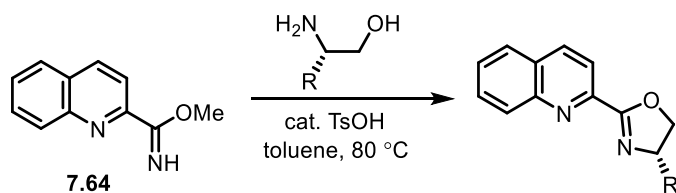
To a 100 mL round bottom flask were added intermediate **7.63** (4.7 mmol, 1.34 g) and 30 mL toluene. To the mixture was added SOCl_2 (7.0 mmol, 0.70 mL) dropwise. The mixture was stirred at 60°C for 1 hour and 90 °C overnight. The reaction was cooled to room temperature and poured into 0 °C 20% KOH solution (100 mL). The organic layer was separated and aqueous extracted with DCM. The combined organics were washed with water and brine. The solvent was removed in vacuo to give chlorination product.

To a 250 mL round bottom flask were added the chlorination product (4.1 mmol, 1.25 g), KOH (10.2 mmol, 574 mg), and 60 mL MeOH. The mixture was heated to reflux for 3 hr. The reaction was cooled to room temperature, concentrated, and water was added to the mixture. The mixture was extracted with DCM. The organics were concentrated in vacuo and flash column chromatography gave **7.35**.

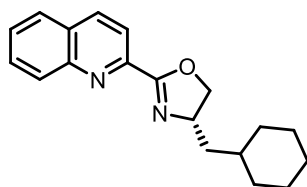
7.35, $^1\text{H NMR}$ (500 MHz, CDCl_3) δ 7.66-7.61 (m, 2H), 7.31 (dd, $J = 10.1, 4.6$ Hz, 2H), 7.26-7.22 (m, 3H), 6.89-6.84 (m, 1H), 4.64 (tdd, $J = 9.4, 7.6, 4.8$ Hz, 1H), 4.43-4.38 (m, 1H), 4.21 (dd, $J = 8.4, 7.7$ Hz, 1H), 4.03 (s, 3H), 3.33 (dd, $J = 13.7, 4.8$ Hz, 1H), 2.74 (dd, $J = 13.7, 9.4$ Hz, 1H).

Procedures for the synthesis of Quinox-type ligands

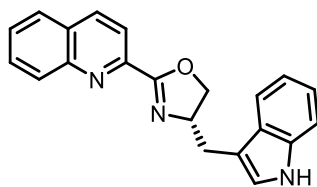
Method A



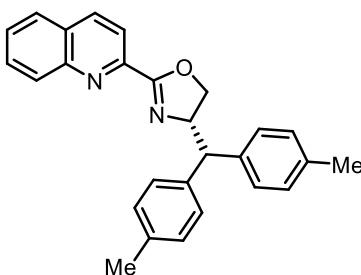
To a 100 mL round bottom flask were added imidate **7.64** (1.0 equiv.), chiral amino alcohol (0.96 equiv.), catalytic amount of *p*-toluenesulfonic acid (5 mol%), and toluene (0.2 M). The mixture was stirred at 80 °C for 3 hours, monitored by TLC. Once completed, the reaction was cooled to room temperature, and quenched with saturated NaHCO₃ solution. The organic layer was separated and the aqueous layer extracted with EtOAc. The organics were combined, washed with water and brine, dried, and filtered. The solvent was removed in vacuo and the residue was submitted to flash column chromatography to yield the desired Quinox-type ligand.



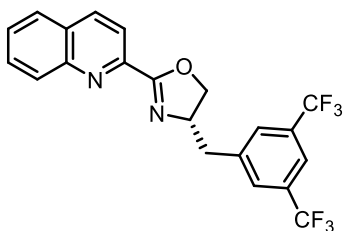
7.46, ¹H NMR (500 MHz, CDCl₃) δ 8.27 (d, *J* = 8.5 Hz, 1H), 8.23 (d, *J* = 8.6 Hz, 1H), 8.19 (d, *J* = 8.5 Hz, 1H), 7.85 (d, *J* = 8.1 Hz, 1H), 7.75 (ddd, *J* = 8.4, 6.9, 1.3 Hz, 1H), 7.63-7.59 (m, 1H), 4.68 (dd, *J* = 9.4, 8.2 Hz, 1H), 4.49 (dq, *J* = 16.0, 8.1 Hz, 1H), 4.16 (t, *J* = 8.2 Hz, 1H), 1.81 (dt, *J* = 13.3, 6.6 Hz, 3H), 1.75-1.65 (m, 3H), 1.54 (dtd, *J* = 10.6, 7.1, 3.6 Hz, 1H), 1.48-1.42 (m, 1H), 1.35-1.14 (m, 3H), 1.04-0.95 (m, 2H).



7.50, ^1H NMR (500 MHz, CDCl_3) δ 8.31-8.20 (m, 3H), 8.10 (s, 1H), 7.86 (d, $J = 8.2$ Hz, 1H), 7.76 (t, $J = 7.7$ Hz, 1H), 7.70 (d, $J = 7.8$ Hz, 1H), 7.62 (t, $J = 7.5$ Hz, 1H), 7.37 (d, $J = 8.1$ Hz, 1H), 7.21 (t, $J = 7.5$ Hz, 1H), 7.14 (t, $J = 7.4$ Hz, 1H), 7.10 (s, 1H), 4.90 – 4.82 (m, 1H), 4.53 (t, $J = 9.0$ Hz, 1H), 4.36 (t, $J = 8.0$ Hz, 1H), 3.47 (dd, $J = 14.5, 4.7$ Hz, 1H), 2.97 (dd, $J = 14.5, 9.1$ Hz, 1H).

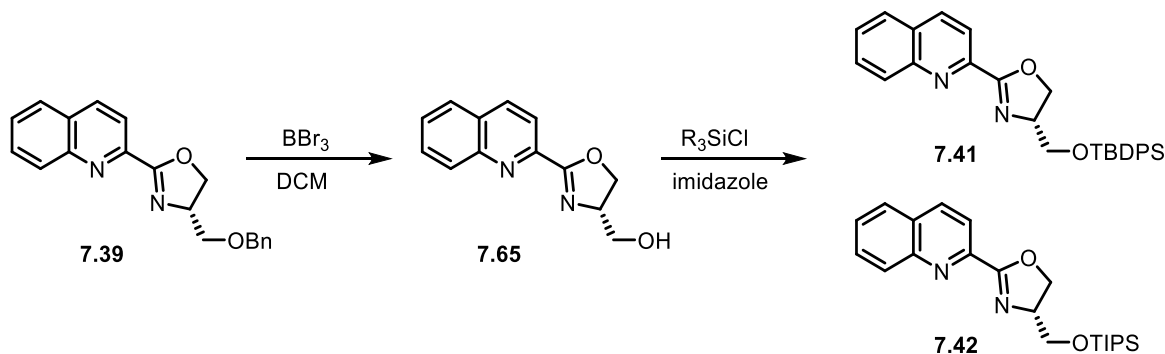


7.43, ^1H NMR (500 MHz, CDCl_3)¹¹ δ 8.26 (d, $J = 8.5$ Hz, 1H), 8.22 (s, 2H), 7.87 (d, $J = 8.1$ Hz, 1H), 7.79 – 7.75 (m, 1H), 7.62 (t, $J = 7.0$ Hz, 1H), 7.28 (d, $J = 6.9$ Hz, 2H), 7.23 (d, $J = 8.0$ Hz, 2H), 7.14 (dd, $J = 7.8, 3.0$ Hz, 4H), 5.22 (dd, $J = 17.7, 9.4$ Hz, 1H), 4.64 (t, $J = 9.2$ Hz, 1H), 4.30 (t, $J = 8.5$ Hz, 1H), 4.10 (d, $J = 9.3$ Hz, 1H), 2.33 (d, $J = 1.6$ Hz, 6H).

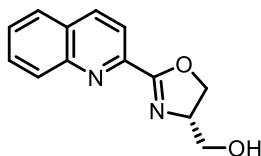


7.51, ^1H NMR (500 MHz, CDCl_3)¹¹ δ 8.29 (dd, $J = 8.3, 4.5$ Hz, 1H), 8.19 (d, $J = 8.6$ Hz, 1H), 7.89 (d, $J = 8.1$ Hz, 1H), 7.82 – 7.78 (m, 2H), 7.67 – 7.63 (m, 1H), 4.78 (ddd, $J = 13.5, 9.5, 7.1$ Hz, 1H), 4.72 – 4.66 (m, 1H), 4.33 – 4.27 (m, 1H), 3.19 (ddd, $J = 20.2, 14.1, 6.6$ Hz, 1H).

Method B

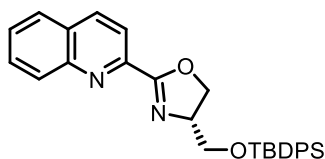


To a 250 mL round bottom flask were added **7.39** (5.3 mmol, 1.67 g) and 120 mL DCM . The mixture was cooled to 0°C , and BBr_3 (15.9 mmol, 1.6 mL) was added dropwise. The reaction was warmed to, and stirred at room temperature, monitored by TLC. Once completed, the reaction was diluted with 100 mL DCM . NaHCO_3 (sat. solution) was added dropwise until pH reached 7-8. The DCM layer was separated and the aqueous was extracted with DCM . The organics were combined, dried, and filtered. The solvent was removed in vacuo and the residue was submitted to flash column chromatography to give **7.65** (507 mg).

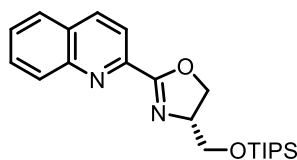


7.65, $^1\text{H NMR}$ (500 MHz, CDCl_3) δ 8.71 (d, $J = 7.7$ Hz, 1H), 8.31 (dd, $J = 21.9, 8.5$ Hz, 2H), 8.15 (d, $J = 8.5$ Hz, 1H), 7.89 (d, $J = 8.1$ Hz, 1H), 7.78 (dd, $J = 11.2, 4.2$ Hz, 1H), 7.64 (t, $J = 7.1$ Hz, 1H), 4.50-4.43 (m, 1H), 4.08 (dd, $J = 11.2, 4.8$ Hz, 1H), 3.94 (dd, $J = 11.2, 5.0$ Hz, 1H), 3.77 (ddd, $J = 16.4, 10.4, 5.4$ Hz, 2H).

To a 10 mL round bottom flask were added **7.65** (1.0 equiv.), SiR₃Cl (2.5 equiv.), imidazole (5.0 equiv.), and 3 mL of DMF. The mixture was stirred at room temperature and monitored by TLC. The reaction was then quenched with water and extracted with EtOAc. The combined organics were washed with water to remove residue DMF, and brine. The organics were dried and concentrated. The residue was submitted to flash column chromatography to give the quinox ligand **7.41** and **7.42**.



7.41, ¹H-NMR, ¹H NMR (500 MHz, CDCl₃) δ 8.31 (d, *J* = 8.5 Hz, 1H), 8.26 (d, *J* = 8.6 Hz, 1H), 8.19 (d, *J* = 8.5 Hz, 1H), 7.88 (d, *J* = 8.1 Hz, 1H), 7.81-7.77 (m, 1H), 7.72-7.69 (m, 4H), 7.63 (dd, *J* = 11.0, 3.9 Hz, 1H), 7.47-7.36 (m, 6H), 4.69 (d, *J* = 8.0 Hz, 2H), 4.63-4.57 (m, 1H), 4.02 (dd, *J* = 10.3, 3.8 Hz, 1H), 3.87 (dd, *J* = 10.3, 6.2 Hz, 1H), 1.04 (s, 9H).



7.42, ¹H-NMR, ¹H NMR (500 MHz, CDCl₃) δ 8.31 (d, *J* = 8.5 Hz, 1H), 8.26 (d, *J* = 8.6 Hz, 1H), 8.19 (d, *J* = 8.5 Hz, 1H), 7.88 (d, *J* = 8.1 Hz, 1H), 7.79 (ddd, *J* = 8.4, 6.9, 1.3 Hz, 1H), 7.65-7.61 (m, 1H), 4.67 (d, *J* = 2.6 Hz, 1H), 4.65 (s, 1H), 4.60-4.54 (m, 1H), 4.11 (dd, *J* = 9.9, 3.9 Hz, 1H), 3.84 (dd, *J* = 9.9, 7.0 Hz, 1H), 1.16-1.05 (m, 21H).

7.6 References

1. Diao, T. N.; Stahl, S. S. *J. Am. Chem. Soc.* **2011**, *133*, 14566
2. Hartwig, J. F., *Organotransition Metal Chemistry: From Bonding to Catalysis*. University Science Books: 2010
3. Fortman, G. C.; Nolan, S. P. *Chem. Soc. Rev.* **2011**, *40*, 5151
4. Lummiss, J. A. M.; Higman, C. S.; Fyson, D. L.; McDonald, R.; Fogg, D. E. *Chem. Sci.* **2015**, *6*, 6739
5. (a) Hadei, N.; Kantchev, E. A. B.; O'Brien, C. J.; Organ, M. G. *Org. Lett.* **2005**, *7*, 3805. (b) Nasielski, J.; Hadei, N.; Achinduh, G.; Kantchev, E. A. B.; O'Brien, C. J.; Lough, A.; Organ, M. G. *Chem. Eur. J.* **2010**, *16*, 10844. (c) Valente, C.; Belowich, M. E.; Hadei, N.; Organ, M. G. *Eur. J. Org. Chem.* **2010**, 4343.
6. (a) Nishikata, T.; Yamamoto, Y.; Miyaura, N. *Adv. Synth. Catal.* **2007**, *349*, 1759. (b) Nishikata, T.; Yamamoto, Y.; Miyaura, N. *Tetrahedron Lett.* **2007**, *48*, 4007
7. Gini, F.; Hessen, B.; Minnaard, A. J. *Org. Lett.* **2005**, *7*, 5309
8. (a) Holder, J. C.; Marziale, A. N.; Gatti, M.; Mao, B.; Stoltz, B. M. *Chem. Eur. J.* **2013**, *19*, 74-77. (b) Holder, J. C.; Zou, L.; Marziale, A. N.; Liu, P.; Lan, Y.; Gatti, M.; Kikushima, K.; Houk, K. N.; Stoltz, B. M. *J. Am. Chem. Soc.* **2013**, *135*, 14996-15007. (c) Kikushima, K.; Holder, J. C.; Gatti, M.; Stoltz, B. M. *J. Am. Chem. Soc.* **2011**, *133*, 6902.
9. Gottumukkala, A. L.; Matcha, K.; Lutz, M.; de Vries, J. G.; Minnaard, A. J. *Chem. Eur. J.* **2012**, *18*, 6907.
10. For a computational study of the rate of protonation of Pd-enolate, see: Peng, Q.; Yan, H.; Zhang, X.; Wu, Y.-D. *J. Org. Chem.* **2012**, *77*, 7487.
11. The corresponding chiral amino alcohols were synthesized using a method reported in literature: Chen, G.; Shigenara, T.; Jain, P.; Zhang, Z.; Jin, Z.; He, J.; Li, S.; Mapelli, C.; Miller, M. M.; Poss, M. A.; Scola, P. M.; Yeung, K.-S.; Yu, J.-Q. *J. Am. Chem. Soc.* **2015**, *137*, 3338.